

CONVERGENT SYNTHETIC STRATEGIES TOWARD
HETERODIMERIC BISINDOLE ALKALOIDS
AND
POLYOXYGENATED DITERPENOIDS

Thesis by
Christopher Elias Reimann

In Partial Fulfillment of the Requirements
for the Degree of
Doctor of Philosophy

CALIFORNIA INSTITUTE OF TECHNOLOGY

Pasadena, California

2020

(Defended: July 14, 2020)

© 2020

Christopher Elias Reimann

All Rights Reserved

To my Mom and Dad

"I've loved, I've laughed, and cried
I've had my fill, my share of losing
And now, as tears subside
I find it all so amusing

To think I did all that
And may I say, not in a shy way
Oh no, oh no, not me
I did it my way"

– Frank Sinatra

ACKNOWLEDGEMENTS

First and foremost, I would like to thank my advisor, Professor Brian Stoltz. After I committed to Caltech, I had dinner with Brian following a lecture at USC and I left that evening with a powerful realization: “this man cares about my development as a human being as much as he does my development as a scientist.” Brian is a brilliant chemist, gifted experimentalist, and fantastic teacher, but what is most outstanding is how he treats us all as colleagues. In a field notorious for characters and egos, the B man has this unbelievable ability to sustain success without losing humanity, and he serves as a template for what good leaders should strive to be. I didn’t make a lot of smart decisions when I was 21, but in reflecting on how much I’ve grown as a member of this lab, I’m glad I made the one that counted. Thanks for not kicking me out when you found out I like the Yankees.

Professor Sarah Reisman and I also had dinner at USC, and though I was substantially more awkward at that one, I’m glad she doesn’t hold that against me. Sarah’s creativity and supernatural ability to simplify complex problems was an inspiration throughout my graduate career, and I appreciate her encouragement to try high-risk, high-impact ideas (and engagement in heated debates during SOTY). Thanks, as well, to Professors Gregory Fu and Alison Ondrus for serving on my committee; as a self-proclaimed synthesis bro, I benefited immensely from having two committee members who made me think critically about physical organic chemistry and biology in the context of work and proposals. I am a much more well-rounded chemist as a result.

My path to Caltech was the direct result of mentorship in chemistry at USC. I owe an immense debt of gratitude to my undergraduate advisor, Professor Nicos Petasis, for taking a chance on some annoying freshman and supporting me all of the way to the present day. I also need to thank my labmates in the Petasis group, especially Steve Glynn, Caitlin DeAngelo, and

Kalyan Nagulapalli-Venkata for teaching me the fundamentals of laboratory research and dealing with me on a regular basis. Professor Travis Williams was a brilliant advisor and friend who provided instrumental advice that led me to Pasadena, and I thank him especially for inspiring me to continue teaching during my graduate career.

Caltech has incredible staff support, and we are indebted to a number of people for enabling our research. Special thanks to Lynne Martinez, Beth Marshall, Agnes Tong, Alison Ross, Paula Higdon, Nate Siladke, Joe Drew, plus the dream team Greg and Armando for keeping day-to-day operations running smoothly. Thanks as well to Dr. Dave Vander Velde, Dr. Mona Shahgholi, Naseem Torian, Dr. Mike Takase, and Larry Henling for maintaining such fantastic facilities that allow us to perform top-of-the-line research. And of course, I can't express enough appreciation for "The Notorious S.C.V.", Dr. Scott Virgil. His vast knowledge of experimental chemistry is matched only by his compassion and willingness to drop everything at once to help a student in need. Thanks to you and Silva for opening your home to us each year at Christmas.

I've overlapped with a number of excellent researchers during the past five years in the Stoltz Group. To the older grad students—Kelly Kim, Nick O'Connor, Seo-jung Han, Chris Haley, Sam Shockley, David Schuman, Alex Sun, Elizabeth Goldstein, Steven Loskot, and Austin Wright—thank you for imparting a significant amount of wisdom and guidance. Shoshana Bachman was an honorary member of our cohort during my first two years, and I am grateful to her for teaching me how important it was to maintain balance in grad school and how far compassion toward those around you really traveled. I'd also like to thank the postdocs, especially Caleb Hethcox, Boger Liu, Max Klatte, Daisuke Saito, Kohei Hayashida, Marchello Cavitt, Denis Kroger, Etienne Donckele, Emma Baker-Tripp, Sebastian "Sea Bass" Lackner, Primali Navaratne, Steffen Gressies, and Lars Suesse for their friendship and guidance during this time. Gerit

Potoschnig and Jaika Doerfler were hands down the two funnest people I met during grad school. Between countless nights bar hopping, Thanksgiving, Pride, the ski trip, and forever ruining the word “escondito,” I could always count on you both to put a smile on my face and a throbbing hangover in my head.

Two individuals in particular deserve special mention. Despite yelling at me during my visit weekend for wanting to study both synthesis and methods, Beau Pritchett has been an amazing friend and mentor since my first day in the Stoltz group. Beau’s intensity was only matched by his empathy, and he helped me become a mature researcher by taking responsibility for my own path and striving to improve the group as a whole. Similarly, Professor Eric “EDubs” Welin was an invaluable source of ideas and support, who inspired a lot of confidence when I was otherwise sure I wasn’t doing well. Over many, many beers, Eric helped me realize how much fun it was to learn and discuss chemistry, and I stand by my statement that I was his unofficial first grad student. Thanks to you both for being like older brothers to me. LSU and Ohio State still suck.

To the younger grad students—Nick Hafeman, Zach Sercel, Tyler “TC” Cassleman, Joel Monroy, Melinda Chan, and Anthony Chen—thank you for being the reason that I wanted to come to work every day. Alexia Kim and Alex Cusumano were especially important friends during my fifth year; during a time where I should have turned into a misanthropic senior grad student, their energy, enthusiasm, and borderline insanity helped me, as Fa so nicely put it, “stay young.” Tyler “TSwift” Fulton, as well, has been a great friend, teacher, and labmate across the board, and I credit him with creating such a fun and supportive environment in the group.

The incredible crew of visiting students and undergrads, especially Remi Laverne, Alvaro Velasco-Rubio, Mokoto Yoriarte, Emil Glibstrup, Yutaro Saito, Marco Wollenburg, and Max Kaiser provided the group with valuable knowledge and fun times. Thanks as well to our

undergrads for always keeping lab interesting. I also had an opportunity to mentor two ambitious younger students, Jaijun Du and Weida Feng, who I know will undoubtedly have exceptional careers in their respective fields. Thank you for teaching me about myself and helping me to develop as a better teacher and communicator.

Throughout my studies, I was blessed with fantastic project partners who helped me grow along the way. Daisuke Saito was a hardworking and fun personality whose synthetic skills were matched only by his deadly softball skills and eccentric taste in sweatpants. Kohei Hayshida was quieter, but instrumental nonetheless in discovering key disconnection strategies towards the alkaloid natural products. Steven “Dirty SAL” Loskot was intense in all senses of the word, but his dedication and focus gave him this incredible ability to make things we thought were ludicrous a reality. Finally, Nick “The Halfman” Hafeman possesses this seemingly impossible combination of brilliant chemical intuition, unbreakable work ethic, and chill outward demeanor; he was an awesome conductor of the Scab Train and I would work with him again 12 times out of 10.

And then, there is my 3F cohort. Eric Alexy¹ joined in the summer a week before I did, and despite our awkward first date at Pieology, I’m going to miss Eric’s lightning-fast wit, classic pranks, and vast knowledge of chemistry. Fa Ngamnithiporn is, simply put, one of the nicest people I’ve ever met, and despite my attempts to bring out “the hate” in her,² I admire her infectious positive energy, caring nature, and in-depth knowledge of great restaurants in LA. Carina Jette and I have built our friendship based on a mutual love of trashy television, gossip, and White Claw, but what I appreciate most about Carina is her unbreakable drive, fierce loyalty to her friends, and frank honesty when I needed somebody to tell me that I was being an ass.³ And finally, what can

¹ Also known as Small Eric, Little Eric, Baby Eric, the Wee Baby Eric, Eric the Snake, Steric Alexy, Saint Eric, EJ, the King of Process, KoP, and King of Popsicles.

² Total synthesis was far more successful at doing that than I ever was

³ Which I needed a lot during my first two years.

I say about Sean Feng that can't be used against her in a court of law; Sean prides herself in pushing everyone out of their comfort zone, but only in a way that makes their lives happier. As much as I love her intimidating, boisterous, outward personality, I respect even more the kind, generous soul who lies angstroms below the surface.⁴

The thing I love most about this group is the fact that I'm pretty sure none of us would've ever been friends in any setting other than grad school; yet after spending five years together, I don't see how I could've done this without you four.

I also owe a hefty debt of gratitude to our colleagues in the Reisman, Fu, Grubbs, and Robb labs for support, including intellectual, material, and emotional. Jordan Beck and Jon Nicolini have been incredibly supportive friends (plus amazing cooks and travel buddies), and I appreciate the number of fun times we've shared, despite the fact my girlfriend likes their dog Quinn more than she likes me. Denise Grünenfelder and Lauren Chapman were also huge helps in the job-hunt process and I thank them for their guidance and advice along the way.

Outside of Caltech, I was happy to remain close with a fair number of undergrad friends. To my trumpet gang—Joycelyn Yip, Natalie Camacho, Kellie Graham, Sean Christensen, Bryan Yee, Giovanni Propersi, and Amy Wang—thank you for simultaneously keeping me sane and driving me crazier, by providing the appropriate balance of fun and support. I also want to thank the Yip and Camacho clans for serving as my adoptive families here in Southern California and truly making it home over the past nine years. A special shoutout is deserved to my roommate of four years, Dylan Visvikis, for being an especially supportive friend. As perhaps the only person with a more obscure work schedule than me, the many late nights we've spent talking about life have been a therapeutic solution to the hardest of days, and I truly appreciate you having my back

⁴ If you have the option of rooming with her at a conference, I highly recommend against it.

through this all. I also couldn't have done it without fellow SSeason ticket holders Kenneth Martin and Kristin Robbio for making gamedays the highlight of my falls, even during the darkest days of the Clay Helton era.

And of course, none of this would have been possible without my family. To my parents, Sue and Bob, thank you for prioritizing education at a young age, nurturing my love of learning, and supporting me emotionally every step of the way. To Gabby and Cole, thank you for listening to my highs and lows, keeping me competitive, and providing a never-ending stream of laughs. To my extended family, especially my late grandparents Fred and Irene, Aunt Laura, Uncle Pete, Aunt Sue, Jordan, Steve, Nate, Rory, and the Porembas, thank you for always being there to support me and celebrate those victories. This dissertation is as much yours as it is mine, and none of this would have been possible without you.

And finally, I'd like to thank my girlfriend, Kelsey Poremba, for providing me with certainty. In this dissertation, you will read about a lot of great discoveries, but I can say—without hesitation or equivocation—that to find a person who is as brilliant, inspirational, supportive, fun, understanding, and compassionate as Kelsey is to me was the greatest discovery I've made in five years. I love you more than words can describe and I can't wait to begin the next chapter of our life back east.

ABSTRACT

Described herein are two projects in the field of natural product synthesis unified by their use of convergent strategies. An introduction into a relevant subclass of natural products, the *bis*(monoterpenoid) indole alkaloids, precedes our synthetic efforts. The molecules in this class are comprised of two monoterpenoid indole alkaloids conjoined by at least one carbon–carbon bond, and we review efforts to construct these dimers using semi-, partial, and total synthesis.

The account of our synthetic work begins with a detailed approach to the *bis*(monoterpenoid) indole alkaloid leucophyllidine. An enantioselective Pd-catalyzed decarboxylative allylic alkylation generates an α -quaternary-substituted lactam, which serves as a building block for both monomeric subunits. The northern fragment, eburnamonine, is constructed through a five-step sequence comprised of Fischer indole synthesis, Bischler–Napieralski cyclization, and diastereoselective hydrogenation. The southern fragment, eucophylline, is constructed through a ten-step formal synthesis comprised of a Friedländer quinoline synthesis, followed by two orthogonal C–H functionalizations that each displayed unexpected reactivity.

We then describe the evolution of a convergent coupling strategy to unify the two polycyclic fragments. While the “biomimetic” Friedel–Crafts and “bio-inspired” organometallic addition approaches failed, a Pd-catalyzed cross-coupling was ultimately successful in forging the key C–C bond. Extensive efforts to install the final stereogenic center with a variety of reducing agents were unsuccessful, and DFT modeling was utilized to probe the recalcitrant nature of the trisubstituted alkene. Preliminary investigations of a directed hydrogenation are then discussed.

Finally, we report an approach to the first total synthesis of the polyoxygenated diterpenoid (–)-scabrolide A. The route begins with the synthesis of an enantioenriched cyclopentendiol building block and an acyclic diyne from (*R*)-linalool and (*R*)-carvone, respectively. A Stieglich esterification and thermal [4+2] cycloaddition affords a tricyclic intermediate bearing all 19 carbons observed in the natural product. The cycloheptenoid motif is installed through a photochemical [2+2]/fragmentation sequence, exploiting an unusual alkene protecting group strategy to counteract unexpected reactivity.

PUBLISHED CONTENT AND CONTRIBUTIONS

1. Hafeman, N.J.; Loskot, S.A.; Reimann, C.E.; Pritchett, B.P.; Virgil, S.C.; Stoltz, B.M. “The Total Synthesis of (–)-Scabrolide A.” *J. Am. Chem. Soc.* **2020**, *142*, 8585–8590. DOI: 10.1021/jacs.0c02513

C.E.R. participated in the strategic planning, experimental work, data analysis, and manuscript preparation.

TABLE OF CONTENTS

Acknowledgements.....	v
Abstract.....	xi
Published Content and Contributions.....	xii
Table of Contents.....	xiii
List of Figures.....	xix
List of Schemes.....	xxxi
List of Tables.....	xxxvii
List of Abbreviations.....	xli

CHAPTER 1 **1**

The Synthesis of Heterodimeric Bis(monoterpenoid) Indole Alkaloids

1.1	Introduction.....	1
1.2	Semi- and Partial Synthesis of Bisindole Alkaloids.....	5
1.2.1	Büchi's Partial Synthesis of Voacamine and Voacorine.....	5
1.2.2	LeQuesne and Cook's Semi-synthesis of Alstonisidine.....	6
1.2.3	LeQuesne and Cook's Semi-synthesis of Villalstonine.....	8
1.2.4	LeQuesne and Cook's Semi-synthesis of Macralstonine.....	9
1.2.5	Portier and Langlois's Partial Synthesis of Vinblastine.....	10
1.2.6	Kutney's Partial Synthesis of Vinblastine.....	12
1.2.7	Kuehne's Partial Synthesis of Vinblastine.....	13
1.2.8	Magnus's Partial Synthesis of Vinblastine.....	15
1.2.9	Cook's Partial Synthesis of Villalstonine.....	16

1.2.10	Cook's Partial Synthesis of Macrocarpamine.....	18
1.2.11	Poupon, Evanno, and Vincent's Semi-Syntheiss of Bipleiophylline...19	
1.3	Total Synthesis of Bisindole Alkaloids.....	20
1.3.1	Magnus's Total Synthesis of Norpleiomutine.....	20
1.3.2	Cook's Total Synthesis of Macralstonidine.....	22
1.3.3	Fukuyama's First Generation Synthesis of Vinblastine.....	23
1.3.4	Fukuyama's Second Generation Synthesis of Vinblastine.....	26
1.3.5	Boger's Total Synthesis of Vinblastine.....	28
1.3.6	Cook's Total Synthesis of Accedinisine.....	31
1.3.7	Fukuyama and Tokuyama's Total Synthesis of Haplophytine.....	33
1.3.8	Nicolaou and Chen's Total Synthesis of Haplophytine.....	36
1.3.9	Fukuyama and Tokuyama's Total Synthesis of Conophylline.....	39
1.3.10	Tokuyama's Second Generation Total Synthesis of Haplophytine.....	41
1.4	Concluding Remarks.....	43
1.5	References.....	45

CHAPTER 2

53

The Divergent Synthesis of Eburnamine and Eucophylline

2.1	Introduction.....	53
2.1.1	Isolation, Bioactivity, and Biosynthetic Hypotheses.....	53
2.1.2	Previous Synthetic Efforts toward Eburnamine.....	56
2.1.3	Previous Synthetic Efforts toward Eucophylline.....	60
2.1.4	Inspiration.....	62

2.1.5	General Synthetic Strategy.....	63
2.2	Total Synthesis of Eburnamine.....	65
2.2.1	Retrosynthetic Analysis.....	65
2.2.2	Scalable Synthesis of the Enantioenriched Lactam Building Block....	66
2.2.3	Advancement to the Bischler–Napieralski Product.....	68
2.2.4	Final Steps.....	71
2.2.5	Concluding Remarks.....	73
2.3	Total Synthesis of Eucophylline.....	74
2.3.1	Retrosynthetic Analysis.....	74
2.3.2	Advancement to the Friedländer quinoline synthesis Product.....	75
2.3.3	Intramolecular C–H Amination: Discovery of a Sn(II)-mediated method.....	77
2.3.4	Intermolecular C–H Alkylation: Investigation of Minisci Alkylation.....	80
2.3.5	Final Steps.....	83
2.3.6	Concluding Remarks.....	84
2.4	References.....	85
2.5	Experimental Section.....	90
2.5.1	Materials and Methods.....	90
2.5.2	Experimental Procedures.....	92
2.5.3	Comparison of NMR Data to Known Samples.....	125
2.5.4	Additional References.....	129

APPENDIX 1	130
<i>Synthetic Summary of Chapter 2</i>	
APPENDIX 2	133
<i>Spectra Relevant to Chapter 2</i>	
CHAPTER 3	199
<i>Progress toward the Convergent Total Synthesis of Leucophyllidine</i>	
3.1 Introduction.....	199
3.2 Biomimetic Friedel-Crafts Strategy.....	201
3.3 Bio-inspired Organometallic Addition Strategy.....	202
3.4 Transition Metal-catalyzed Cross Coupling Strategy.....	207
3.4.1 Suzuki Couplings.....	207
3.4.2 Stille Couplings.....	209
3.5 Investigation of Trisubstituted Olefin Reduction.....	211
3.6 DFT Modelling of Cross-Coupling Substrate.....	214
3.7 Future Directions and Concluding Remarks.....	216
3.8 References	218
3.9 Experimental Section.....	222
3.8.1 Materials and Methods.....	222
3.8.2 Experimental Procedures.....	224
3.8.3 Computational Details.....	245
3.8.4 Additional References.....	246

APPENDIX 3	247
<i>Synthetic Summary of Chapter 3</i>	
APPENDIX 4	250
<i>Spectra Relevant to Chapter 3</i>	
CHAPTER 4	282
<i>The Total Synthesis of (-)-Scabrolide A</i>	
4.1 Introduction.....	282
4.1.1 Isolation, Bioactivity, and Biosynthetic Hypotheses.....	282
4.1.2 Previous Synthetic Efforts toward Polycyclic (Nor)cembranoid Diterpenoids.....	285
4.1.3 Inspiration.....	290
4.1.4 Retrosynthetic Analysis.....	292
4.2 Synthesis of the Cyclohexenone Core.....	294
4.2.1 Synthesis of the Cyclopentendiol.....	294
4.2.2 Synthesis of the Acyclic Diyne.....	296
4.2.3 Convergent Esterification/Diels–Alder.....	297
4.3 Synthesis of the Cycloheptenone Ring.....	298
4.3.1 Initial Investigations of the Photochemical [2+2] Cycloaddition.....	299
4.3.2 Development of an Olefin Protection Strategy.....	300
4.3.3 Synthesis of the Cyclobutanol.....	302
4.3.4 Oxidative Fragmentation of the Cyclobutanol.....	303
4.4 Concluding Remarks.....	306

4.5	References.....	308
4.6	Experimental Section.....	312
4.6.1	Materials and Methods.....	312
4.6.2	Experimental Procedures.....	314
4.6.3	Comparison of Natural and Synthetic Material.....	342
4.6.4	Additional References.....	344
APPENDIX 5		345
<i>Synthetic Summary of Chapter 4</i>		
APPENDIX 6		349
<i>Spectra Relevant to Chapter 4</i>		
APPENDIX 7		402
<i>X-ray Crystallography Reports Relevant to Chapter 4</i>		
A7.1	X-ray Crystal Structure Analysis for Dicyclobutane 500.....	403
A7.2	X-ray Crystal Structure Analysis for Triol 513a.....	421
A7.3	X-ray Crystal Structure Analysis for Triol 513b.....	435
A7.4	X-ray Crystal Structure Analysis for Scabrolide A (416).....	452
Comprehensive Bibliography.....		XX
About the Author.....		XX

LIST OF FIGURES

CHAPTER 1

The Synthesis of Heterodimeric Bis(monoterpenoid) Indole Alkaloids

- Figure 1.1** Representative heterodimeric *bis*(monoterpenoid) indole alkaloids.....2
- Figure 1.2** Vinblastine, vincristine, and their subunits.....10

CHAPTER 2

The Divergent Synthesis of Eburnamine and Eucophylline

- Figure 2.1** Leucophyllidine and its Component Monomers.....54
- Figure 2.2** Conserved structural elements observed in *bis*(monoterpenoid) indole alkaloids.....64
- Figure 2.3** First and second generation Minisci reaction setups.....82
- Figure 2.4** Absorption and emission spectra for Minisci precursor.....83
- Figure 2.5** Reaction setup for large-scale decarboxylative allylic alkylation.....96
- Figure 2.6** Reaction setup for photoredox-mediated Minisci reaction.....121

APPENDIX 2

Spectra Relevant to Chapter 2

- Figure A2.1** ¹H NMR (400 MHz, CDCl₃) of compound **303**.....134
- Figure A2.2** Infrared spectrum (Thin Film, NaCl) of compound **303**.....135
- Figure A2.3** ¹³C NMR (101 MHz, CDCl₃) of compound **303**.....135
- Figure A2.4** ¹H NMR (400 MHz, CDCl₃) of compound **304**.....136
- Figure A2.5** Infrared spectrum (Thin Film, NaCl) of compound **304**.....137

Figure A2.6	^{13}C NMR (101 MHz, CDCl_3) of compound 304	137
Figure A2.7	^1H NMR (400 MHz, CDCl_3) of compound 284	138
Figure A2.8	Infrared spectrum (Thin Film, NaCl) of compound 284	139
Figure A2.9	^{13}C NMR (101 MHz, CDCl_3) of compound 284	139
Figure A2.10	^1H NMR (400 MHz, CDCl_3) of compound 286	140
Figure A2.11	Infrared spectrum (Thin Film, NaCl) of compound 286	141
Figure A2.12	^{13}C NMR (101 MHz, CDCl_3) of compound 286	141
Figure A2.13	^1H NMR (400 MHz, CDCl_3) of compound 300	142
Figure A2.14	Infrared spectrum (Thin Film, NaCl) of compound 300	143
Figure A2.15	^{13}C NMR (101 MHz, CDCl_3) of compound 300	143
Figure A2.16	^1H NMR (400 MHz, CDCl_3) of compound 306	144
Figure A2.17	Infrared spectrum (Thin Film, NaCl) of compound 306	145
Figure A2.18	^{13}C NMR (101 MHz, CDCl_3) of compound 306	145
Figure A2.19	^1H NMR (400 MHz, CDCl_3) of compound 301	146
Figure A2.20	Infrared spectrum (Thin Film, NaCl) of compound 301	147
Figure A2.21	^{13}C NMR (101 MHz, CDCl_3) of compound 301	147
Figure A2.22	^1H NMR (400 MHz, CDCl_3) of compound 307	148
Figure A2.23	Infrared spectrum (Thin Film, NaCl) of compound 307	149
Figure A2.24	^{13}C NMR (101 MHz, CDCl_3) of compound 307	149
Figure A2.25	^1H NMR (600 MHz, CD_2Cl_2) of compound 308	150
Figure A2.26	Infrared spectrum (Thin Film, NaCl) of compound 308	151
Figure A2.27	^{13}C NMR (101 MHz, CDCl_3) of compound 308	151

Figure A2.28	^1H NMR (400 MHz, CDCl_3) of compound 314	152
Figure A2.29	Infrared spectrum (Thin Film, NaCl) of compound 314	153
Figure A2.30	^{13}C NMR (101 MHz, CDCl_3) of compound 314	153
Figure A2.31	^1H NMR (400 MHz, CDCl_3) of compound 315	154
Figure A2.32	Infrared spectrum (Thin Film, NaCl) of compound 315	155
Figure A2.33	^{13}C NMR (101 MHz, CDCl_3) of compound 315	155
Figure A2.34	^1H NMR (500 MHz, CDCl_3) of compound 261	156
Figure A2.35	Infrared spectrum (Thin Film, NaCl) of compound 261	157
Figure A2.36	^{13}C NMR (101 MHz, CDCl_3) of compound 261	157
Figure A2.37	^1H NMR (400 MHz, CDCl_3) of compound 317a	158
Figure A2.38	Infrared spectrum (Thin Film, NaCl) of compound 317a	159
Figure A2.39	^{13}C NMR (101 MHz, CDCl_3) of compound 317a	159
Figure A2.40	^1H NMR (400 MHz, CDCl_3) of compound 317b	160
Figure A2.41	Infrared spectrum (Thin Film, NaCl) of compound 317b	161
Figure A2.42	^{13}C NMR (101 MHz, CDCl_3) of compound 317b	161
Figure A2.43	^1H NMR (400 MHz, CDCl_3) of compound 91	162
Figure A2.44	Infrared spectrum (Thin Film, NaCl) of compound 91	163
Figure A2.45	^{13}C NMR (101 MHz, CDCl_3) of compound 91	163
Figure A2.46	^1H NMR (600 MHz, CDCl_3) of compound 251	164
Figure A2.47	Infrared spectrum (Thin Film, NaCl) of compound 251	165
Figure A2.48	^{13}C NMR (101 MHz, CDCl_3) of compound 251	165
Figure A2.49	^1H NMR (400 MHz, CDCl_3) of compounds 92 and 93	166

Figure A2.50	Infrared spectrum (Thin Film, NaCl) of compounds 92 and 93	167
Figure A2.51	^{13}C NMR (101 MHz, CDCl_3) of compounds 92 and 93	167
Figure A2.52	^1H NMR (400 MHz, CDCl_3) of compound 334	168
Figure A2.53	Infrared spectrum (Thin Film, NaCl) of compound 334	169
Figure A2.54	^{13}C NMR (101 MHz, CDCl_3) of compound 334	169
Figure A2.55	^1H NMR (400 MHz, CDCl_3) of compound 321	170
Figure A2.56	Infrared spectrum (Thin Film, NaCl) of compound 321	171
Figure A2.57	^{13}C NMR (101 MHz, CD_2Cl_2) of compound 321	171
Figure A2.58	^1H NMR (400 MHz, CDCl_3) of compound 326	172
Figure A2.59	Infrared spectrum (Thin Film, NaCl) of compound 326	173
Figure A2.60	^{13}C NMR (101 MHz, CDCl_3) of compound 326	173
Figure A2.61	^1H NMR (400 MHz, CD_2Cl_2) of compound 327	174
Figure A2.62	Infrared spectrum (Thin Film, NaCl) of compound 327	175
Figure A2.63	^{13}C NMR (101 MHz, CD_2Cl_2) of compound 327	175
Figure A2.64	^1H NMR (400 MHz, CDCl_3) of compound 322	176
Figure A2.65	Infrared spectrum (Thin Film, NaCl) of compound 322	177
Figure A2.66	^{13}C NMR (101 MHz, CDCl_3) of compound 322	177
Figure A2.67	^1H NMR (400 MHz, CD_2Cl_2) of compound 320	178
Figure A2.68	Infrared spectrum (Thin Film, NaCl) of compound 320	179
Figure A2.69	^{13}C NMR (101 MHz, d_6 -DMSO) of compound 320	179
Figure A2.70	^1H NMR (400 MHz, CDCl_3) of compound 330	180
Figure A2.71	Infrared spectrum (Thin Film, NaCl) of compound 330	181

Figure A2.72	^{13}C NMR (101 MHz, CDCl_3) of compound 330	181
Figure A2.73	^1H NMR (400 MHz, CDCl_3) of compound 329a	182
Figure A2.74	Infrared spectrum (Thin Film, NaCl) of compound 329a	183
Figure A2.75	^{13}C NMR (101 MHz, CDCl_3) of compound 329a	183
Figure A2.76	^1H NMR (400 MHz, CDCl_3) of compound 329b	184
Figure A2.77	Infrared spectrum (Thin Film, NaCl) of compound 329b	185
Figure A2.78	^{13}C NMR (101 MHz, CDCl_3) of compound 329b	185
Figure A2.79	^1H NMR (400 MHz, CDCl_3) of compound 332	186
Figure A2.80	Infrared spectrum (Thin Film, NaCl) of compound 332	187
Figure A2.81	^{13}C NMR (101 MHz, CDCl_3) of compound 332	187
Figure A2.82	^1H NMR (400 MHz, CDCl_3) of compound 319	188
Figure A2.83	Infrared spectrum (Thin Film, NaCl) of compound 319	189
Figure A2.84	^{13}C NMR (101 MHz, CDCl_3) of compound 319	189
Figure A2.85	NOESY (400 MHz, CDCl_3) of compound 319	190
Figure A2.86	^1H NMR (400 MHz, CD_2Cl_2) of compound 340	191
Figure A2.87	Infrared spectrum (Thin Film, NaCl) of compound 340	192
Figure A2.88	^{13}C NMR (101 MHz, CD_2Cl_2) of compound 340	192
Figure A2.89	^1H NMR (400 MHz, CDCl_3) of compound 342	193
Figure A2.90	Infrared spectrum (Thin Film, NaCl) of compound 342	194
Figure A2.91	^{13}C NMR (101 MHz, CDCl_3) of compound 342	194
Figure A2.92	^1H NMR (400 MHz, CDCl_3) of compound 318	195
Figure A2.93	Infrared spectrum (Thin Film, NaCl) of compound 318	196

Figure A2.94	^{13}C NMR (101 MHz, CDCl_3) of compound 318	196
Figure A2.95	^1H NMR (400 MHz, CDCl_3) of compound 344	197
Figure A2.96	Infrared spectrum (Thin Film, NaCl) of compound 344	198
Figure A2.97	^{13}C NMR (101 MHz, CDCl_3) of compound 344	198

CHAPTER 3

Progress toward the Convergent Total Synthesis of Leucophyllidine

Figure 3.1	DFT models of Stille coupling product.....	215
-------------------	--	-----

APPENDIX 4

Spectra Relevant to Chapter 3

Figure A4.1	^1H NMR (400 MHz, CDCl_3) of compound 364	251
Figure A4.2	Infrared spectrum (Thin Film, NaCl) of compound 364	252
Figure A4.3	^{13}C NMR (101 MHz, CDCl_3) of compound 364	252
Figure A4.4	^1H NMR (400 MHz, CDCl_3) of compound 365	253
Figure A4.5	Infrared spectrum (Thin Film, NaCl) of compound 365	254
Figure A4.6	^{13}C NMR (101 MHz, CDCl_3) of compound 365	254
Figure A4.7	^1H NMR (400 MHz, CD_2Cl_2) of compound 379c	255
Figure A4.8	Infrared spectrum (Thin Film, NaCl) of compound 379c	256
Figure A4.9	^{13}C NMR (101 MHz, CD_2Cl_2) of compound 379c	256
Figure A4.10	^1H NMR (400 MHz, CDCl_3) of compound 367	257
Figure A4.11	Infrared spectrum (Thin Film, NaCl) of compound 367	258

Figure A4.12	^{13}C NMR (101 MHz, CDCl_3) of compound 367	258
Figure A4.13	^1H NMR (400 MHz, CDCl_3) of compound 380	259
Figure A4.14	Infrared spectrum (Thin Film, NaCl) of compound 380	260
Figure A4.15	^{13}C NMR (101 MHz, CDCl_3) of compound 380	260
Figure A4.16	^1H NMR (400 MHz, CDCl_3) of compound 381	261
Figure A4.17	Infrared spectrum (Thin Film, NaCl) of compound 381	262
Figure A4.18	^{13}C NMR (101 MHz, CDCl_3) of compound 381	262
Figure A4.19	^1H NMR (400 MHz, CDCl_3) of compound 385	263
Figure A4.20	Infrared spectrum (Thin Film, NaCl) of compound 385	264
Figure A4.21	^{13}C NMR (101 MHz, CDCl_3) of compound 385	264
Figure A4.22	^1H NMR (400 MHz, CDCl_3) of compound 392	265
Figure A4.23	Infrared spectrum (Thin Film, NaCl) of compound 392	266
Figure A4.24	^{13}C NMR (101 MHz, CDCl_3) of compound 392	266
Figure A4.25	^1H NMR (400 MHz, CDCl_3) of compound 393	267
Figure A4.26	Infrared spectrum (Thin Film, NaCl) of compound 393	268
Figure A4.27	^{13}C NMR (101 MHz, CDCl_3) of compound 393	268
Figure A4.28	^1H NMR (400 MHz, CDCl_3) of compound 391	269
Figure A4.29	Infrared spectrum (Thin Film, NaCl) of compound 391	270
Figure A4.30	^{13}C NMR (101 MHz, CDCl_3) of compound 391	270
Figure A4.31	^1H NMR (600 MHz, C_6D_6) of compound 386	271
Figure A4.32	Infrared spectrum (Thin Film, NaCl) of compound 386	272
Figure A4.33	^{13}C NMR (101 MHz, C_6D_6) of compound 386	272

Figure A4.34 NOESY (600 MHz, C ₆ D ₆) of compound 386	273
Figure A4.35 HSQC (600 MHz, C ₆ D ₆) of compound 386	274
Figure A4.36 ¹ H NMR (400 MHz, CDCl ₃) of compound 396	275
Figure A4.37 Infrared spectrum (Thin Film, NaCl) of compound 396	276
Figure A4.38 ¹³ C NMR (101 MHz, CDCl ₃) of compound 396	276
Figure A4.36 ¹ H NMR (400 MHz, CDCl ₃) of compound 397	277
Figure A4.37 Infrared spectrum (Thin Film, NaCl) of compound 397	278
Figure A4.38 ¹³ C NMR (101 MHz, CDCl ₃) of compound 397	278
Figure A4.39 ¹ H NMR (400 MHz, CDCl ₃) of compound 397	279
Figure A4.40 Infrared spectrum (Thin Film, NaCl) of compound 397	280
Figure A4.41 ¹³ C NMR (101 MHz, CDCl ₃) of compound 397	280
Figure A4.42 NOESY (600 MHz, C ₆ D ₆) of compound 386	273

CHAPTER 4

The Total Synthesis of (-)-Scabrolide A

Figure 4.1 Furanobutenolide-derived norcembranoid diterpenoids.....	282
--	-----

APPENDIX 4

Spectra Relevant to Chapter 3

Figure A6.1 ¹ H NMR (400 MHz, CDCl ₃) of compound 482	349
Figure A6.2 Infrared spectrum (Thin Film, NaCl) of compound 482	350
Figure A6.3 ¹³ C NMR (101 MHz, CDCl ₃) of compound 482	350

Figure A6.4	^1H NMR (400 MHz, C_6D_6) of compound 483	351
Figure A6.5	Infrared spectrum (Thin Film, NaCl) of compound 483	352
Figure A6.6	^{13}C NMR (101 MHz, C_6D_6) of compound 483	352
Figure A6.7	^1H NMR (400 MHz, CDCl_3) of compound 484	353
Figure A6.8	Infrared spectrum (Thin Film, NaCl) of compound 484	354
Figure A6.9	^{13}C NMR (101 MHz, CDCl_3) of compound 484	354
Figure A6.10	^1H NMR (400 MHz, CDCl_3) of compound 490	355
Figure A6.11	Infrared spectrum (Thin Film, NaCl) of compound 490	356
Figure A6.12	^{13}C NMR (101 MHz, CDCl_3) of compound 490	356
Figure A6.13	^1H NMR (400 MHz, CDCl_3) of compound 492	357
Figure A6.14	Infrared spectrum (Thin Film, NaCl) of compound 492	358
Figure A6.15	^{13}C NMR (101 MHz, CDCl_3) of compound 492	358
Figure A6.16	^1H NMR (400 MHz, CDCl_3) of compound 493	359
Figure A6.17	Infrared spectrum (Thin Film, NaCl) of compound 493	360
Figure A6.18	^{13}C NMR (101 MHz, CDCl_3) of compound 493	360
Figure A6.19	^1H NMR (400 MHz, CDCl_3) of compound 472	361
Figure A6.20	Infrared spectrum (Thin Film, NaCl) of compound 472	362
Figure A6.21	^{13}C NMR (101 MHz, CDCl_3) of compound 472	362
Figure A6.22	^1H NMR (400 MHz, CDCl_3) of compound 471	363
Figure A6.23	Infrared spectrum (Thin Film, NaCl) of compound 471	364
Figure A6.24	^{13}C NMR (101 MHz, CDCl_3) of compound 471	364
Figure A6.25	^1H NMR (400 MHz, CDCl_3) of compound 495	365

Figure A6.26	Infrared spectrum (Thin Film, NaCl) of compound 495	366
Figure A6.27	^{13}C NMR (101 MHz, CDCl_3) of compound 495	366
Figure A6.28	^1H NMR (400 MHz, CDCl_3) of compound 496	367
Figure A6.29	Infrared spectrum (Thin Film, NaCl) of compound 496	368
Figure A6.30	^{13}C NMR (101 MHz, CDCl_3) of compound 496	368
Figure A6.31	^1H NMR (400 MHz, CDCl_3) of compound 497	369
Figure A6.32	Infrared spectrum (Thin Film, NaCl) of compound 497	370
Figure A6.33	^{13}C NMR (101 MHz, CDCl_3) of compound 497	370
Figure A6.34	^1H NMR (400 MHz, CDCl_3) of compound 470	371
Figure A6.35	Infrared spectrum (Thin Film, NaCl) of compound 470	372
Figure A6.36	^{13}C NMR (101 MHz, CDCl_3) of compound 470	372
Figure A6.37	^1H NMR (400 MHz, CDCl_3) of compound 499	373
Figure A6.38	Infrared spectrum (Thin Film, NaCl) of compound 499	374
Figure A6.39	^{13}C NMR (101 MHz, CDCl_3) of compound 499	374
Figure A6.40	^1H NMR (400 MHz, CDCl_3) of compound 400	375
Figure A6.41	Infrared spectrum (Thin Film, NaCl) of compound 400	376
Figure A6.42	^{13}C NMR (101 MHz, CDCl_3) of compound 400	376
Figure A6.43	^1H NMR (400 MHz, CDCl_3) of compound 509a	377
Figure A6.44	Infrared spectrum (Thin Film, NaCl) of compound 509a	378
Figure A6.45	^{13}C NMR (101 MHz, CDCl_3) of compound 509a	378
Figure A6.46	^1H NMR (400 MHz, CDCl_3) of compound 509b	379
Figure A6.47	Infrared spectrum (Thin Film, NaCl) of compound 509b	380

Figure A6.48	^{13}C NMR (101 MHz, CDCl_3) of compound 509b	380
Figure A6.49	^1H NMR (400 MHz, CDCl_3) of compound 510a	381
Figure A6.50	Infrared spectrum (Thin Film, NaCl) of compound 510a	382
Figure A6.51	^{13}C NMR (101 MHz, CDCl_3) of compound 510a	382
Figure A6.52	^1H NMR (400 MHz, CDCl_3) of compound 510b	383
Figure A6.53	Infrared spectrum (Thin Film, NaCl) of compound 510b	384
Figure A6.54	^{13}C NMR (101 MHz, CDCl_3) of compound 510b	384
Figure A6.55	^1H NMR (400 MHz, CDCl_3) of compound 511a	385
Figure A6.56	Infrared spectrum (Thin Film, NaCl) of compound 511a	386
Figure A6.57	^{13}C NMR (101 MHz, CDCl_3) of compound 511a	386
Figure A6.58	^1H NMR (400 MHz, CDCl_3) of compound 511b	387
Figure A6.59	Infrared spectrum (Thin Film, NaCl) of compound 511b	388
Figure A6.60	^{13}C NMR (101 MHz, CDCl_3) of compound 511b	388
Figure A6.61	^1H NMR (400 MHz, CDCl_3) of compound 512a	389
Figure A6.62	Infrared spectrum (Thin Film, NaCl) of compound 512a	390
Figure A6.63	^{13}C NMR (101 MHz, CDCl_3) of compound 512a	390
Figure A6.64	^1H NMR (400 MHz, CDCl_3) of compound 512b	391
Figure A6.65	Infrared spectrum (Thin Film, NaCl) of compound 512b	392
Figure A6.66	^{13}C NMR (101 MHz, CDCl_3) of compound 512b	392
Figure A6.67	^1H NMR (400 MHz, CDCl_3) of compound 513a	393
Figure A6.68	Infrared spectrum (Thin Film, NaCl) of compound 513a	394
Figure A6.69	^{13}C NMR (101 MHz, CDCl_3) of compound 513a	394

Figure A6.70	^1H NMR (400 MHz, CDCl_3) of compound 513b	395
Figure A6.71	Infrared spectrum (Thin Film, NaCl) of compound 513b	396
Figure A6.72	^{13}C NMR (101 MHz, CDCl_3) of compound 513b	396
Figure A6.73	^1H NMR (400 MHz, CDCl_3) of compound 527	397
Figure A6.74	Infrared spectrum (Thin Film, NaCl) of compound 527	398
Figure A6.75	^{13}C NMR (101 MHz, CDCl_3) of compound 527	398
Figure A6.76	^1H NMR (400 MHz, CDCl_3) of compound 416	399
Figure A6.77	Infrared spectrum (Thin Film, NaCl) of compound 416	400
Figure A6.78	^{13}C NMR (101 MHz, CDCl_3) of compound 416	400

APPENDIX 7

X-ray Crystallography Reports Relevant to Chapter 4

Figure A7.1	X-ray coordinate of compound 500	402
Figure A7.2	X-ray coordinate of compound 513a	420
Figure A7.3	X-ray coordinate of compound 513b	434
Figure A7.4	X-ray coordinate of compound (416).....	451

LIST OF SCHEMES

CHAPTER 1

The Synthesis of Heterodimeric Bis(monoterpenoid) Indole Alkaloids

Scheme 1.1	Büchi's semi-synthesis of voacamine, voacamidine, and voacorine (1963)....	6
Scheme 1.2	LeQuesne and Cook's semi-synthesis of alstonisidine (1972).....	7
Scheme 1.3	LeQuesne and Cook's semi-synthesis of villalstonine (1972).....	8
Scheme 1.4	LeQuesne and Cook's semi-synthesis of macralstonine (1972).....	9
Scheme 1.5	Portier and Langlois's semi-synthesis of vinblastine (1979).....	11
Scheme 1.6	Kutney's semi-synthesis of vinblastine (1988).....	13
Scheme 1.7	Kuehne's partial synthesis of vinblastine (1991).....	14
Scheme 1.8	Magnus's partial synthesis of vinblastine (1993).....	15
Scheme 1.9	Cook's partial synthesis of villalstonine (1994).....	17
Scheme 1.10	Cook's partial synthesis of macrocarpamine (1996).....	18
Scheme 1.11	Poupon, Evanno, and Vincent's semi-synthesis of bipleiophylline (1996)....	19
Scheme 1.12	Magnus's total synthesis of norpleiomutine (1984).....	21
Scheme 1.13	Cook's total synthesis of macralstonidine (2002).....	22
Scheme 1.14	Fukuyama's total synthesis of vinblastine monomers (2002).....	24
Scheme 1.15	Fukuyama's total synthesis of vinblastine (2002) and vincristine (2003).....	25
Scheme 1.16	Fukuyama's second generation total synthesis of vinblastine (2007).....	27
Scheme 1.17	Boger's total synthesis of vinblastine (2008).....	29
Scheme 1.18	Boger's revised mechanistic proposal and radical cation coupling.....	31
Scheme 1.19	Cook's total synthesis of accedinisine.....	32

Scheme 1.20 Haplophytine and proposed biosynthetic precursors.....	33
Scheme 1.21 Fukuyama and Tokuyama's total synthesis of haplophytine monomers (2009).....	35
Scheme 1.22 Fukuyama and Tokuyama's total synthesis of haplophytine (2009).....	36
Scheme 1.23. Nicolaou and Chen's total synthesis of haplophytine (2009).....	38
Scheme 1.24 Fukuyama and Tokuyama's total synthesis of conophylline monomers (2011).....	40
Scheme 1.25 Fukuyama and Tokuyama's total synthesis of conophylline (2011).....	41
Scheme 1.26 Tokuyama's total synthesis of haplophytine (2016).....	42

CHAPTER 2

The Divergent Synthesis of Eburnamine and Eucophylline

Scheme 2.1 Proposed biosynthesis of eburnamine.....	54
Scheme 2.2 Proposed biosynthesis of eucophylline.....	55
Scheme 2.3 Proposed biosynthesis of leucophyllidine.....	56
Scheme 2.4 Strategically significant bonds in eburnamonine.....	56
Scheme 2.5 Harley Mason's synthesis of (\pm) eburnamonine (1965).....	57
Scheme 2.6 Wenkert's synthesis of (\pm) eburnamonine (1988).....	58
Scheme 2.7 Schlessinger's synthesis of (\pm) eburnamonine (1979).....	59
Scheme 2.8 Landais's synthesis of (\pm) eucophylline (2015).....	60
Scheme 2.9 Panday's synthesis of (\pm) eucophylline (2017).....	61

Scheme 2.10 Application of Pd-catalyzed asymmetric allylic alkylation to the synthesis of monoterpenoid indole alkaloids in the Stoltz laboratory	63
Scheme 2.11 The divergent-convergent strategy to access leucophyllidine.....	65
Scheme 2.12 General retrosynthetic analysis of eburnamonine.....	65
Scheme 2.13 Revised synthesis of enantioenriched lactam building block.....	66
Scheme 2.14 Indole installation via Fischer Synthesis.....	68
Scheme 2.15 Unexpected aza-Prins rearrangement and mechanistic proposal.....	69
Scheme 2.16 Alternate Bischler–Napieralski cyclization.....	70
Scheme 2.17 Issues with diastereoselective reduction.....	71
Scheme 2.18 The effect of solvent on diastereoselectivity.....	72
Scheme 2.19 Retrosynthetic analysis of eucophylline coupling partner.....	74
Scheme 2.20 Synthesis of Friedländer precursors.....	75
Scheme 2.21 Unsuccessful Friedländer attempts.....	76
Scheme 2.22 Initial C(2)–H functionalization studies.....	78
Scheme 2.23 Reported Minisci conditions and application to the eucophylline tetracycle...	80
Scheme 2.24 Formal synthesis of eucophylline.....	84

APPENDIX 1

Synthetic Summary of Chapter 1

Scheme A1.1 Total synthesis of eburnamonine and eburnamine.....	131
Scheme A1.2 Formal synthesis of eucophylline.....	132

CHAPTER 3*Progress toward the Convergent Total Synthesis of Leucophyllidine*

Scheme 3.1	The divergent-convergent strategy to access leucophyllidine.....	200
Scheme 3.2	Proposed coupling strategies toward leucophyllidine.....	201
Scheme 3.3	Literature precedent for biomimetic coupling approach.....	202
Scheme 3.4	Synthesis of eburnamine and eucophylline model substrates.....	203
Scheme 3.5	Literature precedent and proof-of-principle experiment for bio-inspired strategy	204
Scheme 3.6	Unsuccessful model arylations.....	206
Scheme 3.7	Attempted synthesis of Suzuki coupling partners.....	207
Scheme 3.8	Synthesis of Stille coupling partners.....	209
Scheme 3.9	Preparative Stille coupling with vinyl stannane.....	211
Scheme 3.10	Preparative Stille coupling with formyl stannane.....	212
Scheme 3.11	Proposed endgame strategy.....	217

APPENDIX 3*Synthetic Summary of Chapter 3*

Scheme A3.1.	Vinyl Stille coupling and undesired reduction.....	248
Scheme A3.2	Formyl Stille coupling and proposed endgame.....	249

CHAPTER 4*The Total Synthesis of (-)-Scabrolide A*

Scheme 4.1. Proposed biosynthesis of fused tricyclic norcembranoid diterpenoids.....	284
Scheme 4.2. Pattenden's semi-synthesis of ineleganolide and sinulochmodin C (2011).....	285
Scheme 4.3. Yang's asymmetric synthesis of pavidolide B (2017).....	286
Scheme 4.4. Carrier's asymmetric synthesis of sarcophytin (2018).....	287
Scheme 4.5 Ding's asymmetric synthesis of several cembranoids (2018).....	288
Scheme 4.6 Fürstner's asymmetric synthesis of sinulariadiolide (2019).....	289
Scheme 4.7 Zhu's asymmetric synthesis of pavidolide B (2020).....	290
Scheme 4.8 Stoltz's progress toward the synthesis of <i>ent</i> -ineleganolide (2016).....	291
Scheme 4.9 Retrosynthetic analysis.....	293
Scheme 4.10 First generation route to cyclopentendiol building block (2011).....	294
Scheme 4.11 Second generation synthesis of cyclopentendiol from linalool.....	295
Scheme 4.12 Synthesis of acyclic diyne from carvone.....	296
Scheme 4.13 Thermal [4+2] cycloaddition and oxidative manipulations.....	298
Scheme 4.14 Hydrosilylation and unexpected photocycloaddition.....	299
Scheme 4.15 Mechanistic rationale for the observed photocycloaddition.....	300
Scheme 4.16 [2+2] photocycloaddition and subsequent oxidation.....	302
Scheme 4.17 Mechanistic rationale for the trans-fused cyclobutane.....	303

Scheme 4.18 Failed fragmentation/elimination approach.....	304
Scheme 4.19 Unexpected ring contraction and proposed mechanism.....	305
Scheme 4.20 Completion of scabrolide A.....	306

APPENDIX 5

Synthetic Summary of Chapter 4

Scheme A5.1 Synthesis of esterification precursors from chiral pool starting materials.....	346
Scheme A5.2 Synthesis of the tricyclic core of (–)-scabrolide A.....	347
Scheme A5.3 Total synthesis of (–)-scabrolide A.....	348

LIST OF TABLES**CHAPTER 2***The Divergent Synthesis of Eburnamine and Eucophylline*

Table 2.1	Development of a gram-scale decarboxylative allylic alkylation.....	67
Table 2.2	Optimization of one-pot hydrogenation/lactamization.....	73
Table 2.3	Optimization of the Friedländer quinoline synthesis.....	77
Table 2.4	Discovery of Sn(II)-mediated cyclization.....	79
Table 2.5	Control experiments for Minisci alkylation.....	83
Table 2.6	Comparison of eburnamonine ¹ H NMR peaks to previously synthesized material.....	125
Table 2.7	Comparison of eburnamonine ¹³ C NMR peaks to previously synthesized material.....	126
Table 2.8	Comparison of <i>O</i> -methyl eburnamonine ¹ H NMR peaks to previously synthesized material.....	127
Table 2.9	Comparison of <i>O</i> -methyl eburnamonine ¹³ C NMR peaks to previously synthesized material.....	128

CHAPTER 3*The Divergent Synthesis of Eburnamine and Eucophylline*

Table 3.1	Protection of the eburnamine model hemiaminal.....	205
Table 3.2	Synthesis of the organozinc coupling partner.....	206
Table 3.3	Optimization of one-pot Miyaura borylation/Suzuki coupling.....	208
Table 3.4	Optimization of Stille coupling.....	210

Table 3.5	Hydrogenation attempts.....	213
------------------	-----------------------------	-----

CHAPTER 4

The Total Synthesis of (-)-Scabrolide A

Table 4.1	Optimization of the isopropenyl protection strategy.....	301
Table 4.2.	Comparison of scabrolide ¹ H NMR peaks to naturally-isolated material.....	342
Table 4.3.	Comparison of scabrolide ¹³ C NMR peaks to naturally-isolated material....	343

APPENDIX 7

X-ray Crystallography Reports Relevant to Chapter 4

Table A7.1	Crystal data and structure refinement for dicyclobutane 500	403
Table A7.2	Atomic coordinates ($\times 10^5$) and equivalent isotropic displacement parameters ($\approx 2 \times 10^4$) for dicyclobutane 500 . $U(\text{eq})$ is defined as one third of the trace of the orthogonalized U_{ij} tensor.....	405
Table A7.3	Bond lengths [\approx] and angles [∞] for dicyclobutane 500	407
Table A7.4	Anisotropic displacement parameters ($\text{\AA}^2 \times 10^4$) for dicyclobutane 500 . The anisotropic displacement factor exponent takes the form: $-2 \frac{h^2}{a^2} [h^2 a^{*2} U^{11} + 2 h k a^* b^* U^{12}]$	413
Table A7.5.	<i>Hydrogen coordinates ($\times 10^4$) and isotropic displacement parameters ($\approx 2 \times 10^3$) for dicyclobutane 500.....</i>	415
Table A7.6.	Torsion angles [∞] for dicyclobutane 500	417
Table A7.7.	Hydrogen bonds for dicyclobutane 500	420

Table A7.8 Crystal data and structure refinement for triol 513a	421
Table A7.9 Atomic coordinates ($\times 10^5$) and equivalent isotropic displacement parameters ($\approx 2 \times 10^4$) for triol 513a . $U(\text{eq})$ is defined as one third of the trace of the orthogonalized U_{ij} tensor.....	423
Table A7.10 Bond lengths [\approx] and angles [∞] for triol 513a	424
Table A7.11 Anisotropic displacement parameters ($\text{\AA}^2 \times 10^4$) for triol 513a . The anisotropic displacement factor exponent takes the form: $-2 \pi^2 [h^2 a^{*2} U^{11} + 2 h k a^* b^* U^{12}]$	429
Table A7.12 . Hydrogen coordinates ($\times 10^4$) and isotropic displacement parameters ($\text{\AA}^2 \times 10^3$) for triol 513a	430
Table A7.13 . Torsion angles [∞] for triol 513a	431
Table A7.14 . Hydrogen bonds for triol 513a	434
Table A7.15 Crystal data and structure refinement for triol 513b	435
Table A7.16 Atomic coordinates ($\times 10^5$) and equivalent isotropic displacement parameters ($\approx 2 \times 10^4$) for triol 513b . $U(\text{eq})$ is defined as one third of the trace of the orthogonalized U_{ij} tensor.....	437
Table A7.17 Bond lengths [\approx] and angles [∞] for triol 513b	439
Table A7.18 Anisotropic displacement parameters ($\text{\AA}^2 \times 10^4$) for triol 513b . The anisotropic displacement factor exponent takes the form: $-2 \pi^2 [h^2 a^{*2} U^{11} + 2 h k a^* b^* U^{12}]$	445
Table A7.19 . Hydrogen coordinates ($\times 10^4$) and isotropic displacement parameters ($\text{\AA}^2 \times 10^3$) for triol 513b	446

10 ³)for triol 513b	446
Table A7.20. Torsion angles [∞] for triol 513b	448
Table A7.21. Hydrogen bonds for triol 513b	451
Table A7.22 Crystal data and structure refinement for scabrolide a (416).....	452
Table A7.23 Atomic coordinates (x 10 ⁵) and equivalent isotropic displacement parameters (≈2x 10 ⁴) for scabrolide a (416). U(eq) is defined as one third of the trace of the orthogonalized Uij tensor.....	454
Table A7.24 Bond lengths [≈] and angles [∞] for scabrolide a (416).....	455
Table A7.25 Anisotropic displacement parameters (Å ² x 10 ⁴) for scabrolide a (416). The anisotropic displacement factor exponent takes the form: $-2 \frac{h^2}{a^2} [h^2 a^{*2} U^{11} + 2 h k a^* b^* U^{12}]$	460
Table A7.26. Hydrogen coordinates (x 10 ⁴) and isotropic displacement parameters (Å ² x 10 ³) for scabrolide a (416).....	461
Table A7.27. Torsion angles [∞] for scabrolide a (416).....	462
Table A7.28. Hydrogen bonds for scabrolide a (416).....	464

LIST OF ABBREVIATIONS

$[\alpha]_D$	angle of optical rotation of plane polarized light
°C	degrees Celsius
Å	Ångstrom
Ac	acetyl
acac	acetoacetyl
AD-mix	asymmetric dihydroxylation mix
AIBN	azobisisobutyronitrile
aq	aqueous
Ar	aryl group
atm	atmosphere
B	base
BA _{TF}	tetrakis[3,5-bis(trifluoromethyl)phenyl]borate
BBN	borabicyclo[3.3.1.]nonane
Boc	<i>t</i> -butylcarbonyl
BOM	benzyloxymethyl
bp	boiling point
Bpy	2,2'-bipyridine
Bu	butyl
<i>i</i> -Bu	<i>iso</i> -butyl
<i>n</i> -Bu	butyl or <i>norm</i> -butyl
<i>t</i> -Bu	<i>tert</i> -butyl
Bz	benzoyl

<i>c</i>	concentration of sample for measurement of optical rotation
¹³ C	carbon-13 isotope
Cbz	carboxybenzyl
CDI	carbonyldiimidazole
cod	1,5-cyclooctadiene
conc.	concentrated
cm ⁻¹	wavenumber
C.R.E.A.M.	cash rules everything around me
CSA	camphorsulfonic acid
CuTC	copper (I)-thiophene carboxylate
Cy	cyclohexyl
<i>d</i>	dextrorotatory
DBU	1,8-Diazabicyclo[5.4.0]undec-7-ene
DCE	1,2-dichloroethane
DDQ	2,3-Dichloro-5,6-dicyano-1,4-benzoquinone
DEAD	diethyl azodicarboxylate
DHP	dihydropyran
DHPI	dihydropyrido[1,2-a]indolone
DIAD	di- <i>iso</i> -propyl azodicarboxylate
DIBAL-H	diisobutylaluminum hydride
DIC	<i>N,N'</i> -diisopropylcarbodiimide
DMAP	(4-dimethylamino)pyridine
DMA	<i>N,N'</i> -dimethylacetamide

DME	1,2-methoxyethane
DMEDA	<i>N,N'</i> -dimethylethylenediamine
DMF	<i>N,N'</i> -dimethylformamide
DMS	dimethyl sulfide
DNs	<i>di</i> -nitrobenzenesulfonyl
dppe	1,2-bis(diphenylphosphino)ethane
Dtbppy	4,4'- <i>di-tert</i> -butyl-2,2'-dipyridyl
d.r.	diastereomeric ratio
ee	enantiomeric excess
<i>E</i>	<i>trans</i> (entgegen) olefin geometry
E ⁺	electrophile
E1	unimolecular elimination
E2	bimolecular elimination
e.g.	for example (Latin: <i>exempli gratia</i>)
eq	equation
Et	ethyl
<i>et al.</i>	and others (Latin: <i>et alii</i>)
g	gram(s)
h	hour(s)
¹ H	proton
² H	deuterium
[H]	reduction
HG–II	Hoveyda-Grubbs catalyst, 2 nd generation

HMDS	hexamethyldisilazane
HMPA	hexamethylphosphoramide
HPLC	high-pressure liquid chromatography
h ν	light
IBX	2-Iodoxybenzoic acid
IC ₅₀	half maximal inhibitory concentration (50%)
im.	imidazole
IR	infrared spectrometry
<i>J</i>	coupling constant
<i>k</i>	rate constant
kcal	kilocalorie(s)
kg	kilogram(s)
KHMDS	potassium bis(trimethylsilyl)amide
L	liter or neutral ligand
<i>l</i>	levorotatory
LA	Lewis acid
LCMS	liquid chromatography/mass spectrometry
LD ₅₀	median lethal dose (50%)
LDA	Lithium di-isopropylamide
LED	Light emitting diode
LHMDS	lithium bis(trimethylsilyl)amide
LLS	longest linear sequence
LTMP	lithium 2,2,6,6-tetramethylpiperidine

m	Multiplet or meter
M	Molar
<i>m</i>	meta
<i>m</i> -CPBA	meta-chloroperbenzoic acid
Me	methyl
mg	milligram(s)
MHz	Megahertz
min	minute(s)
mol	mole(s)
mp	melting point
Ms	methanesulfonyl (mesyl)
MS	molecular sieves
m/z	mass-to-charge ratio
MTBE	Methyl <i>tert</i> -butyl ether
N	normal or molar
NBS	<i>N</i> -bromosuccinimide
Nf	nonafluorobutanesulfonate (nonaflate)
NIS	<i>N</i> -iodosuccinimide
nm	nanometer(s)
NMI	<i>N</i> -methyl imidazole
NMO	<i>N</i> -methyl morpholine <i>N</i> -oxide
NMR	nuclear magnetic resonance
NOE	nuclear Overhauser effect

NOESY	nuclear Overhauser enhancement spectroscopy
Ns	<i>ortho</i> - or <i>para</i> -nitrosobenzenesulfonyl
Nuc	nucleophile
<i>o</i>	ortho
ox	oxalate
[O]	oxidation
<i>p</i>	para
PCC	pyridinium chlorochromate
PDC	pyridinium dichromate
Ph	phenyl
pH	hydrogen ion concentration in aqueous solution
PHOX	phosphinooxazoline
PIFA	phenyliodine <i>bis</i> (trifluoroacetate)
pKa	acid dissociation constant
PMB	<i>para</i> -methoxybenzyl
PPA	polyphosphoric acid
PPI	protein-protein interactions
ppm	parts per million
PPTS	pyridinium <i>p</i> -toluenesulfonate
ppy	2-phenylpyridine
Pr	propyl
<i>i</i> -Pr	isopropyl
<i>n</i> -Pr	propyl or <i>norm</i> -propyl

psi	pounds per square inch
pyr	pyridine
PyBrOP	Bromotripyrrolidinophosphonium hexafluorophosphate
q	quartet
<i>R</i>	rectus
R	alkyl group
RCAM	ring-closing alkyne metathesis
RCM	ring-closing metathesis
Red-Al	sodium <i>bis</i> (2-methoxyethyl)aluminium hydride
ref	reference
R _f	retention factor
s	singlet or seconds
<i>S</i>	sinister
sat.	saturated
S _E Ar	Electrophilic aromatic substitution
S _N Ar	Nucleophilic aromatic substitution
t	triplet
TBAF	tetrabutylammonium fluoride
TBHP	<i>tert</i> -butyl hydroperoxide
TBS	<i>tert</i> -butyl dimethylsilyl
temp	temperature
TEMPO	2,2,6,6-Tetramethylpiperidin-1-yl)oxyl
TES	triethylsilyl

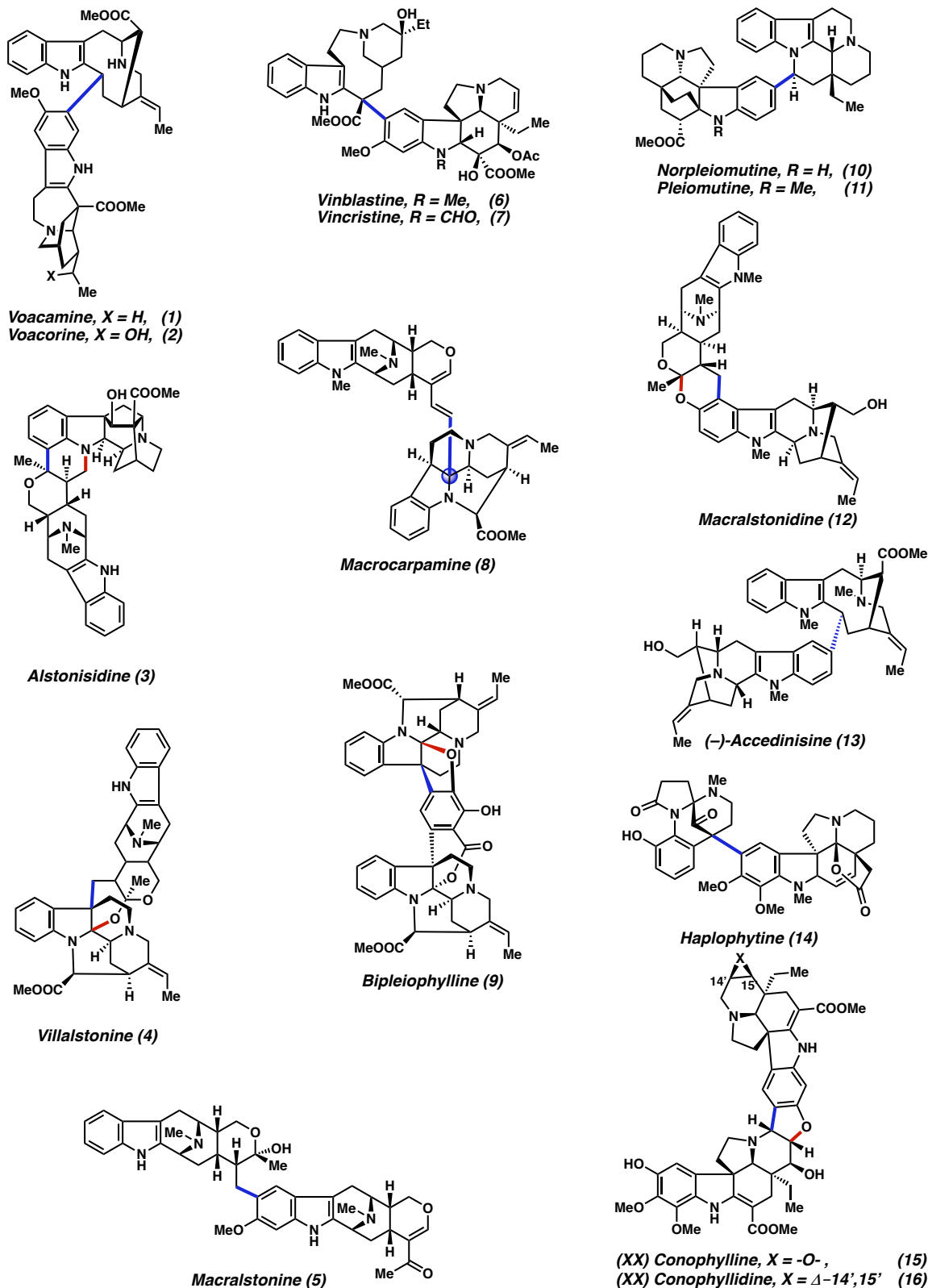
Tf	trifluoromethanesulfonate (triflate)
TFA	trifluoroacetic acid
TFAA	trifluoroacetic anhydride
TFE	2,2,2-trifluoroethanol
THF	tetrahydrofuran
TMAD	tetramethylazodicarboxamide
TMEDA	N,N,N',N'-tetramethylethylenediamine
TMP	2,2,6,6-tetramethylpiperidine
TMS	trimethylsilyl
TOF	time-of-flight
tol	tolyl
TPAP	tetrapropylammonium perruthenate
Ts	<i>para</i> -toluenesulfonyl (tosyl)
UV	ultraviolet
w/v	weight per volume
v/v	volume per volume
X	anionic ligand or halide
Z	cis (zusammen) olefin

CHAPTER 1

The Synthesis of Heterodimeric Bis(monoterpenoid) Indole Alkaloids

1.1 INTRODUCTION

The *bis*(monoterpenoid) indole alkaloids¹ comprise a diverse class of plant-derived natural products with over 200 isolated members to date.² Unlike many natural product families which exhibit a high degree of analogy with respect to their molecular architectures due to conserved biosynthetic pathways, “*bis*(monoterpenoid) indole alkaloid” is a general descriptor which applies to any natural product composed of two monoterpene-derived indole alkaloids joined by at least one C–C bond.^{3,4,5} As a result of this broad definition, the molecules in this class exhibit exceptional variation in structure, reactivity, and function with no one member constituting an “archetypal” bisindole alkaloid (Figure 1.1). Consequently, the chemodiversity within this class has attracted the attention of chemists and biologists from various sub-disciplines for over sixty years.

Figure 1.1 Representative heterodimeric *bis(monoterpenoid)* indole alkaloids.

To the synthetic chemist, dimeric indole alkaloids present a number of challenging aspects, which have limited the number of successful synthetic efforts compared to their monomeric counterparts. Because of the broad definition, the members of this family often display multiple iconic alkaloid architectures—including *aspidosperma*, *corynanthe*, *eburnea*, *macroline*, *vobasine*, and others within a single chemical entity; in effect, one must complete two separate total syntheses en route to one of these higher order monomers, a challenge that is exacerbated by the need to construct or conjoin these two fragments in a single, sterically congested molecule.

Furthermore, while classic retrosynthetic logic indicates that “dimerizing” C–C bonds are strategic disconnections,⁶ the execution in the forward sense is rarely facile. Convergent coupling reactions must construct sterically encumbered bonds with complete chemo-, regio-, and stereoselectivity between densely functionalized natural product frameworks.⁷ For this reason, many synthetic strategies have centered on biomimetic coupling reactions, typically a combination of electrophilic aromatic substitution, condensation, or Michael addition.² However, the ability to replicate this reactivity *ex vivo* is far from guaranteed, while the requirement for distinction between “electron-rich” and “electron-poor” coupling partners can limit the extension to non-natural products and natural-product analogs.

Beyond these intrinsic chemical obstacles, the *bis*(monoterpenoid) alkaloids have also received attention because of their rich biological activity. A number of newly isolated natural products in this class have demonstrated bioactivities including, but not limited to, antileukemic, antimicrobial, antioxidant, antiulcer, cytotoxic, norepinephrine reuptake-inhibiting, platelet inhibiting, and radical scavenging.^{3,4,5} In general, the dimeric alkaloids exhibit more potent activities than their individual component monomers,^{8,9,10,11} which is hypothesized to occur

through higher target affinity or greater stabilization of the protein-ligand complex.^{12,13} For most molecules in this class however, the nature of these biological interactions are poorly understood.

The most well-studied members of this class, vinblastine (**6**) and vincristine (**7**) are FDA-approved to treat a variety of rapidly-dividing cancers like Hodgkin's lymphoma, melanoma, and Non-small-cell lung cancer. Mechanistically,¹⁴ vinblastine (**6**) and vincristine (**7**) inhibit mitotic spindle through disruption of microtubule binding, leading to cell cycle arrest, aberrant division, and necrosis of tumor cells. Small molecule antagonists of protein-protein interactions (PPI's) have been branded "the holy grail of drug discovery,"¹⁵ and natural products that disrupt PPI's have immense value as starting points for the evaluation of new leads.^{16,17} The independent bioactivity of component monomers and structural similarity to established PPI inhibitors have led us to hypothesize that other members of this family could modulate similar interactions.

The goal of this account is to provide a comprehensive review of successful synthetic efforts to date as a resource for chemists who may wish to study *bis*(monoterpenoid) indole alkaloids through semi-, partial-, or total synthesis. Although a number of excellent book chapters have been dedicated to the subject,^{2,3,4,5} most are broadly focused, and they do not provide a comprehensive summary of synthetic efforts in a single resource. Furthermore, a number of other reviews on the topic of synthesis are either out-of-date¹⁸ or focused on specific subclass of bisindole alkaloids.¹⁹ We hope that this resource will help to facilitate future synthetic efforts by highlighting key developments in strategies and tactics.

Our discussion will be limited to *heterodimeric bisindole* alkaloids, which we define as alkaloids composed of two structurally unique monomeric subunits that are each monoterpene-derived in origin; thus, the coupling strategies require an element of *substrate* or *reagent* control to engender cross-selectivity. This serves to distinguish from *homodimeric alkaloids*, which are

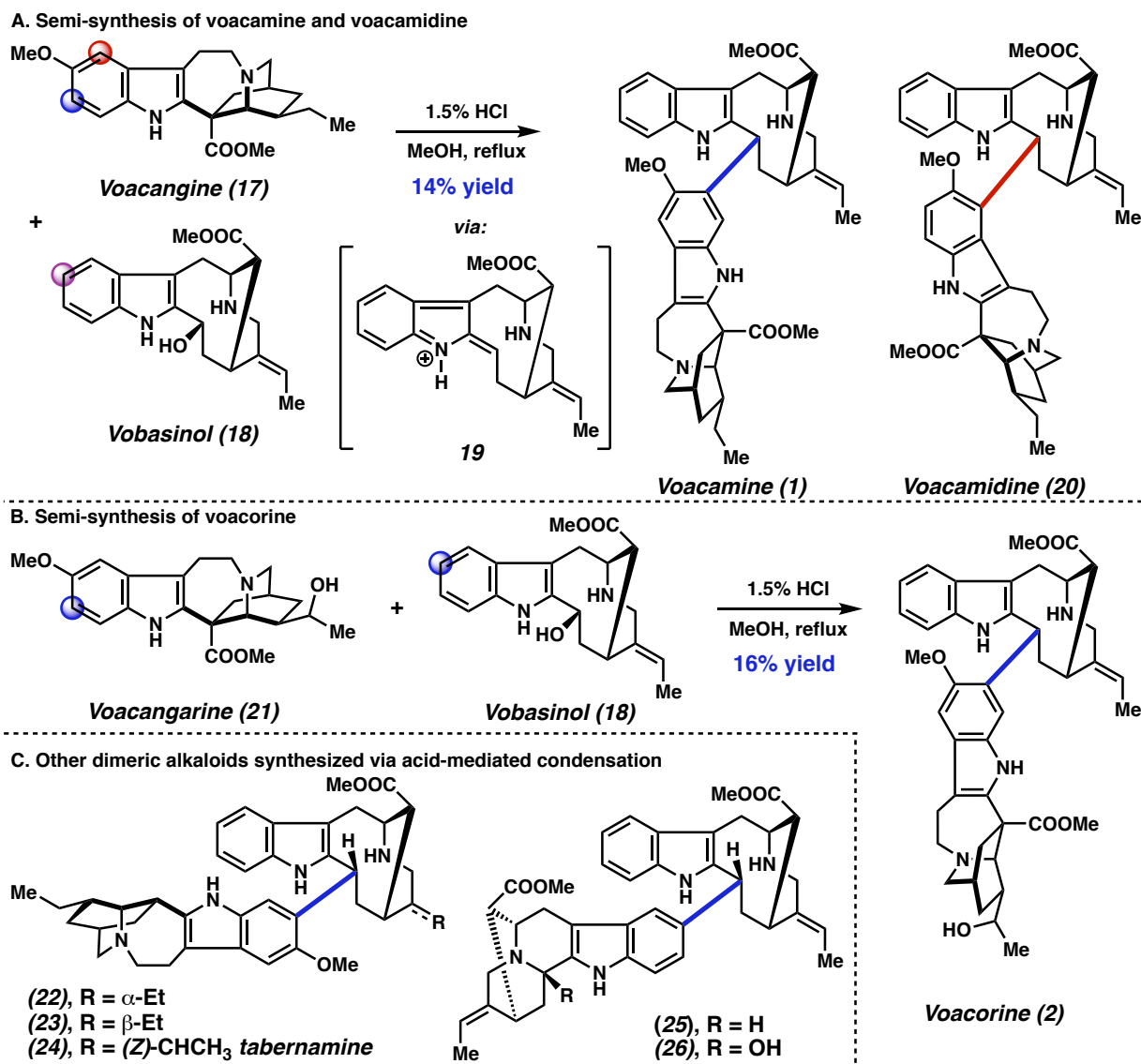
composed of identical subunits resulting from spontaneous dimerization under reaction conditions. Dimeric alkaloids in which one component is not monoterpene-derived (e.g. from a condensed tryptamine or isoquinoline-derived unit) fall out of the scope of this review. Polypyrroloindoline alkaloids also will not be included in this discussion, despite the structural analogy to many of the structures discussed herein, though interested parties may be directed to the following reviews.^{20,21}

1.2 SEMI- AND PARTIAL SYNTHESSES OF BISINDOLE ALKALOIDS

1.2.1 Büchi's Partial Synthesis of Voacamine and Related Alkaloids

The earliest synthesis of a bisindole alkaloid was that of voacamine (**1**) and voacarine (**2**), reported by Büchi in the early 1960's.^{22,23} After performing a number of degradation studies to elucidate the structure of the component monomers, Büchi performed a semi-synthesis to confirm the identity of the dimeric structure. Treating of a mixture of naturally isolated alkaloids voacangine (**17**) and vobasinol (**18**) with 2% HCl in methanol produced voacamine (**1**) in 14% yield, along with an undisclosed quantity of its constitutional isomer voacamidine (**20**) (Scheme 1.1A). This is hypothesized to proceed through the intermediacy of iminium **19** via a Friedel–Crafts alkylation at either the indole C(6) of voacangine (blue) to form voacamine (**1**) or at C(8) (red) to form voacamidine (**20**). It was subsequently shown that the latter isomer can be equilibrated back to voacamine (**1**) under more strongly acidic conditions.²⁴

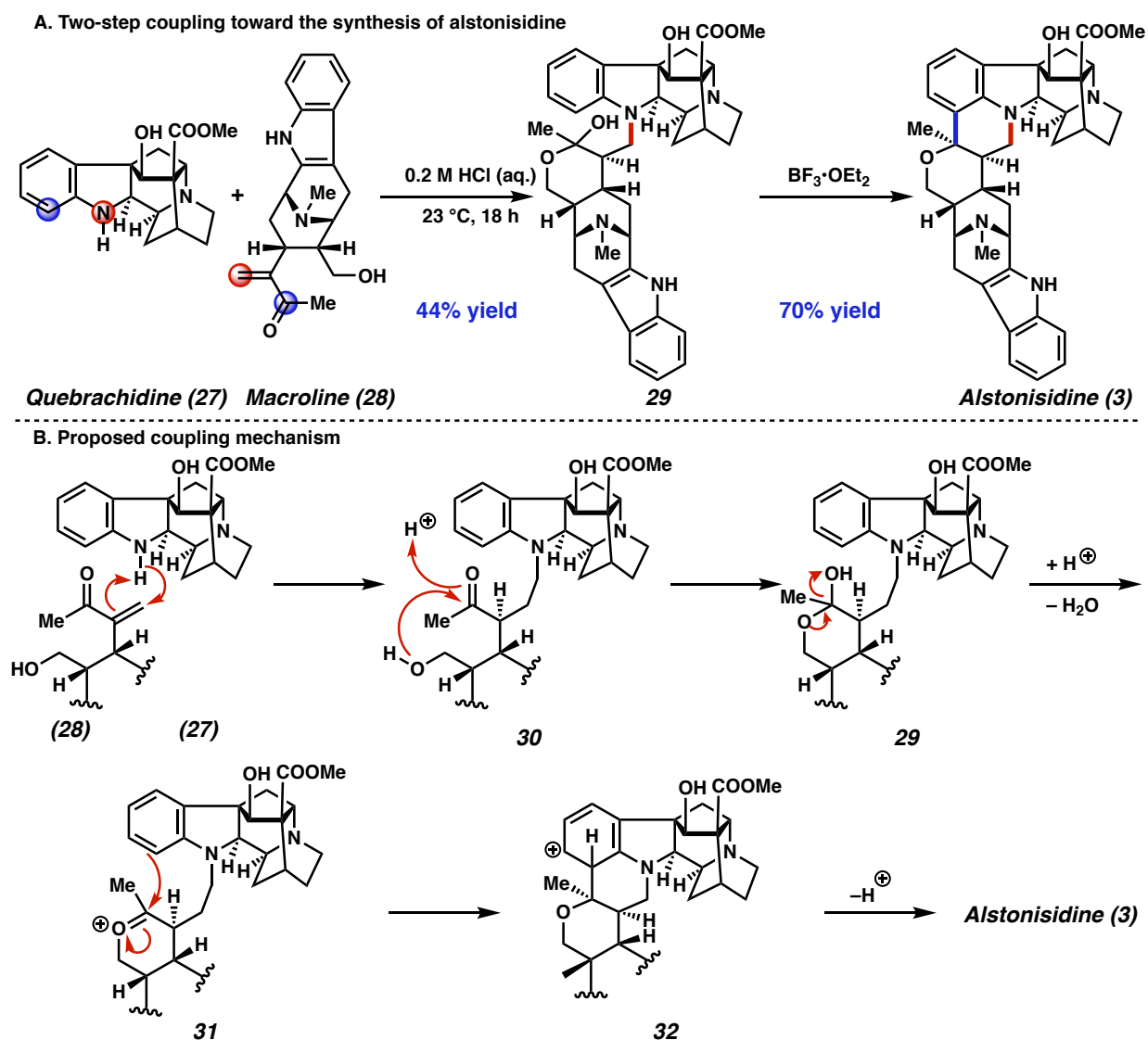
Under identical reaction conditions, Büchi showed that voacarine (**2**) could be accessed through the condensation of voacangarine (**21**) and vobasinol (**18**) (Scheme 1.1B). Analogous acid-mediated condensations would later be utilized to access vobasine-based alkaloids tabernamine²⁵ (**24**), bisindole alkaloids from *E. orientalis*^{26,27} (**22**)–(**23**) and *T. accedens*²⁸ (**25**)–(**26**), ervahaimines A and B,²⁹ and several unnatural dimers³⁰ (Scheme 1.1C).

Scheme 1.1. Büchi's semi-synthesis of voacamine, voacamidine, voacorine (1963).**1.2.2 LeQuesne and Cook's Semi-synthesis of Alstonisidine**

In 1972, LeQuesne and Cook reported the semi-synthesis of alstonisidine (**3**)^{31,32} from naturally isolated quebrachidine (**27**) and macroline (**28**), obtained via the degradation of the related natural product villamine³³ (Scheme 1.2A). In the presence of 0.2 M HCl, quebrachidine (**27**) and macroline (**28**) react to generate hemiketal **29**. Mechanistically, this is proposed to occur

via conjugate addition of the indoline nitrogen into the enone, which following protonation yields ketone **30** (Scheme 1.2B); intramolecular ketalization then occurs to condense the primary alcohol and generate hemiketal **29**. Upon subsequent treatment with $\text{BF}_3 \cdot \text{OEt}_2$ at 0°C , oxocarbenium **31** is generated and intercepted via electrophilic aromatic substitution to afford Wheland intermediate **32**, which upon deprotonation generates alstonisidine (**3**). Although this target has yet to be generated by total synthesis, both quebrachidine precursors³⁴ and macroline (**28**)^{35,36,37,38,39} were later independently accessed through synthetic efforts.⁴⁰

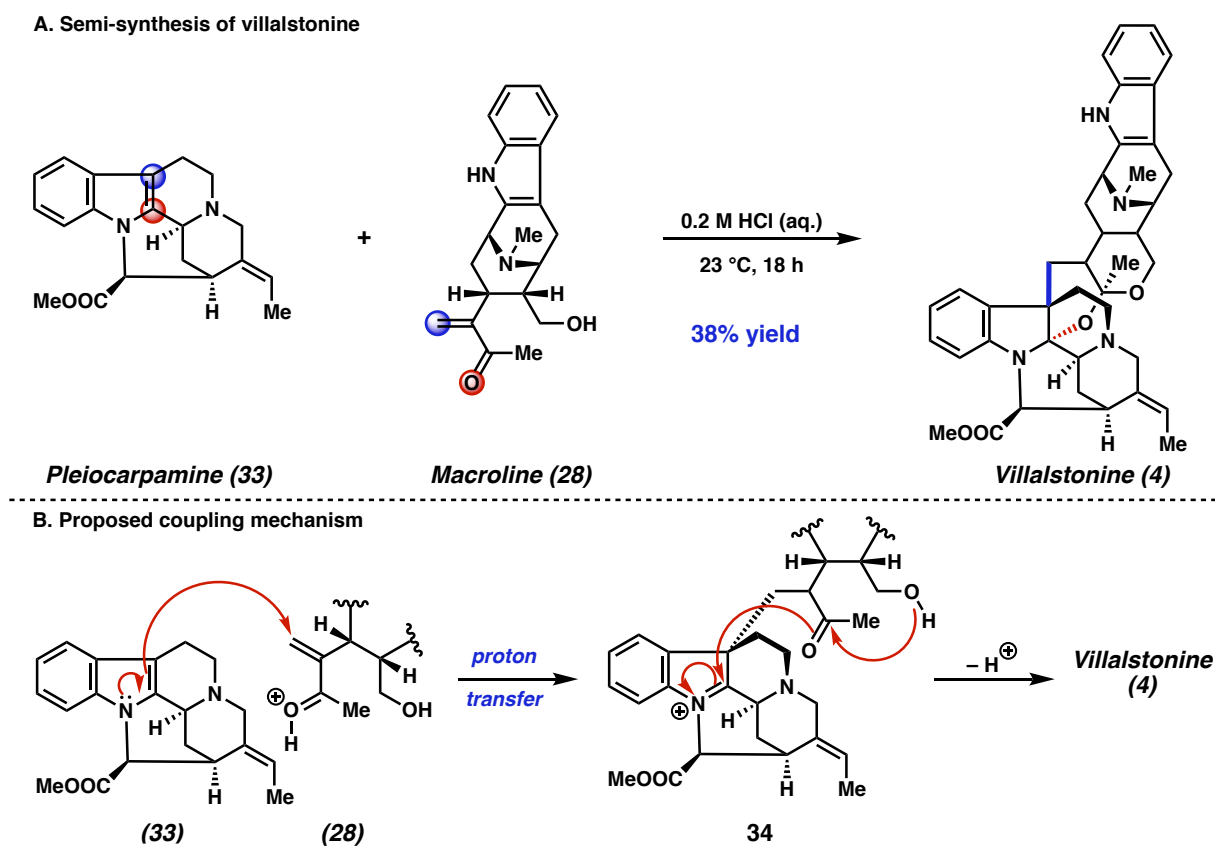
Scheme 1.2. *LeQuesne and Cook's semi-synthesis of alstonisidine (1972).*



1.2.3 *LeQuesne and Cook's Semi-synthesis of Villalstonine*

LeQuesne and coworkers also applied this reactivity to the synthesis of the related alkaloid villalstonine (**4**)^{32,41} from pleiocarpamine (**33**) and macroline (**28**) (Scheme 1.3A). In contrast to quebrachidine (**27**), the *N*-alkylated indole pleiocarpamine (**34**) reacts with the conjugate acceptor of macroline (**28**) at indole C(3), generating ketone **34**; addition of the macroline primary alcohol into the carbonyl then promotes intramolecular amination formation via addition of the oxygen into the C(2) iminium to form villalstonine (**4**) in 38% yield. (Scheme 1.3B)

Scheme 1.3. *LeQuesne's semi-synthesis of villalstonine (1972).*

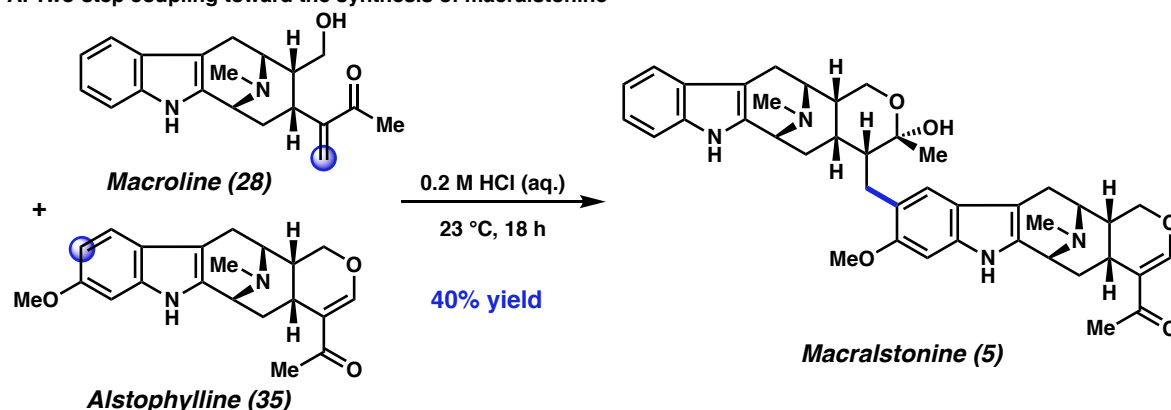


1.2.4 *LeQuesne and Cook's Semi-synthesis of Macralstonine*

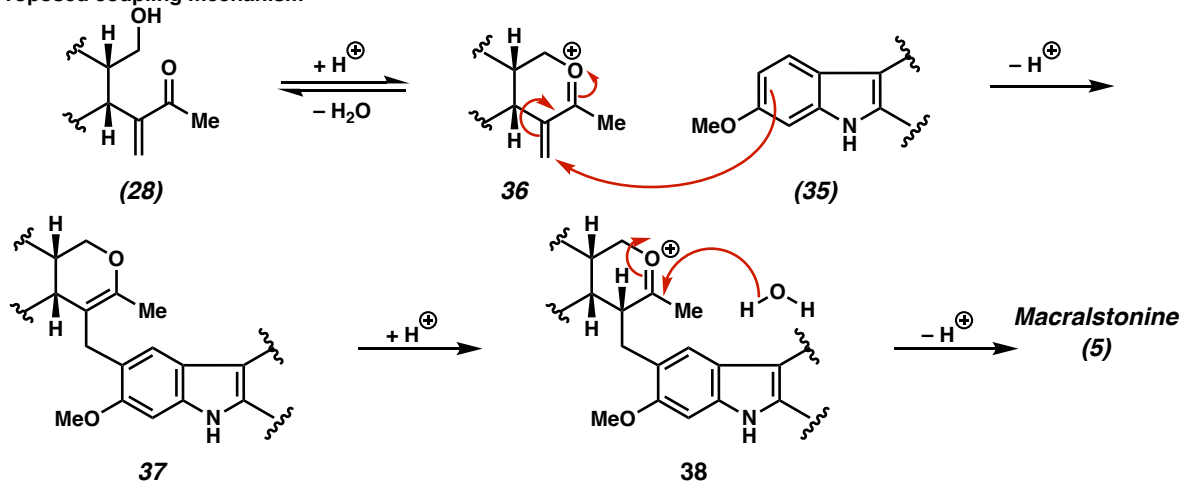
Shortly thereafter, these conditions were applied a third time to the semi-synthesis of macralstonine (**5**)⁴² from macroline (**28**) and alstophylline (**34**) (Scheme 1.4A). Though this initially was proposed to occur via electrophilic aromatic substitution akin to that of villastronine, an alternative mechanism was later proposed⁴³ where macroline (**28**) first equilibrates to oxocarbenium species **36** upon loss of water (Scheme 1.4B). This species is then intercepted by the electron rich indole ring of alstophylline (**35**) to afford conjugate adduct **37**; hydration of the dihydropyran via oxocarbenium **38** then generates the natural product (**5**) in 40% yield. A total synthesis of alstophylline was later accomplished by Cook.^{44,45}

Scheme 1.4. *LeQuesne and Cook's semi-synthesis of macralstonine (1972).*

A. Two-step coupling toward the synthesis of macralstonine



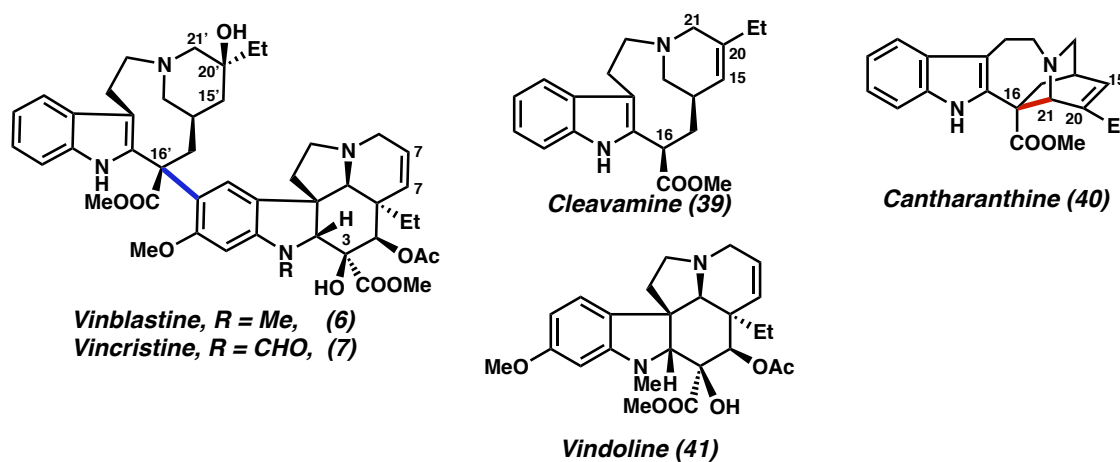
B. Proposed coupling mechanism



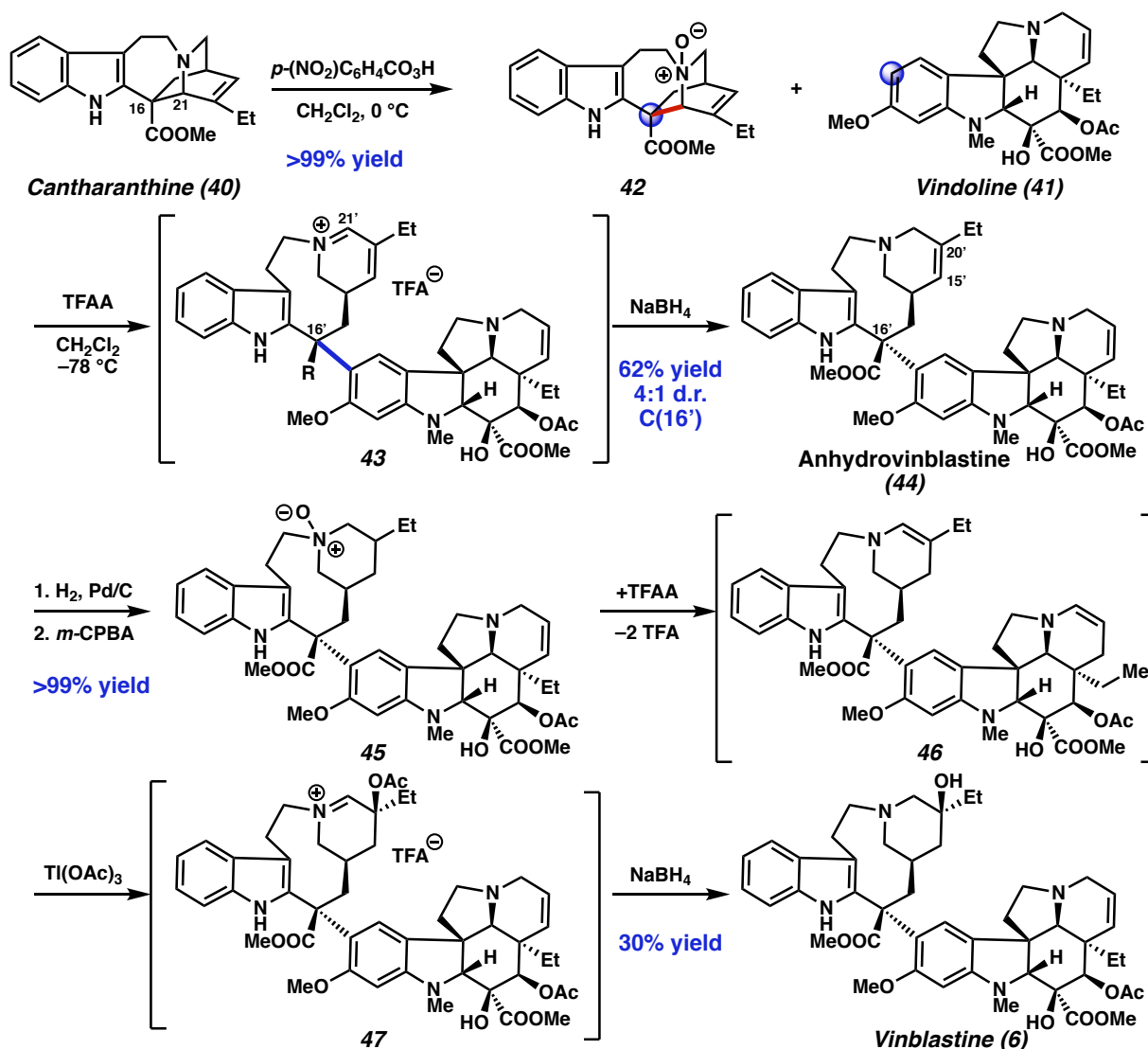
1.2.5 Portier and Langlois's Partial Synthesis of Vinblastine

Vinblastine (6) and vincristine (7) are the most well-studied members of this natural product class from a synthetic perspective (Figure 1.2). Isolated from the Madagascar periwinkle *Cantharanthus roseus* G. don in 1958,^{46,47,48} these natural products are composed of a northern fragment derived from cleavamine (39) —which is synthesized in vivo via C–C bond cleavage of the related natural product cantharanthine (40)—and a southern fragment derived from vindoline (41). Early attempts to couple cleavamine (39) and vindoline (41) directly through S_EAr forged the undesired epimer of vinblastine at C(16') as the exclusive product.⁴⁹

Figure 1.2 Vinblastine, vincristine, and their subunits.



Due to their high potency and treatment in low doses, clinical supplies continue to be derived from natural sources. Nevertheless, the chemical complexity of these molecules, in conjunction with questions about their structure-activity relationship and potential derivatives, have attracted significant attention from the synthetic community over the years, starting from semi-synthetic efforts through the late 20th century and, later, total-synthetic efforts through the early 21st century.

Scheme 1.5. Portier and Langlois's semi-synthesis of vinblastine (1979).

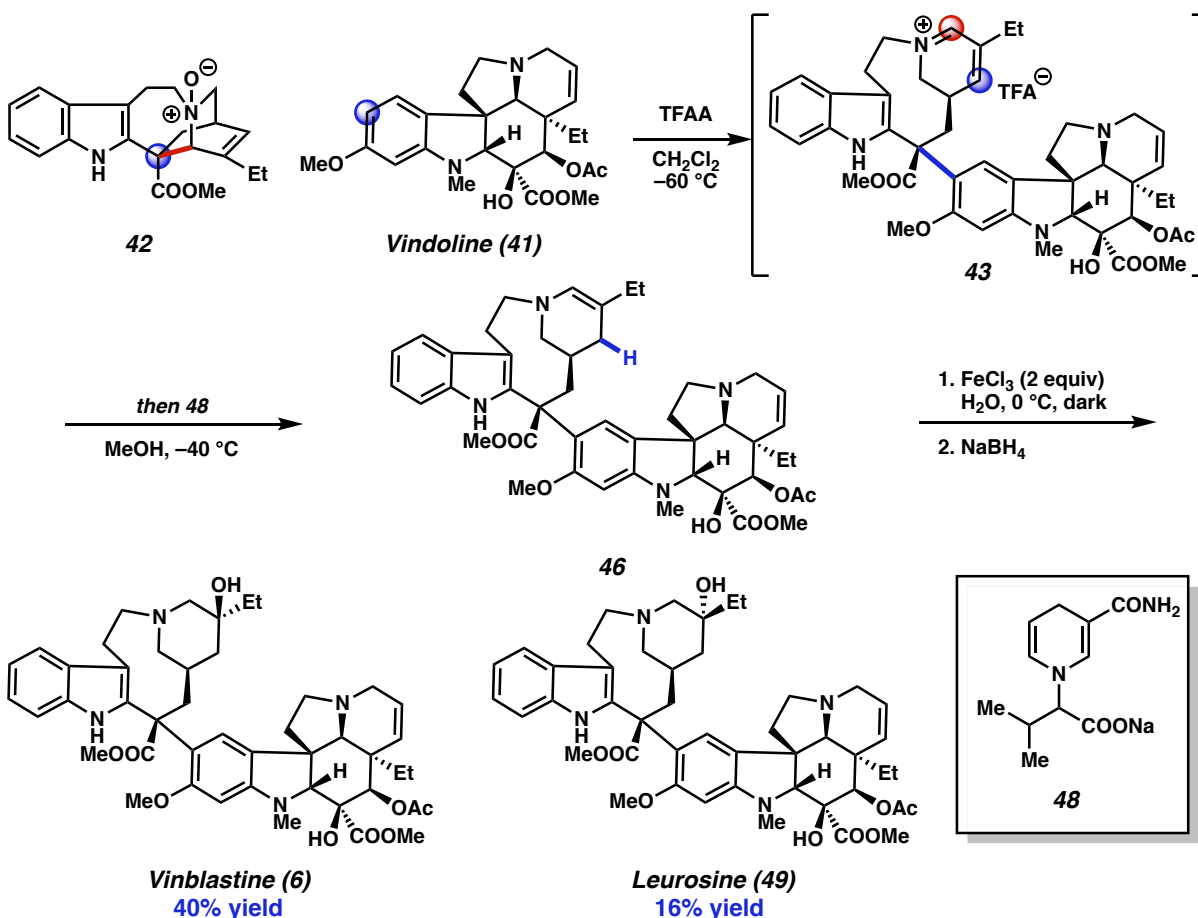
In 1979, Portier and Langlois published the first partial synthesis of vinblastine (**6**) from natural cantharathine (**40**) and vindoline (**41**) (Scheme 1.5).⁵⁰ Following a three-step procedure developed concurrently by the Portier-Langlois^{51,52} and Kutney^{53,54} groups, cantharathine (**40**) is transformed to *N*-oxide **42** before submission to trifluoroacetic anhydride initiates a Polonovski–Portier rearrangement to cleave the C(16)–C(21) bond (red) of the *iboga* framework. The resultant di-cation is intercepted by vindoline (**41**) at C(16) through electrophilic aromatic substitution to generate dimeric iminium **43**, which is reduced by sodium borohydride at C(21') to access

anhydrovinblastine (**44**) in 62% yield. Low temperatures were essential, as warming from -78 to 0 °C eroded the diastereoselectivity from 4:1 to 1:1 d.r. at C(16').⁵²

Anhydrovinblastine (**44**) is then hydrogenated selectively at the $\Delta-15',20'$ olefin and *N*-oxidized with *m*-CPBA to *N*-oxide **45**. TFAA then initiates a second Polonovski-Portier rearrangement to generate enamine **46** upon subsequent elimination. Oxidation with thallium acetate then promotes β -acetloxylation to vinblastine-20'-acetate **47** before reductive deprotection with NaBH_4 generates vinblastine (**6**) in 30% yield. While other oxidants (e.g. OsO_4) oxidized from the less-hindered α -face, the thallium reagent offered the desired β -face oxidation due to direction by the enamine nitrogen lone pair.⁵⁵

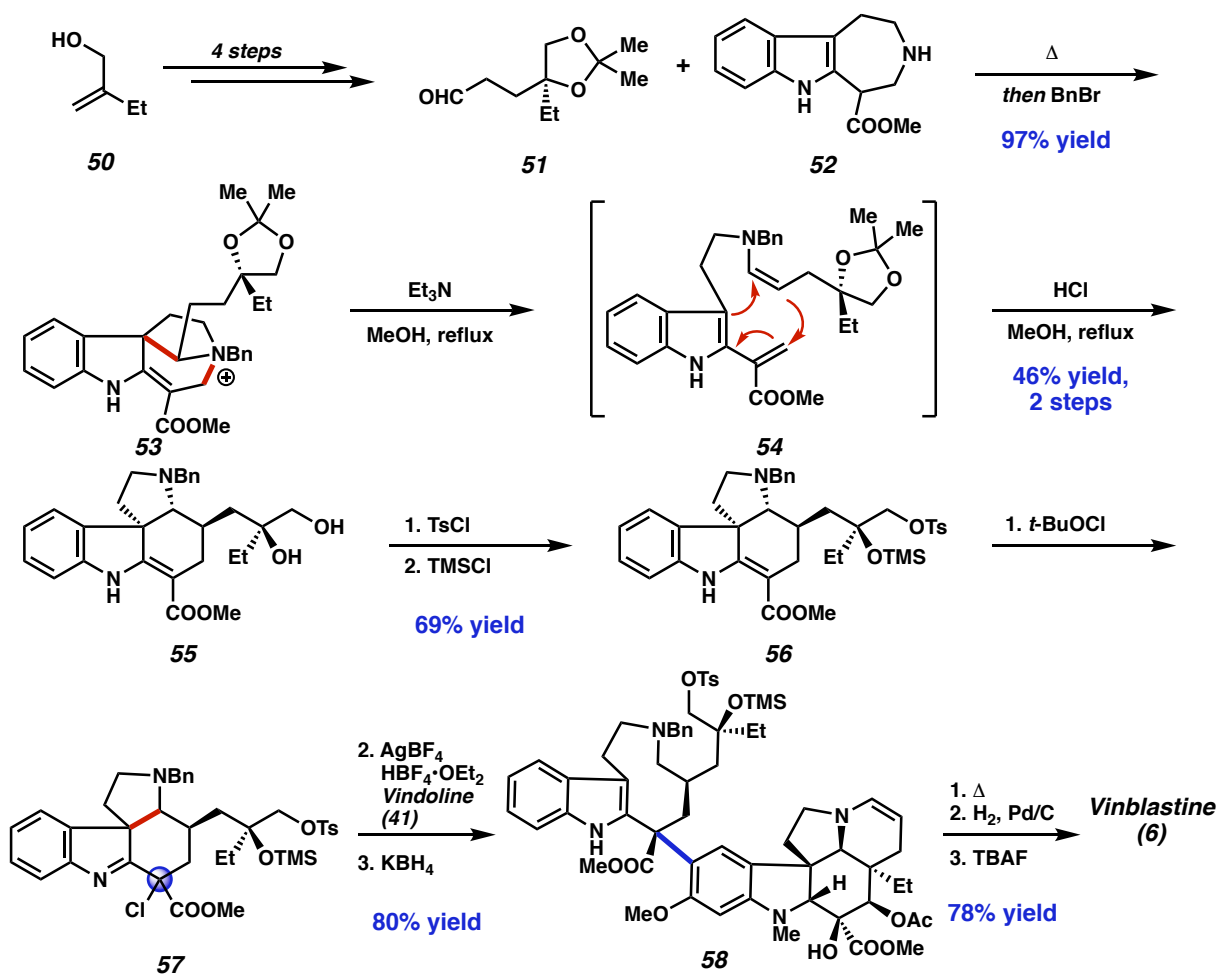
1.2.6 *Kutney's Partial Synthesis of Vinblastine*

Kutney would follow up with an improved route to vinblastine using a similar strategy (Scheme 1.6).⁵⁶ Following the tandem Polonovski-Portier rearrangement of *N*-oxide **42** and electrophilic aromatic substitution with vindoline (**41**), iminium **43** is subsequently treated with nicotinamide derivative **48** to promote 1,4-reduction of α,β -unsaturated iminium **43** preferentially at C(15') (blue) over C(21') (red) and generate enamine **46** directly. Circumventing the use of toxic thallium reagents, Kutney discovered that aerobic oxidation with iron (III) chloride could advance enamine **46** to vinblastine (**6**) following subsequent exposure to sodium borohydride in 40% yield over the sequence. A 16% yield of the alcohol epimer leurosine (**49**) is also obtained.

Scheme 1.6. Kutney's semi-synthesis of vinblastine (1988).

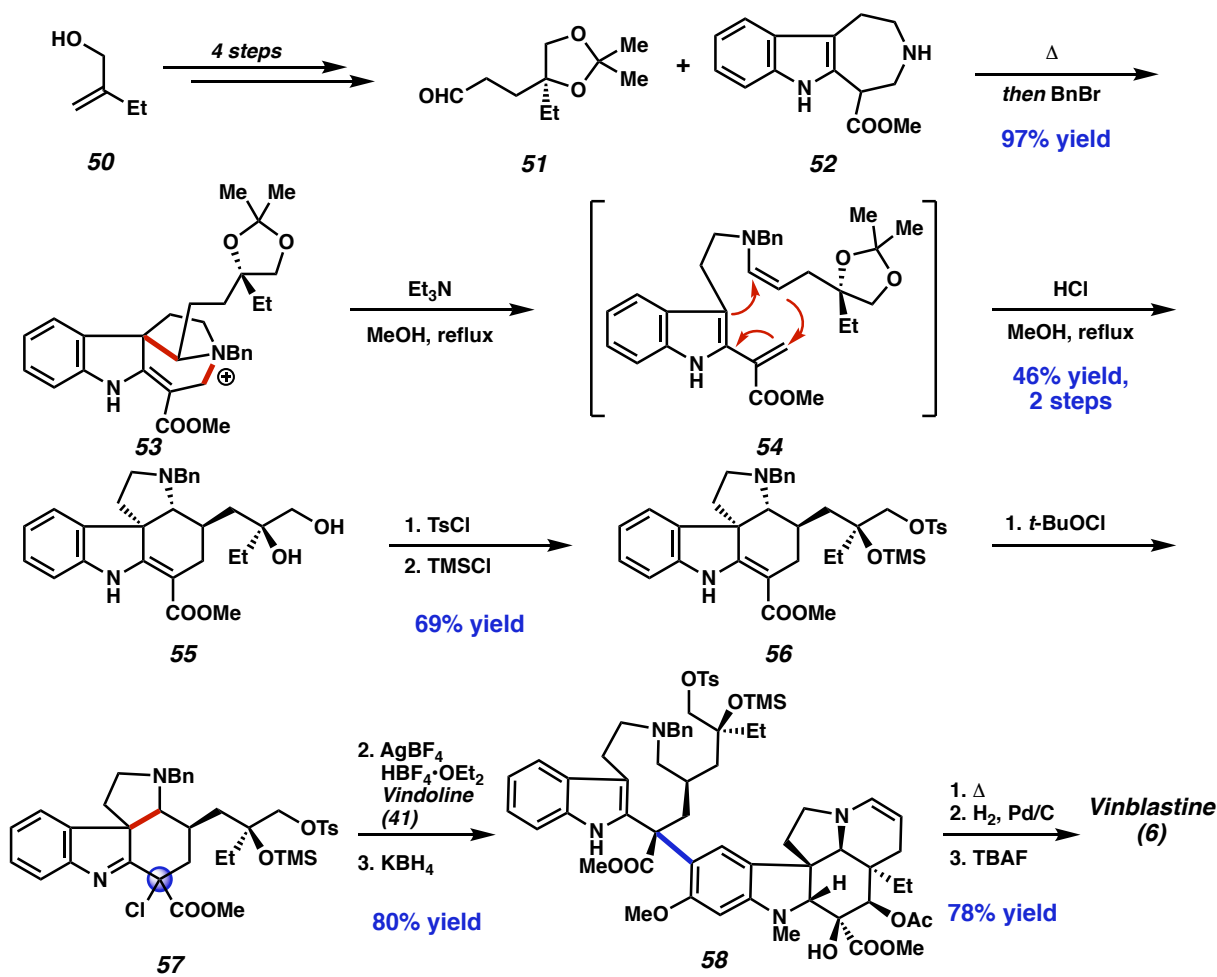
1.2.7 Kuehne's Partial Synthesis of Vinblastine

Kuehne's partial synthesis in 1991⁵⁷ targeted a deconstructed cleavamine unit to be used in the key coupling reaction (Scheme 1.7). Aldehyde **51**, obtained in four steps from 2-ethyl-prop-2-enol **50** via Sharpless epoxidation, was condensed with azepine **52** and alkylated with benzyl bromide to generate quaternary ammonium **53**. Heating promotes C–C bond cleavage (red), which following treatment with base initiates a formal [4+2] cycloaddition of enamine **54**; subsequent diol deprotection affords tetracycle **55** in modest yield, largely due to poor diastereoselectivity in the cycloaddition. Selective tosylation and silylation then affords dimerization precursor **56**.

Scheme 1.7. Kuehne's partial synthesis of vinblastine (1991).

Exposure to *t*-butyl hypochlorite affords chloride **57** which is followed by halide abstraction and heterodimerization; C–C bond cleavage (red) with potassium borohydride produces dimer **58** in 80% yield. While attempts to use cleavamine-derived chloroindenes in coupling reactions had previously⁴⁹ led to poor diastereocontrol at C(16'), this research demonstrated that deconstruction of the piperidine ring was enough to overturn this inherent selectivity. To complete the natural product, dimer **58** is then advanced to vinblastine (**6**) over a three-step sequence consisting of: 1) intramolecular alkylation to generate a quaternary ammonium salt, 2) cleavage of the benzyl protecting group and 3) deprotection of the tertiary alcohol. A second generation approach to the cleavamine unit was published the next year.⁵⁸

1.2.8 Magnus's Partial Synthesis of Vinblastine

Scheme 1.8. Magnus's partial synthesis of vinblastine (1993).

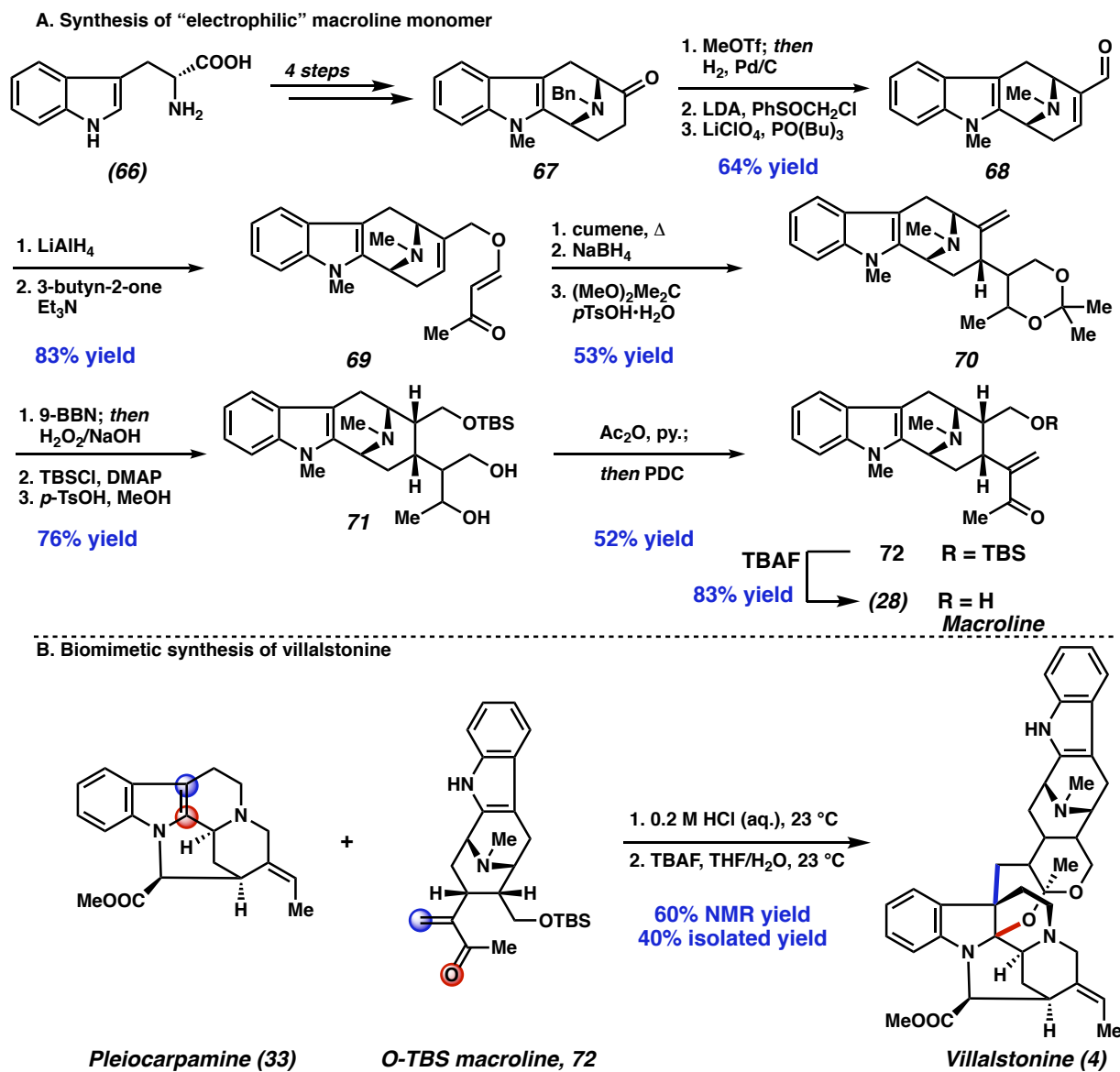
In 1993, Magnus⁵⁹ disclosed an approach to vinblastine relying on “non-oxidative” formation of the electrophilic iminium (Scheme 1.8). *N*-benzyl tryptamine **59** was first advanced to thioamide **60** over a five-step sequence involving Pictet–Spengler cyclization and Barton decarboxylation, while 2-ethyl-prop-2-enol **50** was advanced to aldehyde **61** over a four-step sequence involving Sharpless epoxidation. A tin (II)-mediated aldol first affords alcohol **62** in 75% yield, before tosylation and elimination generates a mixture of alkenes (not shown). Raney nickel-mediated desulfuration reduces thioamide to the tertiary amine before hydrogenation accesses dimerization precursor **63**.

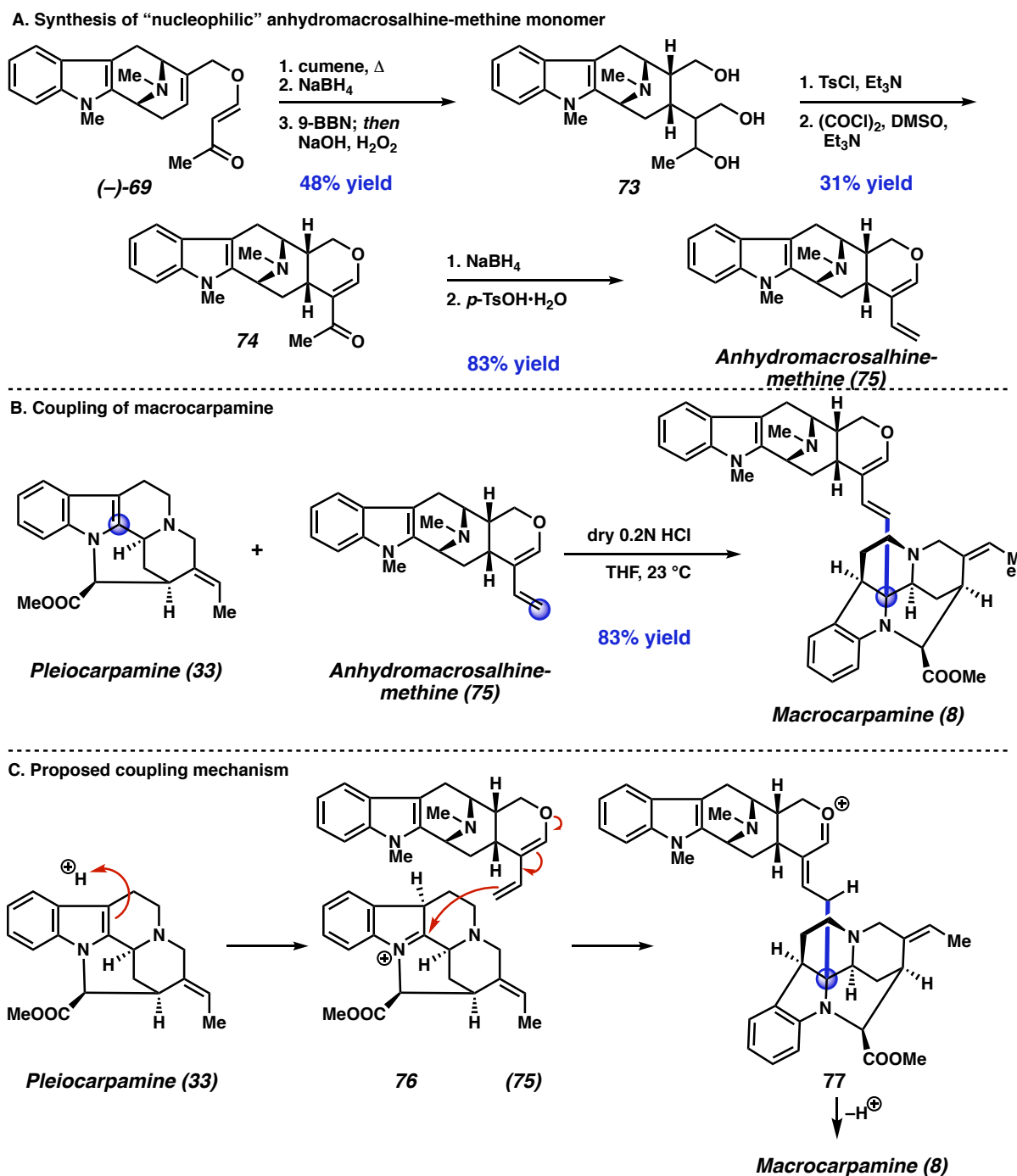
Treatment with nosyl chloroformate and base promotes acylation of the tertiary amine and C–C bond cleavage to indolene **64**, which is intercepted by vindoline (**41**) to generate dimer **65** with ~2:1 d.r. This intermediate is then advanced to vinblastine (**6**) over three-step sequence consisting of: 1) acetonide cleavage, 2) Swern oxidation and 3) carbamate cleavage/reductive amination to close the piperidine ring and complete the natural product.

1.2.9 *Cook's Partial Synthesis of Villalstonine*

In 1994, Cook reported a synthesis^{35,60} of macroline (**28**) en route to the first formal synthesis of villalstonine (**4**) (Scheme 1.9A). Tryptophan (**66**) was first elaborated to bridging lactam **67** over 4 steps via Pictet–Spengler and Dieckman cyclizations.⁶¹ Methylation of the benzyl protected amine is followed by hydrogenolysis and a two-step homologation sequence to access enal **68**. Reduction and oxa-Michael addition affords vinyl ether **69**, which is heated to promote a Claisen rearrangement, doubly reduced, and protected as acetonide **70**. Hydroboration/oxidation of the *exo*-methylene occurs with complete selectivity for the β -face, before silylation and acetonide cleavage affords diol **71**. Acetylation of the primary alcohol, oxidation of the secondary alcohol, and elimination of the acetoxy group affords enone **72**. TBAF deprotection then affords the natural product macroline (**28**).

Using a modified version of conditions described by LeQuesne,³² Friedel–Crafts alkylation generates the C–C bond (blue) before TBAF-triggered C–O bond formation (red) completes the synthesis of villalstonine (**4**) (Scheme 1.9B). Though a high yield is observed via qNMR, the isolated yield was comparable to that of the previously disclosed 38% yield in the one-step coupling (Scheme 1.9B).

Scheme 1.9. Cook's partial synthesis of villalstonine (1994).

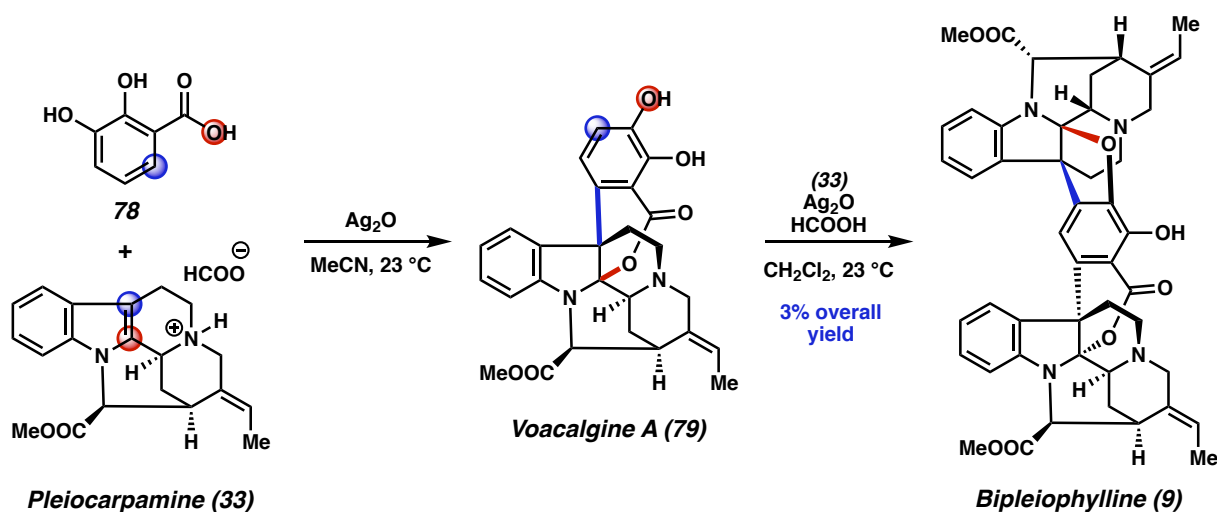
1.2.10 *Magnus's Partial Synthesis of Macroparpamine***Scheme 1.10.** Cook's partial synthesis of macroparpamine (1996).

Shortly thereafter, Cook also completed a partial synthesis of macroparpamine (**8**).

Previously synthesized ether (–)-**69** was first subjected to Claisen rearrangement, followed by

reduction and hydroboration/oxidation to triol **73** (Scheme 1.10A). Mono-tosylation is then followed by Swern oxidation and condensation to dihydropyran **74**. Reduction of the remaining ketone and elimination then affords anhydromacrosalhinine-methine (**75**). Combining this with natural pleiocarpamine (**33**) in anhydrous HCl in methanol then produces macrocarpamine (**8**) in 83% yield (Scheme 1.10B). Mechanistically, this proceeds through protonation of indole C(3), followed by addition of the vinylogous enol ether of (**76**) to the in-situ generated iminium ion, forming oxocarbenium **77**. Deprotonation then affords the natural product (**8**) (Scheme 1.10C).

Scheme 1.11. Poupon, Evanno, and Vincent's semi-synthesis of bipleiophylline (1996).



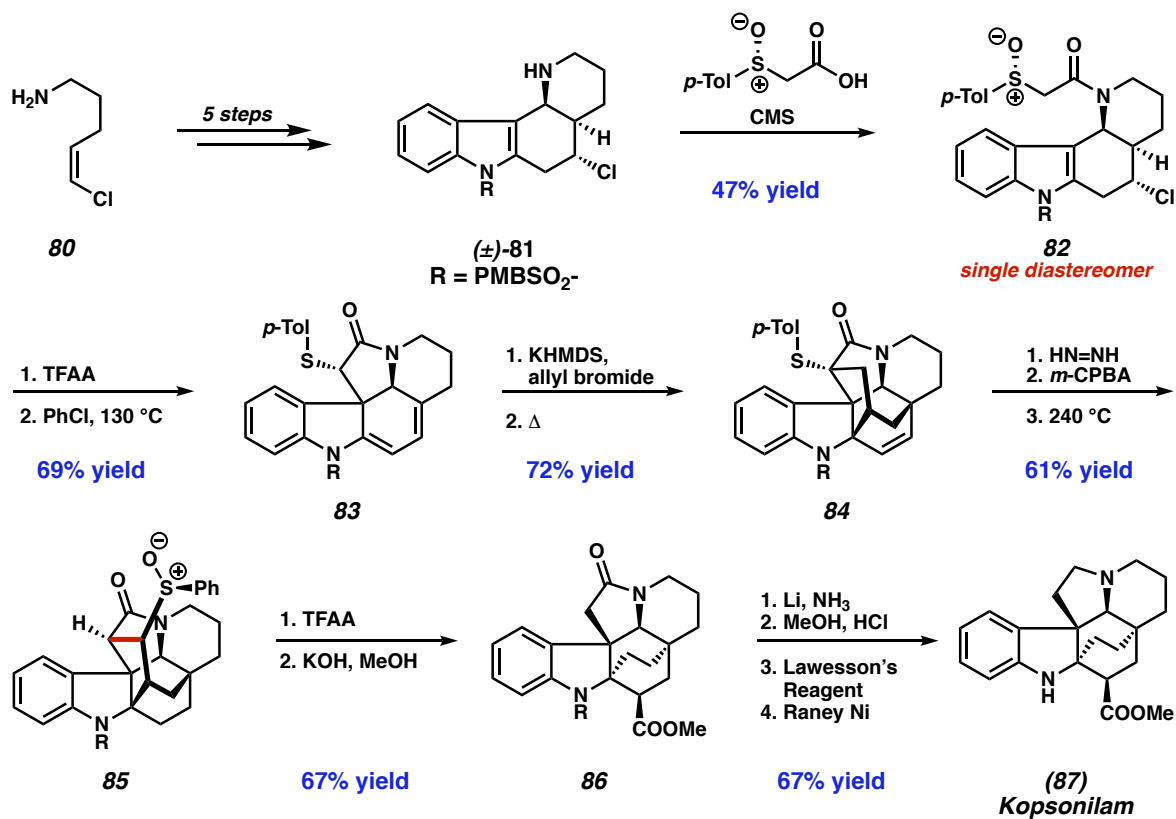
In 2017, Poupon, Evanno, and Vincent published a semi-synthesis⁶² of bipleiophylline (**9**) from pleiocarpamine (**33**) and voacalgine A (**79**) (Scheme 1.11). Though the natural product contains two pleiocarpamine units, classifying it as homodimeric, we were obliged to include it in this account due to the challenge of installing an aromatic spacer unit with the correct regioselectivity. Coupling of 2,3-dihydroxybenzoic acid **78** and the formate salt of pleiocarpamine (**33**) affords voacalgine A (**79**), a structure that was missassigned in the initial report.⁶³ Repeating this procedure in dichloromethane then affords bipleiophylline (**9**) in 3% yield over two steps.

1.3 TOTAL SYNTHESSES OF BISINDOLE ALKALOIDS

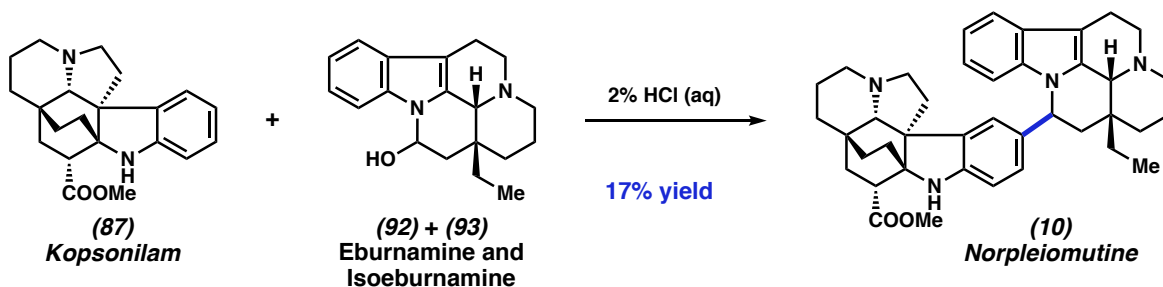
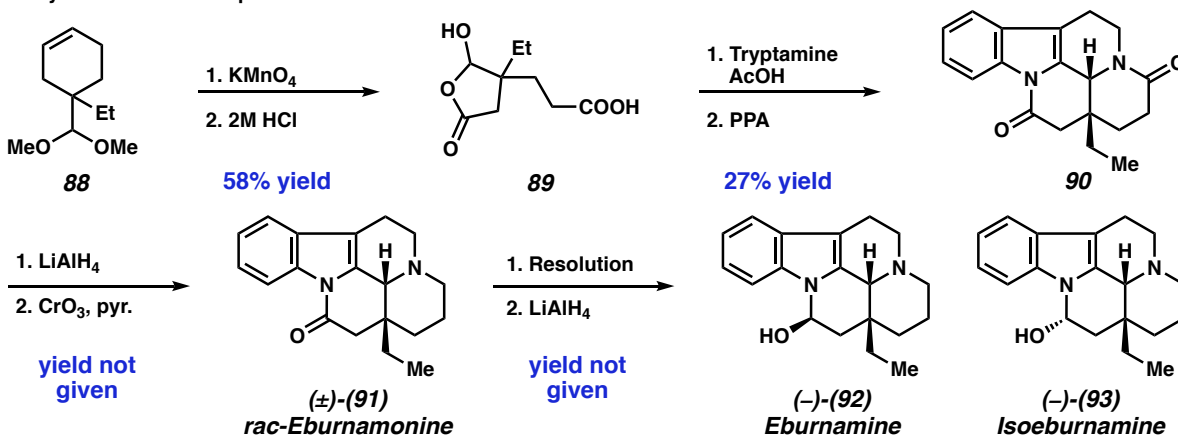
1.3.1 Magnus's Total Synthesis of Norpleiomutine

In 1984, Magnus published a route⁶⁴ to the *eburan-kopsia* dimer norpleiomutine (**10**). Amine **80** is first elaborated to tetracyclic indole **81** through a five-step sequence⁶⁵ involving intramolecular [4+2] cycloaddition (Scheme 1.12A). Esterification with enantioenriched sulfinyl acetic acid and 1-cyclohexyl-3-(2-morpholinoethyl)carbodi-imide-metho-*p*-toluene sulfonate (CMS) allows for chromatographic separation of diastereomers, affording enantiomerically pure **82**. Acylation with TFAA at elevated temperatures generates lactam **83** *via* an interrupted Pummerer rearrangement, before α -alkylation with allyl bromide and heating affords caged Diels–Alder adduct **84** in 72% yield. Following reduction of the olefin with diimide, oxidation of the thioether at 240 °C triggers a formal 1,3-migration to sulfoxide **85**. Oxidation to the ketone followed by methoxide-mediated C–C bond cleavage generates hexacyclic intermediate **86**. Deprotection of the indole nitrogen is followed by reesterification; conversion of the lactam to the thioamide with Lawesson's reagent and desulfurization affords kopsonilam (**87**).

To access the *eburan* fragment, Diels–Alder adduct **88** is subjected to oxidative cleavage and acetal hydrolysis to lactone **89** (Scheme 1.12B). Condensation with tryptamine under acidic conditions promotes a Pictet–Spengler cyclization, affording *cis*-fused pentacycle **90**. A reduction/oxidation sequence then generates *rac*-eburnamonine (**91**), before a classical resolution and lithium aluminum hydride reduction affords a mixture of (–)-eburnamine (**92**) and isoeburnamine (**93**). Subjecting a mixture of the two isomers with kopsanilam (**87**) under acidic conditions then affords norpleiomutine (**10**) in 20 steps LLS from amine **80** (Scheme 1.12C).⁶⁶ This marks the first synthesis of a dimeric indole alkaloid in which both monomeric precursors are synthetically derived and enantioenriched.

Scheme 1.12. Magnus's total synthesis of norpleiomutine (1984).

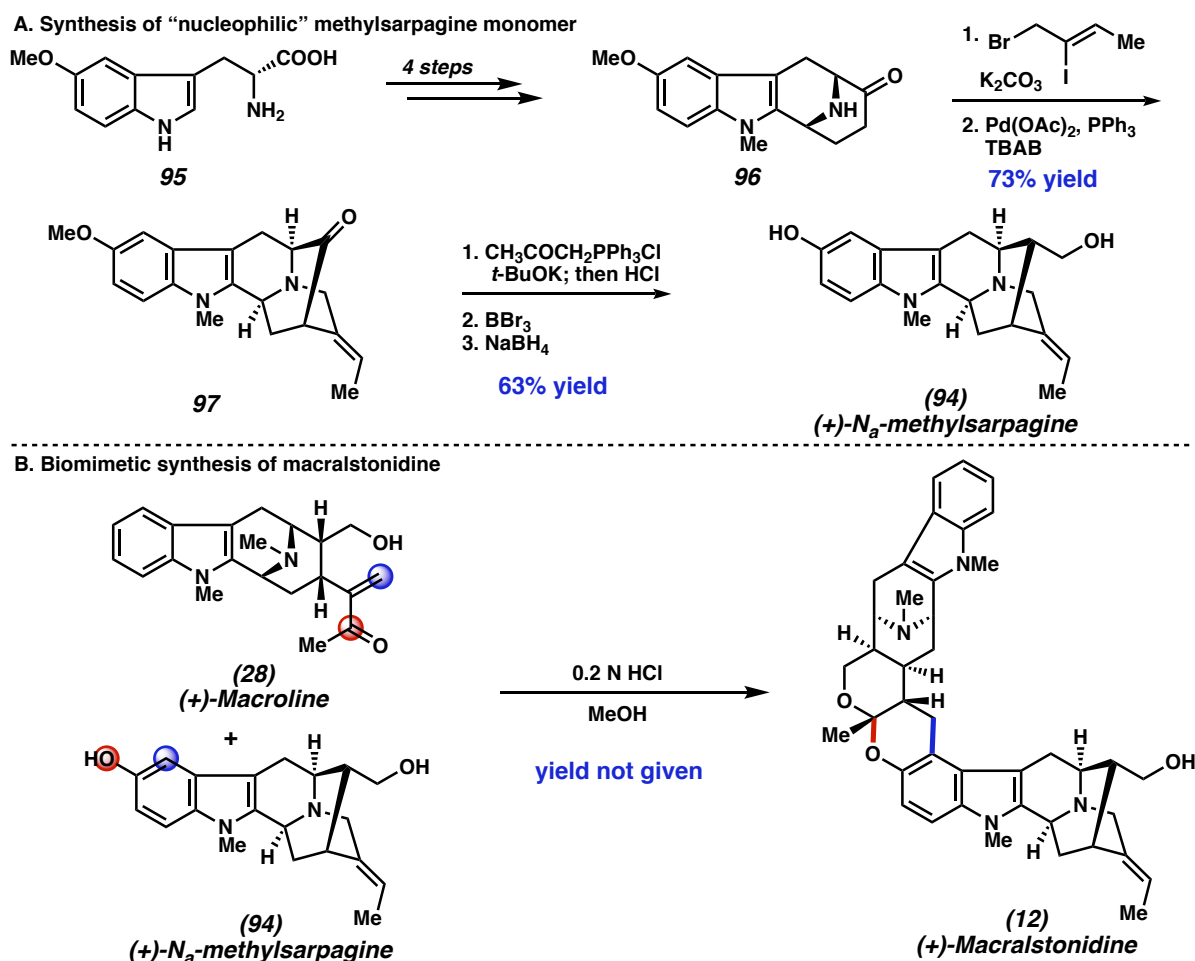
B. Synthesis of "electrophilic" eburnamine monomer



1.3.2 Cook's Total Synthesis of Macralstonidine

In 2002, Cook and coworkers reported the first total synthesis of macralstonidine (**12**) from macroline (**28**) and (+)-*N*_a-methylsarpagine (**94**).⁶⁷ 6-methoxytryptophan **95** was accessed from 4-methoxyaniline through a Japp–Klingemann synthesis⁶⁸ and advanced to lactam **96** (Scheme 1.13A).⁶⁹ *N*-alkylation generates a vinyl iodide, which then undergoes an intramolecular Pd-catalyzed enolate alkenylation to afford bridging ketone **97**. Wittig homologation with acidic workup produces an aldehyde before demethylation and borohydride reduction generates *N*_a-methylsarpagine (**94**). Acid-mediated condensation with synthetic macroline (**28**) under Gannick's conditions⁷⁰ then affords the dimer (+)-macralstonidine (Scheme 1.13B).

Scheme 1.13. Cook's total synthesis of macralstonidine (2002).

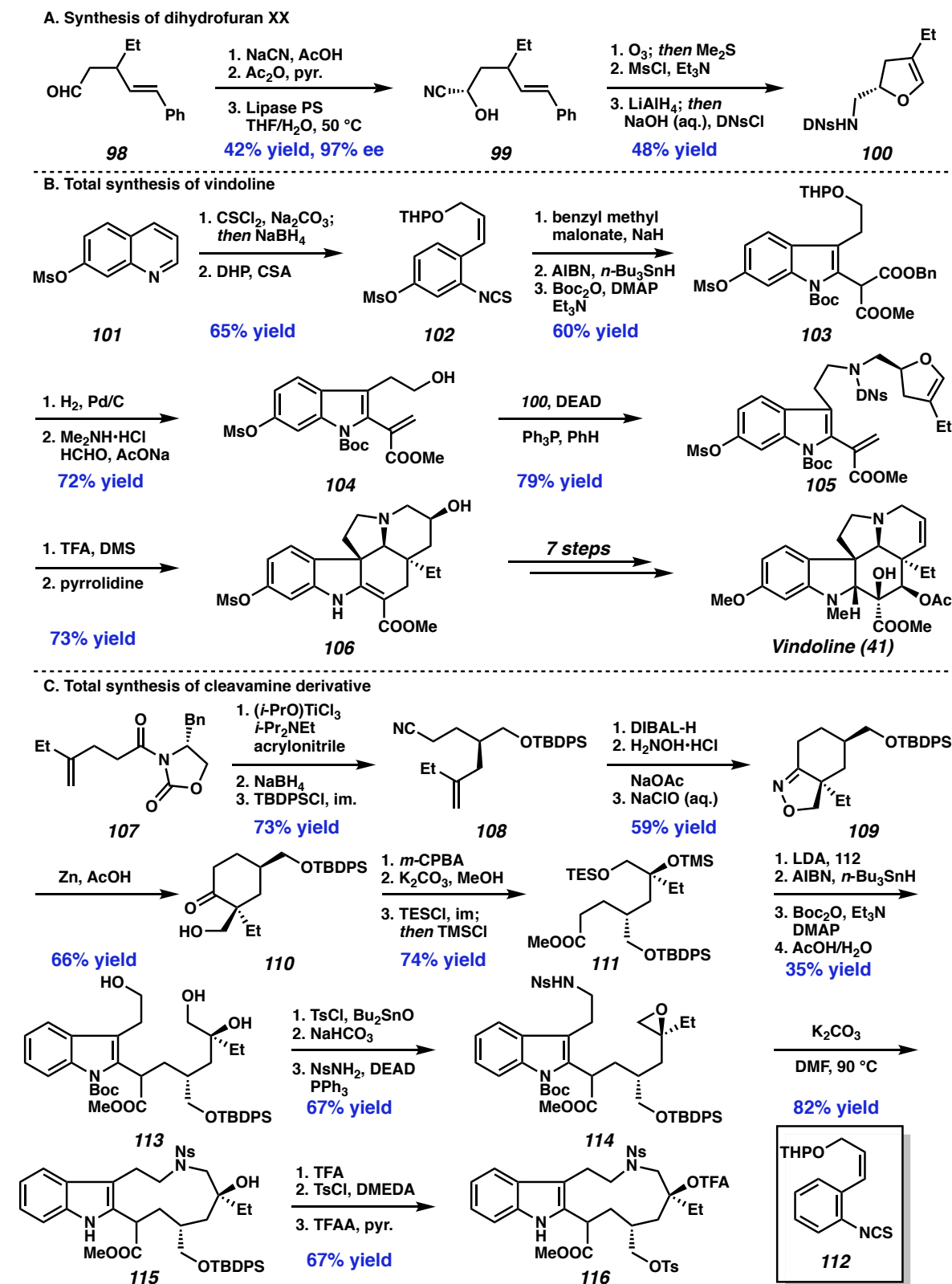


1.3.3 *Fukuyama's First Generation Total Synthesis of Vinblastine*

The first total synthesis of vinblastine (**5**) was completed by the Fukuyama group in 2002.⁷¹ Starting from aldehyde **98**, cyanohydrin formation and acetylation generates a racemic mixture of acetates, which undergoes enzymatic resolution to generate alcohol **99** in 42% yield and 97% ee (Scheme 1.14A). Following ozonolysis of the styrenyl olefin, the alcohol is activated with mesyl chloride before a tandem lithium aluminum hydride reduction and protection sequence advances to dihydrofuran **100**.

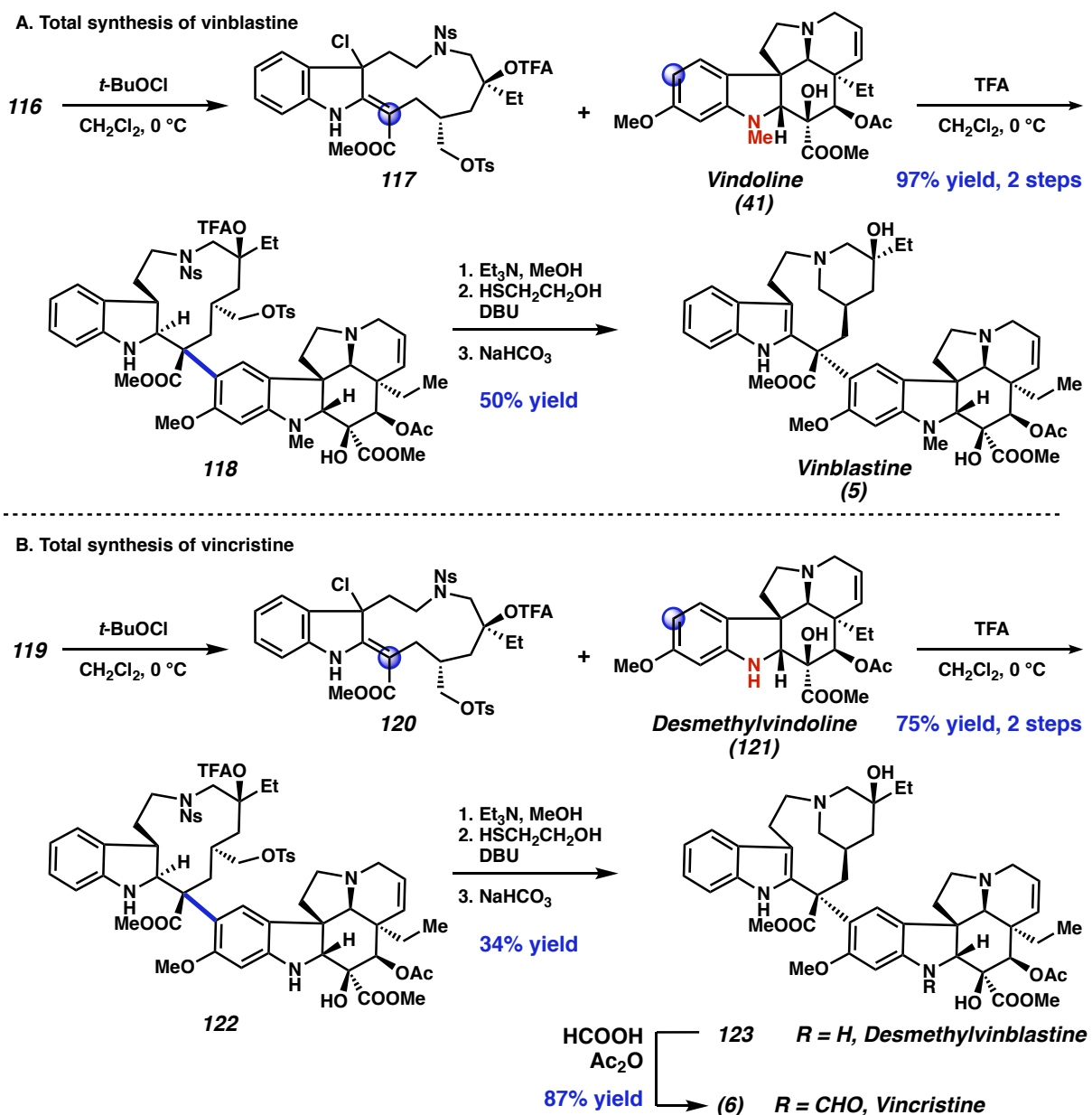
In parallel, quinoline **101** is cleaved with thiophosgene, which following THP-protection affords isocyanate **102** (Scheme 1.14B). Addition of benzyl methyl malonate precedes a Fukuyama indole synthesis⁷² and Boc protection to afford indole **103** in 60% yield. Hydrogenolysis of the benzyl ether is followed by a decarboxylative Mannich reaction with elimination and THP deprotection to form enoate **104**, which is coupled with dihydrofuran **100** through a convergent Mitsunobu reaction to access ether **105**. TFA promotes hydration of the enol ether and Boc deprotection, while addition of pyrrolidine at high temperatures opens the hydrated furan ring and promotes an intramolecular [4+2] cycloaddition to construct pentacycle **106**. This is advanced through a previously published 7-step sequence⁷³ to vindoline (**41**).

To construct the cleavamine-derived northern fragment, oxazolidinone **107** is advanced to nitrile **108** through a diastereoselective Michael addition to acrylonitrile, reductive auxiliary cleavage, and TBDPS-protection (Scheme 1.14C). The nitrile is reduced to the aldehyde and condensed with hydroxylamine to an oxime, which undergoes a nitron-olefin 1,3-dipolar cycloaddition to bicycle **109**; reduction with zinc then unmask β -hydroxy ketone **110**. Baeyer-Villiger oxidation promotes C–C bond cleavage to a lactone (not shown), which is hydrolyzed with basic methanol and orthogonally protected to afford acyclic fragment **111**.

Scheme 1.14. Fukuyama's total synthesis of vinblastine monomers (2002).

Base-mediated addition of ester **111** into isocyanate **112** is followed by an additional three-step sequence to generate indole **113** as a mixture of diastereomers α to the ester. *Bis*-tosylation of the primary alcohols is followed by base-mediated epoxidation and intermolecular S_N2 to afford amine **114**. Treatment with K_2CO_3 at elevated temperatures then affords the 11-membered cyclic amine, **115** which is advanced through an additional three steps to dimerization precursor **116**.

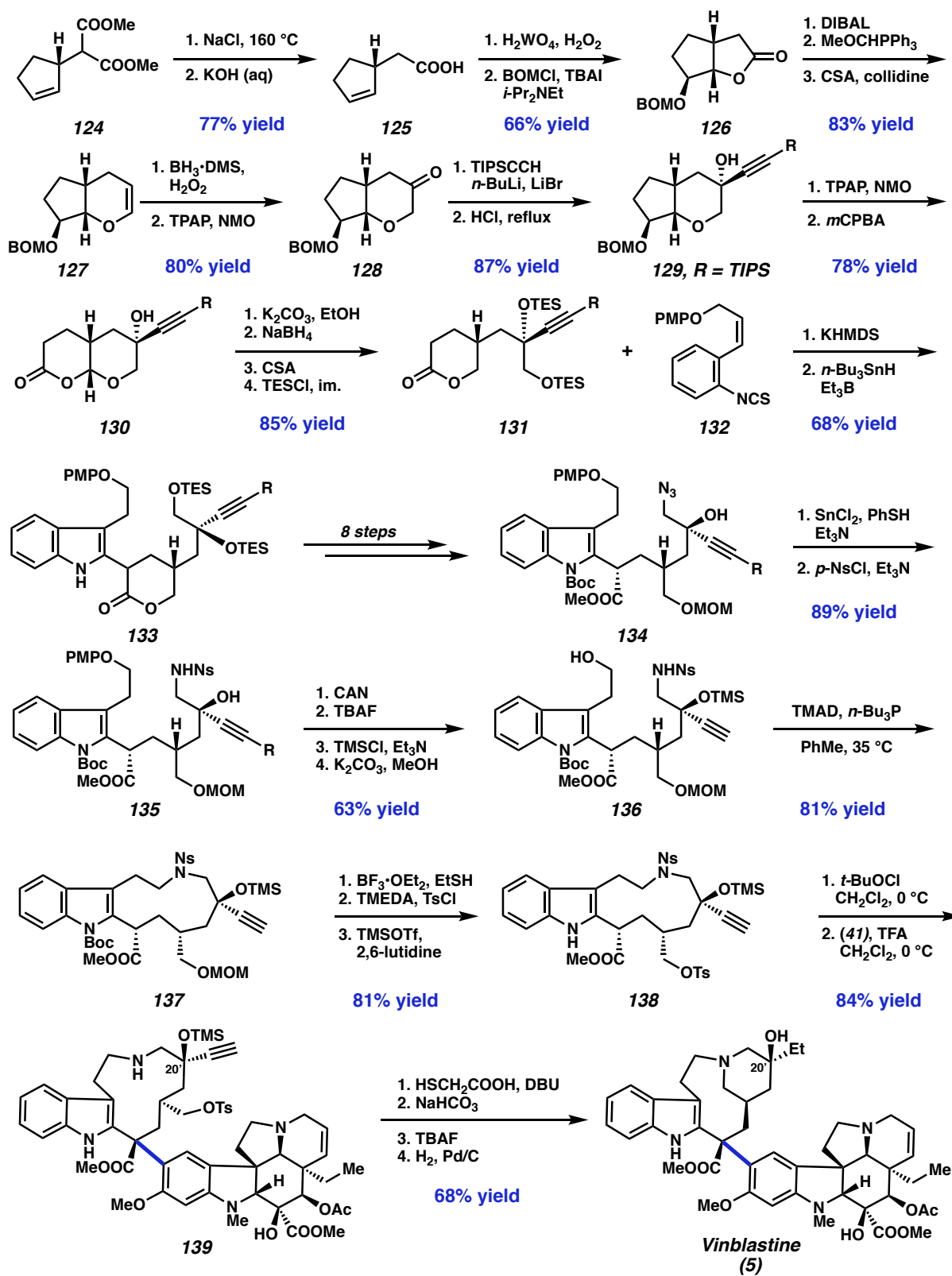
Scheme 1.15. Fukuyama's total synthesis of vinblastine (2002) and vincristine (2003).



To link the two monomeric subunits, indole **116** is treated with *t*-BuOCl to chloroamine **117**, which upon addition of vindoline (**41**) and acid generates dimerized product **118** in 97% yield as a single diastereomer (Scheme 1.15A). Deprotections of the trifluoroacetate and nosyl groups are then followed by base-mediated closure of the 6-membered ring, affording vinblastine (**5**) in 28 steps longest linear sequence from **101**. Fukuyama later showed that an analogous sequence could be used to advance desmethylvindoline **119** to vincristine (**6**) (Scheme 1.15B).⁷⁴

1.3.4 *Fukuyama's Second Generation Total Synthesis of Vinblastine*

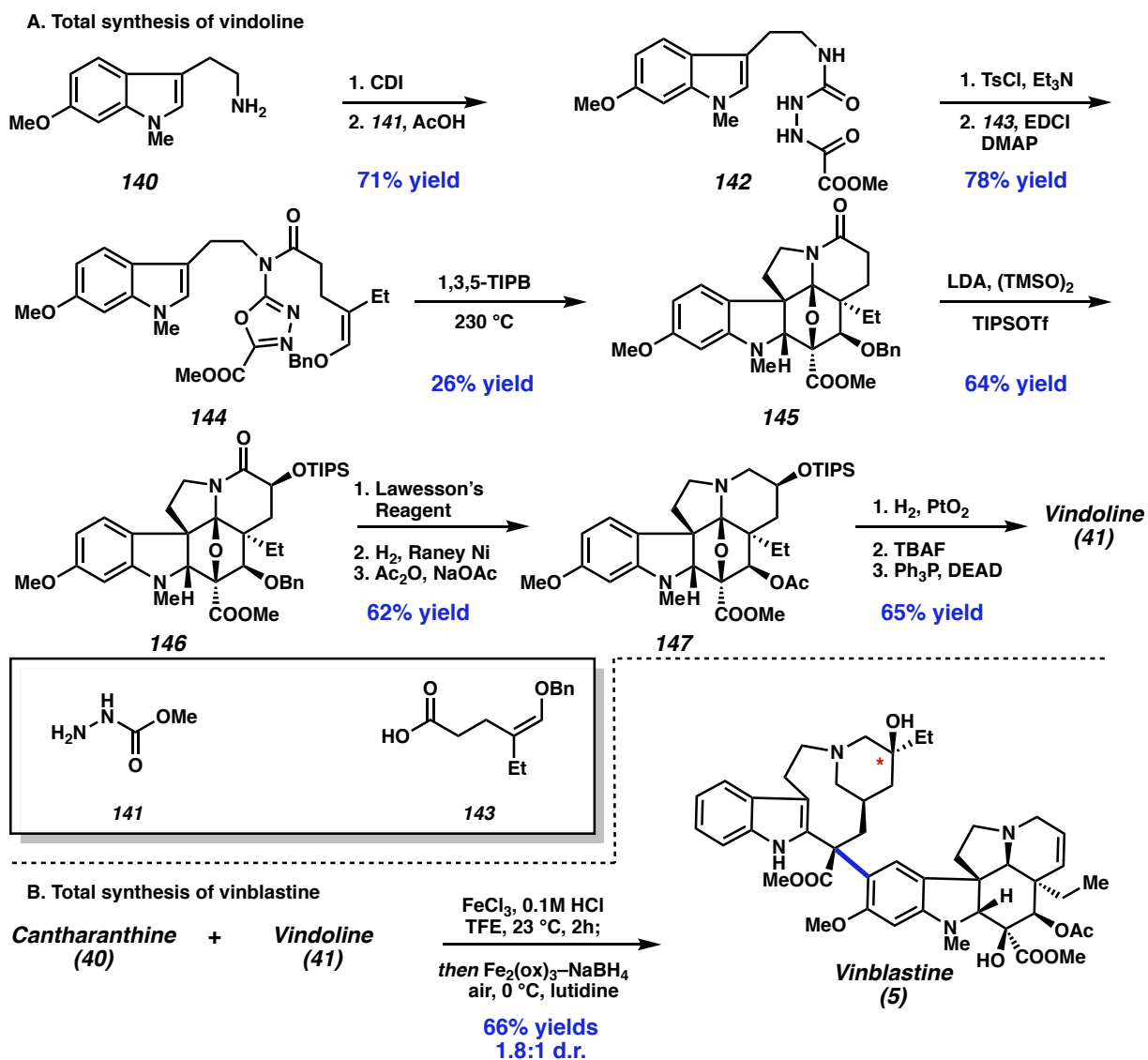
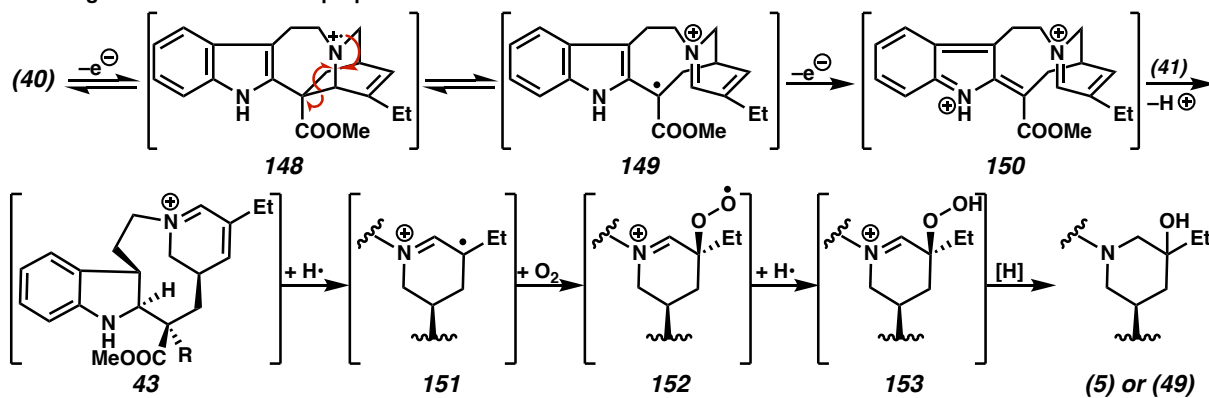
Fukuyama then published a second generation approach to vinblastine in 2007 (Scheme 1.16).⁷⁵ Instrumental to this route was a functional handle at C(20') to allow for derivatization at this position. Starting from enantioenriched cyclopentene **124**, Krapcho decarboxylation and saponification affords acid **125**, which is then lactonized and BOM-protected to afford bicycle **126**. A three-step sequence then advances the intermediate to dihydropyran **127** before hydroboration/oxidation generates ketone **128**. Grignard addition of TMS-acetylene installs the two-carbon handle before acid-mediated BOM-deprotection accesses pyran **129**. Oxidation of the secondary alcohol and Baeyer-Villiger oxidation advances to hemiacetal **130**. Ethanolysis of the lactone, lactol reduction, acid-catalyzed lactonization, and silylation then affords key protected diol **131** in 85% yield. Addition to isothiocyanate **132** and Fukuyama synthesis then generates indole **133** as a mixture of diastereomers.

Scheme 1.16. Fukuyama's second generation total synthesis of vinblastine (2007).

An additional eight steps are required to advance to azide **134**, which is reduced and nosyl protected to amine **135**. Protecting group manipulations are then used to access cyclization precursor **136**, which undergoes a Mitsunobu reaction to generate cyclic amine **137**. MOM-deprotection and tosylation of the primary alcohol is followed by re-protection of the tertiary alcohol to dimerization precursor **138**. The analogous dimerization sequence generates **139** in 84% yield, before an additional four steps afford vinblastine (**5**). Several derivatives of alkyne **139** were generated as well, but all analogs were less biologically active than vinblastine (**5**).

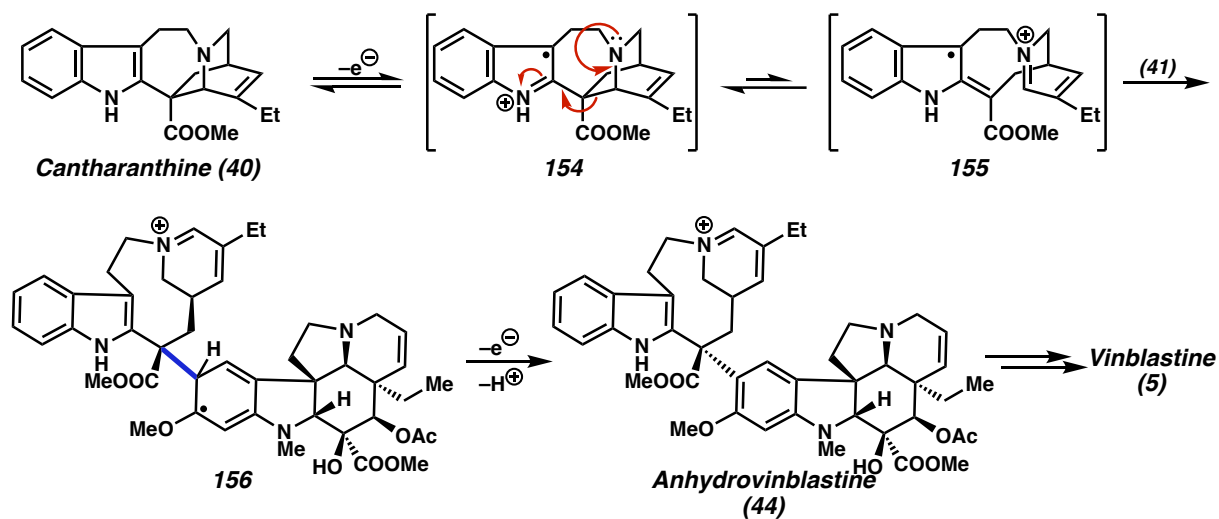
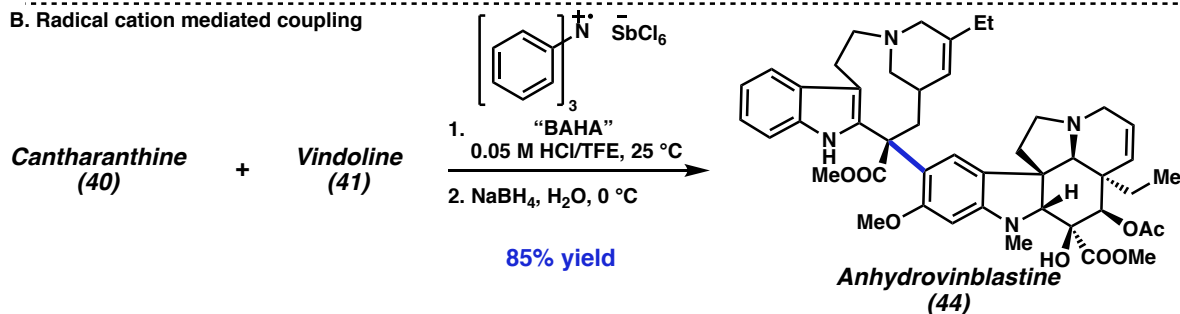
1.3.5 *Boger's Total Synthesis of Vinblastine*

A third total synthesis of vinblastine was reported by Boger in 2008.^{76,77} Their previously reported synthesis of vindoline⁷⁸ begins with 6-methoxytryptamine (**140**), which is treated with CDI and **141** to afford urea **142** (Scheme 1.17A). Tosyl chloride induces cyclization to the 1,3,4-oxadiazole before coupling with acid **143** to afford amide **144**. Heating in 1,3,5-tri-*iso*-propylbenzene (1,3,5-TIPB) at 230 °C promotes a tandem [4+2]/[3+2] cycloaddition to forge the alkaloid core as a mixture of enantiomers which are separated by chiral HPLC to afford enantiomerically pure **145**. α -Oxidation of the lactam is isolated as silyl ether **146** before amide reduction and acetylation generates piperidine **147**. Finally, hydrogenolysis of the cyclic ether, TIPS deprotection, and elimination affords vindoline (**41**) in 11 steps from **140**. A second generation approach was later published starting from the chiral pool.⁷⁹

Scheme 1.17. Boger's total synthesis of vinblastine (2008).**C. First generation mechanistic proposal**

Using cantharanthine (**40**) obtained from Raucher's route^{80,81}, Boger developed a one-pot oxidative coupling/alkene hydration to synthesize vinblastine (**5**) directly from the component monomers (Scheme 1.17B). Originally, Fe(III) was proposed to oxidize cantharanthine (**40**) to radical cation **148**, which undergoes C–C bond cleavage to stabilized radical **149** (Scheme 1.17C); this is oxidized to carbocation **150** before undergoing S_EAr with vindoline (**41**) to iminium **43**. The addition of iron (III) oxalate and sodium borohydride then initiate H• addition to the trisubstituted olefin (via the intermediate Fe–H species), generating a tertiary radical **151** that traps a molecule of singlet oxygen to the peroxide radical **152**. A second hydrogen atom addition then generates the peroxide **153**, which is reduced to vinblastine (**5**) in 42% yield, with 24% of leurosine (**49**) also isolated. The intermediates on this route were then elaborated to a number of analogues to study structure activity relationship.⁸²

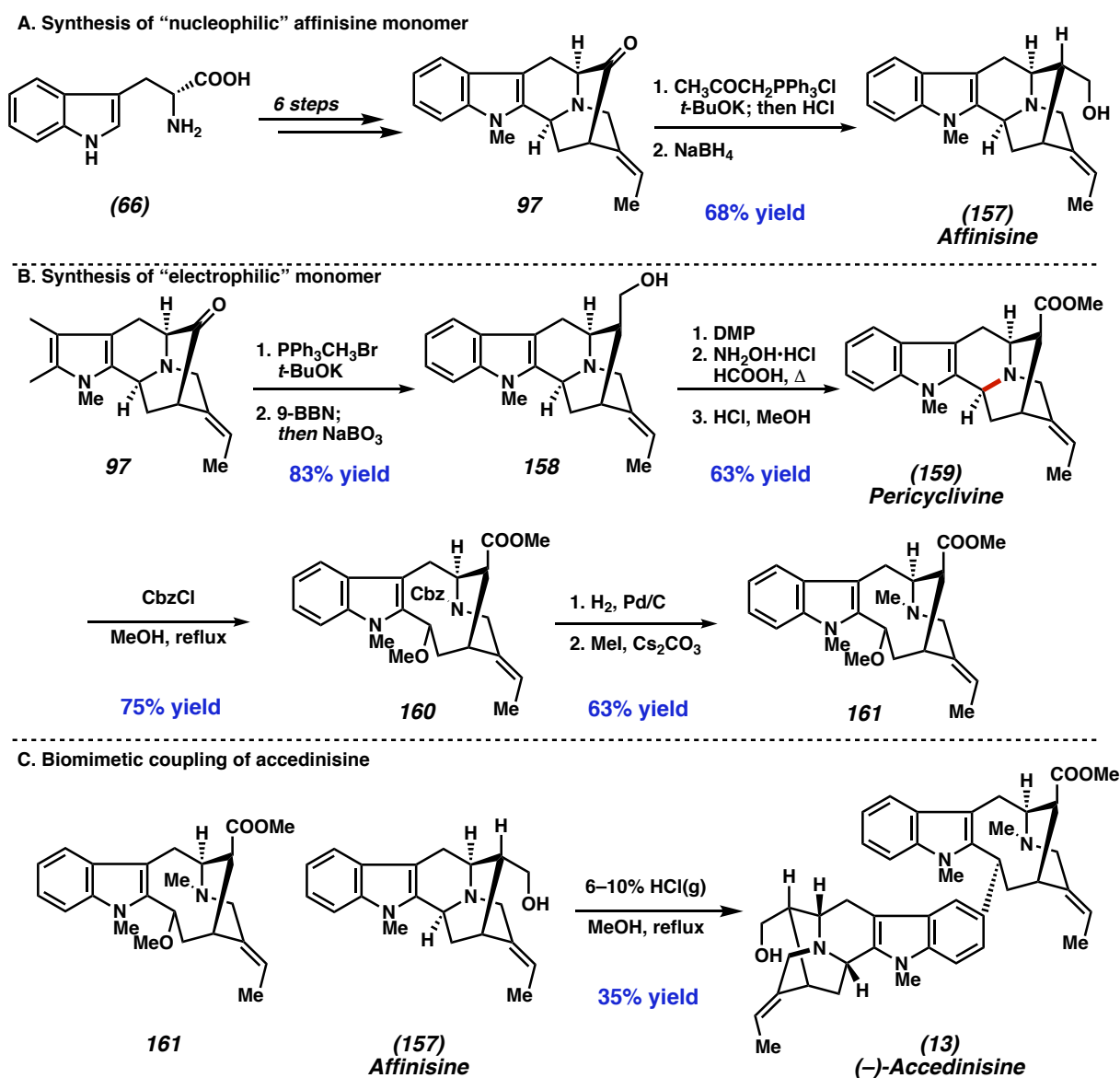
However, this mechanistic proposal failed to explain two key observations: 1) the coupling reaction proceeded with perfect diastereoselectivity at C(16') when conducted at 23 °C, while Kutney and Portier's procedure, which implicated identical intermediates, favored the undesired epimer, and 2) no fragmented cleavamine-type derivatives were observed, as all mass balance returned as unreacted cantharanthine (**40**). A follow-up study⁸³ proposed a new hypothesis where cantharanthine (**40**) is reversibly oxidized to charge-separated radical cation **154** which lies in equilibrium with iminium radical **155**; nucleophilic attack by vindoline forms stabilized radical **156** which is sequentially oxidized and deprotonated to anhydrovinblastine (**44**) and hydrated to vinblastine (**5**) through the mechanism described above (Scheme 1.17C). Boger further supported this hypothesis by publishing a new radical-cation based coupling method in 2019 (Scheme 1.18B)⁸⁴

Scheme 1.18. Boger's revised mechanistic proposal and radical cation coupling (2019).**A. Second generation mechanistic proposal****B. Radical cation mediated coupling****1.3.6 Cook's Total Synthesis of Accedinisine**

In 2008, Cook published the first total synthesis of accedinisine (**13**).^{85,86} Tryptophan (**66**) was advanced to pentacycle **97** over six steps (Scheme 1.19A); in a previous report, Liu and coworkers showed that this intermediate could be advanced to the nucleophilic affinisine (**157**) monomer via Wittig homologation and reduction in the opposite enantiomeric series,⁸⁷ though the correct enantiomer was later correctly accessed en route to macroline (**28**).³⁷ To access the electrophilic coupling partner (Scheme 1.19B), pentacycle **97** was converted to alcohol **158** via hydroboration/oxidation of an intermediate Wittig methylenation product. Conversion to pericyclivine (**159**) over three steps is followed by Cbz-protection and methanol-induced C–C bond cleavage (red) to methyl ether **160**. Deprotection and reductive amination then affords

coupling partner **161**. Mixture of methyl ether **161** and affinisine (**157**) in acidic methanol then affords (–)-accedinisine (**13**) in 35% yield (Scheme 1.19C). Use of Cbz-protected amine **160** in the coupling reaction was also utilized to afford *N*-desmethyl accedinisine.

Scheme 1.19. Cook's total synthesis of accedinisine (2008).

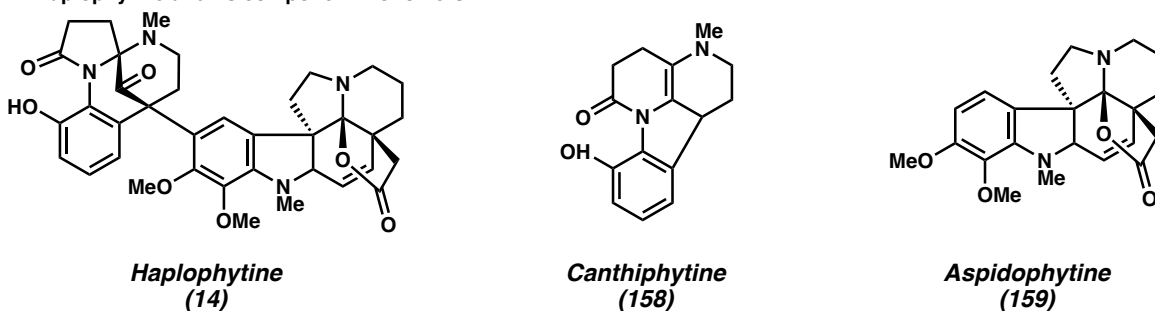


1.3.7 *Fukuyama and Tokuyama's Total Synthesis of Haplophytine*

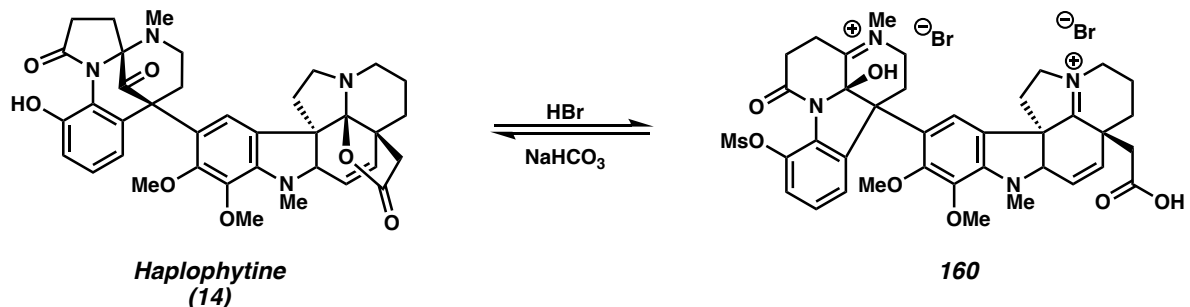
Aside from vinblastine (**5**) and its congeners, haplophytine (**14**) is perhaps the most well-studied *bis*(monoterpenoid) indole alkaloid. Isolated from the leaves of the plant *Haplophyton cimidum* and noted for its insecticidal properties,^{88,89,90,91} it is the dimeric combination of the component alkaloids canthiphytine (**158**) and aspidophytine (**159**) (Scheme 1.20A). Degradation studies by Cava and Yates showed that the western portion of the molecule readily undergoes a reversible rearrangement in the presence of acid or base (Scheme 1.20B).^{92,93} Despite several elegant syntheses of the aspidophytine moiety,^{94,95,96,97,98} all were unsuccessful at advancing directly to haplophytine (**14**). The three published routes to date all utilize simpler precursors in the coupling/rearrangement.

Scheme 1.20. *Haplophytine and proposed biosynthetic precursors.*

A. Haplophytine and its component monomers



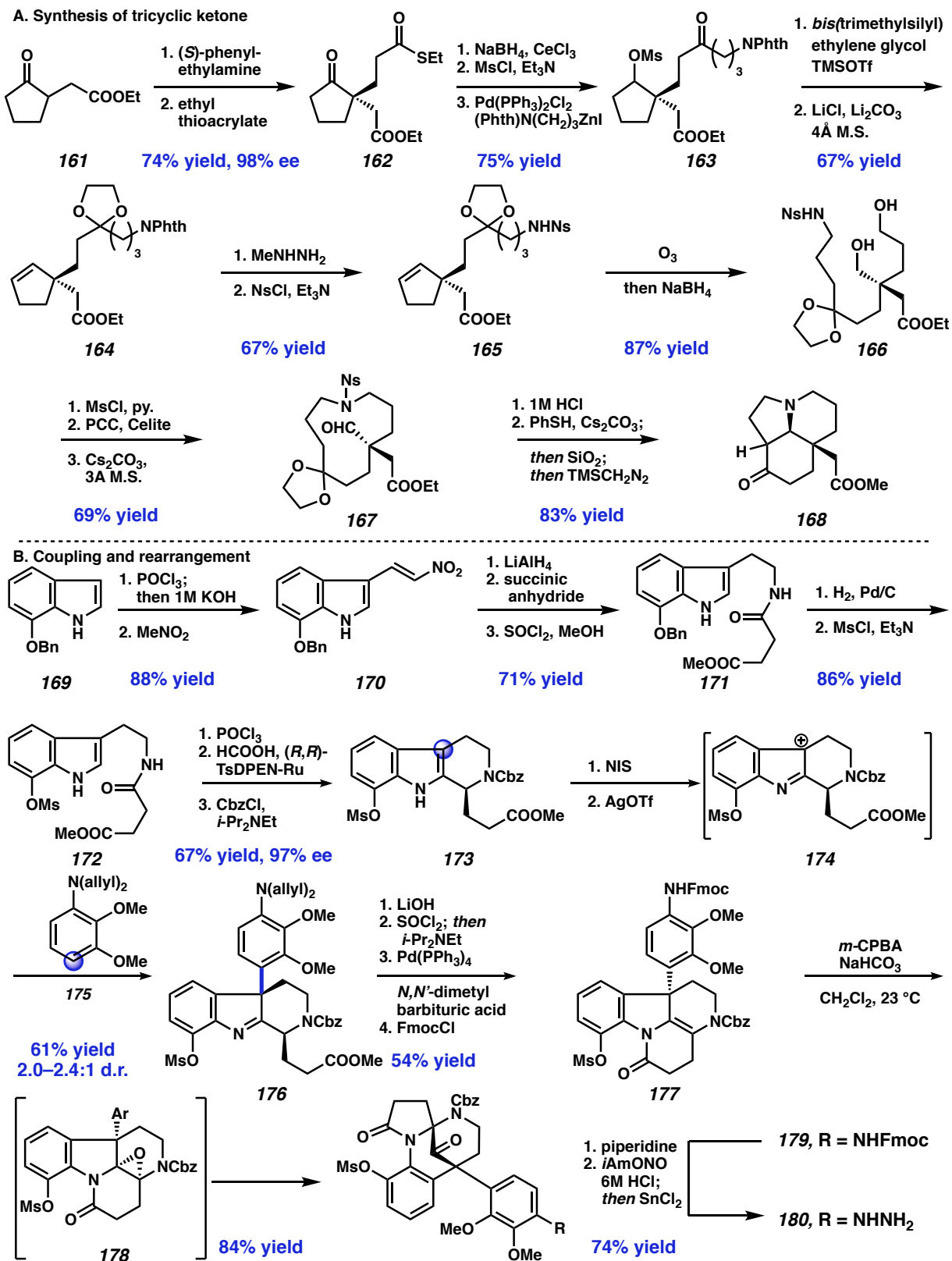
B. Acid-base mediated semi-pinacol rearrangement



The Fukuyama and Tokuyama route⁹⁹ to haplophytine (**15**) begins with auxiliary-controlled diastereoselective conjugate addition of cyclopentanone **161**, generating thioester **162**

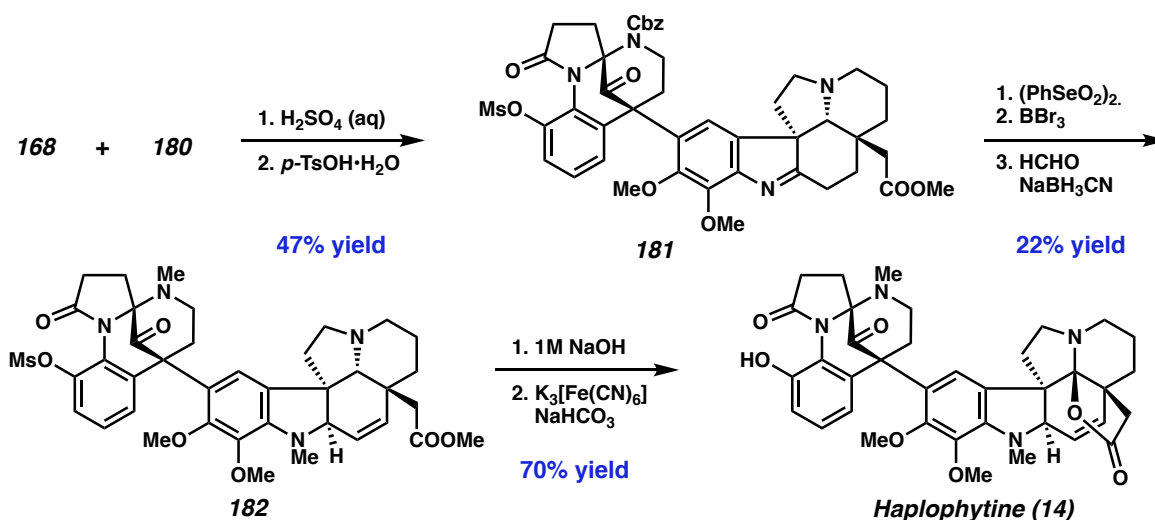
in 74% yield and 98% ee (Scheme 1.21A). Reduction and mesylation are followed by a Fukuyama ketone synthesis¹⁰⁰ to produce phtalamido-ketone **163**, before ketalization and elimination of the mesylate forges cyclopentene **164**. Following a protecting group exchange (**164** → **165**), ozonolysis with reductive workup generates diol **166**. Leveraging the difference in steric environments between two primary alcohols, orthogonal mesylation and oxidation precede alkylation of the nosyl amine to generate cyclic amine **167**. Finally, ketal and nosyl cleavage promotes an intramolecular Mannich reaction, which following reesterification accesses the key tricyclic ketone **168**.

In a separate sequence, Vilsmeier–Haack formylation and Henry addition to indole **169** affords nitroolefin **170** (Scheme 1.21B). Exhaustive reduction with LiAlH₄, followed by acylation and esterification generates amide **171** which undergoes protecting group exchange at the phenol oxygen to mesylate **172**. A Bischler–Napieralski cyclization then accesses the cyclic iminium, which undergoes Noyori-type asymmetric transfer hydrogenation¹⁰¹ and Cbz-protection to afford tricycle **173** in 97% ee. At this juncture, a coupling occurs to install the aryl ring of the southern fragment; iodination of the indole C(3) is followed by treatment with silver (I) to produce carbocation **174** which reacts with aniline derivative **175** to generate quaternary adduct **176** in 61% yield with 2.0–2.4:1 d.r. This is advanced to tetracycle **177** through a lactamization/protecting group exchange sequence. Treatment of the enamine with *m*-CPBA produces an epoxide **178**, which undergoes a spontaneous semi-pinacol rearrangement to forge the rearranged northern fragment **179** in excellent yield. Fmoc deprotection and nitration then affords hydrazine **180**.

Scheme 1.21. Fukuyama and Tokuyama's total synthesis of haplophytine monomers (2009).

To complete the synthesis, fragments **168** and **180** were coupled through a two-step Fischer indole synthesis to access dimer **181** bearing the full skeleton of haplophytine (Scheme 1.22). Desaturation of the imine with benzeneselenenic anhydride and Cbz-deprotection then occur before the final two methyl groups of **182** are installed by reductive amination. Finally, mesyl deprotection/saponification and oxidative lactonization then complete haplophytine (**14**) in 27 steps LLS from indole **169**.

Scheme 1.22. Fukuyama and Tokuyama's total synthesis of haplophytine (2009).

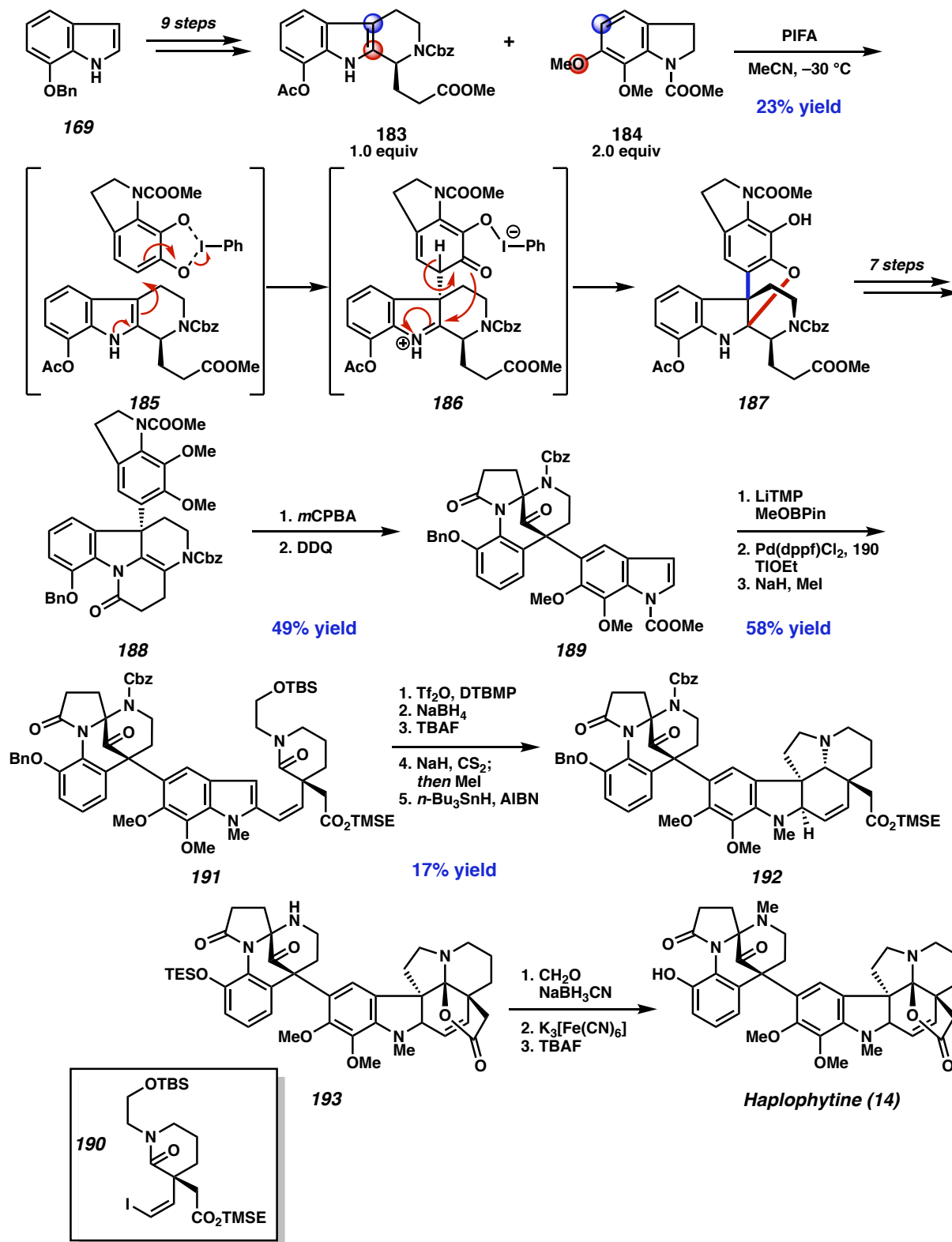


1.3.8 Nicolaou and Chen's Total Synthesis of Haplophytine

The Nicolaou and Chen approach¹⁰² begins with a nearly identical sequence to the Fukuyama route, accessing tricycle **183** (Scheme 1.23). A PIFA-mediated oxidative coupling then occurs with indoline **184**. Mechanistically, this proceeds through ligand exchange between the hypervalent iodine and *ortho*-phenol to generate electrophilic species **185**, which reacts with the C(3) indole of tricycle to afford arylated intermediate **186**. Deprotonation then promotes addition of the oxygen into the newly formed iminium at indole C(2) to forge oxygen bridged product **187**

in 23% yield (albeit with only 25% conversion.) Following a seven-step sequence to advance to lactam **188**, a similar *m*-CPBA initiated rearrangement occurs to forge the bridging tetracyclic fragment on the western fragment. Subsequent treatment with DDQ then oxidizes the intermediate to indole **189**.

Lithiation/borylation at C(2) of the newly formed indole is followed by Suzuki coupling with reported vinyl iodide¹⁰³ **190** and methylation of the indole to afford heptacycle **191**. Amide activation with triflic anhydride promotes intramolecular cyclization with the indole C(3), followed by reduction of the resultant iminium. Deprotection of the primary alcohol and activation as the xanthate allows for a 5-*exo* trig radical cyclization into the indole¹⁰⁴ to access **192**, bearing the full carbocyclic skeleton of haplophytine. Deprotection of the carboxylic acid and oxidative lactonization then occurs, followed by debenzoylation of the phenol oxygen and silylation to intermediate **193**. Reductive amination installs the final methyl group, but it is unfortunately accompanied by reductive lactone opening. This bond is reformed with $K_3[Fe(CN)_6]$ before desilylation affords haplophytine (**14**) in 33 steps from indole **169**.

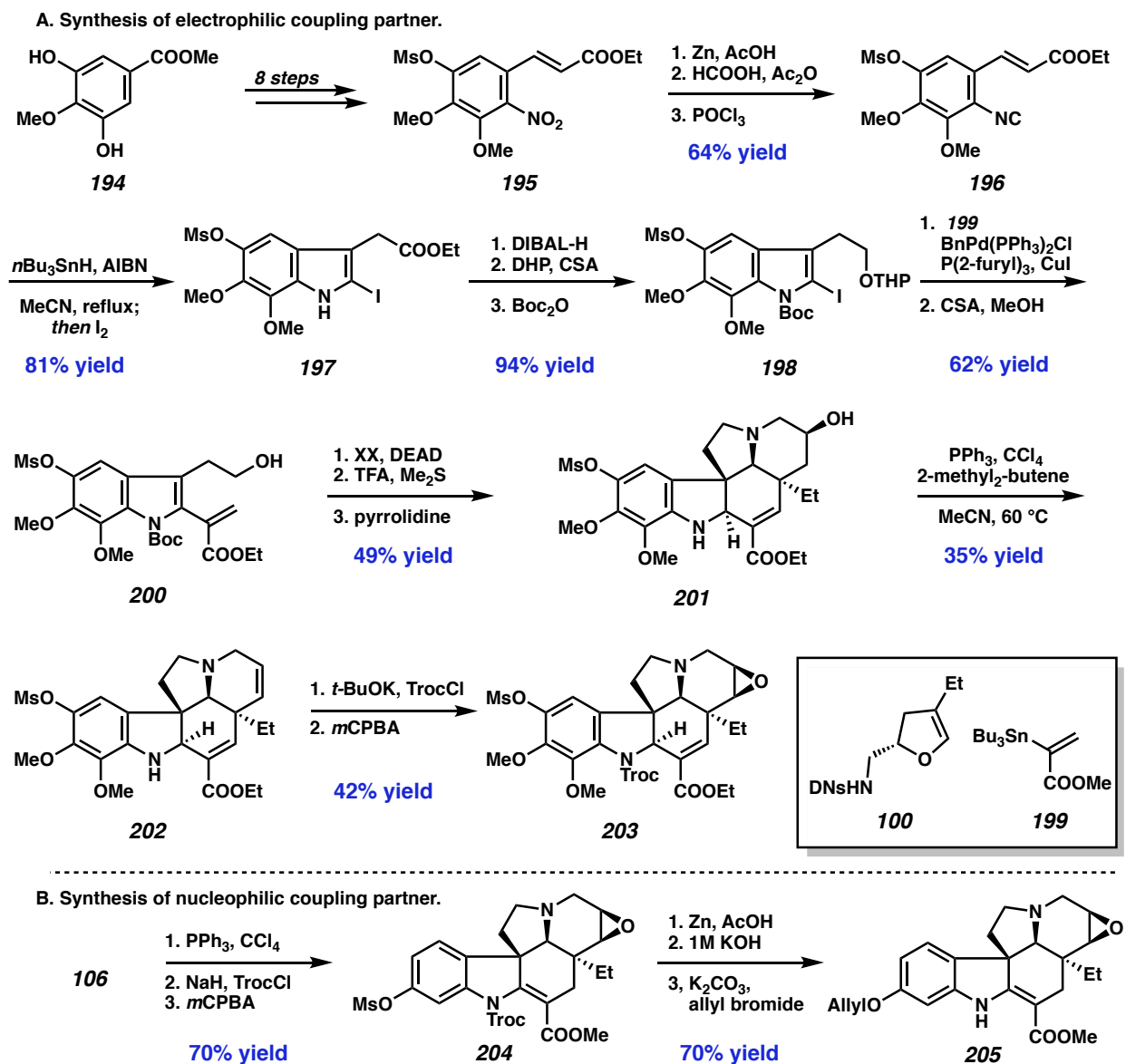
Scheme 1.23. Nicolaou and Chen's total synthesis of haplophytine (2009).

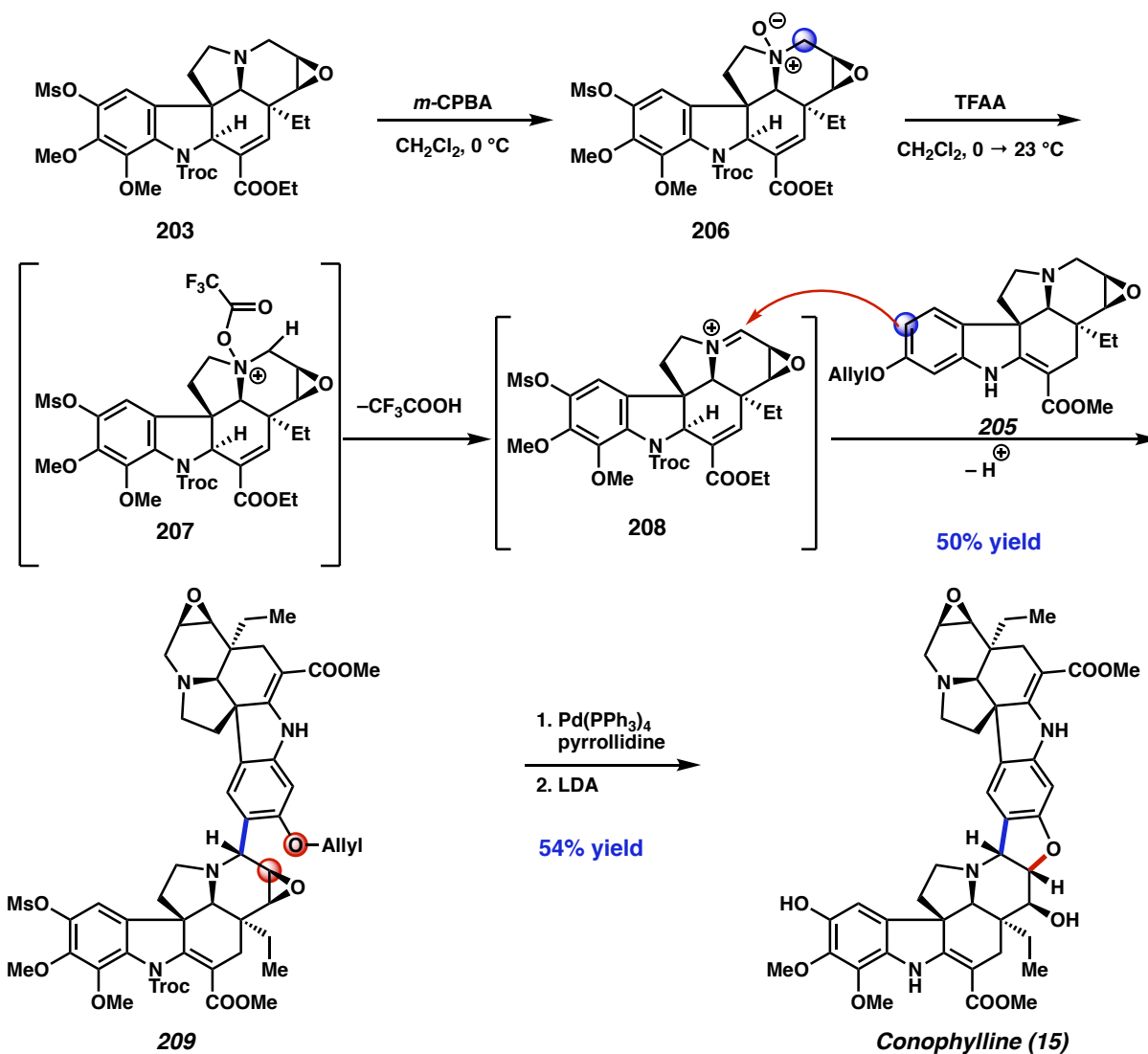
1.3.9 *Fukuyama and Tokuyama's Total Synthesis of Conophylline*

In 2011, Fukuyama and Tokuyama published a route towards the dimeric *aspidosperma* alkaloids conophylline (**15**) and conophyllidine (**16**).¹⁰⁵ Commercial phenol **194** was first advanced to ester **195** over an eight-step sequence (Scheme 1.24A). Nitro reduction, followed by acylation and dehydration affords isocyanate **196** which undergoes a Fukuyama indole synthesis followed by iodine quench to afford 2-iodoindole **197**. After DIBAL reduction and orthogonal protections, indole **198** undergoes Stille coupling with vinylstannane **199** and THP deprotection to afford enoate **200**. This is advanced upon coupling with dihydrofuran **100**, previously implemented in their first-generation vinblastine synthesis,⁷¹ to tetracycle **201** in 49% yield over three steps. Following elimination of the secondary alcohol to pentacycle **202**, indole protection and epoxidation affords the electrophilic coupling partner **203**, a protected version of the natural product taberhanine.

The nucleophilic coupling partner is synthesized from tetracycle **106**, an intermediate that was also accessed during the vinblastine route (Scheme 1.24B).⁷¹ Through an analogous three-step sequence, **106** is advanced to epoxide **204**. Following Troc-deprotection, mesyl group hydrolysis and allylation accesses nucleophilic coupling partner **205**.

To couple the monomeric subunits, electrophilic coupling partner is transformed to *N*-oxide **206** with *m*-CPBA (Scheme 1.25). Subjection to TFAA generates acylated species **207** which undergoes regioselective Polonovski-Portier rearrangement¹⁰⁶ to iminium **208**, which is intercepted by nucleophilic fragment **205** to access dimer **209** in 50% yield over two steps. Allyl deprotection with palladium promotes concomitant epoxide opening to forge the final dihydrofuran ring before global deprotection with LDA affords conophylline (**15**) in 27 steps LLS. A similar procedure is used to access the congener conophylline (**16**).

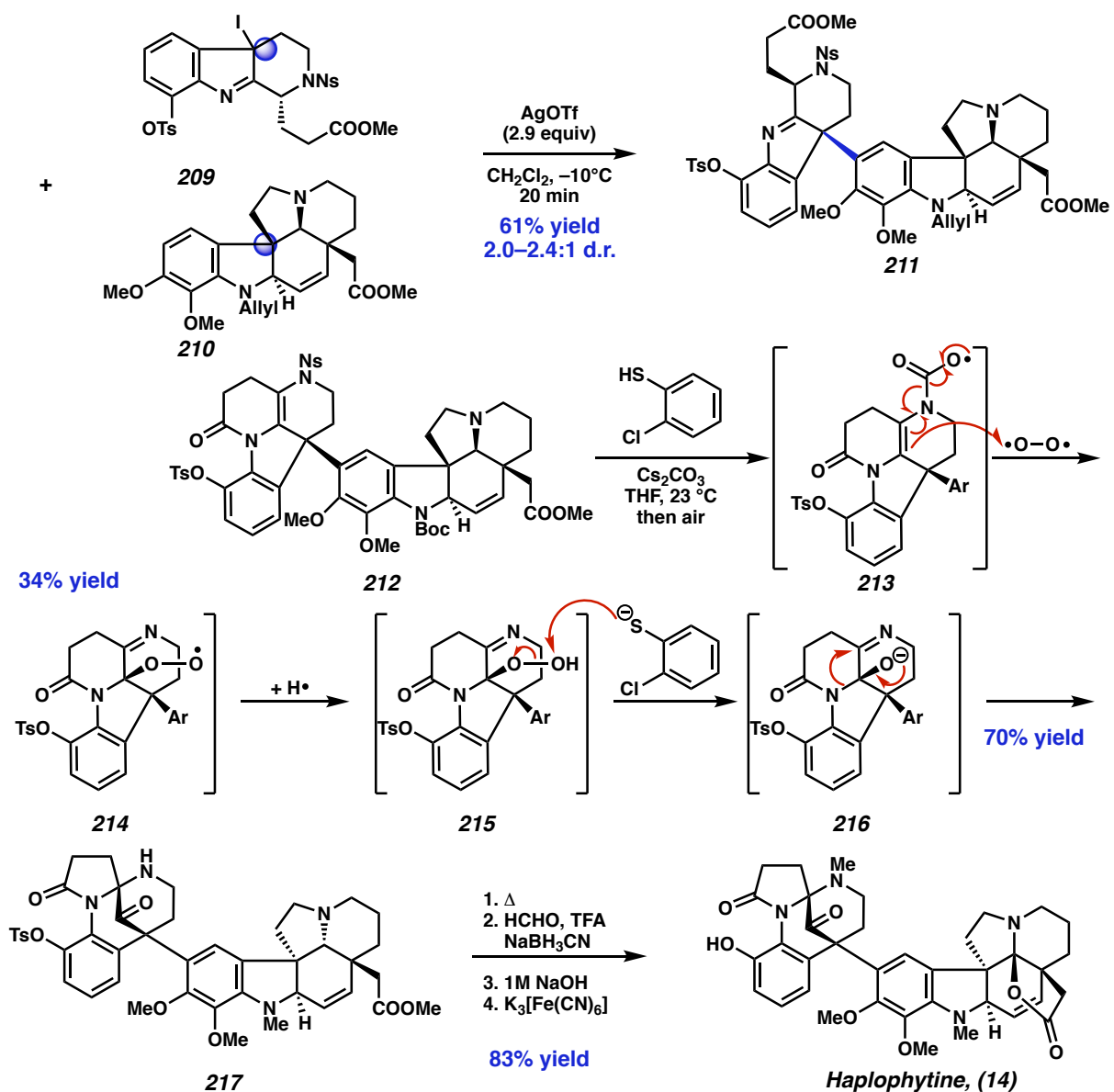
Scheme 1.24. Fukuyama and Tokuyama's total synthesis of conophylline monomers (2011).

Scheme 1.25. Fukuyama and Tokuyama's total synthesis of conophylline (2011).**1.3.10 Tokuyama's Second Generation Total Synthesis of Haplophytine**

In 2016, Tokuyama published a bio-inspired second-generation total synthesis of haplophytine¹⁰⁷, improving upon previously developed chemistry by performing the coupling and rearrangement at a late-stage (Scheme 1.26). Tricyclic **209**⁹⁹ and *aspidosperma* skeleton **210**¹⁰⁸ are subjected to previously optimized Ag-mediated coupling conditions to afford dimer **211**.

Saponification is followed by lactamization and protecting group exchange at the indole nitrogen to afford rearrangement precursor **212**.

Scheme 1.26. Tokuyama's total synthesis of haplophytine (2016).



Using a modified aerobic rearrangement, treatment with 2-chlorothiophenol, cesium carbonate, and air generates carbamate radical **213**, which undergoes decarboxylation and trapping with oxygen to form peroxy radical **214**. Sequential single electron transfers and protonation

affords peroxide **215**, which is reduced to alkoxide **216** before semi-pinacol rearrangement produces the full carbocyclic skeleton **217** in 70% yield. Thermal Boc-deprotection and double reductive amination install the final two carbons, before mesyl deprotection and oxidative lactamization affords haplophytine (**14**) in 15 steps from previously published intermediates.

1.4 CONCLUDING REMARKS

In summary, the *bis*(monoterpenoid) indole alkaloids have inspired a deep and fascinating body of research over the past sixty years. Despite this substantial history, it is surprising that such a storied natural product class remains so dramatically underexplored. While other alkaloid subclasses are subject of dozens of accounts per year, successful bisindole alkaloid syntheses are scarce—especially relative to the continued focus on the monoterpenoid indole alkaloids which frequently compose these dimeric structures. Modern synthetic chemists have largely moved on from the “tour-de-force” approach to natural product total synthesis that were frequently implemented to construct these synthetically challenging targets. By implementing aspects of modern synthetic planning, we can construct these targets with improved efficiency and facilitate the completion of total synthetic efforts.

One such strategy to facilitate studies is the implementation of divergent¹⁰⁹ or diversity-oriented synthesis¹¹⁰ in the construction of monomeric subunits. Inefficient monomer synthesis continues to be the bottleneck of progress, both in material throughput and time invested in optimizing new routes (*vide infra*). Monoterpenoid indole alkaloids, despite substantial structural variation, all arise from the same biosynthetic precursor strictosidine;¹¹¹ these monomers are, thus, particularly well-suited for diversity-oriented synthesis, as evidenced by reports from Zhu,¹¹² MacMillan,¹¹³ and Stoltz.¹¹⁴ Fukuyama’s skillful repurposing of vinblastine intermediates toward

the synthesis of conophylline¹⁰⁵ offers concrete proof-of-principle that this design element can improve the efficiency of route development.

Another area of development is the incorporation of modern advances in cross-coupling to accomplish the convergent linkage of monomeric subunits. Successful efforts to-date have become overreliant on the biomimetic hypotheses to forge the key dimerizing bond; this has thwarted some efforts when these hypotheses have proven unsubstantiated and limited other attempts to expand the scope of coupling partners beyond the natural product. Generalizable cross-couplings can be utilized in multiple natural product syntheses, as evidenced by work on oligomeric polypyrrolidinoindolines by MacMillan¹¹⁵ and Movassaghi.¹¹⁶ Given the recent advances in C(sp³)-C(sp²) cross coupling, the viability of catalyst-controlled coupling strategies has never been greater.

From origins in structural elucidation *via* semi-synthesis to modern implementation in analog development for structure-activity relationship studies, interest in this natural product class has evolved with the changing demands of modern synthetic chemistry. Given the designation of several accounts described herein as landmark syntheses,^{117,118} there remains little doubt that this natural product class will continue to garner interest for years to come.

1.5 REFERENCES

- (1) Also known as “bisindole monoterpenoid alkaloids”, “monoterpene bisindole alkaloids”, “dimeric bisindole alkaloids”, “bisindole alkaloids”, “bis-alkaloids”
- (2) Hesse, M.; Dimeric Alkaloids (Bis-alkaloids). In *Alkaloids: Nature’s Curse or Blessing?*; Wiley-VCH/Weinheim: New York, 2002; pp 91-114.
- (3) Cordell, G.A.; Saxton, J.E. Bisindole Alkaloids. In *The Alkaloids: Chemistry and Physiology*; Manske, R.H.F., Rodrigo, R.G.A., Eds.; Academic Press: New York, 1981; pp 1–295.
- (4) Kam, T-S.; Choo, Y-M. Bisindole Alkaloids. In *The Alkaloids: Chemistry and Biology*; Cordell, G.A. Ed.; Elsevier/Academic Press: New York, 2006; pp 181–387.
- (5) Kitajima, M.; Takayama, H. Monoterpenoid Bisindole Alkaloids. In *The Alkaloids: Chemistry and Biology*; Knölker, H-J. Ed.; Elsevier/Academic Press: Cambridge, MA, 2016; pp 259–310.
- (6) Corey, E.J.; Cheng, X-M. *The Logic of Chemical Synthesis*; John Wiley & Sons: New York, 1989; pp 1-99.
- (7) Ueda, *Chem. Pharm. Bull.* **2020**, *68*, 117–128.
- (8) Wright, C.W.; Allen, D.; Cai, Y.; Philipson, J.D.; Said, I.M.; Kirby, G.C.; Warhurst, D.C.; *Phytother. Res.* **1992**, *6*, 121.
- (9) Keawpradub, N.; Houghton, P.J.; Eno-Amuquaye, E.; Burke, P.J. *Planta. Med.* **1997**, *63*, 97–101.
- (10) Keawpradub, N.; Kirby, G.C.; Steele, J.C.P.; Houghton, P.J.; *Planta. Med.* **1999**, *65*, 690–694.

-
- (11) Deguchi, J.; Shoji, T.; Nugroho, A.; Hirasawa, Y.; Hosoya, T. Shirota, O.; Awang, K.; Hadi, A.H.A.; Morita, H. *J. Nat. Prod.* **2010**, *73*, 1727–1729.
- (12) Voloshchuk, T.; Farina, N.S.; Wauchope, O.R.; Kiprowska, M.; Haberfield, P.; Greer, A. *J. Nat. Prod.* **2004**, *67*, 1141–1146.
- (13) Berube, G.; *Curr. Med. Chem.* **2006**, *13*, 131–154.
- (14) Antitumor Bisindole Alkaloids from *Catharanthus roseus* (L.). *The Alkaloids*; Brossi, A., Suffness, M., Eds.; Academic Press Inc.: San Diego, 1990; Vol. 37, Chapters 3 and 4, pp 133-204.
- (15) Morelli X.; Hupp T. *EMBO Rep.* **2012**, *13*, 877-879.
- (16) Arkin, M.R.; Wells J.A. *Nat. Rev. Drug. Discov.* **2004**, *3*, 301-317.
- (17) Scott, D.E.; Bayly, A.R.; Abell, C.; Skidmore, J. *Nat. Rev. Drug. Discov.* **2016**, *15*, 533-550.
- (18) Lounasmaa, M.; Nemes, A.; *Tetrahedron* **1982**, *38*, 223–243.
- (19) Rahman, M.T.; Tiruveedhula, V.V.N.P.B.; Cook, J.M. *Molecules* **2016**, *21* 1525–1564.
- (20) Steven, A.; Overman, L.E. *Angew. Chem. Int. Ed.* **2007**, *46*, 5488–5508.
- (21) Schmidt, M.A.; Movassaghi, M. *Synlett.* **2008**, *3*, 313–324.
- (22) Büchi, G.; Manning, R.E.; Monti, S.A. *J. Am. Chem. Soc.* **1964**, *85*, 1893–1894.
- (23) Büchi, G.; Manning, R.E.; Monti, S.A. *J. Am. Chem. Soc.* **1964**, *86*, 4631–4641.
- (24) Renner, U.; Fritz, H. *Tetrahedron Lett.* **1964**, *6*, 283–287.
- (25) Kingston, G.I.; Gerhart, B.B.; Ionescu, F. *Tetrahedron Lett.* **1976**, *17*, 649–652.
- (26) Knox, J.R.; Slobbe, J. *Aust. J. Chem.* **1975**, *28*, 1813–1823.
- (27) Knox, J.R.; Slobbe, J. *Aust. J. Chem.* **1975**, *28*, 1825–1841.
- (28) Achenbach, H.; Schaller, E. *Chem. Ber.* **1976**, *109*, 3527–3536.

-
- (29) Feng, X-Z.; Liu, G.; Kan, C.; Portier, P.; Kan, S-W. *J. Nat. Prod.* **1989**, *52*, 928–933.
- (30) Takano, S.; Hatakeyama, S.; Ogasawara, K. *Heterocycles* **1977**, *6*, 1311–1317.
- (31) Burke, D.E.; Cook, J.M.; LeQuesne, P. *J. Chem. Soc. Chem. Commun.* **1972**, 697.
- (32) Burke, D.E.; Cook, J.M.; LeQuesne, P. *J. Am. Chem. Soc.* **1973**, *95*, 546–552.
- (33) Hesse, M.; Bodmer, F.; Gemenden, C.; Joshi, B.; Taylor, W.; Schmid, H. *Helv. Chim. Acta* **1966**, *49*, 1173–1182.
- (34) Yu, J.; Wearing, X.Z.; Cook, J.M. *J. Org. Chem.* **2005**, *70*, 3963–3979.
- (35) First generation total synthesis of (+)- macroline: Bi, Y.; Cook, J.M. *Tetrahedron Lett.* **1993**, *34*, 4501–4504.
- (36) Bi, Y.; Cook, J.M.; *Tetrahedron Lett.* **1994**, *35*, 3877–3878.
- (37) Liao, X.; Zhou, H.; Yu, J.; Cook, J.M. *J. Org. Chem.* **2006**, *71*, 8884–8890.
- (38) Tran, Y.S.; Kwon, O. *Org. Lett.* **2005**, *7*, 4289–4291.
- (39) Total synthesis of (–) macroline: Liu, X.; Zhang, C.; Lio, X. Cook, J.M. *Tetrahedron Lett.* **2002**, *43*, 7373–7377.
- (40) Biomimetic synthesis of (+)-macroline: Esmond, R.W.; LeQuesne, P.W. *J. Am. Chem. Soc.* **1980**, *102*, 7116–7117.
- (41) Burke, D.E.; Cook, J.M.; LeQuesne, P. *J. Chem. Soc. Chem. Commun.* **1972**, 678.
- (42) Burke, D.E.; DeMarkey, C.A.; LeQuesne, P.W.; Cook, J.M. *J. Chem. Soc. Chem. Commun.* **1972**, 1346–1347.
- (43) Liu, X. *Ph.D. Thesis, The University of Wisconsin-Wilwaukee*, **2002**.
- (44) Liu, X.; Deschamp, J.R.; Cook, J.M. *Org. Lett.* **2002**, *4*, 3339–3342.
- (45) Liao, X.; Zhou, H.; Wearing, X.Z.; Ma, J.; Cook, J.M. *Org Lett.* **2005**, *7*, 3501–3504.
- (46) Noble, R. L.; Beer, C. T.; Cutts, J. H. *Ann. N.Y. Acad. Sci.* **1958**, *76*, 882.
- (47) Svoboda, G. H.; Nuess, N.; Gorman, M. *J. Am. Pharm. Assoc. Sci. Ed.* **1959**, *48*, 659.

-
- (48) Noble, R. L. *Lloydia* **1964**, *27*, 280.
- (49) Kutney, J.P.; Beck, J.; Bylsma, F.; Cretney, W.J. *J. Am. Chem. Soc.* **1968**, *90*, 4504–4505
- (50) Mangeney, P.; Andriamialisoa, R.Z.; Langlois, N.; Langlois, Y. *J. Am. Chem. Soc.* **1979**, *101*, 2243–2245.
- (51) Potier, P.; Langlois, N.; Langlois, Y.; Guéritte, F. *J. Chem. Soc. Chem. Comm.* **1975**, 670–671.
- (52) Langlois, N. Guéritte, F.; Langlois, Y.; Potier, P. *J. Am. Chem. Soc.* **1976**, *98*, 7017–7024.
- (53) Kutney, J.P.; Ratcliffe, A.H.; Tresurywala, A.M.; Wunderly, S. *Heterocycles* **1975**, *3*, 639–639.
- (54) Kutney, J.P.; Hibino, T.; Jahngen, E.; Okutani, T.; Ratcliffe, A.H.; Treasurywala, A.M.; Wunderly, S. *Helv. Chim. Acta.* **1976**, *59*, 2858–2882.
- (55) Kuehne, M.E.; Giacobbe, T.J. *J. Org. Chem.* **1968**, *33*, 3359–3369.
- (56) Kutney, J.P.; Choi, L.S.L.; Nakao, J.; Tsukamoto, H.; McHugh, M.; Boulet, C.A. *Heterocycles* **1988**, *27*, 1845–1853.
- (57) Kuehne, M.E.; Matson, P.A.; Bornmann, W.G. *J. Org. Chem.* **1991**, *56*, 513–528.
- (58) Bornman, W.G.; Kuehne, M.E. *J. Org. Chem.* **1992**, *57*, 1752–1760.
- (59) Magnus, P.; Mendoza, J.S.; Stamford, A.; Ladlow, M.; Willis, P. *J. Am. Chem. Soc.* **1992**, *114*, 10232–10245.
- (60) Bi, Y.; Zhang, L.-H.; Hamaker, L.K.; Cook, J.M. *J. Am. Chem. Soc.* **1994**, *116*, 9027–9041.
- (61) Zhang, L.-H.; Cook, J. *Heterocycles* **1988**, *27*, 2795–2802.

-
- (62) Lachkacr, D.; Denizot, N.; Bernadat, G.; Ahamada, K.; Beniddir, M.A.; Dumontet, V.; Gallard, J-F.; Guillot, R.; Leblanc, K.; N'ngang, E.O.; Turpin, V.; Kouklovsky, C.; Poupon, E.; Evanno, L. Vincent, G. *Nature Chem.* **2017**, *9*, 793–798.
- (63) Hirasawa, Y.; Arai, H.; Rahman, A.; Kusumawati, I.; Zaini, N.C.; Shiota, O.; Morita, H. *Tetrahedron* **2013**, *69*, 10869–10875.
- (64) Magnus, P.; Brown, P.; *J. Chem. Soc. Chem. Comm.* **1985**, 184–186.
- (65) Magnus, P.; Gallagher, T.; Brown, P.; Huffman, J.C. *J. Am. Chem. Soc.* **1984**, *106*, 2105–2114.
- (66) Lavaud, C.; Massiot, G.; Vercauteren, J; Le Men-Olivier, L. *Phytochemistry*, **1982**, *21*, 445–446.
- (67) Liu, X.; Deschamp, J.R.; Cook, J.M. *Org. Lett.* **2002**, *4*, 3339–3342.
- (68) Heath-Brown, B.; Philpott, P. *J. Chem. Soc.* **1965** 7185–7193.
- (69) Zhao, S.; Lio, X.; Wang, T.; Flippen-Anderson, J.; Cook, J.M. *J. Org. Chem.* **2003**, *68*, 6279–6295.
- (70) Gannick, R.L.; LeQuesne, P.W. *J. Am. Chem. Soc.* **1978**, *100*, 4213–4219.
- (71) Yokoshima, S.; Ueda, T.; Kobayashi, S.; Sato, A.; Kuboyama, T.; Tokuyama, H.; Fukuyama, T. *J. Am. Chem. Soc.* **2002**, *124*, 2137–2139.
- (72) Fukuyama, T.; Chen, X.; Peng, G. *J. Am. Chem. Soc.* **1994**, 3127–3128.
- (73) Kobayashi, S.; Ueda, T.; Fukuyama, T. *Synlett* **2000**, 883–886.
- (74) Kuboyama, T.; Yokoshima, S.; Tokuyama, H.; Fukuyama, T. *J. Am. Chem. Soc.* **2004**, *101*, 11966–11970.
- (75) Miyazaki, T.; Yokoshima, S.; Simizu, S.; Osada, H.; Tokuyama, H.; Fukuyama, T. *Org. Lett.* **2007**, *9*, 4737–4740.

-
- (76) Ishikawa, H.; Colby, D.A.; Boger, D.L. *J. Am. Chem. Soc.* **2008**, *130*, 420–421. b)
- (77) Ishikawa, H.; Colby, D.A.; Seto, S.; Va, P.; Tam, A.; Kakei, H.; Rayl, T.J.; Hwang, I.; Boger, D.L. *J. Am. Chem. Soc.* **2009**, *131*, 4904–4916.
- (78) Ishikawa, H.; Elliot, G.I.; Velcicky, J.; Choi, Y.; Boger, D.L. *J. Am. Chem. Soc.* **2006**, *128*, 10596–10612.
- (79) Sasaki, Y.; Kato, D.; Boger, D.L. *J. Am. Chem. Soc.* **2010**, *132*, 13533–13544.
- (80) Raucher, S.; Bray, B.L. *J. Org. Chem.* **1985**, *50*, 3236–3237.
- (81) Raucher, S.; Bray, B.L.; Lawrence, R.F. *J. Am. Chem. Soc.* **1987**, *109*, 442–446.
- (82) For summary of vinblastine analog efforts see: Sears, J.E.; Boger, D.L. *Acc. Chem. Res.* **2015**, *48*, 653–662 and references therein.
- (83) Gotoh, H.; Sears, J.E.; Eschenboser, A.; Boger, D.L. *J. Am. Chem. Soc.* **2012**, *134*, 13240–13243.
- (84) Boon, B.A.; Boger, D.L. *J. Am. Chem. Soc.* **2019**, *141*, 14349–14355.
- (85) Edwankar, C.R.; Edwankar, R.V.; Rallapali, S.; Cook, J.M. *Nat. Prod. Commun.* **2008**, *3*, 1837–1870.
- (86) Edwankar, C.R.; Edwankar, R.V.; Namjoshi, O.A.; Rallapalli, S.K.; Yang, J.; Cook, J.M. *Curr. Opin. Drug. Discov. Devel.* **2009**, *12*, 752–771.
- (87) Liu, X.; Wang, T.; Xu, Q.; Ma, C.; Cook, J.M. *Tetrahedron Lett.* **2000**, *41*, 6299–6303.
- (88) Rogers, E.E.; Snyder, H.R.; Fischer, R.F.; *J. Am. Chem. Soc.* **1952**, *74*, 1987–1989.
- (89) Snyder, H.R.; Fischer, R.F.; Walker, J.F.; Els, H.E.; Nussberger, G.A. *J. Am. Chem. Soc.* **1954**, *76*, 2819–2825.
- (90) Snyder, H.R.; Fischer, R.F.; Walker, J.F.; Els, H.E.; Nussberger, G.A. *J. Am. Chem. Soc.* **1954**, *76*, 4601–4605.

-
- (91) Synder, H.R.; Strohmayer, H.F.; Mooney, R.A. *J. Am. Chem. Soc.* **1958**, *80*, 3708–3710.
- (92) Raie, I.D.; Rosenberger, M.; Snabo, A.G.; Willis, C.R.; Yates, P.; Zacharias, D.E.; Jeffrey, G.A.; Douglas, B.; Kirkpatrick, J.L.; Weisbach, J.A.
- (93) Yates, P.; MacLachlan, F.N.; Rai, I.D.; Rosenberger, M.; Szabo, A.G.; Willis, C.R.; Cava, M.P.; Behforouz, M.; Lakshmikantham, M.V.; Zeiger, W. *J. Am. Chem. Soc.* **1973**, *95*, 7842–7850.
- (94) He, F.; Bo, Y.; Atlom, J.D.; Corey, E.J. *J. Am. Chem. Soc.* **1999**, *121*, 6771–6772.
- (95) Sumi, S.; Matusomoto, K.; Tokuyama, h.; Fukuyama, T. *org. Lett.* **2003**, *5*, 1891–1893.
- (96) Sumi, S.; Matsumoto, K.; tokuyama, H.; Fukuyama, T. *Tetrahedron* **2003**, *59*, 8571–8587.
- (97) Mejia-Oneto, J.M.; Padwa, A.; *Org. Lett.* **2006**, *8*, 3275–3278.
- (98) Nicolaou, K.C.; Dalby, S.M.; Majumder, U. *J. Am. Chem. Soc.* **2008**, *130*, 14942–14943.
- (99) Ueda, H.; Satoh, H.; Matsumoto, K.; Sugimoto, K.; Fukuyama, T.; Tokuyama, H. *Angew Chem. Int. Ed.* **2009**, *48*, 7600–7603.
- (100) Tokuyama, H.; Yokoshima, S.; Yamashita, T.; Fukuyama, T.; *tetrahedron Lett.* **1998**, *39*, 3189–3192.
- (101) Uematsu, N.; Fujii, A.; Hashiguchi, H.; Ikariya, T.; Noyori, R. *J. Am. Chem. Soc.* **1996**, *118*, 4916–4917.
- (102) Nicolaou, K.C.; Dalby, S.M.; Li, S.; Suzuki, T.; Chen, D.Y.K. *Angew. Chem. Int. Ed.* **2009**, *48*, 7616–7620.
- (103) Nicolaou, K.C.; Dalby, S.M.; Majumder, U. *J. Am. Chem. Soc.* **2008**, *130*, 14942–14943.
- (104) Yang, C.C.; Chang, H.T.; Fang, J.M. *J. Org. Chem.* **1993**, *58*, 3100–3105.
- (105) Han-ya, Y.; Tokuyama, H.; Fukuyama, T. *Angew. Chem. Int. Ed.* **2011**, *50*, 4884–4887.

-
- (106) Ahond, A.; Cavé, A.; Kan-Fan, C.; Housson, H-P.; de Rostolan, J.; Portier, P. *J. Am. Chem. Soc.* **1968**, *90*, 5622.
- (107) Satoh, H.; Ojima, K.; Ueda, H.; Tokuyama, H. *Angew. Chem. Int. Ed.* **2016**, *55*, 15157–15161.
- (108) Satoh, H.; Ueda, H.; Tokuyama, H. *Tetrahedron* **2013**, *69*, 89–95.
- (109) Li, L. Chen, Z.; Zhang, X.; Jia, Y. *Chem. Rev.* **2018**, *118*, 3752–3832
- (110) Burke, M.D.; Schreiber, S.L. *Angew. Chem. Int. Ed.* **2004**, *43*, 46–58.
- (111) O'Connor, S.E.; Maresh, J.J. *Nat. Prod. Rep.* **2006**, *23*, 532–547.
- (112) Xu, Z.; Wang, Q.; Zhu, J. *Chem. Soc. Rev.* **2018**, *47*, 7882–7898.
- (113) Jones, S.B.; Simmons, B.; Mastracchio, A.; MacMillan, D.W.C. *Nature* **2011**, *475*, 183–188.
- (114) Pritchett, B.P.; Donckele, E.J.; Stoltz, B.M. *Angew. Chem. Int. Ed.* **2017**, *56*, 12624–12627.
- (115) Jamison, C.R.; Badillo, J.J.; Lipshultz, J.M.; Comito, R.J.; Macmillan, D.W.C. *Nature Chem.* **2017**, *9*, 1165–1169.
- (116) Lindovska, P.; Movassaghi, M. *J. Am. Chem. Soc.* **2017**, *139*, 17590–17596.
- (117) Nicolaou, K.C.; Snyder, S.A. Vinblastine. In *Classics in total synthesis II: more targets, strategies, methods*; Wiley-VCH: Weinheim, Germany, 2003; pp 505–532.
- (118) Nicolaou, K.C.; Chen, J.S. Haplophytine. In *Classics in total synthesis III: further targets, strategies, methods*; Wiley-VCH: Weinheim, Germany, 2011; pp. 689–718.

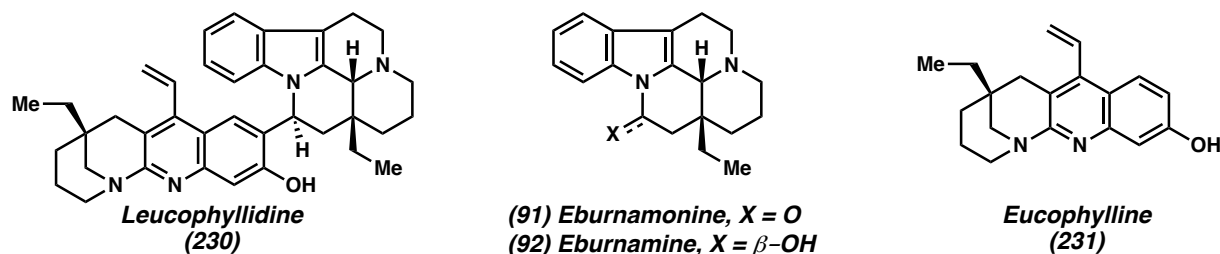
CHAPTER 2

Divergent Synthesis of Eburnamonine and Eucophylline

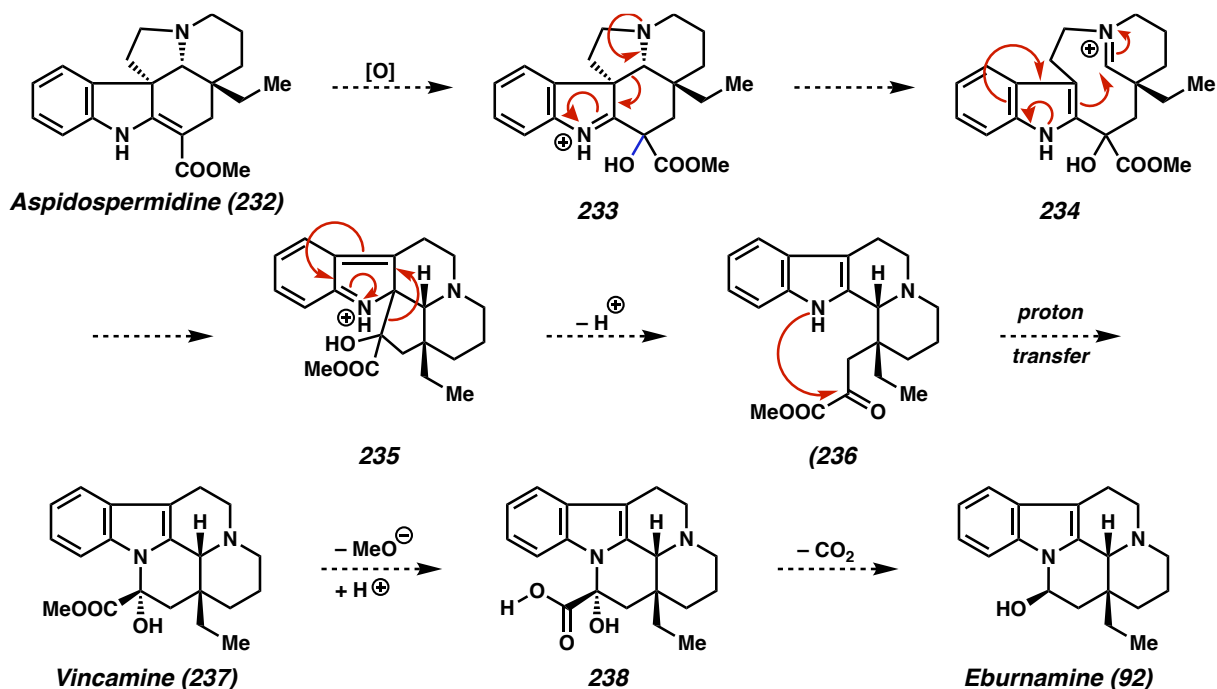
2.1 INTRODUCTION

2.1.1 Isolation, Bioactivity, and Biosynthetic Hypotheses

Leucophyllidine (**230**) is a *bis*(monoterpenoid) indole alkaloid that was first isolated from the bark of the Malaysian woody climber *Leuconotis griffithi* in 2009.¹ It is composed of two polycyclic fragments: a northern pentacyclic indole-containing fragment derived from eburnamonine (**91**) and a southern tetracyclic vinylquinoline fragment derived from eucophylline (**231**) (Figure 2.1). Structurally, the molecule contains nine rings, four stereogenic carbons (including two all-carbon quaternary stereogenic centers) and a sterically hindered C(sp)³–C(sp)² bond which joins the two polycyclic fragments. The molecule demonstrates *in vitro* cytotoxicity toward drug-sensitive and drug-resistant human KB cells (IC₅₀ = 5.16, 5.10 μM) while also acting as a dose-dependent inhibitor of nitrous oxide (NO) synthase.²

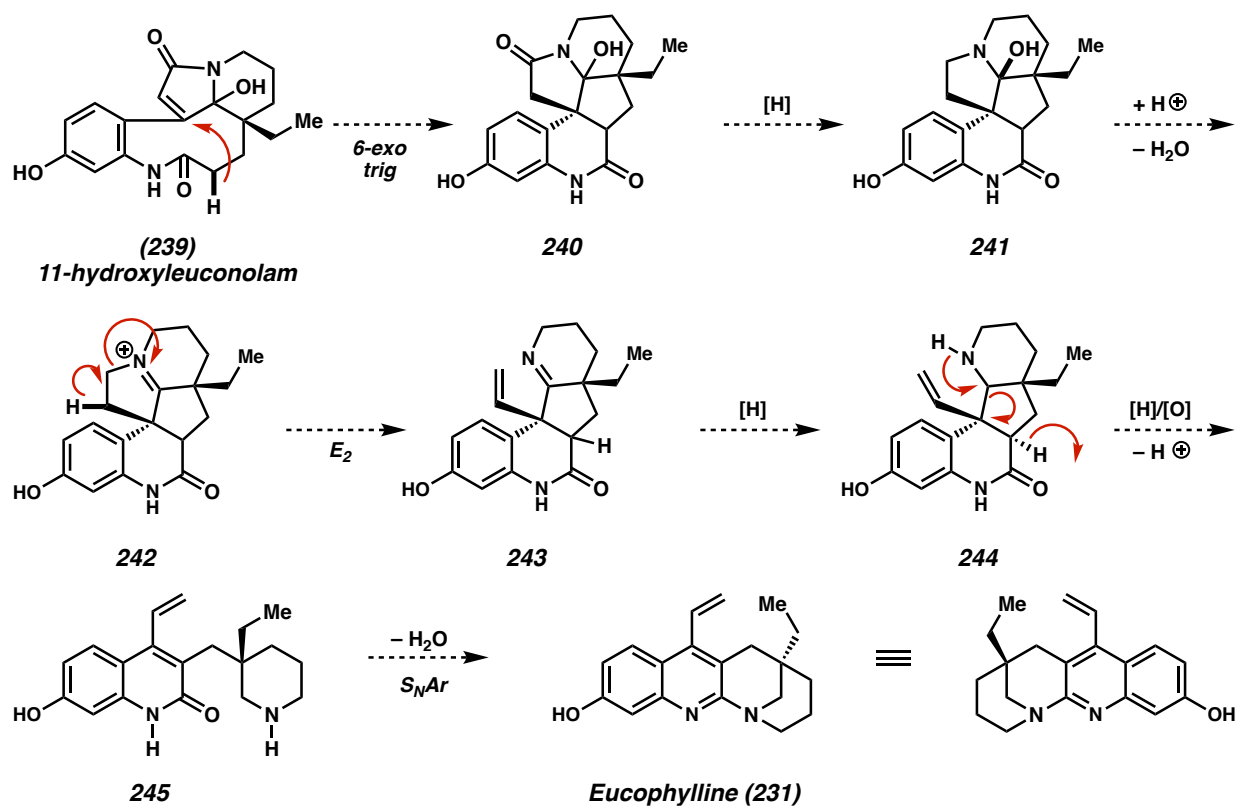
Figure 2.1 Leucophyllidine and its component monomers.

The two monomeric components of leucophyllidine (230) have each been independently isolated from separate biological sources (Figure 2.1). Eburnamonine (91) and its reduced form eburnamine (92) were first isolated in 1959 by Bartlett and Taylor³ from the plant *Hunteria eburnea*, and it was later demonstrated to show anticholinergic⁴ and cerebratonic⁵ properties. Eucophylline (231) was first isolated in 2010 from the related plant species *Leuconotis eugenifolius*. Though noteworthy for its unique tetrahydro-benzo[*b*][1,8]naphthyridine core, eucophylline (231) displays no known biological activity to date.

Scheme 2.1. Proposed biosynthesis of eburnamine.

Biosynthetically, eburnamine (**92**) is hypothesized to arise from aspidospermidine (**232**), which is first oxidized to hydroxylated alkaloid **233** (Scheme 2.1). A fragmentation then occurs to reform iminium **234**, which undergoes subsequent attack from indole C(2) to form rearranged pentacycle **235**. Cleavage of the five-membered ring affords α -ketoester **236**, before nucleophilic attack of the indole nitrogen closes the 6-membered ring of vincamine (**237**), thus completing the pentacyclic framework. Methyl ester hydrolysis to acid **238**, followed by decarboxylation then affords eburnamine (**91**).⁶

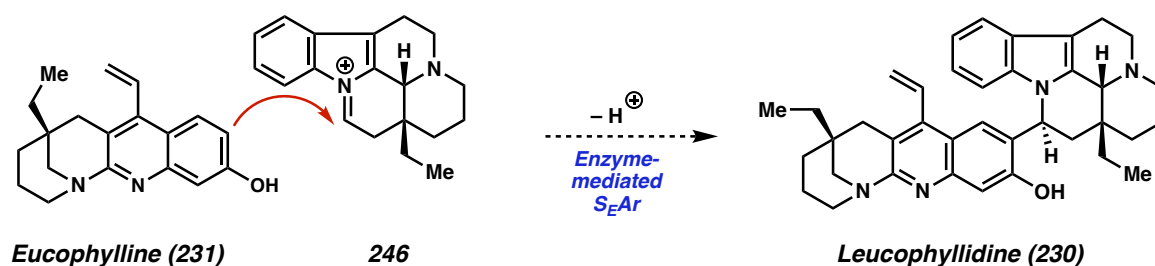
Scheme 2.2. Proposed biosynthesis of eucophylline.



Eucophylline (**92**) is hypothesized to arise from 11-hydroxyleuconolam (**239**), which undergoes an intramolecular *6-exo trig* conjugate addition to form pentacycle **240**, which is reduced to hemiaminal **241** (Scheme 2.2).² Formation of iminium **242** precedes an E_2 elimination to generate the vinyl fragment of imine **243**, which is subsequently reduced to the *Melodinus* type

alkaloid **244**. At this juncture, reduction of the piperidine motif occurs before a fragmentation/oxidation establishes aromatic quinolone **246**. This then participates in nucleophilic aromatic substitution to complete the tetrahydro[*b*][1.8]naphthyridine core of eucophylline (**231**).

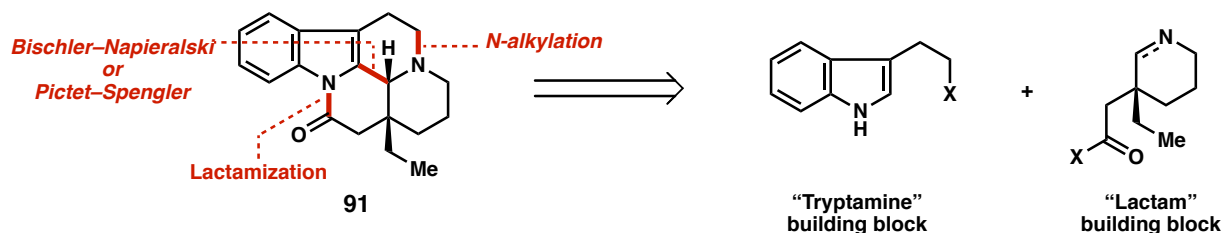
Scheme 2.3. Proposed biosynthesis of leucophyllidine.



The coupling of monomers is proposed to occur upon dehydration of eburnamine (**92**) to the corresponding iminium ion **246**, followed by electrophilic aromatic substitution with the electron-rich eucophylline (**231**) to complete leucophyllidine (**230**) (Scheme 2.3). Based on synthetic work by Panday, the C(6) position of eucophylline is much less nucleophilic than C(8) to Friedel-Crafts type reactivity due to greater stabilization of the Weiland intermediate. Therefore, it is very likely that the corresponding dimerization event is enzyme-mediated.⁷

2.1.2. Previous Synthetic Efforts toward Eburnamine

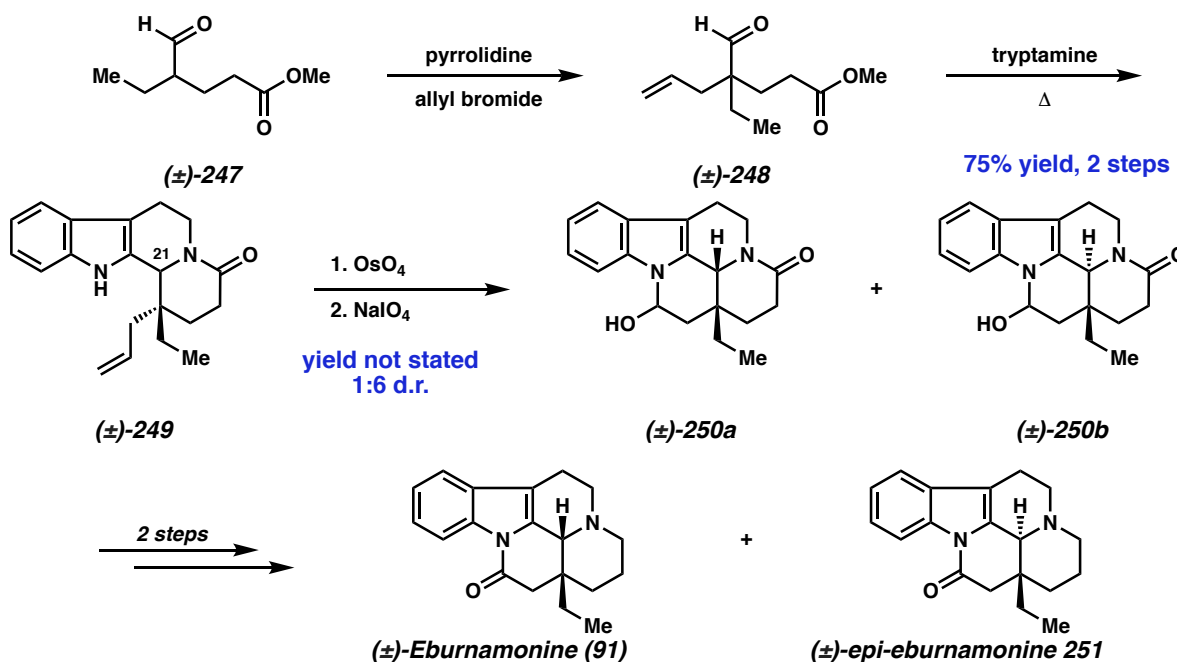
Scheme 2.4. Strategically significant bonds in eburnamonine.



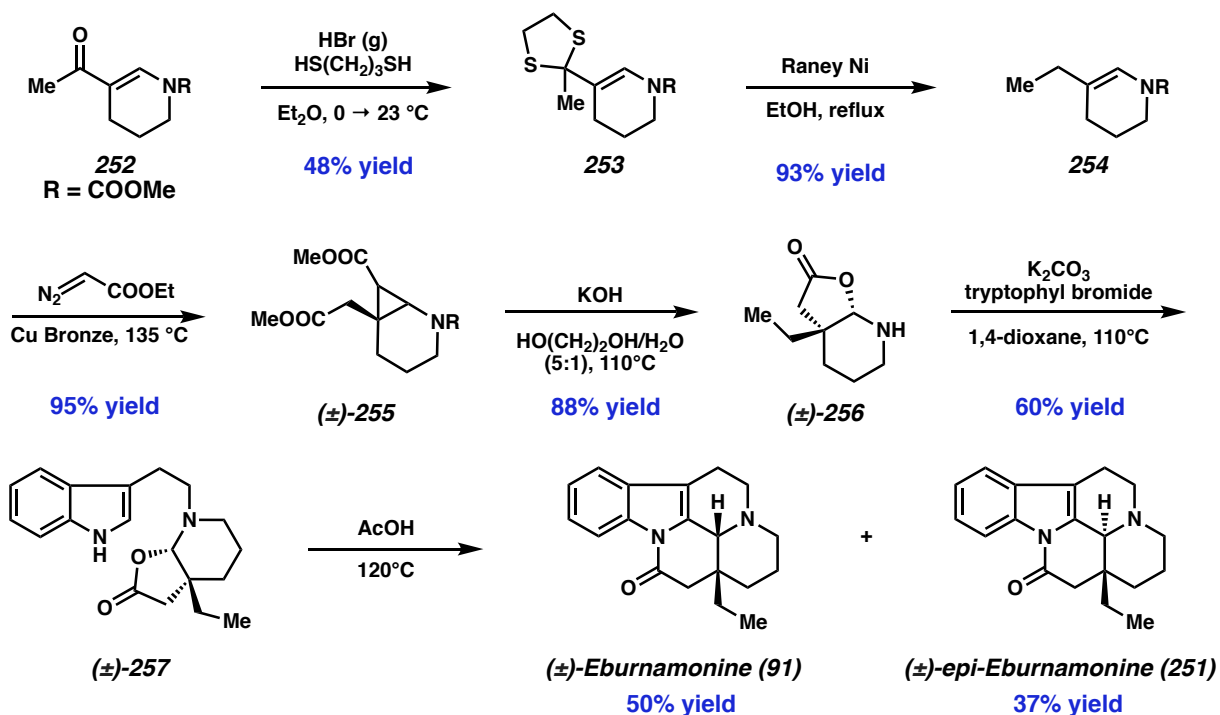
In the 60 years since its initial discovery, there have been over two dozen reported syntheses of racemic⁸ and enantioenriched^{7,9,10} eburnamonine (**91**) and eburnamine (**92**). Rather

than discuss each synthesis individually, we will focus on select examples that identified three strategic bonds (Scheme 2.4), disconnecting the pentacycle into a “tryptamine” and “lactam”-derived fragments. These examples were the most influential in our retrosynthetic analysis.

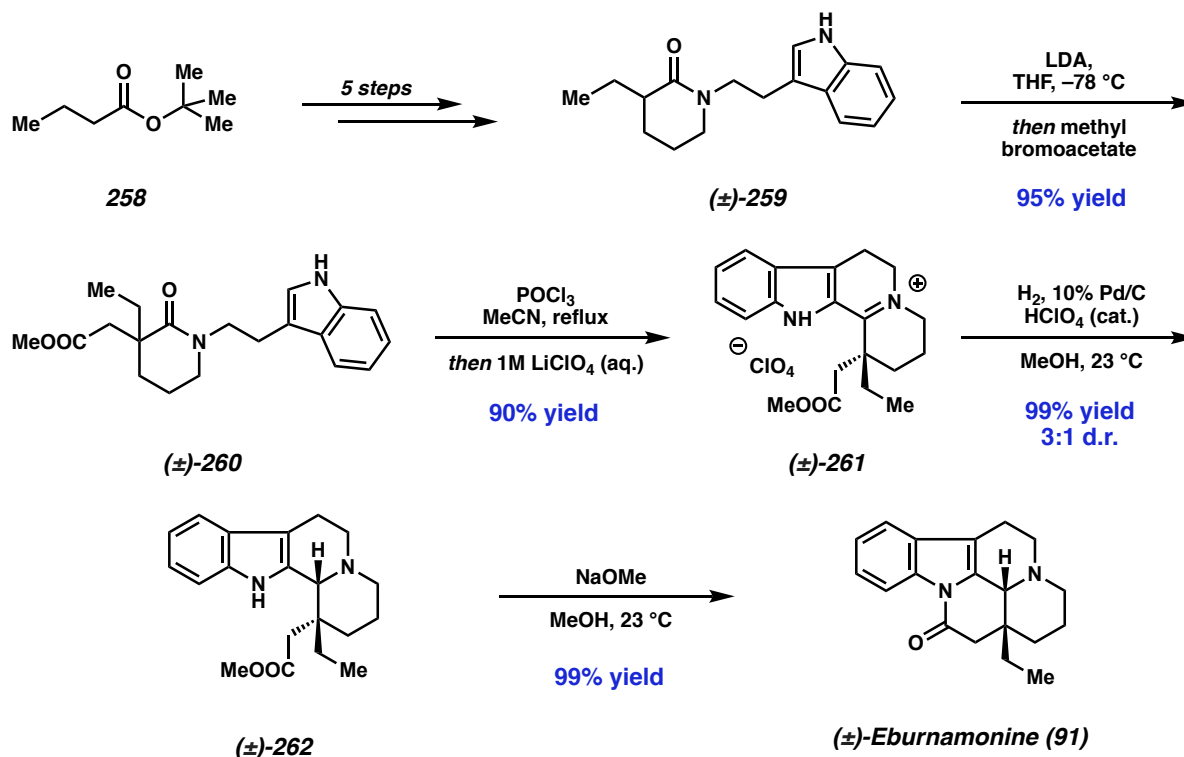
Scheme 2.5. Harley-Mason’s synthesis of (\pm) eburnamonine (1965).



The first noteworthy example by Barton and Harley-Mason^{8b} exploits a Pictet-Spengler approach to construct the *eburnan* core (Scheme 2.5). Starting from 4-formylhexanoate **247**, enamine alkylation with allyl bromide generates quaternary adduct **248** in racemic fashion (Scheme 2.5). Treatment with tryptamine promotes a tandem condensation/Pictet-Spengler cyclization to lactam **249** in 75% yield. While this was initially believed to forge a single C(21) diastereomer, additional studies¹¹ revealed that following Johnson-Lemieux oxidation and careful chromatography affords eburnamine N(b) lactam **250a** and its C(21) epimer **250b** as a 1:6 mixture. These intermediates were then advanced in two steps to eburnamonine (**91**) and *epi*-eburnamonine **251**, respectively.

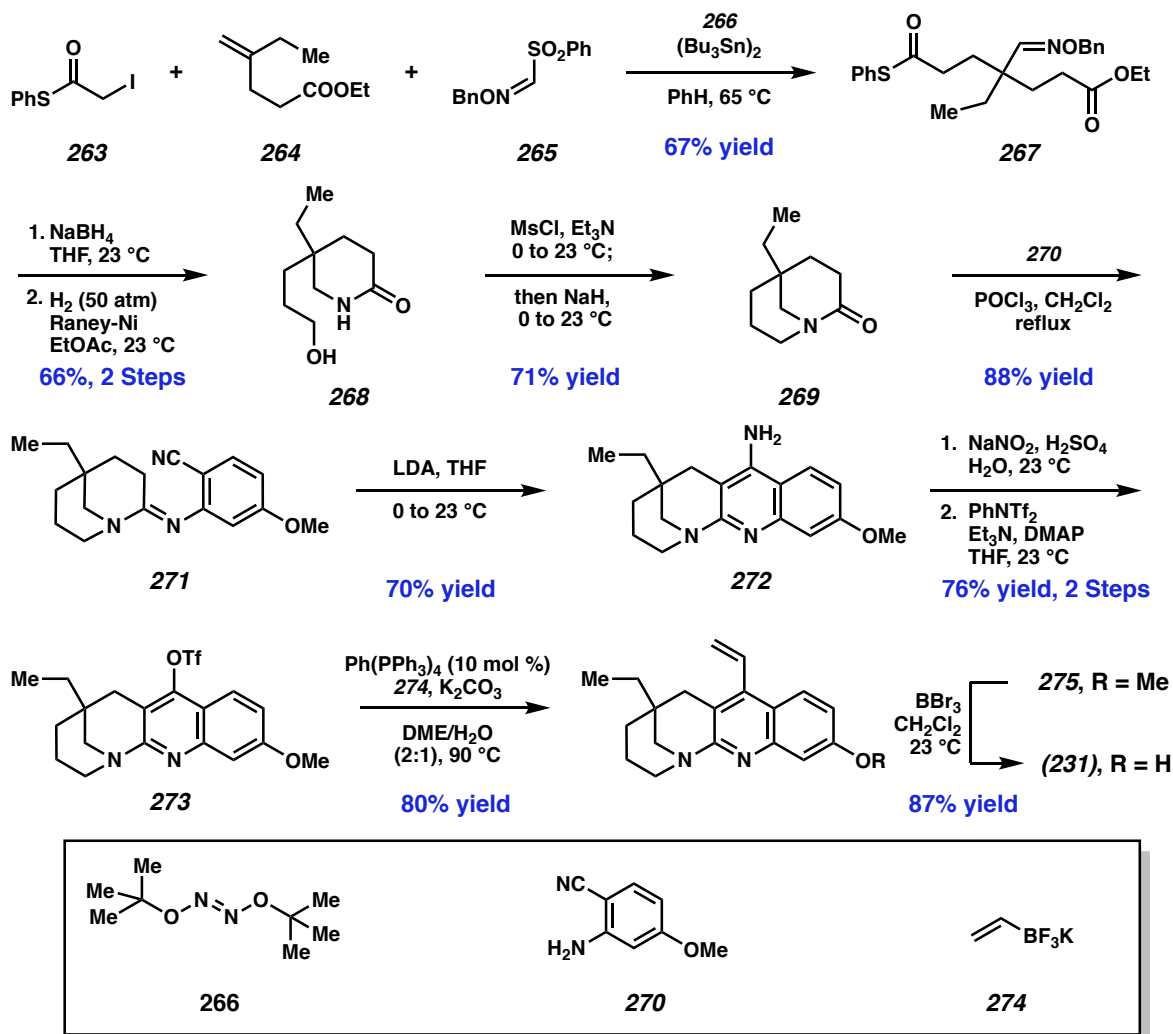
Scheme 2.6. Wenkert's synthesis of (\pm) eburnamonine (1988).

Wenkert and coworkers⁸¹ later disclosed a route that utilizes a Pictet-Spengler cyclization into a cyclic iminium rather than an acyclic iminium (Scheme 2.6). Enaminone **252** is first converted to dithiolane **253**, which is followed by Raney Nickel-mediated desulfurization to access cyclic enamine **254** (Scheme 2.6). Treatment with ethyl diazoacetate in the presence of copper bronze generates cyclopropane **255** in racemic fashion before base-mediated hydrolysis produces lactone **256**. Alkylation with tryptophyl bromide affords tetracycle **257**, and heating in glacial acetic acid generates eburnamonine (**91**) and *epi*-eburnamonine (**251**) in good yield but low diastereoselectivity (1.4:1). Degradation studies by Lounasmaa¹² determined that the unnatural *trans*-ring fusion is thermodynamically preferred, leading us to hypothesize that the further optimization of this diastereoselective cyclization would be challenging.

Scheme 2.7. Schlessinger's synthesis of (\pm) eburnamonine (1979).

The route by Schlessinger and coworkers,^{8f} in contrast, utilized a Bischler–Napieralski cyclization to access the *eburnan* core (Scheme 2.7). *t*-Butyl butyrate **258** is advanced over five steps to indole-substituted lactam **259**. Enolate alkylation with methyl bromoacetate generates quaternary lactam **260** in racemic fashion, which is subsequently subjected to Bischler–Napieralski cyclization conditions and anion exchange to yield iminium perchlorate **261**. Hydrogenation with 10% palladium on carbon yields tertiary amine **262** in quantitative yield as a 3:1 mixture of diastereomers in favor of the *cis*-ring fusion; this selectivity arises from preferential addition of hydrogen from the less-hindered β -face of the natural product, generating the kinetically favorable *cis* product as the major diastereomer. Base-mediated lactamization then produces eburnamonine (**91**) in quantitative yield.

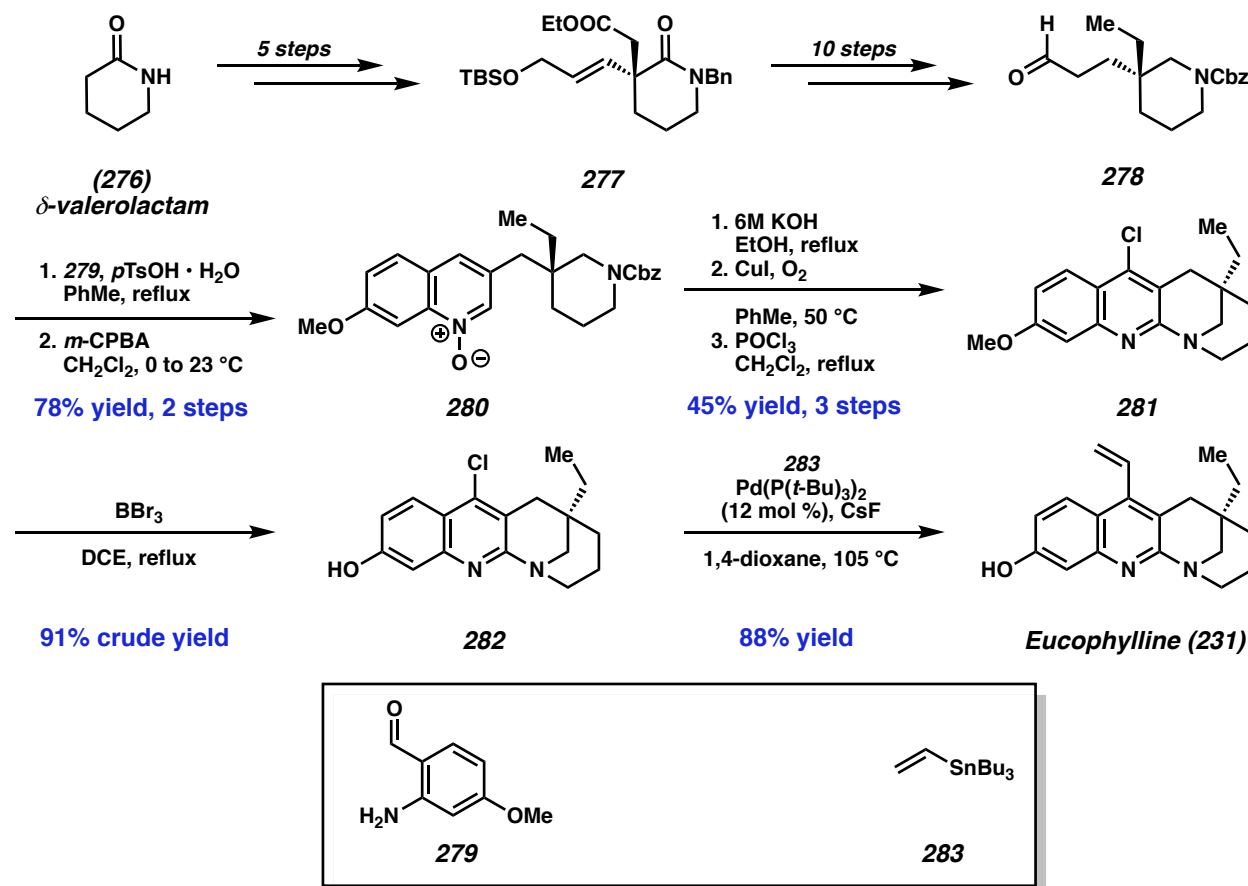
2.1.3. Previous Synthetic Efforts toward Eucophylline

Scheme 2.8. Landais's synthesis of (\pm) eucophylline (2015).

In sharp contrast to eburnamonine (**91**), eucophylline (**231**) has only been synthesized twice since its initial isolation. The first report by Landais and coworkers¹³ begins with a three-component radical coupling of alkyl iodide **263**, alkene **264**, and *O*-benzyloxime **265** to afford quaternary adduct **267** in racemic fashion (Scheme 2.8). Treatment with sodium borohydride, followed by hydrogenolysis with Raney-Ni affords cyclized lactam **268** in 66% yield over two steps. A one-pot mesylation/S_N2 displacement generates fused bicyclic intermediate **269** which, upon treatment with phosphorous oxychloride in the presence of aniline **270**, affords the unusual amidine **271**.

Cyclization is then initiated with LDA to generate 4-aminopyridine **272**, then advanced to triflate **273** over two steps. Suzuki coupling with **274** appends the vinyl fragment in *O*-methylleucophylline **275** before demethylation affords eucophylline (**231**) in 10% yield over 10 steps.

Scheme 2.9. Panday's asymmetric synthesis of eucophylline (2017).



In 2017, Panday and coworkers described the first asymmetric synthesis of eucophylline (**231**) as part of their unsuccessful efforts toward leucophyllidine (**230**) (Scheme 2.9). δ -valerolactam **276** is advanced to α -quaternary lactam **277** in five steps through a stereospecific Johnson-Claisen rearrangement from chiral pool starting materials, then advanced ten additional steps to aldehyde **278**. A Friedländer synthesis with amino aldehyde **279** forges the quinoline core before treatment with m -CPBA affords quinoline *N*-oxide **280**. This intermediate is then subjected to a three-step sequence involving Cbz-deprotection, C–N coupling, and chlorination to access 4-

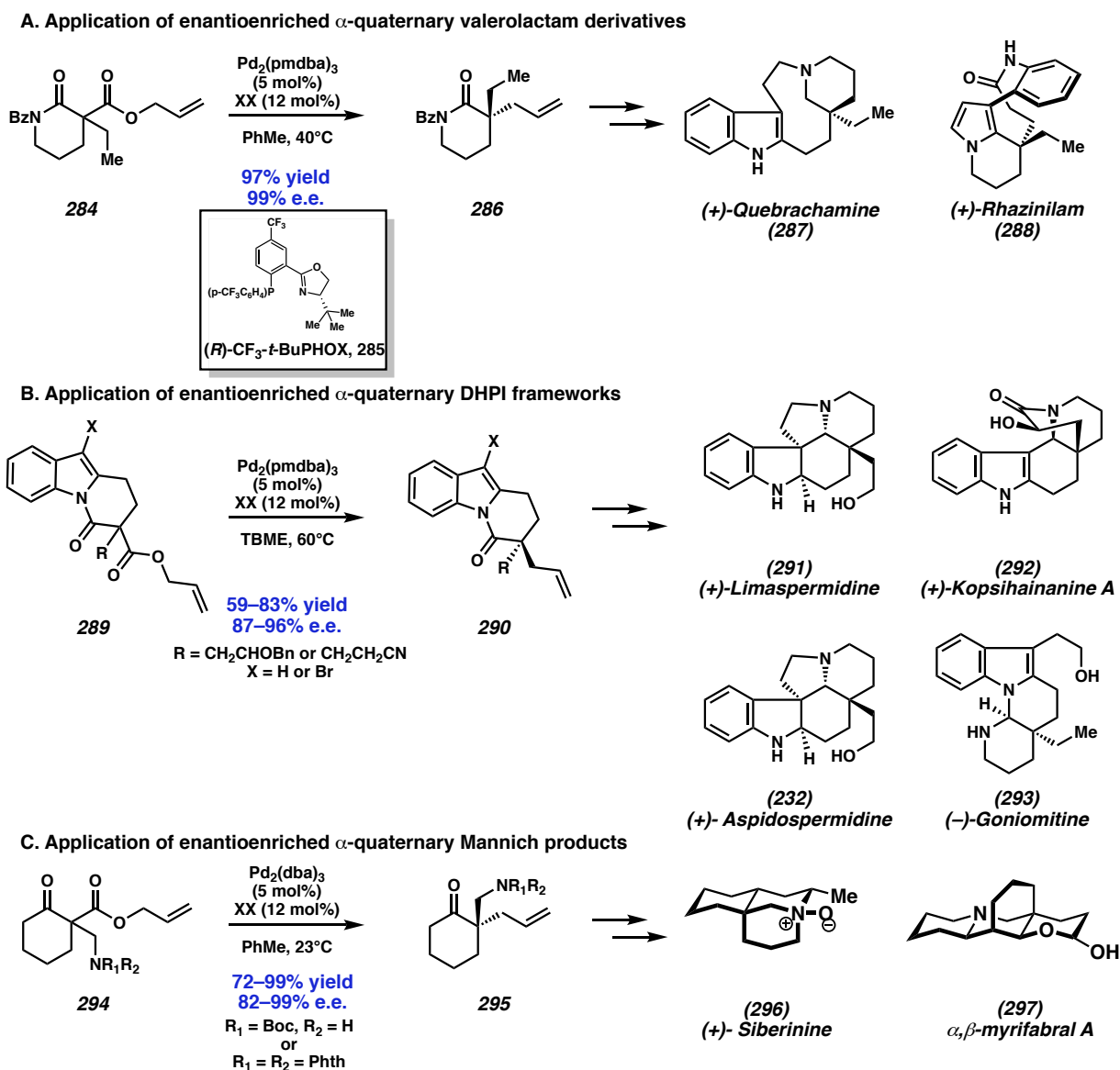
chloroquinoline **281** in modest yield. Demethylation under forcing conditions accesses phenol **282** before a final Stille coupling stannane **283** with appends the vinyl fragment, accessing eucophylline (**231**) in 22 steps from commercial material.

2.1.4. *Inspiration*

For nearly two decades, our laboratory has studied the transition-metal catalyzed asymmetric allylic alkylation of prochiral enolates;¹⁴ these powerful methods allow us to access substrates bearing all-carbon quaternary stereogenic centers in good yield and enantioselectivity. The functionality incorporated in these products has enabled their utility as building blocks and inspired new disconnection strategies in natural products total synthesis.

Recent advances in our technology has allowed the incorporation of nitrogenated functionality, providing new entry points into alkaloid total synthesis (Scheme 2.10). Our first extension of this methodology to *N*-containing heterocycles in 2012 used the decarboxylation allylic alkylation of racemic carboxylactam **284** to access enantioenriched lactam **286** in excellent yield and enantioselectivity while accomplishing formal syntheses of the natural products quebrachamine (**287**) and rhazinilam (**288**)¹⁵ (Scheme 2.10A). In subsequent years, we illustrated that decarboxylative allylic alkylation of dihydropyrido[1,2-*a*]indolone (DHPI) frameworks (**289** → **290**) could be elaborated into *cis*-fused *Aspidosperma* alkaloids limaspermidine (**291**) and aspidospermidine (**232**), *trans*-fused *Kopsia* alkaloids kopsihainanine A (**292**), and the rearranged alkaloid goniomatine (**293**) via stereodivergent cyclizations (Scheme 2.10B).¹⁶ The allylic alkylation of racemic Mannich adducts (**294** → **295**) has also enabled efficient syntheses of sibirinine (**296**) and α,β -myrifabral A (**297**) (Scheme 2.10C).¹⁷

Scheme 2.10. Application of Pd-catalyzed asymmetric allylic alkylation to the synthesis of monoterpene indole alkaloids in the Stoltz laboratory.

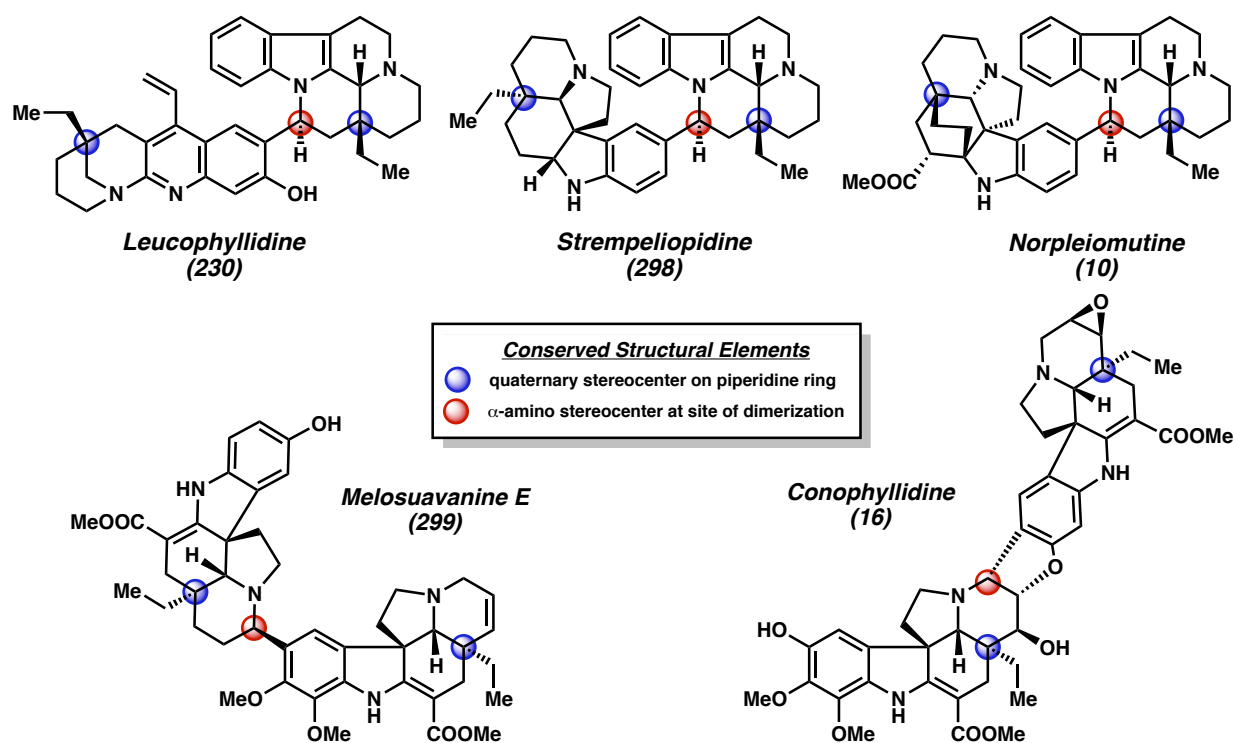


2.1.5. General Synthetic Strategy

Given the diverse range of monoterpene indole alkaloids accessible from these enantioenriched building blocks, we hypothesized that a similar strategy could be utilized to access dimeric indole alkaloids, which have remained far more elusive to synthetic efforts (see Chapter

1). Numerous *bis*(monoterpenoid) indole alkaloids including leucophyllidine (**230**) contain all-carbon quaternary stereogenic center at the three position of a piperidine ring in both monomeric subunits (blue, Figure 2.2), and the *eburnan* monomer is conserved in several natural products such as strempeliopidine (**298**) and norpleiomutine (**11**). Furthermore, many alkaloids are joined at an α -amino stereogenic center (green, Figure 2.2). The conserved structural analogy between these fragments suggests that our technology, in combination with a generalized cross-coupling method, could provide a foundation for a general strategy to access *bis*(monoterpenoid) indole alkaloids.

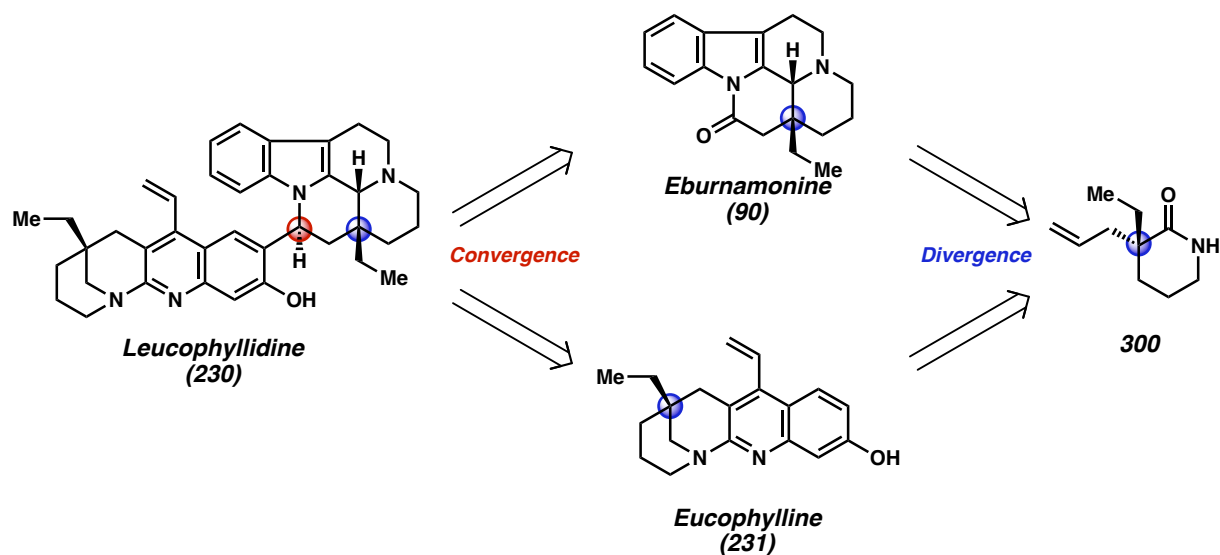
Figure 2.2. Conserved structural elements observed in *bis*(monoterpenoid) indole alkaloids.



Retrosynthetically, we envision constructing leucophyllidine (**290**) through a “convergent-divergent” strategy. Leucophyllidine (**290**) would be forged in a *convergent* manner through late-stage cross-coupling of eburnamonine (**91**) and eucophylline (**231**) or a close-derivative through a

method to forge the α -amino stereogenic center. The monomeric subunits would be synthesized through *divergent* routes to access both natural product cores from a conserved building block, enantioenriched lactam **300**.

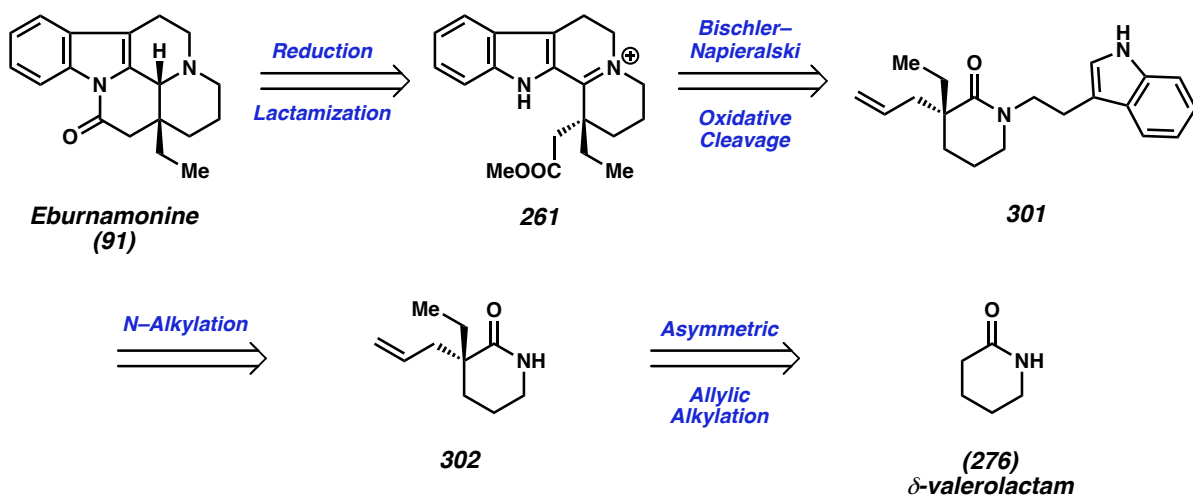
Scheme 2.11. The divergent-convergent strategy to access leucophyllidine.



2.2 TOTAL SYNTHESIS OF EBURNAMINE

2.2.1. Retrosynthetic Analysis

Scheme 2.12. Retrosynthetic analysis of eburnamonine.

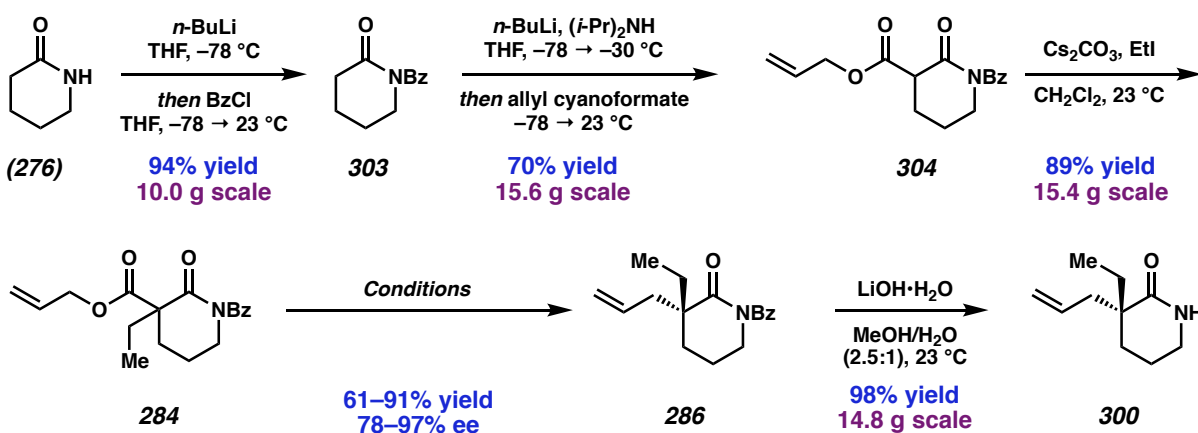


Retrosynthetically, we envisioned that eburnamonine (**91**) could be accessed through a reduction of iminium perchlorate **261** with subsequent lactamization as is observed in the Schlessinger route (Scheme 2.12).^{8f} This would be formed via the oxidative cleavage and Bischler–Napieralski cyclization of indole substituted lactam **301**. The indole would be installed through *N*- with a tryptophol-derived electrophile alkylation of building block **300** that, in turn, is accessible from δ -valerolactam (**276**) using our asymmetric allylic alkylation methodology.

2.2.2. Scalable Synthesis of the Enantioenriched Lactam Building Block

Though the synthesis of lactam **300** had been previously reported, we elected to develop a modified route that would be both shorter and more efficient to perform on large-scale.^{15,18} Starting from δ -valerolactam (**276**), we first perform benzoyl protection to generate lactam **303**. This is followed by *C*-acylation using allyl cyanofornate to produce allyl ester **304**, which is then alkylated with ethyl iodide to generate racemic β -keto ester **284**. Our decarboxylative allylic alkylation then generates the enantioenriched α -quaternary lactam **286** before benzoyl deprotection accesses key lactam precursor **300** in only five steps.

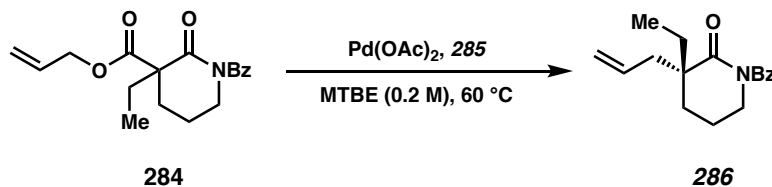
Scheme 2.13. Revised synthesis of enantioenriched lactam building block.



While our first generation conditions were effective at generating lactam **300** in high yield and ee, there were several aspects of this reaction that were prohibitive to perform on large scale.¹⁵ First, the conditions required 5 mol% loading of Pd(0) precatalyst with a pmdba ligand that would frequently co-elute with desired products upon purification. Second, the conditions also required 12.5 mol % loading of ligand **285**, which was accessible through a scalable, yet tedious 7-step route.¹⁹ Finally, the dilute concentrations of toluene greatly complicated the setup and workup.

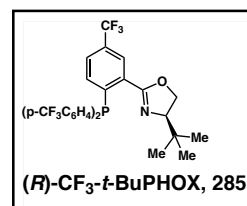
To solve these problems, we sought to adapt our low-catalyst loading conditions, which required a less-expensive and robust Pd(II) source, lower ligand loadings, and higher concentrations in MTBE.²⁰ While the yield was slightly lower, the enantioselectivity of this transformation was retained in the reported examples. Furthermore, the facile purification allowed excess ligand to be recovered and reused.

Table 2.1. Development of gram-scale decarboxylative allylic alkylation.



Entry	Pd(OAc) ₂ (mol%)	(<i>R</i>)-CF ₃ -PHOX (mol%)	time (d)	scale (g)	yield	ee	Reaction Setup
1	0.3	3.0	0.75	0.063	85%	97%	Sealed vial
2	0.3	3.0	2.5	9.5	61%	76%	Flask with reflux condenser
3	0.5	5.0	3.0	8.8	66%	94%	Schlenk Flask
4	1.5*	7.5*	4.0	15.0	88%	93%	Schlenk Flask
5	1.0	5.0	2.0	14.8	91%	92%	Schlenk Flask

*Initial loading: 0.5 mol% Pd, 2.5% ligand. Equimolar amounts of each added after 2 and 3 days



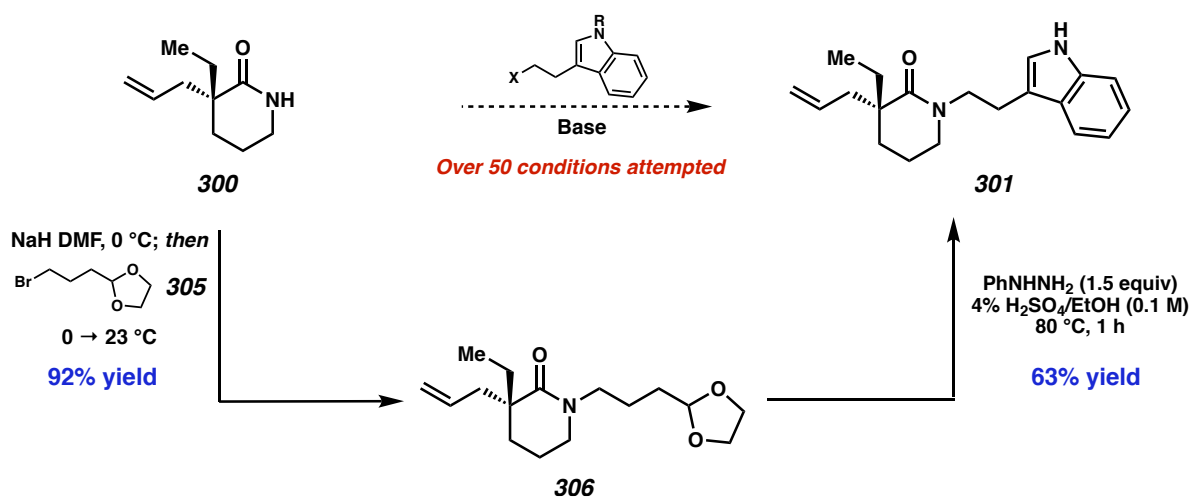
While we were able to replicate the results of our initial publication on 60 mg scale (Table 2.1, Entry 1), we were disappointed to notice a sharp decrease in yield and enantioselectivity when conducted on 9.5 gram scale (Entry 2). Reasoning that the lower concentrations of active catalyst may be more air-sensitive, we were pleased to see that switching to a Schlenk flask greatly improved the enantioselectivity of the transformation, albeit with only minimal increase in yield

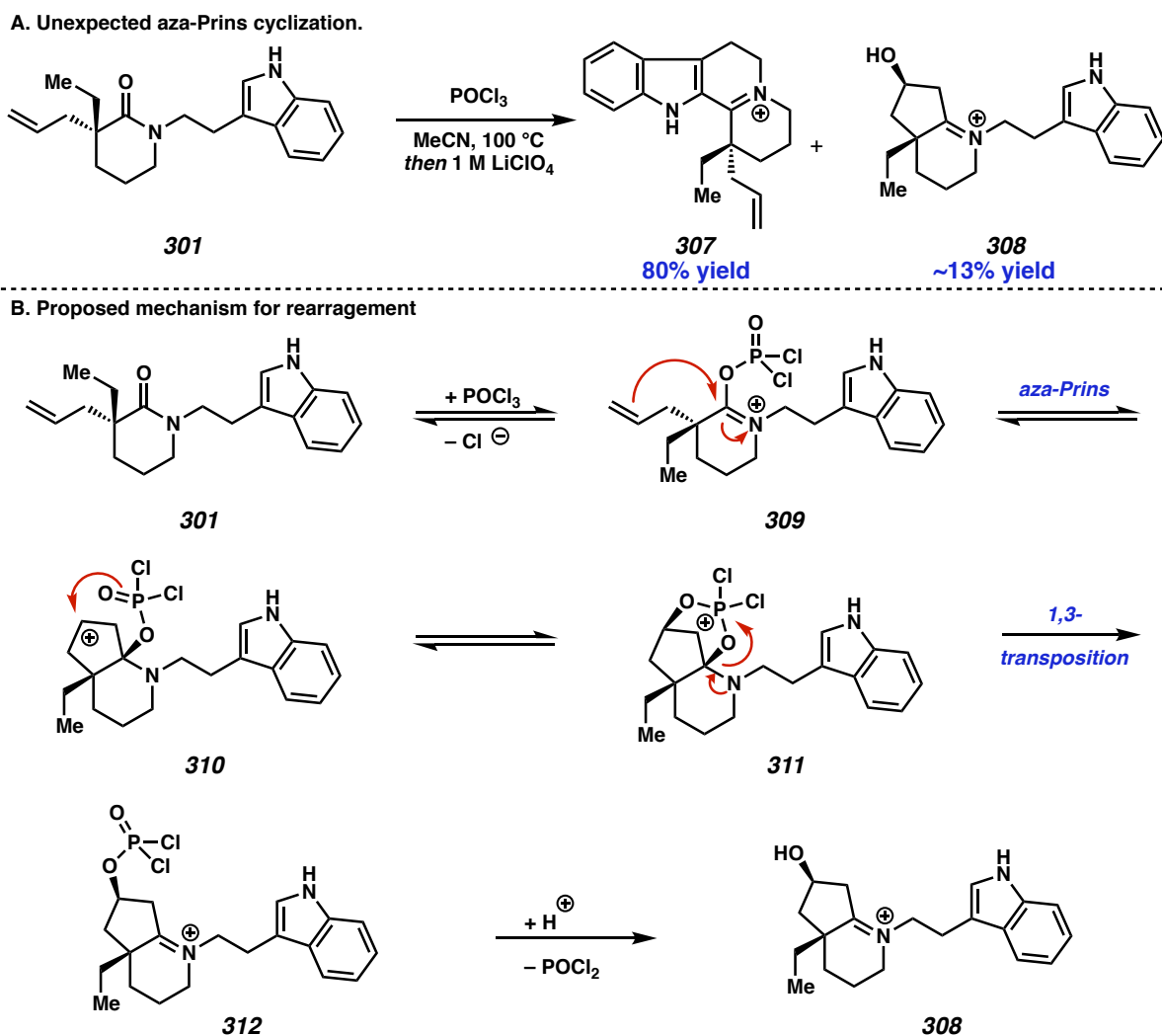
(Entry 3). As the remainder of mass balance returned as starting material, we found that adding equimolar amounts of Pd and ligand **285** at 2 and 3 days, respectively, allowed us to restart the reaction and improve conversion and yield (Entry 4). By increasing the initial Pd and ligand loading to 1 mol % and 5 mol %, respectively, we obtained the desired product in 91% yield and 92 % ee on 15-gram scale (Entry 5).

2.2.3. Advancement to the Bischler–Napieralski Product

With sufficient quantities of lactam **300** in hand, we turned our attention to advancing this intermediate to indole **301**. We were disappointed to observe that all attempts to *N*-alkylate lactam **300** with tryptophol-derived electrophiles failed to deliver the product in our hands; though we had successfully alkylated similar nucleophiles, we determined that the β -indolyl electrophiles were unstable under the basic conditions required for these reactions. Thus, we first *N*-alkylated indole with known²¹ dioxolane **305** in excellent yield, which was advanced to indole **306** through an optimized Fischer synthesis.

Scheme 2.14. Indole installation via Fischer synthesis.



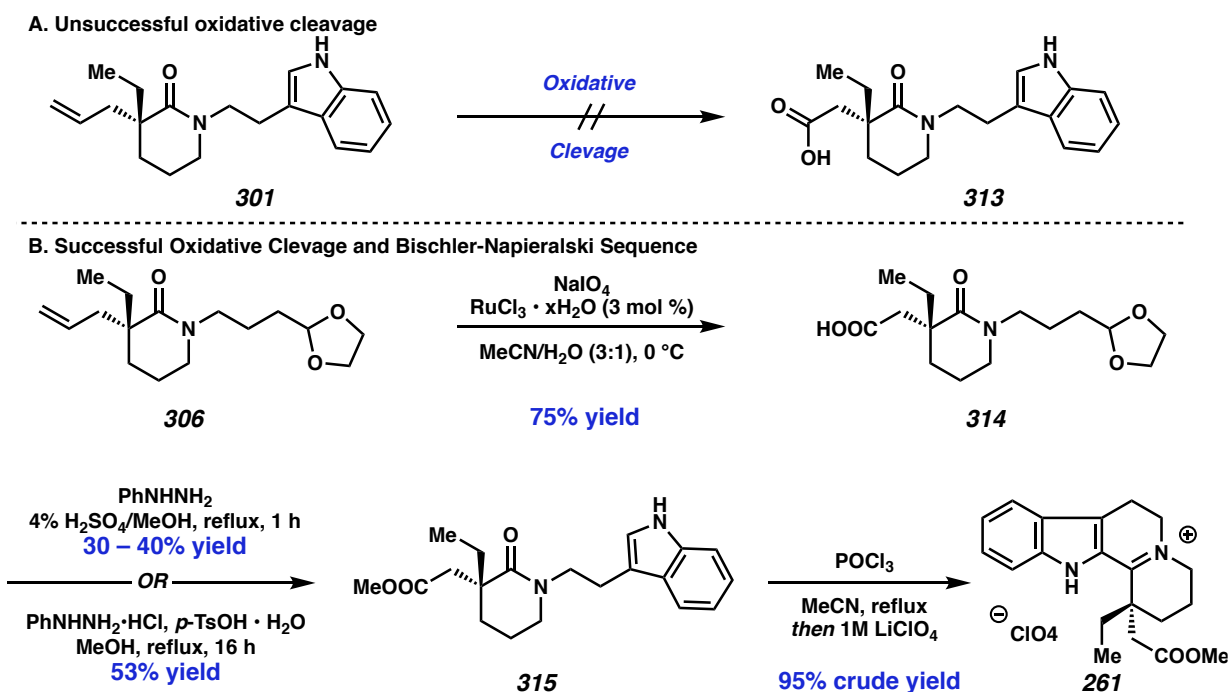
Scheme 2.15. Unexpected aza-Prins rearrangement and mechanistic proposal.

We then turned our attention to the key Bischler–Napieralski cyclization. Though we did successfully obtain our desired iminium perchlorate **307** as the major product, we were surprised to observe variable amounts of a minor side product, which we later determined to be fused [5,6] system **308** as a single diastereomer (Scheme 2.15A). Mechanistically, one can envision this forming from activated amide **309** through an aza-Prins cyclization of the allyl fragment to carbocation **310**, which reacts with the phosphonate to form bridged species **311** (Scheme 2.15B). 1,3-transposition accompanies reformation of iminium **312**, which upon hydrolysis of the

phosphonate affords secondary alcohol **313**. Though this was a minor component, it could not be purified without careful HPLC separation, complicating analysis of the subsequent reaction.

To avoid this issue, we decided to perform oxidative cleavage of the allyl fragment first prior to the Bischler–Napieralski rearrangement, assuming that an ester or carboxylate at that position would be less nucleophilic or reversibly nucleophilic. Despite Harley–Mason’s precedent using Johnson–Lemieux conditions,^{8a} we were disappointed to see that all attempts to perform oxidative functionalization in the presence of the indole ring (**301** → **313**) were unsuccessful (Scheme 2.16A). Though we briefly investigated protecting the indole nitrogen, this would add numerous steps to what was previously a very efficient sequence.

Scheme 2.16. Alternate Bischler–Napieralski cyclization.



To solve this problem, we first performed oxidative cleavage on dioxolane intermediate **306**, affording the carboxylic acid in 75% yield (Scheme 2.16B). Though our previously optimized Fischer indolization conditions were low yielding and inconsistent, we found after brief

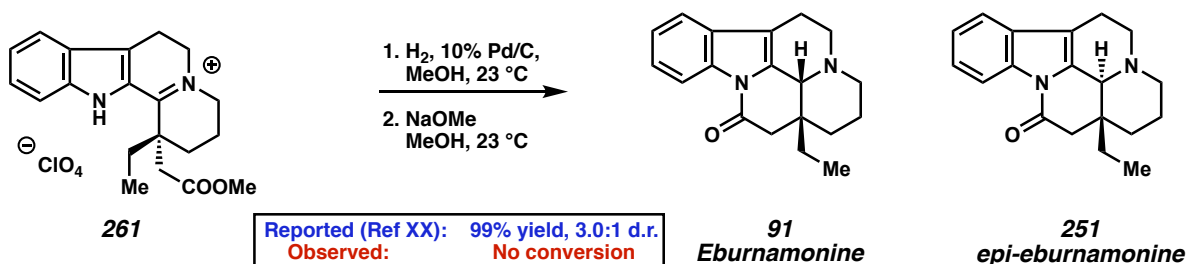
optimization that use of a milder acid (p -TsOH \cdot H₂O) and the hydrochloride salt of phenylhydrazine afforded our desired product **315** in good yield. Using Schlessinger's conditions,^{8f} the Bischler–Napieralski cyclization and anion exchange proceeded smoothly to perchlorate **261**.

2.2.4. Final Steps

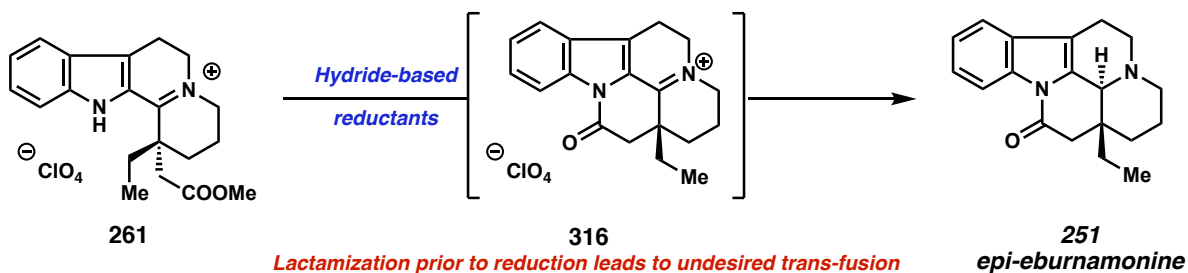
Although we had completed a formal synthesis of eburnamonine (**91**) according to Schlessinger's route,^{8f} we were disappointed to observe that the reported diastereoselective hydrogenation failed to produce any reduced amine in our hands (Scheme 2.17A). Though this was surprising at first, we later learned of other reports which had difficulty reproducing these conditions.²² Attempts to reduce the iminium ion with hydride-based reductants (e.g. LiAlH₄, NaBH₄, (n -Bu)₃SnH, and Li(O - t -Bu)₃AlH) led to lactamization prior to reduction, and afforded the trans-fused *epi*-eburnamonine **251** as the exclusive product (Scheme 2.17B).

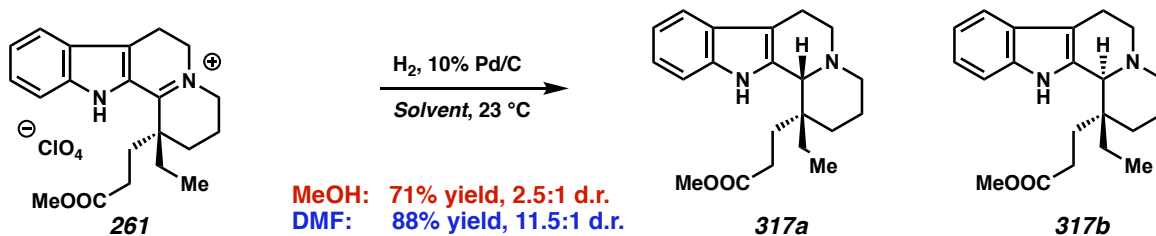
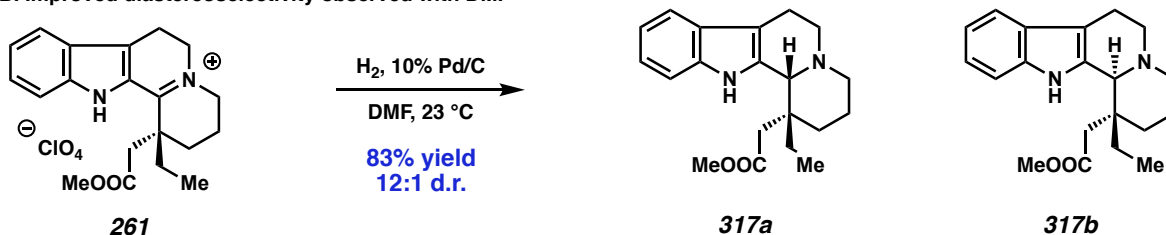
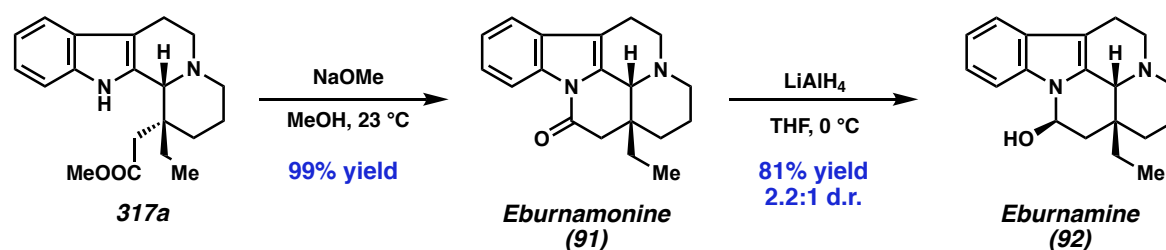
Scheme 2.17. Issues with diastereoselective reduction.

A. Irreproducible diastereoselective iminium hydrogenation.



B. Undesired reduction with hydride-based reagents.



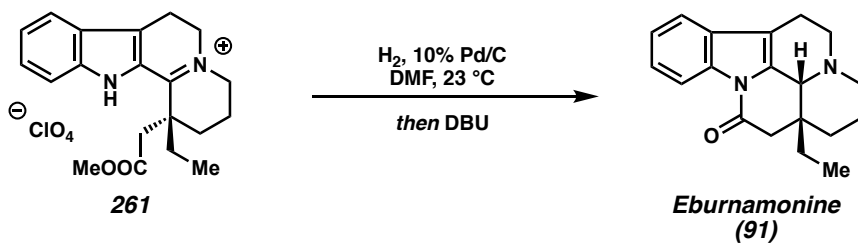
Scheme 2.18. The effect of solvent on diastereoselectivity.**A. Szabo: Solvent effect on diastereoselective hydrogenations of Vinca-type alkaloids (1983)****B. Improved diastereoselectivity observed with DMF****C. Completion of eburnamonine and eburnamine**

Seeking to optimize the hydrogenation, we found a report by Szabo and coworkers²³ describing a solvent effect in the diastereoselective hydrogenation of homologous intermediates (Scheme 2.18A). The authors note that while hydrogenation in methanol afforded modest diastereoselectivity, performing the reduction in DMF offered a dramatic improvement in yield and d.r.; furthermore, while the diastereoselectivity in methanol was highly sensitive to the sterics of the non-ethyl chain, comparable degrees of *cis*-selectivity was observed in DMF regardless of the substituent at this position, provided it was larger than ethyl. Applying these conditions in our system, we were delighted to find that the hydrogenation proceeded in excellent yield and selectivity for *cis*-fused **317a** over *trans*-fused tetracycle **317b** (Scheme XB). *Cis*-fused

intermediate could then undergo lactamization with basic methanol to afford eburnamonine (**91**) in quantitative yield and reduction with lithium aluminum hydride to form eburnamine (**92**).

Gratifyingly, treatment with DBU following the hydrogenation also allowed for lactamization in one-pot, synthesizing eburnamonine (**91**) and *epi*-eburnamonine **251** in 78% combined yield on gram-scale, but a modest 3.4:1 d.r on gram scale. (Table 2.2, entry 1). The lower diastereoselectivity and reaction times could be prevented on smaller scale using more dilute concentrations in DMF (entry 2), yet further dilutions were found to decrease yields (entry 3), potentially due to greater product loss on workup. Nevertheless, this route has allowed us to successfully synthesize up to 700 mg of eburnamonine in a single pass, facilitating studies of the subsequent late-stage chemistry.

Table 2.2. Optimization of one-pot hydrogenation/lactamization.



**700 mg of
eburnamonine
prepared!**

Entry	Scale (g)	Concentration (M)	DBU (equiv)	yield	d.r.
1	1.1	0.5	2.1	71%	3.4:1
2	0.5	0.2	4.1	84%	8.0:1
3	1.3	0.15	5.0	65%	6.1:1

2.2.5 Concluding Remarks

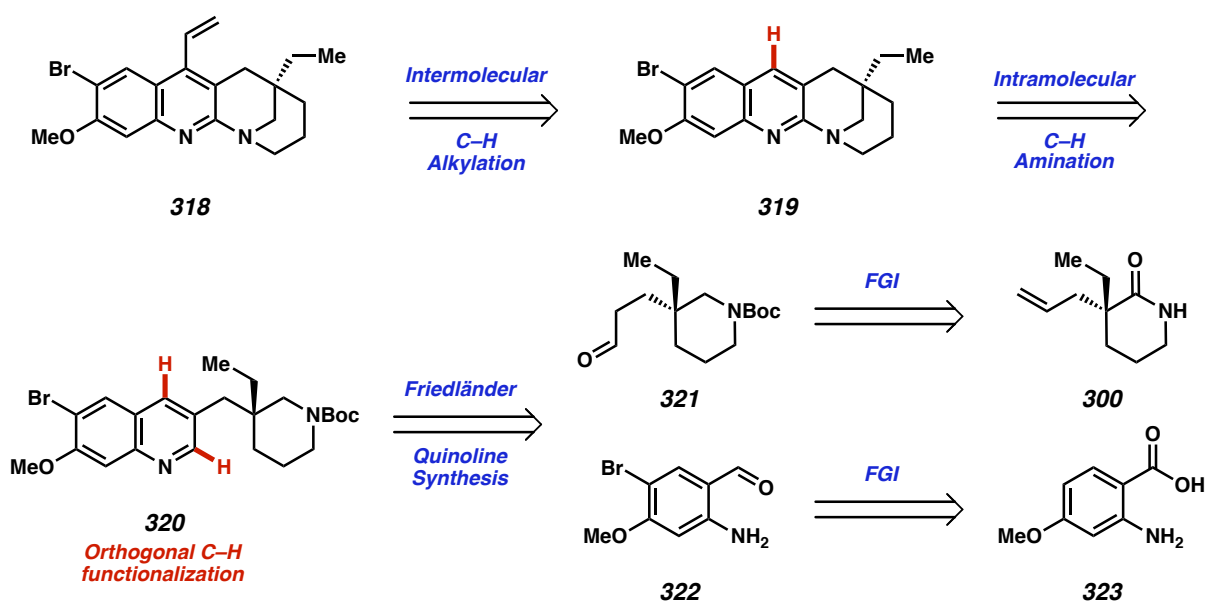
In summary, we have completed an 11-step synthesis of eburnamine (**91**) from δ -valerolactam (6 steps from conserved lactam building block (**300**)). Key steps in this route include a Fischer indole synthesis, Bischler–Napieralski cyclization, and diastereoselective hydrogenation. With the exception of the final reduction, all reactions have been performed on gram-scale. To

date, this marks the shortest asymmetric synthesis of eburnamonine (**91**) or eburnamine (**92**) and the first to utilize asymmetric catalysis.

2.3 TOTAL SYNTHESIS OF EUCOPHYLLINE

2.3.1. Retrosynthetic Analysis

Scheme 2.19. Retrosynthetic analysis of eucophylline coupling partner.



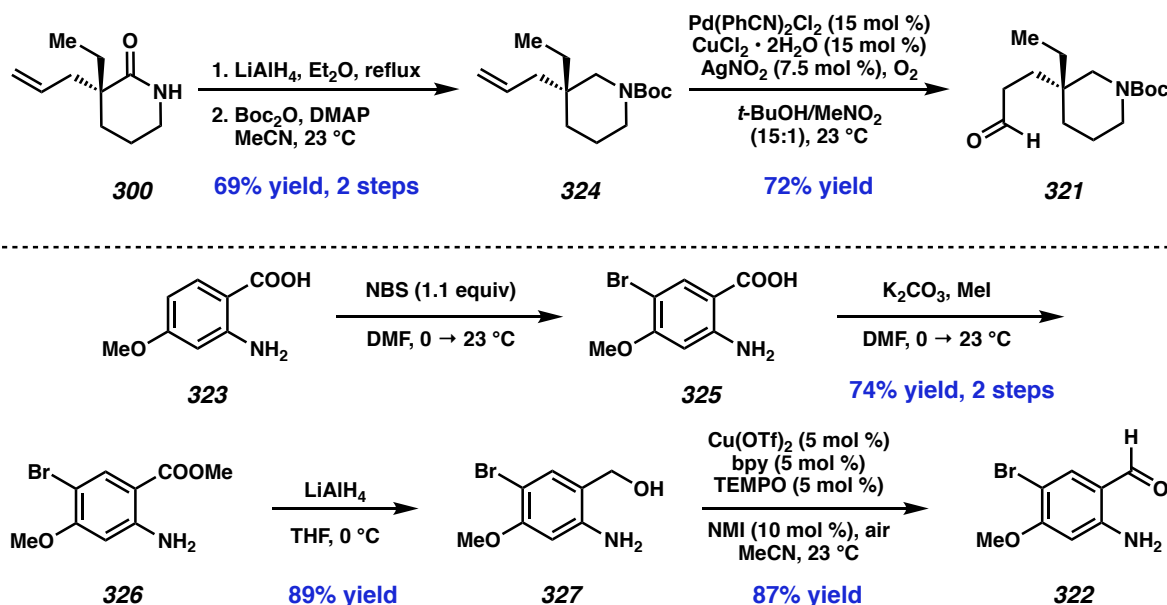
To facilitate our eventual late-stage coupling to access leucophyllidine (**203**), we elected to target brominated coupling partner **318** to provide a functional handle at the eventual site of dimerization (Scheme 2.20). Retrosynthetically, we envisioned appending the vinyl fragment through an *intermolecular* alkylation at C(4) from tetracycle **319**, and constructing the C–N bond through an *intramolecular* amination at C(2) from quinoline **320**, we believed this orthogonal C–H functionalization strategy would remove a number of inefficient functional group interconversion (FGI) steps and allow for a broader range of quinoline synthesis methods to be applied. The quinoline would be formed through a Friedländer synthesis, disconnecting across the

central heterocyclic ring to aldehyde **321** and *o*-aminoaldehyde **322**. The former would be accessed from enantioenriched lactam **300**, while the latter would be synthesized from commercially available 2-amino-4-methoxybenzoic acid **323**.

2.3.2. Advancement to the Friedländer Quinoline Synthesis Product

Starting from lactam **300**, reduction with lithium aluminum hydride followed by Boc protection affords piperidine **324** in 69% yield over two steps (Scheme 2.20). Our initial attempts to functionalize the allyl fragment using hydroboration/oxidation reactions were met with surprisingly low yields. However, we found that the anti-Markovnikov selective Wacker oxidation developed by the Grubbs²⁴ and Stoltz²⁵ groups could provide aldehyde **321** directly on gram-scale with no detectable amount of the ketone isomer.

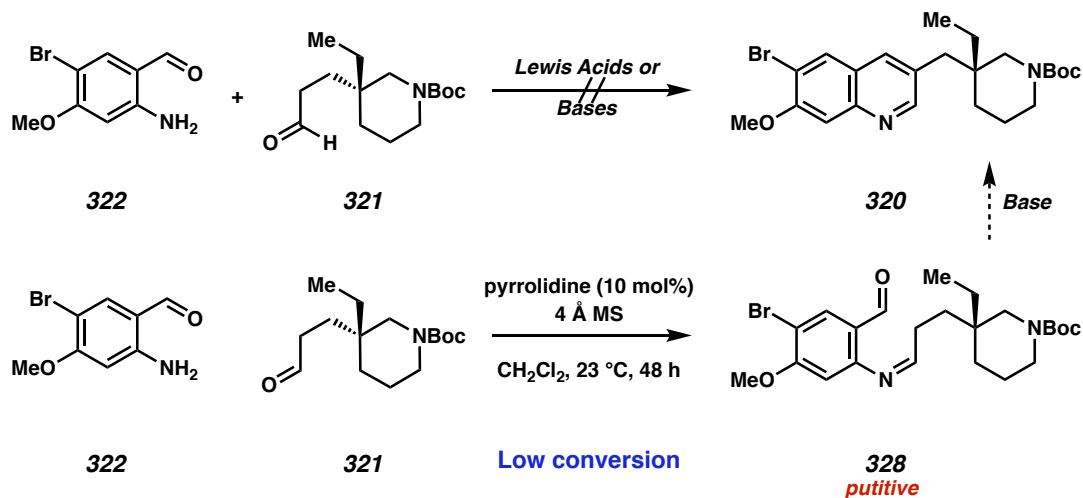
Scheme 2.20. Synthesis of Friedländer precursors.



To access the aryl coupling partner, 2-amino-4-methoxybenzoic acid **323** is advanced to bromide **325** with NBS, then alkylated to afford methyl ester **326**. The ester is then reduced with

lithium aluminum hydride to benzyl alcohol **327** then oxidized to *o*-aminoaldehyde **322** under conditions described by Stahl.²⁶

Scheme 2.21. Unsuccessful Friedländer attempts.

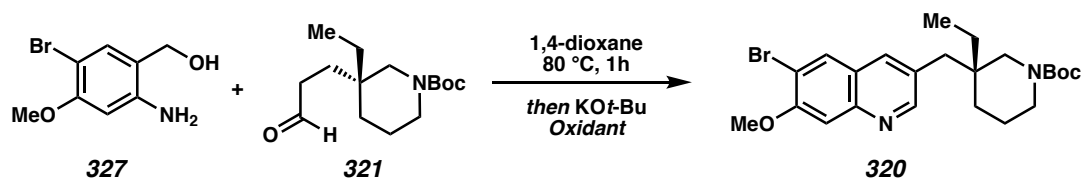


After a screen of Lewis acidic and Brønsted basic conditions, we were unable to successfully synthesize the quinoline **320** from our precursors **321** and **322** (Scheme 2.21).²⁷ Attempts to perform this reaction stepwise—first through condensation to form the *N*-aryl imine **328**, then subjection to basic conditions to cyclize—revealed that imine condensation with the desired aniline derivative was extremely slow. Even under conditions described by the Cid group to catalyze aldimine formations²⁸ yielded only trace condensation.

To circumvent this issue, we implemented conditions described by Verpoort and coworkers for the synthesis of 3-monosubstituted quinolines²⁹ starting from amino alcohol **327**; mechanistically, the benzyl alcohol is hypothesized to participate more readily in imine condensations before an in-situ Oppenauer-Woodward oxidation³⁰ (*KOt*-Bu and benzophenone) generates the carbonyl prior to cyclization. While Verpoort's standard conditions were unsuccessful (entry 1), we found that the desired quinoline **320** could be obtained in good yield by increasing the proportion of base and oxidant (entry 2-4), with 2.5 equivalents of *KOt*-Bu and 5.0

equivalents of benzophenone proving optimal. Changing the oxidant to fluorenone (entry 5) or DDQ (entry 6) diminished the yield, and no product was observed when the temperature was lowered to 60 °C (Entry 7). When scaled to 0.5 mmol of aldehyde however, we observed a decrease to 45% yield (entry 8). By adding the base as a solution in 1,4-dioxane over 30 minutes (entry 9), we improved the yield to 74% on gram-scale.

Table 2.3. Optimization of the Friedländer quinoline synthesis.



Entry	KOt-Bu	Oxidant	t (h)	T (°C)	Yield	Notes
1	1.1 equiv	Benzophenone (1.2 equiv)	2	80	0%	Standard conditions
2	2.5 equiv	Benzophenone (5.0 equiv)	2	80	61%	--
3	3.0 equiv	Benzophenone (10.0 equiv)	2	80	48%	--
4	2.5 equiv	Fluorenone 5.0 equiv)	2	80	20%	Incomplete oxidation
5	1.1 equiv	DDQ (1.2 equiv)	2	80	16%	Multiple side products
6	2.5 equiv	Benzophenone (5.0 equiv)	2	60	0%	Incomplete oxidation
7	2.5 equiv	Benzophenone (5.0 equiv)	1	80	45%	0.5 mmol scale.
8	2.5 equiv	Benzophenone (5.0 equiv)	1	80	69%	1.0 mmol scale. Slow addition of KOt-Bu
9	2.5 equiv	Benzophenone (5.0 equiv)	1	80	74%	3.6 mmol scale. Slow addition of KOt-Bu

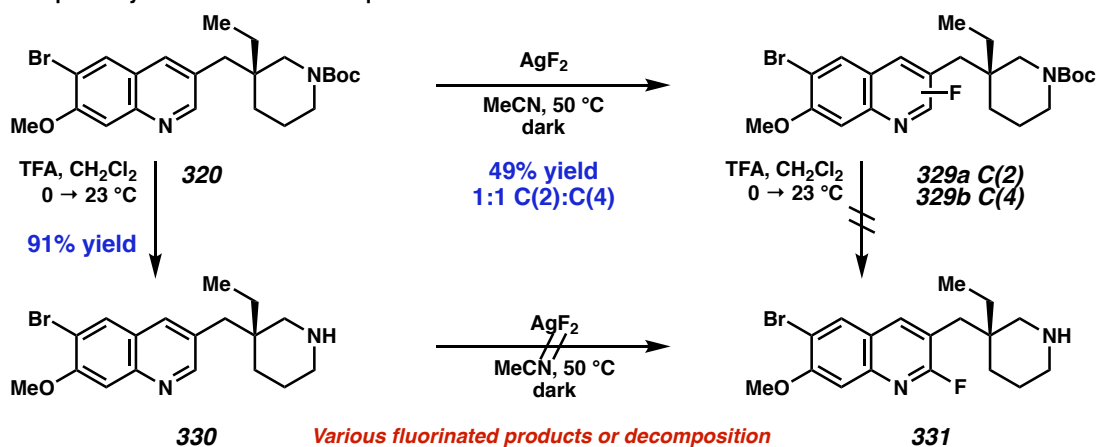
*0.1 mmol scale unless otherwise noted

2.3.3. Intramolecular C–H Amination: Discovery of a Sn(II)-mediated method

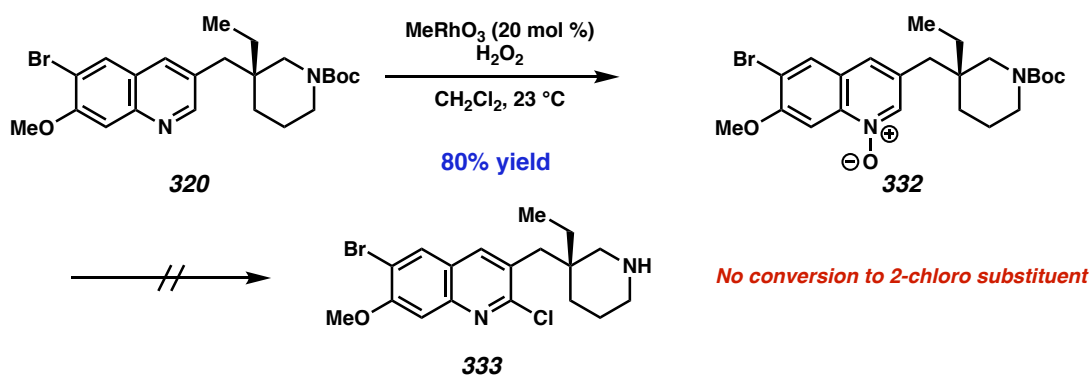
With quinoline **320** in hand, we turned our attention to the first of two C–H functionalizations. Though 2-fluoroquinoline **329a** and 4-fluoroquinoline **329b** could be accessed using the Ag(II) protocol described by Hartwig,³¹ the yield was modest and subsequent deprotection led only to decomposition (Scheme 2.22A). While Boc-deprotection afforded free amine **330** in excellent yield, the subsequent treatment with AgF₂ led to a complex mixture of fluorinated and bisfluorinated products.

Scheme 2.22. Initial C(2)-H functionalization studies.

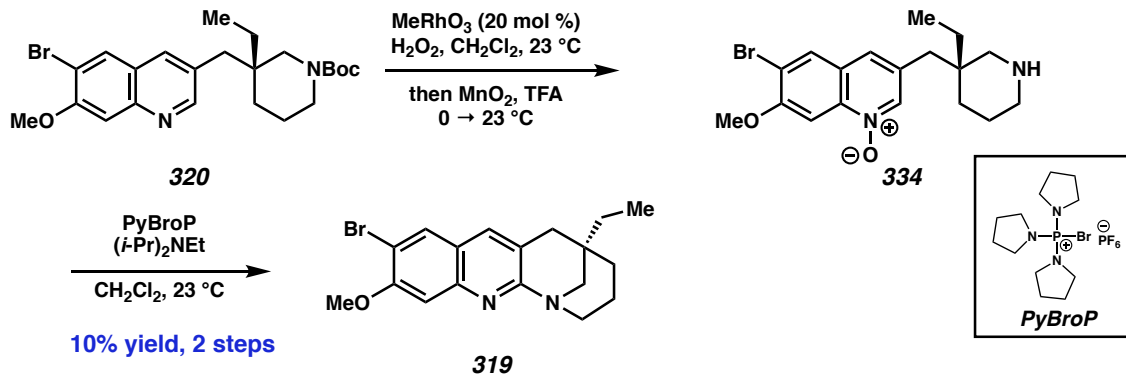
A. Attempts to synthesize 2-fluorinated quinolines



B. Attempts to synthesize 2-chlorinated quinolines



C. Direct N-oxide functionalization

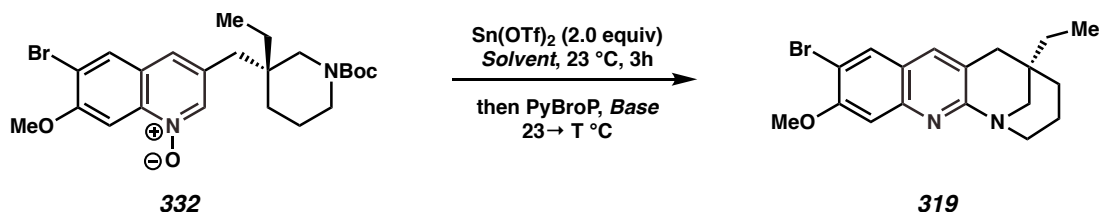


We then turned our attention to quinoline N-oxide functionalization. Quinoline **320** was successfully oxidized under Sharpless' conditions to access N-oxide **332**,³² but advancement to the corresponding 2-chloroquinoline **333** was not successful (Scheme 2.22B). Motivated by recent

advances in direct *N*-oxide functionalization, we performed the Re-catalyzed *N*-oxidation followed by Boc-deprotection in one-pot (Scheme 2.22C). Intermediate **334** then was subjected to the PyBroP-mediated amination³³ developed by Londregan and coworkers to afford tetracycle **319**, albeit in 10% yield over 2 steps.

Due to the polarity and instability of Boc-protected *N*-oxide **334**, we elected to modify our order of steps to avoid the direct isolation of this product. First, we subjected Boc-protected *N*-oxide **319** to Sn(OTf)₂ deprotection as described by Reddy³⁴, then added PyBroP and Hünig's base in the same pot to promote the subsequent cyclization. Though no product was observed at room temperature (Table 2.4, entry 1), increasing to 40 °C generated tetracycle **319** in 41% yield (Entry 2), though further heating caused yield to diminish (Entry 3); switching to other solvents like THF led to a complete shutdown of cyclization (Entry 4). Triethylamine boosted the yield slightly (entry 5), while utilizing a 1M NaOH workup led to a significant improvement (entry 6).

Table 2.4. Discovery of Sn(II)-mediated cyclization.



Entry ^a	PyBroP	Base	Solvent	T (°C)	Yield ^b
1	1.3 equiv	<i>i</i> -Pr ₂ NEt (3.8 equiv)	CH ₂ Cl ₂	23	0%
2	1.3 equiv	<i>i</i> -Pr ₂ NEt (3.8 equiv)	CH ₂ Cl ₂	40	41%
3	1.3 equiv	<i>i</i> -Pr ₂ NEt (3.8 equiv)	CH ₂ Cl ₂	50	36%
4	1.3 equiv	<i>i</i> -Pr ₂ NEt (3.8 equiv)	THF	50	0%
5	1.3 equiv	Et ₃ N (3.8 equiv)	CH ₂ Cl ₂	40	46%
6 ^c	1.3 equiv	Et ₃ N (3.8 equiv)	CH ₂ Cl ₂	40	56%
7 ^c	None	Et ₃ N (3.8 equiv)	CH ₂ Cl ₂	40	57%
8 ^{c,d,e}	None	Et ₃ N (5.0 equiv)	CH ₂ Cl ₂	40	81%
9 ^{c,d,e,f}	None	Et ₃ N (5.0 equiv)	CH ₂ Cl ₂	40	79%

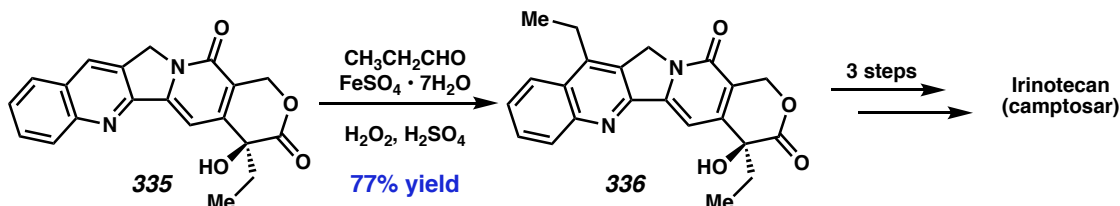
a) 0.1 mmol scale reactions unless noted. b) NMR yields using 1,3,5-trimethoxybenzene as internal standard unless noted. c) 1N NaOH workup. d) 2.5 equiv Sn(OTf)₂. e) isolated yield, f) Combined yield of twelve 0.1mmol reactions run in parallel.

While performing order-of-addition studies, we observed trace product formation by LCMS when base was added before PyBroP. Upon heating this reaction, we were surprised to observe identical yields in the absence of PyBroP altogether (Entry 7), suggesting Sn(II) was the *N*-oxide activating agent. Finally, we found rigorous exclusion of water and an increase of reagent equivalents could generate the desired tetracycle in 81% yield (Entry 8). Though scalability issues were experienced due to the heterogeneous nature of the reactions, we were able to obtain 750 mg of tetracycle **319** by conducting a series of reactions in parallel (Entry 9).

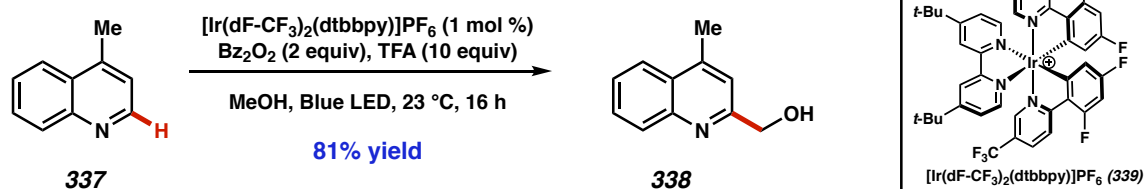
2.3.4. Intermolecular C–H Alkylation: Investigation of a Minisci Alkylation

Scheme 2.23. Reported Minisci conditions and application to the eucophylline tetracycle.

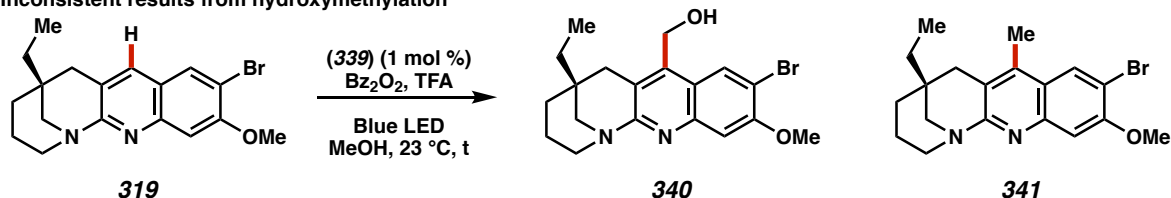
A. Sawada (1991): Synthesis of camptothecin derivatives using Minisci Reaction



B. DiRocco and Kraska (2016): Photoredox-mediated Minisci addition of hydroxymethyl radicals



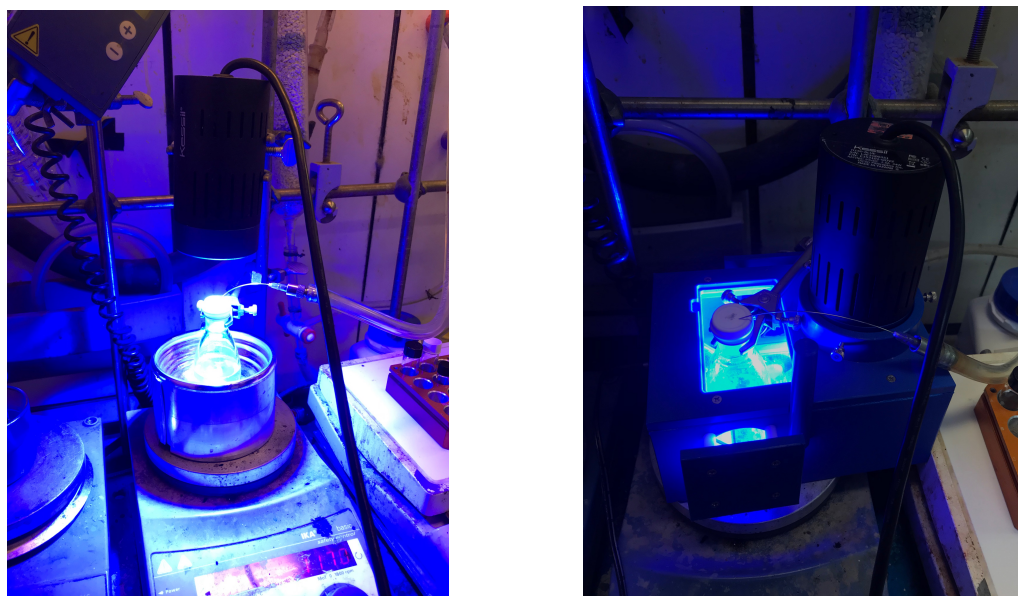
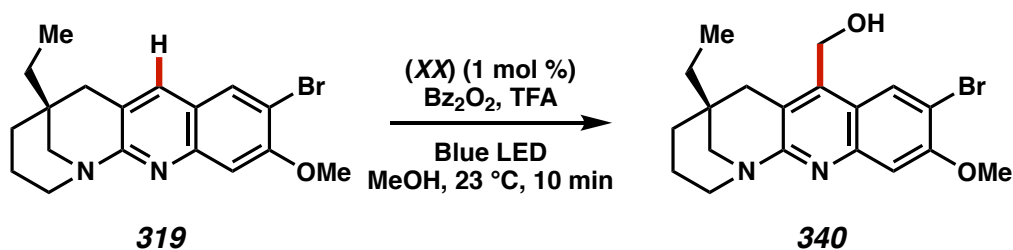
C. Inconsistent results from hydroxymethylation



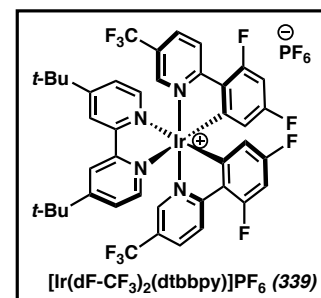
Trial	Yield 339	Yield 334	<i>t</i> (min)
1	56%	0%	10
2	0%	55%	15
3	0%	80%	120

To accomplish our second C–H functionalization, we elected to investigate the Minsci reaction³⁵ due to its established utility in C(4) quinoline functionalization of densely functionalized natural products such as camptothecin³⁶ ((**335**) → **336**, Scheme 2.23A). While “classical” conditions lead to numerous oxidized side products, we were delighted to find that the mild photoredox-mediated conditions described by DiRocco and Krska³⁷ (Scheme 2.23B) were much more tolerant of our system. While we successfully obtained alcohol **340** on our first attempt, we were disappointed to observe that the reaction was poorly reproducible and frequently generated methylated product **341** as the exclusive product (2.23B). Attributing this issue to inconsistencies in reaction setup, we found that switching our reaction setup from a Dewar with suspended LED to a Hepatochem photobox with an internal fan consistently provided alcohol **340** as the major product in good yield (Figure 1.2).

While a consistent reaction was obtained, we noted that the reaction remained unusually fast (40 minutes) in comparison to the reported examples (~16 hours), and we began to suspect that a background reaction may be occurring. Upon conducting control experiments (Table 2.5), we were surprised to discover that the reaction proceeded in the absence of iridium complex (**339**), suggesting that our substrate itself is serving as its own photocatalyst for this reaction. Electron-deficient quinolines have been reported to promote hydroxyalkylations under photochemical conditions,³⁸ and DiRocco and Krska note that this “autophotocatalysis” occurs with several reported substrates when the intensity of the light source is increased.³⁷

Figure 2.3. First and second generation Minisci reaction setup.**Table 2.5.** Control experiments for Minisci alkylation.

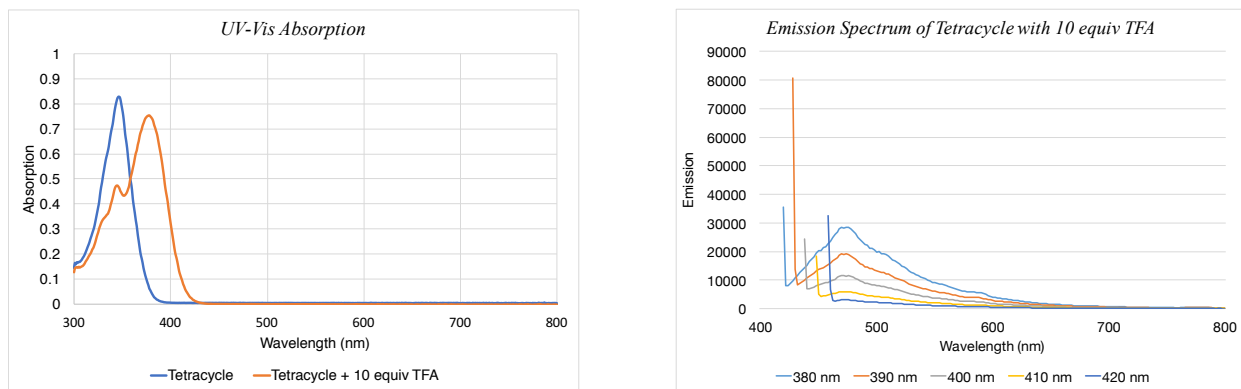
Entry	Variation	Product Observed?
1	None	Yes
2	No [Ir(dF-CF ₃) ₂ (dtbbpy)]PF ₆	Yes
3	No Bz ₂ O ₂	No
4	No Blue LED (dark)	No
5	No Blue LED (ambient light)	No



We acquired UV/vis data for tetracycle **319** (Figure 2.4) to better understand its photophysical properties. While the maximum wavelength of absorption (λ_{abs}) for tetracycle **319** lies soundly in the ultraviolet region, the addition of 10 equivalents of TFA to mimic reaction conditions caused a significant red shift ($\lambda_{\text{abs}} = 346 \rightarrow 378$ nm); when the protonated tetracycle

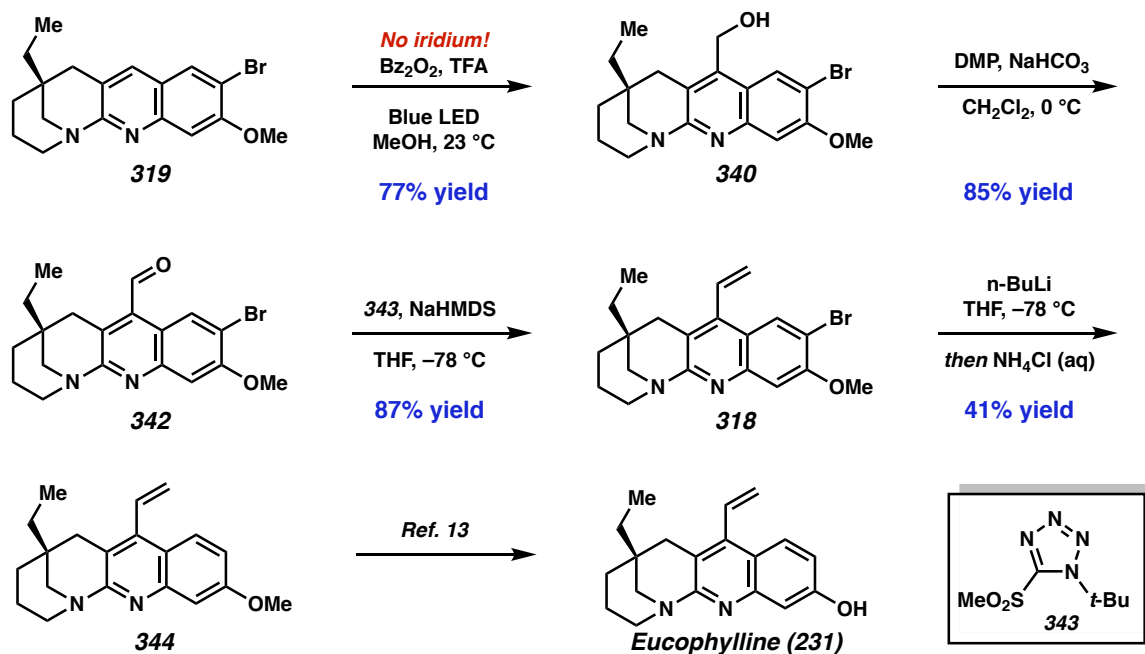
was irradiated at 380 nm, it recorded a maximum wavelength of emission (λ_{em}) at 476 nm. These values are remarkably similar to iridium complex (**339**) ($\lambda_{abs} = 380$ nm and 470 nm in MeCN),³⁹ lending support to this “autophotocatalytic” hypothesis. Further investigations of this transformation are ongoing.

Figure 2.4. Absorption and emission spectra for Minsici precursor.



2.3.5 Final Steps

Following our Minsici investigations, we found that the hydroxymethylation could be easily scaled to access alcohol **340**. This intermediate is subsequently oxidized to aldehyde **342** with DMP. Though methylenation under Wittig conditions were low yielding, we found that the modified Julia-Kocienski methylenation with sulfone **343** described by Aïssa⁴⁰ could afford the targeted coupling partner, alkene **318**, in 87% yield. To complete the formal synthesis, we performed lithiation/protonation to access *O*-methyleucophylline **344** as had been reported in the Landais route.¹³

Scheme 2.24. Formal synthesis of eucophylline.**2.3.6 Concluding Remarks**

In summary, we have completed a 16-step formal synthesis of eucophylline (**231**) from δ -valerolactam (11 steps from conserved lactam building block **300**). Key steps in this route include a Friedländer quinoline synthesis, an unprecedented Sn(II)-mediated C–H amination, and a photoredox-mediated Minisci hydroxymethylation promoted by a photoactive substrate. This route provides us with ample access to key coupling partner **318** to investigate our key cross-coupling en route to leucophyllidine (**230**).

2.4 References

-
- (1) Gan, C-Y.; Robinson, W.T.; Etoh, T.; Hayashi, M.; Komiyama, K.; Kam, T-S. *Org. Lett.* **2009**, *11*, 3962 – 3965.
 - (2) Deguichi, J.; Shosji, T.; Nugroho, A.E.; Hirasawa, Y.; Hosoya, T.; Shirota, O.; Awang, K.; Hadi, A.H.A.; Morita, H. *J. Nat. Prod.* **2010**, *73*, 1727–1729.
 - (3) Bartlett, M.F.; Taylor, W.I.; Hamet, R. *C.R. Acad. Sci. Paris.* **1959**, *249*, 1259.
 - (4) Naaz, H.; Singh, S.; Pandey, V.P.; Singh, P.; Swivedi, U.N. *Indian Journal of Biochemistry & Biophysics* **2013**, *50*, 120–125.
 - (5) Lounasmaa, M.; Tolvanen, A. In *The Alkaloids*; Cordell, G. A., Ed.; Academic Press: New York, **1992**; Vol. 42, p 1.
 - (6) Kutney, J.P.; Beck, J.F.; Nelson, V.R.; Sood, R.S. *J. Am. Chem. Soc.* **1971**, *92*, 255–257.
 - (7) Pandey, G.; Mishra, A.; Khamrai, J. *Org. Lett.* **2017**, *19*, 3267 – 3270.
 - (8) For racemic total syntheses of eburnamonine or eburnamine, see: (a) Bartlett, M. F.; Taylor, W. I. *J. Am. Chem. Soc.* **1960**, *82*, 5941–5942. (b) Barton, J.E.D.; Harley-Mason, J.; *J. Chem. Soc. Chem. Comm.* **1965**, 298–299. (c) Wenkert, E.; Wickberg, B. *J. Am. Chem. Soc.* **1965**, *87*, 1580–1589. (d) Cartier, D.; Lévy, J.; LeMen, *J. Bull. Soc. Chim. Fr.* **1976**, 1961. (e) Costerousse, G.; Buendia, J.; Toromanoff, E.; Martell, J.; *J. Bull. Soc. Chim. Fr.* **1978**, II-355. (f) Hermann, J. L.; Cregge, R. J.; Richman, J. E.; Kieczkowski, G. R.; Normandin, S. N.; Quesada, M. L.; Semmelhack, C. L.; Poss, A. J.; Schlessinger, R. H. *J. Am. Chem. Soc.* **1979**, *101*, 1540–1544. (g) Bólsing, E.; Klatte, F.; Rosentreter, V.; Winterfeldt, E. *Chem. Ber.* **1979**, *112*, 1902–1912. (h) Irie, K.; Okita, M.; Wakamatsu, T.; Ban, Y. *Nouv. J. Chem.* **1980**, *4*, 275. (i) Irie, K.; Ban, Y. *Heterocycles* **1981**, *15*, 201–206. (i) Kalas, G.; Malkieh, N.; Katona, I.; Kajtar-Peredy, M.; Koritsanszky, T.; Kalman, A.;

-
- Szabo, L.; Szantay, C. *J. Org. Chem.* **1985**, *50*, 3760–3767. (j) Magnus, P.; Pappalardo, P.; Southwell, I. *Tetrahedron* **1986**, *42*, 3215–3222. (k) Shono, T.; Matsumura, H.; Ogaki, M.; Onomura, O. *Chem. Lett.* **1987**, *16*, 1447–1450. (l) Wenkert, E.; Hudlicky, T. *J. Org. Chem.* **1988**, *53*, 1953–1957. (m) Wasserman, H. H.; Kuo, G.-H. *Tetrahedron Lett.* **1989**, *30*, 873–876. (n) Meyers, A. I.; Romine, J.; Robichaud, A. J. *Heterocycles* **1990**, *30*, 339–340. (o) Gmeiner, P.; Feldman, P. L.; Chu-Moyer, M. Y.; Rapoport, H. *J. Org. Chem.* **1990**, *55*, 3068–3074. (p) Ihara, M.; Takahashi, M.; Taniguchi, N.; Yasui, K.; Niitsuma, H.; Fukumoto, K. *J. Chem. Soc., Perkin Trans. 1*, **1991**, 525–535. (o) Lounasmaa, M.; Karvinen, E. *Heterocycles* **1992**, *34*, 1773–1782. (p) Ghosh, A. K.; Kawahama, R. *J. Org. Chem.* **2000**, *65*, 5433–5435.
- (9) For asymmetric syntheses of eburnamonine or eburnamine, see: (a) Takano, S.; Yonaga, M.; Morimoto, M.; Ogasawara, K. *J. Chem. Soc., Perkin Trans. 1*, **1985**, 305–309. (b) Hakam, K.; Thielmann, M.; Thielmann, T.; Winterfeldt, E. *Tetrahedron* **1987**, *43*, 2035–2044. (c) Node, M.; Nagasawa, H.; Fuji, K. *J. Am. Chem. Soc.* **1987**, *109*, 7901–7903. (d) Node, M.; Nagasawa, H.; Fuji, K. *J. Org. Chem.* **1990**, *55*, 517–521. (e) Schultz, A. G.; Pettus, L. *J. Org. Chem.* **1997**, *62*, 6855–6861. (e) Wee, A. G. H.; Yu, Q. *Tetrahedron Lett.* **2000**, *41*, 587–590. (f) Wee, A. G. H.; Yu, Q. *J. Org. Chem.* **2001**, *66*, 8935–8943. (g) Iwabuchi, Y.; Hayashi, M.; Satoh, A.; Shibuya, M.; Ogasawara, K. *Heterocycles* **2009**, *77*, 855–863. (h) Prasad, K. R.; Nidhiry, J. E. *Synlett* **2012**, *23*, 1477–1480.
- (10) Following the initiation of these studies, Trost and coworkers published a route to related C19-oxoeburane alkaloids through Pd-catalyzed asymmetric allylic alkylation. See: Trost, B.M.; Bai, Y.; Bai, W.-J.; Schultz, J.E. *J. Am. Chem. Soc.* **2019**, *141*, 4811–4814.
- (11) Castedo, L.; Harley-Mason, J.; Leeny, T.J. *J. Chem. Soc. Chem. Comm.* **1968**, 1168.

-
- (12) Lounasmaa, M.; Berner, M.; Brunner, M.; Soumalainen, H.; Tolvanen, A. *Tetrahedron* **1998**, *54*, 10205–10216.
- (13) Hassan, H.; Mohammed, S.; Robert, F.; Landais, Y. *Org. Lett.* **2015**, *17*, 4518–4521.
- (14) For select reviews, see: (a) Korch, K. M., Loskot, S. A. and Stoltz, B. M. (2017). Asymmetric Synthesis of Quaternary Stereocenters via Metal Enolates. In PATAI'S Chemistry of Functional Groups, Z. Rappoport (Ed.).
doi:10.1002/9780470682531.pat0858. (b) Liu, Y.; Han, S-J.; Liu, W-B.; Stoltz, B.M. *Acc. Chem. Res.* **2015**, *48*, 740–751. (c) Behenna, D.C.; Mohr, J.T.; Sherden, N.H.; Marinescu, S.C.; Harnet, A.M.; Tani, K.; Seto, M.; Ma, S.; Novák, Z.; Krout, M.R.; McFadden, R.M.; Roizen, J.L.; Enquist, J.A.; White, D.E.; Levine, S.R.; Petrova, K.V.; Iwashita, A.; Virgil, S.C.; Stoltz, B.M. *Chem. –Eur. J.* **2011**, *17*, 14199–14223.
- (15) Behenna D.C.; Liu Y.; Yurino T.; Kim J.; White D.E.; Virgil S.C.; Stoltz B.M. *Nature Chem.* **2012**, *4*, 130–133.
- (16) (a) Pritchett B.P.; Kikuchi J.; Numajiri Y.; Stoltz B.M. *Angew Chem. Int. Ed* **2016**, *56*, 13529–13532. (b) Pritchett B.P.; Donckele E.J.; Stoltz B.M. *Angew. Chem. Int. Ed.* **2017**, *56*, 12624-12627.
- (17) (a) Numajiri Y. Pritchett B.P.; Chiyoda K.; Stoltz B.M. *J. Am. Chem. Soc.* **2015**, *137*, 1040-1043. (b) Fulton T.J.; Chen A.Y.; Stoltz B.M. *ChemRxiv. Preprint. DOI: 10.26434/chemrxiv.11900331.v1.*
- (18) The previously reported route was longer by three steps, required several challenging separations by flash column chromatography and utilized superstoichiometric trimethylaluminum.

-
- (19) McDougal, N.T.; Streuff, J.; Mukherjee, H.; Virgil, S.C.; Stoltz, B.M. *Tetrahedron Lett.* **2010**, *51*, 5550–5554.
- (20) Marziale, A.N.; Duquette, D.C.; Craig II, R.A.; Kim, K.E.; Liniger, M.; Numajira Y.; Stoltz B.M. *Adv. Synth Catal.* **2015**, *357*, 2238 – 2245.
- (21) Varseev, G.N.; Maier, M.E. *Org. Lett.* **2005**, *7*, 3881–3885.
- (22) Lancefield, C.S.; Zhou, L.; Lébl, T.; Slawin, A.M.Z.; Westwood, N.J. *Org. Lett.* **2012**, *14*, 6166–6169.
- (23) Szabo, L.; Kalaus, G.; Szantay C. *Archiv der Pharmazie*, **1983**, *316*, 629 –638.
- (24) (a) Wickens, Z.K.; Morandi, B.; Grubbs, R.H. *Angew. Chem. Int. Ed.* **2013**, *52*, 11257–11260. (b) Wickens, Z.K.; Skakuj, K.; Morandi, B.; Grubbs, R.H. *J. Am. Chem. Soc.* **2014**, *136*, 890–893.
- (25) Kim, K.E.; Li, J.; Stoltz, B.M.; Grubbs R.H.; *J. Am. Chem. Soc.* **2016**, *138*, 13179 – 13182.
- (26) Steves, J. E.; Stahl, S. S. *J. Am. Chem. Soc.* **2013**, *135*, 15742–15745.
- (27) Marco-Contelles, J.; Perez-Mayoral, E.; Samadi, A.; do Carmo Carrieras, M.; Soriano, E. *Chem. Rev.* **2009**, *109*, 2652–2671.
- (28) Morales, S.; Guijarro, F.G.; Garcia Ruano, J.L.; Cid, M.B. *J. Am. Chem. Soc.* **2014**, *136*, 1082–1089.
- (29) Vander Mierde, H.; Van Der Poort, P.; Verpoort, F. *Tetrahedron Lett.* **2009**, *50*, 201–203.
- (30) Woodward, R.B.; Wendler, N.L.; Brutschy, F.J. *J. Am. Chem. Soc.* **1945**, *67*, 1425–1429.
- (31) (a) Fier, P.S.; Hartwig, J.F. *Science* **2013**, *342*, 956–960. (b) Fier, P.S.; Hartwig, J.F. *J. Am. Chem. Soc.* **2014**, *136*, 10139–10147.

-
- (32) Coperet C.; Adolfsson H.; Chiang J.P.; Yudin A.K.; Sharpless K.B. *Tetrahedron Lett.* **1998**, *39*, 761–764.
- (33) Londregan A.T.; Jennings S.; Wei L. *Org. Lett.* **2011**, *13*, 1840–1843
- (34) Bose, D.S.; Kumar, K.K.; Reddy, A.V.N. *Synth. Commun.*, **33**, 445–450.
- (35) Duncton, M.A.J. *Med. Chem.. Commun.* **2011**, *2*, 1135–1161.
- (36) Sawada, S., Okajima, S., Aiyama, R. Nokata, K., Furuta, T., Yokokura, T., Sugino, E., Yamaguchi, K., Miyasaka, T. *Chem. Pharm. Bull.* **1991**, *39*, 1446–1454.
- (37) Huff C.A.; Cohen R.D.; Dykstra K.D.; Steckfuss E.; DiRocco D.A.; Krska S.W.; *J. Org. Chem.* **2016**, *81*, 6980 – 6987.
- (38) Ono, I.; Hata, N. *Bull. Chem. Soc. Jpn.* **1987**, *60*, 2891–2897.
- (39) (a) Lowry, M. S.; Goldsmith, J. I.; Slinker, J. D.; Rohl, R.; Pascal, R. A.; Malliaras, G. G.; Bernhard, S. *Chem. Mater.* **2005**, *17*, 5712–5719. (b) Prier, C.K.; Rankic, D.A.; MacMillan, D.W.C. *Chem. Rev.* **2015**, *113*, 5322–5363.
- (40) Aissa C. *J. Org. Chem.* **2006**, *71*, 360–363.

2.5 EXPERIMENTAL SECTION

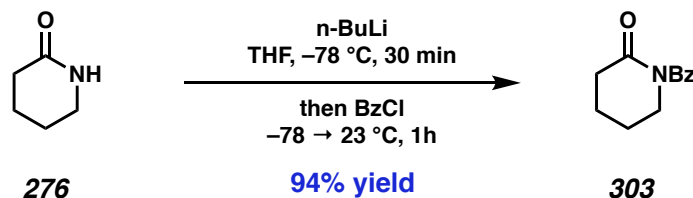
2.5.1 Materials and Methods

Unless otherwise stated, reactions were performed in flame-dried glassware under an argon or nitrogen atmosphere using dry, deoxygenated solvents. Solvents were dried by passage through an activated alumina column under argon.¹ Reaction progress was monitored by thin-layer chromatography (TLC) or Agilent 1290 UHPLC-LCMS. TLC was performed using E. Merck silica gel 60 F254 precoated glass plates (0.25 mm) and visualized by UV fluorescence quenching, *p*-anisaldehyde, CAM, or KMnO₄ staining. Silicycle SiliaFlash® P60 Academic Silica gel (particle size 40–63 nm) was used for flash chromatography. ¹H and ¹³C NMR spectra were recorded on a Varian Inova 500 (500 MHz and 126 MHz, respectively) and a Bruker AV III HD spectrometer equipped with a Prodigy liquid nitrogen temperature cryoprobe (400 MHz and 101 MHz, respectively) and are reported in terms of chemical shift relative to CHCl₃ (δ 7.26 and δ 77.16, respectively), CD₂Cl₂ (δ 5.32 and δ 53.84, respectively), (CD₃)₂SO (δ 2.50 and δ 39.52, respectively) and CD₃CN (δ 1.94 and 118.26). Data for ¹H NMR are reported as follows: chemical shift (δ ppm) (multiplicity, coupling constant (Hz), integration). Multiplicities are reported as follows: s = singlet, d = doublet, t = triplet, q = quartet, p = pentet, sept = septuplet, m = multiplet, br s = broad singlet, br d = broad doublet, br t = broad triplet, app = apparent. Some reported spectra in CDCl₃ include minor solvent impurities of water (δ 1.56 ppm), ethyl acetate (δ 4.12, 2.05, 1.26 ppm), dichloromethane (δ 5.30 ppm), acetone (δ 2.17 ppm), grease (δ 1.26, 0.86 ppm), and/or silicon grease (δ 0.07 ppm), which do not impact product assignments.² Data for ¹³C NMR are reported in terms of chemical shifts (δ ppm). IR spectra were obtained by use of a Perkin Elmer Spectrum BXII spectrometer using thin films deposited on NaCl plates and reported in frequency of absorption (cm⁻¹). Optical rotations were measured with a Jasco P-2000

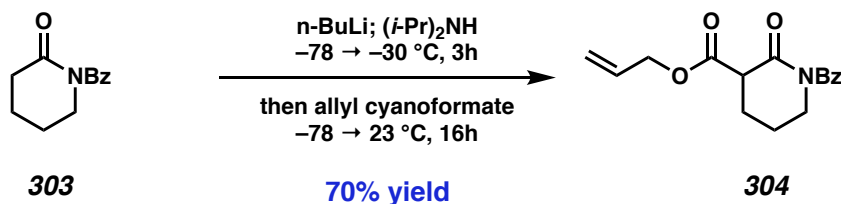
polarimeter operating on the sodium D-line (589 nm), using a 100 mm path-length cell, and are reported as $[\alpha]_T$ (concentration in g/100 mL, solvent). Analytical SFC was performed with a Mettler SFC supercritical CO₂ analytical chromatography system utilizing Chiralpak OD-J column (4.6 mm x 25 cm) obtained from Daicel Chemical Industries, Ltd. High resolution mass spectra (HRMS) were obtained from the Caltech Mass Spectral Facility using a JEOL JMS-600H High Resolution Mass Spectrometer in fast atom bombardment (FAB+) or electron ionization (EI+) mode, or Agilent 6200 Series TOF with an Agilent G1978A Multimode source in mixed ionization mode (MM: ESI/APCI).

Reagents were purchased from Sigma-Aldrich, Acros Organics, Strem, or Alfa Aesar and used as received unless otherwise stated. *n*-butyllithium was titrated prior to use according to the method of Gilman.³ Di-*iso*-propylamine was distilled from calcium hydride immediately prior to use. NBS was purchased from Sigma Aldrich, recrystallized from H₂O, and stored in a -25 °C freezer. PhNHNH₂•HCl was purchased from Sigma Aldrich, recrystallized from H₂O and EtOH, and stored in a -25 °C freezer. MeOH was distilled from magnesium methoxide immediately prior to use. Allyl cyanoformate⁴, (*R*)-(CF₃)₃-*t*-Bu-PHOX **285**⁵, dioxolane⁶ **305** and tetrazole⁷ **343** were prepared by known methods.

2.4.2 Experimental Procedures



***N*-Benzoyl δ -valerolactam 303:** Following a modified procedure described by Gigant,⁸ a flame-dried 1L flask with stir bar was charged with δ -valerolactam **276** (9.9 g, 100.0 mmol, 1.0 equiv) and THF (500 mL, 0.2 M), then cooled to -78 °C. *n*-butyllithium (2.30M in hexanes, 43.0 mL, 99.0 mmol, 0.99 equiv) was added slowly and the solution was stirred at -78 °C for 30 minutes. Benzoyl chloride (12.8 mL, 110.0 mmol, 1.1 equiv) was added dropwise, then stirred at -78 °C for 30 minutes, removed from the cooling bath, and warmed to 23 °C over 30 minutes. The reaction was quenched with saturated ammonium chloride, transferred to a separatory funnel, and extracted with ether three times. The combined organic extracts were washed with brine, dried with magnesium sulfate, and concentrated in vacuo to produce an amorphous solid. This solid was recrystallized from toluene to afford *N*-benzoyl δ -valerolactam **303** (18.41 grams, 94%) as a white crystalline solid. ¹H NMR (400 MHz, CDCl₃) δ 7.61 – 7.52 (m, 2H), 7.52 – 7.42 (m, 1H), 7.42 – 7.33 (m, 2H), 3.80 (ddd, $J = 6.3, 5.0, 1.0$ Hz, 2H), 2.63 – 2.49 (m, 2H), 2.06 – 1.88 (m, 4H); ¹³C NMR (101 MHz, CDCl₃) δ 174.8, 173.6, 136.2, 131.6, 128.26, 128.0, 77.5, 77.4, 77.2, 76.8, 46.3, 34.8, 23.0, 21.6; IR (Neat Film, NaCl) 2961, 1673, 1388, 1286, 1265, 1159, 1146, 734 cm⁻¹; HRMS (FAB+) m/z calculated for C₁₂H₁₃NO₂ [M+H⁺]: 204.1025, found 204.1024. Data were consistent with literature values.⁸

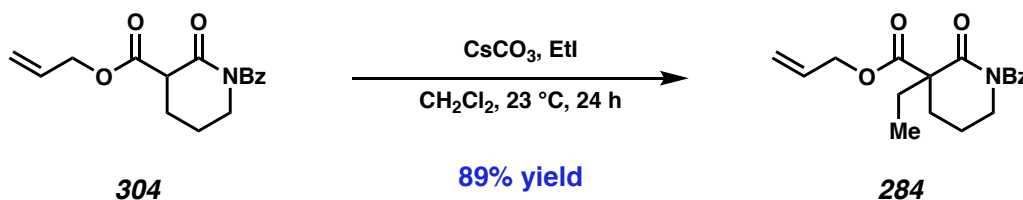


Allyl ester 304: Following the procedure described by Behenna,⁹ a flame-dried 1L three-neck round bottom flask equipped with low temperature thermometer and stir bar was charged with THF (460 mL) and freshly distilled di-*iso*-propylamine (12.93 mL, 91.62 mmol, 1.2 equiv). The flask was cooled to -78 °C and a solution of *n*-butyllithium (2.44M in hexanes, 34.4 mL, 84.0 mmol, 1.1 equiv) was added slowly. The flask was warmed to 0 °C and stirred for 30 minutes, at which point the solution turns pale yellow, then re-cooled to -78 °C.

A separate 250-mL round-bottom flask was charged with benzoyl lactam **303** (15.50 g, 76.4 mmol, 1.0 equiv) and THF (95 mL). The solution was slowly transferred to the reaction flask via cannula (NOTE: the internal temperature of the reaction should not exceed -70 °C). Upon complete addition, the reaction mixture was stirred for 2 hours at -78 °C, then 1 hour at -30 °C. The flask was re-cooled to -78 °C before neat allyl cyanoformate was added dropwise (9.33g, 84.0 mmol, 1.1 equiv). The reaction mixture was stirred at -78 °C for 2 hours, then slowly warmed up to 23 °C over 14 hours.

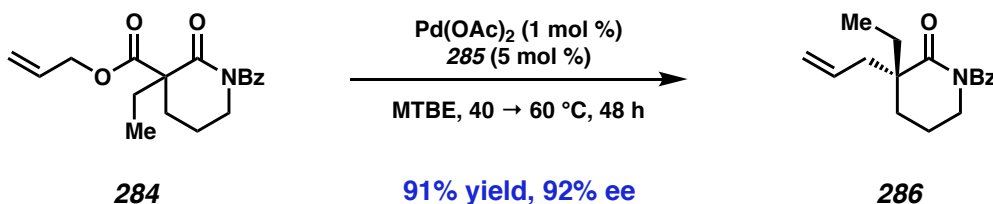
The reaction was quenched with saturated ammonium chloride, transferred to a separatory funnel, and extracted with diethyl ether (3X). The combined organic extracts were washed with brine, dried with sodium sulfate, and concentrated in vacuo. Flash column chromatography (15→20 → 25 → 30% ethyl acetate/hexanes) afforded allyl ester **304** (15.34 g, 70% yield) as a colorless oil. ¹H NMR (400 MHz, CDCl₃) δ 7.72 – 7.66 (m, 2H), 7.51 – 7.45 (m, 1H), 7.41 – 7.35 (m, 2H), 5.95 (ddt, *J* = 17.2, 10.4, 5.9 Hz, 1H), 5.37 (dq, *J* = 17.2, 1.5 Hz, 1H),

5.29 (dq, $J = 10.4, 1.2$ Hz, 1H), 4.69 (dq, $J = 5.9, 1.4$ Hz, 2H), 3.88 – 3.76 (m, 2H), 3.59 (t, $J = 6.3$ Hz, 1H), 2.39 – 2.30 (m, 1H), 2.22 – 2.13 (m, 1H), 2.12 – 2.02 (m, 1H), 2.01 – 1.90 (m, 1H). ^{13}C NMR (101 MHz, CDCl_3) δ 174.6, 169.6, 169.3, 135.4, 131.9, 131.4, 128.3, 128.2, 119.3, 66.4, 51.1, 46.3, 25.5, 20.7. IR (Neat Film, NaCl) 2960, 1737, 1674, 1448, 1389, 1285, 1259, 1146, 986, 946, 824, 799, 732, 704, 670 cm^{-1} ; HRMS (FAB+) m/z calculated for $\text{C}_{16}\text{H}_{18}\text{NO}_4$ [$\text{M}+\text{H}^+$]: 288.1236, found 288.1265. Data were consistent with literature values.⁹



β -amidoester 284: To a flame-dried 1L round-bottom flask with stir bar was added allyl ester **304** (15.33 g, 53.4 mmol, 1.0 equiv) and dichloromethane (390 mL). Cesium carbonate (76.7 g, 235.5 mmol, 4.4 equiv) was added, and the heterogeneous mixture was stirred for 10 minutes. Ethyl iodide (18.8 mL, 235.5 mmol, 4.4 equiv) was then added dropwise, and the reaction mixture was stirred for 24 hours. The reaction was quenched with ammonium chloride and extracted with dichloromethane (5X). The combined organic extracts were washed with brine, dried with sodium sulfate, and concentrated in vacuo. Flash column chromatography (15%→20%→25%→30% diethyl ether/hexanes) afforded the desired β -ketoester **304** (14.95g, 89% yield) as a light yellow oil. ^1H NMR (400 MHz, CDCl_3) δ 7.73 – 7.68 (m, 2H), 7.50 – 7.44 (m, 1H), 7.40 – 7.34 (m, 2H), 5.98 (ddt, $J = 17.2, 10.4, 5.9$ Hz, 1H), 5.40 (dq, $J = 17.2, 1.5$ Hz, 1H), 5.33 (dq, $J = 10.4, 1.2$ Hz, 1H), 4.73 (dt, $J = 5.9, 1.3$ Hz, 2H), 3.86 – 3.71 (m, 2H), 2.47 – 2.38 (m, 1H), 2.05 – 1.82 (m, 5H), 0.91 (t, $J = 7.4$ Hz, 3H). ^{13}C NMR (101 MHz, CDCl_3) δ

175.1, 172.1, 171.9, 136.0, 131.7, 131.5, 128.1 (2C), 119.7, 66.5, 57.0, 46.6, 29.9, 28.7, 20.4, 9.2. IR (Neat Film, NaCl) 2963, 1731, 1680, 1448, 1386, 1264, 1187, 1136, 1025, 797, 723, 694, 660 cm^{-1} HRMS (FAB+) m/z calculated for $\text{C}_{18}\text{H}_{22}\text{NO}_4$ $[\text{M}+\text{H}^+]$: 316.1549, found 316.1547. Data were consistent with literature values.⁹



Enantioenriched *N*-benzoyl lactam 286: A 500-mL Schlenk flask with stir bar was flame-dried and brought into a nitrogen-filled glove box. The flask was charged with palladium (II) acetate (103.5 mg, 0.461 mmol, 0.010 equiv), (*R*)- CF_3 -*t*-Bu-PHOX **285** (1.37g, 2.31 mmol, 0.05 equiv), and MTBE (190 mL) before it was sealed, removed from the glovebox, and heated to 40 $^\circ\text{C}$ for 30 minutes.

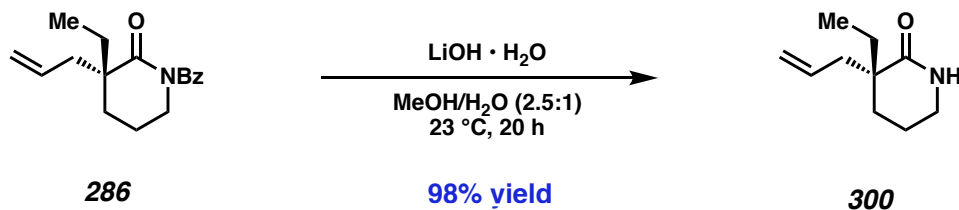
In a separate flask, racemic β -amidoester **284** (14.53 g, 46.1 mmol, 1.00 equiv) was dissolved in MTBE, then transferred to the Schlenk flask via cannula. The Schlenk flask was sealed once again and heated to 60 $^\circ\text{C}$ for 48 hours; to remove the overpressure of carbon dioxide generated during the reaction, the flask was connected to a nitrogen-containing Schlenk line and vented for about 3 seconds every hour for the first eight hours, then every 12 hours thereafter.

After complete consumption of the starting material, as determined by TLC, the flask was cooled to room temperature, transferred to a round-bottom flask, and concentrated in vacuo. Flash column chromatography (15% \rightarrow 20% \rightarrow 25% diethyl ether/hexanes) then afforded enantioenriched lactam **286** (11.40 g, 91% yield, 92% ee) as a colorless oil. ^1H NMR (400 MHz,

CDCl_3) δ 7.54 – 7.49 (m, 2H), 7.49 – 7.43 (m, 1H), 7.41 – 7.35 (m, 2H), 5.73 (dddd, $J = 16.5$, 10.6, 7.6, 7.0 Hz, 1H), 5.17 – 5.04 (m, 2H), 3.85 – 3.71 (m, 2H), 2.51 (ddt, $J = 13.8$, 7.0, 1.3 Hz, 1H), 2.27 (ddt, $J = 13.7$, 7.6, 1.1 Hz, 1H), 2.08 – 1.92 (m, 2H), 1.92 – 1.78 (m, 3H), 1.78 – 1.63 (m, 1H), 0.91 (t, $J = 7.4$ Hz, 3H); ^{13}C NMR (101 MHz, CDCl_3) δ 178.2, 175.8, 136.9, 133.8, 131.4, 128.3, 127.6, 118.9, 47.6, 47.1, 41.5, 30.5, 30.4, 19.7, 8.4. IR (Neat Film, NaCl) 3075, 2940, 2881, 1679, 1448, 1384, 1281, 1148, 916, 726, 658 cm^{-1} ; ^1H HRMS (FAB+) m/z calculated for $\text{C}_{17}\text{H}_{22}\text{NO}_2$ [$\text{M}+\text{H}^+$]: 272.1651, found 272.1675; $[\alpha]_{\text{D}}^{22.2}$ 35.3 (c 0.24, CHCl_3 , 92% ee); SFC conditions: 3% MeOH, 3.5 mL/min, Chiralpak OJ-H column, $\lambda = 210$ nm, t_{R} (min): major = 4.07, minor = 6.42. Data were consistent with literature values.⁹

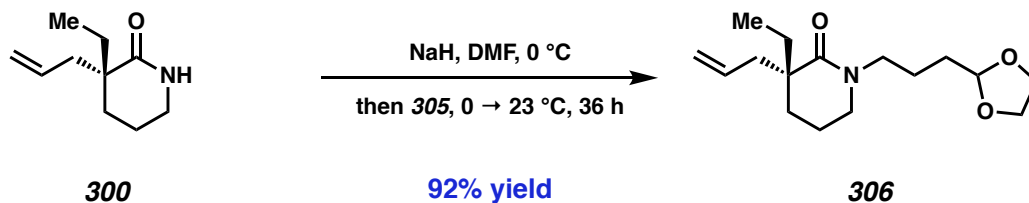
Figure 2.5. Reaction setup for large-scale decarboxylative allylic alkylation.





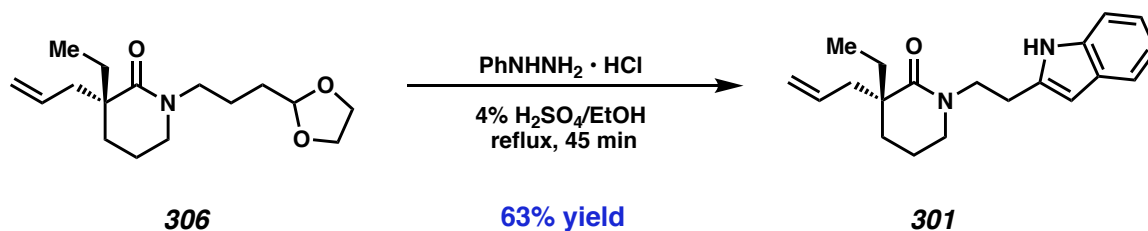
Lactam 300: Following a modified procedure by Behenna and coworkers,⁸ a 2L round-bottom flask with stir bar was charged with *N*-benzoyl lactam **286** (5.44 g, 20.1 mmol, 1.0 equiv) in methanol (500 mL). A solution of lithium hydroxide monohydrate (1.25 g, 30.1 mmol, 1.5 equiv) water (200 mL) was added, and the reaction mixture was stirred at $23\text{ }^\circ\text{C}$, for 20 hours.

The reaction was then partially concentrated in vacuo to remove methanol, then transferred to separatory funnel. The reaction mixture was diluted with ethyl acetate and saturated sodium bicarbonate, then extracted with ethyl acetate (4X). The combined organic extracts were washed with brine, dried with sodium sulfate, and concentrated in vacuo to afford neat lactam **300** (3.26 g, 98% yield) as a light yellow oil without any further purification. ^1H NMR (400 MHz, CDCl_3) δ 6.03 (br s, 1H), 5.88 – 5.68 (m, 1H), 5.12 – 5.03 (m, 2H), 3.26 (td, $J = 5.9, 2.5$ Hz, 2H), 2.49 (ddt, $J = 13.6, 6.7, 1.3$ Hz, 1H), 2.27 – 2.12 (m, 1H), 1.87 – 1.65 (m, 5H), 1.50 (dq, $J = 13.7, 7.4$ Hz, 1H), 0.89 (t, $J = 7.5$ Hz, 3H); ^{13}C NMR (101 MHz, CDCl_3) 176.8, 134.8, 110.0, 45.0, 42.9, 42.9, 31.2, 28.7, 31.2, 28.7, 19.9, 8.8. IR (Neat Film, NaCl) 2972, 1718, 1286, 1147, 700, 676, 649 cm^{-1} ; $[\alpha]_{\text{D}}^{25}$ 5.3 (c 0.09, CHCl_3 , 92% ee). Data were consistent with literature values.⁹



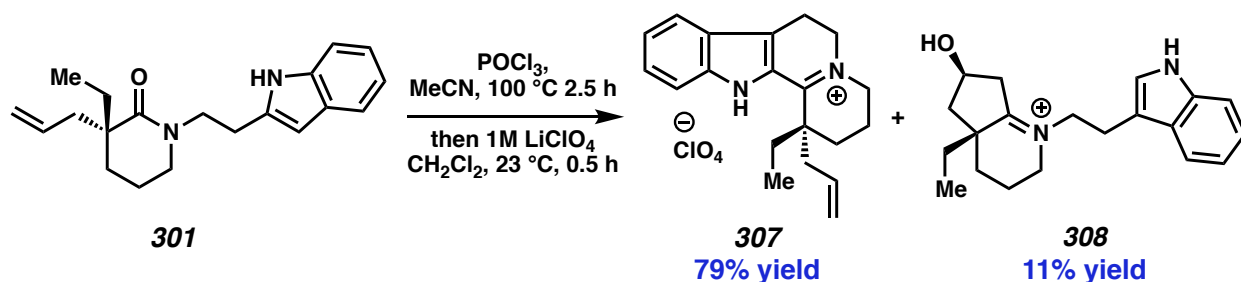
Acetal 306: To a flame-dried 100 mL round bottom flask with stir bar was added lactam **300** (4.00 g, 24.0 mmol, 1.0 equiv) and DMF (24.0 mL). The flask was cooled to 0 °C before sodium hydride (1.41 g, 60% dispersion in mineral oil, 35.3 mmol, 1.47 equiv) was added portionwise (CAUTION: Evolution of hydrogen gas). The reaction mixture was stirred at 0 °C for 1 hr before dioxolane **305** (6.88 g, 35.28 mmol, 1.47 equiv) was added dropwise. The flask was slowly warmed to 23 °C over 36 hours.

When the starting material was consumed, as determined by TLC, the flask was re-cooled to 0 °C, then quenched with water. The mixture was transferred to a separatory funnel and extracted with ethyl acetate (5X). The organic extracts were combined and washed with 10% lithium chloride solution (2X), brine (1X), and dried with sodium sulfate, then concentrated in vacuo. Flash column chromatography (30% → 40% → 50% ethyl acetate/hexanes) afforded desired acetal **306** (6.28g, 92% yield) as a colorless oil. ¹H NMR (400 MHz, CDCl₃) δ 5.82 – 5.67 (m, 1H), 5.09 – 5.00 (m, 2H), 4.92 – 4.82 (m, 1H), 4.00 – 3.91 (m, 2H), 3.90 – 3.79 (m, 2H), 3.46 – 3.30 (m, 2H), 3.24 (td, *J* = 5.9, 1.8 Hz, 2H), 2.48 (ddt, *J* = 13.5, 6.6, 1.4 Hz, 1H), 2.14 (ddt, *J* = 13.5, 8.1, 0.9 Hz, 1H), 1.84 – 1.72 (m, 3H), 1.71 – 1.59 (m, 6H), 1.45 (dq, *J* = 13.5, 7.4 Hz, 1H), 0.84 (t, *J* = 7.5 Hz, 3H).; ¹³C NMR (101 MHz, CDCl₃) δ 174.2, 135.2, 117.7, 104.3, 65.0, 48.5, 47.5, 45.2, 43.5, 31.7, 31.3, 29.0, 21.8, 20.1, 8.9. IR (Neat Film, NaCl) 3072, 2941, 2876, 1632, 1490, 1490, 1461, 1429, 1359, 1284, 1239, 11197, 1138, 1041, 944, 912; HRMS (FAB+) *m/z* calculated for C₁₆H₂₈NO₃ [M+H⁺] 282.2069, found 282.2069. [α]_D^{22.4} 8.9° (*c* 0.49, CHCl₃, 92% ee).



Indole 301: To a 50-mL flask with stir bar was added acetal **306** (144 mg, 0.50 mmol, 1.0 equiv) in 4% sulfuric acid in ethanol (10.0 mL) and phenylhydrazine (0.10 mL, 1.0 mmol, 2.0 equiv). The flask was equipped with a reflux condenser and heated to 80 °C for 45 minutes.

After completion, as determined by LCMS, the reaction was quenched with bicarbonate and transferred to a separatory funnel, and extracted with ethyl acetate (3X). The combined organic extracts were washed with brine, dried with sodium sulfate, and concentrated in vacuo. Flash column chromatography (30 → 40 → 50% ethyl acetate/hexanes) afforded indole **301** (97.0 mg, 63% yield) as a yellow oil. ^1H NMR (400 MHz, CDCl_3) δ 8.15 (s, 1H), 7.69 (ddt, $J = 7.8, 1.4, 0.8$ Hz, 1H), 7.36 (dt, $J = 8.1, 1.0$ Hz, 1H), 7.19 (ddd, $J = 8.2, 7.0, 1.3$ Hz, 1H), 7.12 (ddd, $J = 8.1, 7.1, 1.1$ Hz, 1H), 7.08 – 7.03 (m, 1H), 5.74 (dddd, $J = 16.8, 10.2, 8.1, 6.6$ Hz, 1H), 5.10 – 4.99 (m, 2H), 3.72 – 3.61 (m, 2H), 3.28 – 3.15 (m, 2H), 3.02 (ddd, $J = 8.3, 6.1, 0.9$ Hz, 2H), 2.51 (ddt, $J = 13.6, 6.6, 1.4$ Hz, 1H), 2.18 (ddt, $J = 13.4, 8.1, 1.0$ Hz, 1H), 1.86 – 1.61 (m, 5H), 1.48 (dq, $J = 13.6, 7.4$ Hz, 1H), 0.86 (t, $J = 7.5$ Hz, 3H); ^{13}C NMR (101 MHz, CDCl_3) δ 174.1, 136.3, 135.1, 127.5, 122.0, 121.9, 119.3, 118.9, 117.6, 113.3, 111.1, 49.0, 48.7, 45.0, 43.4, 31.5, 28.8, 23.2, 20.0, 8.8. IR (Neat Film, NaCl) 3261, 3072, 2937, 2876, 1611, 1490, 1458, 1340, 1292, 1234, 1119, 1168, 1103, 999, 914, 876, 741, 687; HRMS (FAB+) m/z calculated for $\text{C}_{20}\text{H}_{26}\text{N}_2\text{O}$ [$\text{M} + \text{H}^+$] 311.2123, found 311.2130; $[\alpha]_{\text{D}}^{22.4}$ 13.4° (c 0.82, CHCl_3 , 92% ee).



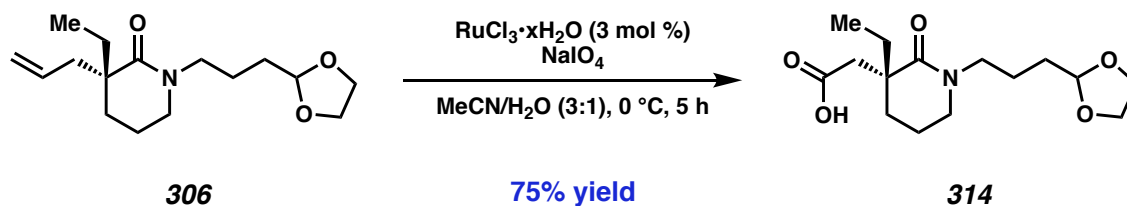
Iminiums 307 and 308: To an oven-dried 20-mL scintillation vial was added indole **301** (60.0 mg, 0.193 mmol, 1.0 equiv) in acetonitrile (0.4 mL). Phosphorous (V) oxychloride (0.54 mL, 5.8 mmol, 30.0 equiv) was added dropwise and the reaction was sealed with a Teflon-lined cap and stirred for 2.5 hours. When starting material was consumed, as determined by LCMS, the reaction mixture was cooled to room temperature and concentrated in vacuo. Residual phosphoryl chloride was removed azeotropically with acetonitrile (3 x 1.0 mL) to yield a brown, amorphous solid.

The crude mixture was redissolved in dichloromethane (1.0 mL), transferred to a one-dram vial, and stirred at $23\text{ }^\circ\text{C}$. 1M aq. lithium perchlorate (0.4 mL) was added and the heterogeneous mixture was rapidly stirred for 30 minutes. The mixture was transferred to a separatory funnel and extracted with dichloromethane (3X). The combined organic extracts were washed with 1M lithium perchlorate (2 X), dried with sodium sulfate, and concentrated in vacuo to afford crude iminium perchlorate as a light yellow oil. Preparative HPLC afforded both iminium perchlorate **307** (62.3 mg, 0.152 mmol, 79%) and rearranged product **308** (9.0 mg, 0.021 mmol, 11% with grease impurity), both as light yellow solids.

Iminium Perchlorate 307: $^1\text{H NMR}$ (400 MHz, CDCl_3) δ 13.03 (s, 1H), 7.86 (dt, $J = 8.6, 1.0$ Hz, 1H), 7.46 (d, $J = 8.2$ Hz, 1H), 7.37 (ddd, $J = 8.3, 6.9, 1.1$ Hz, 1H), 7.13 (ddd, $J = 8.1, 7.0, 0.9$ Hz, 1H), 5.50 – 5.32 (m, 1H), 4.92 (dd, $J = 10.1, 1.8$ Hz, 1H), 4.80 (dd, $J = 17.0, 1.7$ Hz, 1H), 3.97 (t, $J = 8.2$ Hz, 2H), 3.88 (s, 2H), 3.02 (t, $J = 8.2$ Hz, 2H), 2.84 (dd, $J = 14.2, 7.8$ Hz, 1H), 2.60 (dd, J

= 14.2, 7.1 Hz, 1H), 2.17 (dq, $J = 14.6, 7.4$ Hz, 1H), 2.03 (dt, $J = 14.6, 7.4$ Hz, 1H), 1.92 (d, $J = 6.1$ Hz, 2H), 1.82 – 1.73 (m, 2H), 0.69 (t, $J = 7.4$ Hz, 3H); ^{13}C NMR (101 MHz, CDCl_3) ^{13}C NMR (101 MHz, CDCl_3) δ 172.9, 142.3, 131.6, 129.1, 125.2, 124.4, 122.8, 121.7, 120.6, 120.4, 115.1, 54.8, 53.7, 44.7, 41.0, 29.8, 26.3, 19.3, 17.7, 8.0.; IR (Neat Film, NaCl) 2924, 1682, 1593, 1521, 1434, 1337, 1198, 1168, 926, 798, 753, 716, 620 cm^{-1} ; + HRMS (FAB+) m/z calculated for $\text{C}_{20}\text{H}_{25}\text{N}_2$ [M] XXX, found YYY.

Alcohol 308: ^1H NMR (600 MHz, CD_2Cl_2) δ 10.64 (s, 1H), 7.48 (t, $J = 8.2$ Hz, 2H), 7.20 – 7.11 (m, 2H), 7.07 (td, $J = 7.5, 6.4$ Hz, 1H), 4.76 (dt, $J = 11.2, 5.6$ Hz, 1H), 4.04 (dt, $J = 13.2, 6.5$ Hz, 1H), 3.78 (dt, $J = 12.8, 6.2$ Hz, 1H), 3.57 – 3.51 (m, 2H), 3.19 (t, $J = 6.4$ Hz, 2H), 2.34 (dd, $J = 13.1, 4.8$ Hz, 1H), 2.04 (dt, $J = 13.7, 4.1$ Hz, 1H), 1.93 (d, $J = 14.5$ Hz, 1H), 1.86 – 1.76 (m, 0H), 1.46 (q, $J = 11.7, 11.2$ Hz, 2H), 1.32 – 1.27 (m, 1H), 1.20 (q, $J = 7.4$ Hz, 2H), 1.16 (d, $J = 6.1$ Hz, 3H), 0.81 (t, $J = 7.4$ Hz, 3H); ^{13}C NMR (101 MHz, CD_3CN) δ 172.7, 141.9, 132.9, 129.7, 126.5, 126.3, 124.1, 122.6, 122.3, 120.4, 114.3, 55.7, 54.8, 45.3, 42.2, 31.0, 27.3, 19.5, 18.3, 8.4. IR (Neat Film, NaCl) 3223, 2924, 2853, 1775, 1690, 1459, 1421, 1199, 1131, 1036, 916, 798, 746, 718 cm^{-1} ; HRMS (FAB+) m/z calculated for $\text{C}_{20}\text{H}_{27}\text{N}_2\text{O}$ [M^+] XXX, found YYY.

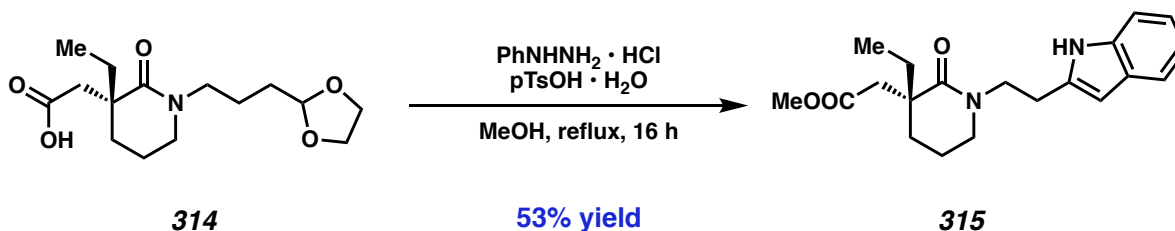


Carboxylic acid 314: To a 500-mL round-bottom flask with stir bar was added acetal **306** (2.00 g, 6.97 mmol, 1.0 equiv) in acetonitrile (105 mL). Water (35 mL) was added and the flask cooled to 0 °C. Ruthenium (III) trichloride hydrate (43.4 mg, 0.21 mmol, 0.03 equiv) was added,

followed by sodium periodate (7.42 g, 34.8 mmol, 5.0 equiv) in a single portion. The heterogeneous mixture was rapidly stirred for 5 hours and monitored closely by LCMS.

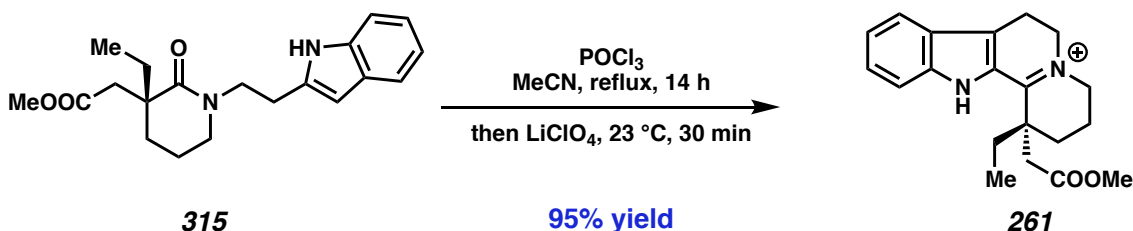
Upon completion, the reaction mixture was quickly filtered through a plug of Celite (washing with acetonitrile) and concentrated in vacuo to remove organic solvents. The aqueous mixture was extracted with dichloromethane (5X), dried with sodium sulfate, and concentrated in vacuo. Flash column chromatography (1 → 2 → 3 → 4 → 5% methanol/dichloromethane) afforded acid **314** (1.58 g, 75% yield) as a colorless oil. ¹H NMR (400 MHz, CDCl₃) δ 4.87 (t, *J* = 4.0 Hz, 1H), 4.04 – 3.93 (m, 2H), 3.93 – 3.77 (m, 2H), 3.55 – 3.46 (m, 1H), 3.32 (tt, *J* = 13.3, 6.1 Hz, 3H), 2.66 (d, *J* = 15.7 Hz, 1H), 2.48 (d, *J* = 15.7 Hz, 1H), 1.95 – 1.63 (m, 7H), 1.63 – 1.52 (m, 1H), 1.33 – 1.21 (m, 1H), 0.90 (dt, *J* = 17.8, 7.4 Hz, 4H); ¹³C NMR (101 MHz, CDCl₃) δ 177.4, 172.3, 103.9, 65.0, 48.2, 48.0, 44.5, 42.8, 30.8, 30.5, 28.0, 21.1, 18.7, 7.8; IR (Neat Film, NaCl) 2948, 2880, 1729, 1630, 1598, 1579, 1498, 1456, 1438, 1359, 1290, 1186, 1142, 1030, 946; HRMS (FAB+) *m/z* calculated for C₁₅H₂₆NO₅ [M + H⁺] 300.1811, found 300.1810; [α]_D^{22.2} –17.4° (*c* 0.31, CHCl₃, 92% ee).

NOTE: We have observed that the times of this reaction were highly variable (between 1 and 6 hours) depending on the scale and bottle of RuCl₃·xH₂O used. It is important to quench the reaction as soon as the starting material is consumed, as other oxidized byproducts will begin to form.



Indole 315: To a flame-dried 500-mL round-bottom flask with stir bar was added carboxylic acid **314** (3.02 g, 10.1 mmol, 1.0 equiv) and methanol (210 mL). Phenylhydrazine hydrochloride salt (3.10 g, 21.4 mmol, 2.0 equiv) and *p*-toluenesulfonic acid monohydrate (4.78 g, 32.1 mmol, 3.0 equiv) were added sequentially. The flask was equipped with a reflux condenser and heated to reflux for 12 hours. After this, additional phenylhydrazine hydrochloride salt was added (1.00g, 6.89 mmol, 0.68 equiv) and the reaction was stirred at reflux for an additional four hours. Upon completion, as determined by LCMS analysis, the reaction was cooled to room temperature, quenched with 1M aqueous hydrochloric acid, and transferred to a separatory funnel. The mixture was extracted with dichloromethane (5X), before the combined organic extracts were washed with brine, dried with sodium sulfate, and concentrated in vacuo onto silica gel. Flash column chromatography (50% ethyl acetate/hexanes) afforded indole **315** (1.85 g, 53% yield) as a viscous orange oil. ^1H NMR (400 MHz, CDCl_3) δ 8.03 (s, 1H), 7.69 (ddt, $J = 7.8, 1.5, 0.7$ Hz, 1H), 7.36 (dt, $J = 8.1, 1.0$ Hz, 1H), 7.19 (ddd, $J = 8.1, 7.0, 1.2$ Hz, 1H), 7.15 – 7.10 (m, 1H), 7.09 – 7.06 (m, 1H), 3.68 – 3.62 (m, 5H), 3.44 – 3.36 (m, 1H), 3.20 (dtd, $J = 10.9, 4.7, 2.2$ Hz, 1H), 3.07 – 3.00 (m, 2H), 2.96 (d, $J = 16.1$ Hz, 1H), 2.35 (d, $J = 16.0$ Hz, 1H), 1.99 – 1.89 (m, 1H), 1.83 – 1.60 (m, 5H), 0.88 (t, $J = 7.5$ Hz, 3H); ^{13}C NMR (101 MHz, CDCl_3) δ 173.8, 172.6, 136.2, 127.5, 122.0, 121.9, 119.3, 118.9, 113.6, 111.1, 51.4, 49.0, 48.8, 43.4, 42.0, 31.5, 29.1, 23.0, 19.9, 8.6; IR (Neat Film, NaCl) 3265, 2947, 2870, 1736, 1614, 1492, 1457,

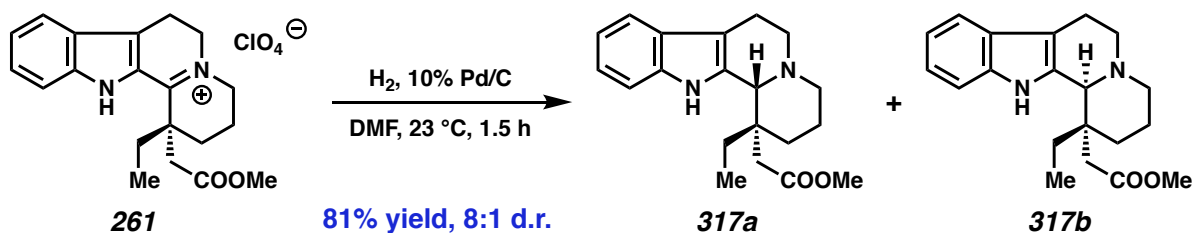
1434, 1358, 1290, 1198, 1172, 1011, 744, cm^{-1} ; HRMS (FAB+) m/z calculated for $\text{C}_{20}\text{H}_{26}\text{N}_2\text{O}_3$ $[\text{M} + \text{H}^+]$ 343.2022, found 343.2006; $[\alpha]_{\text{D}}^{22.4} -10.3^\circ$ (c 0.28, CHCl_3 , 92% ee).



Iminium perchlorate 261: To a flame-dried, 250-mL round-bottom flask with stir bar was added indole **315** (1.85g, 5.39 mmol, 1.0 equiv) in acetonitrile (110 mL). Freshly distilled phosphoryl chloride (15.0 mL, 153 mmol, 30.0 equiv) was then added, before the flask was equipped with a reflux condenser and heated to 100 °C for 14 hours. When the starting material was consumed, as determined by LCMS, the reaction mixture was cooled to room temperature and concentrated in vacuo. Residual phosphoryl chloride was removed azeotropically with acetonitrile (3 X 20 mL) to yield a brown, amorphous solid.

The crude mixture was redissolved in dichloromethane (27 mL) and stirred at room temperature. 1M aq. lithium perchlorate was added and the heterogeneous mixture was rapidly stirred for 30 minutes. The mixture was transferred to a separatory funnel and extracted with dichloromethane (3X). The combined organic extracts were washed with 1M lithium perchlorate (2X), dried with sodium sulfate, and concentrated in vacuo to afford crude iminium perchlorate **261** (2.18 g, 95% crude yield) as a light brown solid without any further purification. ^1H NMR (500 MHz, CD_2Cl_2) δ 10.34 (s, 1H), 7.83 (dt, $J = 8.6, 0.9$ Hz, 1H), 7.59 (dq, $J = 8.2, 0.9$ Hz, 1H), 7.46 (ddd, $J = 8.4, 6.9, 1.1$ Hz, 1H), 7.20 (ddd, $J = 8.1, 7.0, 0.9$ Hz, 1H), 4.08 – 3.94 (m, 3H), 3.87 (d, $J = 14.9$ Hz, 1H), 3.61 (dd, $J = 18.6, 2.8$ Hz, 1H), 3.45 (s, 3H), 3.20 (dd, $J = 9.9, 6.6$ Hz,

2H), 2.84 (d, $J = 18.4$ Hz, 1H), 2.30 – 2.20 (m, 1H), 2.14 – 1.98 (m, 4H), 1.93 – 1.82 (m, 1H), 1.09 (t, $J = 7.4$ Hz, 3H); ^{13}C NMR (101 MHz, CDCl_3) δ 172.2, 171.9, 141.2, 129.0, 125.4, 124.9, 123.0, 121.7, 121.1, 114.7, 54.6, 53.7, 52.1, 42.3, 42.0, 28.9, 27.8, 19.1, 17.8, 8.2; IR (Neat Film, NaCl) 3332, 2954, 1731, 1600, 1527, 1435, 1336, 1236, 1201, 1096, 752, 622 cm^{-1} ; HRMS (FAB+) m/z calculated for $\text{C}_{20}\text{H}_{25}\text{N}_2\text{O}_2$ [$\text{M} - \text{OCH}_3$] XXX, found 295.1835; $[\alpha]_{\text{D}}^{22.4}$ 10.4° (c 2.1, CHCl_3 , 92% ee).



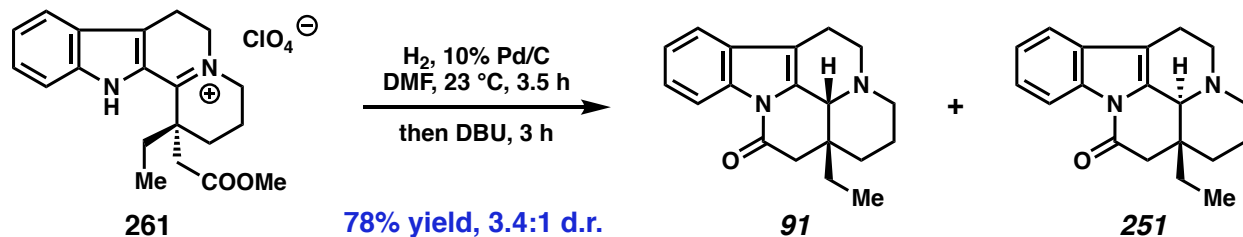
Amines 317a and 317b: To an oven-dried one-dram vial with stir bar was added iminium perchlorate **261** (21.2 mg, 0.050 mmol, 1.0 equiv) and DMF (0.1 mL). 10% palladium on carbon (11.6 mg, 0.010 mmol with respect to palladium, 0.2 equiv) was added, and the vial was evacuated and backfilled with hydrogen (5X). The solution was sparged with hydrogen for 1 minute, then allowed to stir at 23 °C for 1 hour.

After the reaction was complete (as determined by HPLC), the mixture was diluted with ethyl acetate and filtered through a pad of Celite. The solution was transferred to a separatory funnel, washed with 10% lithium chloride, brine, and water, dried with sodium sulfate, and concentrated in vacuo. Flash column chromatography (10 → 20 → 50 → 100% ethyl acetate) afforded *cis*-fused amine **317a** (11.7 mg, 71% yield) and *trans*-fused amine **317b** (1.5 mg, 9% yield) as colorless oils.

***cis*-fused amine 317a:** ^1H NMR (400 MHz, CDCl_3) δ 7.83 (s, 1H), 7.47 (dd, $J = 7.7, 1.1$ Hz, 1H), 7.32 (dt, $J = 8.0, 0.9$ Hz, 1H), 7.15 (ddd, $J = 8.1, 7.0, 1.3$ Hz, 1H), 7.09 (ddd, $J = 8.0, 7.0, 1.1$ Hz,

1H), 3.49 (s, 3H), 3.38 (t, $J = 1.9$ Hz, 1H), 3.07 – 2.97 (m, 3H), 2.94 – 2.84 (m, 1H), 2.66 – 2.59 (m, 1H), 2.56 (dd, $J = 11.2, 3.5$ Hz, 1H), 2.40 (ddd, $J = 12.4, 11.1, 2.8$ Hz, 1H), 2.08 – 1.87 (m, 4H), 1.85 – 1.76 (m, 1H), 1.67 – 1.55 (m, 2H), 1.18 (t, $J = 7.7$ Hz, 3H); ^{13}C NMR (101 MHz, CDCl_3) δ 173.8, 136.1, 132.7, 126.8, 121.8, 119.5, 118.0, 112.5, 110.9, 66.3, 57.0, 54.0, 51.2, 40.5, 38.2, 32.4, 31.5, 22.3, 22.1, 8.2; IR (Neat Film, NaCl) 3432, 2943, 1729, 1463, 1346, 1319, 1295, 1196, 1017, 743 cm^{-1} ; HRMS (FAB+) m/z calculated for $\text{C}_{20}\text{H}_{27}\text{N}_{22}\text{O}$ [$\text{M} + \text{H}^+$] 327.2073, found 327.2084; $[\alpha]_{\text{D}}^{22.4}$ 6.8° (c 0.44, CHCl_3 , 92% ee).

trans-fused amine 317b: ^1H NMR (400 MHz, CDCl_3) δ 9.51 (s, 1H), 7.47 (ddt, $J = 7.7, 1.4, 0.7$ Hz, 1H), 7.36 (dt, $J = 8.0, 0.9$ Hz, 1H), 7.16 – 7.05 (m, 2H), 3.81 (s, 3H), 3.31 (d, $J = 1.7$ Hz, 1H), 3.02 – 2.87 (m, 3H), 2.82 (d, $J = 13.0$ Hz, 1H), 2.66 – 2.54 (m, 2H), 2.51 – 2.37 (m, 2H), 2.22 (dd, $J = 14.8, 7.6$ Hz, 1H), 1.90 – 1.65 (m, 3H), 1.56 – 1.48 (m, 1H), 1.02 (ddd, $J = 14.7, 7.6, 1.1$ Hz, 1H), 0.67 (t, $J = 7.7$ Hz, 3H); ^{13}C NMR (101 MHz, CDCl_3) δ 175.2, 136.9, 133.8, 127.4, 121.3, 119.2, 117.9, 112.5, 111.4, 67.0, 56.7, 53.6, 52.2, 43.1, 41.5, 32.9, 25.0, 22.6, 22.5, 7.3; IR (Neat Film, NaCl) 3333, 2934, 2796, 2749, 1709, 1456, 1341, 1305, 1195, 1160, 936, 738 cm^{-1} ; HRMS (FAB+) m/z calculated for $\text{C}_{20}\text{H}_{27}\text{N}_{22}\text{O}$ [$\text{M} + \text{H}^+$] 327.2073, found 327.2078; $[\alpha]_{\text{D}}^{22.4}$ 13.4° (c 0.17, CHCl_3 , 92% ee).



Eburnamonine (91) and epi-eburnamonine (251): To a flame-dried, 100 mL round-bottom flask with stir bar was added iminium perchlorate **261** (1.92 g, 4.52 mmol, 1.0 equiv) and DMF (9.0 mL). 10% palladium on carbon (960 mg, 0.90 mmol with respect to palladium, 0.2 equiv)

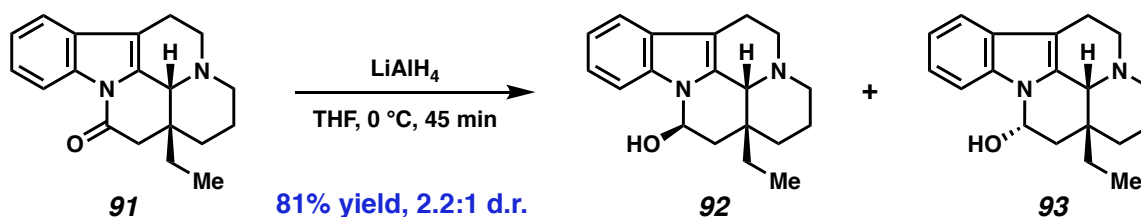
was added, and the flask was evacuated and backfilled with hydrogen (5X). The solution was sparged with hydrogen for 10 minutes, then allowed to stir at 23 °C for 3.5 hours.

The flask was then evacuated and backfilled with nitrogen (3X) and sparged for 5 minutes. DBU (1.42 mL, 9.49 mmol, 2.1 equiv) was added dropwise, and the reaction was stirred at 23 °C for 2.5 hours. Additional DBU was added (0.27 mL, 1.81 mmol, 0.4 equiv) and the reaction was stirred at 23 °C for another 0.5 hours.

After the reaction was complete (as determined by HPLC), the mixture was diluted with ethyl acetate and filtered through a pad of Celite. The solution was transferred to a separatory funnel, washed with 10% lithium chloride, brine, and water, dried with sodium sulfate, and concentrated in vacuo. Flash column chromatography (5 → 25% ethyl acetate/chloroform) afforded eburnamonine **91** (0.82 g, 62%) as a light brown solid and *epi*-eburnamonine **251** (0.23g, 17%) as an orange solid. Eburnamonine **91** was recrystallized from methanol to afford a white solid.

Eburnamonine: ^1H NMR (400 MHz, CDCl_3) δ 8.39 – 8.35 (m, 1H), 7.46 – 7.41 (m, 1H), 7.37 – 7.27 (m, 2H), 4.05 (s, 1H), 3.38 (dd, $J = 13.9, 6.7$ Hz, 1H), 3.29 (ddd, $J = 13.9, 11.3, 5.8$ Hz, 1H), 2.92 (dddd, $J = 16.9, 11.3, 6.7, 2.9$ Hz, 1H), 2.69 (d, $J = 16.8$ Hz, 1H), 2.66 (bs, 1H), 2.60 (d, $J = 16.8$ Hz, 1H), 2.58 – 2.41 (m, 2H), 2.09 (dq, $J = 15.1, 7.6$ Hz, 1H), 1.81 (qt, $J = 13.2, 3.9$ Hz, 1H), 1.68 (dq, $J = 14.7, 7.4$ Hz, 1H), 1.51 (ddt, $J = 13.6, 3.6, 1.9$ Hz, 1H), 1.46 – 1.38 (m, 1H), 1.05 (td, $J = 13.6, 3.9$ Hz, 1H), 0.94 (t, $J = 7.6$ Hz, 3H); ^{13}C NMR (101 MHz, CDCl_3) δ 167.6, 134.4, 131.6, 130.0, 124.7, 124.1, 118.3, 116.4, 112.7, 57.9, 50.9, 44.5, 44.4, 38.7, 28.5, 26.9, 20.6, 16.7, 7.8; IR (Neat Film, NaCl) 3051., 2933, 2856, 1704, 1627, 1454, 1375, 1332, 1262, 1208, ; HRMS (FAB+) m/z calculated for $\text{C}_{19}\text{H}_{23}\text{N}_2\text{O}$ [$\text{M} + \text{H}^+$] 295.1810, found 295.1787; $[\alpha]_{\text{D}}^{22.4}$ 93.1° (c 0.55, CHCl_3 , 92% ee). Data were consistent with literature values.¹⁰

epi-Eburnamonine: ^1H NMR (600 MHz, CDCl_3) δ 8.35 – 8.31 (m, 1H), 7.40 (dd, $J = 7.3, 1.6$ Hz, 1H), 7.31 – 7.24 (m, 3H), 3.14 – 3.05 (m, 3H), 3.03 (s, 1H), 2.88 (s, 1H), 2.80 (d, $J = 16.7$ Hz, 1H), 2.65 (dq, $J = 15.9, 2.5, 2.0$ Hz, 1H), 2.52 (td, $J = 11.4, 4.3$ Hz, 1H), 2.37 – 2.28 (m, 2H), 1.89 (hd, $J = 8.4, 4.4$ Hz, 3H), 1.63 (dtd, $J = 13.5, 4.9, 4.3, 2.3$ Hz, 1H), 1.23 – 1.15 (m, 1H), 0.87 – 0.80 (m, 1H), 0.78 (t, $J = 7.3$ Hz, 3H); ^{13}C NMR (101 MHz, CDCl_3) δ 167.6, 135.1, 133.3, 129.9, 124.1, 123.8, 118.1, 116.2, 113.0, 66.0, 55.4, 52.3, 44.3, 39.4, 31.8, 21.6, 21.3, 20.7, 7.4; IR (Neat Film, NaCl) 3050, 2935, 2796, 1708, 1655, 1600, 1457, 1365, 1324, 1301, 1149, 1118, 1042, 958, 746, 688 cm^{-1} ; HRMS (FAB+) m/z calculated for for $\text{C}_{19}\text{H}_{23}\text{N}_2\text{O}$ [$\text{M} + \text{H}^+$] 295.1810, found 295.1834; $[\alpha]_{\text{D}}^{22.4} -120.2$ (c 0.78, CHCl_3). Data were consistent with literature values.¹⁰



Eburnamine (92) and isoeburnamine (93): To a flame-dried 25 mL flask with stir bar was added lithium aluminum hydride (6.8 mg, 0.20 mmol, 2.0 equiv) and THF (1.18 mL). The flask was cooled to $0\text{ }^\circ\text{C}$ and a solution of eburnamonine (91) (29.5 mg, 0.10 mmol, 1.0 equiv) in THF (1.78 mL) was slowly added dropwise. The solution was stirred at $0\text{ }^\circ\text{C}$ for 45 minutes.

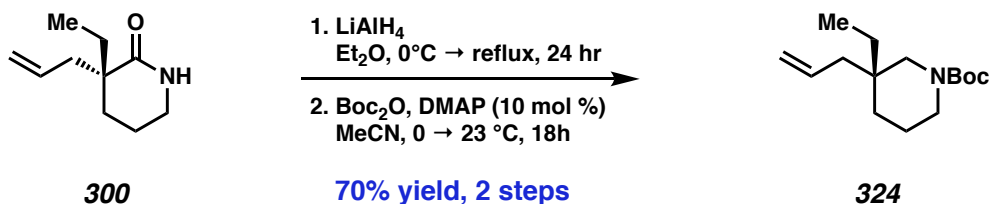
The reaction mixture was quenched with cool brine, transferred to a separatory funnel, and extracted with ethyl acetate (3X). The combined organic extracts were washed once with cool brine, dried with sodium sulfate, and concentrated in vacuo. Flash column chromatography afforded an inseparable mixture of eburnamine (92) and isoeburnamine (93) (24.1 mg, 81%

yield, 2.2:1 d.r.). The ratio of eburnamine to *epi*-eburnamine was determined by integration of the diagnostic peaks in the ^1H NMR for **92** (5.59) and **93** (6.05), respectively. Data were consistent with literature values.¹¹

Eburnamine **92** (major diastereomer): ^1H NMR (400 MHz, CDCl_3) δ 7.78 – 7.71 (m, 1H), 7.54 – 7.45 (m, 1H), 7.25 – 7.14 (m, 2H), 5.59 (dd, $J = 9.5, 5.2$ Hz, 1H), 3.84 (bs, 1H), 3.37 – 3.15 (m, 2H), 3.05 – 2.88 (m, 1H), 2.69 – 2.47 (m, 3H), 2.39 – 2.27 (m, 1H), 2.25 – 2.13 (m, 1H), 2.12 – 1.95 (m, 1H), 1.85 – 1.24 (m, 4H), 0.96 – 0.80 (m, 4H). ^{13}C NMR (101 MHz, CDCl_3) δ 136.8, 132.8, 128.8, 121.4, 120.3, 118.2, 112.3, 105.8, 76.8, 58.9, 50.9, 44.5, 43.7, 37.0, 28.7, 25.3, 20.6, 16.9, 7.7.

iso-Eburnamine **93** (minor diastereomer): ^1H NMR (400 MHz, CDCl_3) δ 7.78 – 7.71 (m, 1H), 7.54 – 7.45 (m, 1H), 7.43 – 7.37 (m, 1H), 7.25 – 7.14 (m, 2H), 6.05 (dd, $J = 4.8, 1.3$ Hz, 0H), 5.59 (dd, $J = 9.5, 5.2$ Hz, 1H), 3.87 – 3.82 (m, 1H), 3.37 – 3.15 (m, 2H), 3.05 – 2.88 (m, 1H), 2.69 – 2.47 (m, 3H), 2.39 – 2.27 (m, 2H), 2.25 – 2.13 (m, 1H), 2.12 – 1.95 (m, 1H), 1.85 – 1.62 (m, 1H), 1.62 – 1.42 (m, 2H), 1.42 – 1.24 (m, 2H), 0.96 – 0.80 (m, 4H). ^{13}C NMR (101 MHz, CDCl_3) δ 134.8, 131.3, 129.0, 121.4, 120.3, 118.6, 109.9, 105.7, 74.8, 59.4, 51.4, 45.0, 40.0, 34.8, 29.1, 26.7, 21.1, 16.9, 7.8.

IR (Neat Film, NaCl) 3356, 2921, 2714, 1694, 1668, 1455, 1366, 1301, 1272, 1165, 1057, 741 cm^{-1} ; HRMS (FAB+) m/z calculated for $\text{C}_{19}\text{H}_{24}\text{N}_2\text{O}$ $[\text{M} + \text{H}^+]$ XXX, found YYY; $[\alpha]_{\text{D}}^{22.4} -7.6$ (c 0.89, CHCl_3).



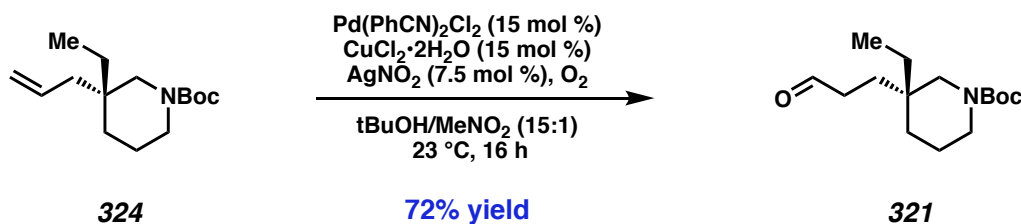
Piperidine 324: To a flame-dried 500 mL round-bottom flask with stir bar was added lactam **300** (2.47 g, 14.8 mmol, 1.0 equiv) in diethyl ether (150 mL). The flask was cooled to 0 °C before lithium aluminum hydride (1.64 g, 44.4 mmol, 3.0 equiv) was added portionwise. The flask was equipped with a reflux condenser and heated to reflux for 24 hours.

After the reaction is complete, as determined by TLC, the flask is re-cooled to 0 °C and quenched with saturated sodium carbonate. The flask was then removed from the bath and stirred at 23 °C for 20 minutes. The mixture was transferred to a separatory funnel and extracted with diethyl ether (5X). The combined organic extracts were washed with brine (2X), dried with sodium sulfate, and concentrated in vacuo to yield a brown oil, which was used immediately in the next step without further purification.

The 500 mL round bottomed flask was equipped with a stir bar, placed under nitrogen atmosphere, and charged with acetonitrile (75 mL). The flask was cooled to 0 °C before di-*tert*-butyldicarbonate (4.08 mL, 17.8 mmol, 1.2 equiv) and DMAP (180 mg, 1.48 mmol, 0.1 equiv) were added sequentially. The flask was warmed slowly to 23 °C over 12 hours. Additional di-*tert*-butyldicarbonate (2.0 mL, 8.9 mmol, 0.6 equiv) was added and the reaction was stirred for an additional 6 hours.

After the reaction was complete, as determined by TLC, the reaction was quenched with 2,2,2-trifluoroethanol (~ 5mL) and stirred for 30 minutes. The stir bar was then removed and the reaction mixture is concentrated in vacuo onto silica gel. Flash column chromatography (5% ethyl acetate/hexane) afforded piperidine **324** (2.59 grams, 70% yield) as a colorless oil. ¹H

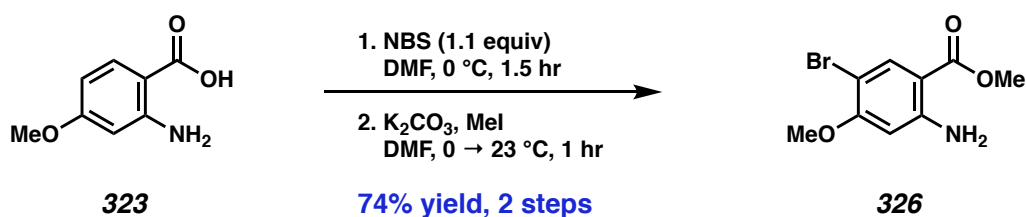
NMR (400 MHz, CDCl₃) δ 5.77 (ddt, $J = 15.6, 11.6, 7.5$ Hz, 1H), 5.08 – 4.98 (m, 2H), 3.34 (t, $J = 5.8$ Hz, 2H), 3.10 (m, 2H), 2.05 (dd, $J = 14.1, 7.1$ Hz, 1H), 1.95 (bs, 1H), 1.51 (m, 2H), 1.46 (bs, 9H), 1.38 (t, $J = 6.2$ Hz, 2H), 1.33 – 1.14 (m, 2H), 0.82 (t, $J = 7.5$ Hz, 3H); ¹³C NMR (101 MHz, CDCl₃) δ 155.2, 134.3, 117.4, 79.2, 52.5, 52.0, 44.9, 44.0, 38.7, 36.1, 33.9, 33.5, 28.6, 27.2, 21.1, 7.4; IR (Neat Film, NaCl) 2973, 2933, 2857, 1695, 1426, 1365, 1274, 1250, 1162, 1101, 912, 767 cm⁻¹; HRMS (FAB+) m/z calculated for C₁₅H₂₈NO₂ [M + H⁺] 254.2120, found 254.2101; [α]_D^{22.5} 9.3° (*c* 1.8, CHCl₃, 92% ee).



Aldehyde 321: To a flame-dried 500-mL round-bottom flask with stir bar was added bis(benzonitrile) palladium(II) chloride (460 mg, 1.2 mmol, 0.15 equiv), copper (II) chloride dihydrate (205 mg, 1.2 mmol, 0.15 equiv), and silver (I) nitrite (92.4 mg, 0.6 mmol, 0.075 equiv). Nitromethane (10 mL) and *tert*-butanol (150 mL) were sequentially added and stirred at 23 °C. The flask was evacuated and backfilled with oxygen (3X) before the reaction mixture was sparged for 10 minutes. Piperidine **321** (2.02 g, 8.0 mmol, 1.0 equiv) was added neat, and the reaction was sparged at 23 °C for another 5 minutes. The reaction mixture was stirred at 23 °C for 16 hours.

The reaction was quenched with water, transferred to a separatory funnel, and extracted with ethyl acetate (4X). The combined organic extracts were washed with brine, dried with sodium sulfate, and concentrated in vacuo (rotary evaporator with bath at 40 °C to remove *t*-BuOH). Flash column chromatography (15 → 20% ethyl acetate/hexanes) afforded aldehyde **321**.

(1.52 g, 72% yield) as a colorless oil ^1H NMR (400 MHz, CD_2Cl_2) δ 9.75 (s, 1H), 3.17 (m, 4H), 2.51 – 2.15 (m, 2H), 1.70 – 1.46 (m, 4H), 1.42 (s, 9H), 1.34 – 1.10 (m, 4H), 0.80 (t, $J = 7.5$ Hz, 3H); ^{13}C NMR (101 MHz, CD_2Cl_2) δ 202.7, 155.1, 79.4, 52.5, 51.7, 45.3, 44.2, 38.5, 35.6, 34.4, 28.7, 28.5, 27.5, 27.1, 25.9, 25.5, 21.4, 7.4. IR (Neat Film, NaCl) 2973, 2933, 2857, 1695, 1426, 1365, 1274, 1250, 1162, 1101, 912, 767 cm^{-1} ; HRMS (FAB+) m/z calculated for $\text{C}_{15}\text{H}_{28}\text{NO}_3$ [$\text{M} + \text{H}^+$] 270.2069, found 270.2056; $[\alpha]_{\text{D}}^{25}$ 13.0° (c 1.92, CHCl_3).



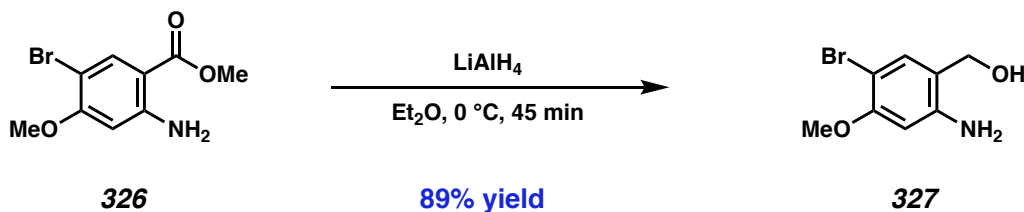
Methyl 2-amino-5-bromo-4-methoxybenzoate 326: To a flame-dried 250 mL round-bottom flask with stir bar was added 2-amino, 4-methoxybenzoic acid **323** (3.00 g, 18.0 mmol, 1.0 equiv) and DMF (90 mL). The flask was cooled to 0 °C, and *N*-bromosuccinimide (1.1 equiv, 19.8 mmol, 1.1 equiv) was added in a single portion. The flask was removed from the bath and warmed to 23 °C over 90 minutes.

The reaction was quenched with saturated sodium sulfite and acidified to pH ~3 with concentrated hydrochloric acid. The solution was transferred to a separatory funnel and extracted with diethyl ether (3X). The combined organic extracts were washed with 10% sat. lithium chloride, water, and brine, then concentrated in vacuo to yield a white solid. This was used in the next reaction immediately without further purification.

To a flame-dried 250 mL round-bottom flask with stir bar was added the crude reaction mixture and DMF (45 mL). The flask was cooled to 0 °C before potassium carbonate (4.97 g,

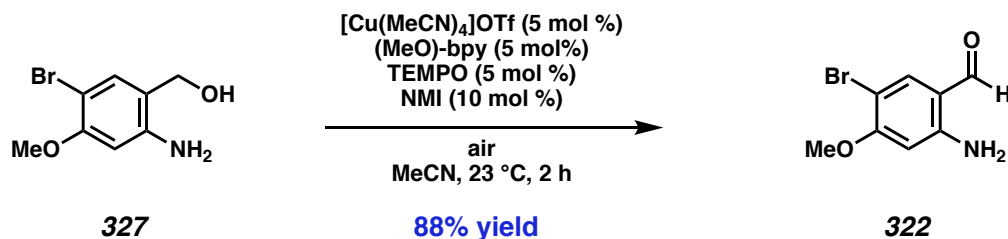
36.0 mmol, 2.0 equiv) and methyl iodide (1.68 mL, 27.0 mmol, 1.5 equiv) were added sequentially. The flask was removed from the cooling bath and warmed to 23 °C over 1 hour.

The reaction was quenched with cool water, transferred to a separatory funnel, and extracted with ethyl acetate (3x). The combined organic extracts were washed with 10% saturated lithium chloride and brine, dried with sodium sulfate, and concentrated in vacuo. Flash column chromatography (20 → 30% ethyl acetate/hexanes) afforded methyl ester **326** as a light yellow, amorphous solid (3.47 g, 74% yield over 2 steps). ¹H NMR (400 MHz, CDCl₃) δ 8.00 (s, 1H), 6.11 (s, 1H), 5.85 (s, 2H), 3.86 (s, 3H), 3.84 (s, 3H); ¹³C NMR (101 MHz, CDCl₃) δ 167.5, 160.1, 151.8, 135.7, 105.2, 98.7, 98.3, 56.3, 51.7, 31.1; IR (Neat Film, NaCl) 3478, 3467, 2948, 1687, 1610, 1589, 1485, 1446, 1277, 1224, 1109, 1050, 822, 555 cm⁻¹; HRMS (FAB+) m/z calculated for C₉H₁₀BrNO₃ [M + •] 258.9844, found 258.9851.



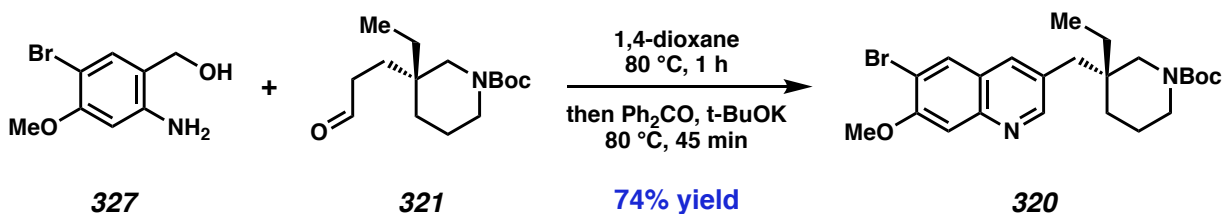
(2-amino-5-bromo-4-methoxyphenyl)methanol 327: To a flame-dried 250 mL round-bottom flask with stir bar was charged lithium aluminum hydride (798 mg, 21.0 mmol, 800 mg) and diethyl ether (30 mL). The flask was cooled to 0 °C before a solution of ester **326** (2.60 g, 10.0 mmol, 1.0 equiv) in diethyl ether (30 mL) was added dropwise via cannula. The flask was stirred at 0 °C for 10 minutes. The reaction was quenched with methanol and saturated Rochelle's salt solution, then warmed to 23 °C over 20 minutes. The mixture was transferred to a separatory funnel and extracted with diethyl ether (3X). The combined organic extracts are washed with brine, dried with magnesium sulfate, and concentrated to afford alcohol **327** (2.06 g, 89%) as a

white solid with no further purification. ^1H NMR (400 MHz, CD_2Cl_2) δ 7.17 (s, 1H), 6.29 (s, 1H), 4.54 (s, 2H), 3.81 (s, 3H); ^{13}C NMR (101 MHz, CD_2Cl_2) δ 156.74, 147.45, 133.53, 119.01, 100.28, 98.18, 63.44, 56.51; IR (Neat Film, NaCl) 3370, 2926, 1605, 1501, 1446, 1407, 1307, 1217, 1050, 999, 888, 827 cm^{-1} ; HRMS (FAB+) m/z calculated for $\text{C}_8\text{H}_{10}\text{BrNO}_2$ [$\text{M} + \bullet$] 230.9895, found 230.9908.



2-amino-4-methoxybenzaldehyde 322: To prepare a stock solution, an oven-dried 20 mL scintillation vial with stir bar was charged with 4-4'-dimethoxy-2-2'-bipyridine (108 mg), TEMPO (78 mg), NMI (92 mg) and acetonitrile (2.5 mL). A separate flame-dried 100 mL round-bottom flask was charged sequentially with alcohol **327** (232 mg, 1.0 mmol, 1.0 equiv), acetonitrile (10 mL), and *tetrakis*(acetonitrile) copper (I) triflate (18.8 mg, 0.050 mmol, 0.050 equiv). 0.25 mL of stock solution was then added and the reaction was stirred under air for 2 hours.

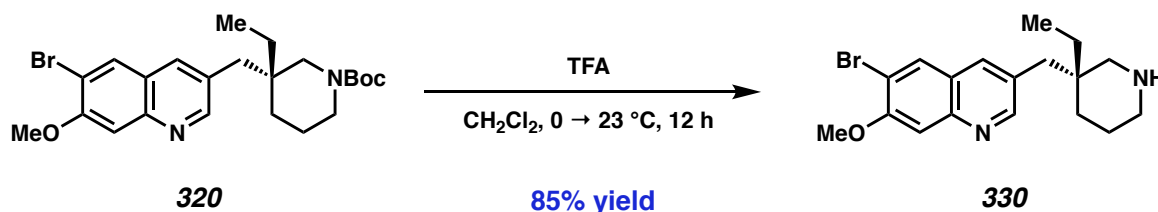
The reaction was diluted with ethyl acetate, filtered through a plug of silica gel, and concentrated in vacuo. Flash column chromatography (20 \rightarrow 25 \rightarrow 30% ethyl acetate/hexanes) yielded aldehyde **322** as a white solid (200 mg, 87% yield). ^1H NMR (400 MHz, CDCl_3) δ 9.66 (d, $J = 0.6$ Hz, 1H), 7.59 (s, 1H), 6.28 (s, 2H), 6.09 (s, 1H), 3.90 (s, 3H); ^{13}C NMR (101 MHz, CDCl_3) δ 191.1, 161.0, 151.4, 139.7, 114.4, 98.5, 97.9, 56.4; IR (Neat Film, NaCl) 3431, 3313, 2843, 1652, 1611, 1228, 1198, 1048, 818 cm^{-1} ; HRMS (FAB+) m/z calculated for $\text{C}_8\text{H}_8\text{BrNO}_2$ [$\text{M} + \text{H}^+$] 229.9817, found 229.9842.



Quinoline 320: To a flame-dried 50 mL round-bottom flask with stir bar was added alcohol **327** (1.10 g, 4.75 mmol, 1.3 equiv) and a solution of aldehyde **321** (985 mg, 3.66 mmol, 1.0 equiv) in 1,4-dioxane (11 mL). The reaction was then heated to 80 °C for 1 hour. Benzophenone (3.33 g, 18.3 mmol, 5 equiv) was then added at 80 °C in a single portion, and the reaction mixture was stirred at that temperature for 5 minutes. A solution of potassium *tert*-butoxide (1.03g, 9.15 mmol, 2.5 equiv) in 1,4-dioxane (9.2 mL) was then added over 30 minutes via syringe pump. The reaction mixture was then stirred for an additional 15 minutes.

Upon completion, the reaction mixture was cooled to 23 °C, quenched with saturated sodium bicarbonate solution, and transferred to a separatory funnel. The mixture was extracted with ethyl acetate (3X) before the combined organic extracts were washed with brine, dried with sodium sulfate, and concentrated in vacuo. Flash column chromatography (30% ethyl acetate/hexanes) afforded quinoline **320** (1.26 g, 74% yield) as a yellow foam. ^1H NMR (400 MHz, CDCl_3) δ 8.63 (d, $J = 2.2$ Hz, 1H), 7.99 (s, 1H), 7.76 (s, 1H), 7.41 (s, 1H), 4.00 (s, 3H), 3.48 – 3.06 (m, 4H), 2.75 (d, $J = 13.8$ Hz, 1H), 2.65 (d, $J = 13.8$ Hz, 1H), 1.67 – 1.51 (m, 2H) (H_2O peak overlapping), 1.42 (s, 9H), 1.40 – 1.34 (m, 12), 1.22 (m, 2H), 0.95 (t, $J = 7.5$ Hz, 3H); ^{13}C NMR (101 MHz, DMSO) δ 155.3, 154.1, 153.4, 146.8, 135.1, 131.3, 129.4, 123.2, 113.1, 108.3, 78.5, 56.6, 51.3, 50.8, 37.4, 36.8, 32.4, 28.0, 25.5, 20.8, 7.5; IR (Neat Film, NaCl) 2969, 2933, 2855, 1688, 1614, 1598, 1477, 1427, 1365, 1323, 1273, 1247, 1207, 1157, 1042, 919, 849,

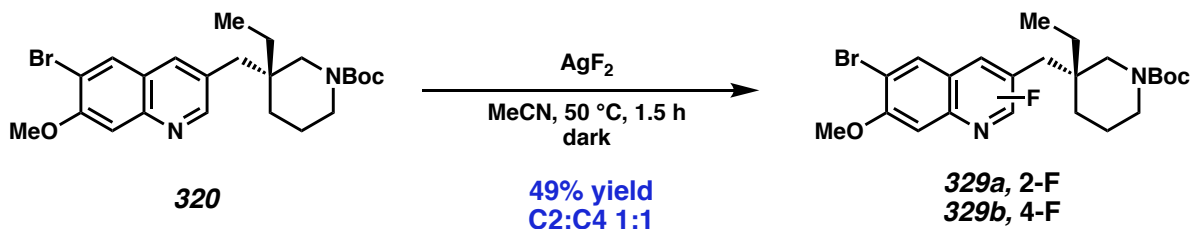
732 cm^{-1} ; HRMS (FAB+) m/z calculated for $\text{C}_{23}\text{H}_{32}\text{BrN}_2\text{O}_3$ [$\text{M} + \text{H}^+$] 463.1596, found 463.1623; $[\alpha]_{\text{D}}^{22.60}$ 21.2° (c 0.21, CHCl_3).



Amine 330: To a 10-mL round-bottom flask with stir bar was added quinoline **320** (46.3 mg, 0.10 mmol, 1.0 equiv) in dichloromethane (1.8 mL). The flask was cooled to 0 °C and trifluoroacetic acid (0.2 mL) was added dropwise. The flask was warmed slowly to 23 °C over 12 hours.

Upon completion, as determined by LCMS analysis, the solution was diluted with water, transferred to a scintillation vial, and extracted with diethyl ether (3X). The mixture was then basified to $\text{pH} = 7$ by addition of 1M NaOH. The aqueous layer was extracted with dichloromethane (3X), then 3:1 chloroform/isopropanol (3X), dried with sodium sulfate, then concentrated in vacuo. Preparative TLC (5% methanol/dichloromethane) afforded amine **330** (30.8 mg, 85% yield) as a white, amorphous solid. ^1H NMR (400 MHz, CDCl_3) δ 8.67 (d, $J = 2.2$ Hz, 1H), 7.98 (s, 1H), 7.78 (d, $J = 2.2$ Hz, 1H), 7.41 (s, 1H), 4.03 (s, 3H), 3.33 – 3.00 (bs, 1H), 2.91 – 2.83 (m, 3H), 2.77 (d, $J = 13.8$ Hz, 1H), 2.70 – 2.60 (m, 2H), 1.80 – 1.69 (m, 1H), 1.68 – 1.57 (m, 1H), 1.43 (t, $J = 6.2$ Hz, 2H), 1.33 (q, $J = 7.8$ Hz, 2H), 0.97 (t, $J = 7.5$ Hz, 3H); ^{13}C NMR (101 MHz, CDCl_3) δ 156.2, 153.6, 147.4, 135.3, 131.3, 129.9, 123.8, 114.3, 108.3, 56.6, 53.8, 46.5, 38.0, 36.6, 32.9, 27.2, 21.6, 14.3, 8.2, 7.6; IR (Neat Film, NaCl) 2932, 2855, 1614, 158, 1477, 1341, 1248, 126, 1042, 917, 850, 756, 612 cm^{-1} ;

HRMS (FAB+) m/z calculated for $C_{23}H_{32}BrN_2O_3$ $[M + H^+]$ 363.1072, found 363.1098;; $[\alpha]_D^{22.6}$ 3.5 (c 1.21, $CHCl_3$).



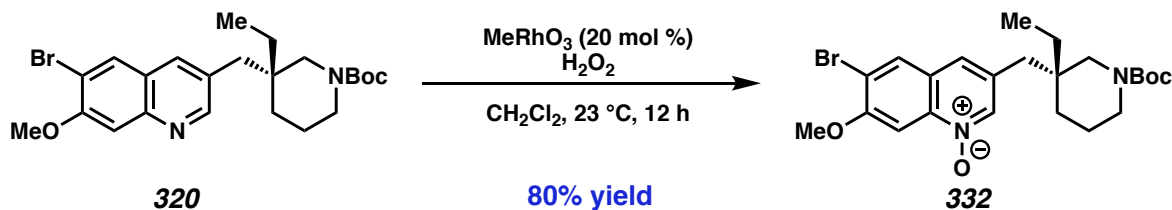
Fluoroquinolines 327a and 327: To an oven-dried one-dram vial with stir bar in a nitrogen filled glove box was added quinoline **320** (27.5 mg, 0.0593 mmol, 1.0 equiv) and acetonitrile (2.4 mL). Silver (II) fluoride (43.0 mg, 0.297 mmol, 5.0 equiv) was then added in a single portion. The vial was removed from the glovebox and heated to 50 °C in the dark for 1.5 hours.

After completion of the reaction, the reaction mixture was filtered through a pad of Celite and concentrated in vacuo. The crude mixture was dissolved in ethyl acetate and treated with saturated sodium bicarbonate. The organic extracts were separated and the aqueous layer was extracted with ethyl acetate (5X). The combined organic extracts were then washed with brine, dried with sodium sulfate, and concentrated in vacuo. Preparative TLC (30% ethyl acetate/hexanes) afforded both 2-fluoroquinoline **329a** (7.0mg, 24% yield) and 4-fluoroquinoline **329b** (6.8 mg, 24% yield) both as amorphous white solids.

2-fluoroquinoline 329a: ^1H NMR (400 MHz, CDCl_3) δ 8.00 (s, 1H), 7.86 (s, 1H), 7.27 (s, 1H), 4.01 (s, 3H), 3.78 – 3.25 (m, 2H), 3.00 (d, $J = 70.6$ Hz, 2H), 2.72 (s, 2H), 1.60 (s, 1H), 1.46 (s, 11H), 1.33 (dt, $J = 13.4, 6.9$ Hz, 3H), 0.95 (t, $J = 7.5$ Hz, 3H); ^{13}C NMR (101 MHz, CDCl_3) ^{13}C NMR (101 MHz, CDCl_3) δ 162.6, 160.2, 157.2, 155.3, 145.7, 141.4, 131.0, 122.9, 118.4, 113.3, 107.4, 79.6, 56.7, 51.2, 37.9, 34.6, 32.6, 28.6, 26.4, 21.3, 7.8.; IR 2932, 1688, 1480, 1428, 1366,

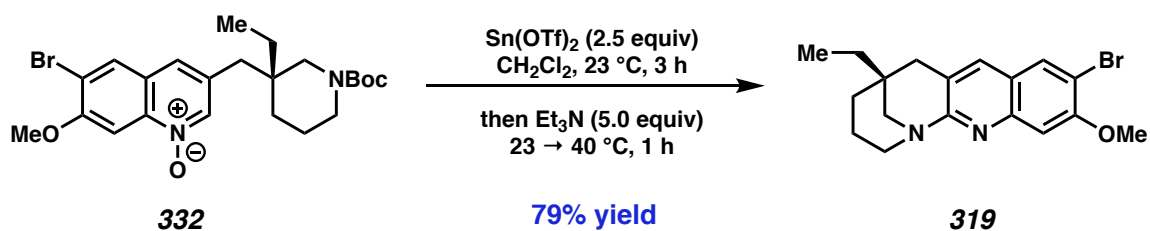
1249, 1157, 1041, 758 cm^{-1} (Neat Film, NaCl); HRMS (FAB+) m/z calculated for $\text{C}_{23}\text{H}_{31}\text{FBrN}_2\text{O}_3$ $[\text{M} + \text{H}^+]$ 481.1502, found 481.1523; $[\alpha]_{\text{D}}^{25}$ 27.2° (c 0.35, CHCl_3).

4-fluoroquinoline 327a: ^1H NMR (400 MHz, CDCl_3) ^1H NMR (400 MHz, Chloroform- d) δ 8.74 (d, $J = 2.1$ Hz, 1H), 7.82 (d, $J = 2.0$ Hz, 1H), 7.80 (s, 1H), 4.15 (d, $J = 2.1$ Hz, 3H), 3.35 (d, $J = 108.0$ Hz, 4H), 2.80 (d, $J = 14.0$ Hz, 1H), 2.71 (d, $J = 13.8$ Hz, 1H), 1.71 – 1.61 (m, 1H), 1.46 (s, 10H), 1.38 (dd, $J = 11.0, 5.1$ Hz, 1H), 1.29 – 1.16 (m, 2H), 0.97 (t, $J = 7.4$ Hz, 3H); ^{13}C NMR (101 MHz, CDCl_3) ^{13}C NMR (101 MHz, CDCl_3) δ 155.3, 153.6, 151.0, 148.4, 143.7, 137.7, 135.1, 131.9, 125.7, 125.5, 117.6, 79.7, 62.1, 52.3, 38.0, 37.6, 33.1, 28.6, 26.8, 21.4, 7.8; IR 2930, 2862, 1686, 1474, 1428, 1365, 1273, 1248, 1154, 1039, 754 cm^{-1} (Neat Film, NaCl); HRMS (FAB+) m/z calculated for $\text{C}_{23}\text{H}_{31}\text{FBrN}_2\text{O}_3$ $[\text{M} + \text{H}^+]$ 481.1502, found 481.1491; $[\alpha]_{\text{D}}^{22.6}$ 17.9° (c 0.32, CHCl_3).



Quinoline N-oxide 332: To a 50-mL round-bottom flask with stir bar was added quinoline **320** (1.60 g, 3.44 mmol, 1.0 equiv) and dichloromethane (3.5 mL). 35% hydrogen peroxide solution (1.67 mL, 17.2 mmol, 5.0 equiv) was added, followed by methyltrioxorhenium(VII) (171 mg, 0.688 mmol, 0.20 equiv). The biphasic reaction mixture was rapidly stirred at 23 °C for 12 hours. The reaction was quenched with 5 mg of manganese dioxide and stirred rapidly for 30 minutes until evolution of oxygen ceased. The solution was transferred to a separatory funnel and extracted with dichloromethane, before the combined organic extracts were dried with sodium sulfate and concentrated in vacuo to yield a yellow oil. Addition of ethyl acetate caused

quinoline N-oxide **332** to precipitate as a white, amorphous solid (1.32 g, 80% yield). ^1H NMR (400 MHz, CDCl_3) δ 8.38 (d, $J = 1.5$ Hz, 1H), 8.06 (s, 1H), 8.04 (s, 1H), 7.40 (s, 1H), 4.08 (s, 3H), 3.52 – 3.00 (m, 4H), 2.71 (d, $J = 13.9$ Hz, 1H), 2.58 (d, $J = 13.9$ Hz, 1H), 1.59 (dp, $J = 14.0$, 7.3, 6.8 Hz, 2H), 1.47 (s, 9H), 1.43 – 1.36 (m, 2H), 1.26 (m, 2H), 0.95 (t, $J = 7.5$ Hz, 3H); ^{13}C NMR (101 MHz, CDCl_3) ^{13}C NMR (101 MHz, CDCl_3) δ 157.5, 155.2, 140.3, 138.2, 131.9, 130.6, 126.3, 125.6, 117.0, 99.3, 79.9, 57.2, 51.9, 44.8, 43.9, 38.1, 37.5, 33.2, 28.6, 26.9, 21.4, 7.8; IR (Neat Film, NaCl) 2967, 2934, 2868, 1687, 1573, 1470, 1428, 1343, 1306, 1273, 1247, 1203, 1155, 1038, 863, 754 cm^{-1} ; HRMS (FAB+) m/z calculated for $\text{C}_{23}\text{H}_{31}\text{BrN}_2\text{O}_4$ [$\text{M} + \text{H}^+$] 479.1545, found 479.1538; $[\alpha]_{\text{D}}^{25}$ 16.8° (c 0.46, CHCl_3).



Tetracycle 332: To an oven-dried 1-dram vial in a nitrogen-filled glove box was added *N*-oxide **332** (96.0 mg, 0.20 mmol, 1.0 equiv), dichloromethane (1.0 mL), and tin (II) trifluoromethanesulfonate (2.5 equiv, 0.50 mmol, 2.5 equiv). This was repeated nine times and the reactions were stirred rapidly for 3 hours, during which time the solution turned from a clear yellow to a cloudy white. Triethylamine (1.39 mL, 1.00 mmol, 5.0 equiv) was added to each of the vials, which were then quickly sealed and heated to 40 °C for 1 hour.

After the reaction was complete, the vials were removed from the glovebox, diluted with dichloromethane, and transferred to a separatory funnel containing 0.5M aqueous sodium hydroxide. The solution was extracted with dichloromethane (5X), before the combined organic extracts were washed with brine, dried with sodium sulfate, and concentrated in vacuo. Flash

column chromatography (1% methanol/0.5% triethylamine/ethyl acetate → 3% methanol/0.5% triethylamine/ethyl acetate) afforded tetracycle **319** as a white solid. ^1H NMR (600 MHz, CDCl_3) δ 7.88 (s, 1H), 7.70 (s, 1H), 7.32 (s, 1H), 3.99 (s, 3H), 3.77 – 3.69 (m, 1H), 3.26 – 3.16 (m, 1H), 3.08 (dd, $J = 13.3, 2.2$ Hz, 1H), 2.94 (ddd, $J = 13.4, 2.9, 1.2$ Hz, 1H), 2.89 (dt, $J = 17.4, 1.7$ Hz, 1H), 2.73 (dt, $J = 17.3, 1.5$ Hz, 1H), 1.84 – 1.74 (m, 1H), 1.62 – 1.53 (m, 1H), 1.38 – 1.29 (m, 4H), 0.95 (t, $J = 7.5$ Hz, 3H); ^{13}C NMR (101 MHz, CDCl_3) δ 162.9, 156.1, 147.1, 134.5, 130.5, 126.1, 122.1, 112.0, 107.5, 58.1, 56.5, 56.0, 37.4, 36.1, 35.1, 30.9, 19.7, 7.3; IR (Neat Film, NaCl) 2928, 1612, 1477, 1449, 1371, 1234, 11127, 1040, 859, 755, 674, 649 cm^{-1} ; HRMS (FAB+) m/z calculated for $\text{C}_{18}\text{H}_{22}\text{N}_2\text{OBr}$ [$\text{M} + \text{H}^+$] 361.0916, found 363.0936; $[\alpha]_{\text{D}}^{22.7}$ 83.7° (c 0.99, CHCl_3 , 92% ee).



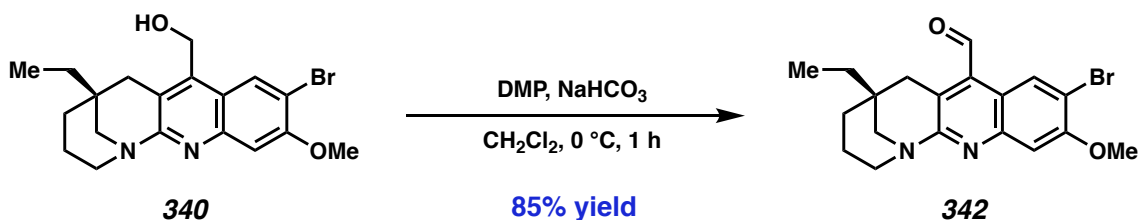
Alcohol 340: To a flame-dried, 25 mL round-bottom flask with stir bar was added tetracycle **319** (337 mg, 0.93 mmol, 1.0 equiv), benzoyl peroxide (451 mg, 1.87 mmol, 2.0 equiv), and methanol (9.3 mL). The reaction mixture is sparged with argon for 20 minutes before trifluoroacetic acid (0.71 mL, 9.34 mmol, 10.0 equiv) is added dropwise. The flask is placed in a Hepatochem© setup and irradiated with blue LED's for 45 minutes.

The mixture was quenched with sodium bicarbonate solution, transferred to a separatory funnel, and extracted with dichloromethane (3X). The combined organic extracts were washed with brine, dried, and concentrated in vacuo. Flash column chromatography (1 → 2 → 3 → 4 → 5% methanol/0.5% triethylamine/ethyl acetate) afforded alcohol **340** (280 mg, 77% yield) as a

white amorphous solid. ^1H NMR (400 MHz, CD_2Cl_2) δ 8.24 (s, 1H), 7.16 (s, 1H), 5.03 – 4.88 (m, 2H), 3.90 (s, 3H), 3.62 (ddt, $J = 13.1, 4.2, 2.1$ Hz, 1H), 3.12 – 3.03 (m, 1H), 3.03 – 2.91 (m, 1H), 2.88 – 2.64 (m, 3H), 2.39 – 1.97 (bs, 1H), 1.72 – 1.60 (m, 1H), 1.57 – 1.44 (m, 1H), 1.29 (q, $J = 7.5$ Hz, 2H), 1.22 (dd, $J = 6.3, 3.5$ Hz, 2H), 0.88 (t, $J = 7.6$ Hz, 3H); ^{13}C NMR (101 MHz, CD_2Cl_2); δ 163.1, 156.1, 147.8, 142.0, 128.3, 124.6, 120.9, 112.2, 108.0, 57.6, 57.3, 56.7, 56.3, 36.2, 35.8, 35.5, 31.1, 20.1, 7.4. IR (Neat Film, NaCl) 3178, 2923, 2853, 1606, 0580, 1463, 1451, 1410, 1369, 1236, 1046, 756 cm^{-1} ; HRMS (FAB+) m/z calculated for $\text{C}_{19}\text{H}_{24}\text{BrN}_2\text{O}_2$ [$\text{M} + \text{H}^+$] 391.1021, found 391.1013; $[\alpha]_{\text{D}}^{22.7}$ 83.6 (c 0.19, CHCl_3 , 92% ee).

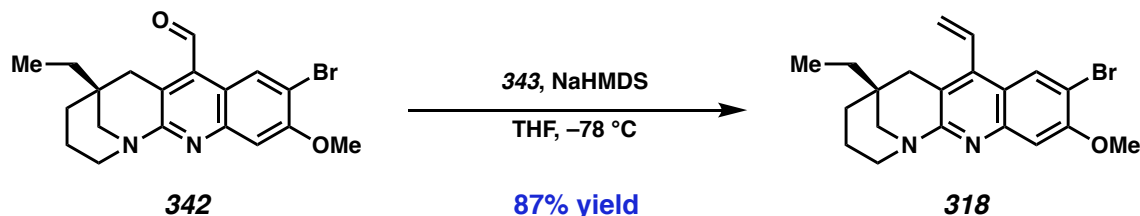
Figure 2.6. Reaction Setup for Photoredox-mediated Minisci Reaction.





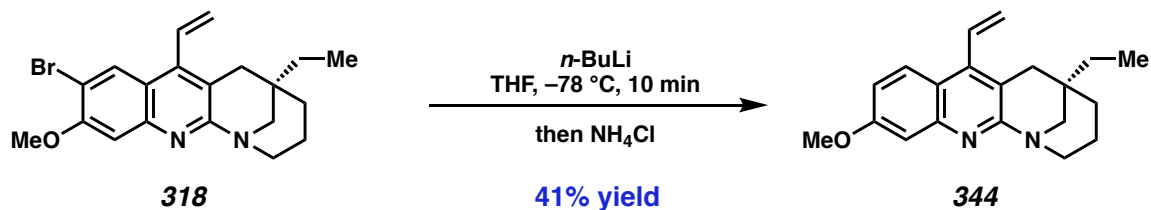
Aldehyde 342: To a 50-mL round bottom flask with stir bar was added alcohol **340** (280 mg, 0.716 mmol, 1.0 equiv), non-dried dichloromethane (14.2 mL), and sodium bicarbonate (420 mg, 5.01 mmol, 7.0 equiv). The flask was cooled to 0 °C and Dess-Martin periodinane (424 mg, 1.00 mmol, 1.4 equiv) was added as a single portion. The reaction mixture was stirred at 0 °C for 1 hour.

The reaction mixture was quenched with water, transferred to a separatory funnel, and extracted with dichloromethane (3X). The combined organic extracts were washed with brine, dried with sodium sulfate, and concentrated in vacuo. Flash column chromatography (0 → 20 → 30% ethyl acetate/dichloromethane) afforded aldehyde **342** (235 mg, 85% yield) as an amorphous, yellow solid. ^1H NMR (600 MHz, CD_2Cl_2) δ 10.88 (s, 1H), 8.82 (s, 1H), 7.31 (s, 1H), 4.01 (s, 3H), 3.79 – 3.74 (m, 1H), 3.25 (dd, $J = 18.1, 1.5$ Hz, 1H), 3.23 – 3.17 (m, 1H), 3.12 (dd, $J = 13.3, 2.3$ Hz, 1H), 3.02 (dd, $J = 18.1, 2.3$ Hz, 1H), 2.94 (ddd, $J = 13.5, 2.8, 1.3$ Hz, 1H), 1.80 – 1.73 (m, 1H), 1.66 – 1.59 (m, 1H), 1.41 (q, $J = 7.6$ Hz, 2H), 1.34 (tt, $J = 10.5, 3.1$ Hz, 2H), 0.98 (t, $J = 7.6$ Hz, 3H); ^{13}C NMR (101 MHz, CD_2Cl_2) δ 193.6, 163.6, 156.5, 148.5, 133.8, 128.5, 128.4, 117.7, 114.7, 107.9, 57.2, 56.79, 56.46, 36.0, 35.8, 35.4, 31.1, 20.2, 7.4; IR (Neat Film, NaCl) 2926, 1692, 1603, 1567, 1478, 1363, 1230, 1215, 1043, 752 cm^{-1} ; HRMS (FAB+) m/z calculated for $\text{C}_{19}\text{H}_{22}\text{BrN}_2\text{O}_2$ [$\text{M} + \text{H}^+$] 389.0865, found 389.0854; $[\alpha]_{\text{D}}^{22.7}$ 311.7° (c 0.05, CHCl_3 , 92% ee).



Alkene 318: To an oven-dried 1-dram vial with stir bar was added aldehyde **342** (50 mg, 0.128 mmol, 1.0 equiv), sulfone **343** (31.5 mg, 0.154 mmol, 1.2 equiv), and tetrahydrofuran (1.28 mL). The vial is cooled to $-78\text{ }^{\circ}\text{C}$ and sodium hexamethyldisilazane (30.4 mg, 0.166 mmol, 1.3 equiv) was added quickly as a single portion. The reaction mixture was stirred at $-78\text{ }^{\circ}\text{C}$ for 30 minutes and monitored by TLC.

The reaction was quenched with saturated ammonium chloride and warmed up to $23\text{ }^{\circ}\text{C}$. The mixture was extracted with ethyl acetate (5X) before the combined organic extracts were washed with brine, dried with sodium sulfate, and concentrated in vacuo. Flash column chromatography (0.5% triethylamine in ethyl acetate) afforded alkene **318** (42.7 mg, 87% yield) as a light yellow oil. ^1H NMR (400 MHz, CDCl_3) δ 8.21 (s, 1H), 7.32 (s, 1H), 6.80 (ddt, $J = 17.9, 11.7, 0.9$ Hz, 1H), 5.88 (dd, $J = 11.7, 1.6$ Hz, 1H), 5.56 (dd, $J = 18.0, 1.7$ Hz, 1H), 4.00 (s, 3H), 3.79 (dd, $J = 14.0, 3.8$ Hz, 1H), 3.20 (ddd, $J = 13.4, 11.3, 4.8$ Hz, 1H), 3.07 (dd, $J = 13.3, 2.2$ Hz, 1H), 2.93 (ddd, $J = 13.5, 2.7, 1.3$ Hz, 1H), 2.72 (dt, $J = 17.9, 1.2$ Hz, 1H), 2.58 – 2.51 (m, 1H), 1.81 – 1.71 (m, 1H), 1.62 – 1.50 (m, 1H), 1.41 – 1.27 (m, 4H), 0.95 (t, $J = 7.5$ Hz, 3H); ^{13}C NMR (101 MHz, CDCl_3) δ 162.1, 156.0, 147.4, 142.9, 131.6, 129.1, 123.4, 122.8, 120.1, 111.9, 107.8, 57.6, 56.5, 56.0, 36.8, 36.2, 35.3, 30.9, 19.8, 7.4; IR (Neat Film, NaCl) 2957, 2932, 1603, 1560, 1479, 1449, 1412, 1367, 1229, 1045, 1001, 847, 754 cm^{-1} ; HRMS (FAB+) m/z calculated for $\text{C}_{20}\text{H}_{24}\text{BrN}_2\text{O}$ [$\text{M} + \text{H}^+$] 387.1073, found 387.1072; $[\alpha]_{\text{D}}^{22.7}$ 186.5° (c 0.20, CHCl_3 , 92% ee).



***O*-methyleucophylline 344:** To an oven-dried, 1-dram vial with stir bar was added alkene **318** (15.5 mg, 0.040 mmol, 1.0 equiv) in THF (0.4 mL). The vial was cooled to $-78\text{ }^\circ\text{C}$ and stirred for 10 minutes. *n*-BuLi (2.30 M in hexanes, 0.0480 mmol, 24 μL , 1.1 equiv) was added dropwise and the reaction mixture was stirred for an additional 10 minutes.

The reaction was then diluted with diethyl ether, quenched with saturated ammonium chloride solution and warmed to $23\text{ }^\circ\text{C}$ over 30 minutes. The organic extracts were separated and the aqueous layer was extracted with ethyl acetate (3X). The combined organic extracts were washed with brine, dried with sodium sulfate, and concentrated in vacuo. Preparative TLC (100% ethyl acetate) affords *O*-methyleucophylline **344** (5.1 mg, 41% yield) as a light yellow oil. ^1H NMR (400 MHz, CDCl_3) δ 7.92 (d, $J = 9.2$ Hz, 1H), 7.27 (d, $J = 2.6$ Hz, 1H), 7.03 (dd, $J = 9.2, 2.6$ Hz, 1H), 6.84 (ddt, $J = 17.9, 11.6, 0.9$ Hz, 1H), 5.84 (dd, $J = 11.7, 1.8$ Hz, 1H), 5.54 (dd, $J = 18.0, 1.8$ Hz, 1H), 3.91 (s, 3H), 3.81 – 3.72 (m, 1H), 3.18 (ddd, $J = 13.5, 12.4, 3.7$ Hz, 1H), 3.07 (dd, $J = 13.2, 2.1$ Hz, 1H), 2.94 (ddd, $J = 13.2, 3.0, 1.1$ Hz, 1H), 2.72 (dt, $J = 17.7, 1.3$ Hz, 1H), 2.60 – 2.51 (m, 1H), 1.80 – 1.31 (m, 6H), 0.95 (t, $J = 7.6$ Hz, 3H); ^{13}C NMR (101 MHz, CDCl_3) δ 161.8, 160.1, 148.5, 143.7, 132.1, 126.1, 122.7, 121.9, 119.4, 117.7, 106.7, 57.8, 55.9, 55.5, 36.8, 36.3, 35.3, 30.8, 19.7, 7.4; IR (Neat Film, NaCl) 3730, 2919, 1620, 1557, 1452, 1370, 1226, 1159, 1026, 941, 848 cm^{-1} ; HRMS (FAB+) m/z calculated for $\text{C}_{20}\text{H}_{54}\text{N}_2\text{O}$ [$\text{M} + \text{H}^+$] 309.1967, found 309.1950; $[\alpha]_{\text{D}}^{22.7}$ 117.0° (c 0.26, CHCl_3). Data were consistent with literature values.¹²

2.5.3 Comparison of NMR Data to Known Samples

Table 2.6. Comparison of eburnamonine ¹H NMR peaks to previously synthesized material

Synthetic Eburnamonine (This research, 400 MHz)	Synthetic Eburnamonine (Panday)
8.37 (m, 1H)	8.38 (m, 1H)
7.44 (m, 1H)	7.45 (m, 1H)
7.32 (m, 2H)	7.33 (m, 2H)
4.05 (bs)	3.99 (bs, 1H)
3.38 (dd, $J = 13.9, 6.7$ Hz)	3.30 (m, 2H)
3.29 (ddd, $J = 13.9, 11.3, 5.8$ Hz)	3.30 (m, 2H)
2.92 (dddd, $J = 16.9, 11.3, 6.7, 2.9$ Hz, 1H)	2.91 (m, 1H)
2.69 (d, $J = 16.8$ Hz, 1H)	2.64 (m, 3H)
2.66 (bs, 1H)	2.64 (m, 3H)
2.60 (d, $J = 16.8$ Hz, 1H)	2.64 (m, 3H)
2.50 (m, 2H)	2.46 (m, 2H)
2.09 (dq, $J = 15.1, 7.6$ Hz, 1H)	2.06 (m, 1H)
1.81 (qt, $J = 13.2, 3.9$ Hz, 1H)	1.72 (m, 2H)
1.68 (dq, $J = 14.7, 7.4$ Hz, 1H)	1.72 (m, 1H)
1.51 (ddt, $J = 13.6, 3.6, 1.9$ Hz, 1H)	1.50 (d, $J = 13.7$, 1H)
1.42 (m, 1H)	1.40 (m, 1H)
1.05 (td, $J = 13.6, 3.9$ Hz, 1H)	1.05 (dt, $J = 13.5, 3.8$ Hz, 1H)
0.94 (t, $J = 7.6$ Hz, 3H)	0.94 (t, $J = 7.6$ Hz, 3 H)

Table 2.7. Comparison of eburnamonine ^{13}C NMR peaks to previously synthesized material.

Synthetic Eburnamonine (This research, 101 MHz)	Synthetic Eburnamonine (Panday, 100 MHz)
167.6	167.6
134.4	134.2
131.6	132.0
130.0	130.1
124.7	124.3
124.1	123.8
118.3	118.1
116.4	116.2
112.7	112.6
57.9	57.7
50.9	50.6
44.5	44.4
44.4	44.3
38.7	38.4
28.5	28.3
26.9	26.9
20.6	20.6
16.7	16.5
7.8	7.6

Table 2.8. Comparison of *O*-methyl eucophylline ¹H NMR peaks to previously synthesized material.

Synthetic <i>O</i> -methyleucophylline (This research, 400 MHz)	Synthetic <i>O</i> -methyleucophylline (Landais, 300 MHz)
7.92 (d, <i>J</i> = 9.2 Hz, 1H)	7.91 (d, 1H, <i>J</i> = 9.3 Hz)
7.27 (d, <i>J</i> = 2.6 Hz, 1H),	7.27 (d, 1H, <i>J</i> = 2.7 Hz)
7.03 (dd, <i>J</i> = 9.2, 2.6 Hz, 1H)	7.02 (dd, 1H, <i>J</i> = 2.7, 9.3 Hz)
6.84 (ddt, <i>J</i> = 17.9, 11.6, 0.9 Hz, 1H)	6.83 (dd, 1H, <i>J</i> = 11.7, 18 Hz)
5.84 (dd, <i>J</i> = 11.7, 1.8 Hz, 1H)	5.83 (dd, 1H, <i>J</i> = 1.8, 11.7 Hz)
5.54 (dd, <i>J</i> = 18.0, 1.8 Hz, 1H)	5.53 (dd, 1H, <i>J</i> = 1.8, 18 Hz)
3.91 (s, 3H)	3.90 (s, 3H),
3.81 – 3.72 (m, 1H)	3.84-3.73 (m, 1H)
3.18 (ddd, <i>J</i> = 13.5, 12.4, 3.7 Hz, 1H)	3.24-3.12 (m, 1H)
3.07 (dd, <i>J</i> = 13.2, 2.1 Hz, 1H)	3.06 (dd, 1H, <i>J</i> = 1.8, 13.2 Hz),
2.94 (ddd, <i>J</i> = 13.2, 3.0, 1.1 Hz, 1H)	2.93 (dd, 1H, <i>J</i> = 1.5, 13.2 Hz)
2.72 (dt, <i>J</i> = 17.7, 1.3 Hz, 1H)	2.71 (d, 1H, <i>J</i> = 17.7 Hz),
2.60 – 2.51 (m, 1H)	2.54 (dd, 1H, <i>J</i> = 1.5, 17.7 Hz)
1.80-1.31 (m, 6H)	1.80-1.25 (m, 4H)
“	1.35 (q, 2H, <i>J</i> = 7.5 Hz),
0.95 (t, <i>J</i> = 7.6 Hz, 4H).	0.94 (t, 3H, <i>J</i> = 7.5 Hz).

Table 2.9. Comparison of *O*-methyl eucophylline ^{13}C NMR peaks to previously synthesized material.

Synthetic <i>O</i> -methyleucophylline (This research, 101 MHz)	Synthetic <i>O</i> -methyleucophylline (Landais, 75 MHz)
161.8	161.6
160.1	160.0
148.5	148.4
143.7	143.6
132.1	131.9
126.1	126.0
122.37	122.6
121.9	121.8
119.4	119.2
117.7	117.5
106.7	106.5
57.8	57.6
55.9	55.7
55.5	55.4
36.8	36.6
36.3	36.1
35.3	35.1
30.8	30.6
19.7	19.5
7.4	7.2

2.5.4 Additional References

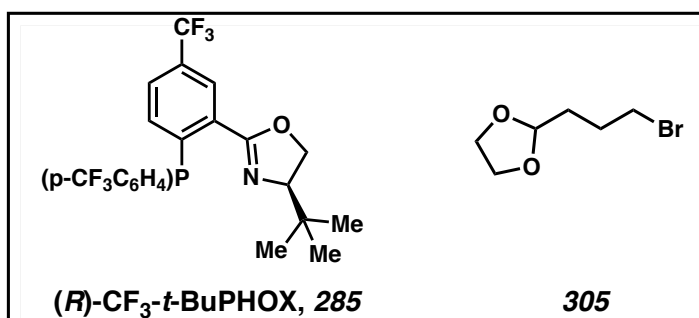
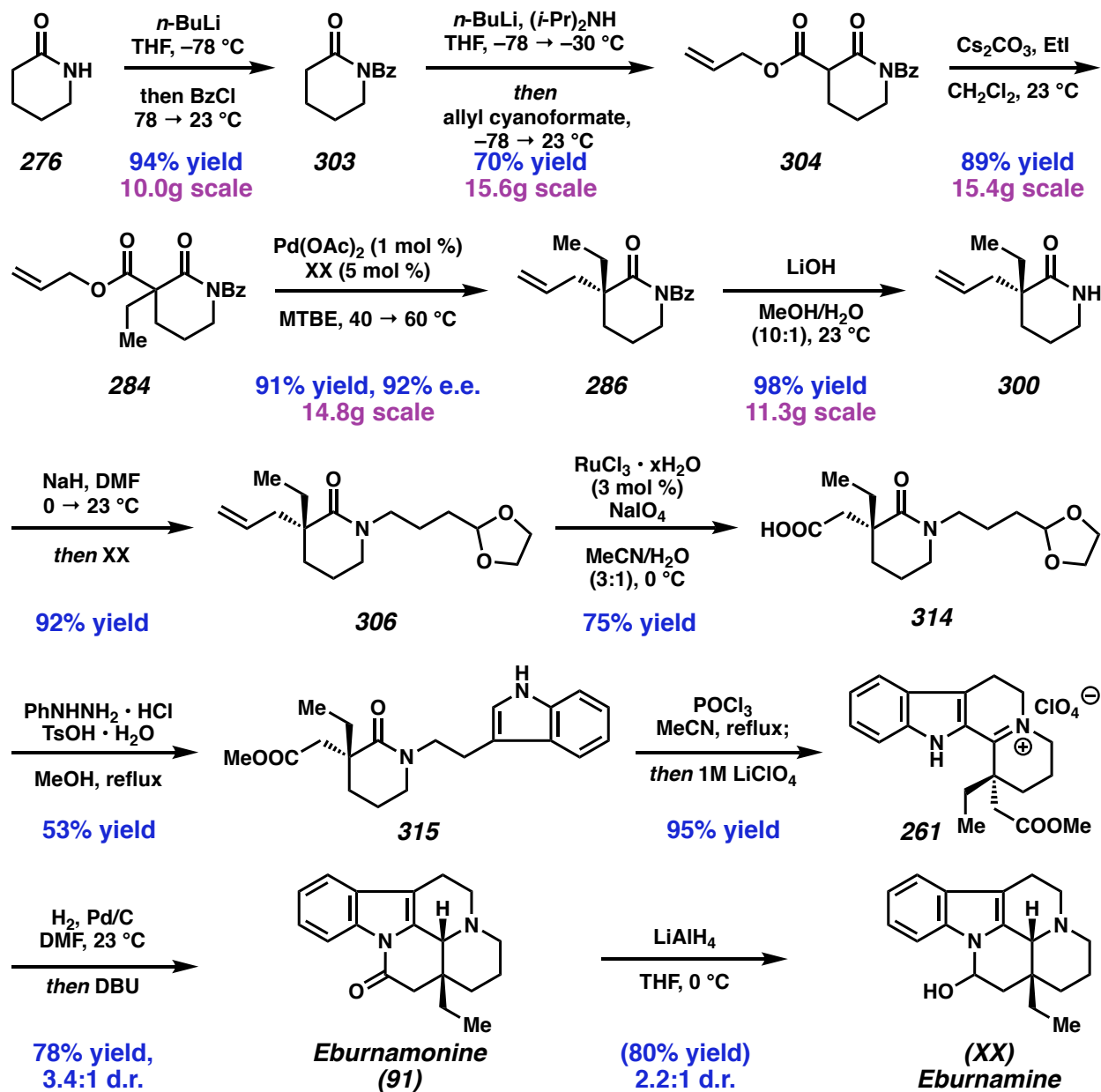
- (1) Pangborn, A. M.; Giardello, M. A.; Grubbs, R. H.; Rosen, R. K.; Timmers, F. J. *Organometallics* **1996**, *15*, 1518–1520.
- (2) Fulmer, G.R, Miller, A.J.M.; Sherden, N.H.; Gottlieb, H.E.; Nudelman, A.; Stoltz, B.M.; Bercaw, J.E.; Goldberg, K.I. *Organometallics* **2010**, *29*, 2176–2179.
- (3) Gilman, H.; Cartledge, F.K. *J. Organomet. Chem.* **1964**, *2*, 447–454.
- (4) Childs, M. E.; Weber, W. P. *J. Org. Chem.* **1976**, *41*, 3486–3487
- (5) McDougal, N. T.; Streuff, J.; Mukherjee, H.; Virgil, S. C.; Stoltz, B. M. *Tetrahedron Lett.* **2010**, *51*, 5550–5554.
- (6) Varseev, G.N.; Maier, M.E. A Novel. *Org. Lett.* **2005**, *7*, 3881 – 3884.
- (7) Aissa C. *J. Org. Chem.* **2006**, *71*, 360–363.
- (8) Gigant, N.; Chausset-Boissarie, L.; Belhomme, M-C.; Poisson, T.; Pannecoucke, X.; Gillaizeau, I. *Org. Lett.* **2012**, *15*, 278–281.
- (9) Behenna, D.C.; Liu, Y.; Taiga, Y.; Kim, J.; White, D.E.; Virgil, S.C.; Stoltz, B.M. *Nature Chem.* **2012**, *4*, 130–133.
- (10) Pandey, G.; Mishra, A.; Dhamrai, J. *Org. Lett.* **2017**, *19*, 3267–3270.
- (11) Ho, T-L.; Chen, C-K. *Helv. Chim. Act.* **2005**, *88*, 2764-2770.
- (12) Hassan, H.; Mohammed, S.; Robert, F.; Landais, Y. *Org. Lett.* **2015**, *17*, 4518–4521.

APPENDIX 1

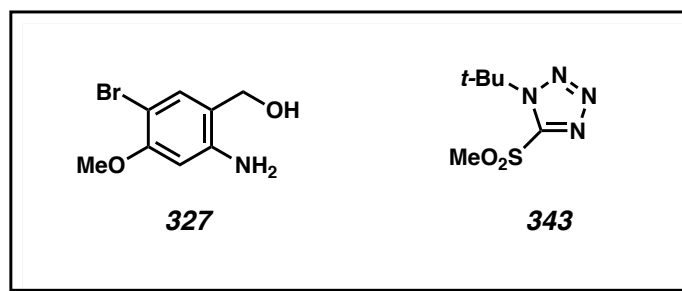
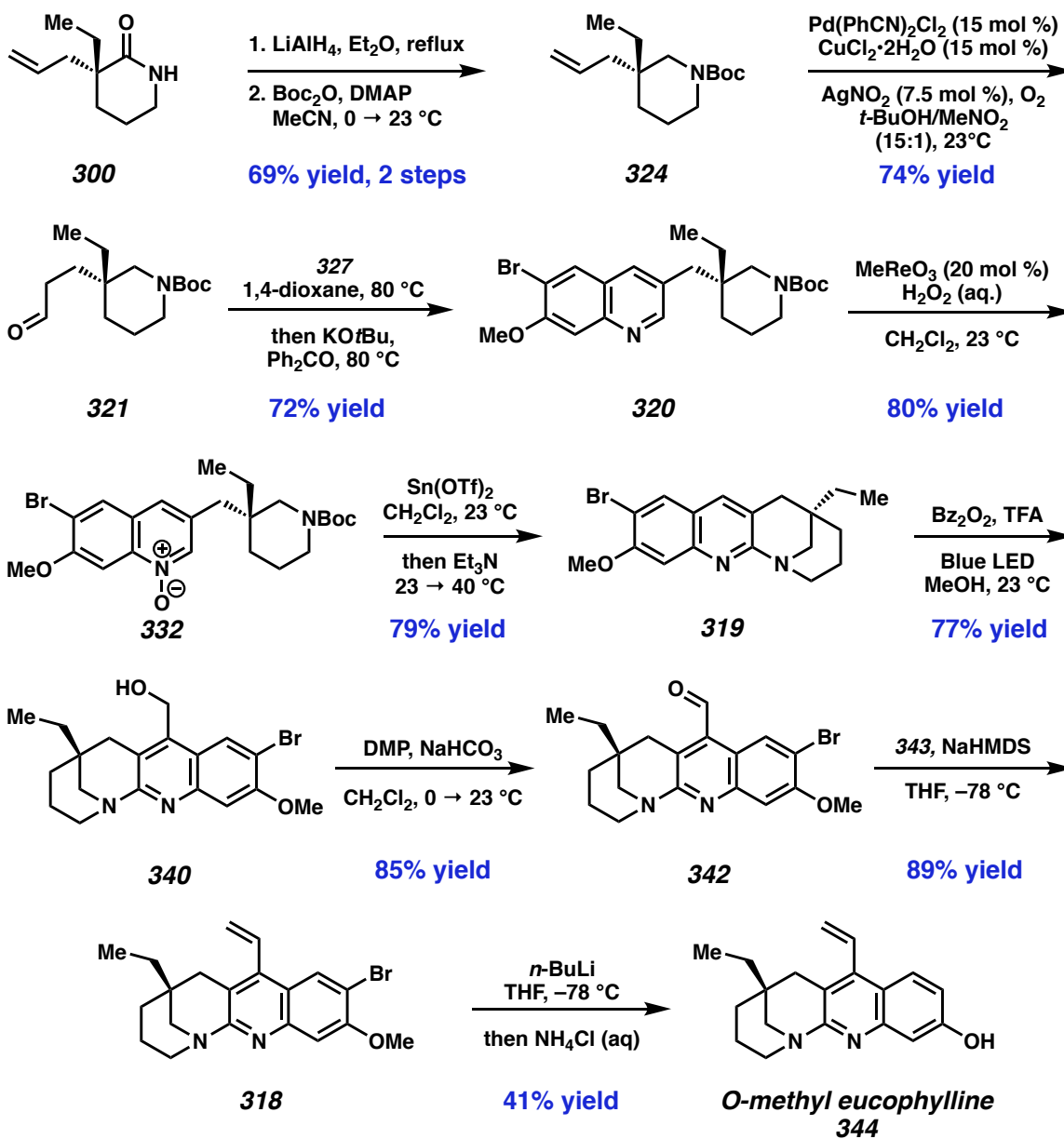
Synthetic Summary for Chapter 2:

*The Divergent Synthesis of
Eburnamine and Eucophylline*

Scheme A1.1. Total synthesis of eburnamine and eburnamonine



Scheme A1.2. Total synthesis of 6-bromoecucophylline

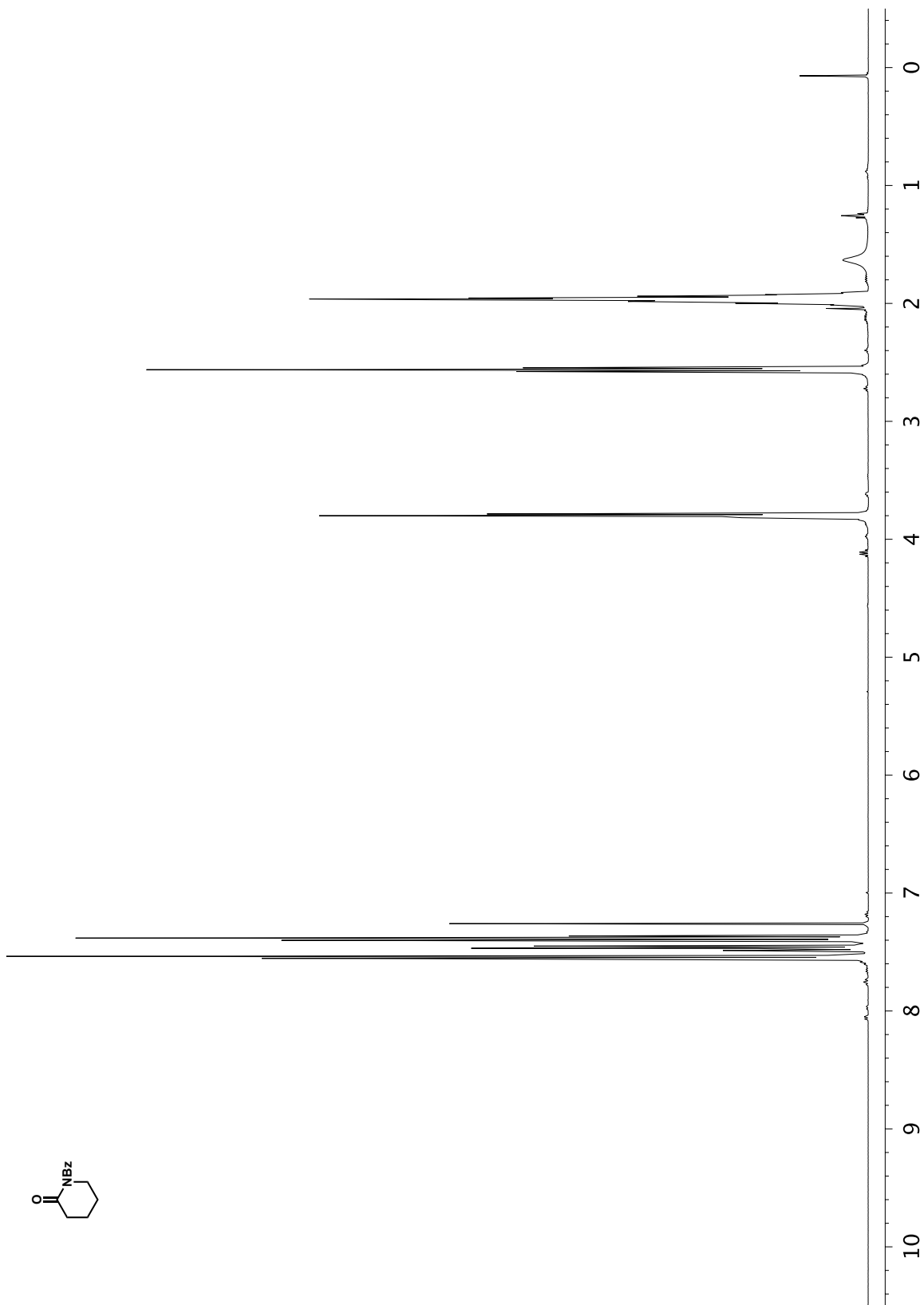


APPENDIX 2

Spectra Relevant to Chapter 3:

Divergent Synthesis of

Eburnamine and Eucophylline



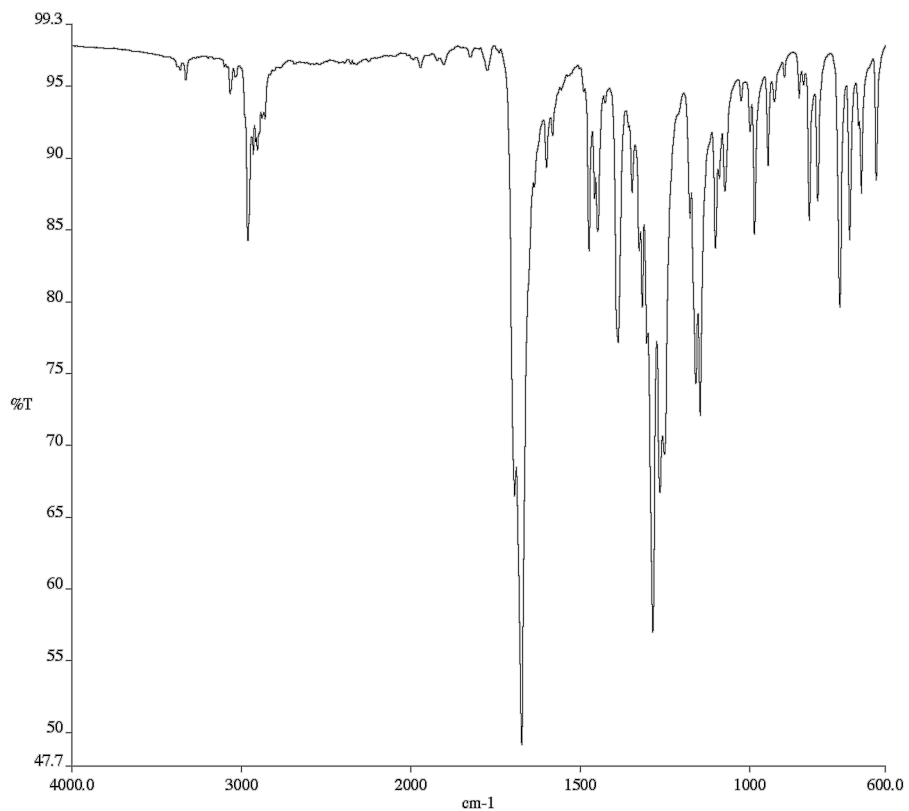


Figure A2.2. Infrared spectrum (Thin Film, NaCl) of compound **303**.

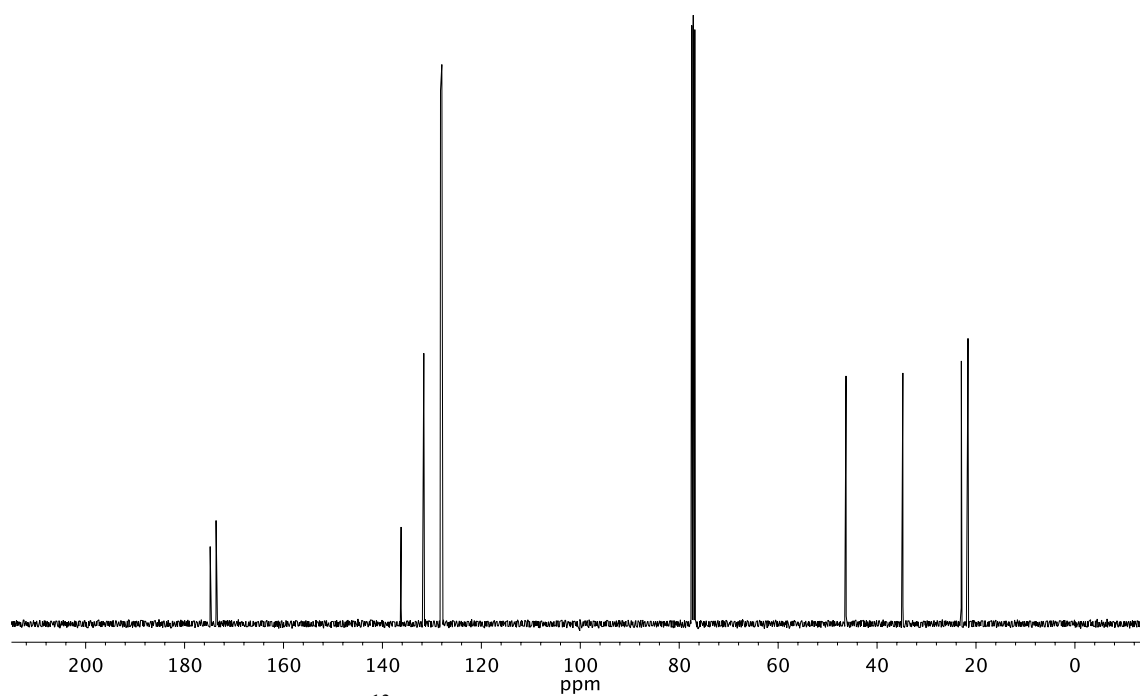


Figure A2.3. ¹³C NMR (101 MHz, CDCl₃) of compound **303**.

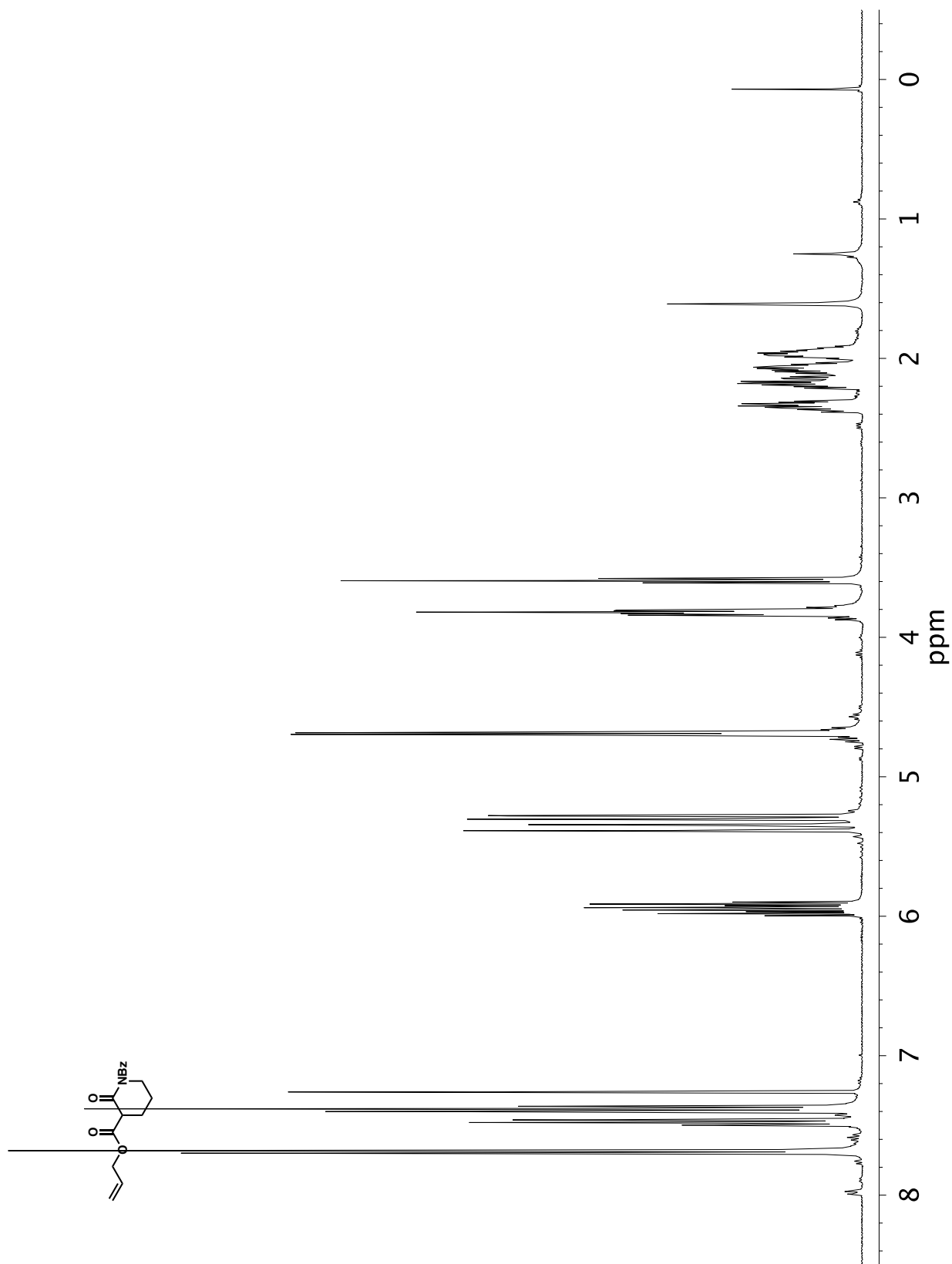


Figure A2.4. ^1H NMR (400 MHz, CDCl_3) of compound 304.

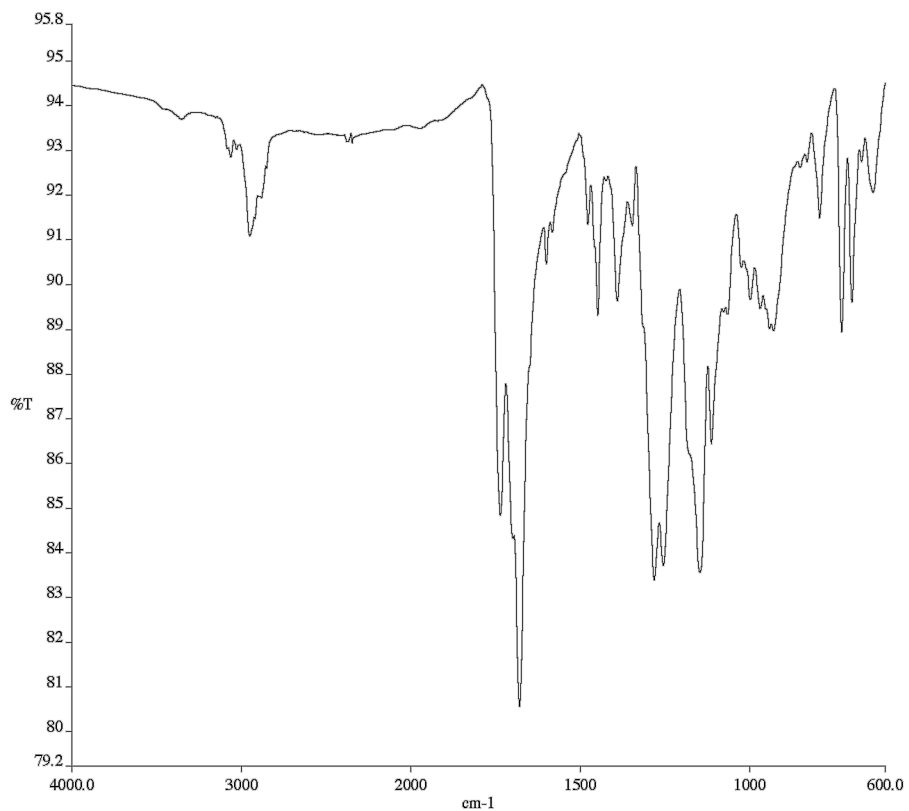


Figure A2.5. Infrared spectrum (Thin Film, NaCl) of compound **304**.

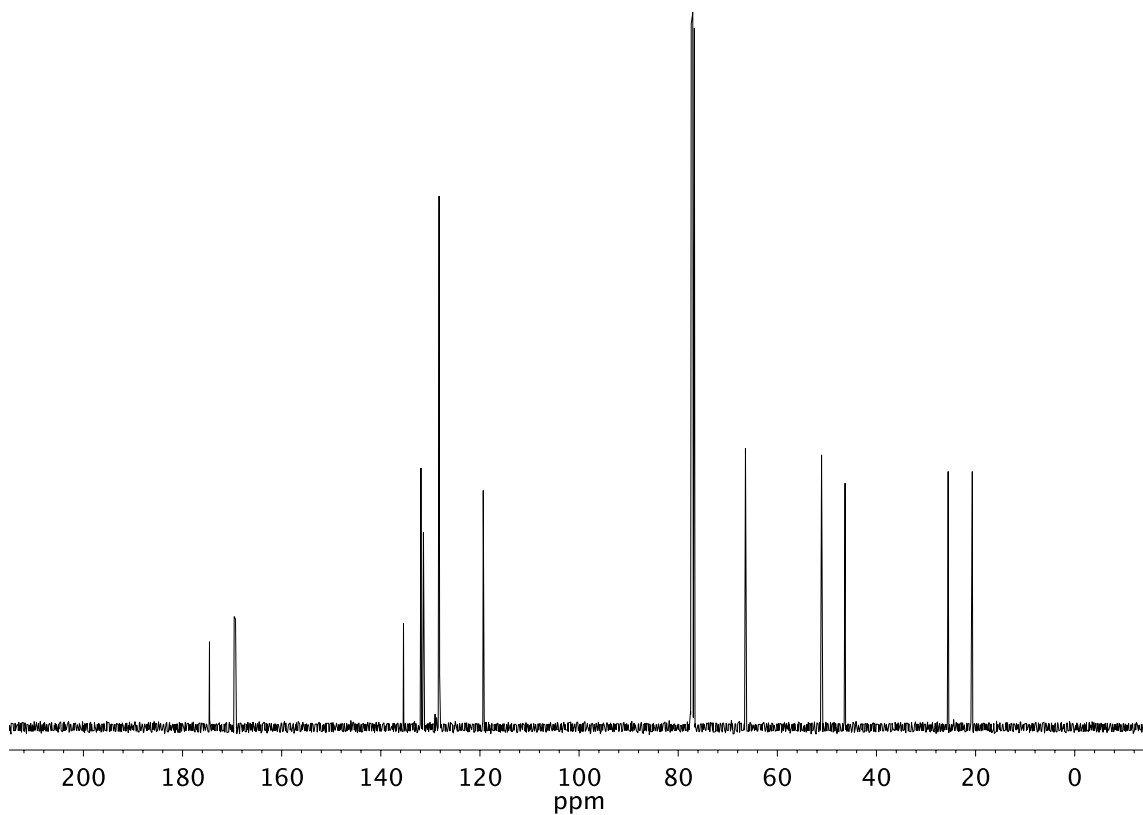


Figure A2.6. ¹³C NMR (101 MHz, CDCl₃) of compound **304**.

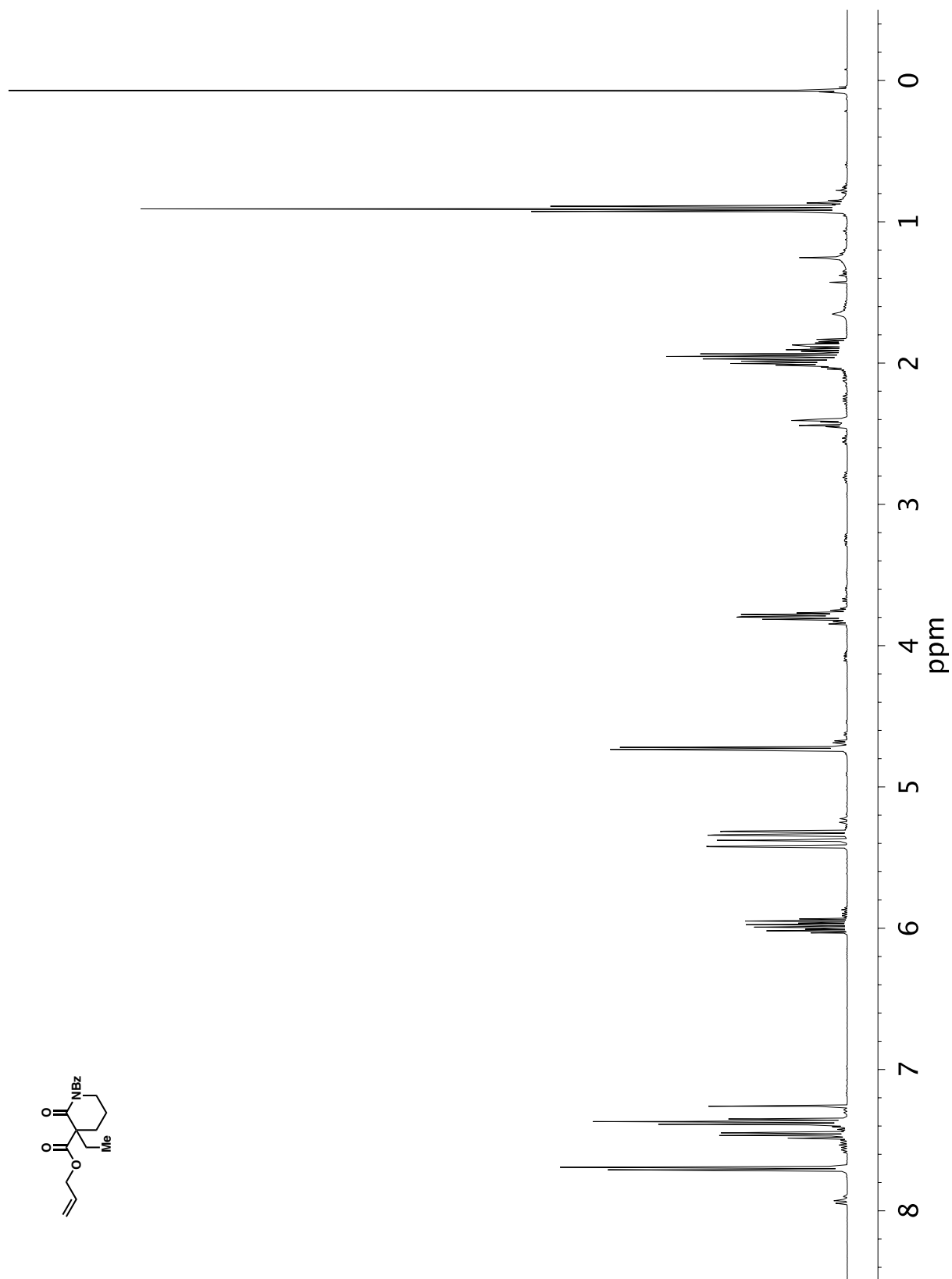


Figure A2.7. ¹H NMR (400 MHz, CDCl₃) compound **284**.

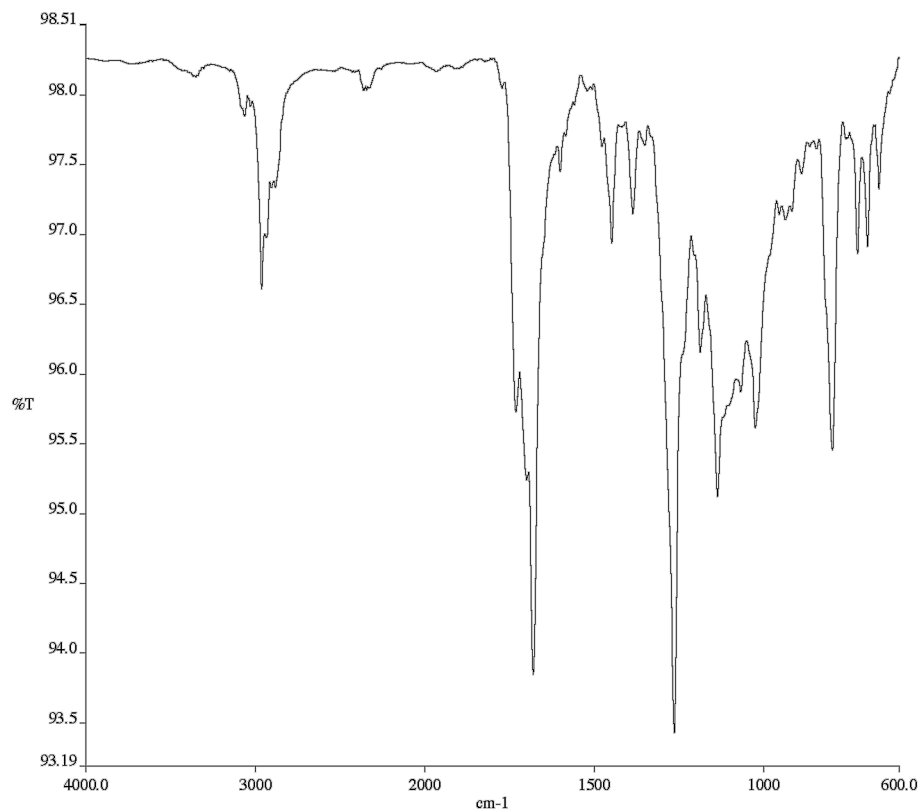


Figure A2.8. Infrared spectrum (Thin Film, NaCl) of compound **284**.

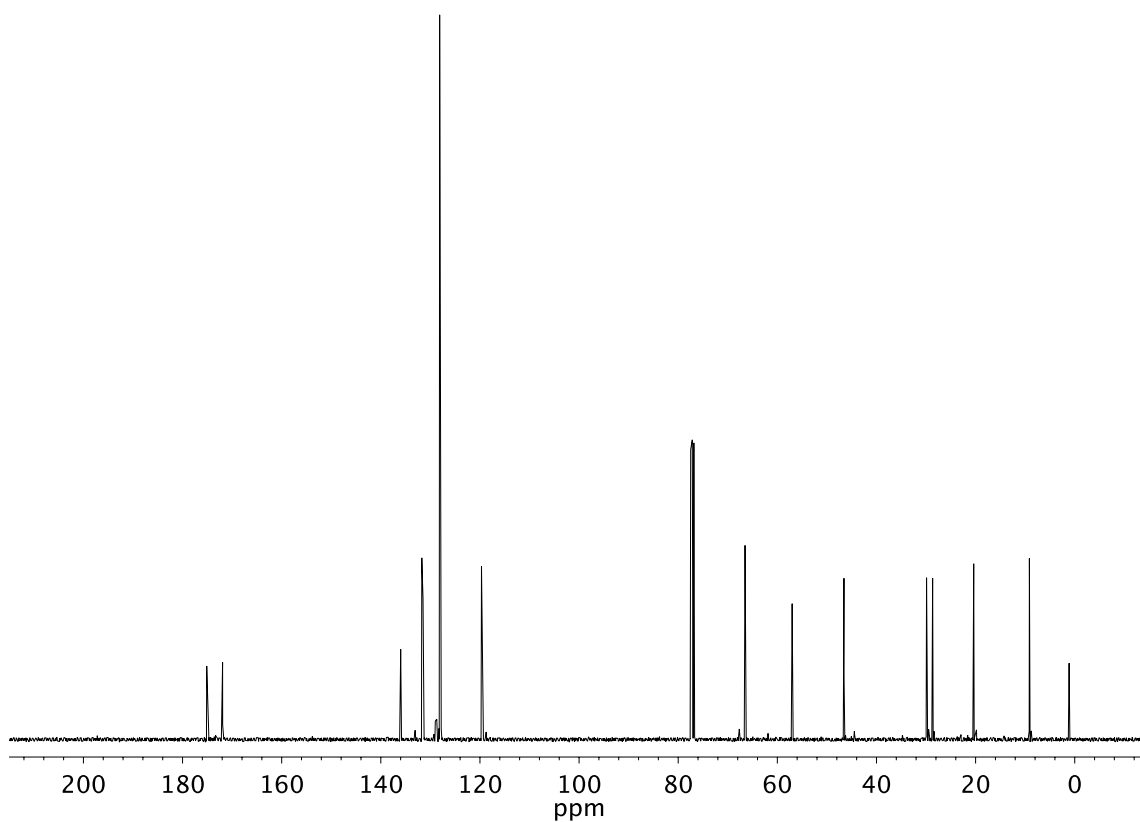


Figure A2.9. ¹³C NMR (101 MHz, CDCl₃) of compound **284**.

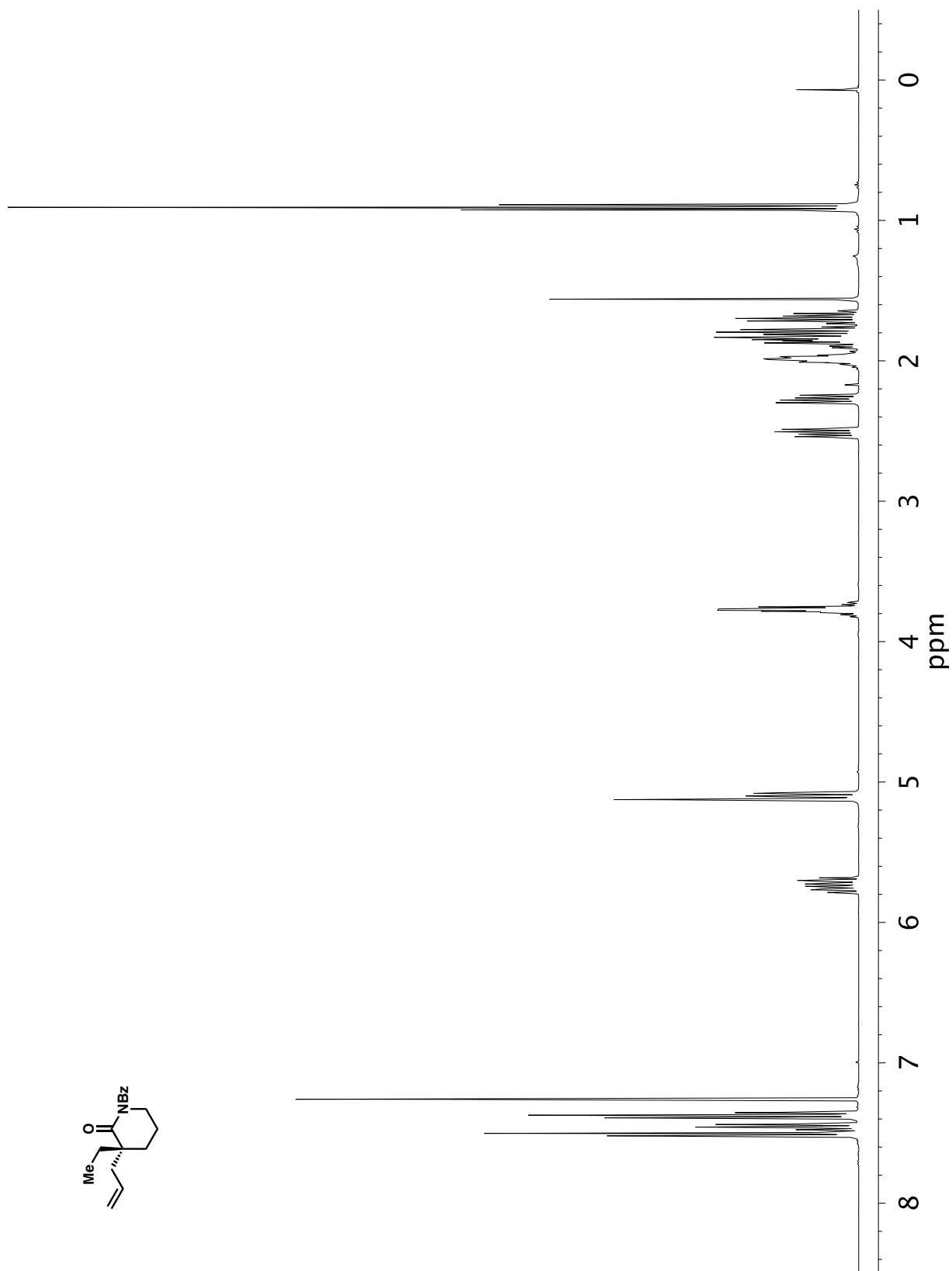


Figure A2.10. ^1H NMR (400 MHz, CDCl_3) of compound 286.

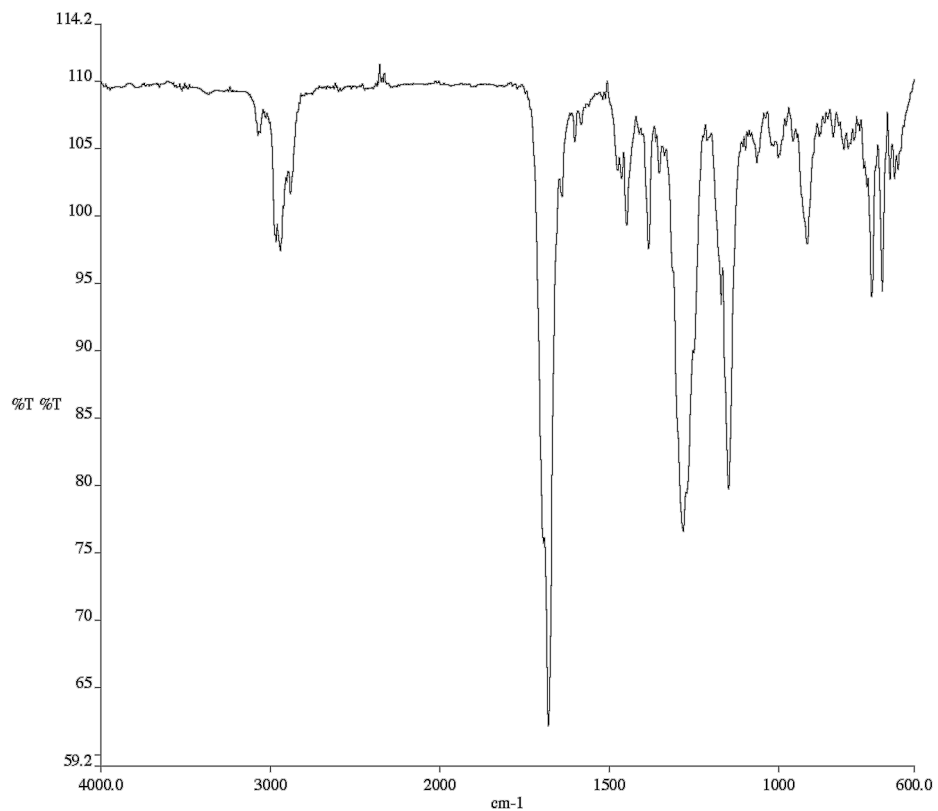


Figure A2.11. Infrared spectrum (Thin Film, NaCl) of compound **286**.

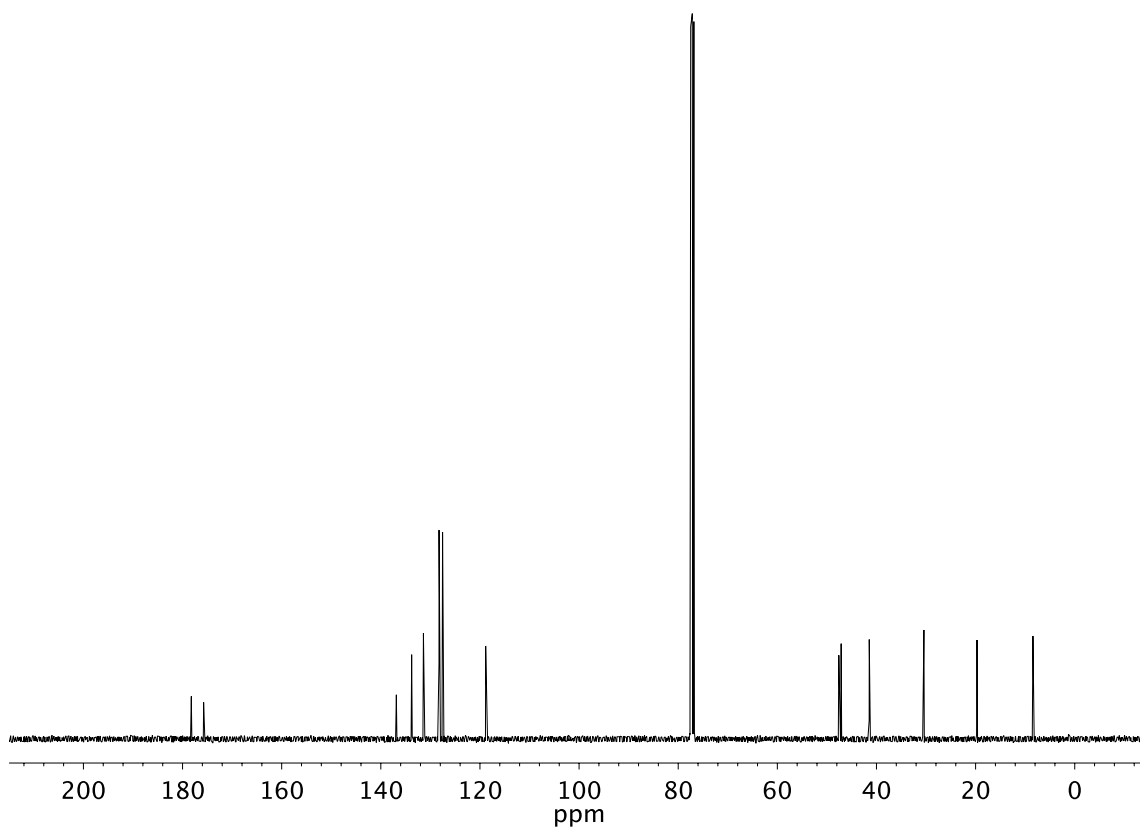


Figure A2.12. ¹³C NMR (101 MHz, CDCl₃) of compound **286**.

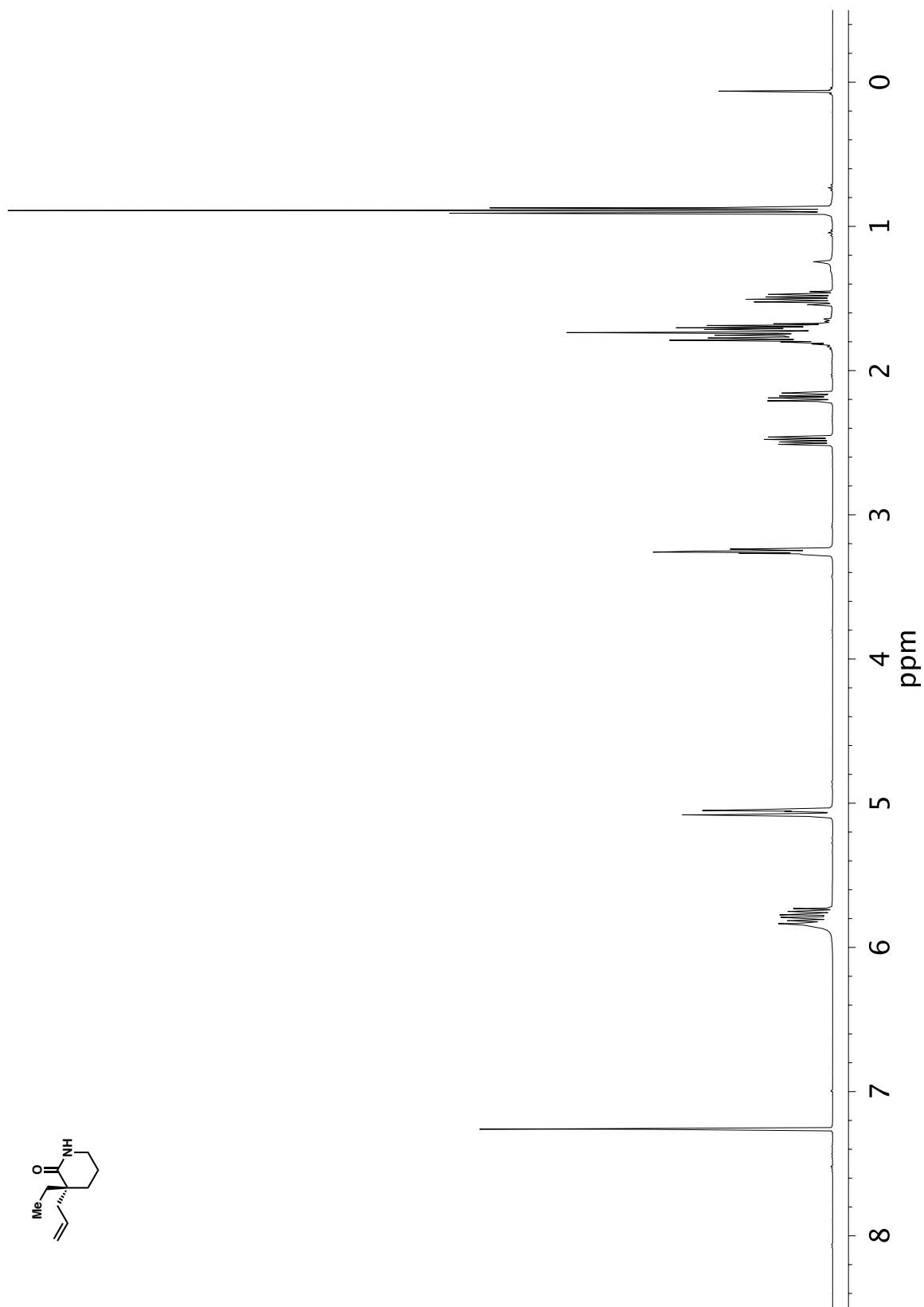
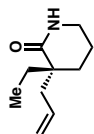


Figure A2.13. ^1H NMR (400 MHz, CDCl_3) of P compound 300.



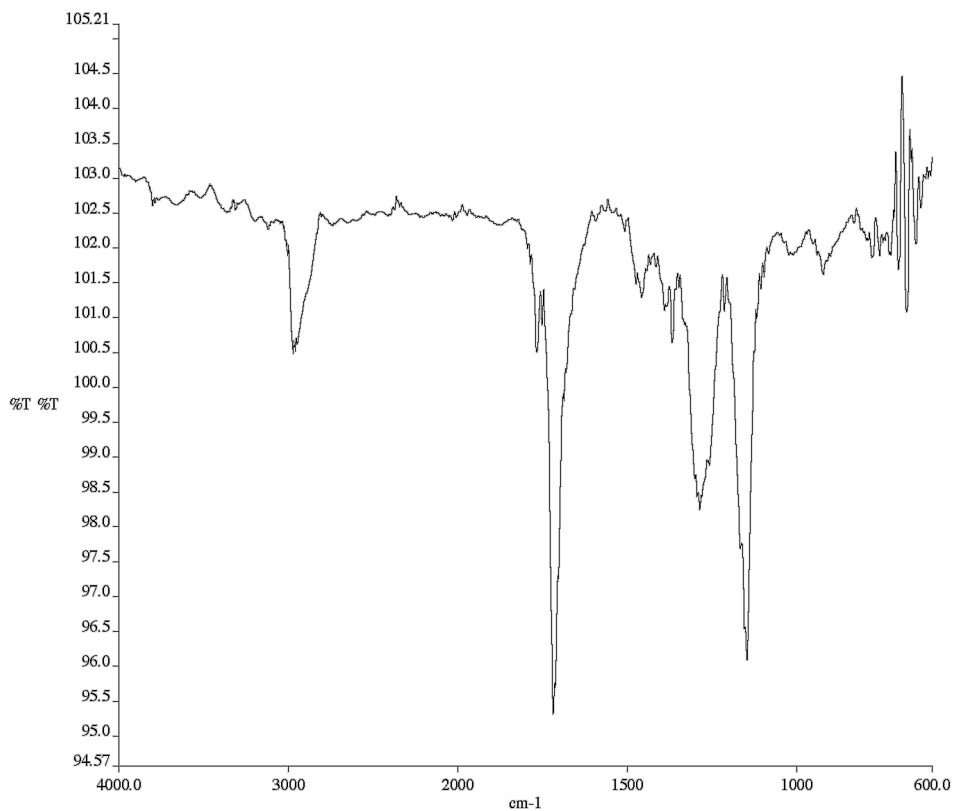


Figure A2.14. Infrared spectrum (Thin Film, NaCl) of compound **300**.

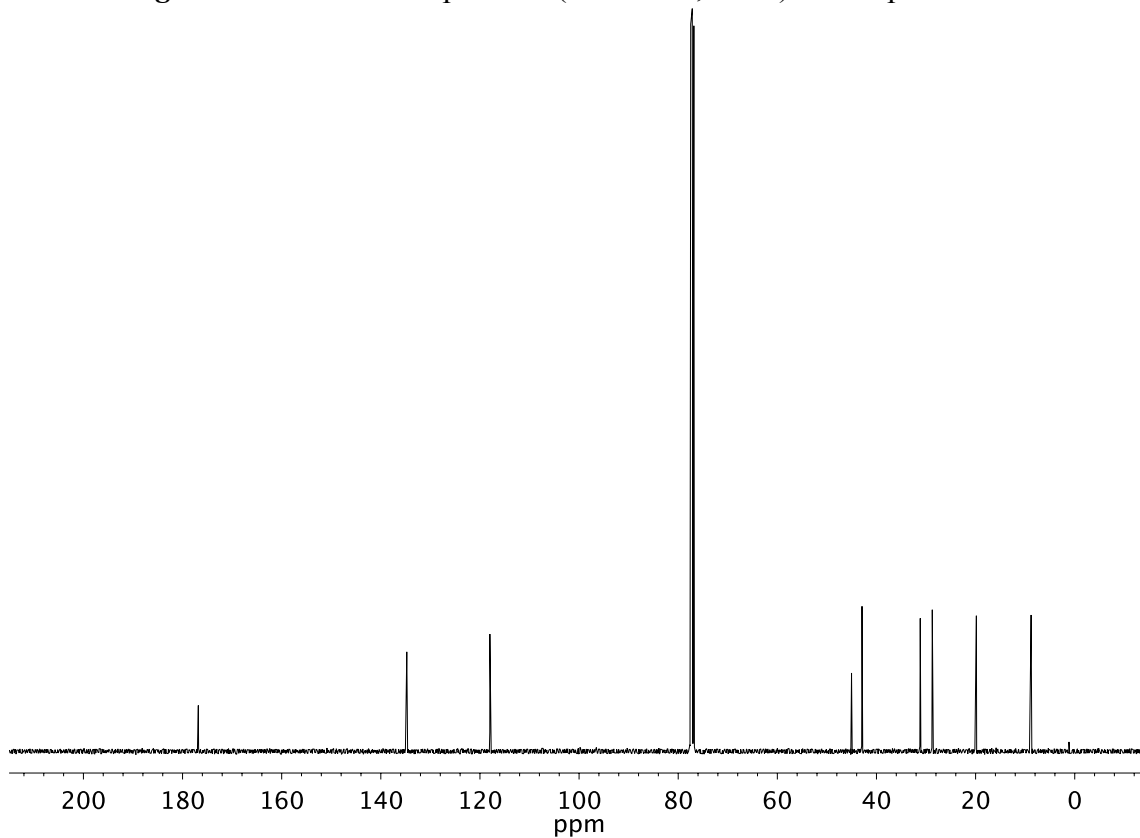


Figure A2.15. ¹³C NMR (101 MHz, CDCl₃) of compound **300**.

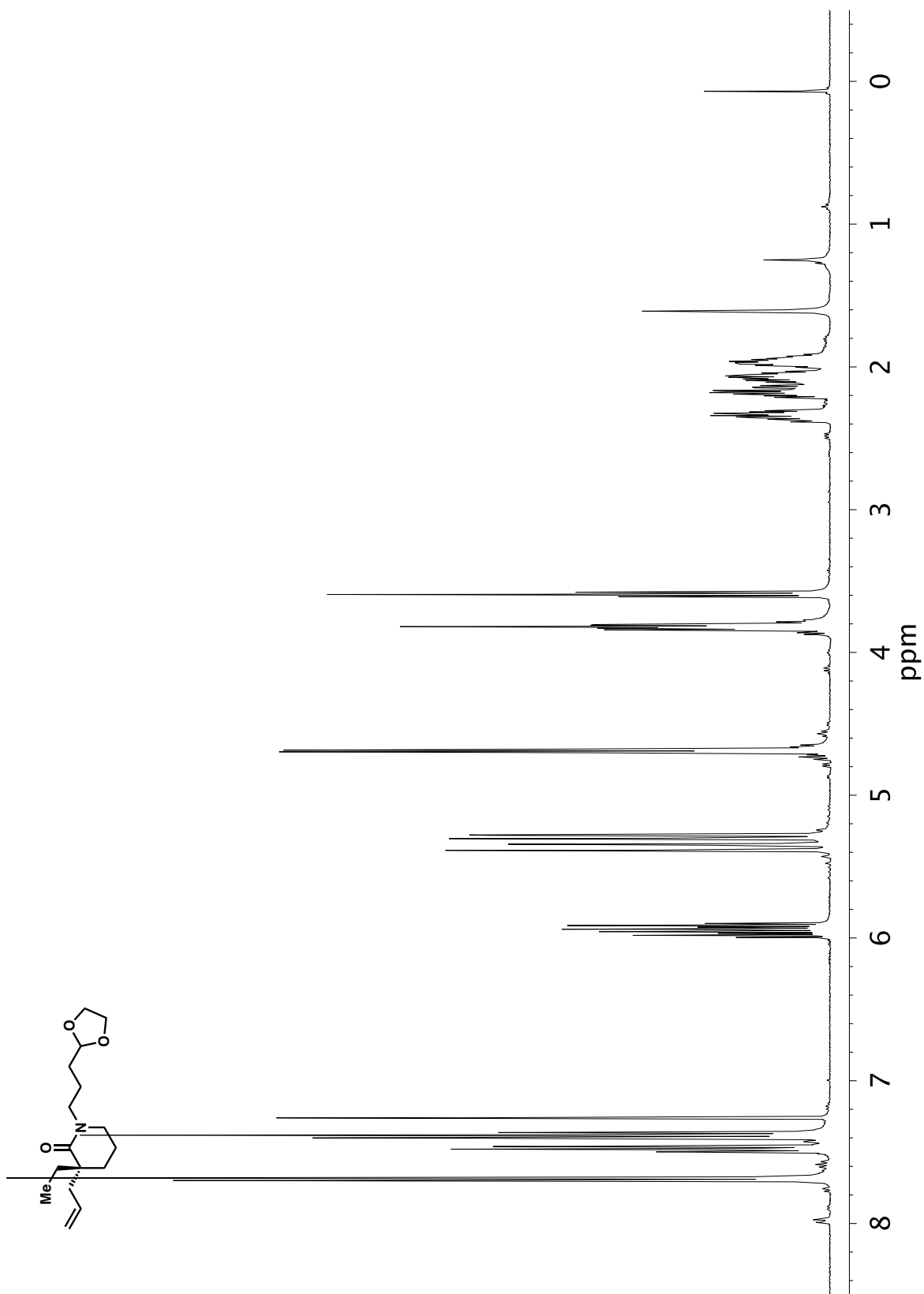


Figure A2.16. ^1H NMR (400 MHz, CDCl_3) of compound 306.

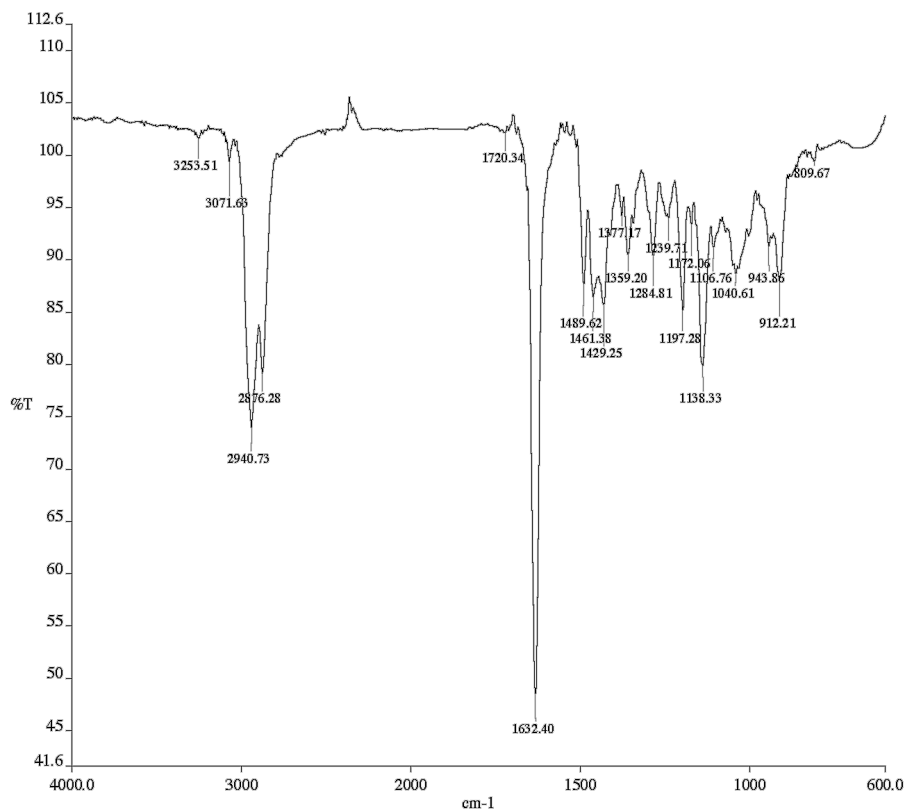


Figure A2.17. Infrared spectrum (Thin Film, NaCl) of compound **306**.

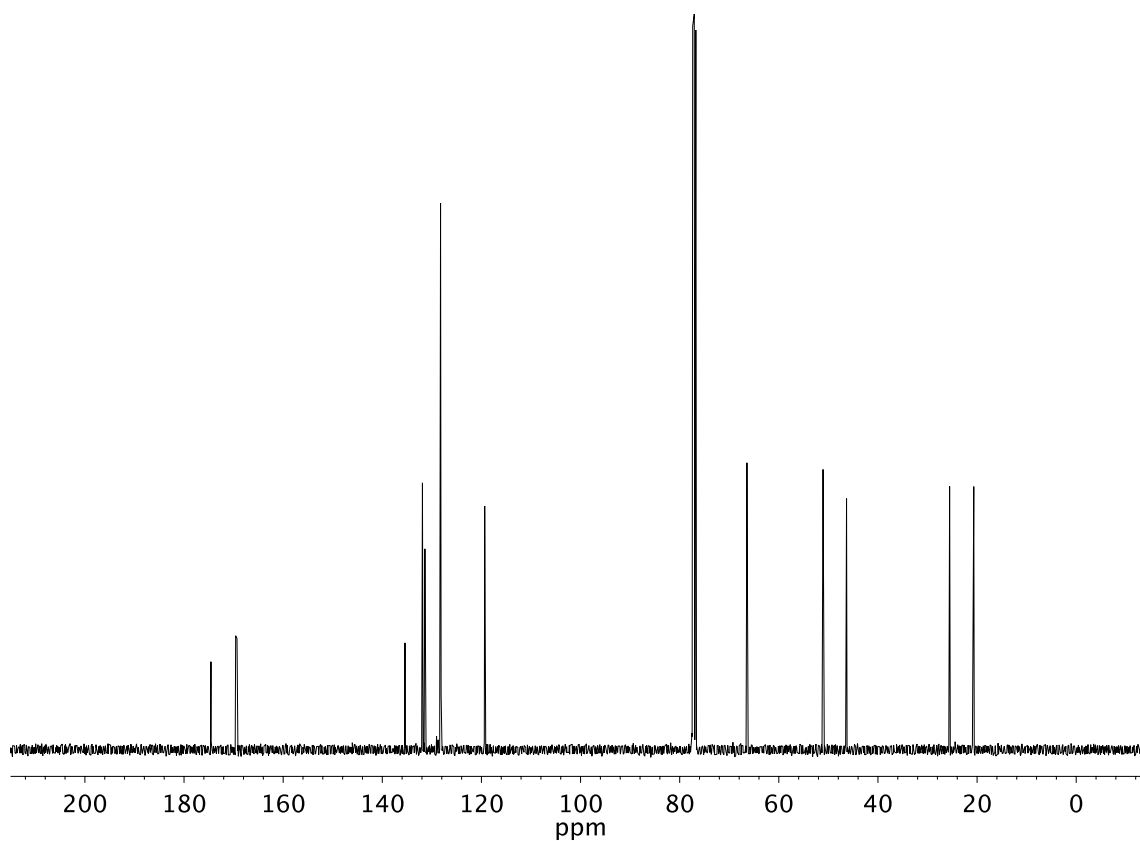


Figure A2.18. ¹³C NMR (101 MHz, CDCl₃) of compound **306**.

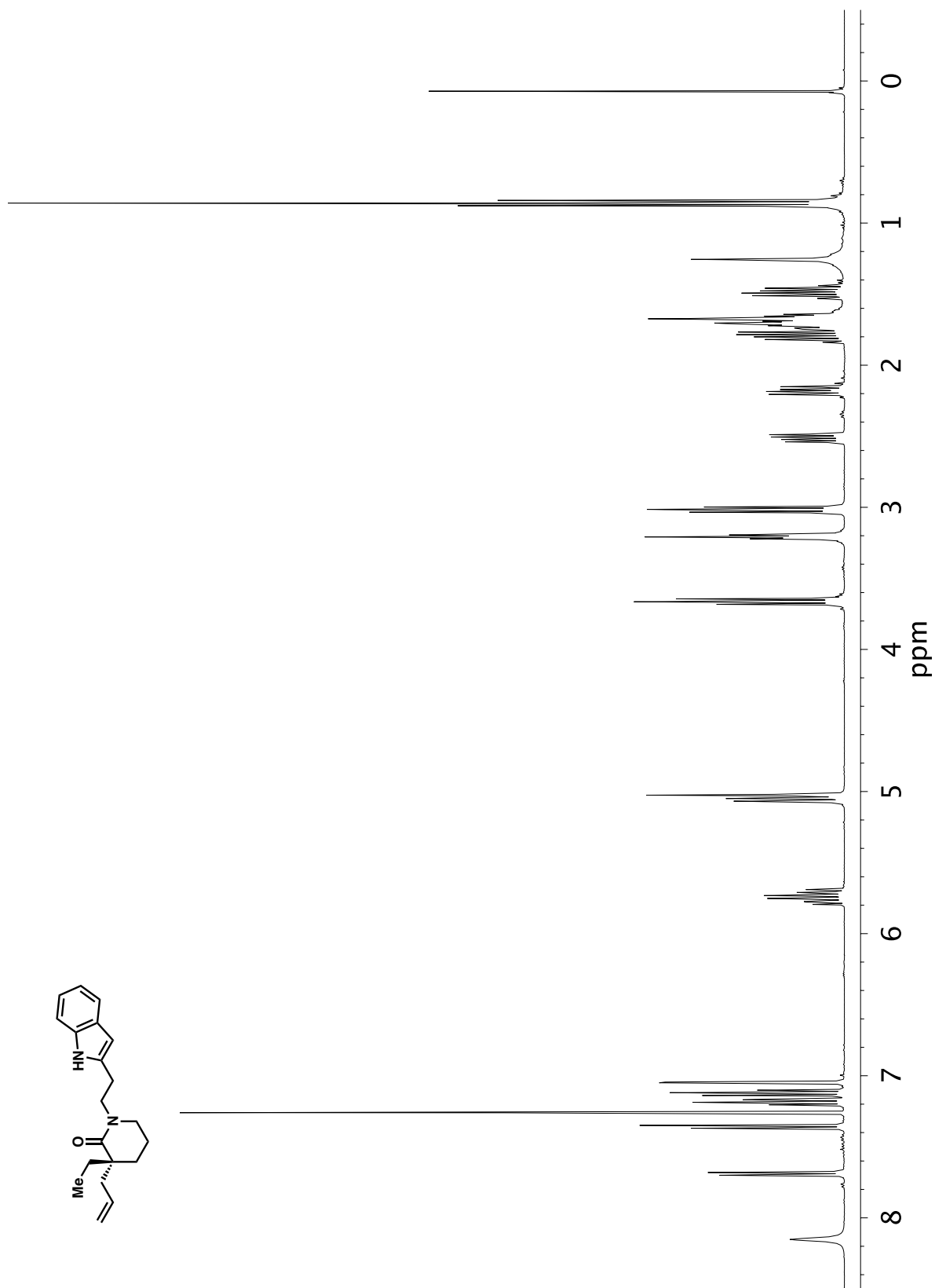


Figure A2.19. ^1H NMR (400 MHz, CDCl_3) of compound 301.

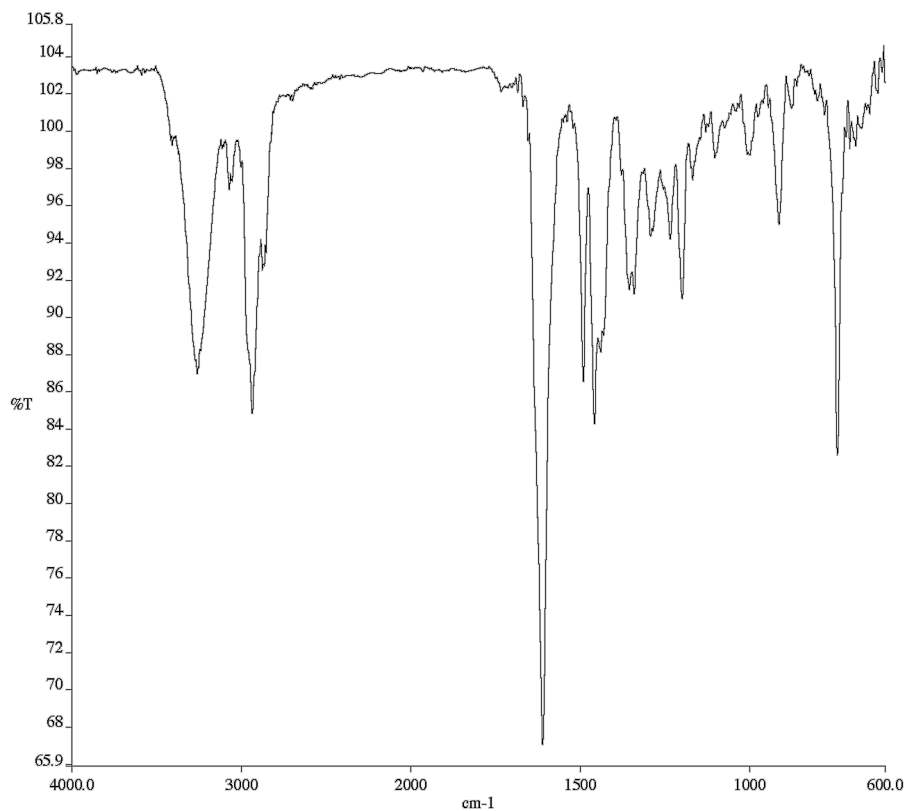


Figure A2.20. Infrared spectrum (Thin Film, NaCl) of compound **301**.

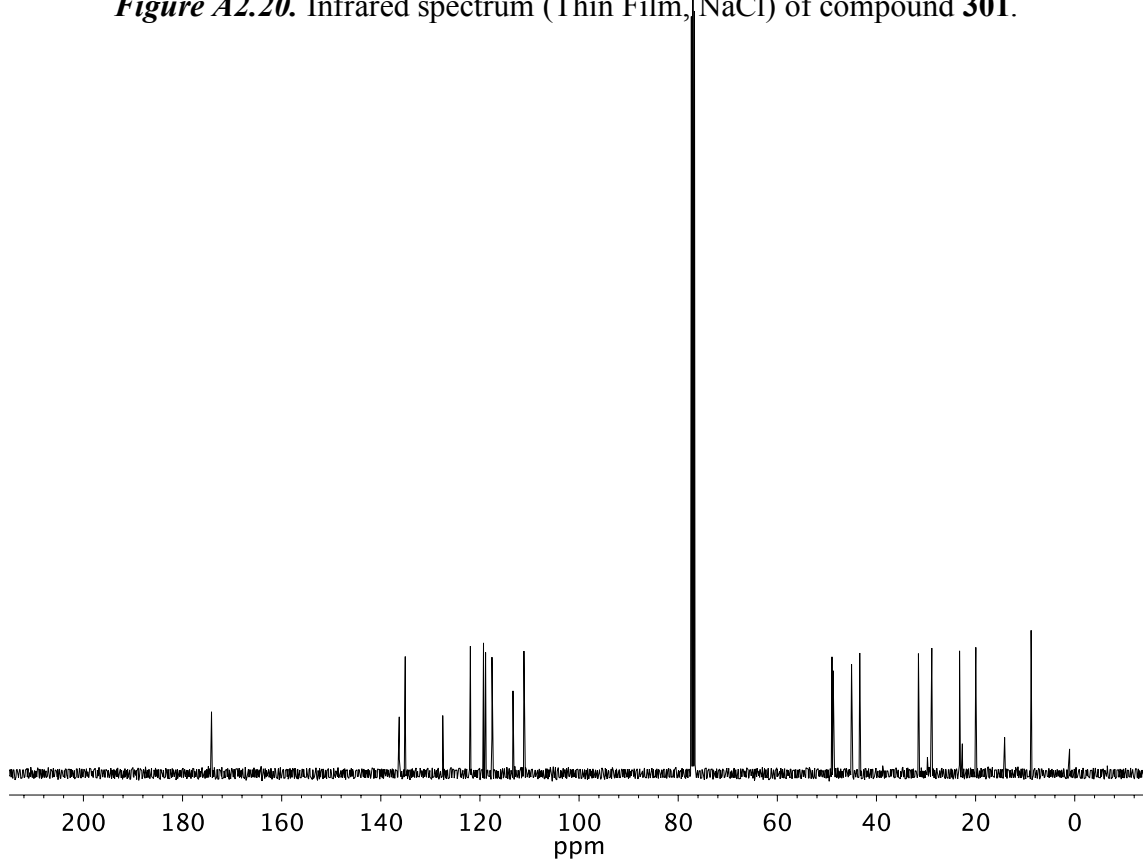


Figure A2.21. ¹³C NMR (101 MHz, CDCl₃) of compound **301**.

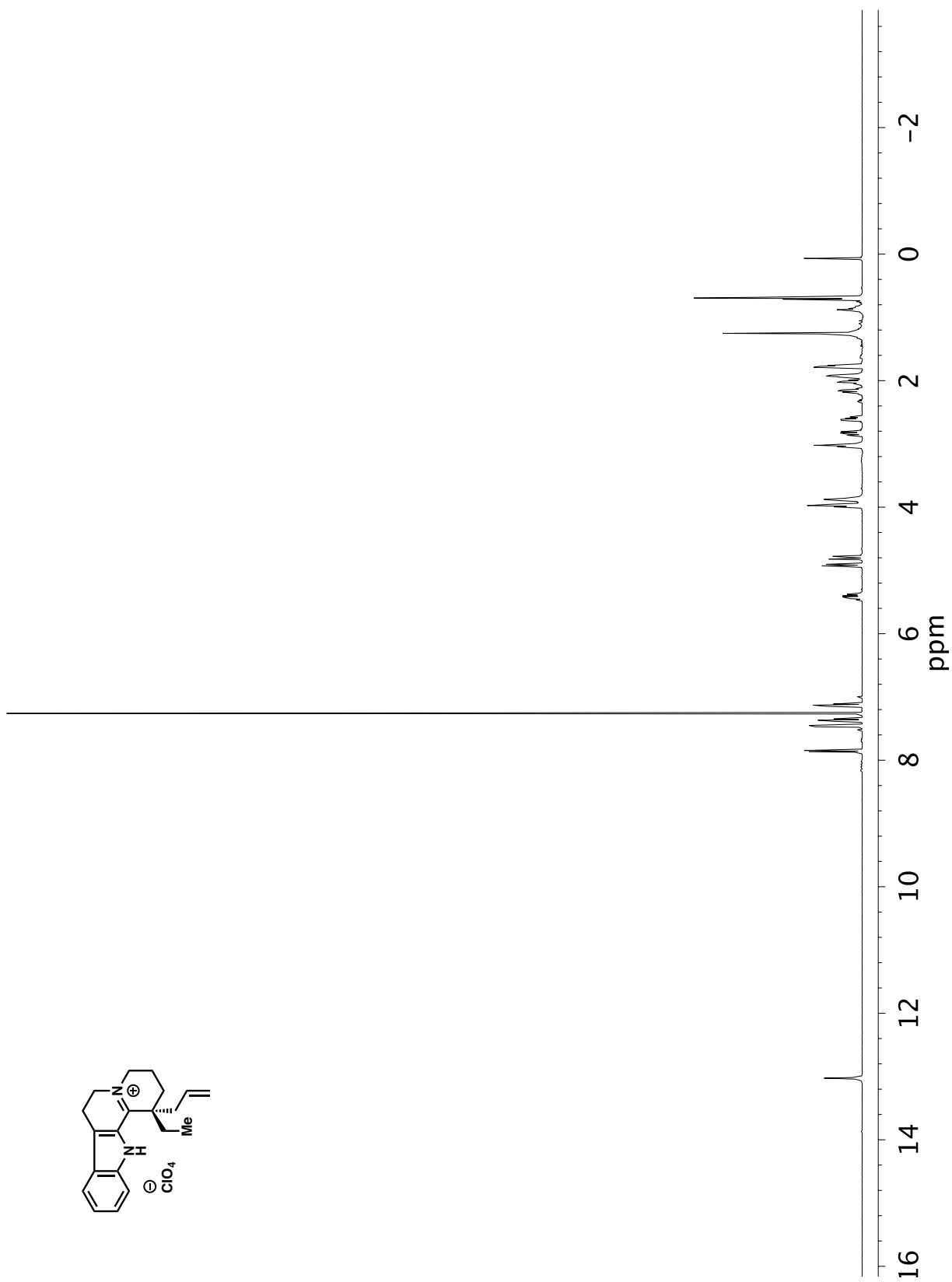


Figure A2.22. ¹H NMR (400 MHz, CDCl₃) of compound 307.

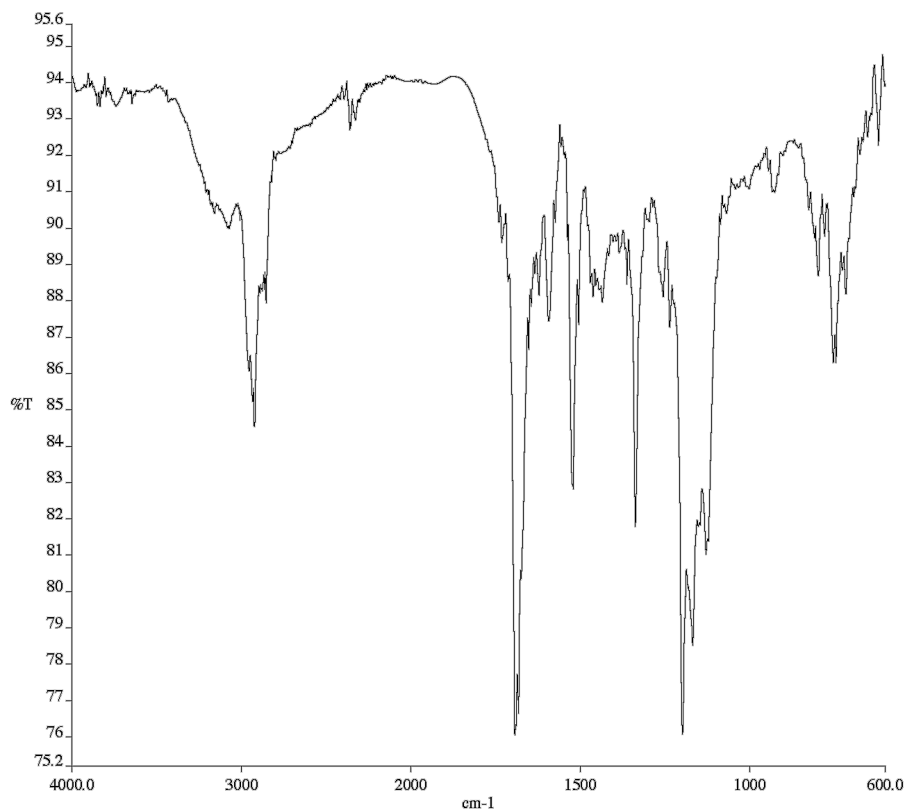


Figure A2.23. Infrared spectrum (Thin Film, NaCl) of compound **307**.

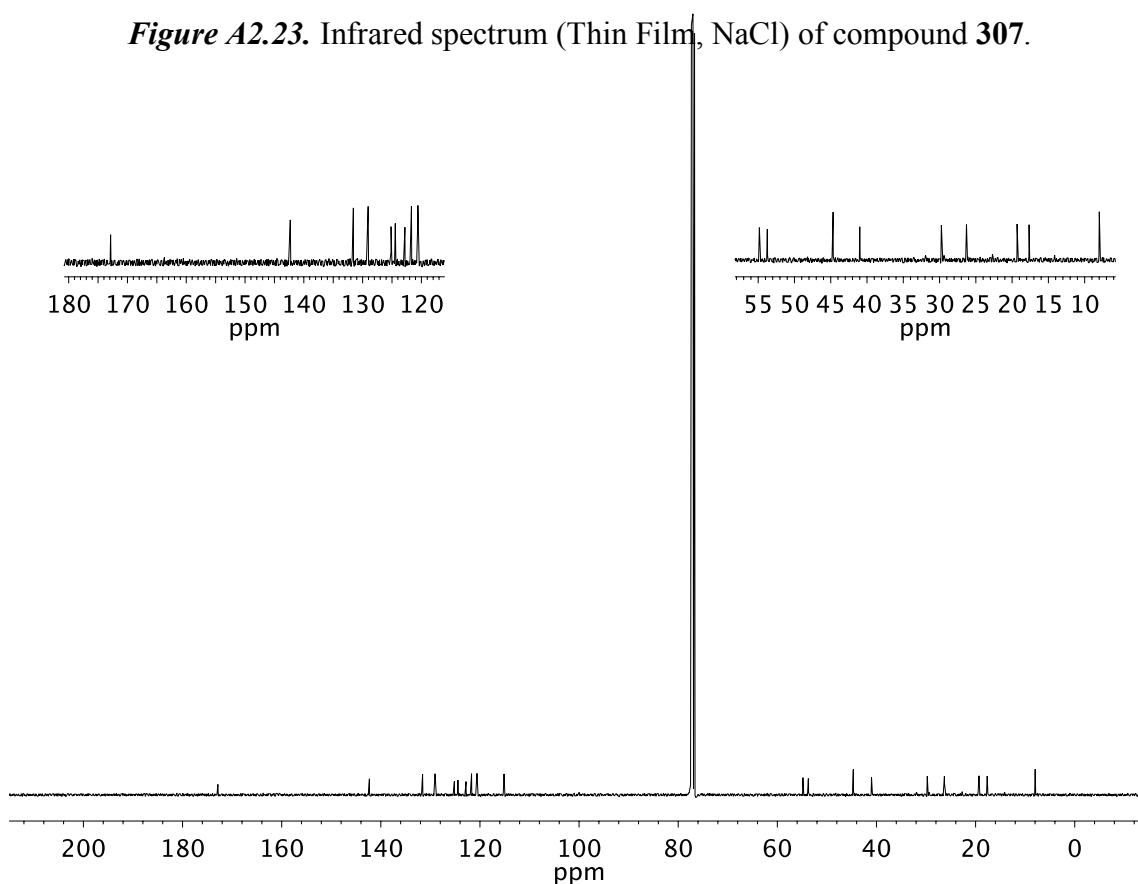


Figure A2.24. ¹³C NMR (101 MHz, CDCl₃) of compound **307**.

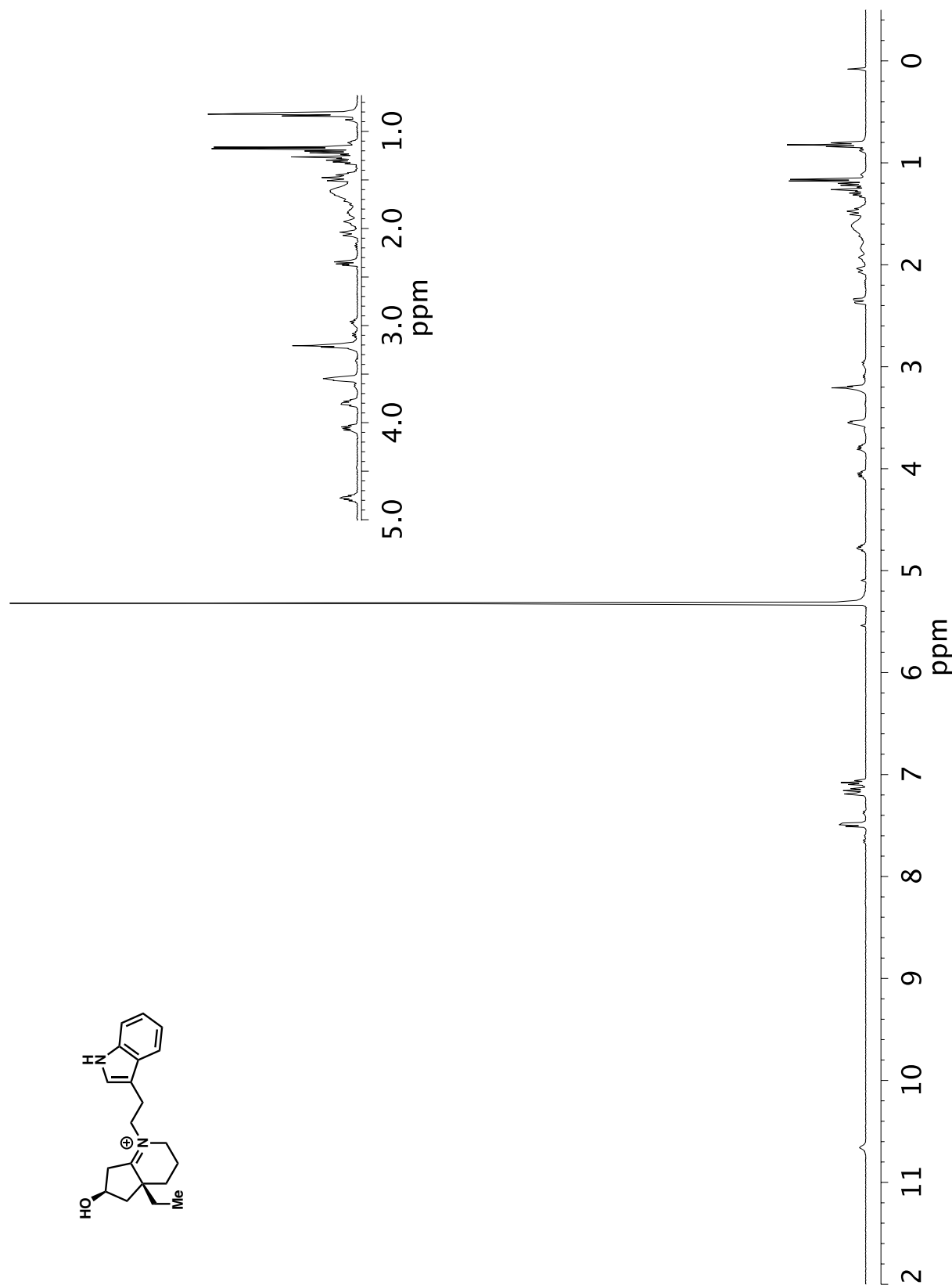


Figure A2.25. ^1H NMR (600 MHz, CD_2Cl_2) of compound 308.

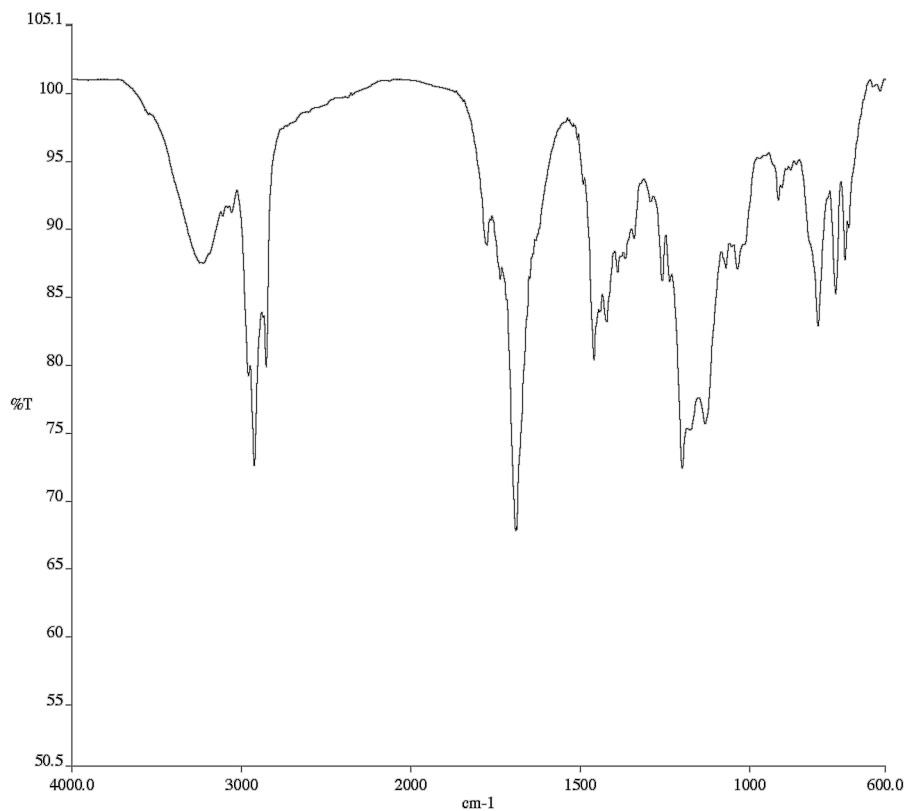


Figure A2.26. Infrared spectrum (Thin Film, NaCl) of compound **308**.

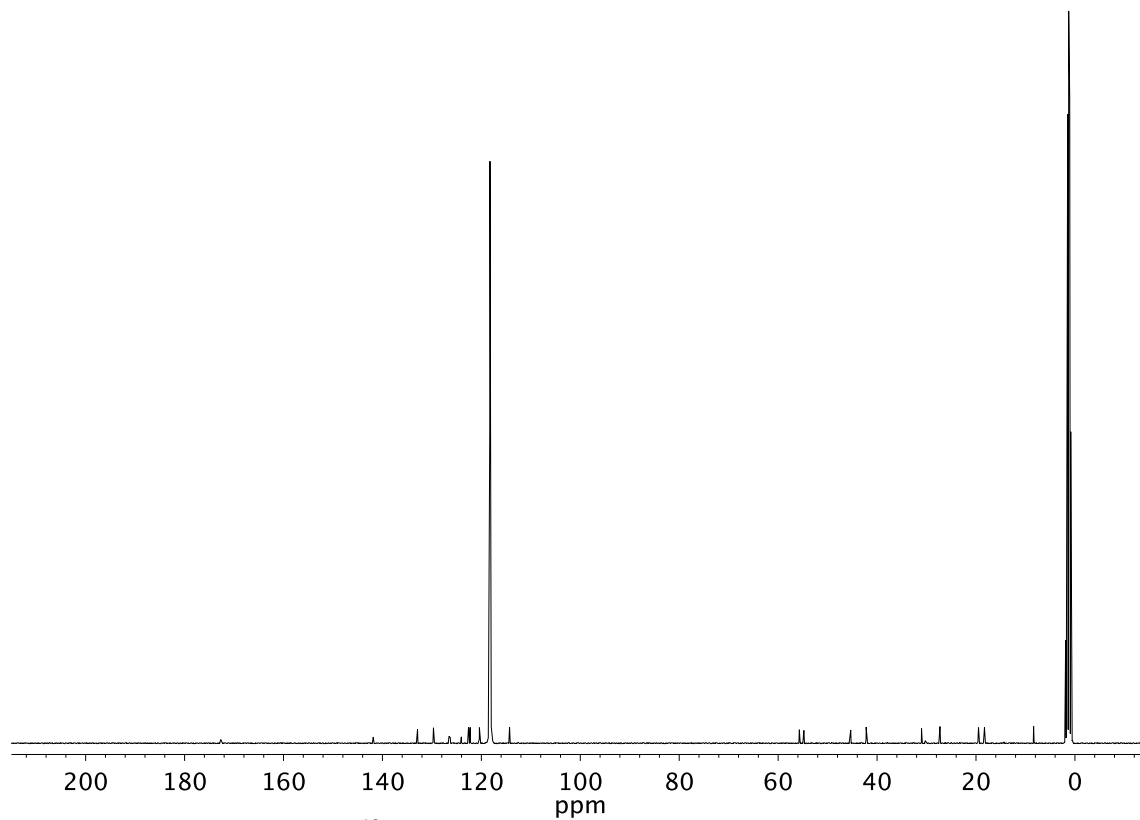


Figure A2.27. ¹³C NMR (101 MHz, CD₃CN) of compound **308**.

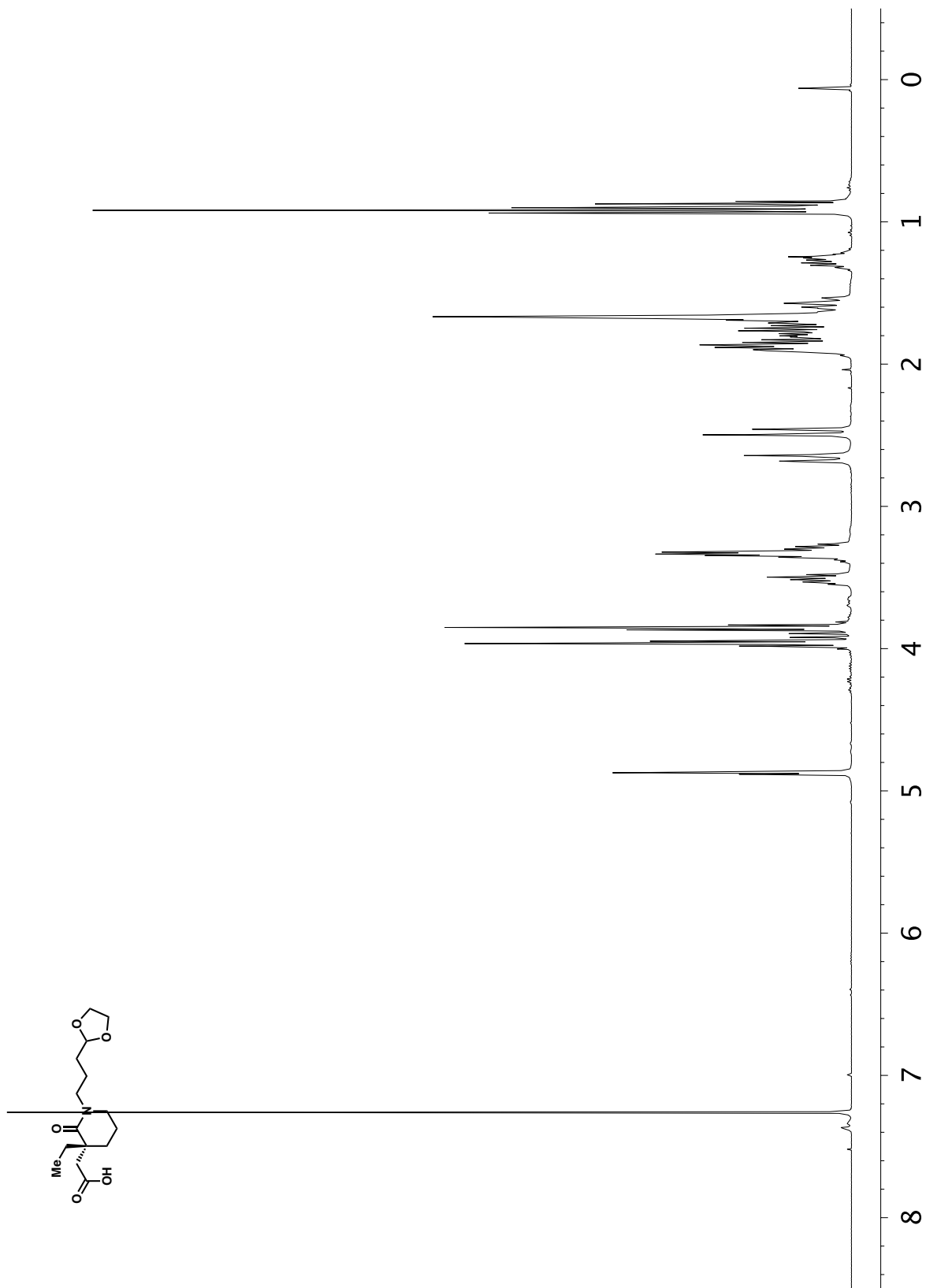


Figure A2.28. ¹H NMR (400 MHz, CDCl₃) of compound 314.

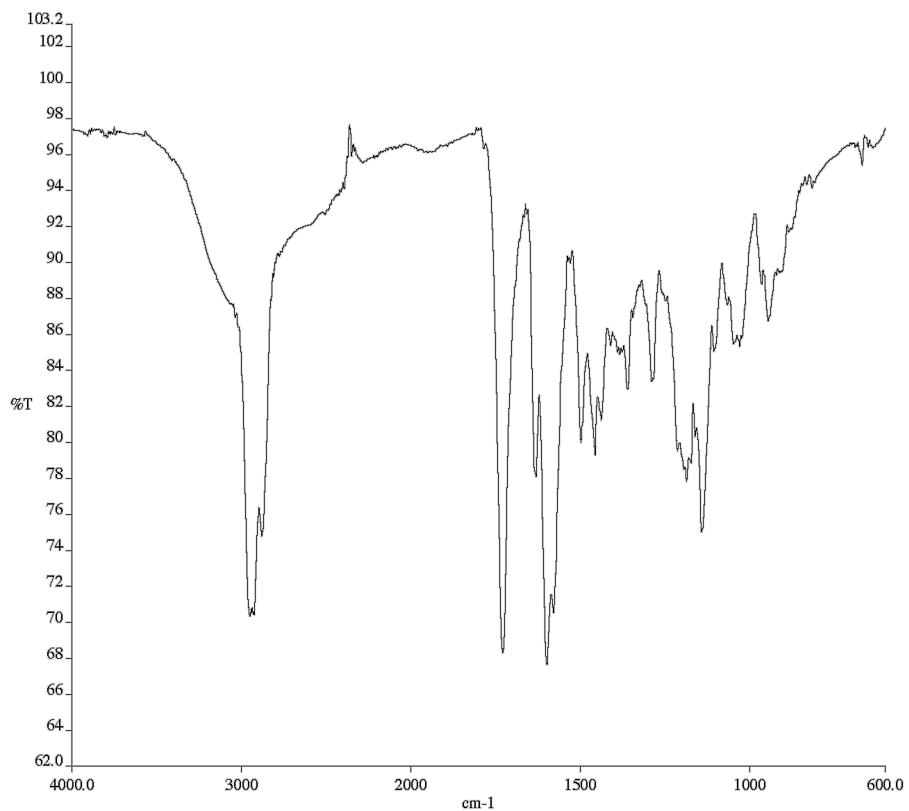


Figure A2.29. Infrared spectrum (Thin Film, NaCl) of compound **314**.

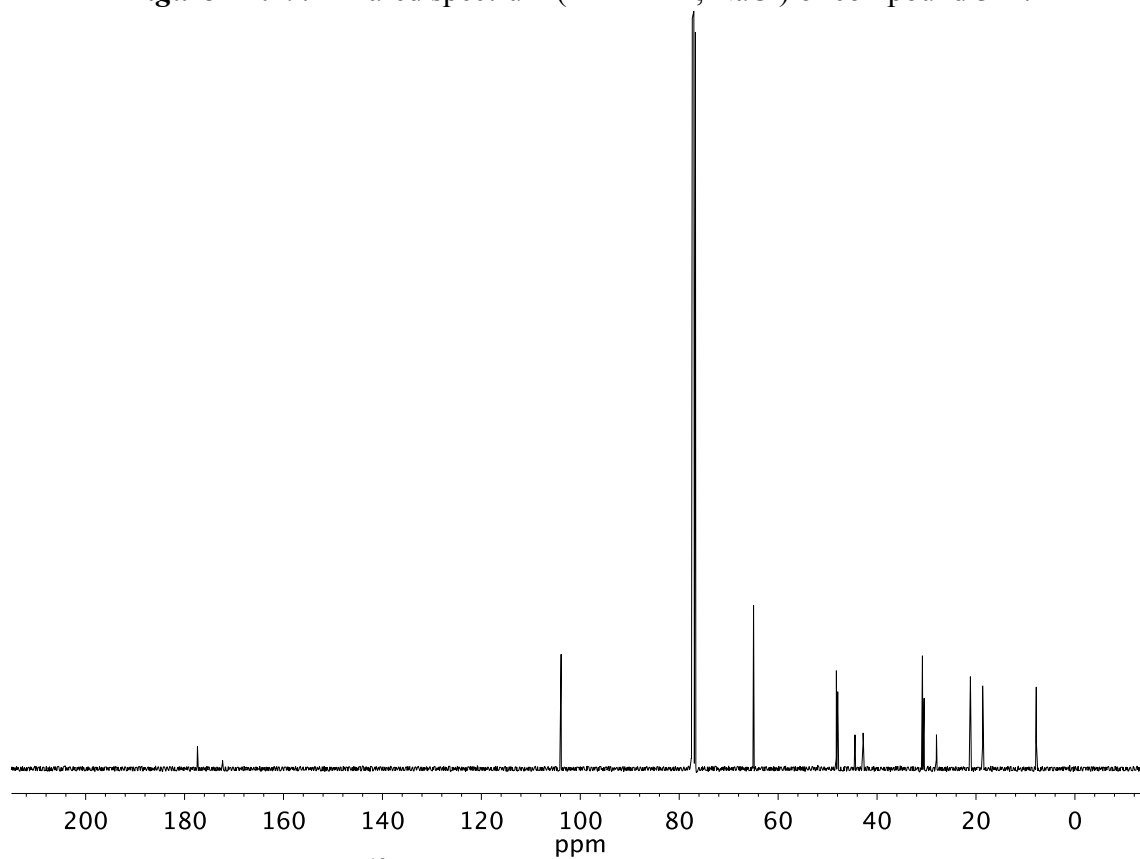


Figure A2.30. ¹³C NMR (101 MHz, CDCl₃) of compound **314**.

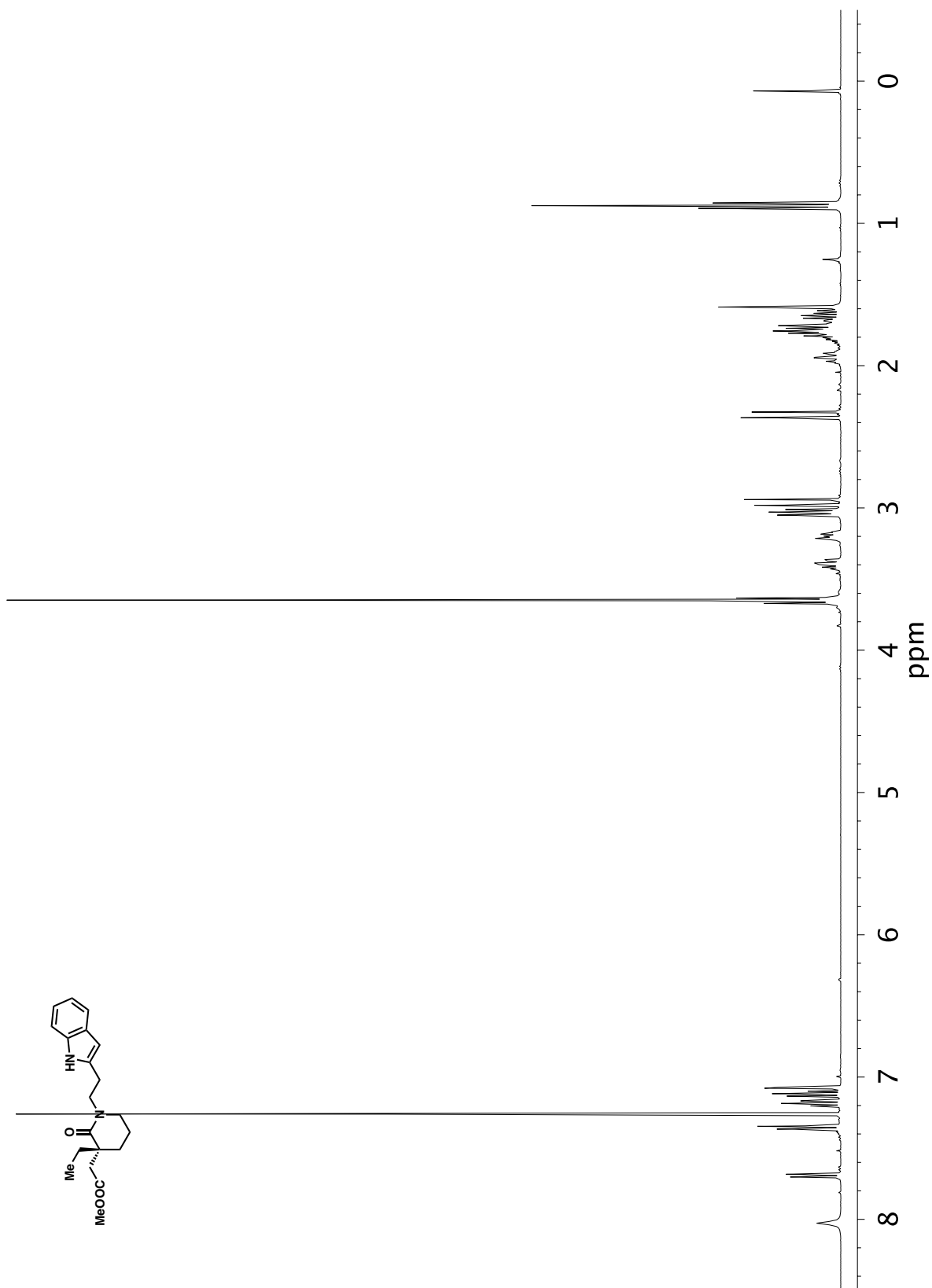


Figure A2.31. ¹H NMR (400 MHz, CDCl₃) of compound 315.

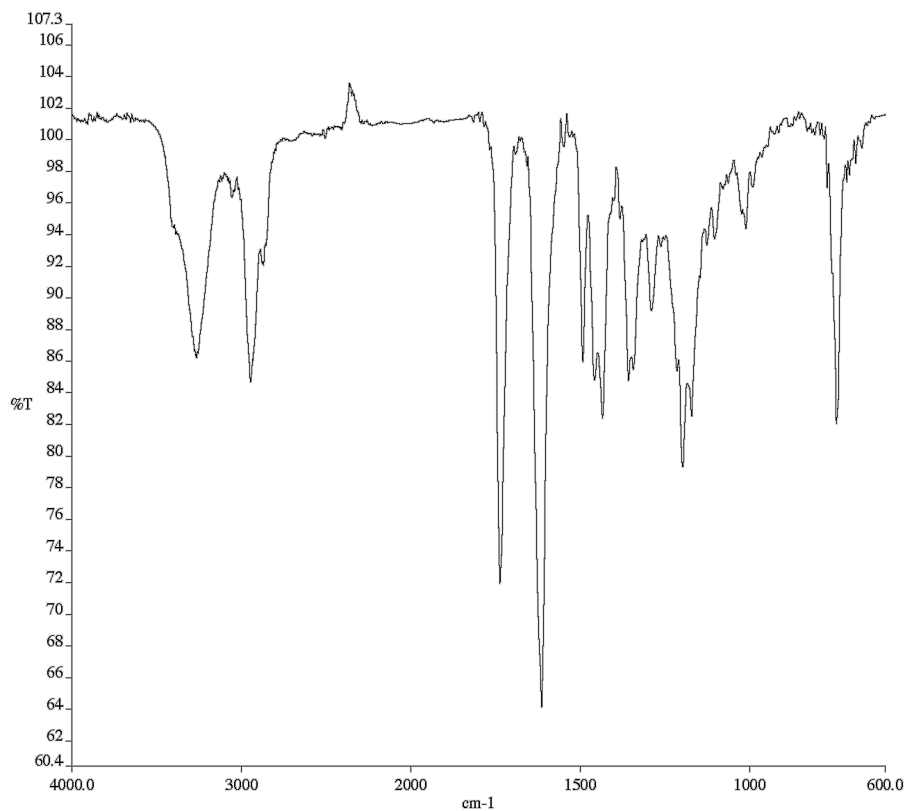


Figure A2.32. Infrared spectrum (Thin Film, NaCl) of compound **315**.

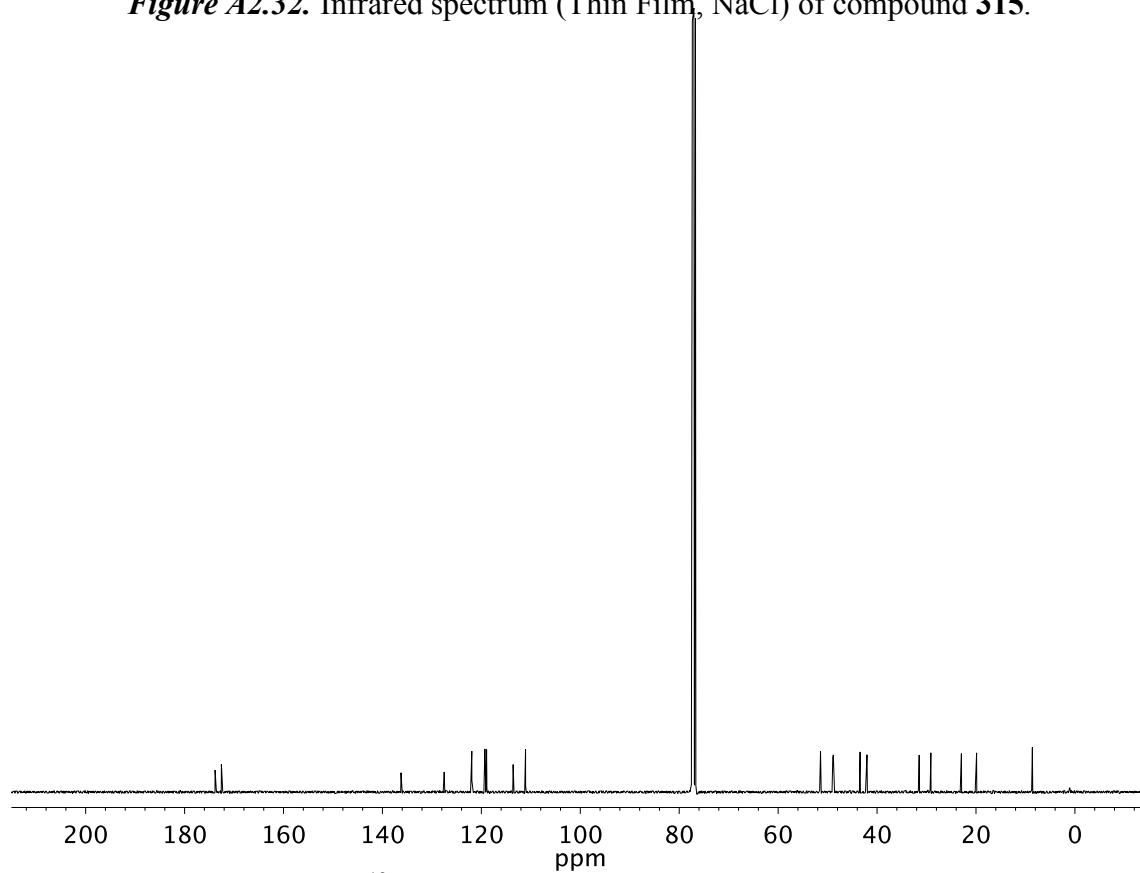


Figure A2.33. ^{13}C NMR (101 MHz, CDCl_3) of compound **315**.

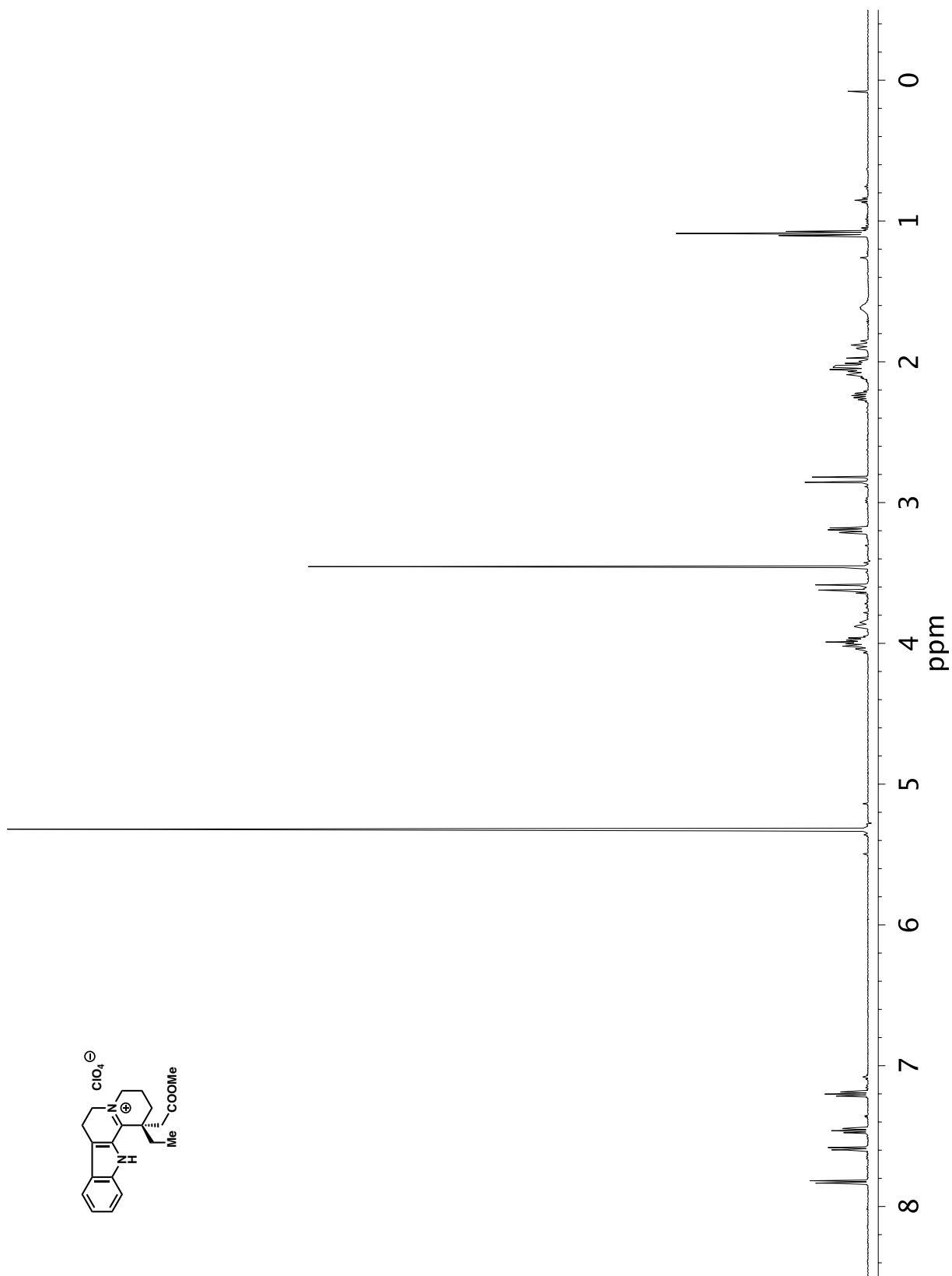


Figure A2.34. ¹H NMR (500 MHz, CD₂Cl₂) of compound 261.

Figure A2.35. Infrared spectrum (Thin Film, NaCl) of compound **261**.

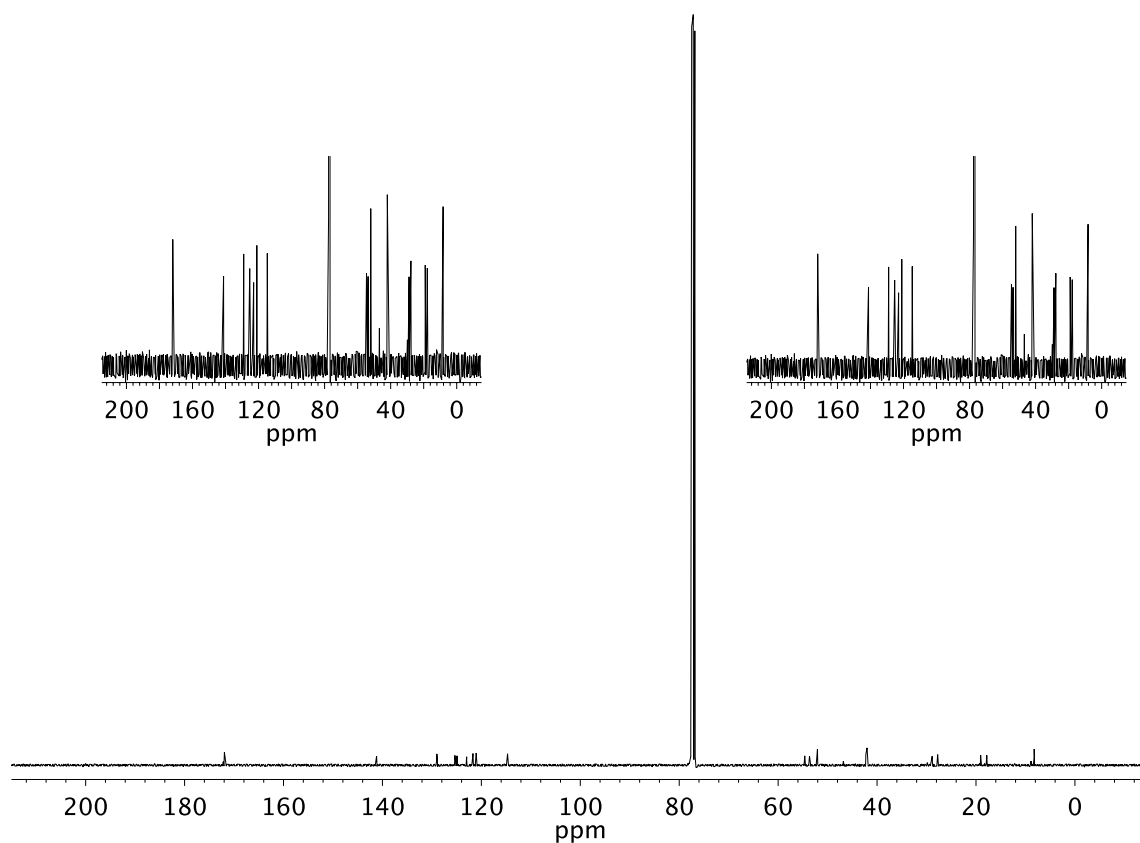


Figure A2.36. ^{13}C NMR (101 MHz, CDCl_3) of compound **261**.

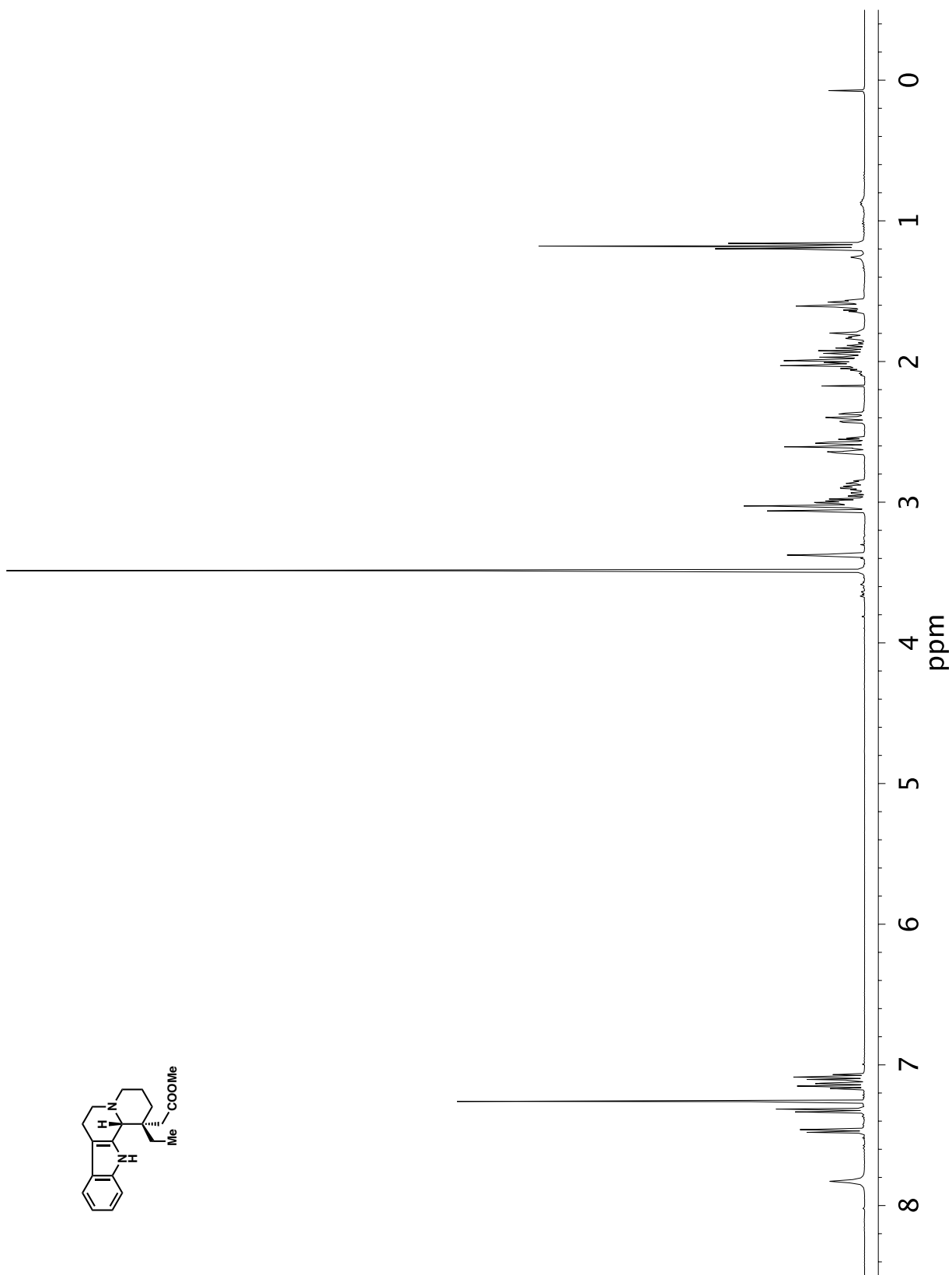


Figure A2.37. ¹H NMR (400 MHz, CDCl₃) of compound **317a**.

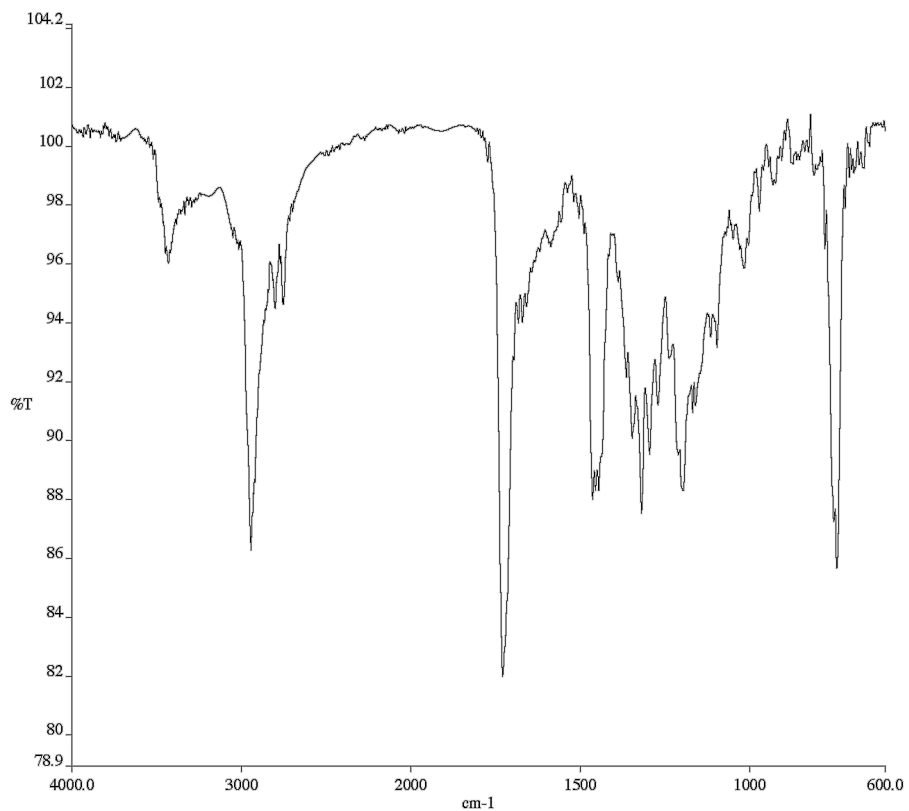


Figure A2.38. Infrared spectrum (Thin Film, NaCl) of compound **317a**.

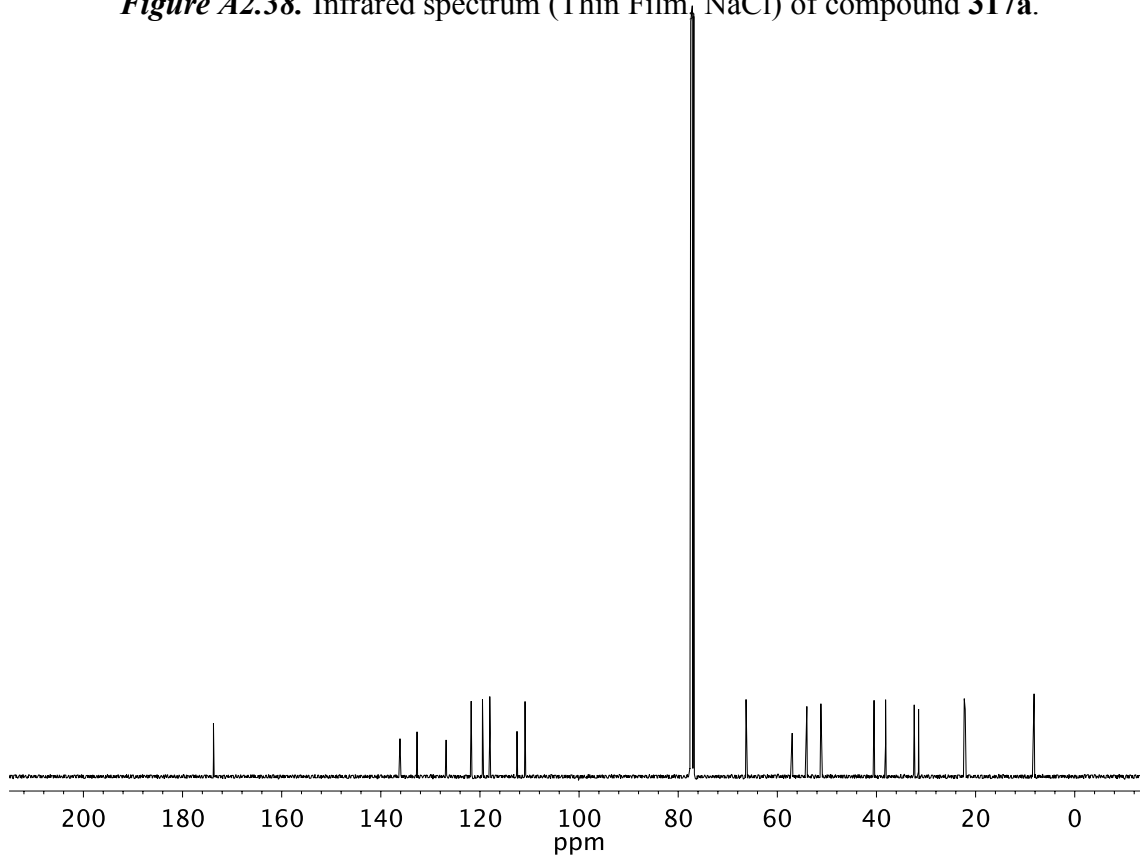


Figure A2.39. ¹³C NMR (101 MHz, CDCl₃) of compound **317b**.

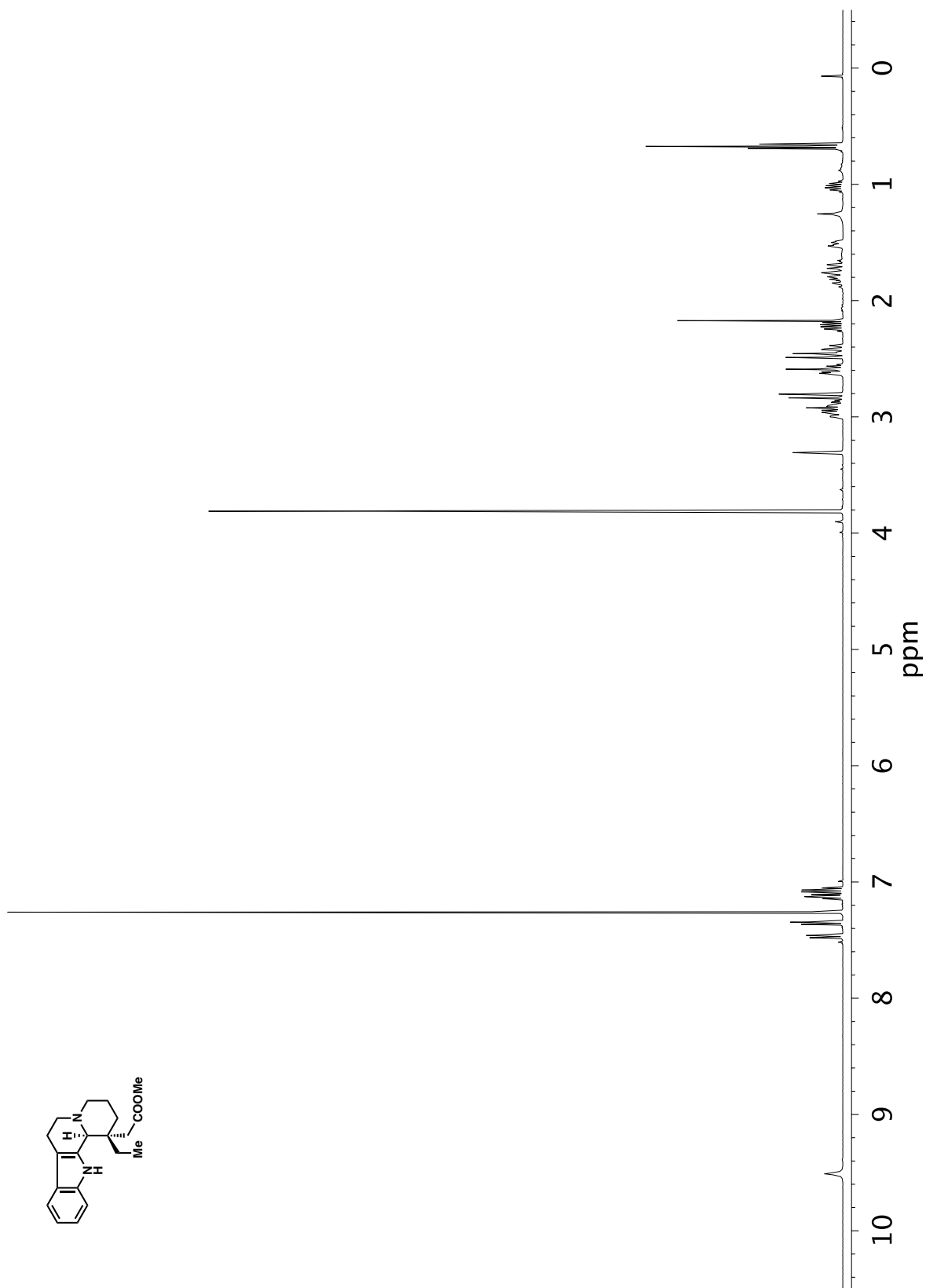


Figure A2.40. $^1\text{H NMR}$ (400 MHz, CDCl_3) of compound **317b**.

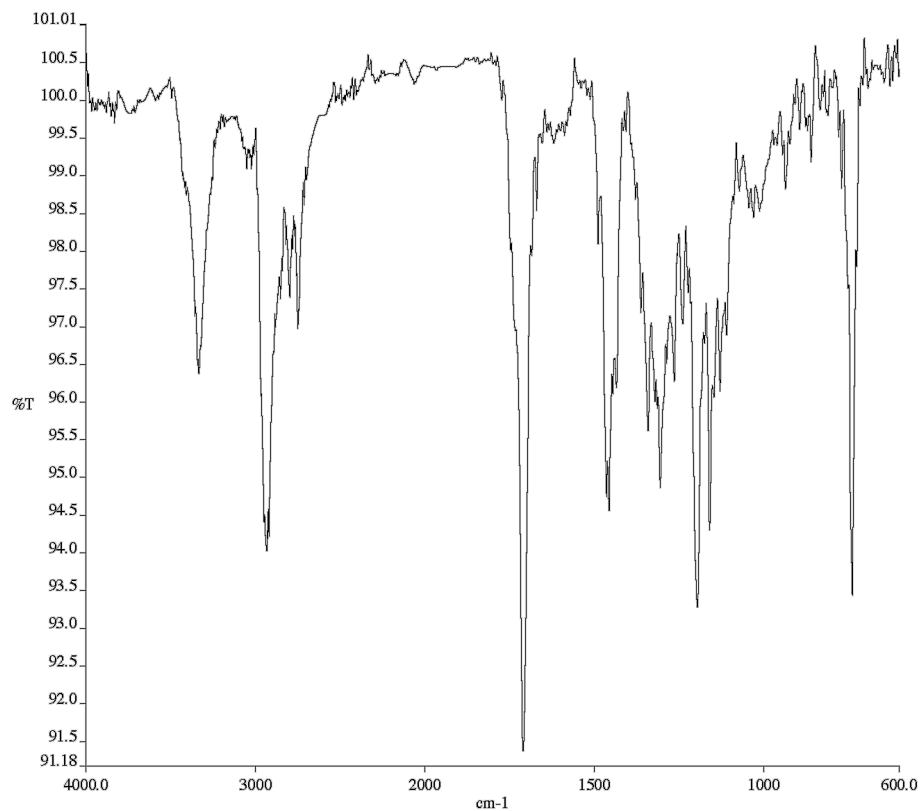


Figure A2.41. Infrared spectrum (Thin Film, NaCl) of compound **317b**.

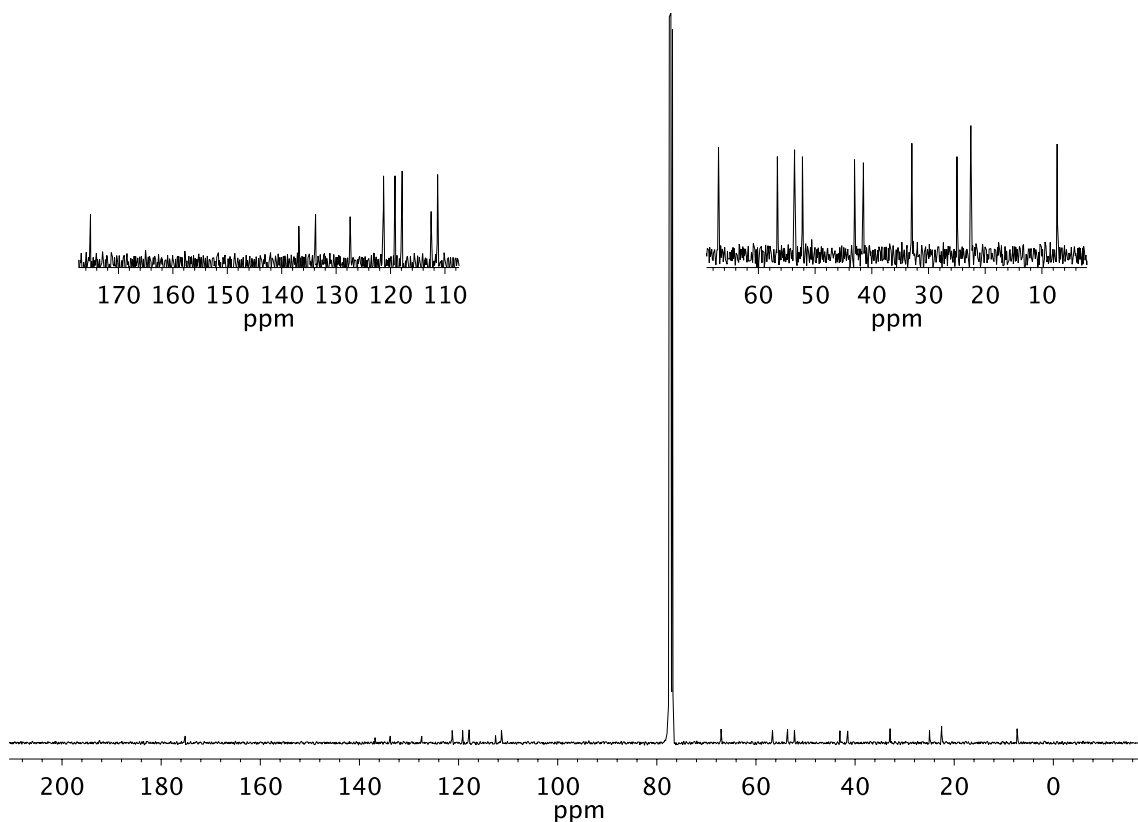


Figure A2.42. ¹³C NMR (101 MHz, CDCl₃) of compound **317b**.

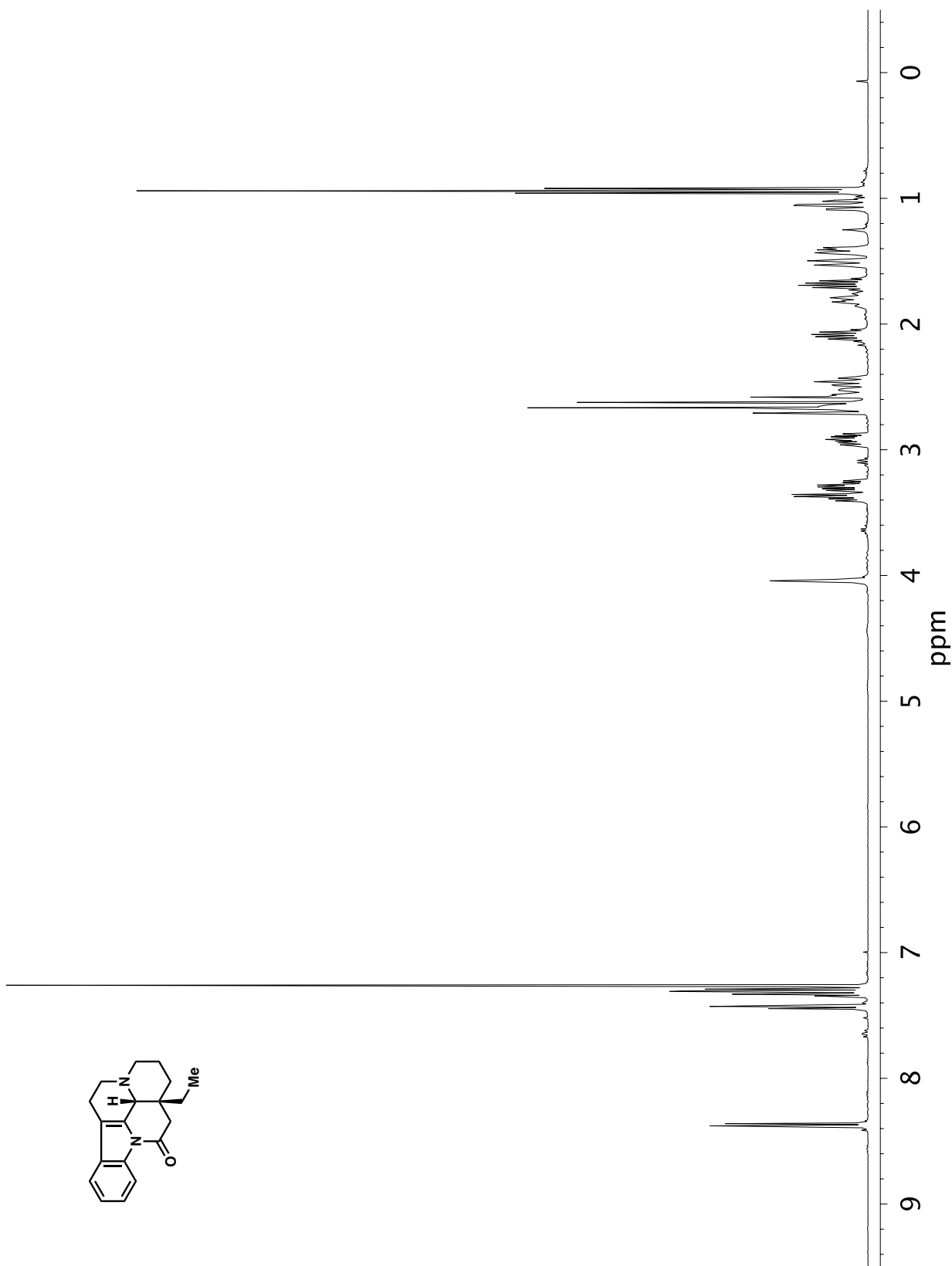


Figure A2.43. ¹H NMR (400 MHz, CDCl₃) of compound 91.

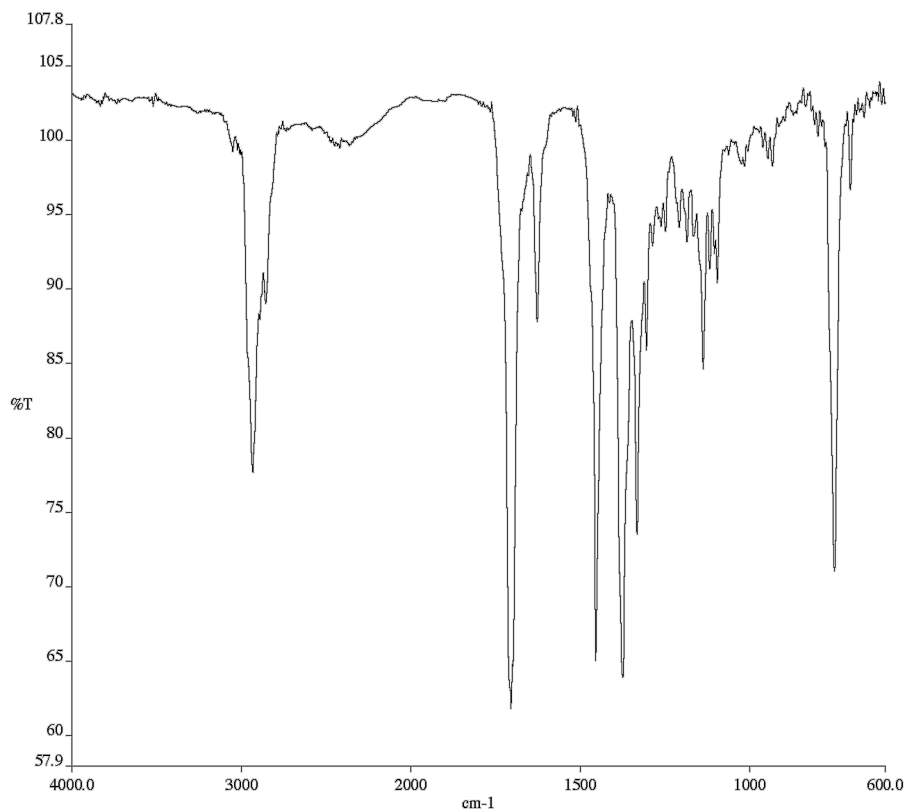


Figure A2.44. Infrared spectrum (Thin Film, NaCl) of compound **91**.

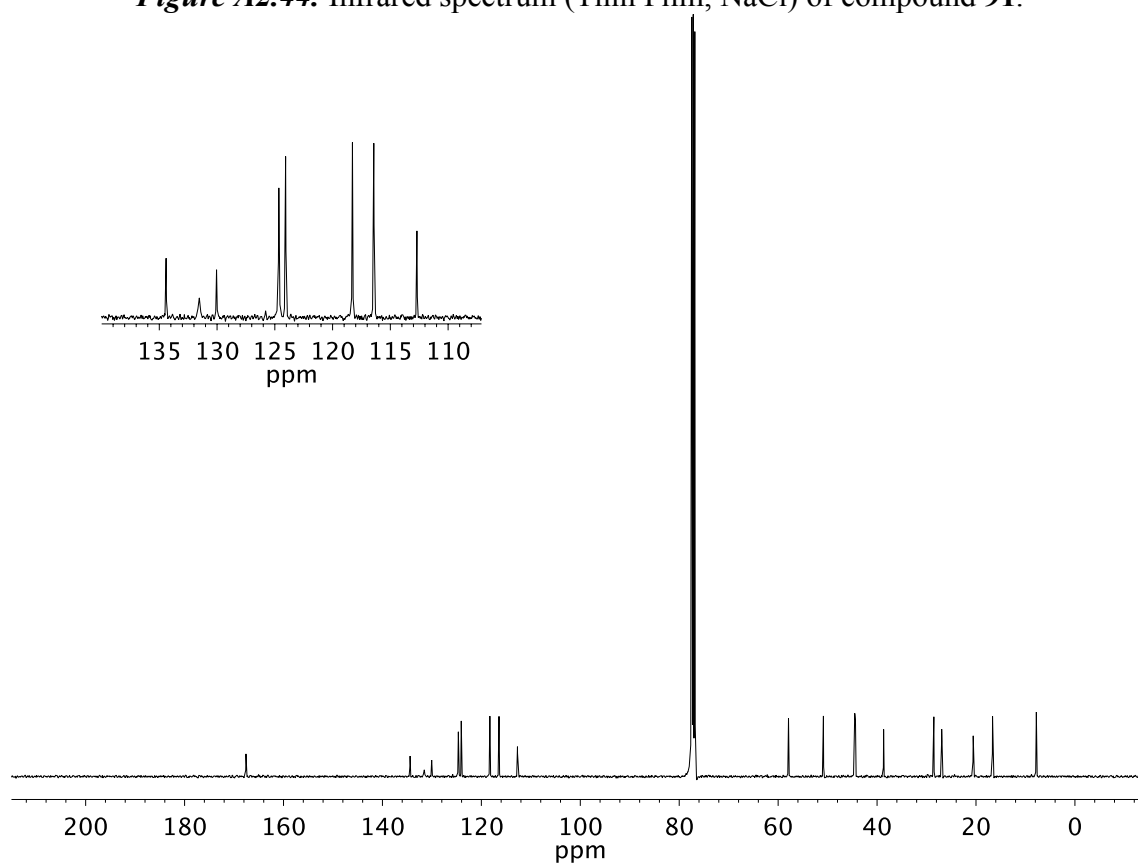


Figure A2.45. ¹³C NMR (101 MHz, CDCl₃) of compound **91**.

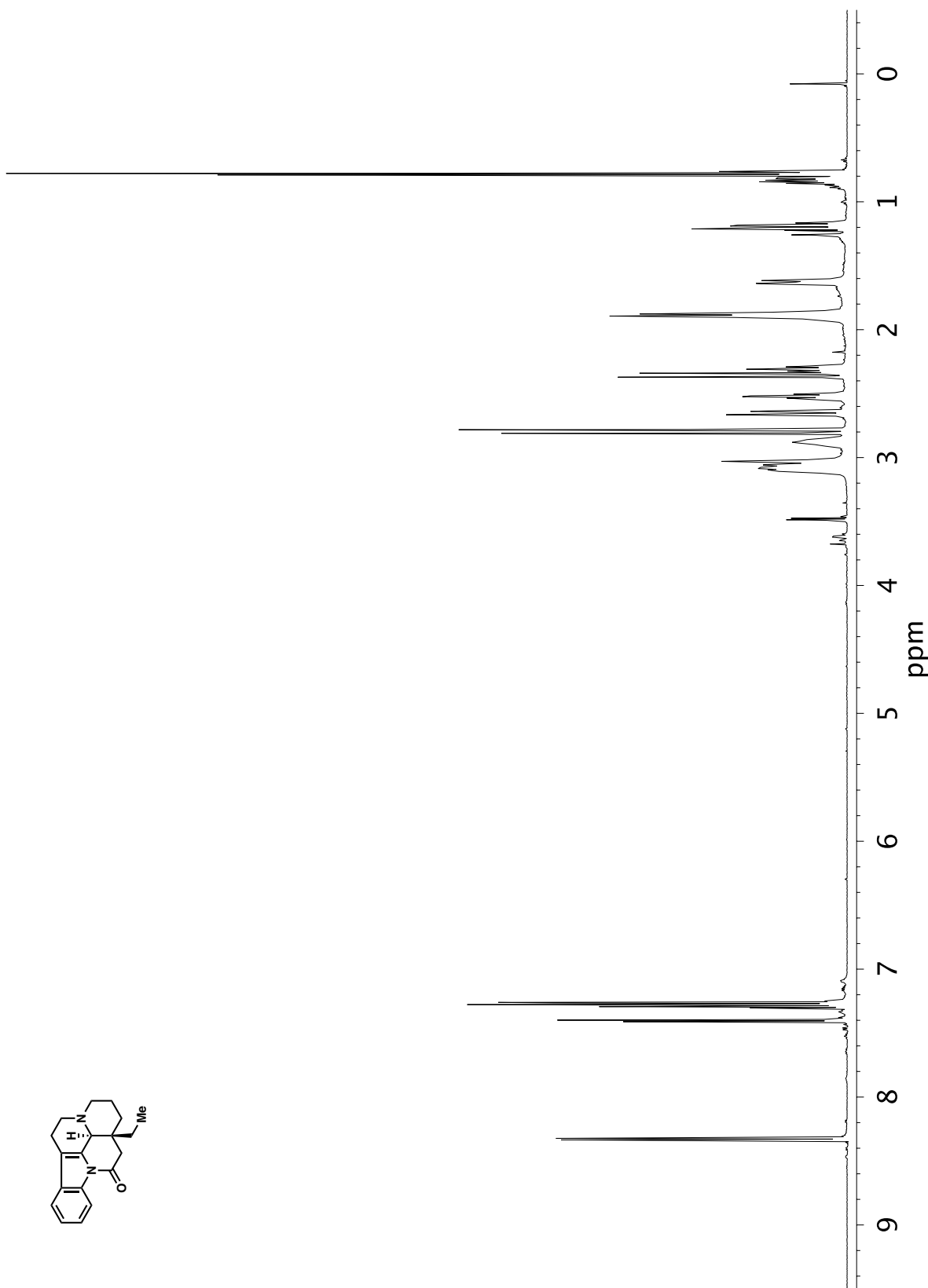


Figure A2.46. ¹H NMR (600 MHz, CDCl₃) of compound 251.

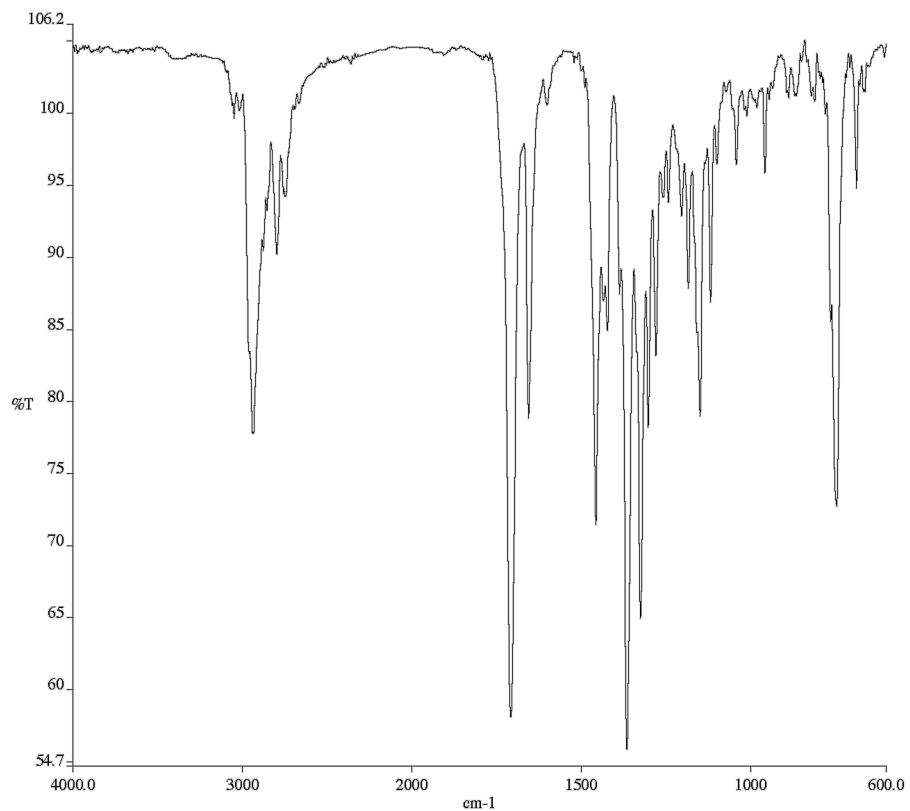


Figure A2.47. Infrared spectrum (Thin Film, NaCl) of compound **251**.

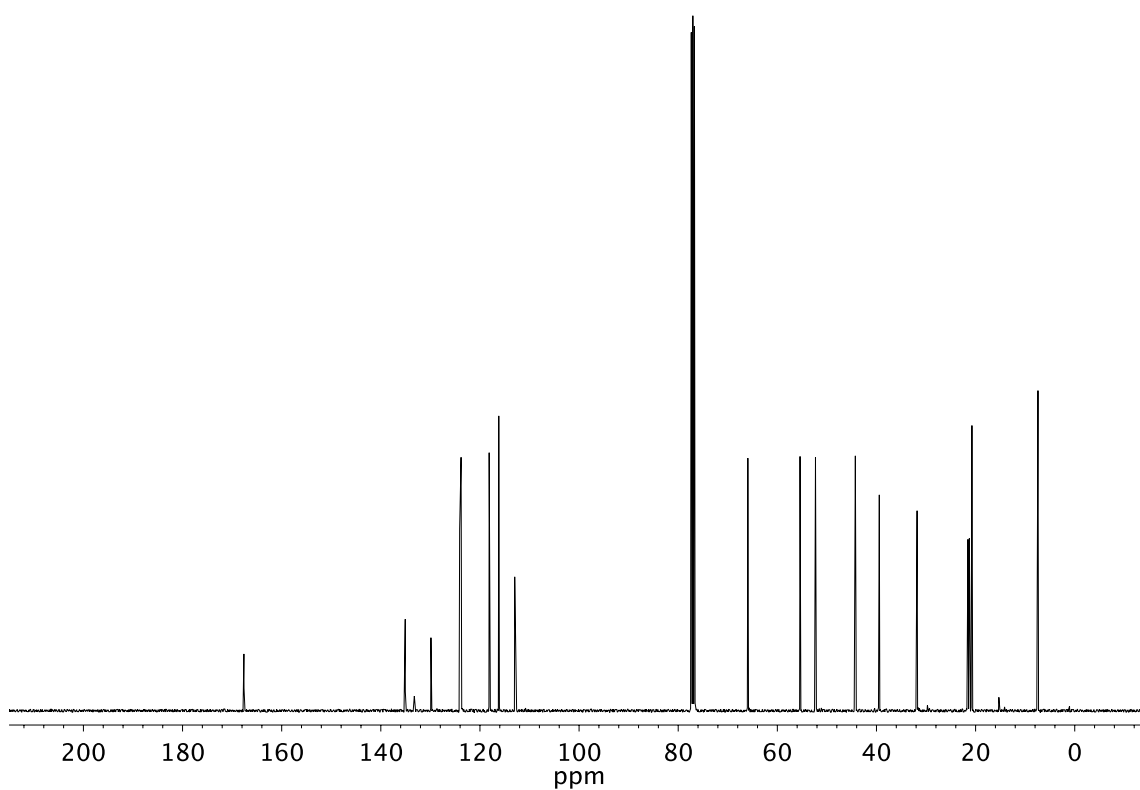


Figure A2.48. ¹³C NMR (101 MHz, CDCl₃) of compound **251**.

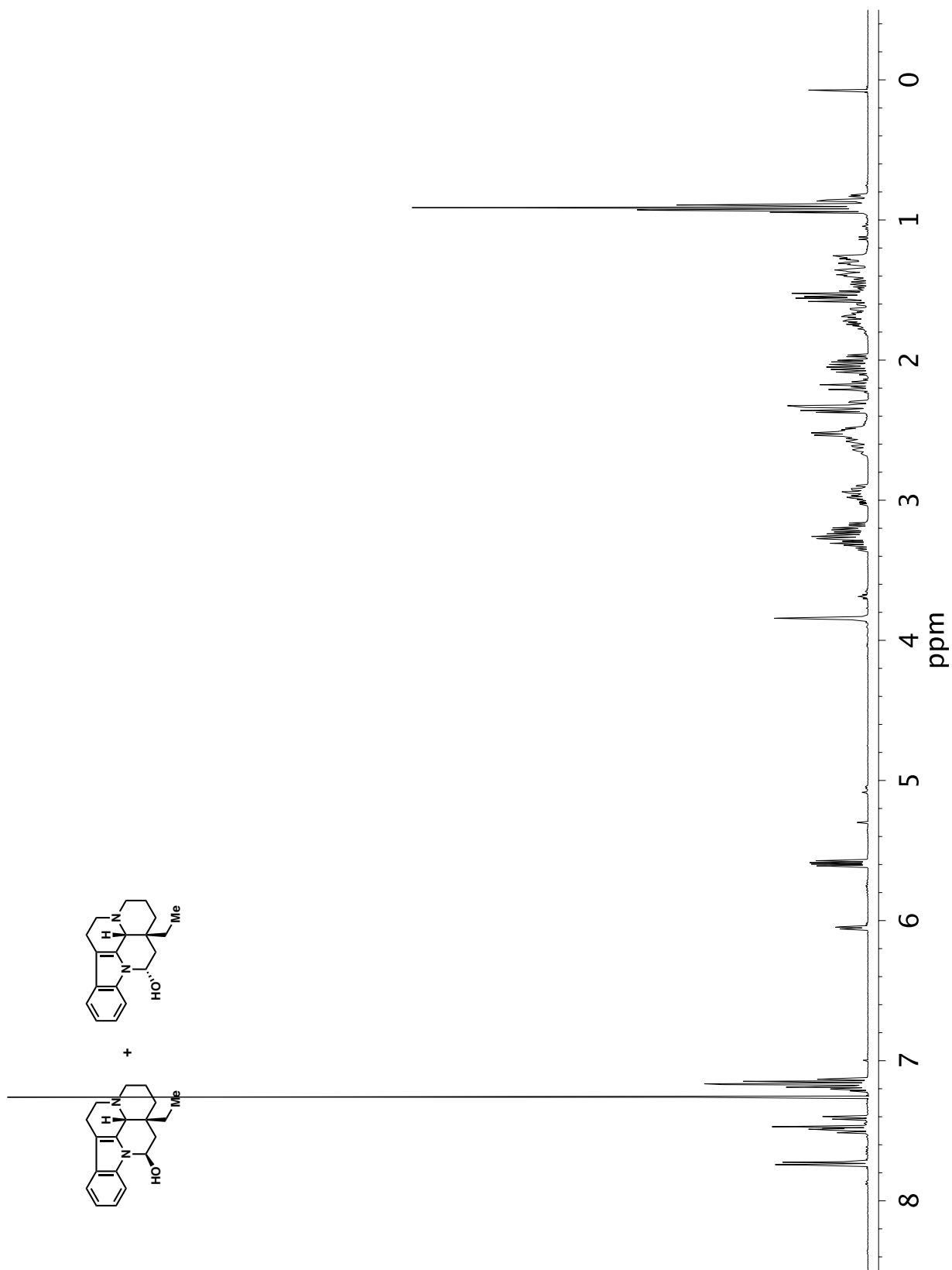


Figure A2.49. ¹H NMR (400 MHz, CDCl₃) of compound **92** and **93**.

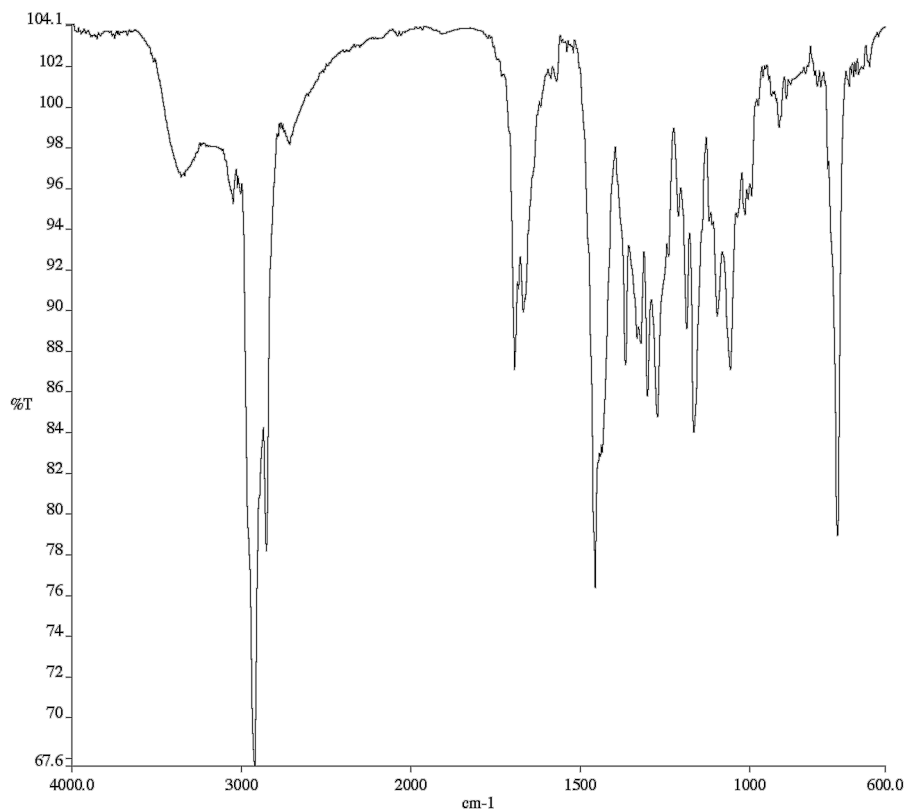


Figure A2.50. Infrared spectrum (Thin Film, NaCl) of compound **92** and **93**.

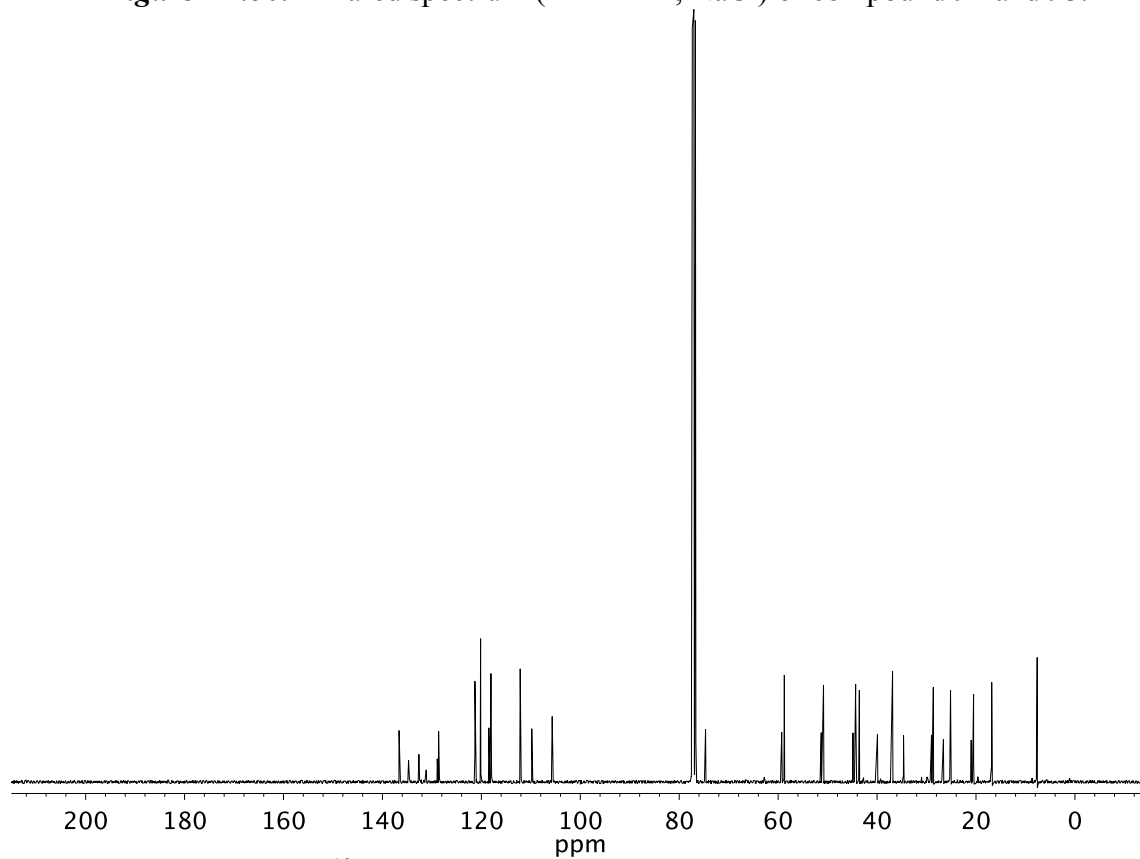


Figure A2.51. ¹³C NMR (101 MHz, CDCl₃) of compound **92** and **93**.

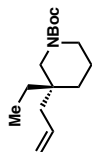
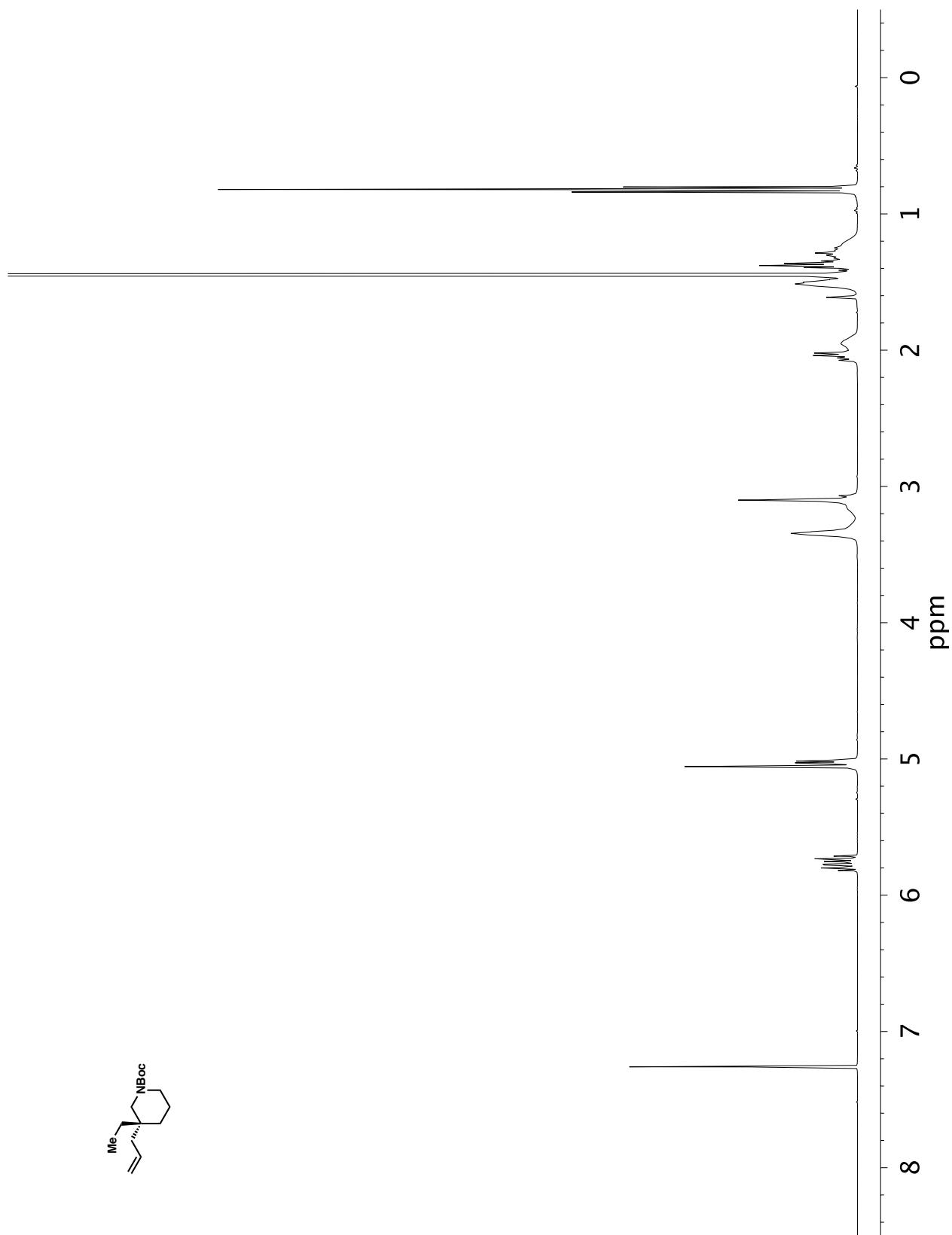


Figure A2.52. ^1H NMR (400 MHz, CDCl_3) of compound 324.

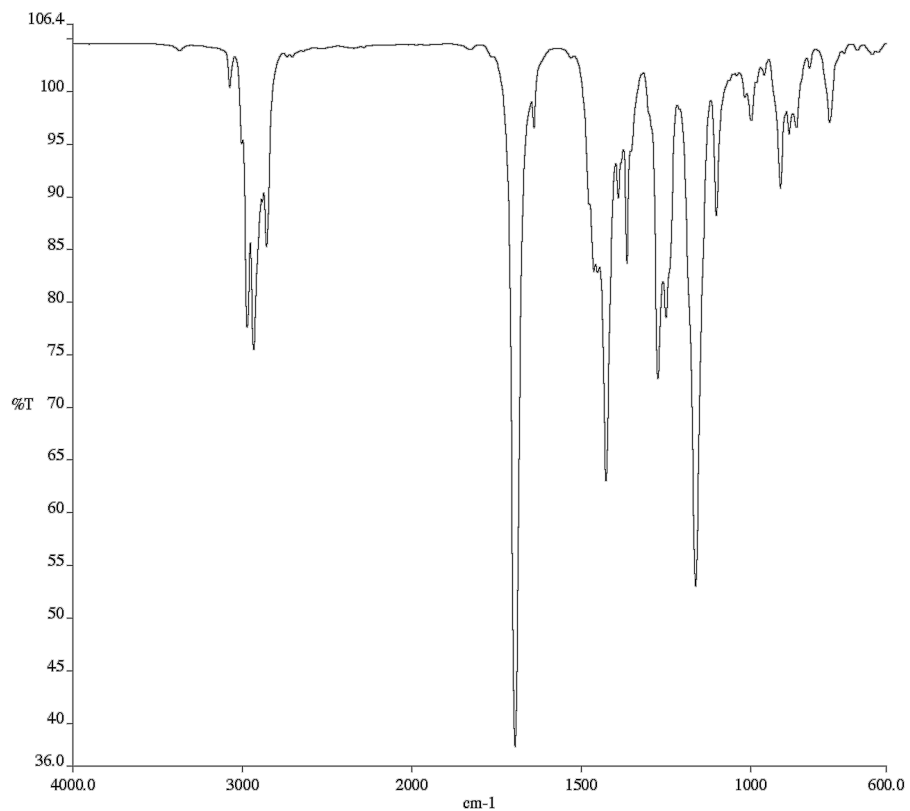


Figure A2.53. Infrared spectrum (Thin Film, NaCl) of compound **324**.

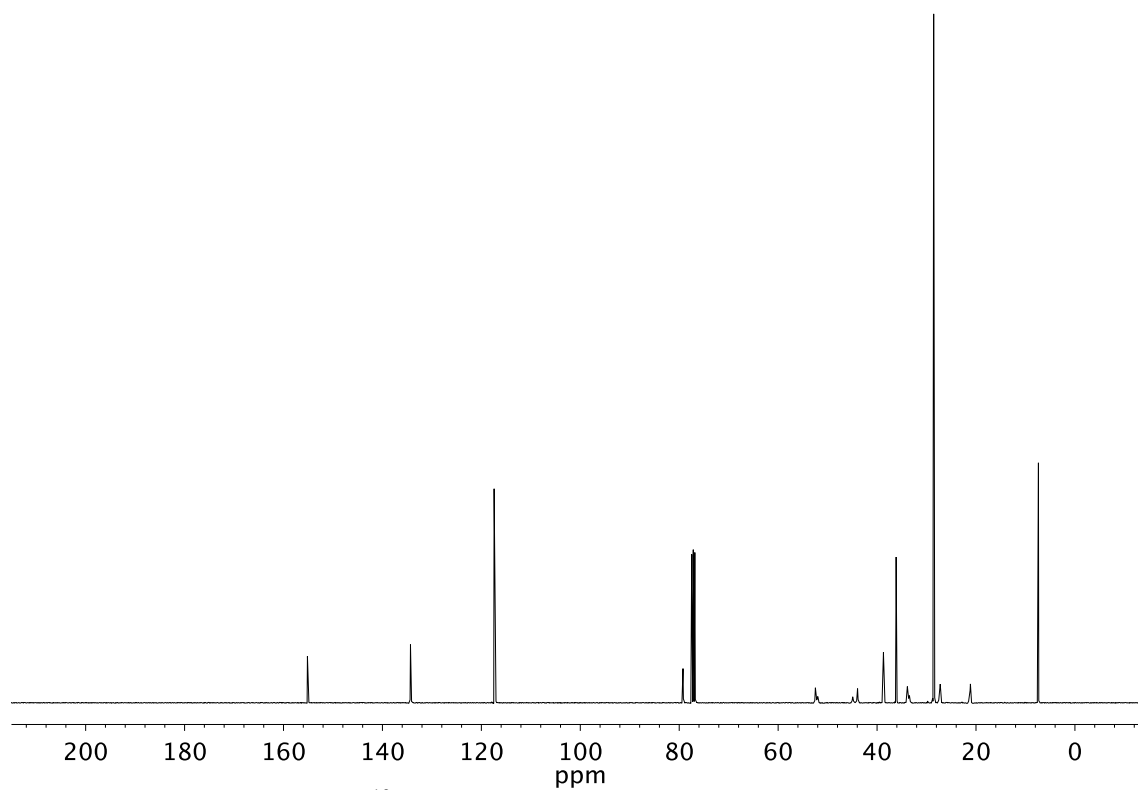


Figure A2.54. ¹³C NMR (101 MHz, CDCl₃) of compound **324**.

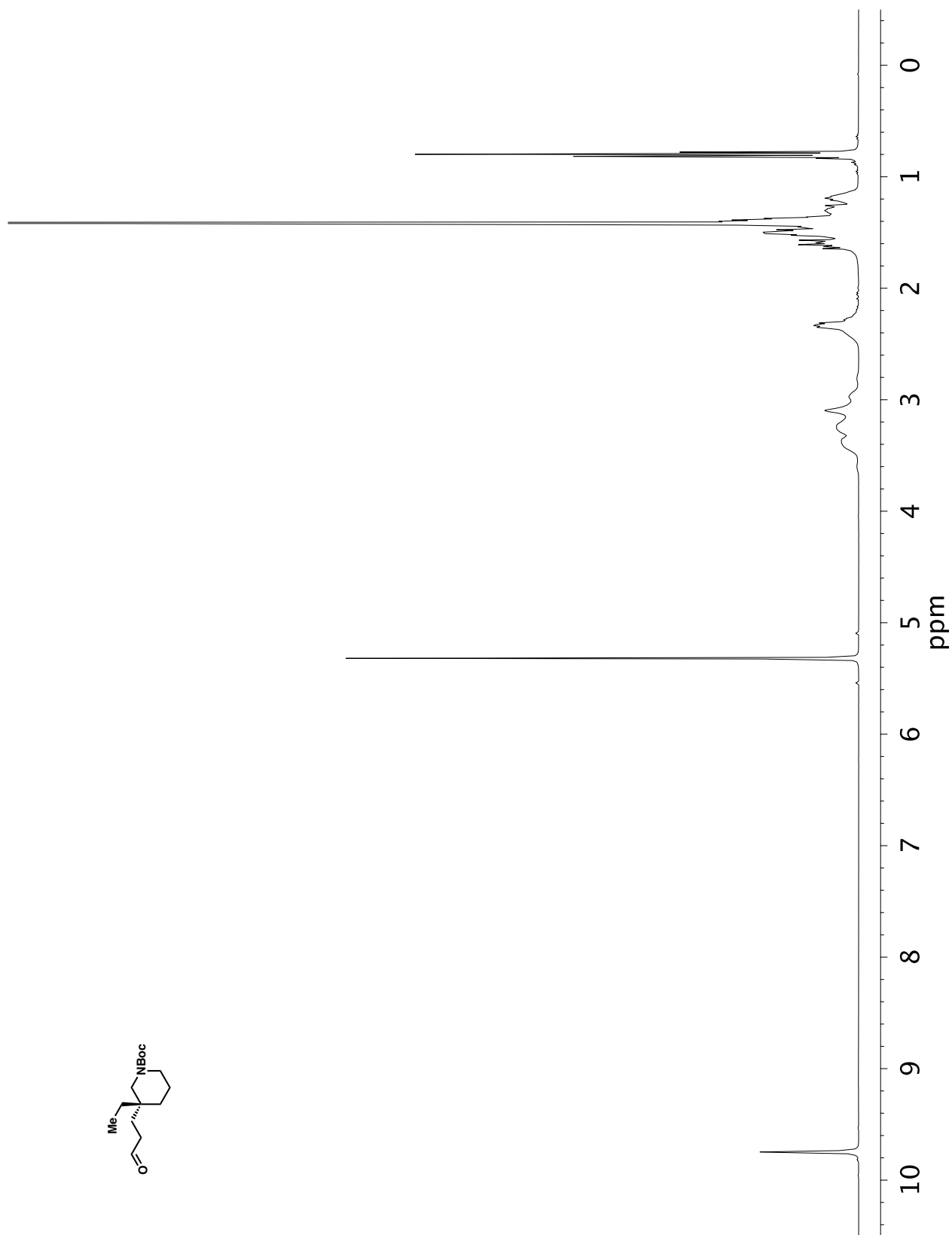


Figure A2.55. ^1H NMR (400 MHz, CDCl_3) of compound 321.

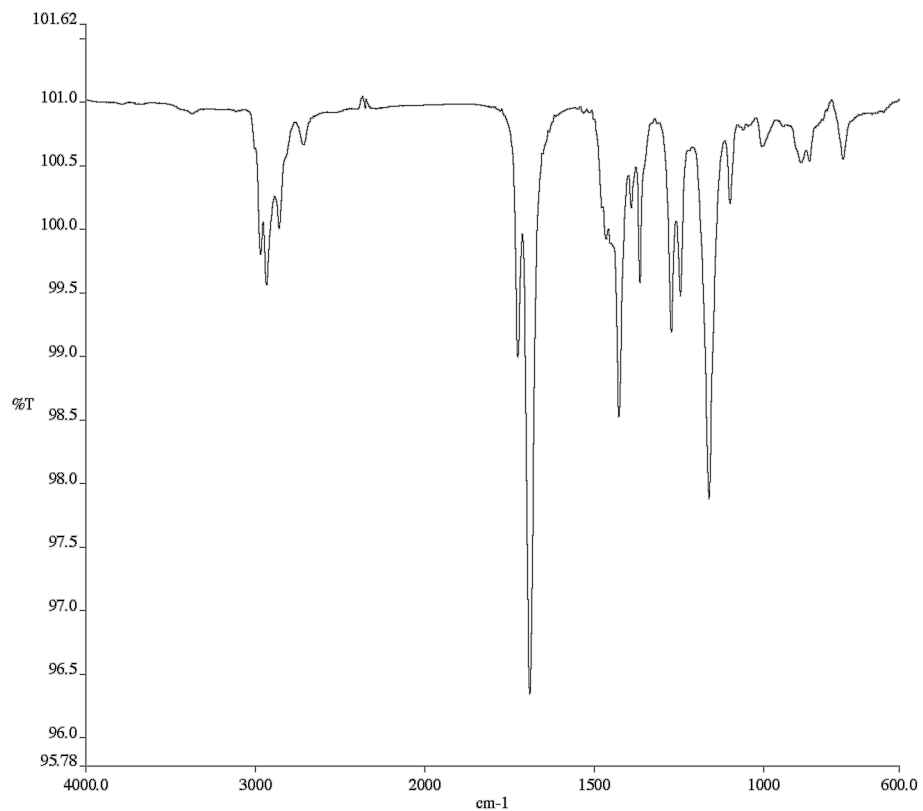


Figure A2.56. Infrared spectrum (Thin Film, NaCl) of compound **321**.

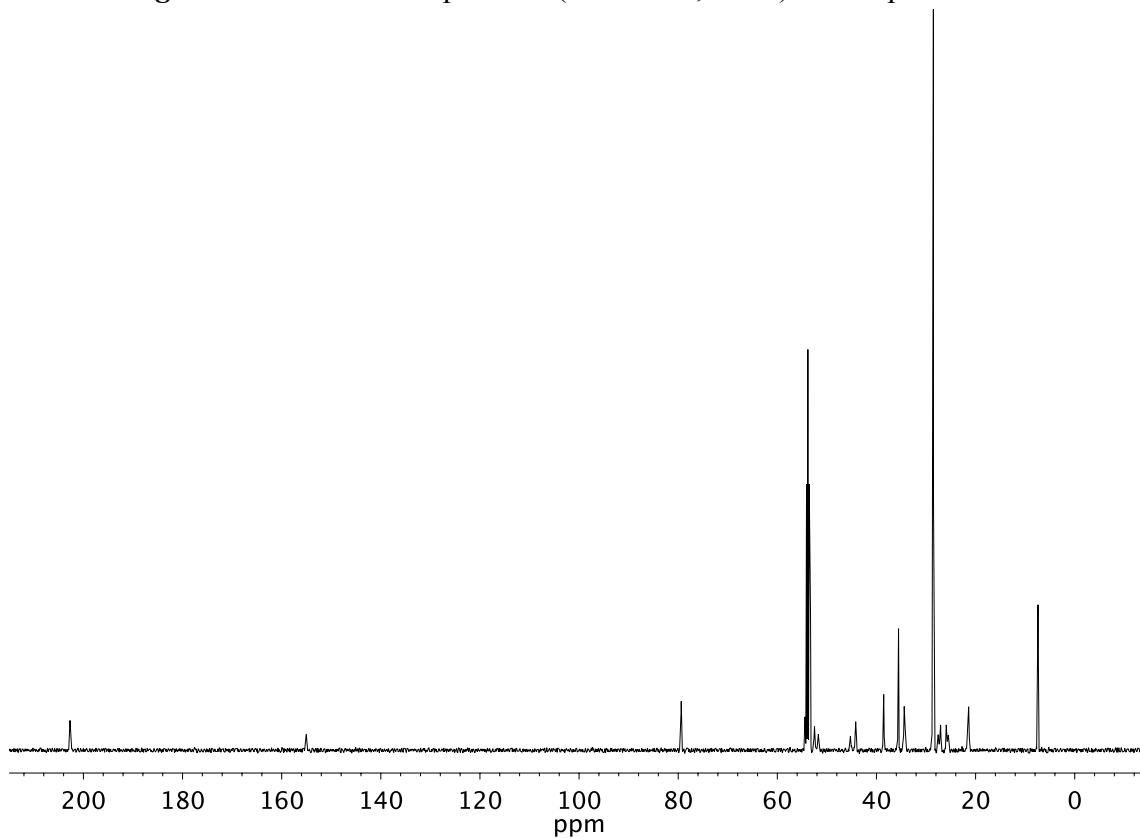


Figure A2.57. ¹³C NMR (101 MHz, CD₂Cl₂) of compound **321**.

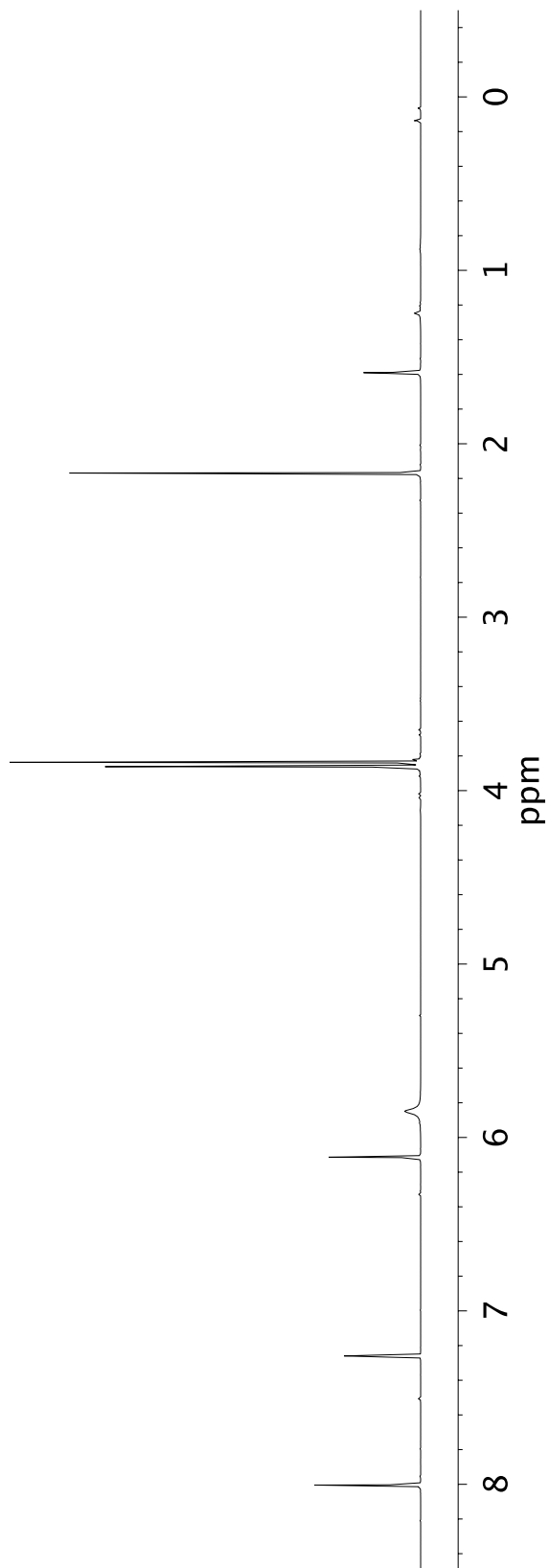
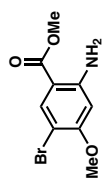


Figure A2.58. ¹H NMR (400 MHz, CD₂Cl₂) of compound 326.

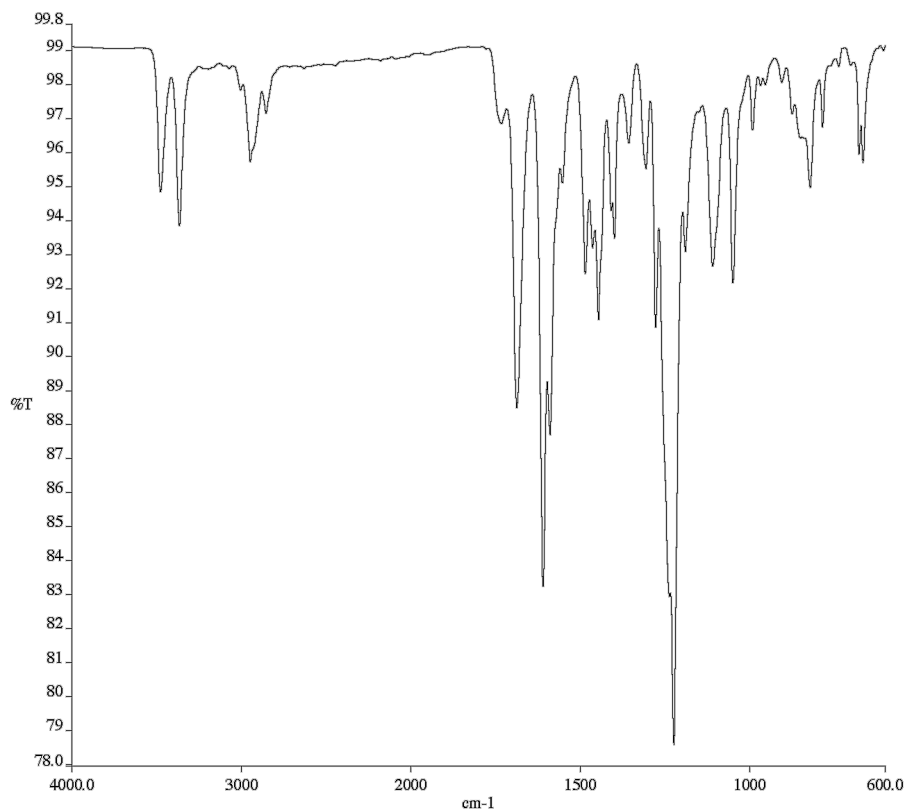


Figure A2.59. Infrared spectrum (Thin Film, NaCl) of compound **326**.

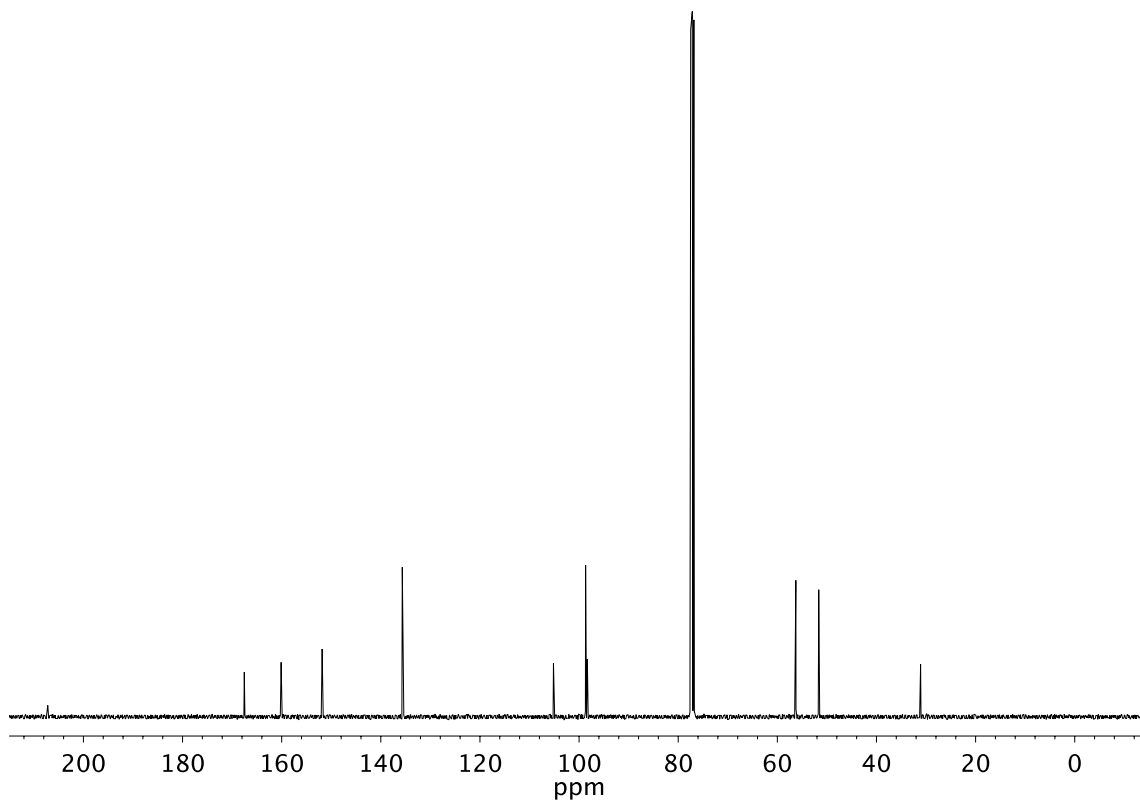


Figure A2.60. ¹³C NMR (101 MHz, CDCl₃) of compound **326**.

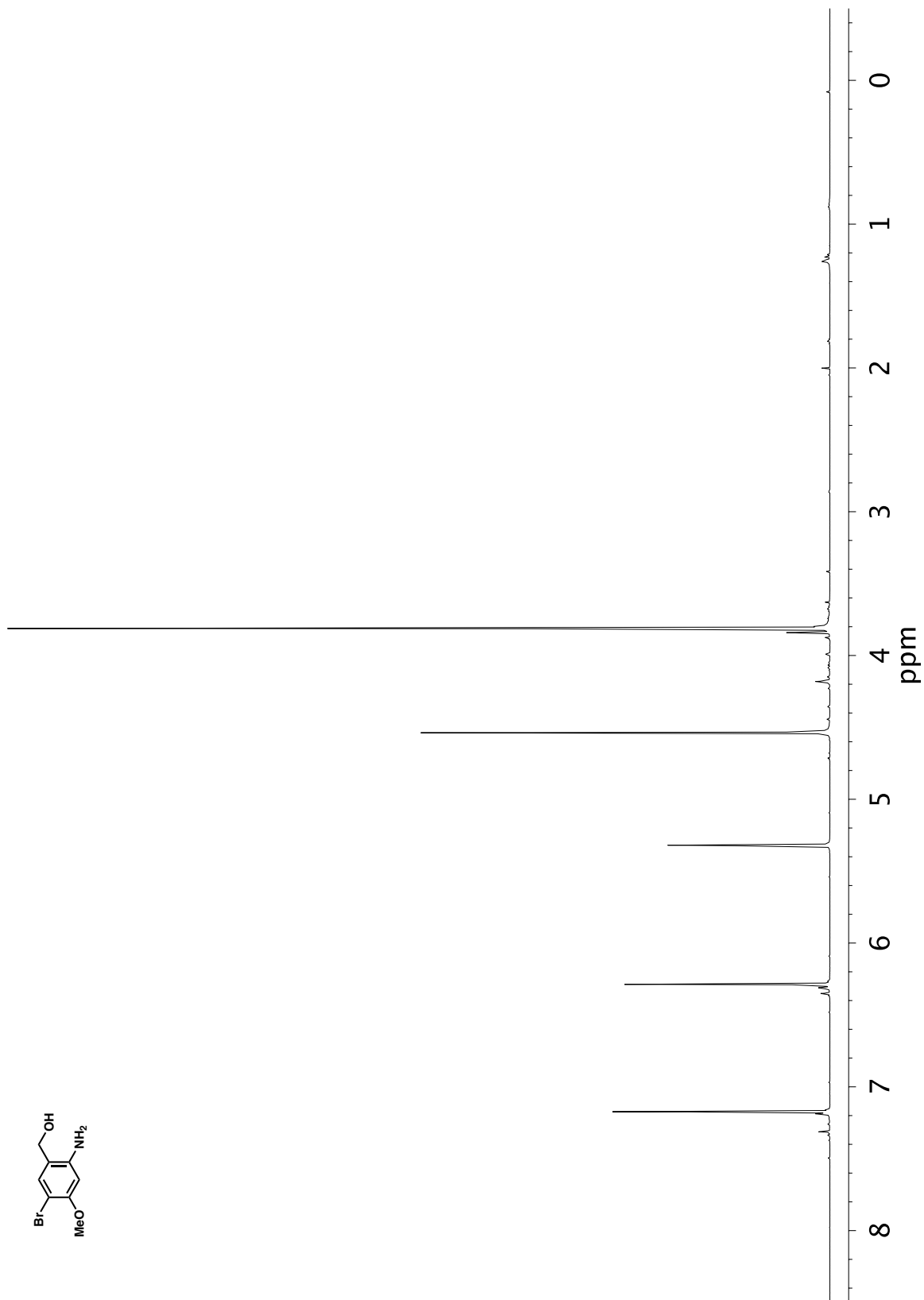


Figure A2.61. ¹H NMR (400 MHz, CD₂Cl₂) of compound 327.

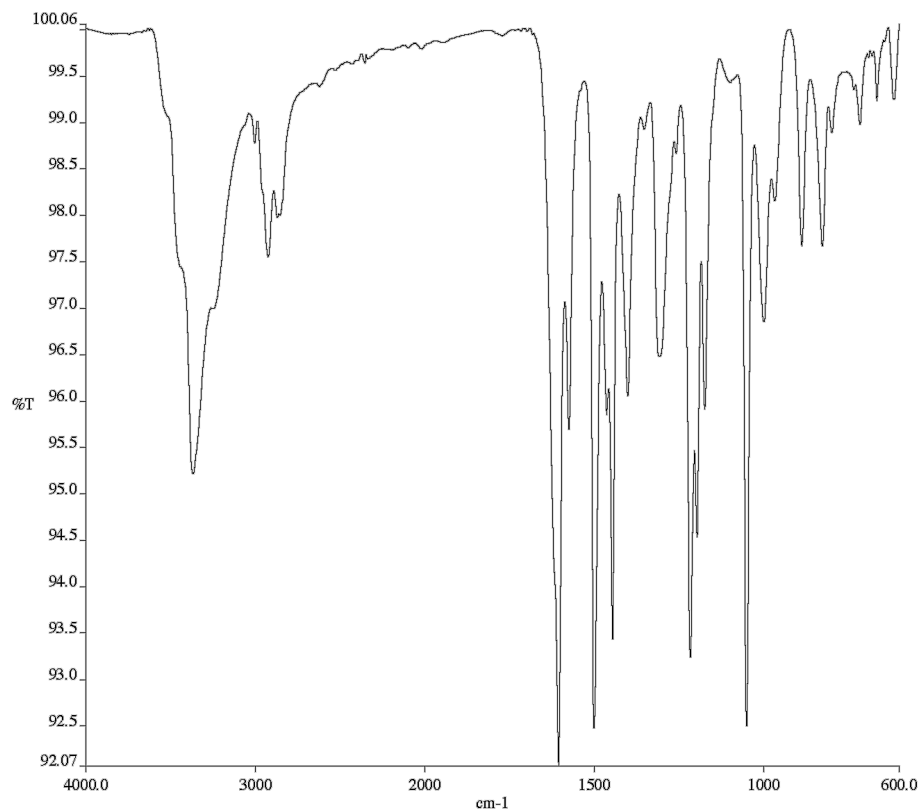


Figure A2.62. Infrared spectrum (Thin Film, NaCl) of compound **327**.

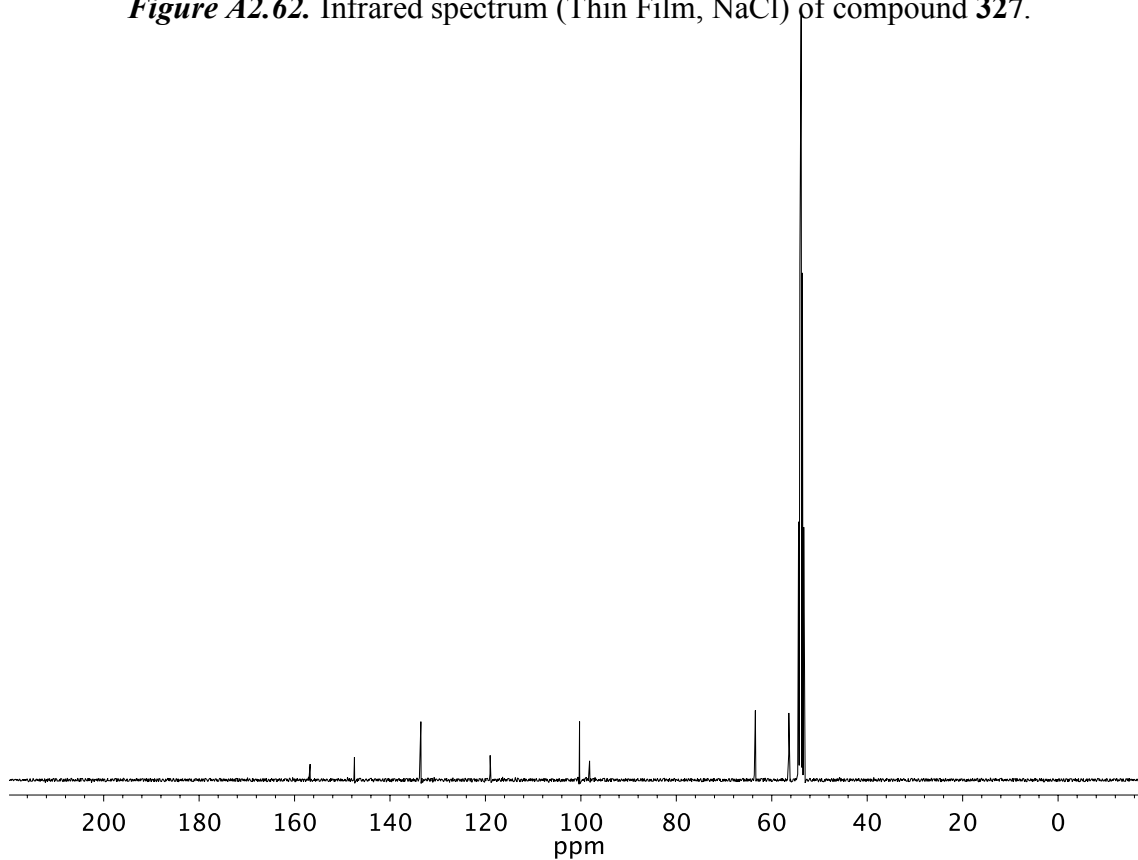


Figure A2.63. ¹³C NMR (101 MHz, CD₂Cl₂) of compound **327**.

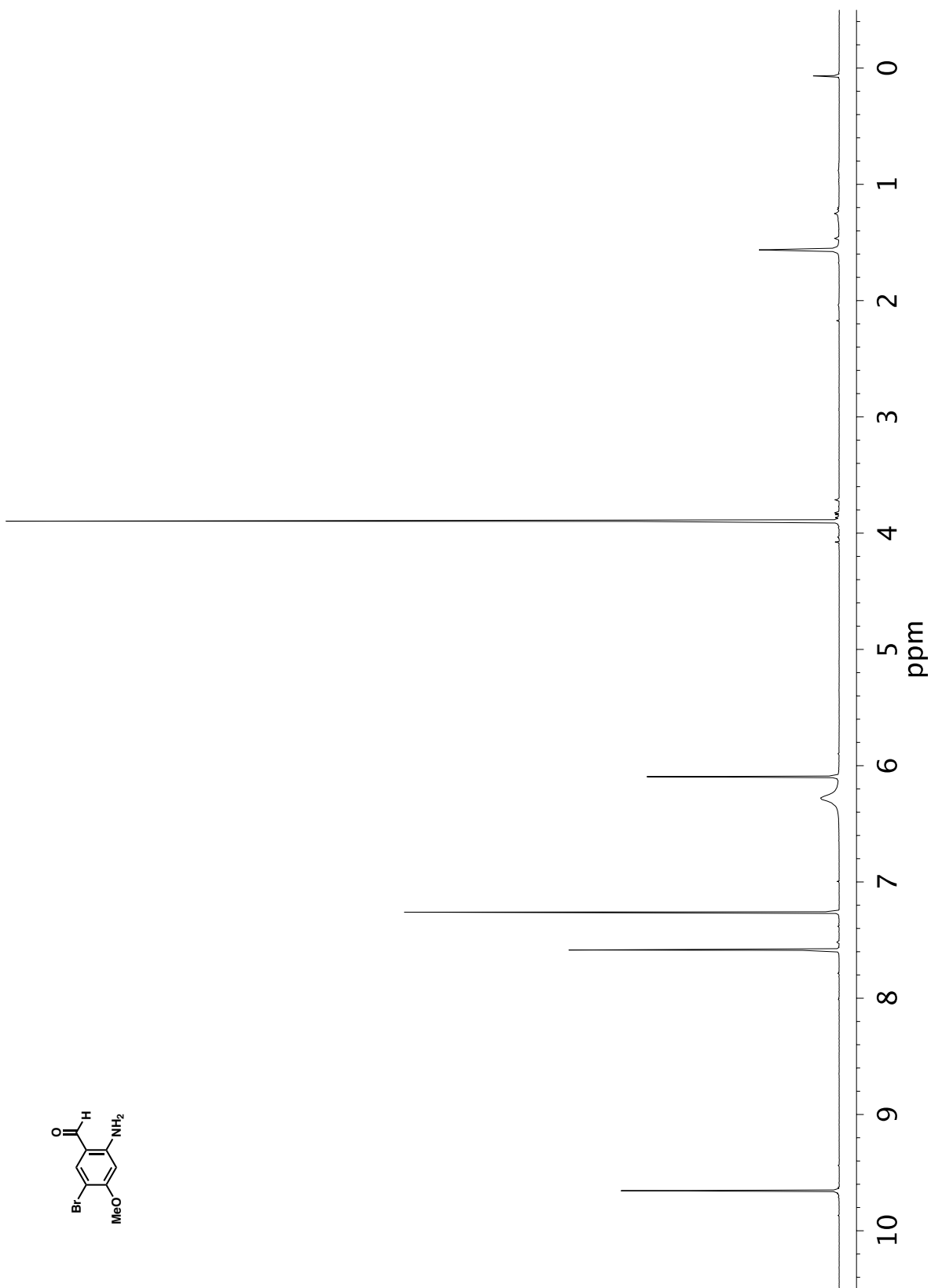


Figure A2.64. ^1H NMR (400 MHz, CDCl_3) of compound 322.

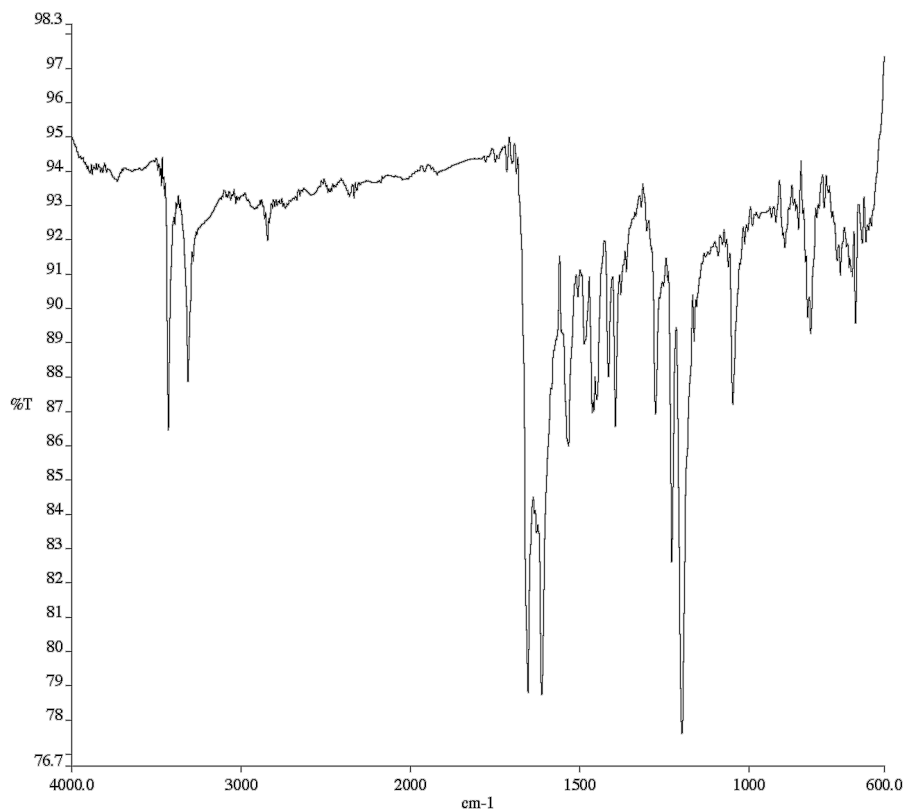


Figure A2.65. Infrared spectrum (Thin Film, NaCl) of compound **322**.

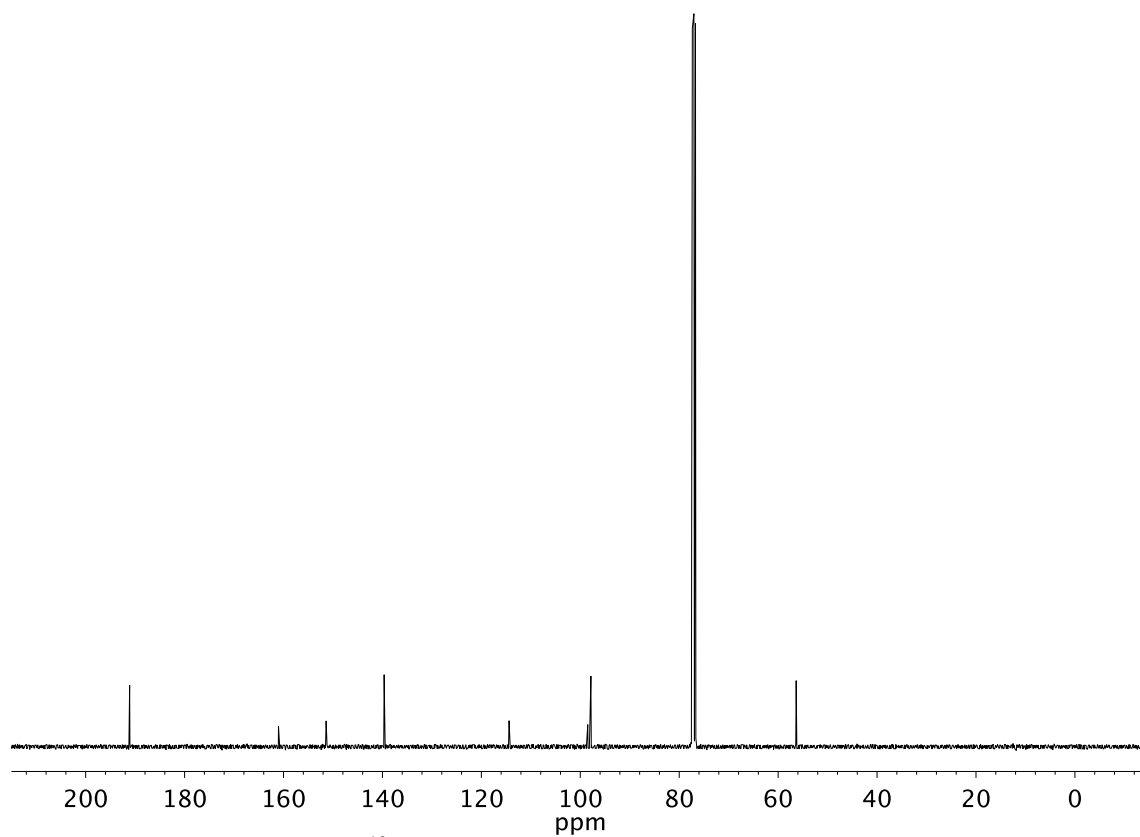


Figure A2.66. ¹³C NMR (101 MHz, CDCl₃) of compound **322**.

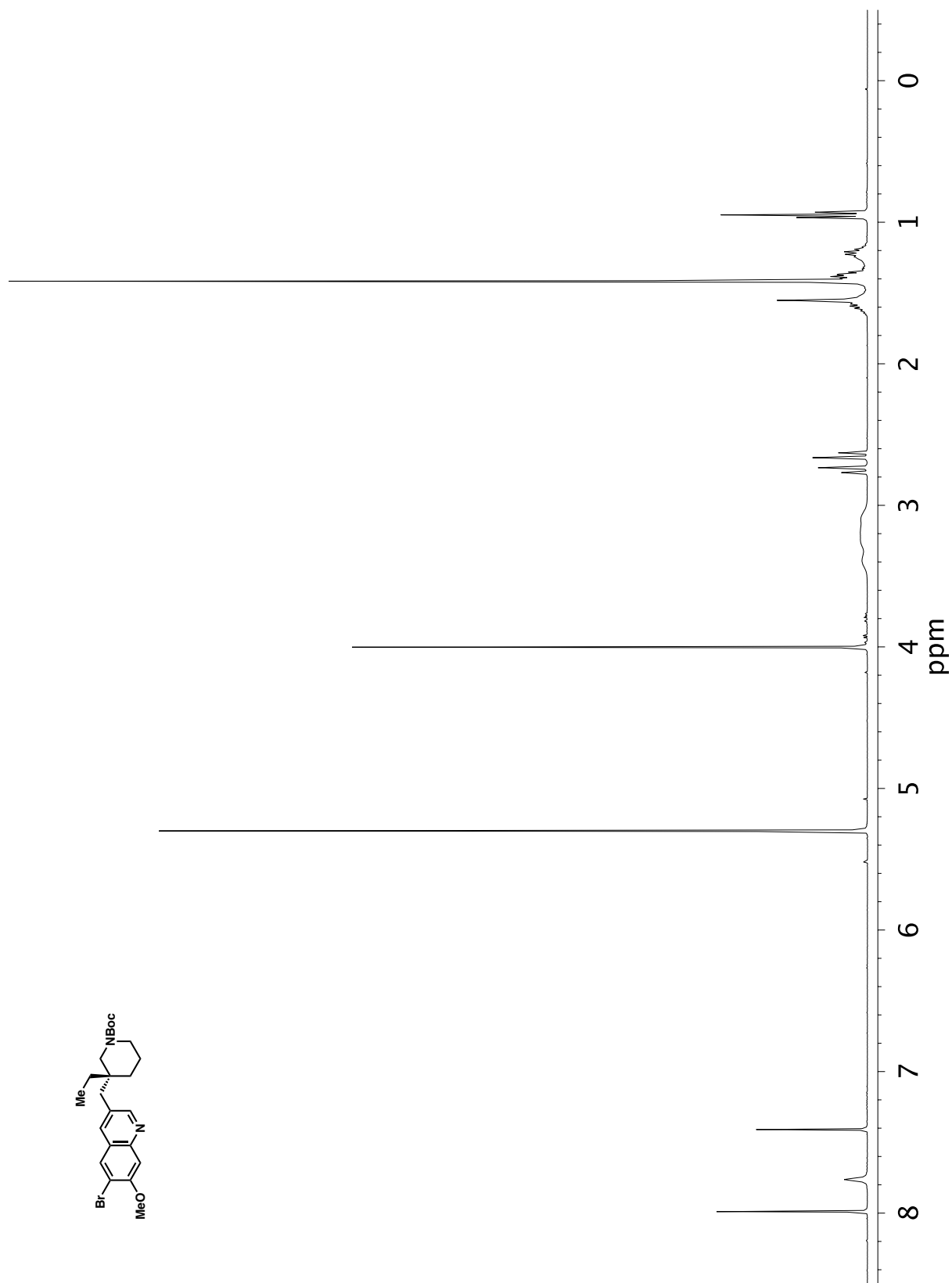


Figure A2.67. ¹H NMR (400 MHz, CD₂Cl₂) of compound 320.

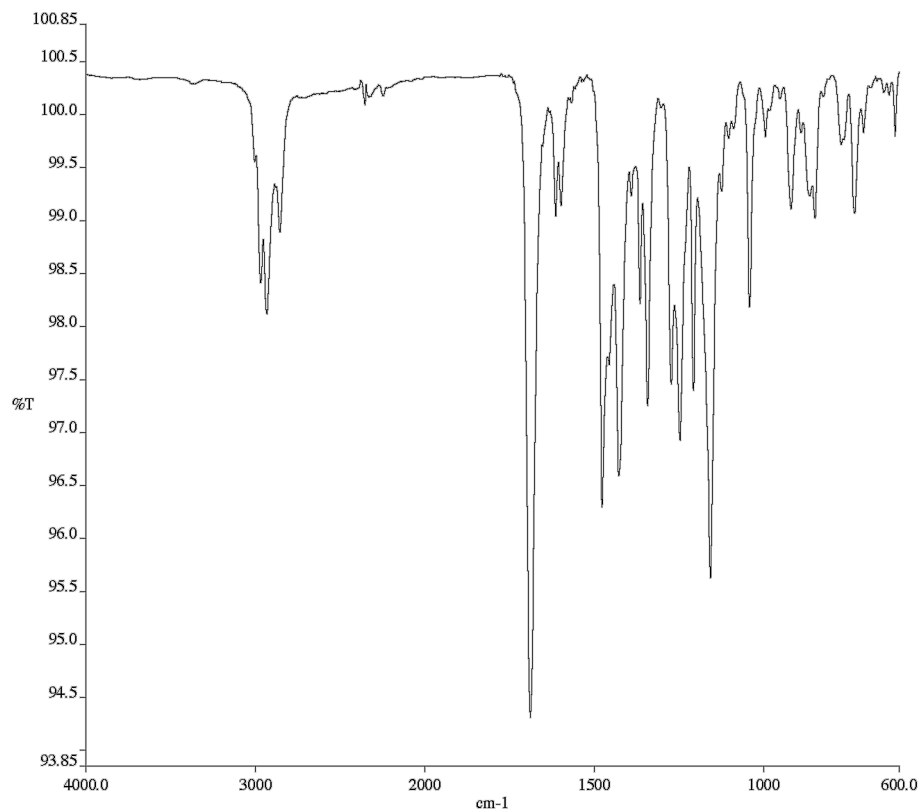


Figure A2.68. Infrared spectrum (Thin Film, NaCl) of compound **320**.

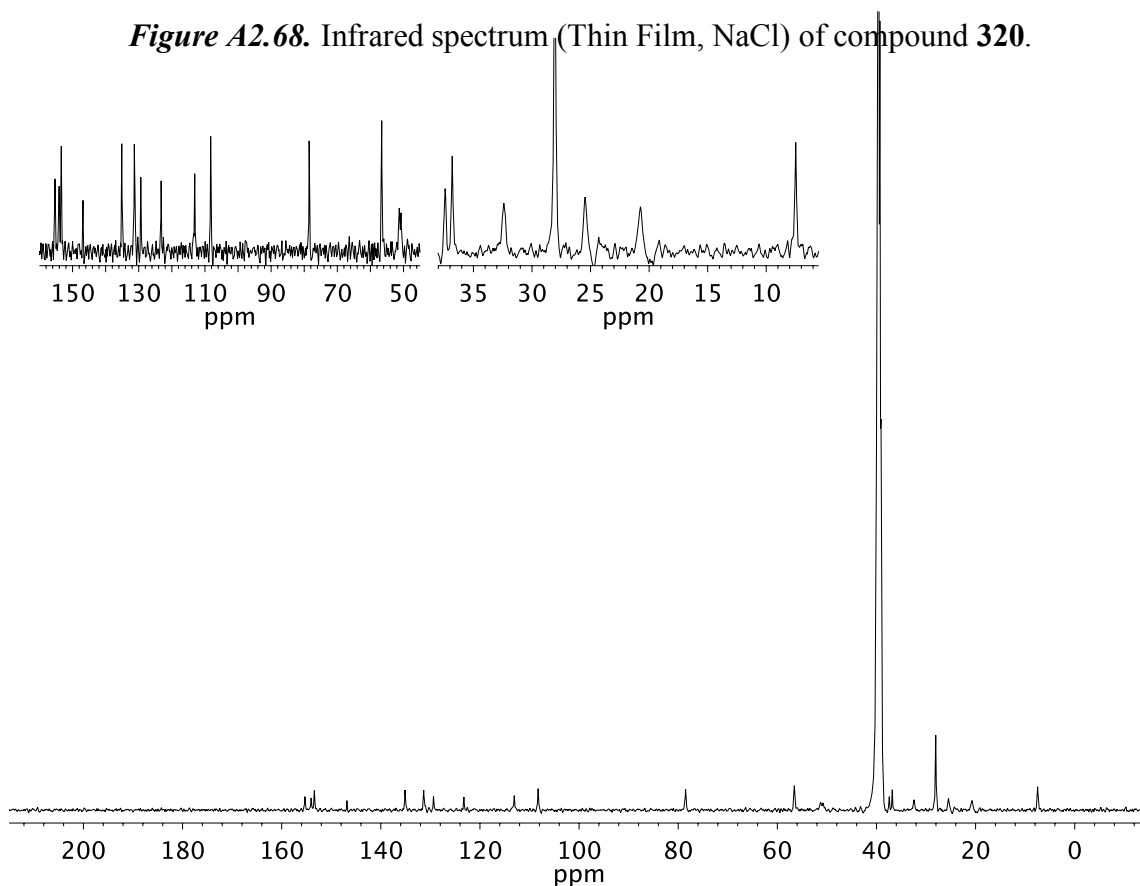


Figure A2.69. ^{13}C NMR (101 MHz, d_6 -DMSO) of compound **320**.

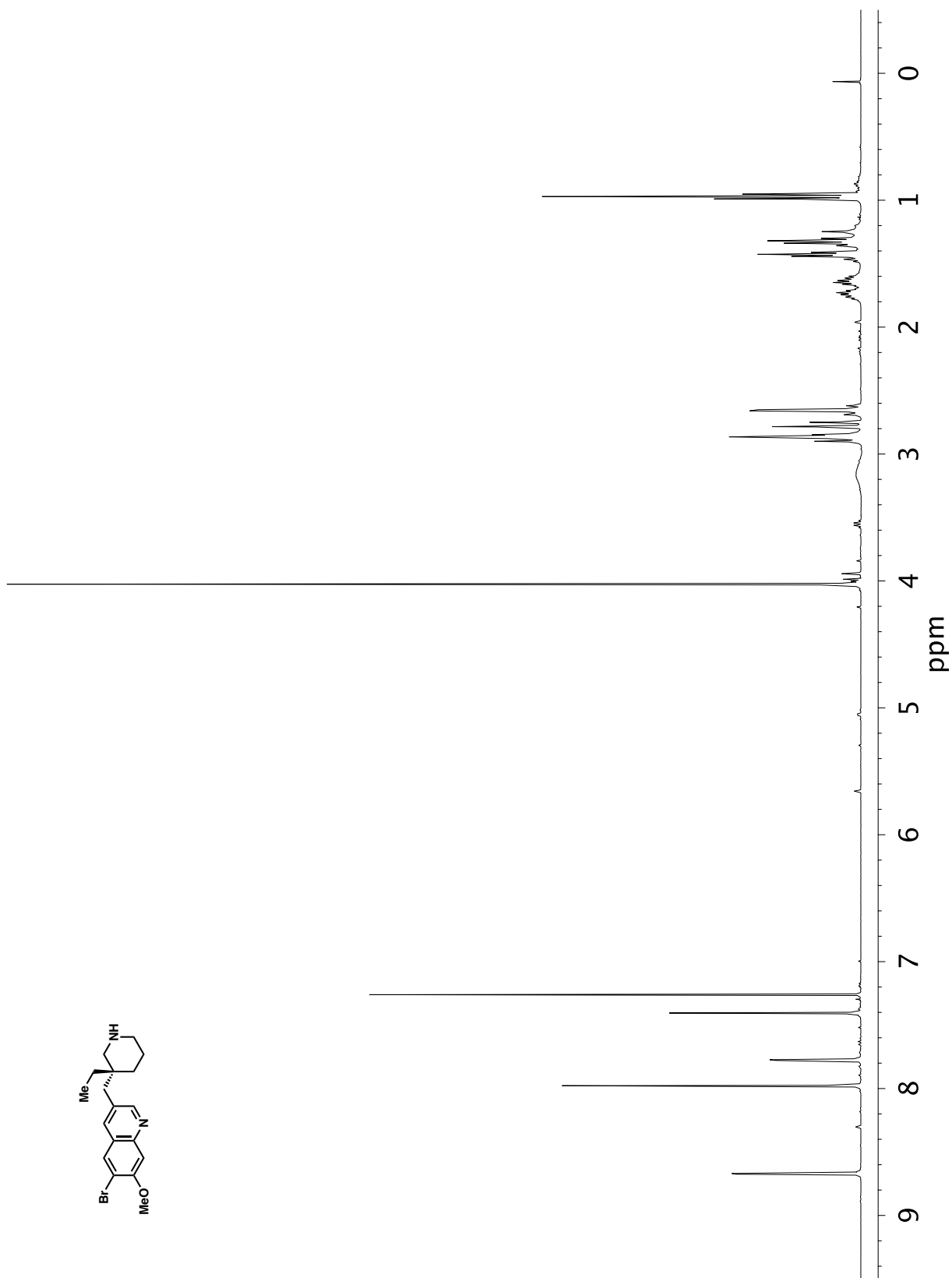


Figure A2.70. ¹H NMR (400 MHz, CDCl₃) of compound 330.

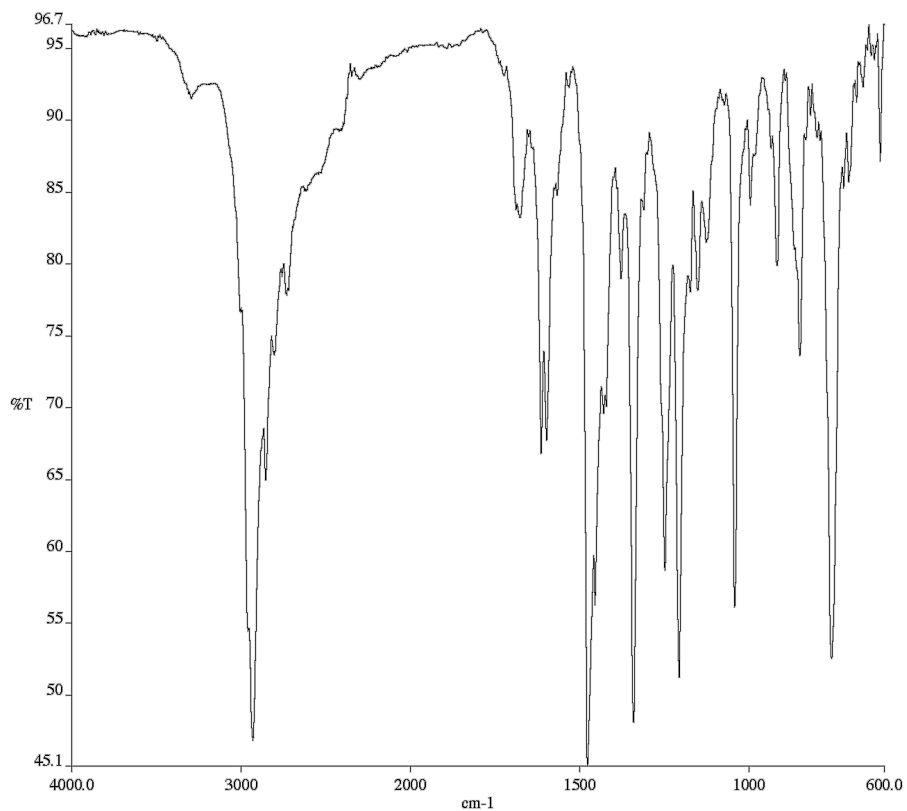


Figure A2.71. Infrared spectrum (Thin Film, NaCl) of compound **330**.

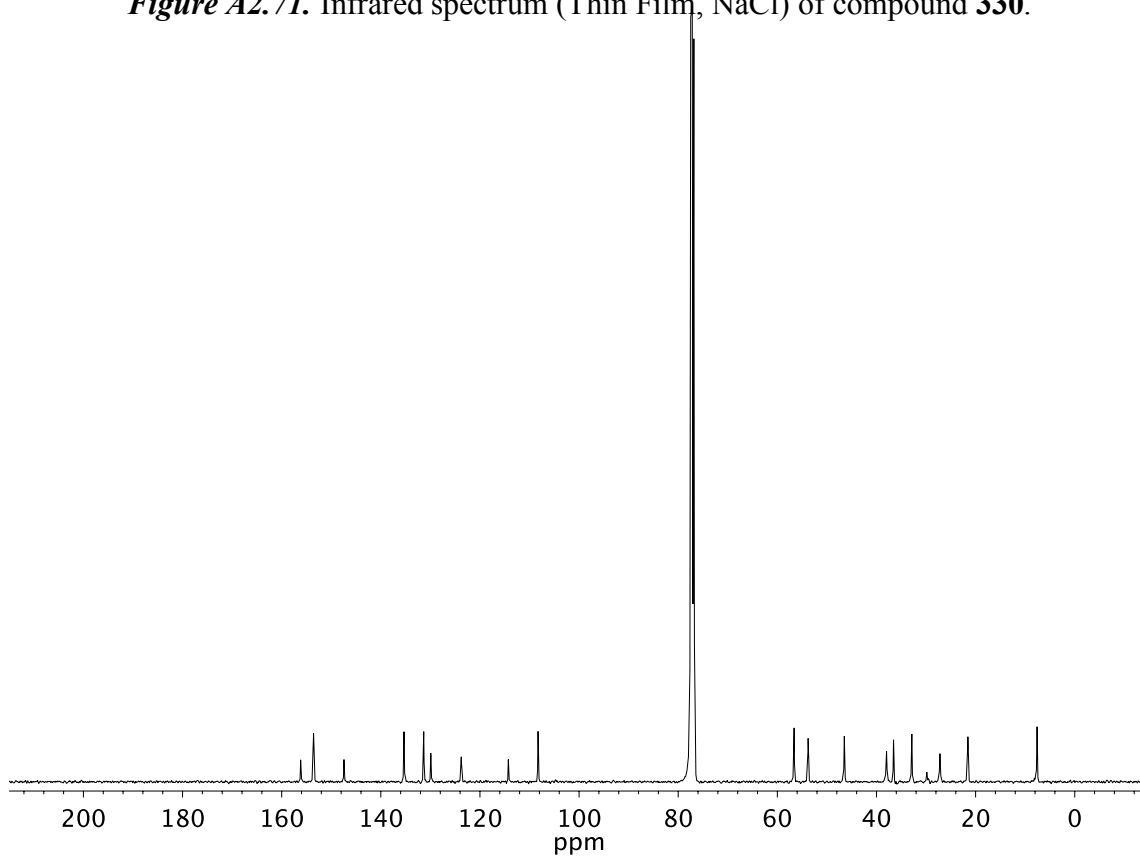


Figure A2.72. ¹³C NMR (101 MHz, CDCl₃) of compound **330**.

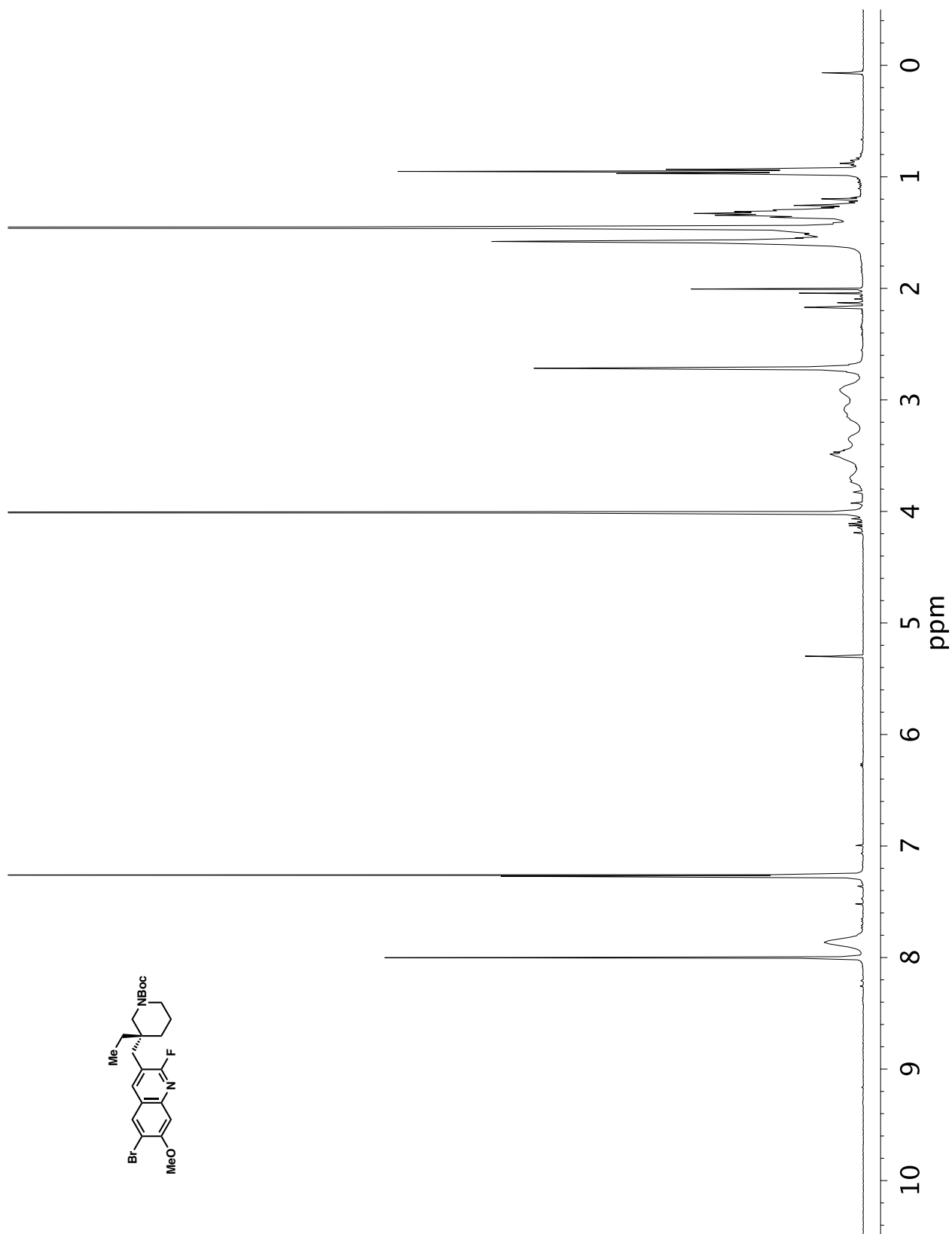


Figure A2.73. ^1H NMR (400 MHz, CDCl_3) of compound 329a.

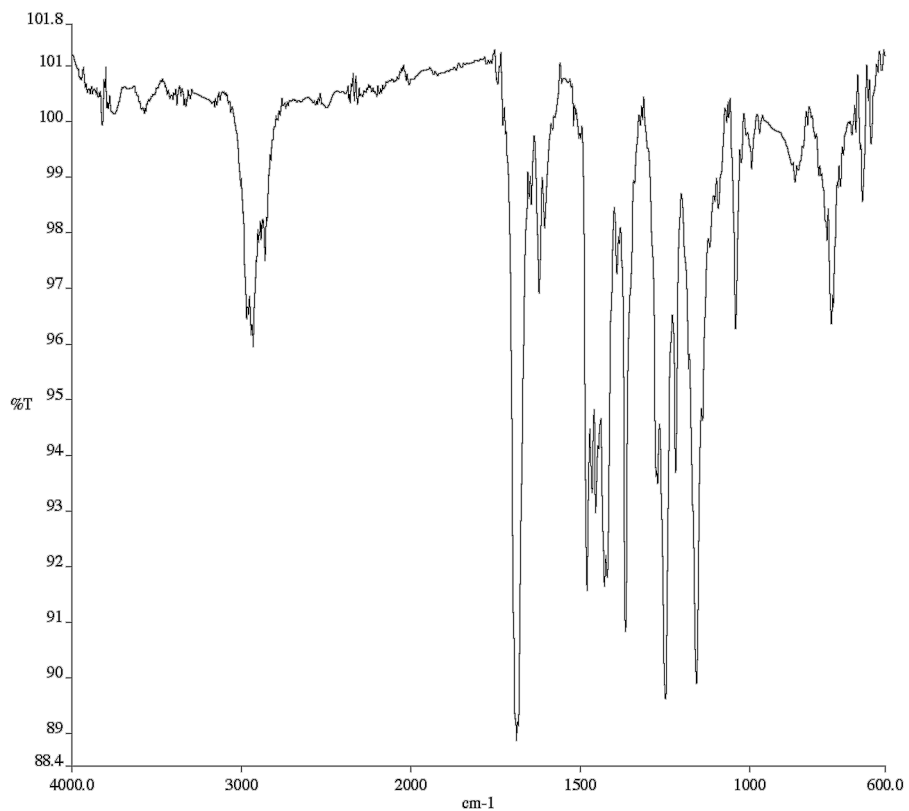


Figure A2.74. Infrared spectrum (Thin Film, NaCl) of compound **329a**.

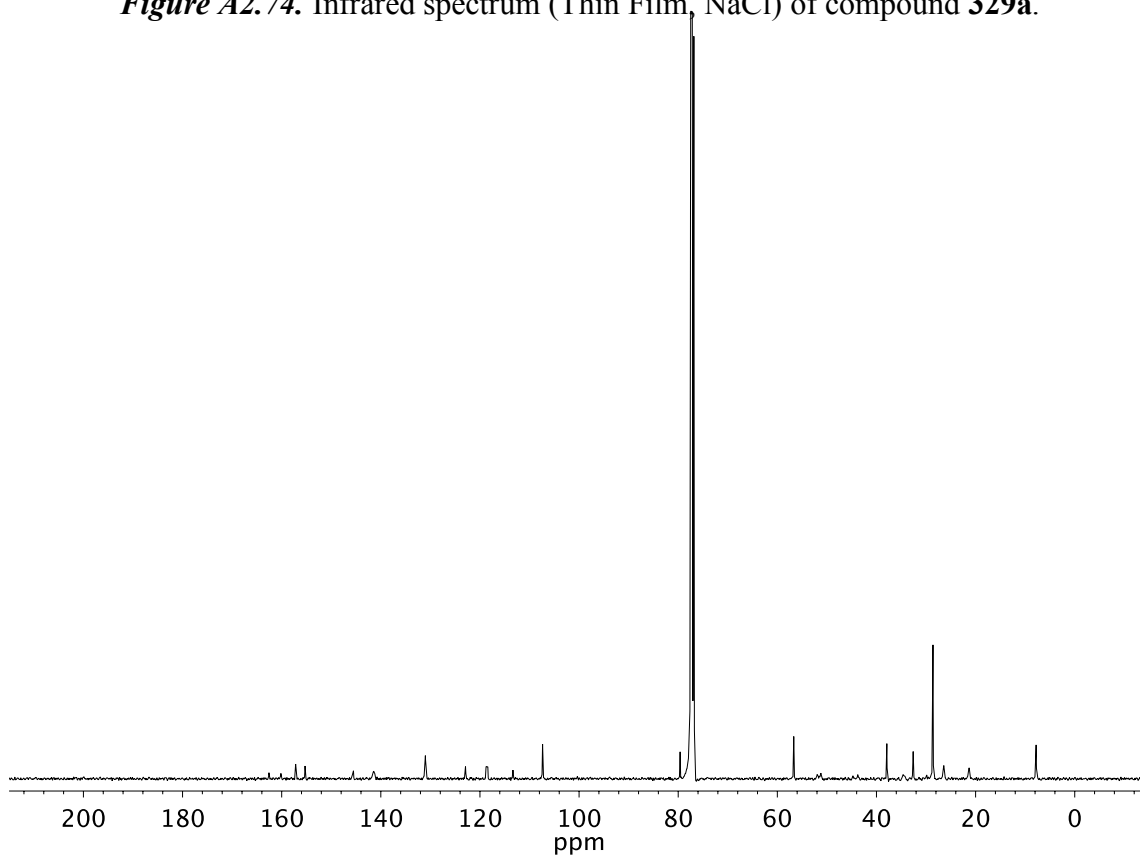


Figure A2.75. ¹³C NMR (101 MHz, CDCl₃) of compound **329a**.

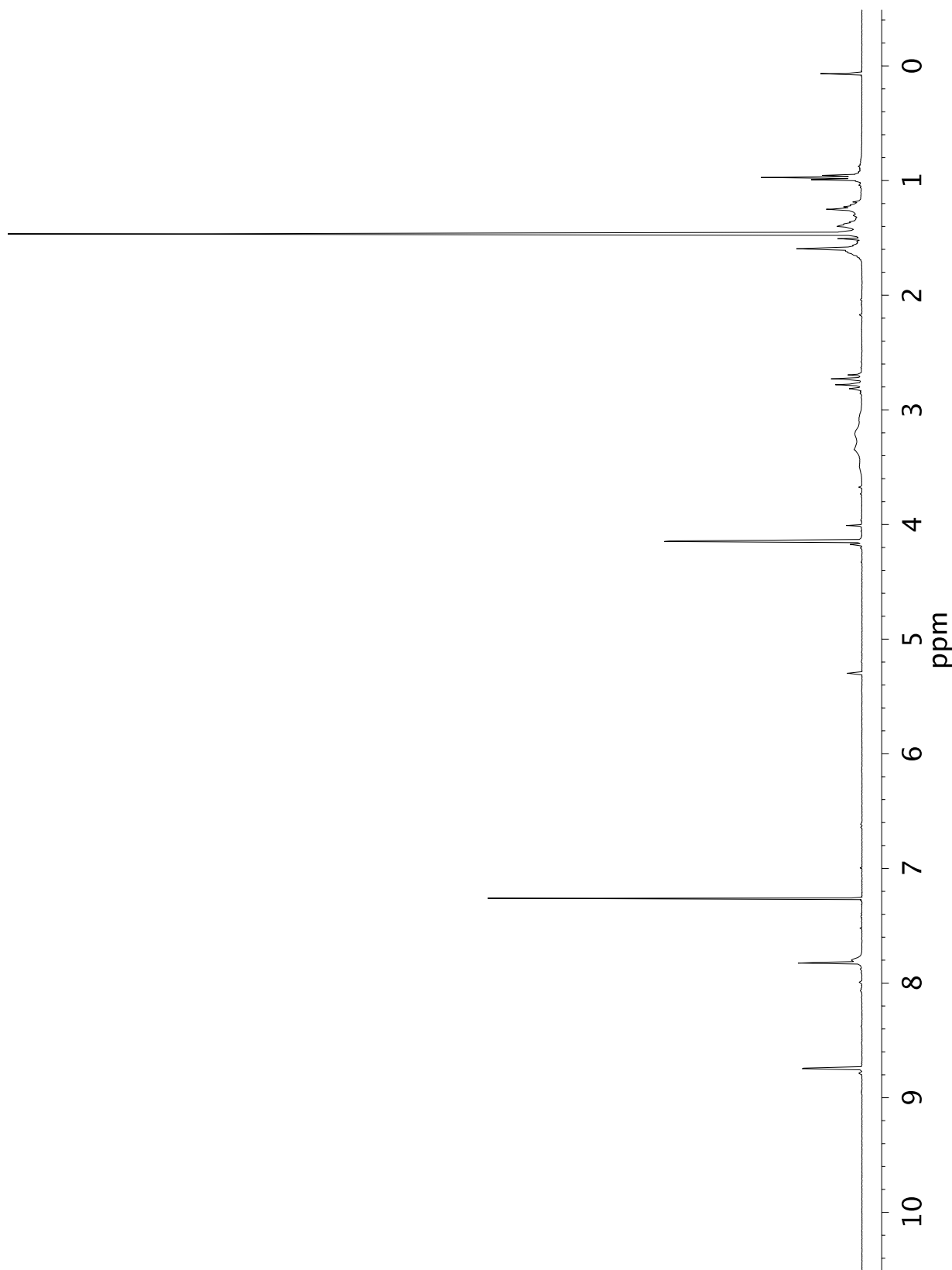


Figure A2.76. ^1H NMR (400 MHz, CDCl_3) of compound 329b.

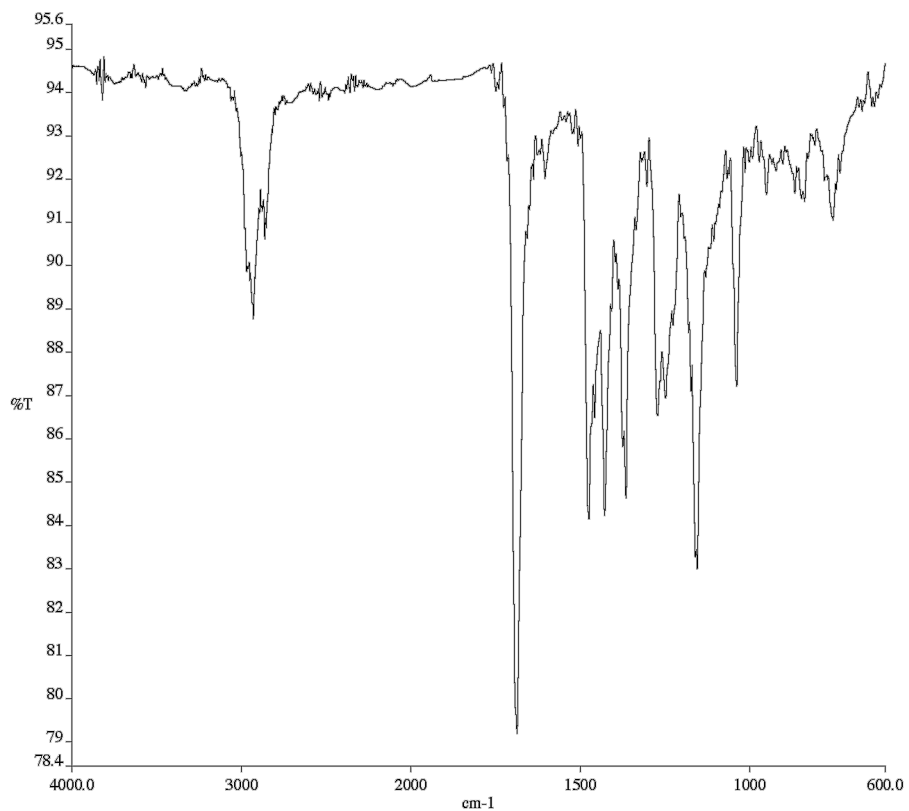


Figure A2.77. Infrared spectrum (Thin Film, NaCl) of compound **329b**.

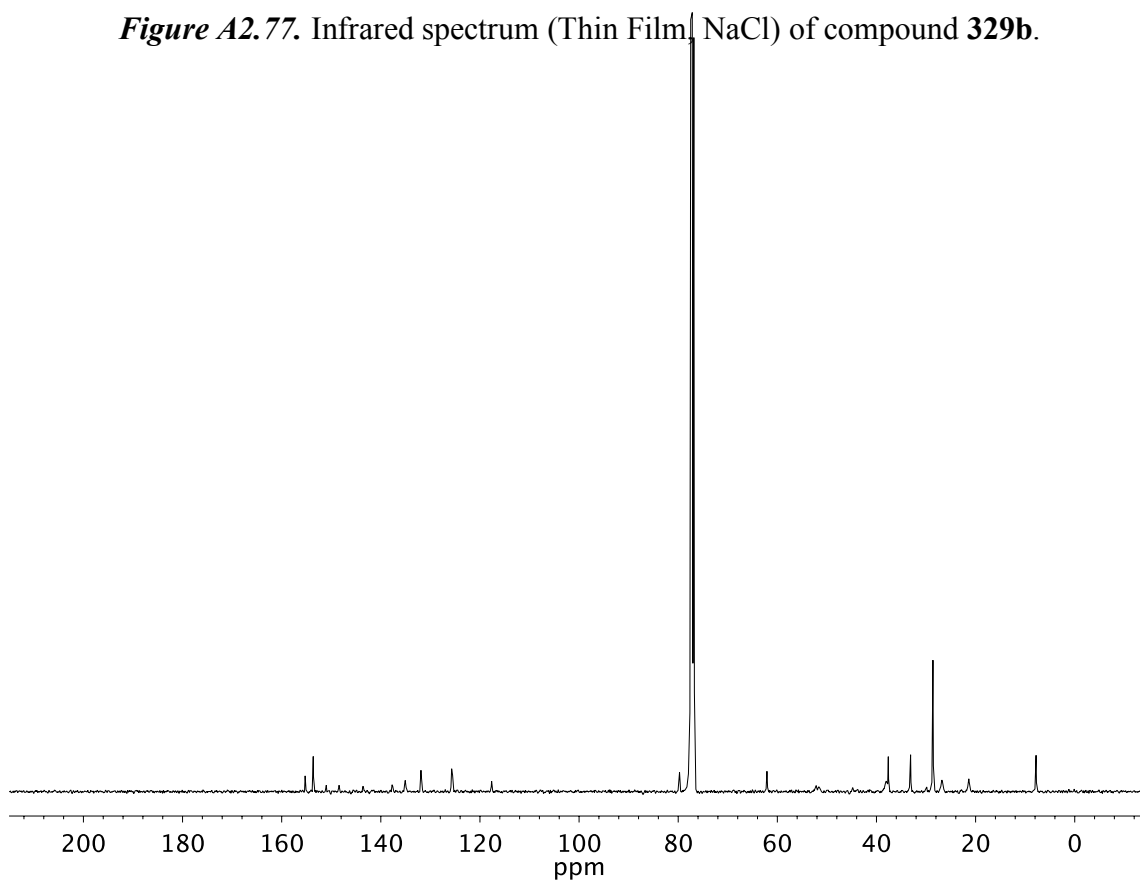


Figure A2.78. ¹³C NMR (101 MHz, CDCl₃) of compound **329b**.

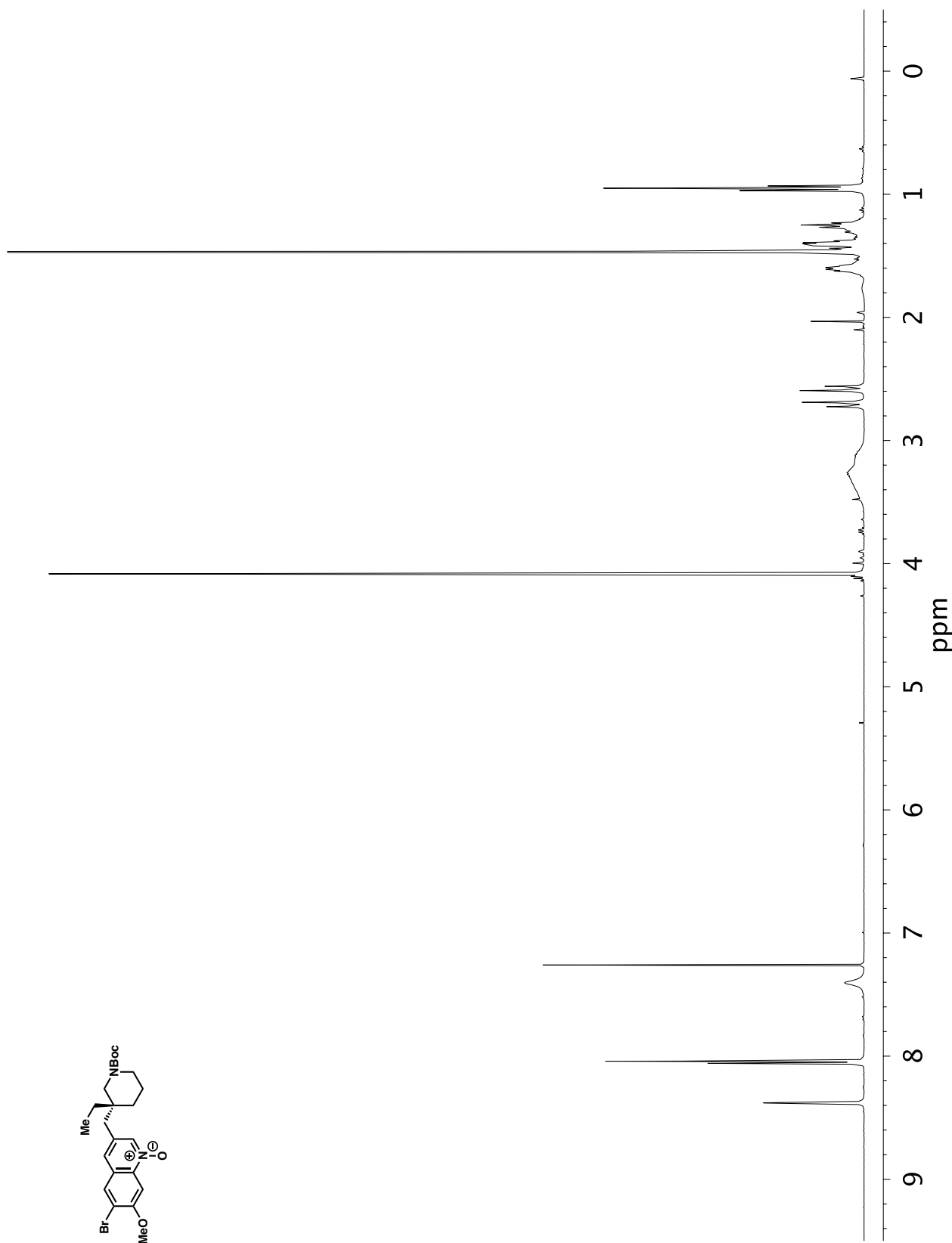


Figure A2.79. $^1\text{H NMR}$ (400 MHz, CDCl_3) of compound 332.

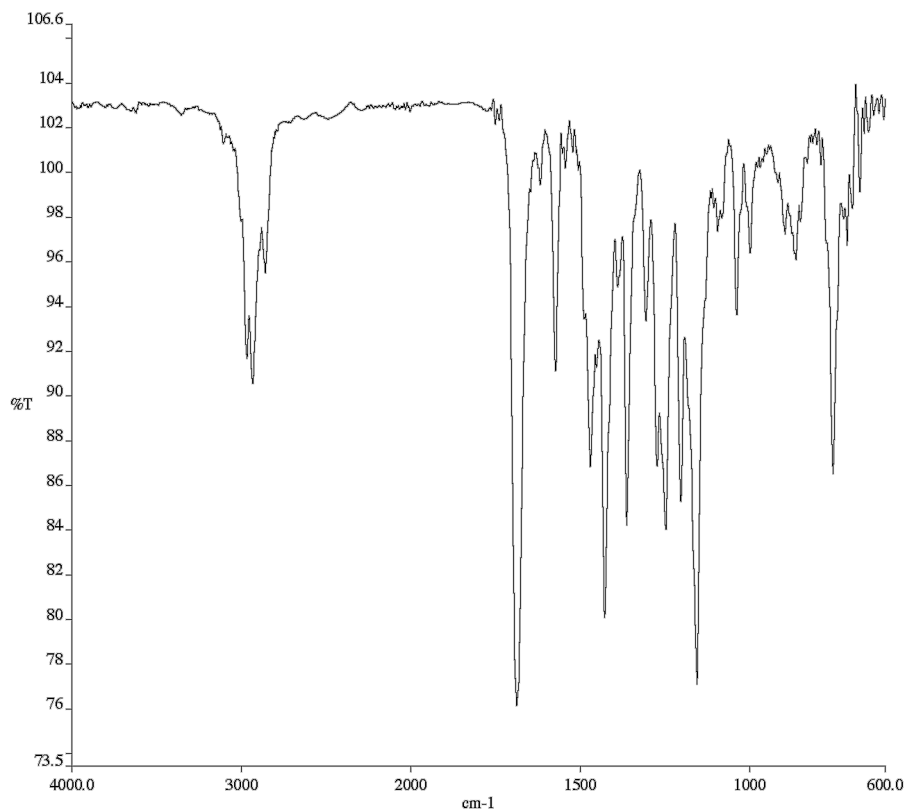


Figure A2.80. Infrared spectrum (Thin Film, NaCl) of compound **332**.

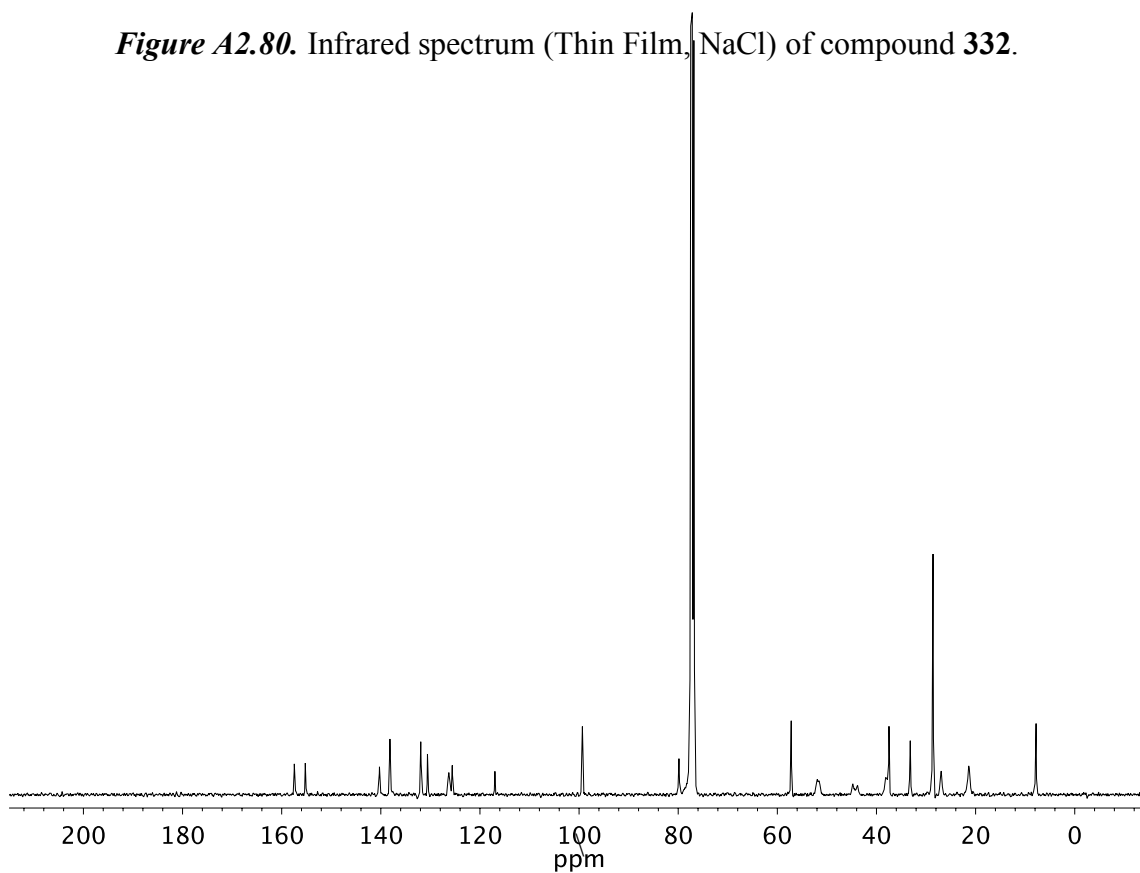


Figure A2.81. ¹³C NMR (101 MHz, CDCl₃) of compound **332**.

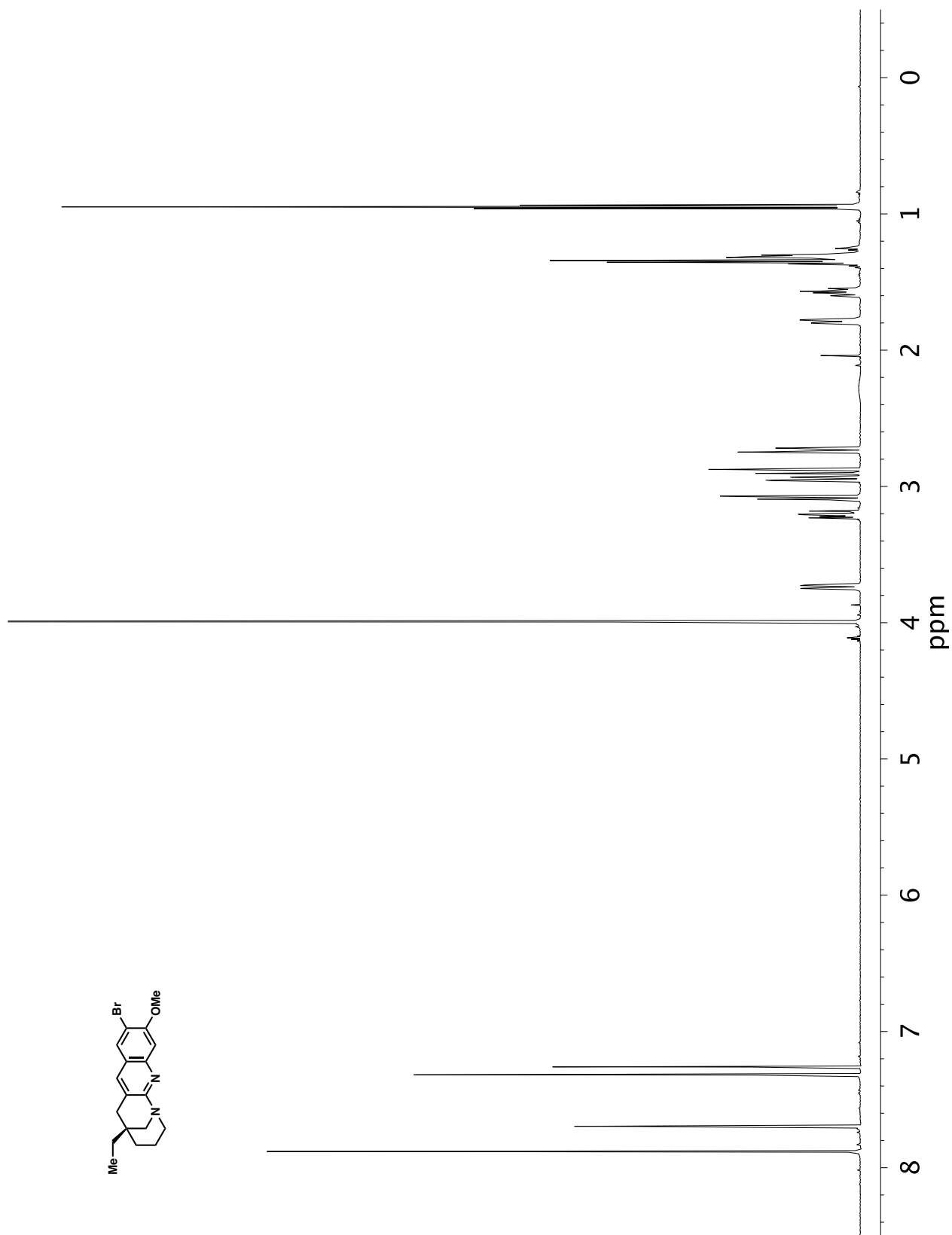


Figure A2.82. ¹H NMR (600 MHz, CDCl₃) of compound 319.

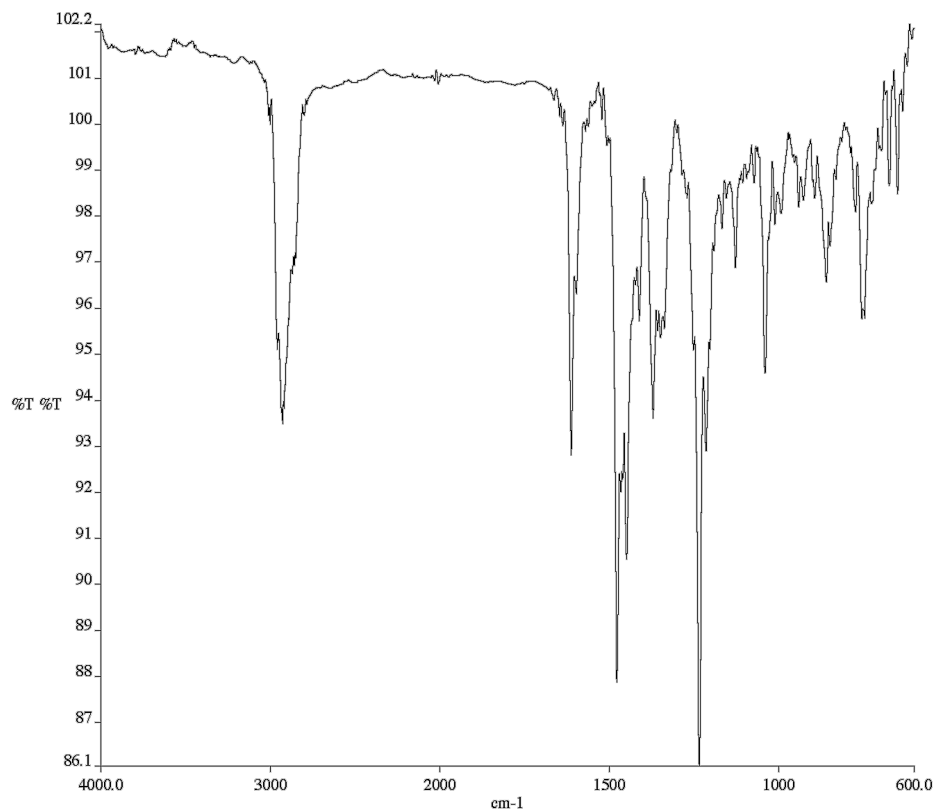


Figure A2.83. Infrared spectrum (Thin Film, NaCl) of compound **319**.

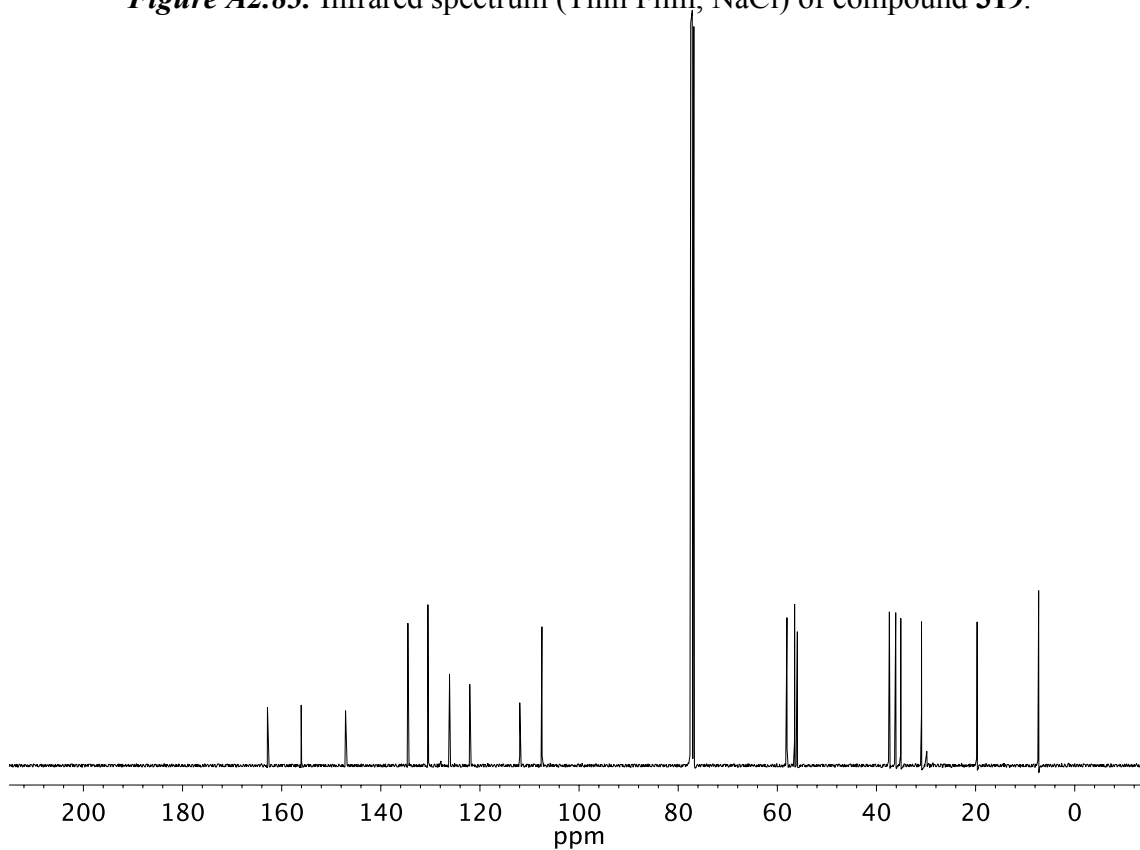


Figure A2.84. ¹³C NMR (101 MHz, CDCl₃) of compound **319**.

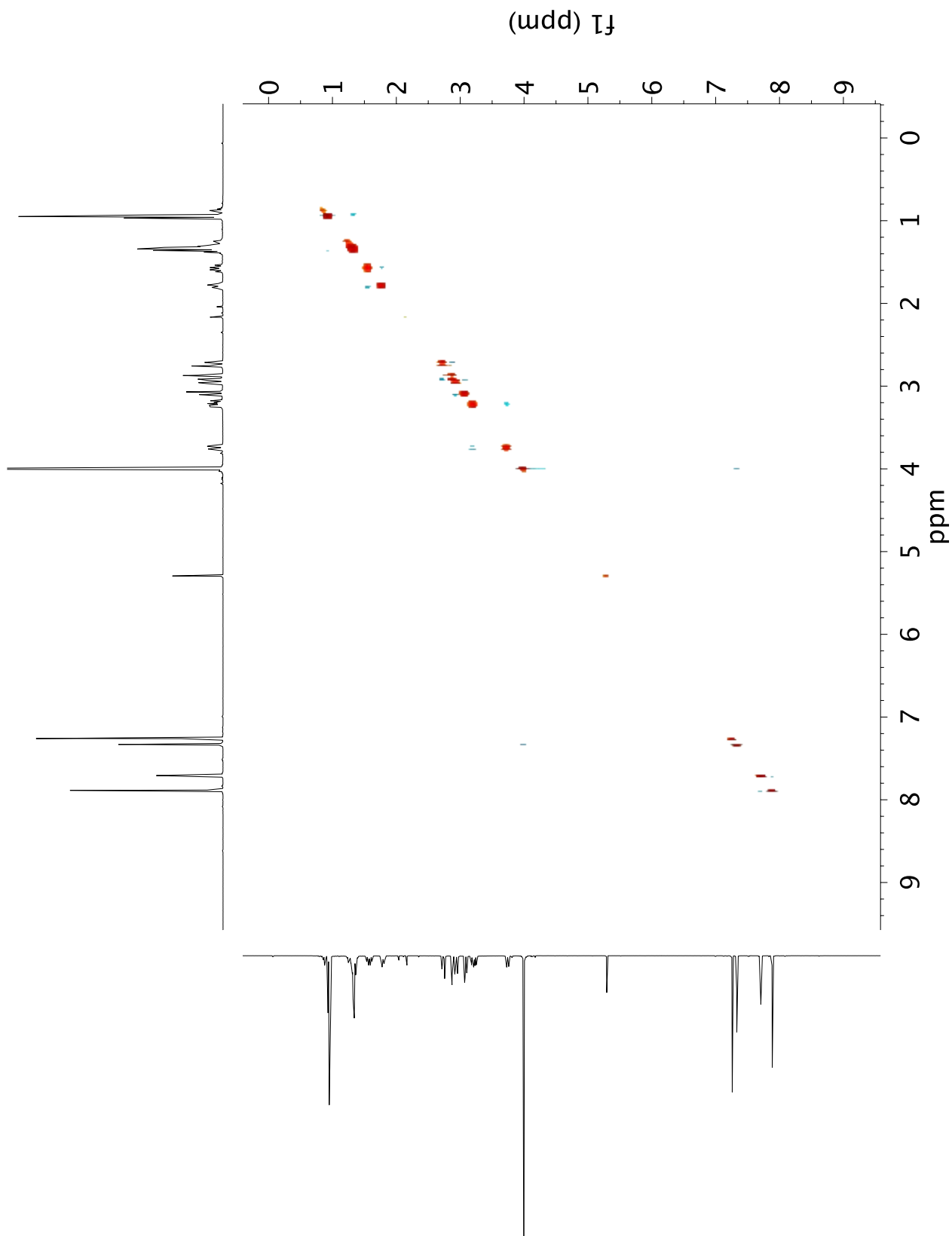


Figure A2.85. NOESY (400 MHz, CD₂Cl₂) of compound 319.

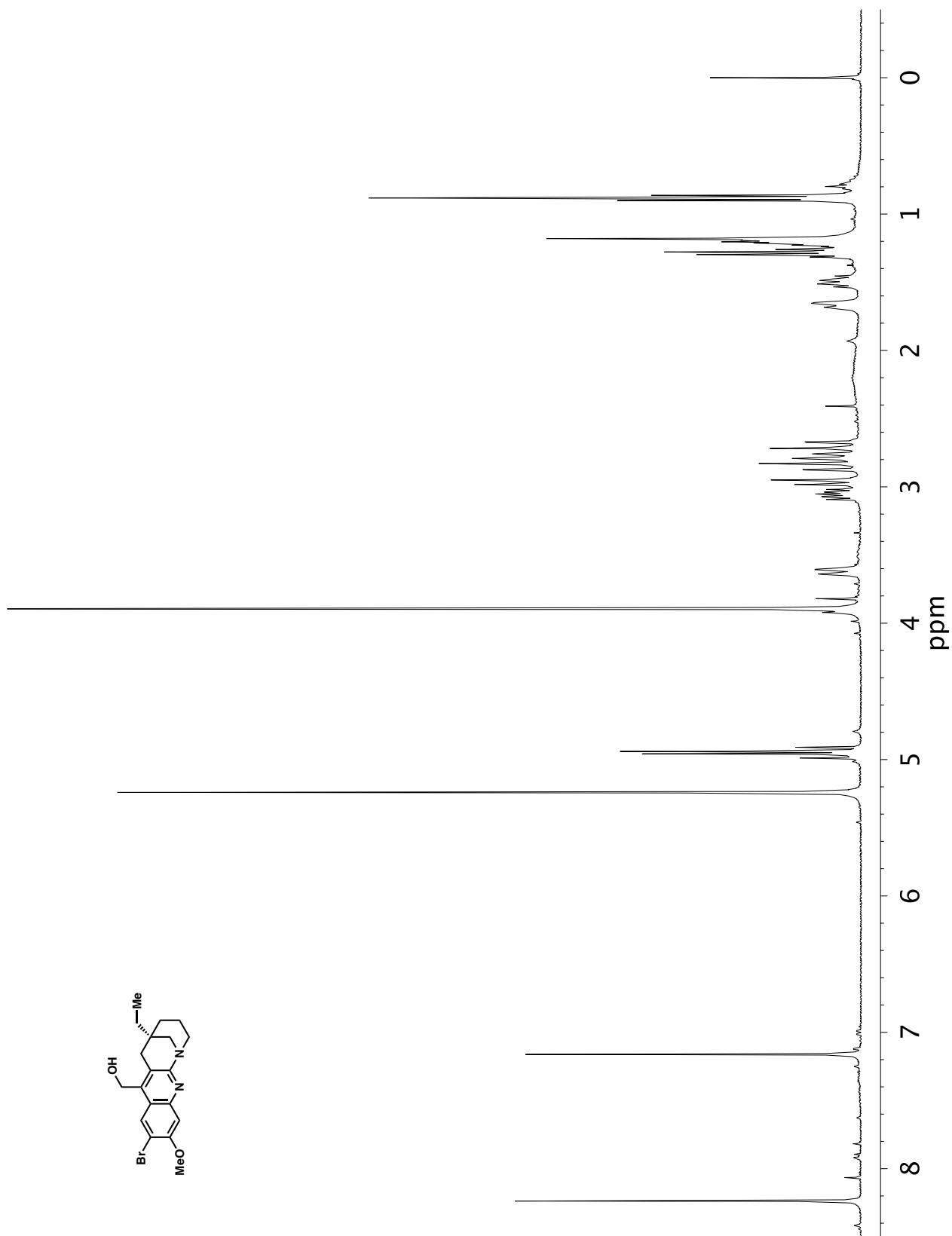


Figure A2.86. $^1\text{H NMR}$ (400 MHz, CD_2Cl_2) of compound 340.

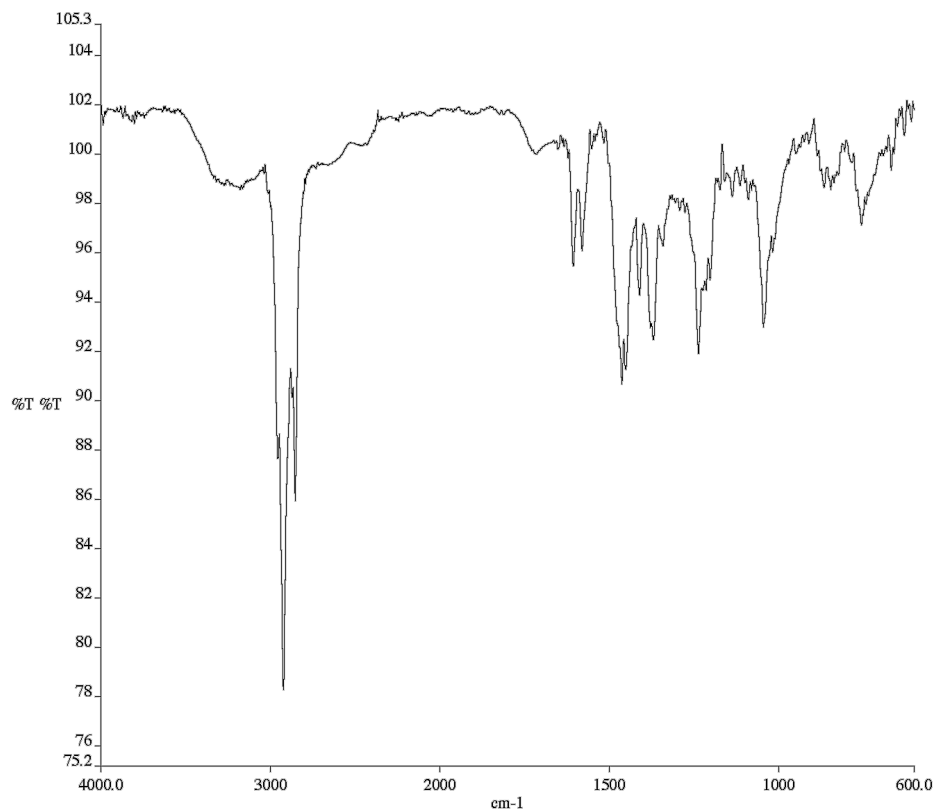


Figure A2.87. Infrared spectrum (Thin Film, NaCl) of compound **340**.

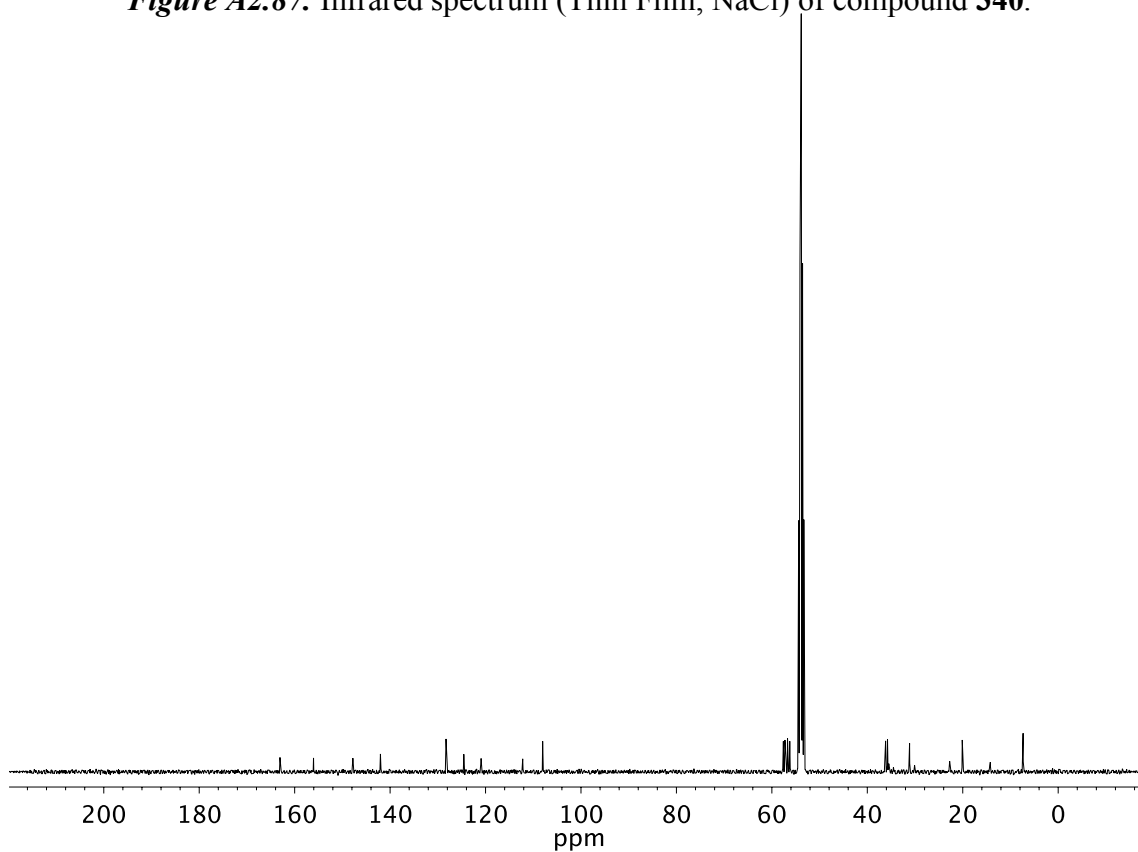


Figure A2.88. ¹³C NMR (101 MHz, CD₂Cl₂) of compound **340**.

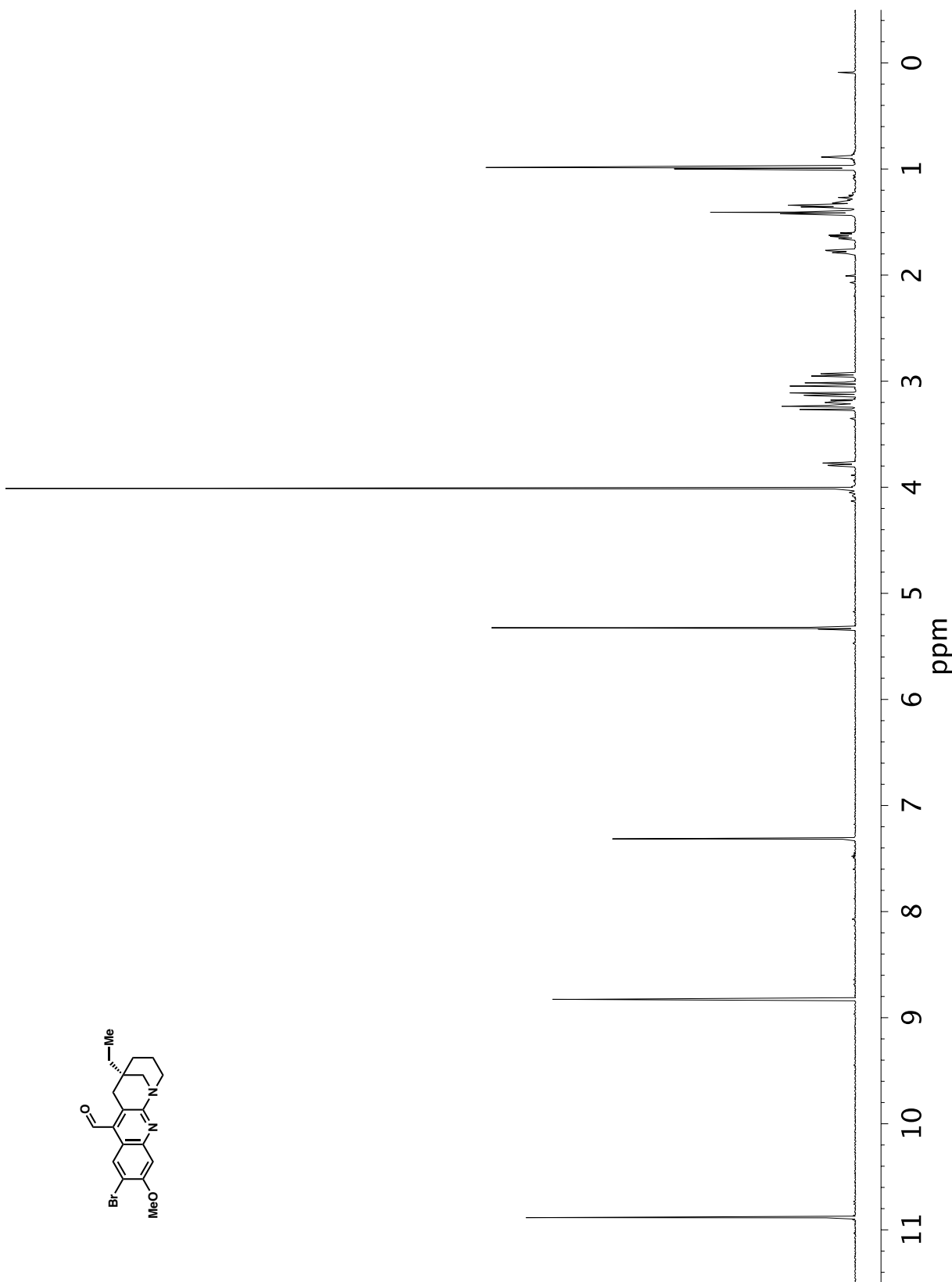


Figure A2.89. ¹H NMR (400 MHz, CD₂Cl₂) of compound 342.

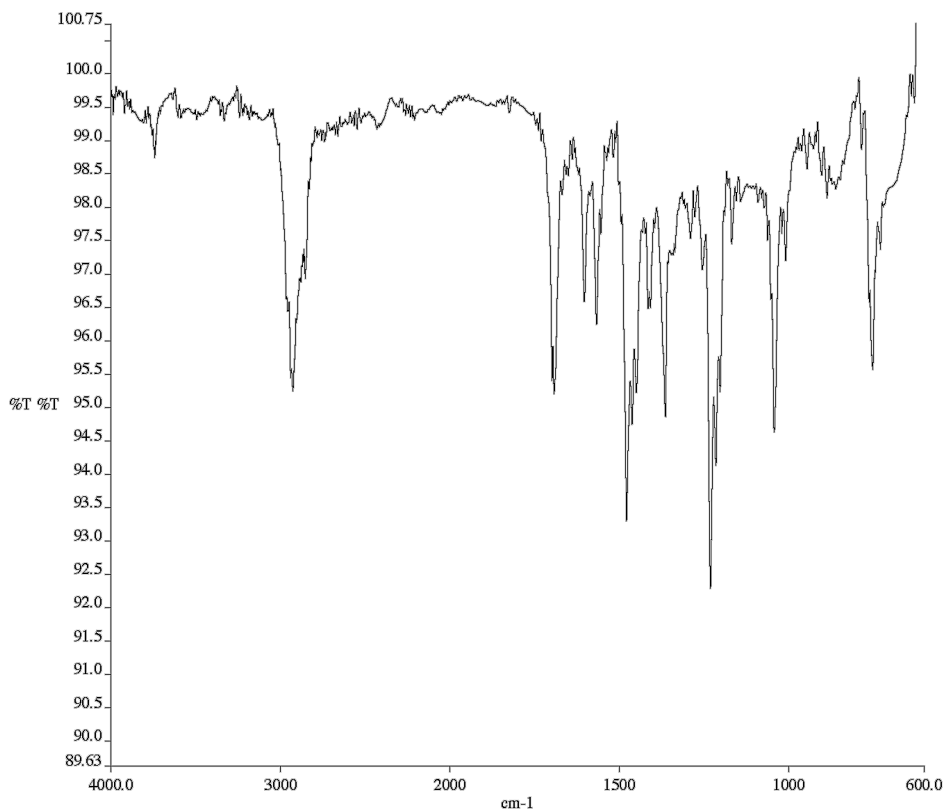


Figure A2.90. Infrared spectrum (Thin Film, NaCl) of compound **342**.

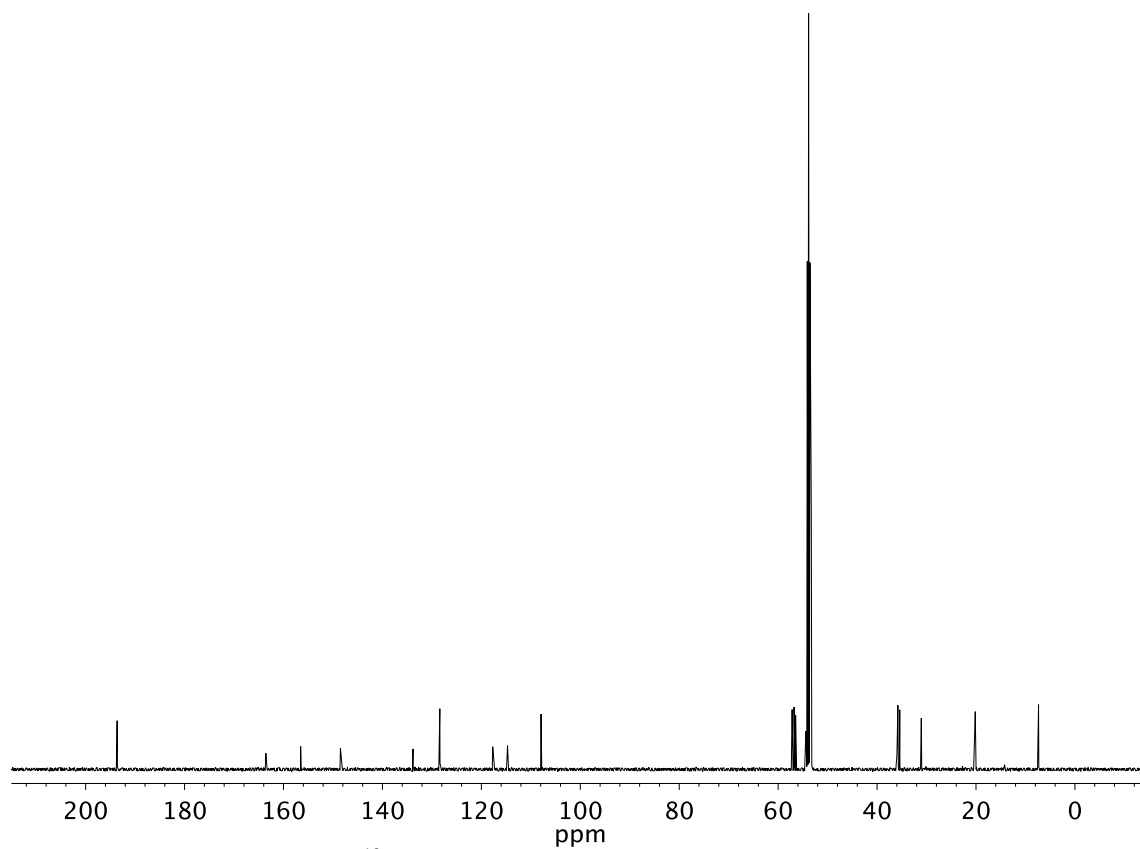


Figure A2.91. ¹³C NMR (101 MHz, CD₂Cl₂) of compound **342**.

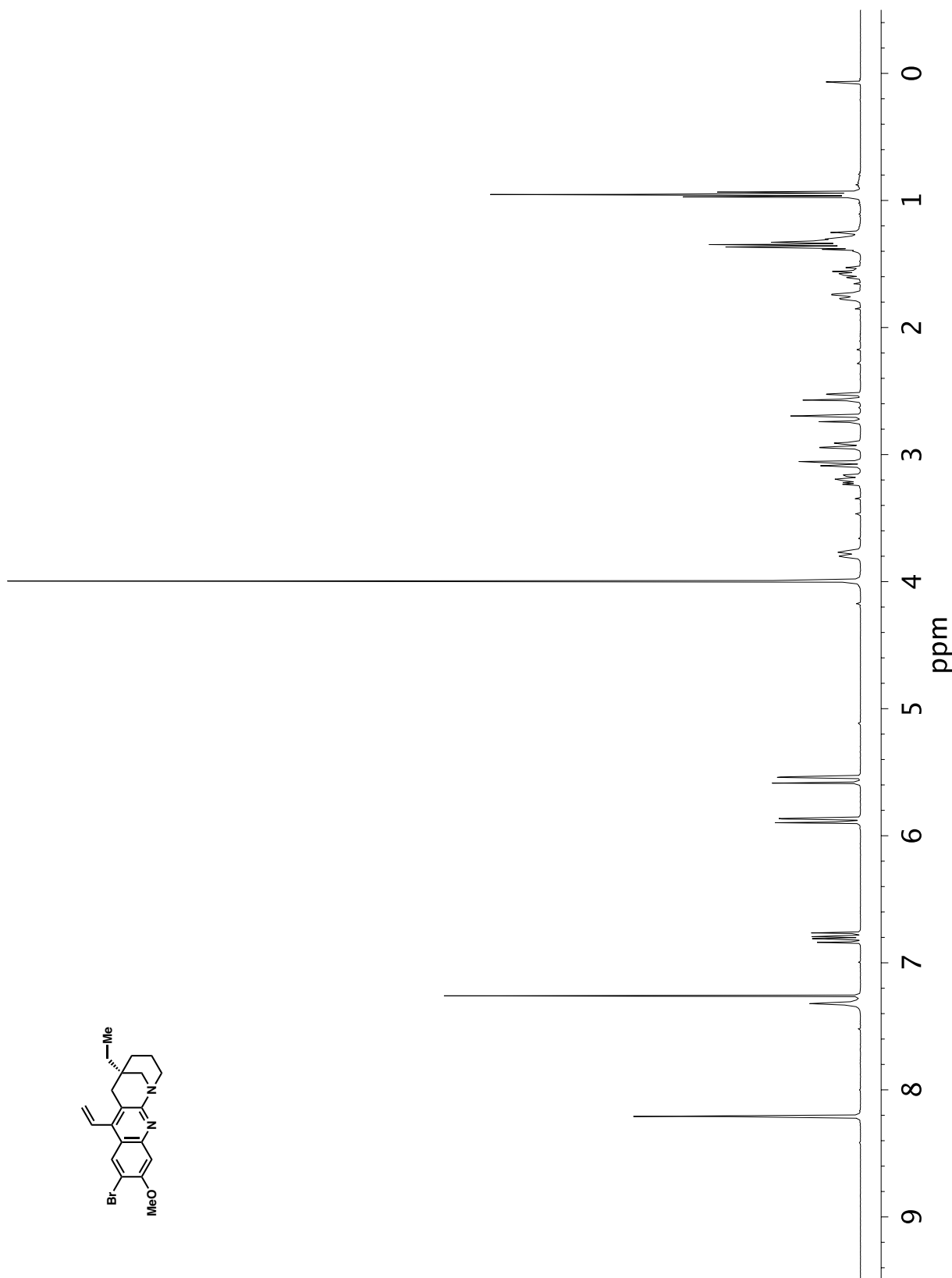


Figure A2.92. $^1\text{H NMR}$ (400 MHz, CDCl_3) of compound **318**.

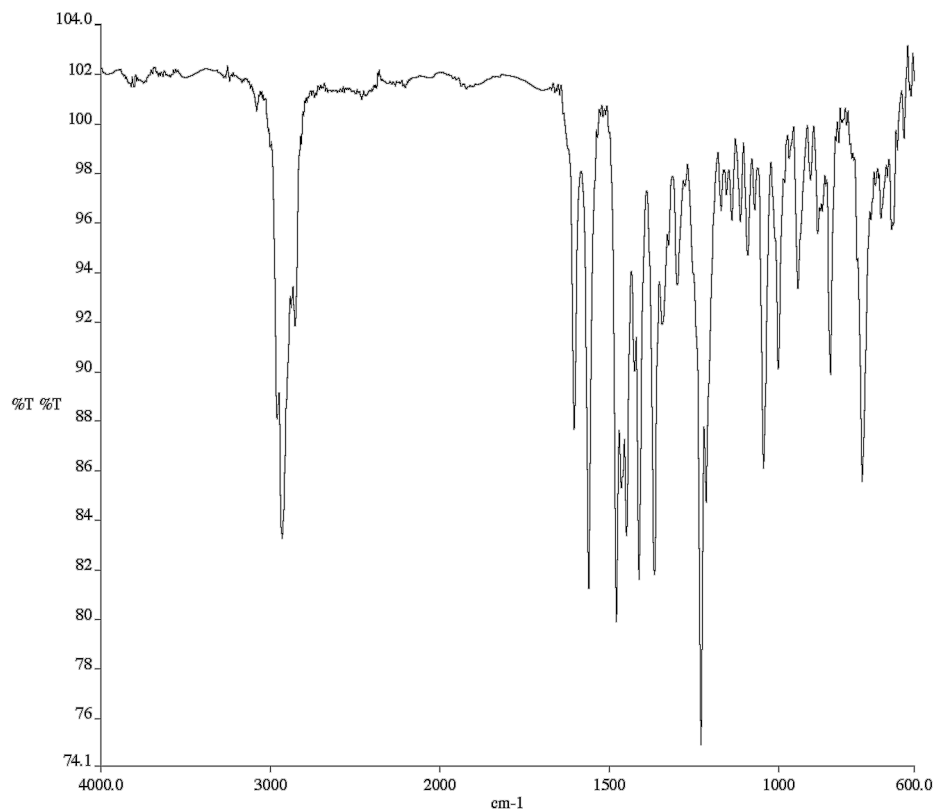


Figure A2.93. Infrared spectrum (Thin Film, NaCl) of compound **318**.

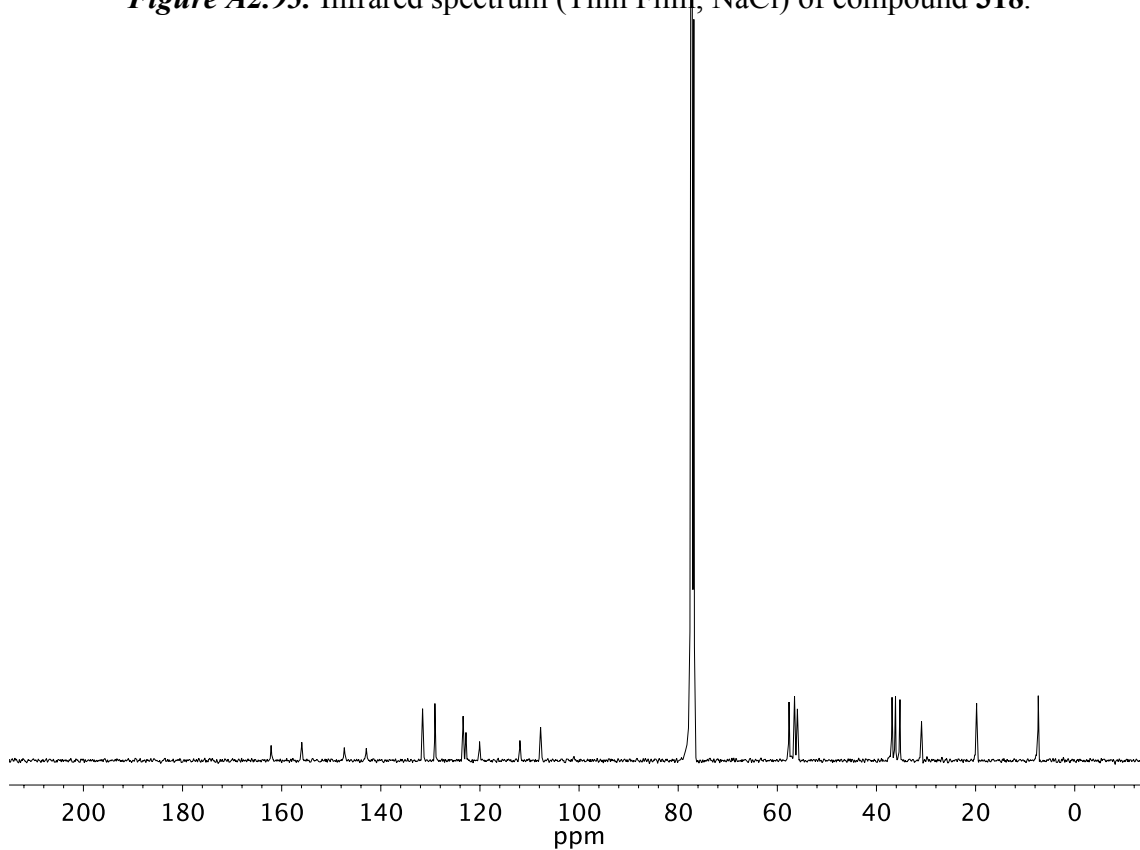


Figure A2.94 ¹³C NMR (101 MHz, CDCl₃) of compound **318**.

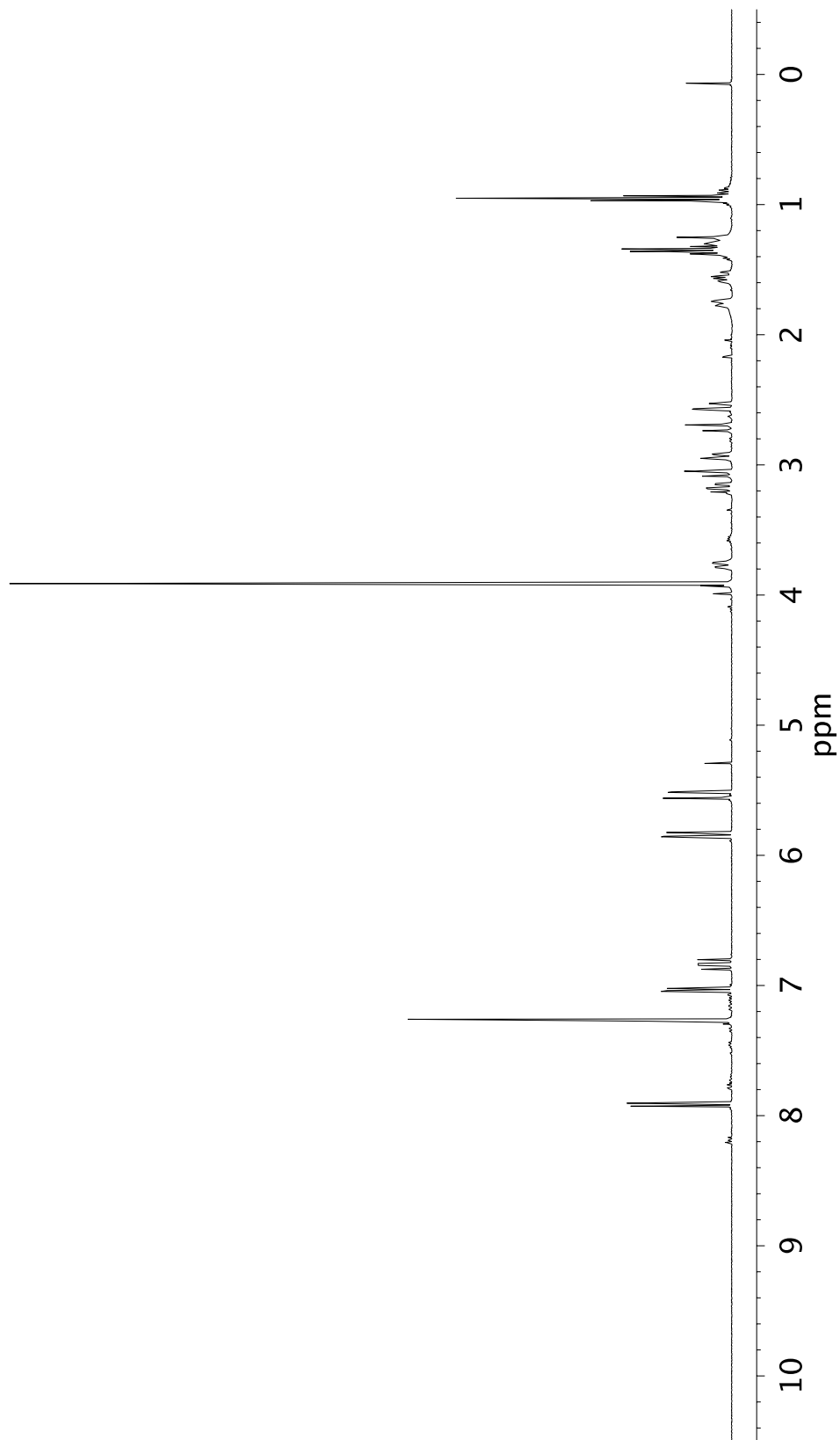
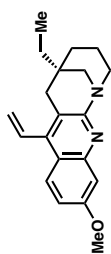


Figure A2.95 ¹H NMR (400 MHz, CDCl₃) of compound 344.

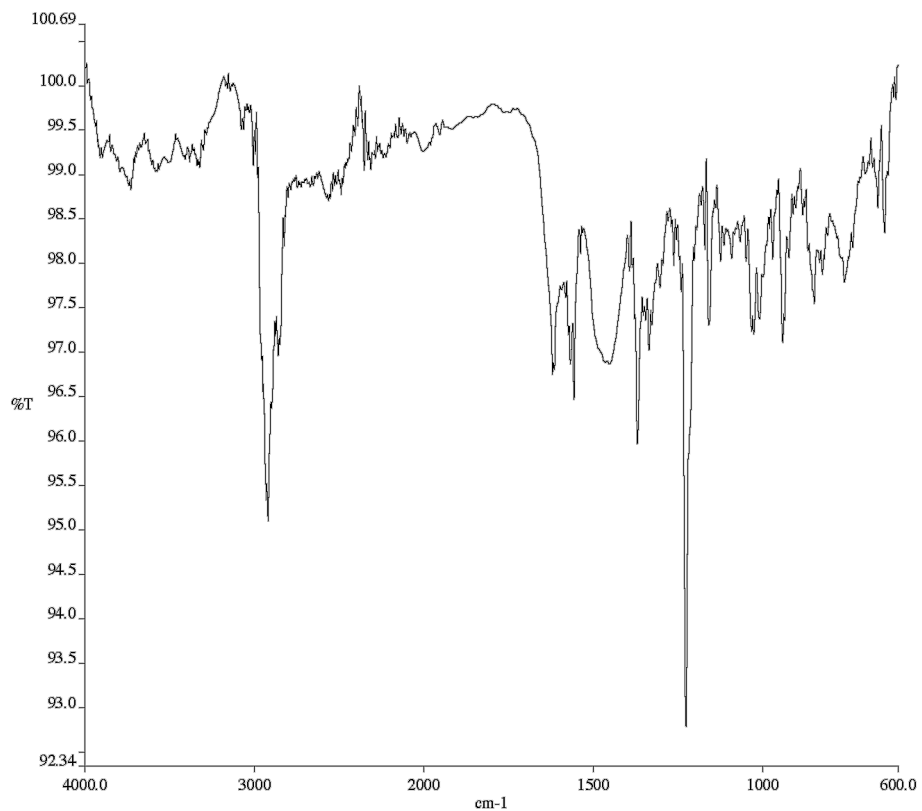


Figure A2.96 Infrared spectrum (Thin Film, NaCl) of compound **344**.

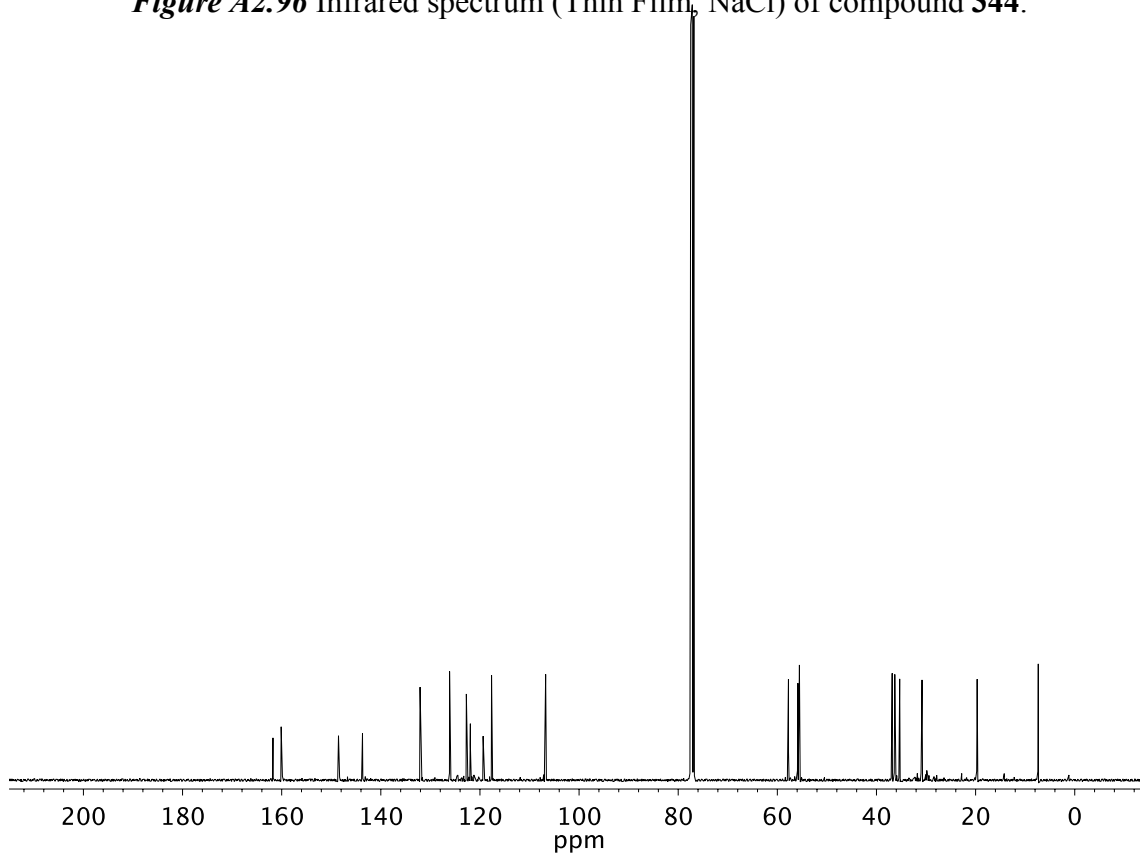


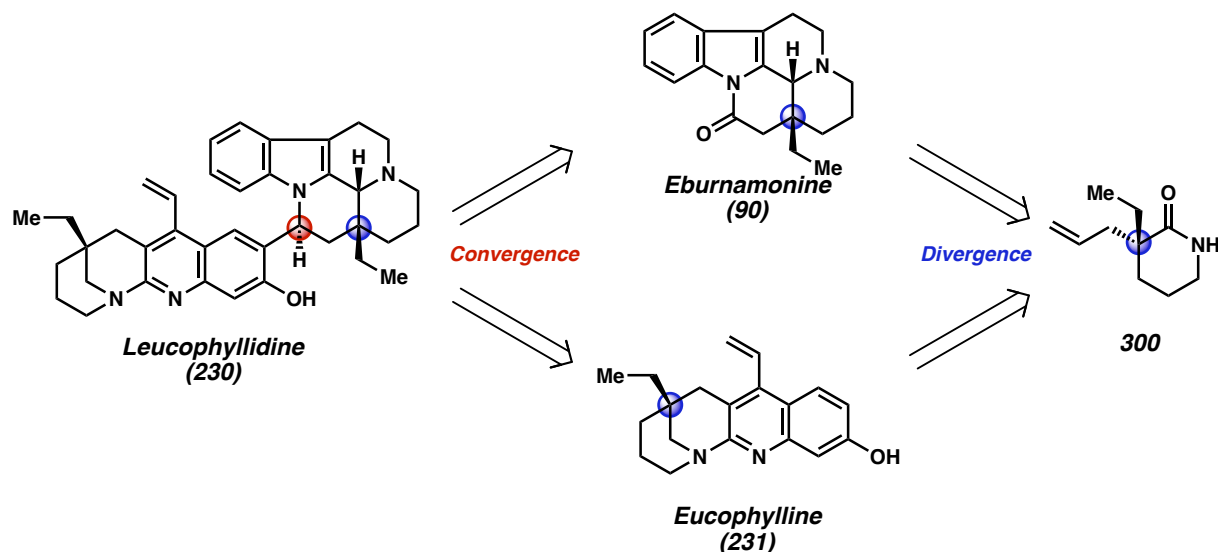
Figure A2.97. ^{13}C NMR (101 MHz, CDCl_3) of compound **344**.

CHAPTER 3

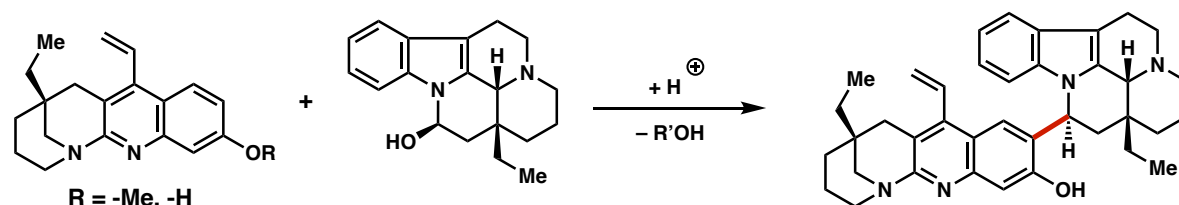
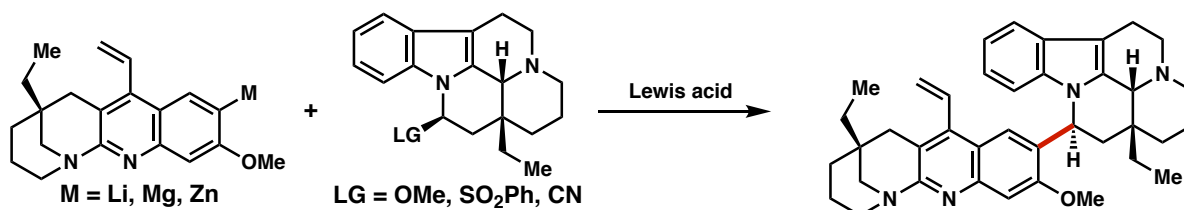
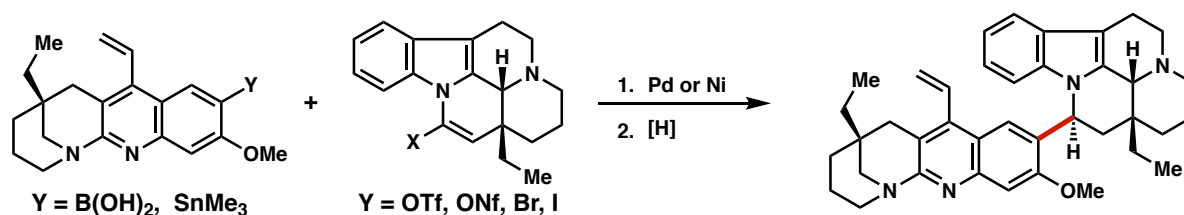
Progress toward a Convergent Total Synthesis of Leucophyllidine

3.1 INTRODUCTION

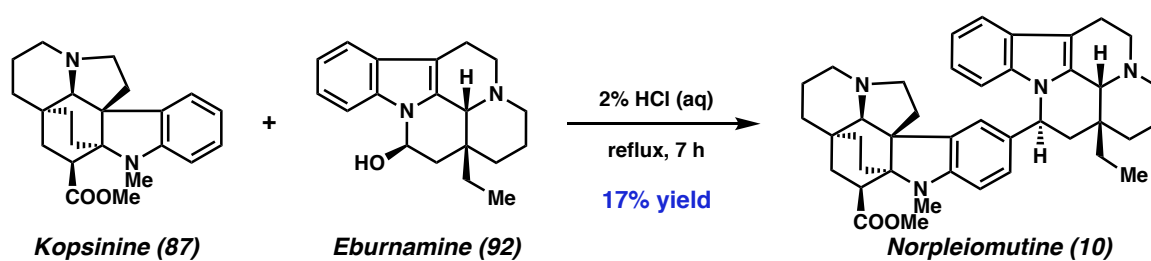
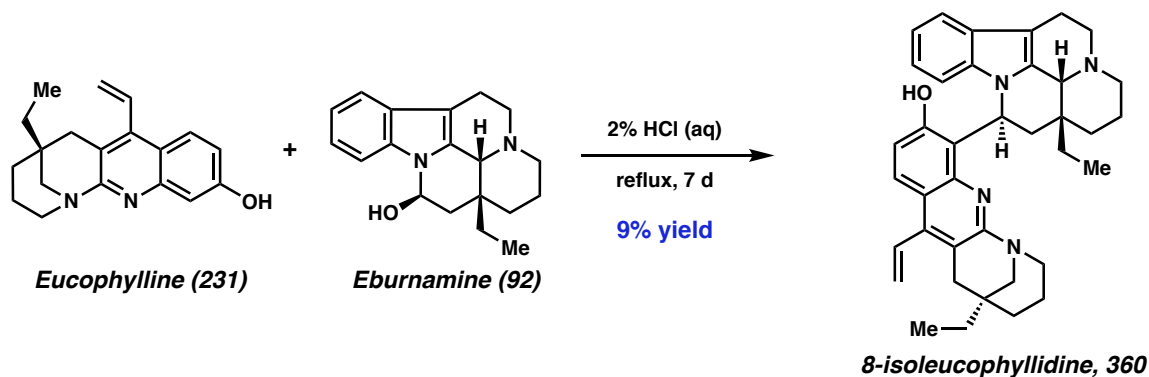
Having successfully completed the synthesis of both monomeric precursors, eburnamonine (**91**) and eucophylline (**231**), we then turned our attention toward the second phase of our synthetic endeavor: the convergent coupling and completion of the dimeric bisindole alkaloid leucophyllidine (**230**) (Scheme 3.1).¹ As our long-term goal remained to develop a general strategy for the synthesis of other related natural products and synthetic analogues, we remained cognizant of the fact that the α -amino stereogenic center was a conserved motif at the site of heterodimerization; as such, the development of a generalizable coupling strategy that was reliant on *reagent-* or *catalyst-*control, rather than *substrate-*control, would have immense benefit if applied to future synthetic efforts.

Scheme 3.1. The divergent-convergent strategy to access leucophyllidine.

At the onset of this project, we identified three broad coupling strategies that could potentially be exploited to access leucophyllidine (**230**). The first was a “biomimetic” Friedel-Crafts acylation strategy from eburnamine (**91**) and eucophylline (**231**) directly (Scheme 3.2A); this would rely on an electrophilic aromatic substitution at C(6) of eucophylline into an in-situ generated iminium ion under acidic conditions to forge both the final C–C bond and stereogenic center of the natural product in a single operation. The second was a “bio-inspired” organometallic addition strategy from a metallated eucophylline-derivative and a masked eburnamine hemiaminal (Scheme 3.2B); this strategy would exploit reactive organometallic species generated at C(6) of eucophylline and add it into the eburnamine-derived iminium ion under Lewis acidic conditions. The third was a “transition metal-catalyzed” cross-coupling approach between an isolable eucophylline organometallic and an eburnamine-derived alkenyl electrophile (Scheme 3.2C). This would first involve a $C(sp)^2-C(sp)^2$ cross coupling to build the final C–C bond before a subsequent reduction would set the final stereogenic center and complete the natural product.

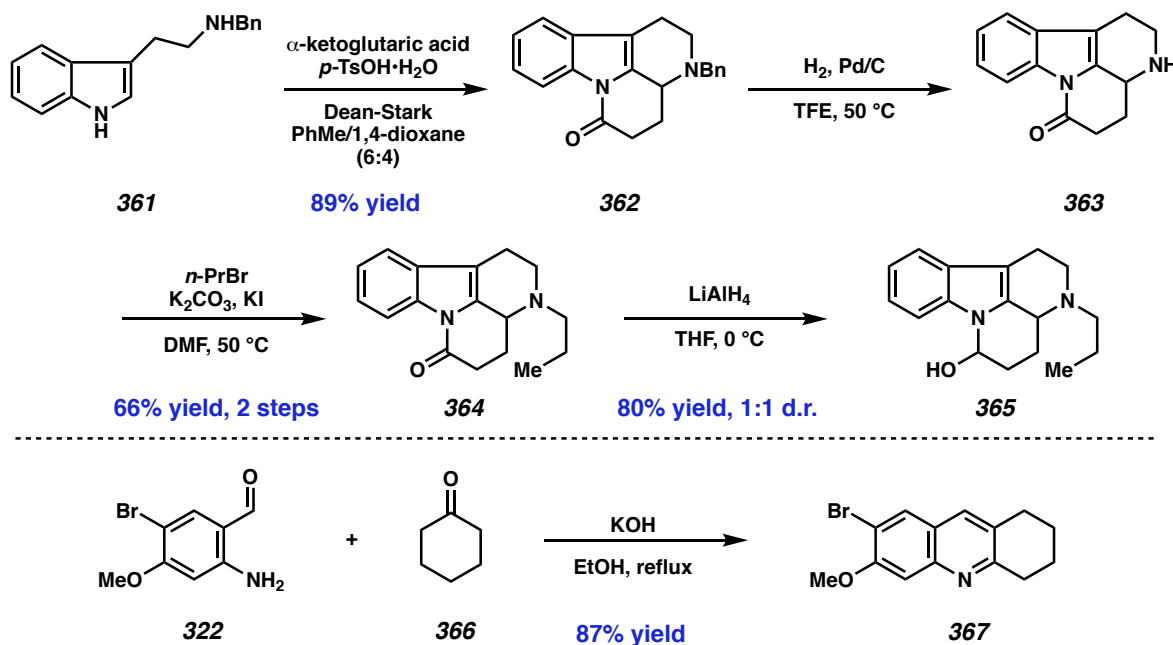
Scheme 3.2. Proposed coupling strategies toward leucophyllidine.**Strategy 1: "Biomimetic" Friedel-Crafts Acylation****Strategy 2: "Bio-inspired" Organometallic Addition****Strategy 3: "Transition-metal catalyzed" cross-coupling and reduction****3.2 BIOMIMETIC FRIEDEL-CRAFTS STRATEGY**

The first strategy we planned to investigate was a biomimetic Friedel-Crafts approach. We were encouraged by reports from Magnus² and coworkers who successfully accessed the bisindole alkaloid norpleiomutine (**10**) from the component alkaloids kopsinine (**87**) and eburnamine (**91**) in aqueous acid (Scheme 3.3A). Though this strategy would be insufficient for a general coupling strategy, we predicted this would have the highest probability of success, while providing some information about the inherent reactivity of the substrates. Before we could test this hypothesis, however, the Panday group³ reported a failed biomimetic coupling of leucophyllidine, which generated C(8) coupling product **360** (Scheme 3.3B). As the authors attributed this regioselectivity to greater stabilization of the Wheland intermediate, we did not investigate further.

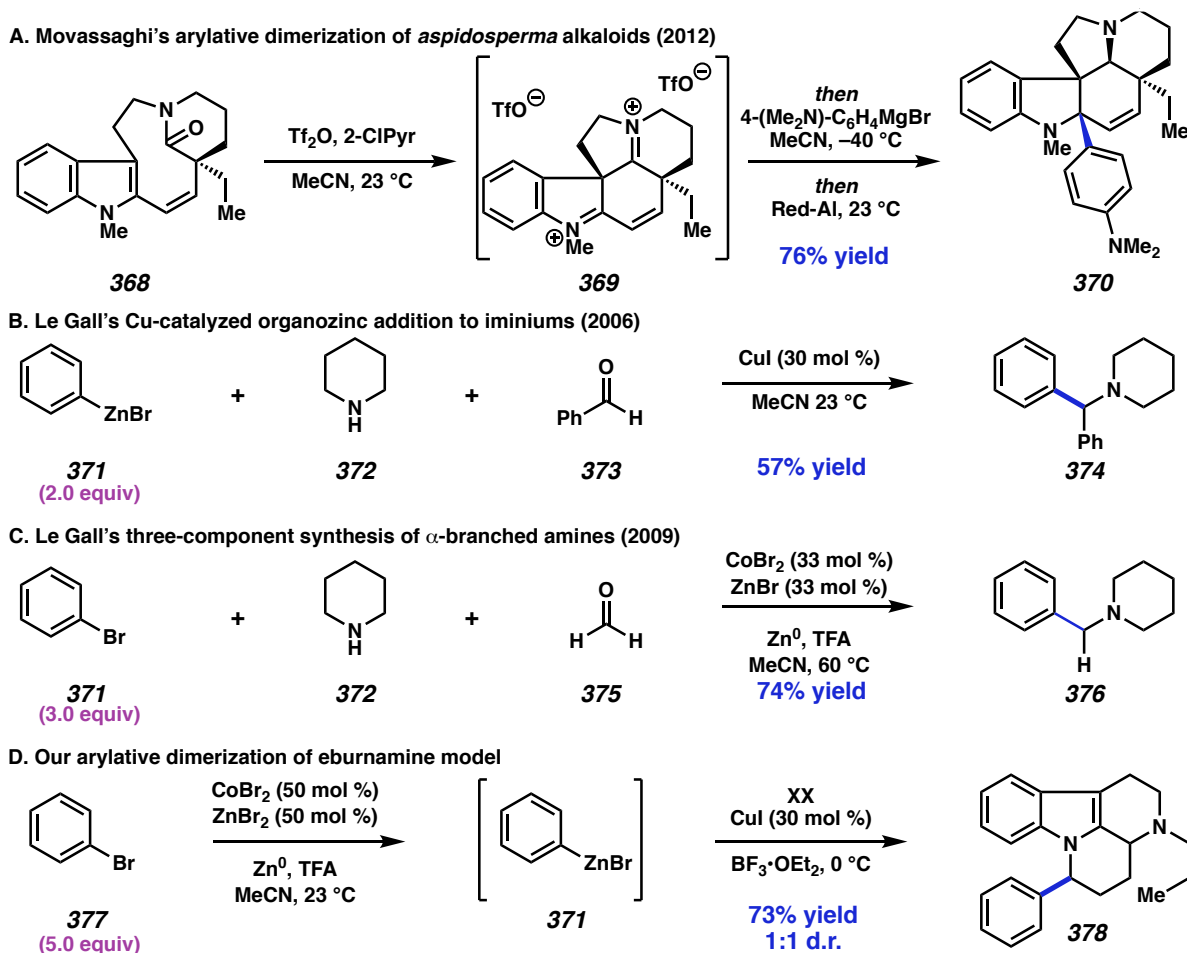
Scheme 3.3. Literature precedent for biomimetic coupling approach.**A. Magnus's acid-mediated "biomimetic" coupling of norpleiomutine (1985)****B. Panday's unsuccessful "biomimetic" coupling of leucophyllidine (2017)**

3.3 BIOINSPIRED ORGANOMETALLIC ADDITION STRATEGY

We subsequently turned our attention to the organometallic addition strategy. In order to investigate this reactivity while material access to monomeric subunits was limited, we developed model systems to investigate bond formation through this manifold. Following a procedure described by Wang,⁴ *N*-benzyl tryptamine **361** was condensed with α -ketoglutaric acid to promote a tandem Pictet-Spengler/lactamization sequence and afford tetracycle **362** in 89% yield (Scheme 3.4). Hydrogenolysis of the benzyl protecting group generates secondary amine **363** before subsequent *N*-alkylation with *n*-propyl bromide affords eburnamonine model **364** which is then reduced to eburnamine model **365**. A eucophylline model is accessed by condensation of our previously synthesized aldehyde **322** with cyclohexanone **366** to afford quinoline **367**.

Scheme 3.4. Synthesis of eburnamine and eucophylline model substrates.

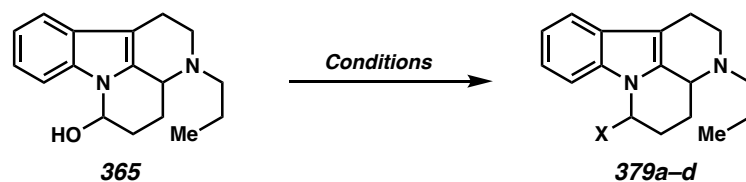
We were encouraged by a report from Movassaghi⁵ showing that alkaloid-derived iminium electrophiles (368 \rightarrow 369, Scheme 3.5A) could be intercepted by a Grignard reagent to afford quaternary adduct 370 (Scheme 3.5A); however, as our desired iminium is enolizable, we surmised that milder, less basic organometallic reagents would be necessary to conduct the desired transformation. We were surprised to find few reports of organometallic additions into in-situ formed iminium ions, as the majority of reported examples required α -directing groups (e.g Petasis reactions)⁶ to promote this reactivity. However, we did find two accounts illustrating that organozinc reagents could perform the requisite addition in the presence of copper at room temperature (Scheme 3.5B)⁷ or in the absence of copper at elevated temperature (Scheme 3.5C).⁸ Much to our delight, we found that phenylzinc bromide, generated through the cobalt-mediated procedure developed by Périchon (377 \rightarrow 378),⁹ could effectively be added into model eburnamine 365 to generate arylated product XX, albeit as a mixture of diastereomers (Scheme 3.5D). This offered proof-of-principle that such a strategy could be realized.

Scheme 3.5. Literature precedent and proof-of-principle experiment for bio-inspired strategy.

Encouraged by this result, we then sought to investigate a coupling reaction that more closely represented our desired system. To avoid the need for excess organometallic reagent, we first sought to mask the hemiaminal with a different iminium surrogate. While O-methyl iminal **379a** formation could be conducted easily,¹⁰ we found that this intermediate rapidly decomposed while neat under vacuum (Table 3.1, entry 1); ethylation under phase transfer conditions¹¹ afforded ethoxylated model **379b** (entry 2) but with little improvement in stability. Gratifyingly, we found that the ethoxyethyl group **379c**¹² offered better stability at lower temperatures (entry 3). The corresponding aminonitrile¹³ **379d** (entry 4) could also be generated, however, this intermediate

proved to be too stable and any attempts to remove the cyano group in the presence of Lewis acids and silver salts were ultimately unsuccessful.

Table 3.1. Protection of the eburnamine model hemiaminal.



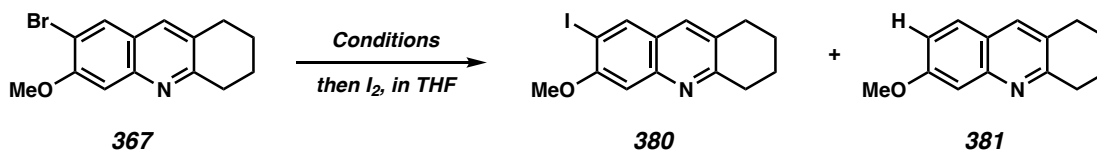
Entry	X-	Conditions	Yield	Notes
1	Me	PPTS, MeOH, reflux	–	Decomposes neat
2	Et	TBAI, EtI, PhH/NaOH (aq), 23 °C	–	Decomposes neat
3	EtOCH ₂ CH ₂ O	TBAB, MeOCH ₂ CH ₂ Br, PhH/NaOH(aq), 23 °C	71%	Stable at –20 °C
4	Me	TMSCN, BF ₃ ·OEt ₂ , CH ₂ Cl ₂ , –78 °C	85%	

We then turned to formation of the organozinc reagent from model bromide **367** using an iodine quench to quantify the active amount of organometallic species (as iodide **380**), protodemetalation (as iodide **381**), and recovered starting material **365**.¹⁴ Using previously implemented cobalt conditions⁹ led to modest conversions (Table 3.2, entry 1), while Périchon's second generation conditions¹⁵ (entry 2) effected an increase in zincation and protohalogenation. Reike zinc¹⁶ (entry 3) lead to limited yield while lithiation-transmetallation¹⁷ (entry 4) resulted in complete protodemetalation. Returning to the cobalt conditions, increasing the temperature lead to greater rates of zincation (entry 5), and doubling the catalyst loading improved our ideal conversion to 86% (entry 6).

With individual conditions for nucleophile and electrophile optimized, we turned our attention to coupling the two fragments. Despite an extensive screen of parameters including solvent mixtures, copper catalysts, and Lewis acids, the desired coupling product **XX** was not observed. We hypothesize that the *ortho*-methoxy quinoline was significantly more sterically

hindered, which caused the α -deprotonation pathway to outcompete the corresponding 1,2-addition. Discouraged by these results, we elected not to investigate further.

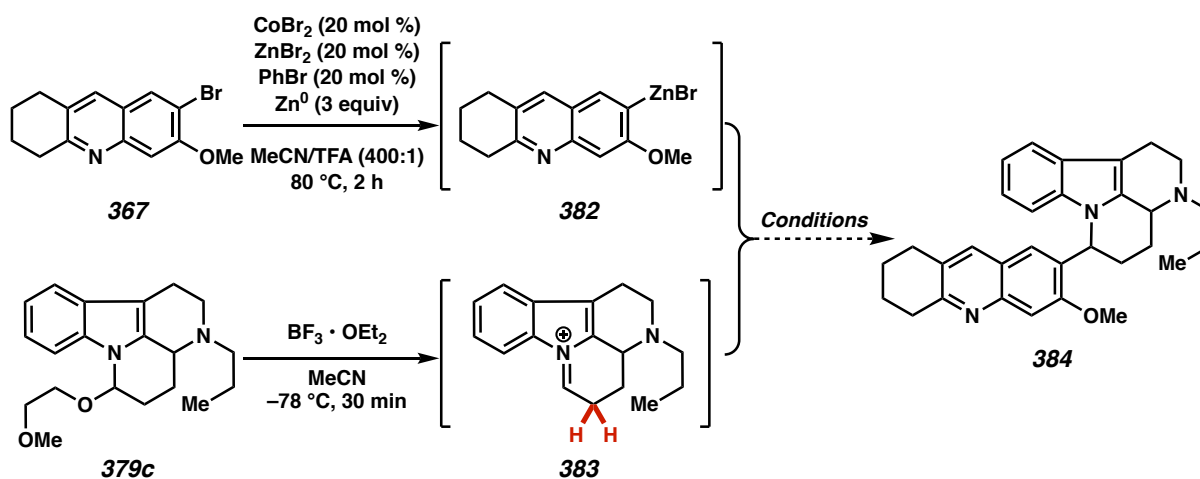
Table 3.2. Synthesis of organozinc coupling partner.



Entry	Conditions	380	381	367
1	CoBr ₂ (10 mol %), ZnBr ₂ (10 mol %) PhBr (10 mol %) Zn (3 equiv), MeCN/TFA (400:1), 23 °C, 1.5 h	23%	2%	75%
2	CoBr ₂ (5 mol %), AllylCl (15 mol %) Zn (3 equiv), MeCN/TFA (400:1), 23 °C, 3 h	51%	14%	35%
3	Reike Zn (5 equiv) THF, 23 → 65 °C, 3 h	39%	0%	61%
4	<i>n</i> -BuLi, THF, -78 °C, 1 h then ZnCl ₂ , -78 → 0 °C, 3 h	0%	100%	0%
5	CoBr ₂ (10 mol %), ZnBr ₂ (10 mol %) PhBr (10 mol %) Zn (3 equiv), MeCN/TFA (400:1), 80 °C, 1.5 h	58%	18%	24%
6	CoBr ₂ (20 mol %), ZnBr ₂ (20 mol %) PhBr (20 mol %) Zn (3 equiv), MeCN/TFA (400:1), 80 °C, 2 h	86%	6%	8%

*Relative conversion, monitored by integration of 254 nm peak on LCMS, which roughly correlates to the distribution of products as determined by qNMR.

Scheme 3.6. Unsuccessful model arylations.

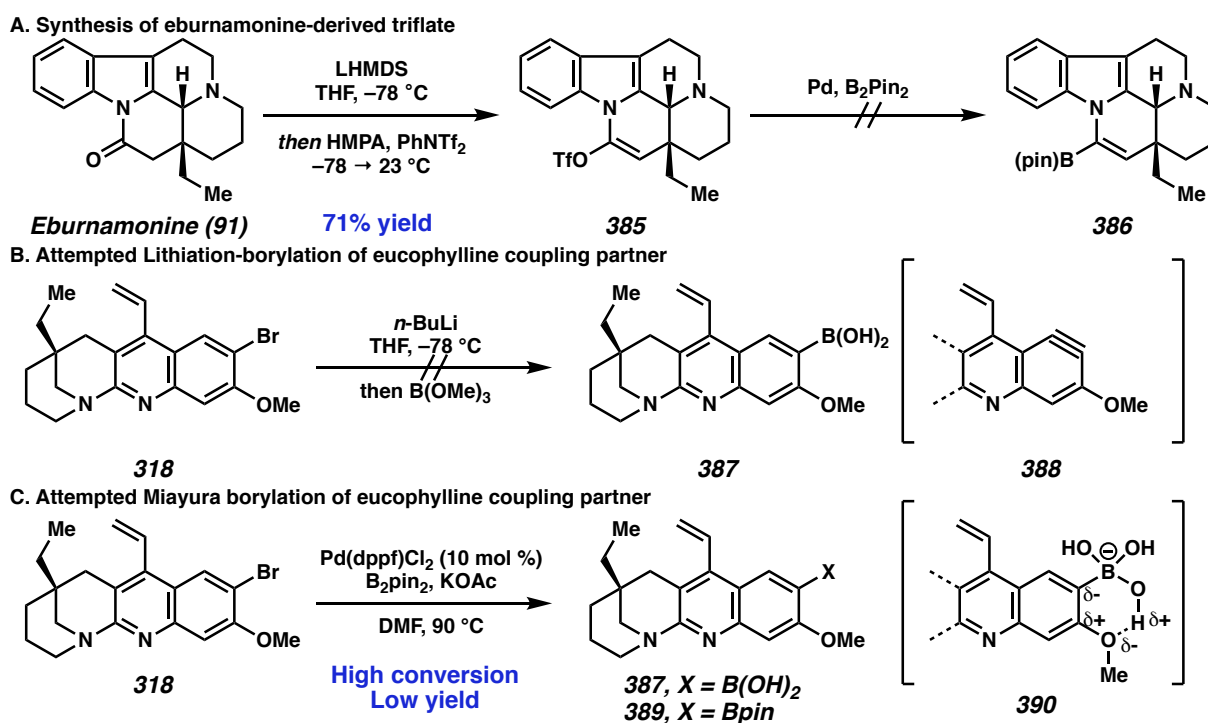


3.4 TRANSITION METAL-CATALYZED CROSS-COUPLING STRATEGY

3.4.1 Suzuki Couplings

After evaluating the organometallic addition strategy with no success, we turned our attention to transition metal-catalyzed cross-coupling strategy. First, we attempted to investigate Suzuki coupling conditions due to their established history of success with highly functionalized substrates.¹⁸ Eburnamonine (**91**) was easily advanced to the corresponding trifloxyenamine **385** under optimized conditions for lactam-derived enolates¹⁹ (Scheme 3.7A), but attempts to convert this to a boronic ester,²⁰ and later a stannane at this position using Pd-catalysis led to complex mixtures of products, which we hypothesize is due to severe steric hindrance imposed by the benzenoid ring of the indole motif.

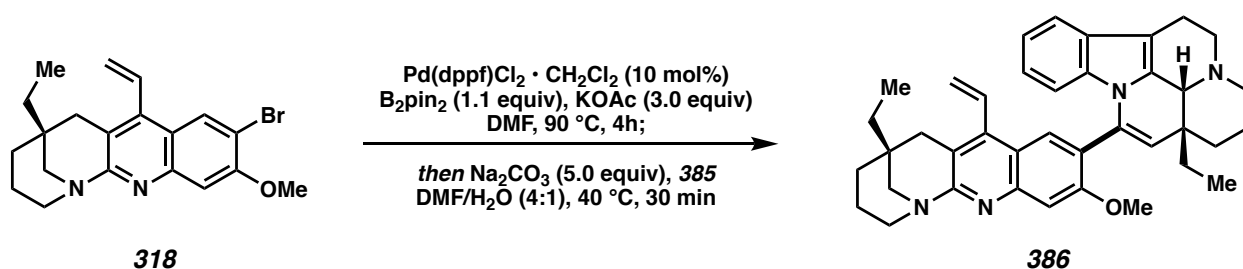
Scheme 3.7. Attempted synthesis of Suzuki coupling partners.



We then elected to install the organometallic handle on the eucophylline-derived fragment. Our attempts to perform lithiation/borylation on bromide **318** were unsuccessful in affording

boronic acid **387**, leading only to proto-dehalogenation, as was observed in our aforementioned zincation attempts (Scheme 3.7B); we attribute this challenge to likely formation of aryne intermediate **388** which competes with the exchange process.²¹ While Miyaura borylation²² did lead to high conversion and significant amount of ester **389**, we found that this intermediate was unstable to purification, and a significant amount of hydrolyzed boronic acid **387** and protodeboronated product was observed via LCMS (Scheme 3.7C). We attribute this decomposition to the formation of internal hydrogen bonding with the *ortho*-methoxy group in **390**, contributing to the build-up of negative charge at quinoline C(6) and boron, which resulted in *ipso* protonation and hydrolysis, respectively.²³

Table 3.3. Optimization of one-pot Miyaura borylation/Suzuki coupling.



Entry	Condition 1 Modifications	Condition 2 Modifications	Yield* 386	Notes
1	Standard	Standard	24%	Protodeborylation and triflate hydrolysis
2	“	DMF/H ₂ O (10:1), 16 h	21%	“
3	“	NMP/H ₂ O (4:1), 16 h	20%	“
4	“	DMSO/H ₂ O (10:1), 16 h	24%	“
5	“	Na ₂ CO ₃ (anhydrous), 16 h	0%	Slow decomposition of coupling partners
6	“	K ₂ CO ₃ (anhydrous), 16 h	0%	“
7	“	Cs ₂ CO ₃ (anhydrous), 16 h	4%	Triflate hydrolysis
8	“	K ₃ PO ₄ (anhydrous), 16 h	0%	Triflate hydrolysis
9	“	CsF (anhydrous), 10 min	0%	Rapid triflate hydrolysis
10	“	Et ₃ N (anhydrous), 16 h	0%	Triflate hydrolysis

* HPLC yields calculated using 2,3,5,6-tetrachloronitrobenzene as an internal standard.

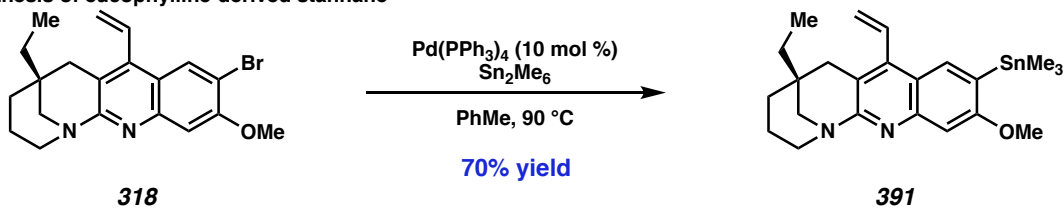
To avoid these isolation issues, we explored a one-pot Miyaura borylation/Suzuki coupling. Much to our delight, we found that successful borylation, with Pd(dppf)Cl₂ and B₂(pin)₂, could be

followed by the addition of aqueous base and triflate **385** to afford the cross-coupled product in 24% yield (Table 3.3, entry 1). The remainder of mass balance returned as protodeborylated nucleophile **344** and hydrolyzed triflate in the form of eburnamonine (**91**). Decreasing the DMF/water ratio lead to a slight decrease in yield (entry 2). While other polar aprotic solvents led to comparable yields (entry 3–4), less polar solvents such as THF and toluene decreased the efficiency of the borylation. Attempts to use anhydrous sodium carbonate slowed both the decomposition and cross coupling pathways (entry 5). Use of other stronger inorganic bases (entry 6–8), non-basic fluoride (entry 9), and organic base (entry 10) drastically hindered reactivity in almost all cases, causing rapid decomposition of the triflate electrophile.

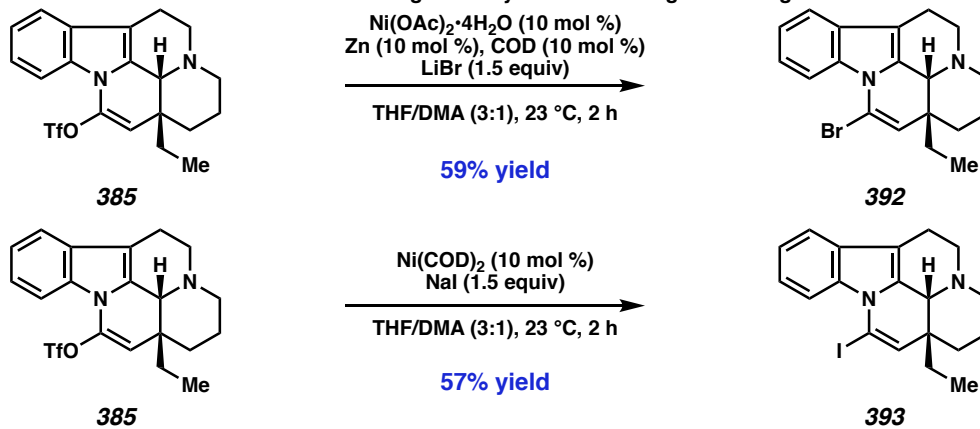
3.4.2 Stille Couplings

Scheme 3.8. Synthesis of Stille coupling partners.

A. Synthesis of eucophylline-derived stannane

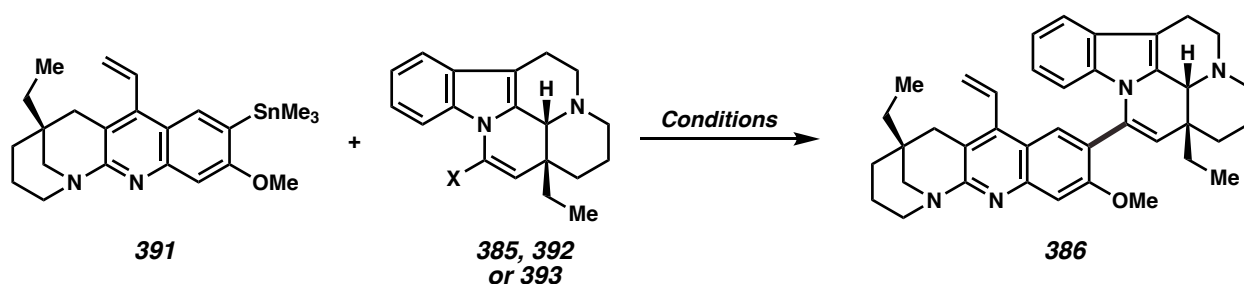


B. Synthesis of eburnamonine-derived halides using Ni-catalyzed triflate/halogen exchange



Disappointed by this unsuccessful optimization, we turned our attention to Stille couplings. Stannylation of bromide **318** afforded trimethylstannane **391** in good yield (Scheme 3.8A). Around this time, we became aware of research by Reisman and coworkers²⁴ detailing the conversion of alkenyl triflates into their coresponding halides under Ni-catalysis; gratifyingly, conditions using Ni(II) and Ni(0) precatalysts were applied to access both the vinyl bromide **392** and vinyl iodide **393** in moderate yield (Scheme 3.8B).

Table 3.4. Optimization of Stille Coupling.



Entry	-X	Conditions	Yield* 391
1	OTf	Pd(PPh ₃) ₂ Cl ₂ (10 mol%), 1,4-dioxane, 90 °C	0%
2	OTf	Pd(PPh ₃) ₄ (10 mol%), LiCl (4 equiv), 1,4-dioxane, 100 °C	0%
3	OTf	Pd(PPh ₃) ₄ (10 mol %), CuI (8 mol %), LiCl (4 equiv), dioxane, 100 °C	< 5%
4	OTf	Pd ₂ (dba) ₃ (2.5 mol %), Ph ₃ As (10 mol %), DMF, 60 °C	19%
5	OTf	Pd(PPh ₃) ₄ (10 mol %), CuCl (5 equiv), LiCl (6 equiv), DMSO, 60 °C	41%
6	OTf	Pd(PPh ₃) ₄ (10 mol %), CuTC (1.5 equiv), NMP, 23 °C	53%
7	I	CuTC (1.5 equiv), NMP, 23 °C	24%
8	Br	Pd(OAc) ₂ (5 mol%), XPhos (15 mol%), CsF (2.0 equiv), dioxane, 80 °C	< 5%
9	Br	Pd ₂ (dba) ₃ (1 mol %), P(<i>t</i> -Bu) ₃ (2 mol %), CsF (2 equiv) NMP, 80 °C	< 5%

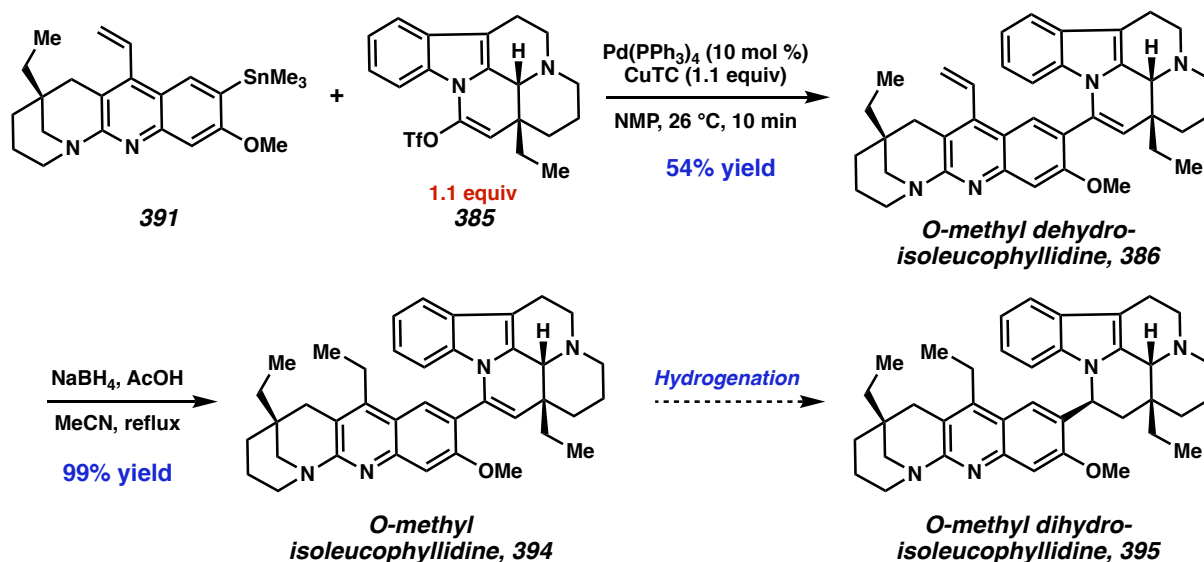
* Yields recorded by ¹H NMR with 2,3,5,6-tetrachloronitrobenzene as an internal standard

Turning to our key cross-coupling event, we were disappointed to find canonical Stille conditions with triflate **385** in 1,4-dioxane produced little to no cross-coupled product **386** (Table 3.4, entry 1–3). Implementing Farina's conditions²⁵ in DMF, we were delighted to observe a boost in cross-coupling product (entry 4), though LCMS analysis suggested that methyl transfer from the stannane was competitive with aryl transfer of sterically encumbered fragment. To circumvent this problem, we investigated copper additives and were delighted to see that use of CuCl²⁶ and CuTC²⁷ produced the desired product in 41% and 53% yield, respectively. With the analogous

vinyl iodide electrophile **393** (entry 7), we found that background coupling reactions proceeded in the absence of palladium at greatly decreased yield.²⁸ With the vinyl bromide **392**, we attempted conditions described by Buchwald²⁹ (entry 8) and Fu³⁰ (entry 9), but no reactivity could be observed in these cases.

3.5 INVESTIGATION OF TRISUBSTITUTED OLEFIN REDUCTION

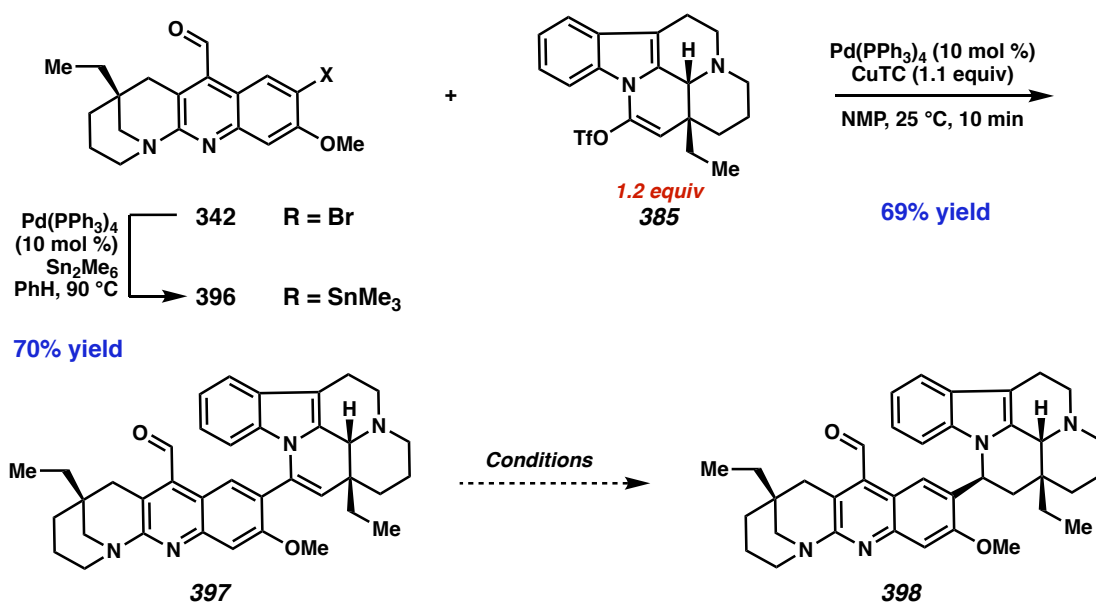
Scheme 3.9. Preparative Stille coupling with vinyl stannane.



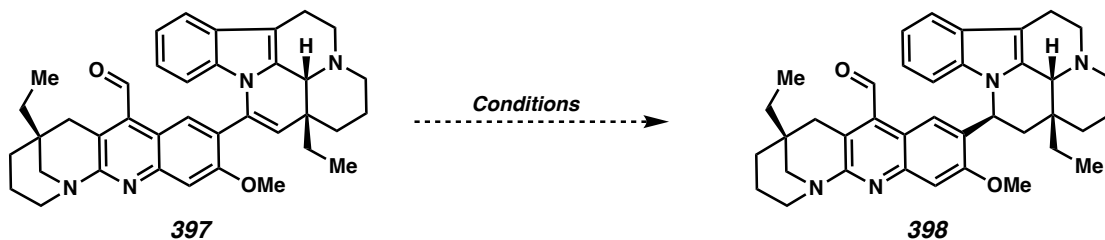
With optimized conditions in hand, we demonstrated that the Stille coupling could be performed on preparative scale by decreasing CuTC loading and using a slight excess of triflate **385**,³¹ accessing sufficient quantities of our cross-coupled product **386**, which we termed *O*-methyldehydro-leucophyllidine (Scheme 3.9). We hypothesized that the enamine-like trisubstituted olefin could be reduced selectively over the monosubstituted vinyl group using reductive amination-type conditions to leverage the electron-rich nature of the *N*-substituted alkene. However, we were disappointed to observe quantitative reduction of the exocyclic olefin, generating *O*-methyl isoleucophyllidine **394**. Returning to the literature, we discovered that 4-

vinylpyridines are active conjugate acceptors for a variety of soft nucleophiles³² and are frequently exploited in polymerization processes.³³ Attempts to over-reduce to *O*-methyl dihydro-leucophyllidine **395** were unsuccessful, indicating that chemoselective olefin differentiation was not likely a viable approach to the desired natural product.

Scheme 3.10. Preparative Stille coupling with formyl stannane.

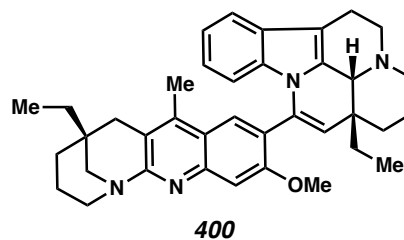
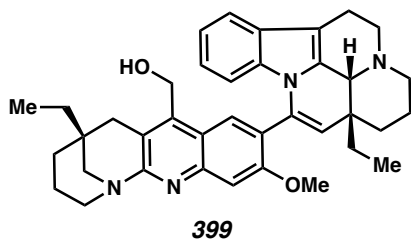


To circumvent this issue, we advanced aldehyde **342** to the corresponding trimethylstannane **396** (Scheme 3.10). We observed an improvement in the yield of coupling product **397**, which we attribute to two principle factors: 1) a greater electron-withdrawing influence of the formyl substituent improves transmetallation rates with CuTC to decrease the formation of homocoupled byproducts; 2) undesired decomposition pathways due to the presence of the vinylpyridine motif, which led to minor amounts of decomposition observed in acidic solvents such as chloroform.

Table 3.5. Hydrogenation attempts.

Entry*	Conditions	Result
1	H ₂ (60 atm), 10% Pd/C, EtOAc, 23 °C, 24 h	Aldehyde reduction
2	H ₂ (10 atm), 5% Rh/C, MeOH, 23 °C, 24 h	Aldehyde reduction
3	HCHO (6.5 equiv), 10% Pd/C, MeOH/DMF (7:1), 23 to 50 °C	Deoxygenation
4	NH ₄ HCHO, 10% Pd/C, EtOH, 80 °C, 10 min	Complex mixture
5	H ₂ , PtO ₂ , AcOH, 50 °C	Complex mixture
6	Raney Ni (20 wt equiv), <i>i</i> -PrOH/H ₂ O (10 : 1), 80 °C,	Deoxygenation
7	H ₂ , (1 → 50 bar) [Ir(COD)pyr(PCy ₃)]PF ₆ , CH ₂ Cl ₂ , 23 °C, 12 h	Aldehyde reduction (incomplete)
8	H ₂ , (1 → 50 bar) [Ir(COD)pyr(PCy ₃)]BARF, CH ₂ Cl ₂ , 23 °C, 12 h	Aldehyde reduction (incomplete)
9	H ₂ , (1 → 50 bar), Ir(COD)Cl ₂ (1 mol %), I ₂ (20 mol %), CH ₂ Cl ₂ , 23 °C	Complex Mixture
10	H ₂ , (^{<i>i</i>} PrDINiH) ₂ (1 equiv), HBpin (8 equiv), PhMe	Aldehyde reduction
11	BH ₃ · THF, Magic Blue, CH ₂ Cl ₂ , 0 to 23 °C	Epimerization
12	NaBH ₃ CN, HCl/MeOH, 23 to reflux	Aldehyde reduction
13	RuCl ₃ · xH ₂ O, NaBH ₄ , DMA/H ₂ O, 23 °C	Decomposition
14	Md(dpm) ₃ (20 mol %), PhSiH ₃ 3 equiv), TBHP (3 equiv), <i>i</i> -PrOH	Aldehyde reduction
15	Fe(acac) ₃ (10 equiv), PhSiH ₃ (25 equiv), EtOH, 60 °C	Aldehyde reduction
16	Co(acac) ₂ , Et ₃ SiH (100 equiv), 1,4-CHD (100 equiv), <i>n</i> -PrOH, 40 °C	Complex mixture
17	Fe(acac) ₂ ·6H ₂ O, NaBH ₄ , TFE/H ₂ O (1:300)	Aldehyde reduction
18	Li(0), NH ₃ , THF, -78 °C	Decomposition
19	Na-SG, THF, 23 °C, then MeOH	No reaction
20	Sml ₂ , Et ₃ N, H ₂ O, THF, 23 °C	Deoxygenation
21	Sml ₂ , H ₂ O, THF, 23 °C	No reaction

* Test reactions run with 1.0 mg of aldehyde XX and observed by LCMS.



With our key substrate in hand, we then turned our attention to the final diastereoselective hydrogenation. Homogeneous hydrogenation (Table 3.5, entry 1–6) quickly caused an undesired reduction, likely of the aldehyde motif, while a deoxygenation occurred upon use of acid additives (formic acid, entry 3)³⁴ or more active catalysts (Raney Ni, entry 6).³⁵ Alternative transfer hydrogenations (entry 4) and platinum catalysts (entry 5) led to complex mixtures, likely due to additional reduction of the heterocyclic motifs. Homogeneous hydrogenation (entry 7–10) with iridium³⁶ or nickel-³⁷ based catalysts were also unsuccessful, which we attributed to catalyst poisoning by the basic amines.

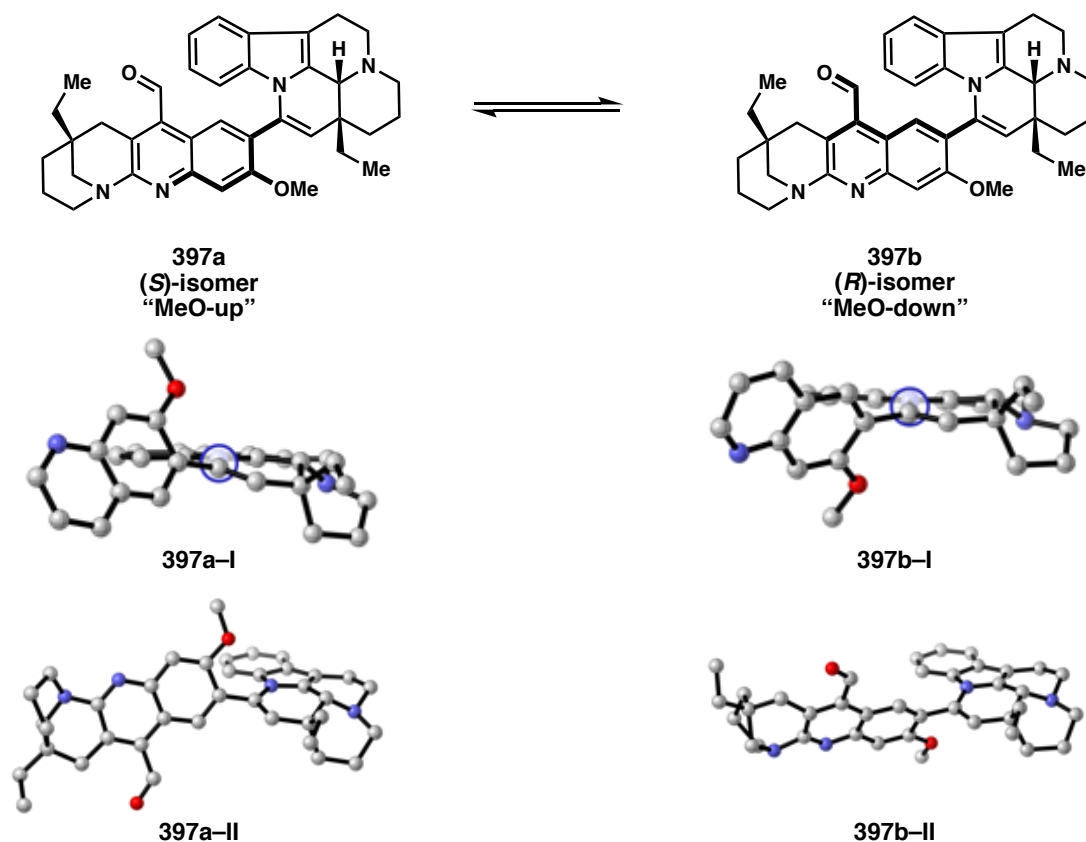
Moving away to non-hydrogenation approaches, we found that attempts to use hydroboration/protonation (entry 11), reductive amination (entry 12), or in-situ formed metal hydrides (entry 13) were likewise unsuccessful. Shifting to single electron reductants, we were disappointed to see that hydrogen atom transfer reductions described by Shenvi,³⁸ Baran,³⁹ Herzon,⁴⁰ and Boger⁴¹ (entry 14–17) all failed to reduce the olefin despite their established effectiveness in the reduction of highly substituted olefins. Dissolving metal reduction⁴² (entry 18) led to rapid overreduction, while milder silica-supported reductants (entry 19) led to complete recovery of starting material. Finally, samarium-based reductions led once again to either deoxygenation (entry 20) or no reaction⁴³ (entry 21) based on additive.

3.6 DFT MODELING OF CROSS-COUPLING SUBSTRATE

Puzzled by this lack of reactivity, we elected to model formyl substrate **397** computationally using density functional theory (DFT) to investigate the nature of this recalcitrant olefin. Our calculations revealed two major atropisomers with respect to the central C–C bond, corroborating our observed experimental results by NMR (Figure 3.1). Relaxed surface scans

along the biaryl dihedral offer an initial estimation to the rotational barrier of $12.6 \text{ kcal mol}^{-1}$, and the “MeO-up” atropisomer $0.6 \text{ kcal mol}^{-1}$ (gas phase) is slightly lower in energy.

Figure 3.1. DFT models of Stille coupling product.

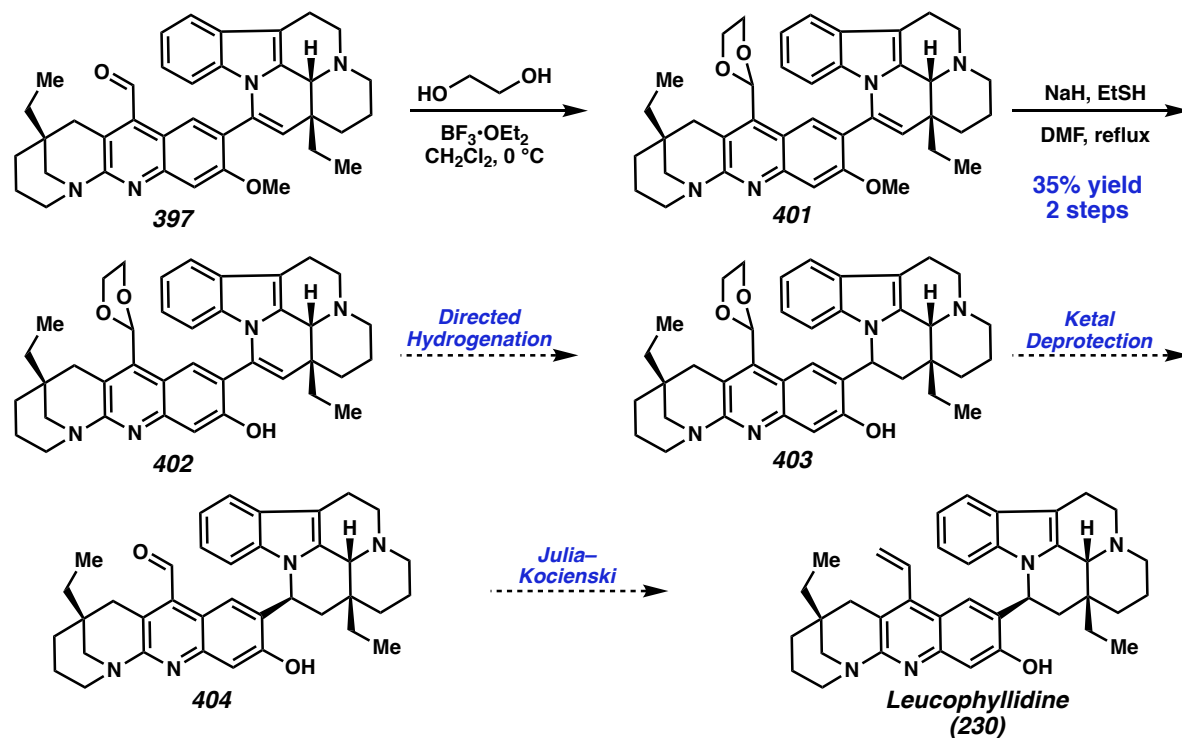


In these models, we observed two unexpected phenomena. The first is that the trisubstituted olefin lies slightly out of conjugation with the π -system of the indole ring, as observed in Newman projections **397a-I** and **397b-I**. The strain of the lactam-derived ring, due to the rigid conformation of the *eburnan* monomer and presence of the bulky eucophylline substituent, forces the two carbons of the “enamine” olefin to buckle, thus deactivating the alkene and contributing to the lack of expected reactivity. The second observation is that the piperidine ring of the *eburan* monomer adopts a boat-like configuration in both the lowest energy conformations **397a-II** and **397b-II**, pushing the ethyl substituent of the quaternary center into a *pseudo*-axial position. While

we were concerned that hydrogenation would be preferred from the α -face due to the concave nature of the cis-ring fusion, the boat-configuration opens up the desired face of reduction while creating an unfavorable flagpole interaction on the undesired face. Furthermore, the close proximity of the quinoline C(7) methoxy group in the **397b-II** configuration suggests that, following demethylation, this oxygen could be used to direct hydrogenation from the desired face, thus setting the correct diastereomer.

3.7 *FUTURE DIRECTIONS AND CONCLUDING REMARKS*

To complete the synthesis of leucophyllidine (**230**), our strategy moving forward is to apply a directed hydrogenation approach to install the final stereogenic center of leucophyllidine. Given the facile reduction of the formyl group, we first protected it with ethylene glycol to ketal **401**, then demethylated to afford the hydrogenation precursor **402**, albeit in low yield over two steps. We plan to investigate a number of hydrogenation catalysts to access reduced product **403**. Of particular interest are Ir-based Crabtree-Pfaltz catalysts^{36a} in the presence of acid to prevent poisoning by the substrate's tertiary amines,⁴⁴ Rh/phosphines due to success in similar reports by Amgen in phenol-directed hydrogenations,⁴⁵ and organocatalytic transfer hydrogenations.⁴⁶ If the appropriate stereochemistry can be set, only ketal deprotection to aldehyde **XX** and methylenation will be required to complete leucophyllidine (**230**).

Scheme 3.11. Endgame strategy.

In conclusion, we have developed a highly convergent Stille coupling to cross-couple the eburnamine and eucophylline-derived fragments to install the full carbocyclic skeleton of leucophyllidine. Initial attempts to forge the key C–C bond and stereogenic center using biomimetic and bio-inspired strategies were unsuccessful in model systems. A challenging hydrogenation currently prohibits us from completing the natural product. Nevertheless, we believe that use of an intramolecular directing group will ultimately help us to achieve the synthesis of the final target.

3.8 REFERENCES

- (1) Gan, C-Y.; Robinson, WT.; Etoh, T.; Hayashi, M.; Komiyama, K.; Kam, T-S. *Org. Lett.* **2009**, *11*, 3962 – 3965.
- (2) Magnus, P; Brown, P. *J. Chem. Soc. Chem. Commun.* **1985**, 184–186.
- (3) Pandey, G.; Mishra, A.; Khamrai, J. *Org. Lett.* **2017**, *19*, 3267 – 3270.
- (4) Dai, J-K.; Dan, W-J.; Du, H-T.; Zhang, J-W.; Wang, J-R. *Bioorg. Med. Chem. Lett.* **2016**, *26*, 580–583.
- (5) Medley, J.W; Movassaghi, M. *Angew. Chem. Int. Ed.* **2012**, *51*, 4572–4576.
- (6) Wu, P.; Givskov, M.; Nielsen, T.E. *Chem. Rev.* **2019**, *119*, 11245–11290.
- (7) Le Gall, E.; Troupel, M.; Nédélec, J-Y. *Tetrahedron* **2006**, *62*, 9953–9965.
- (8) Le Gall, E.; Haurena, C.; Sengmany, S.; Martens, T.; Troupel, M. *J. Org. Chem.* **2009**, *20*, 7970–7973.
- (9) Fillon, H.; Gosmini, C.; Périchon, J. *J. Am. Chem. Soc.* **2003**, *125*, 3867–3870.
- (10) Bruno, D.; Lesma, G.; Mauro, M.; Palmisano, G.; Passarella, D. *J. Org. Chem.* **1995**, *60*, 2506–2513.
- (11) Lancefield, C.S.; Zhou, L.; Lébl, T.; Slawn, A.M.Z.; Westwood, N.J. *Org. Lett.* **2012**, *14*, 6166–6169.
- (12) Chapman, L.M.; Beck, J.C.; Wu, L.; Reisman, S.E. *J. Am. Chem. Soc.* **2016**, *138*, 9803–9806.
- (13) Enders, D.; Shilvock, J.P. *Chem. Soc. Rev.* **2000**, *29*, 359–373.
- (14) A standard of protonation product **XX** was prepared using lithium/halogen exchange, followed by aqueous workup. A standard of quinoline iodide **XX** was prepared under

- aromatic Finkelstein conditions (See: Suzuki, H.; Kondo, A.; Ogawa, T. *Chem Lett.* **1985**, *14*, 411–412.)
- (15) Kazmierski, I.; Gosmini, C.; Paris, J-M.; Périchon, J. *Tetrahedron Lett.* **2003**, *44*, 6417–6420.
- (16) Rieke, R.D.; Uhm, S.J.; Hudnall, P.M. *J. Chem. Soc. Chem. Comm.* **1973**, 269–270.
- (17) Schley, N.D.; Fu, G.C. *J. Am. Chem. Soc.* **2014**, *136*, 16588–16593.
- (18) Nicolaou, K.C.; Bulger, P.G.; Sarlah, D. *Angew. Chem. Int. Ed.* **2005**, *44*, 4442–4489.
- (19) Occhiato, E.G.; Trabocchi, A.; Guarna, A. *J. Org. Chem.* **2001**, *66*, 2459–2465.
- (20) Ferrali, A.; Guarna, A.; Lo Galbo, F.; Occhiato, E.G. *Tetrahedron Lett.* **2004**, 5271–5274.
- (21) Tadross, P.A.; Stoltz, B.M. *Chem. Rev.* **2012**, *112*, 3550 – 3577.
- (22) Ishiyama, T.; Murata, M.; Miyaura, N. *J. Org. Chem.* **1995**, *60*, 7508–7510.
- (23) a) Cox, P.A.; Leach, A.G.; Campbell, A.D.; Lloyd-Jones, G.C. *J. Am. Chem. Soc.* **2016**, *138*, 9145–9157. b) Cox, P.A.; Reid, M.; Leach, A.G.; Campbell, A.D.; King, E.J.; Lloyd-Jones, G.C. *J. Am. Chem. Soc.* **2017**, *139*, 13156 – 13165.
- (24) Hofstra, J.L.; Poremba, K.E.; Shomozono, A.M.; Reisman, S.E. *Angew. Chem. Int. Ed.* **2019**, *58*, 14901–14905.
- (25) a) Farina, V.; Krishnan, B. *J. Am. Chem. Soc.* **1991**, *113*, 9585-9595. b) Farina, V.; Krishnan, B.; Marshall, D.R.; Roth, G.P. *J. Org. Chem.* **1993**, *58*, 5434-5444.
- (26) Xan, H; Stoltz, B.M.; Corey E.J.; *J. Am. Chem. Soc.* **1999**, *121*, 7600 – 7605.
- (27) a) Li, H.; Chen, Q.; Lu, Z.; Li, A. *J. Am. Chem. Soc.* **2016**, *138*, 15555–15558. b) Furstner, A.; Funel, J-A.; Tremblay, M.; Bouchez, L.C.; Nevado, C.; Waser, M.; Ackerstaff, J.; Stimson, C.C. *Chem Comm.* **2008**, 2873 – 2875.
- (28) Allred, G. D.; Liebeskind, L. S. *J. Am. Chem. Soc.* **1996**, *118*, 2748–2749.

-
- (29) Naber, J.R.; Buchwald, S.L. *Adv. Synth. Catal.* **2008**, *350*, 957–961.
- (30) Littke, A.F.; Fu, G.C. *Angew. Chem. Int. Ed.* **1999**, *38*, 2411–2413.
- (31) Palani, V.; Hugelshofer, C.L.; Sarpong, R. *J. Am. Chem. Soc.* **2019**, *141*, 14421–14432.
- (32) Katiritzky, A.R.; Khan, G.R.; Schwarz, O.A. *Tetrahedron Lett.* **1984**, *25*, 1223–1226.
- (33) Xia, S.; Yang, B.; Li, G.; Zhu, X.; Wang, A.; Zhu, J. *Polym. Chem.* **2011**, *2*, 2356–2359.
- (34) Czibula, L.; Nemes, A.; Visky, G.; Farkas, M.; Szombathelyi, Z.; Kárpáti, E.; Sohár, P.; Kessel, M. Kreidl, J. *Liebigs Annalen der Chemie* **1993**, *3*, 221–230.
- (35) Shenvi, R.A.; Guerrero, C.A.; Shi, J.; Li, C.-C.; Baran, P.S. *J. Am. Chem. Soc.* **2008**, *130*, 7241–7243.
- (36) (a) Crabtree, R.H. *Acc. Chem. Res.* *12*, 331–338. b) Wüstenberg, B.; Pfaltz, A. *Adv. Synth. Cat.* **2008**, *350*, 174–178. c) Kim, A.N.; Ngamnithiporn, A.; Welin, E.R.; Daiger, M.T.; Grünanger, C.U.; Bartberger, M.D.; Virgil, S.C.; Stoltz, B.M. *ACS Catal.* **2020**, *10*, 3241–3248.
- (37) Léonard, N.G.; Chirik, P.J. *ACS Catal.* **2018**, *8*, 342–348.
- (38) Iwasaki, K.; Wan, K.K.; Oppedisano, A.; Crossley, S.W.M.; Shenvi, R.A. *J. Am. Chem. Soc.* **2014**, *136*, 1300–1303.
- (39) Lo, J.C.; Yabe, Y.; Baran, P.S. *J. Am. Chem. Soc.* **2014**, *136*, 1304–1307.
- (40) Ma, X.; Herzon, S.B. *Chem. Sci.* **2015**, *6*, 6250–6255.
- (41) Leggans, E.K.; Barker, T.J.; Duncan, K.K.; Boger, D.L. *Org. Lett.* **2012**, *14*, 1428–1431.
- (42) Cleve, A.; Fritzeimerer, K.-H.; Klar, U.; Müller-Farnow, Neef, G.; Ottow, E.; Schwede, W. *Tetrahedron* **1996**, *52*, 1529–1542.
- (43) Kolmar, S.S.; Mayer, J.M. *J. Am. Chem. Soc.* **2017**, *129*, 10687–10692.
- (44) Crabtree, R.H.; Iridium. In *The Handbook of Homogeneous Hydrogenation*; de Vries,

-
- J.G.; Elsevier, C.J. (Eds.); Wiley-VCH: Weinheim, Germany, 2007. pp 31–43.
- (45) a) Wang, X.; Guram, A.; Caille, S.; Hu, J.; Preston, J.P.; Ronk, M.; Walker, S. *Org. Lett.* **2011**, *13*, 1881–1883. b) Caille, S.; Crockett, R.; Ranganathan, K.; Wang, X.; Woo, J.C.S.; Walker, S.D. *J. Org. Chem.* **2011**, *76*, 5198-5206.
- (46) Wang, Z.; Ai, F.; Wang, Z.; Zhao, W.; Zhu, G.; Lin, Z.; Sun, J. *J. Am. Chem. Soc.* **2015**, *137*, 383–389.

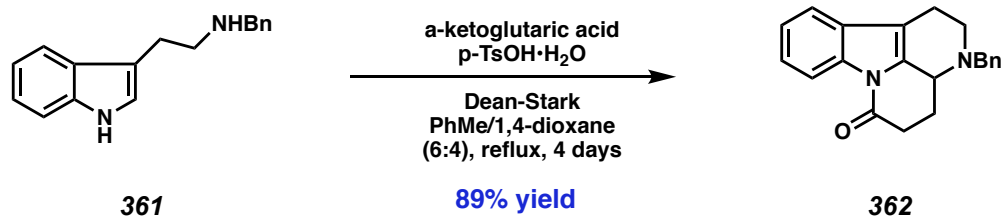
3.8 EXPERIMENTAL SECTION

3.8.1 Materials and Methods

Unless otherwise stated, reactions were performed in flame-dried glassware under an argon or nitrogen atmosphere using dry, deoxygenated solvents. Solvents were dried by passage through an activated alumina column under argon.¹ Reaction progress was monitored by thin-layer chromatography (TLC) or Agilent 1290 UHPLC-LCMS. TLC was performed using E. Merck silica gel 60 F254 precoated glass plates (0.25 mm) and visualized by UV fluorescence quenching, *p*-anisaldehyde, CAM, or KMnO₄ staining. Silicycle SiliaFlash® P60 Academic Silica gel (particle size 40–63 nm) was used for flash chromatography. ¹H and ¹³C NMR spectra were recorded on a Varian Inova 500 (500 MHz and 126 MHz, respectively) and a Bruker AV III HD spectrometer equipped with a Prodigy liquid nitrogen temperature cryoprobe (400 MHz and 101 MHz, respectively) and are reported in terms of chemical shift relative to CHCl₃ (δ 7.26 and δ 77.16, respectively) and C₆D₆ (δ 7.16 and δ 128.06, respectively). Data for ¹H NMR are reported as follows: chemical shift (δ ppm) (multiplicity, coupling constant (Hz), integration). Multiplicities are reported as follows: s = singlet, d = doublet, t = triplet, q = quartet, p = pentet, sept = septuplet, m = multiplet, br s = broad singlet, br d = broad doublet, br t = broad triplet, app = apparent. Some reported spectra in chloroform include minor solvent impurities of water (δ 1.56ppm), ethyl acetate (δ 4.12, 2.05, 1.26 ppm), methylene chloride (δ 5.30 ppm), acetone (δ 2.17 ppm), grease (δ 1.26, 0.86 ppm), and/or silicon grease (δ 0.07 ppm), which do not impact product assignments.² Data for ¹³C NMR are reported in terms of chemical shifts (δ ppm). IR spectra were obtained by use of a Perkin Elmer Spectrum BXII spectrometer using thin films deposited on NaCl plates and reported in frequency of absorption (cm⁻¹). Optical rotations were measured with a Jasco P-2000 polarimeter operating on the sodium D-line (589 nm), using a 100 mm path-length cell, and are

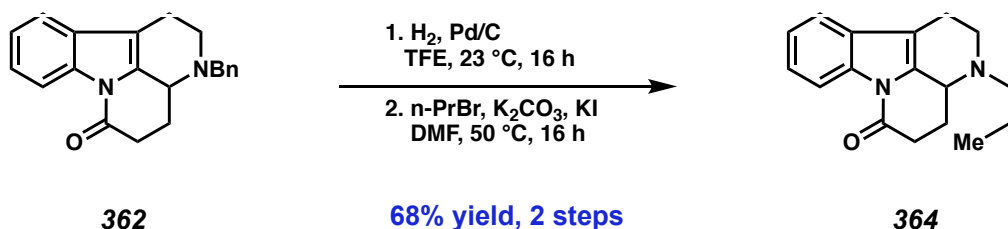
reported as $[\alpha]_D$ (concentration in g/100 mL, solvent). Analytical SFC was performed with a Mettler SFC supercritical CO₂ analytical chromatography system utilizing Chiralpak OD-J column (4.6 mm x 25 cm) obtained from Daicel Chemical Industries, Ltd. High resolution mass spectra (HRMS) were obtained from the Caltech Mass Spectral Facility using a JEOL JMS-600H High Resolution Mass Spectrometer in fast atom bombardment (FAB⁺) or electron ionization (EI⁺) mode, or Agilent 6200 Series TOF with an Agilent G1978A Multimode source in mixed ionization mode (MM: ESI/APCI). Reagents were purchased from Sigma-Aldrich, Acros Organics, Strem, or Alfa Aesar and used as received unless otherwise stated. Copper (I) thiophene carboxylate was prepared by known methods.³

3.8.2 Experimental Procedures



Lactam 362: Following the procedure described by Wang, to a 1L round-bottom flask equipped with stir bar was added *N*-benzyltryptamine **361** (6.25g, 25.0 mmol, 1.0 equiv), α -ketoglutaric acid (5.11g, 35.0 mmol, 1.4 equiv), benzene (340 mL), and 1,4-dioxane (225 mL). The flask was equipped with a Dean-Stark apparatus and heated to 100 °C for 4 days.

After completion, the flask was cooled to room temperature, diluted with ethyl acetate, and washed successively with saturated sodium bicarbonate, water, and brine. The organics were dried with ethyl acetate, and concentrated in vacuo to afford tetracycle **362** a green solid (7.03g, 89% yield). The material is carried forward without further purification. Characterization data are in accordance with published values.⁴



Model lactam 364: To a flame dried 100-mL flask with stir bar was charged lactam **362** (1.0 g, 3.16 mmol, 1.0 equiv) in trifluoroethanol (32 mL). The headspace was evacuated and backfilled with nitrogen and stirred for 5 minutes before 10% palladium on carbon (0.5 g) was added in a

single portion. The headspace was then evacuated and backfilled with hydrogen gas (3X) before the flask was stirred for 16 hours.

Following completion, as determined by LCMS analysis, the solution was sparged with nitrogen gas for five minutes. The reaction mixture was then filtered through a pad of Celite, washing the filter cake with methanol. The combined organics were then concentrated in vacuo to afford a green, amorphous solid. The product was used directly in the next reaction without further purification.

To a separate, flame-dried 100-mL flask with stir bar was added the crude starting material in DMF (15 mL), potassium iodide (786 mg, 4.74 mmol, 1.5 equiv), and potassium carbonate (1.31 g, 9.48 mmol, 3.0 equiv). The reaction mixture was stirred at 23 °C for five minutes before *n*-propyl bromide (0.43 mL, 4.74 mmol, 1.5 equiv) was added dropwise. The reaction mixture was heated to 50 °C for 16 hours.

Following completion, as determined by LCMS analysis, the reaction mixture was cooled to room temperature and diluted with ethyl acetate. The organic layer was washed sequentially with water (1X) and brine (1X), dried with sodium sulfate, and concentrated in vacuo. Flash column chromatography (50% → 100% ethyl acetate/hexanes) afforded model lactam **364** (580 mg, 68% yield as a white, amorphous solid. ¹H NMR (400 MHz, CDCl₃) δ 8.41 – 8.33 (m, 1H), 7.44 – 7.36 (m, 1H), 7.33 – 7.22 (m, 2H), 3.46 (ddt, *J* = 12.0, 4.9, 2.7 Hz, 1H), 3.34 (ddd, *J* = 11.7, 6.0, 1.3 Hz, 1H), 2.90 – 2.80 (m, 3H), 2.79 – 2.65 (m, 2H), 2.59 (td, *J* = 11.6, 4.4 Hz, 1H), 2.47 – 2.36 (m, 2H), 1.80 (dtd, *J* = 13.6, 12.2, 4.3 Hz, 1H), 1.71 – 1.50 (m, 2H), 0.95 (t, *J* = 7.4 Hz, 3H); ¹³C NMR (101 MHz, CDCl₃) δ 168.3, 135.0, 134.9, 129.5, 124.5, 124.0, 118.2, 116.3, 113.5, 56.9, 55.2, 50.2, 33.1, 27.4, 21.6, 20.1, 12.1; IR (neat film, NaCl) 2961, 2801, 1708, 1456, 1385, 1362,

1329, 1344, 750 cm^{-1} (Neat Film, NaCl); HRMS (ESI/APCI) m/z calculated for $\text{C}_{17}\text{H}_{21}\text{N}_2\text{O}$ [$\text{M} + \text{H}^+$]: 269.1654, found, 269.1669.

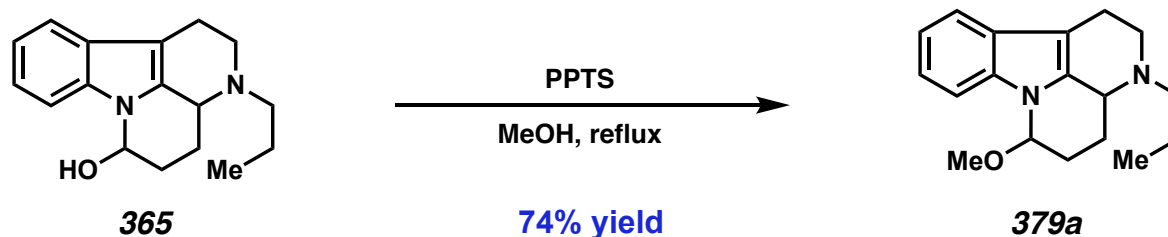


Model hemiaminal XX: To a flame-dried 100-mL flask with stir bar was added lithium aluminum hydride (358 mg, 9.44 mmol, 2.0 equiv) and THF (24 mL) at 0 °C. In a separate flask, eburnan model **XX** (1.27 g, 4.72 mmol, 1.0 equiv) was dissolved in THF (23 mL) and cooled to 0 °C. The starting material was added to the flask dropwise via cannula over 10 minutes, and the reaction mixture was allowed to stir at 0 °C for 35 additional minutes.

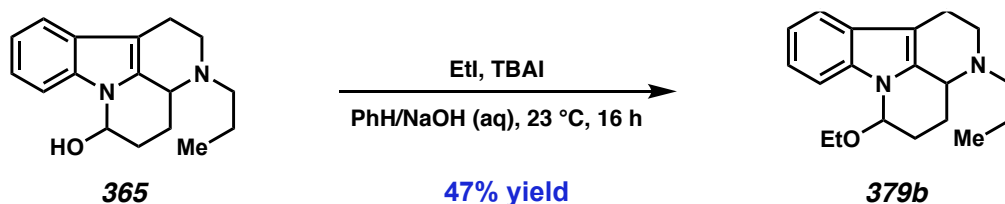
After the reaction was complete, as determined by TLC, the reaction was quenched with cool brine, transferred to a separatory funnel, and extracted with ethyl acetate (3X). The combined organics were washed once with cool brine, dried with sodium sulfate, and concentrated in vacuo. Flash column chromatography (50% \rightarrow 100% ethyl acetate/hexanes) afforded a mixture model hemiaminal **XX** epimers (1.02 g, 80% yield, 17.5:1 d.r.) as a white, amorphous solid. The ratio of major and minor diastereomers was determined by integration of the diagnostic peaks in the ^1H NMR for and 5.41 and 5.95, respectively.

Major diastereomer: ^1H NMR (400 MHz, CDCl_3) δ 7.68 – 7.58 (m, 1H), 7.50 – 7.42 (m, 1H), 7.21 – 7.08 (m, 2H), , 5.41 (dd, $J = 9.2, 5.6$ Hz), 3.25 (tdd, $J = 11.0, 5.2, 1.7$ Hz, 2H), 2.93 – 2.62 (m, 4H), 2.61 – 2.50 (m, 1H), 2.49 – 2.37 (m, 1H), 2.32 (ddd, $J = 12.7, 9.7, 5.0$ Hz, 1H), 2.15 (dtd, $J = 12.3, 4.6, 2.9$ Hz, 1H), 1.72 – 1.45 (m, 3H), 1.35 – 1.14 (m, 1H), 0.92 (t, $J = 7.4$ Hz, 3H); ^{13}C NMR (101 MHz, CDCl_3) δ 138.0, 135.7, 128.3, 121.6, 120.3, 118.2, 112.0, 107.3, 78.9, 58.1, 55.0,

50.4, 33.4, 26.1, 21.7, 19.9, 12.2. IR (Neat Film, NaCl); HRMS (ESI/APCI) m/z calculated for $C_xH_xN_xO_x$ [$M + H^+$]: $C_{17}H_{23}N_2O$, found, YYY.

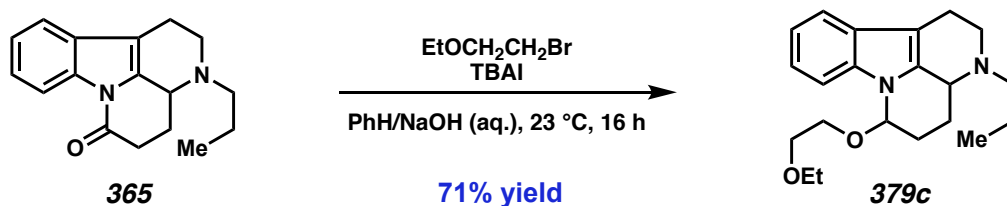


Aminal 379a: To a flame-dried, one-dram vial with stir bar was added hemiaminal model **365** (27.0 mg, 0.10 mmol, 1.0 equiv), pyridinium *p*-toluenesulfonate (2.5 mg, 0.010 mmol, 0.10 equiv) and methanol (0.2 mL). The vial was sealed and heated to reflux for 16 hours. Upon completion, the reaction mixture was cooled to room temperature, diluted with ethyl acetate, filtered through a plug of Celite, and concentrated in vacuo. Preparative TLC (50% ethyl acetate/hexanes) affords aminal **379a** as a colorless oil. Product characterization data was not obtained due to the Spring 2020 COVID-19 shutdown of research facilities.



Aminal 379b: To a 25 mL round-bottom flask with stir bar was added hemiaminal model **365** (108 mg, 0.4 mmol, 1.0 equiv) and toluene (10 mL) and 50% aqueous NaOH (10 mL). Tetrabutylammonium iodide (664 mg, 1.8 mmol, 4.5 equiv) was added in a single portion before and the biphasic mixture was rapidly stirred for 10 minutes. Ethyl iodide (2.17 mL, 27.2 mmol, 68 equiv) was added dropwise and the reaction was slowly warmed to 23 °C for 16 hours.

The reaction mixture was diluted with diethyl ether and transferred to a separatory funnel. The organic layer was washed with water (3X) and brine (3X), dried with sodium sulfate, and concentrated in vacuo. Flash column chromatography on silica gel (0 → 40 → 50% ethyl acetate/hexanes) afforded aminal **379c** (56.0 mg, 47% yield) as a colorless oil. Product characterization data was not obtained due to the Spring 2020 COVID-19 shutdown of research facilities.



Aminal 379c: To a 25 mL round-bottom flask with stir bar was added hemiaminal model **365** (108 mg, 0.4 mmol, 1.0 equiv) and toluene (10 mL) and 50% aqueous NaOH (10 mL). Tetrabutylammonium iodide (664 mg, 1.8 mmol, 4.5 equiv) was added in a single portion before being cooled to $0\text{ }^\circ\text{C}$ and rapidly stirred for 10 minutes. 2-bromoethyl ethyl ether (3.96 mL, 28 mmol, 70 equiv) was added dropwise and the reaction was slowly warmed to $23\text{ }^\circ\text{C}$ for 16 hours.

The reaction mixture was diluted with diethyl ether and transferred to a separatory funnel. The organic layer was washed with water (3X) and brine (3X), dried with sodium sulfate, and concentrated in vacuo. Flash column chromatography on silica gel pre-treated with 0.5% triethylamine/hexanes (0 → 30 → 40 → 50% ethyl acetate/hexanes) afforded aminal **379c** (97.2 mg, 71% yield) as a colorless oil which was stored in a $-20\text{ }^\circ\text{C}$ freezer to avoid decomposition.

Major Diastereomer: $^1\text{H NMR}$ (400 MHz, CD_2Cl_2) δ , 7.50 – 7.36 (m, 2H), 7.19 – 7.04 (m, 2H), 5.50 (dd, $J = 8.1, 5.6$ Hz, 1H), 3.79 – 3.55 (m, 3H), 3.54 – 3.23 (m, 5H), 2.93 – 2.74 (m, 2H), 2.73 – 2.63 (m, 1H), 2.55 (td, $J = 11.5, 4.4$ Hz, 1H), 2.43 – 2.28 (m, 3H), 2.17 – 1.99 (m, 1H), 1.68 –

1.50 (m, 2H), 1.42 – 1.26 (m, 1H), 1.18 (dt, $J = 18.2, 7.0$ Hz, 3H), 0.94 (td, $J = 7.4, 5.6$ Hz, 3H).

^{13}C NMR (101 MHz, CD_2Cl_2) δ 137.9, 136.4, 128.0, 121.1, 119.8, 117.8, 111.5, 107.1, 83.7, 69.8, 66.5, 63.9, 57.6, 55.0, 50.2, 27.7, 25.7, 21.8, 20.1, 15.0, 11.8.

Minor Diastereomer: ^1H NMR (400 MHz, CD_2Cl_2) δ 7.60 (ddd, $J = 8.0, 1.4, 0.8$ Hz, 2H), 7.19 – 7.04 (m, 2H), 5.66 (dd, $J = 3.0, 2.1$ Hz, 1H), 3.79 – 3.55 (m, 3H), 3.54 – 3.23 (m, 5H), 2.93 – 2.74 (m, 2H), 2.73 – 2.63 (m, 1H), 2.55 (td, $J = 11.5, 4.4$ Hz, 1H), 2.43 – 2.28 (m, 2H), 2.17 – 1.99 (m, 2H), 1.84 – 1.70 (m, 1H), 1.68 – 1.50 (m, 1H), 1.42 – 1.26 (m, 1H), 1.18 (dt, $J = 18.2, 7.0$ Hz, 3H), 0.94 (td, $J = 7.4, 5.6$ Hz, 3H). ^{13}C NMR (101 MHz, CD_2Cl_2) δ 136.8, 136.4, 128.4, 120.8, 119.8, 118.0, 110.9, 107.1, 81.3, 70.0, 67.7, 66.5, 58.6, 55.0, 50.8, 27.1, 25.7, 21.5, 20.0, 15.0, 11.8.

Combined: IR (Neat Film, NaCl): 2959, 2866, 2800, 1458, 1345, 1309, 1159, 1120, 743 cm^{-1} .

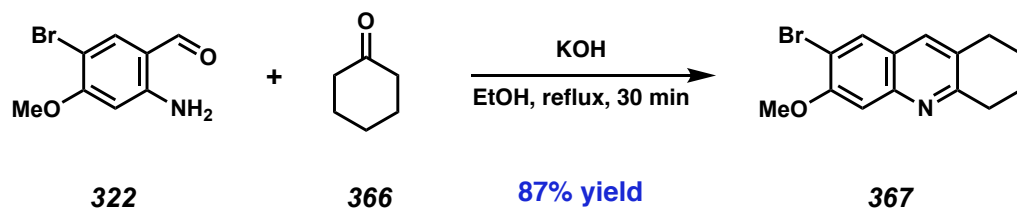
HRMS (ESI/APCI) m/z calculated for $\text{C}_{21}\text{H}_{31}\text{N}_2\text{O}_2$ [$\text{M} + \text{H}^+$]: 342.2386, found, 343.2368.



Aminonitrile 379d: To a flame-dried one-dram vial with stir bar was added hemiaminal **365** (30 mg, 0.111 mmol, 1.0 equiv) in dichloromethane (1.1 mL). The vial was cooled to -78°C before trimethylsilyl cyanide (21.1 μL , 0.167 mmol, 1.5 equiv) and boron trifluoride diethyl etherate (21.0 μL , 0.167 mmol, 1.5 equiv) were successively added. The cooling bath was removed and the vial was allowed to warm to 23°C over 1.5 hours.

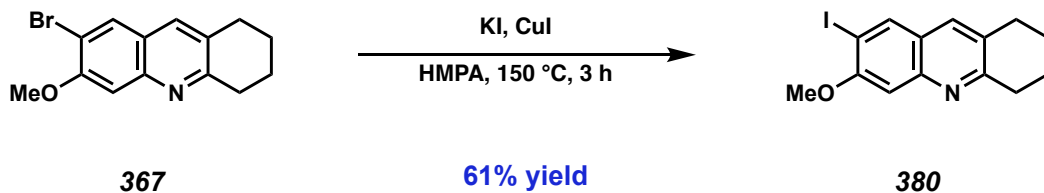
After the reaction was complete, the solution was quenched with saturated sodium bicarbonate solution and extracted with dichloromethane (3X). The combined organic extracts

were dried with sodium sulfate and concentrated in vacuo. Flash column chromatography (30% → 40% ethyl acetate/hexanes) afforded aminonitrile **379d** (26.8 mmol, 85% yield) as an amorphous white solid. Product characterization data was not obtained due to the Spring 2020 COVID-19 shutdown of research facilities.



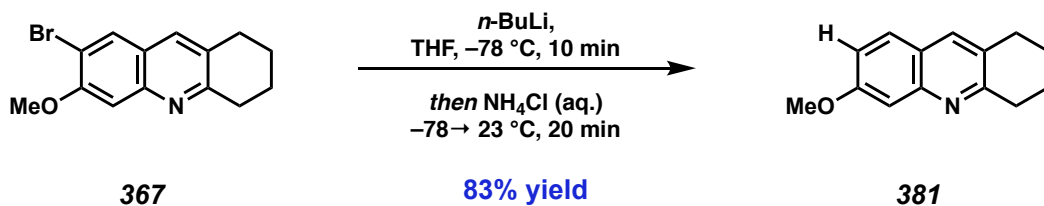
Bromoquinoline 367: To a 100-mL round-bottom flask equipped with stir bar was added aldehyde **322** (1.20 g, 5.2 mmol, 1.0 equiv), absolute ethanol (17.8 mL), and cyclohexanone **366** (0.59 mL, 5.7 mmol, 1.1 equiv). Powdered potassium hydroxide (350 mg, 6.3 mmol, 1.2 equiv) was added in one portion. The flask was fitted with a reflux condenser and heated to reflux for 30 minutes.

Following the completion of the reaction, the flask was cooled to room temperature, filtered through Celite (washing the cake with absolute ethanol), and concentrated in vacuo. The crude mixture was purified by flash column chromatography (40% ethyl acetate/hexanes) to afford bromoquinoline **367** (1.34 g, 88% yield) as a light brown, amorphous solid. ^1H NMR (500 MHz, CD_3OD) δ 8.02 (s, 1H), 7.85 (s, 1H), 7.29 (s, 1H), 4.00 (s, 3H), 3.04 (t, $J = 6.5$ Hz, 2H), 2.98 – 2.94 (m, 2H), 2.02 – 1.96 (m, 2H), 1.93 – 1.86 (m, 2H); ^{13}C NMR (126 MHz, CD_3OD) δ 161.0, 157.7, 147.7, 136.1, 132.2, 131.2, 124.6, 114.3, 107.0, 56.9, 33.9, 29.8, 24.0, 23.9; IR (Neat Film, NaCl) 2937, 2862, 1614, 1599, 1481, 1454, 1361, 1318, 1318, 1240, 1205, 1040, 838 cm^{-1} ; HRMS (ESI/APCI) m/z calculated for $\text{C}_{14}\text{H}_{15}\text{NOBr}$ [$\text{M} + \text{H}^+$]: 292.0337, found 292.0327.



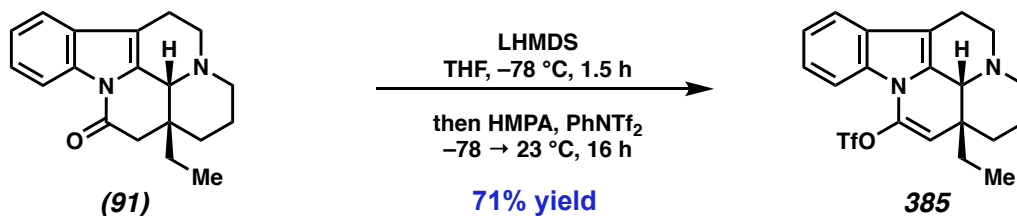
Iodoquinoline 380: To an oven-dried 1-dram vial with stir bar was added bromide **367** (100 mg, 0.33 mmol, 1.0 equiv), potassium iodide (846 mg, 5.1 mmol, 15.0 equiv), and copper (I) iodide (323 mg, 1.7 mmol, 5.0 equiv). The vial was evacuated and backfilled with nitrogen three times before HMPA (1.0 mL) was added to the solution. The vial was heated to 150 °C for 3 hours.

The reaction mixture was transferred to a 20-mL scintillation vial and diluted with 1M HCl until homogeneous. The solution was then basified with 1 M NaOH and extracted with ethyl acetate (5X). The combined organic extracts were washed with brine, dried with sodium sulfate, and concentrated in vacuo. Flash column chromatography (25% → 30% → 40% ethyl acetate/hexanes) afforded iodoquinoline **380** (71 mg, 61% yield) as a light brown solid. ¹H NMR (400 MHz, (1.34 g, 88% yield)) δ 8.17 (s, 1H), 7.62 (d, *J* = 1.2 Hz, 1H), 7.27 (s, 1H), 3.98 (s, 3H), 3.07 (t, *J* = 6.5 Hz, 2H), 2.98 – 2.88 (m, 2H), 2.02 – 1.94 (m, 2H), 1.91 – 1.84 (m, 2H). ¹³C NMR (101 MHz, CDCl₃) δ 160.2, 157.4, 147.8, 137.6, 133.6, 129.4, 123.9, 106.5, 87.4, 56.5, 33.6, 29.1, 23.2, 22.9. IR (Neat film, NaCl) 2933, 1858, 1611, 1593, 1473, 1452, 1407, 1316, 1238, 1207, 1035 cm⁻¹; HRMS (ESI/APCI) *m/z* calculated for C₁₄H₁₅NOI [M + H⁺]: 340.0199, found, 340.0226.



Quinoline 381: To a flame-dried, 25-mL round-bottom flask with stir bar was added bromoquinoline **367** (146 mg, 0.5 mmol, 1.0 equiv) and THF (5.0 mL). The flask was cooled to $-78\text{ }^{\circ}\text{C}$ and *n*-BuLi (0.26 mL, 2.3 M, 1.2 equiv) was added dropwise, turning the solution from colorless to red. The reaction mixture was stirred at that temperature for an additional ten minutes. Saturated aqueous ammonium chloride (2.0 mL) was then added and the reaction was warmed to room temperature over 20 minutes.

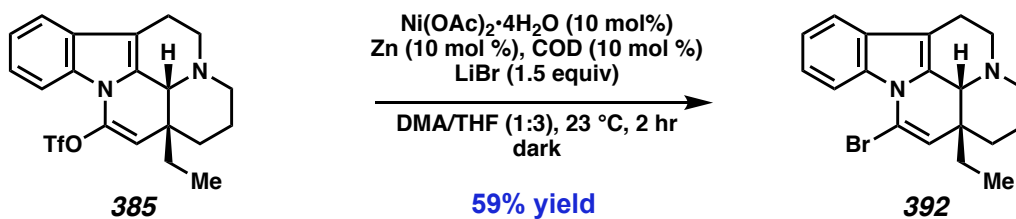
The reaction mixture was diluted with diethyl ether and the organic layer was separated. The aqueous layer was washed with ether (3X) before the combined organic extracts were dried with sodium sulfate and concentrated in vacuo. Flash column chromatography (30% \rightarrow 40% \rightarrow 50% ethyl acetate/hexanes) afforded quinoline **381** (89 mg, 83% yield) as a light brown oil. ^1H NMR (400 MHz, CDCl_3) δ 7.72 (d, $J = 1.2$ Hz, 1H), 7.56 (d, $J = 8.9$ Hz, 1H), 7.33 (d, $J = 2.5$ Hz, 1H), 7.09 (dd, $J = 8.9, 2.5$ Hz, 1H), 3.91 (s, 3H), 3.09 (t, $J = 6.5$ Hz, 2H), 2.99 – 2.82 (m, 2H), 2.06 – 1.91 (m, 2H), 1.91 – 1.78 (m, 2H); ^{13}C NMR (101 MHz, CDCl_3) δ 160.1, 159.2, 147.9, 135.1, 128.6, 127.9, 122.4, 118.9, 106.1, 55.5, 33.4, 29.0, 23.3, 23.0; IR (Neat Film, NaCl) 2928, 1624, 1602, 1452, 1317, 1231, 1210 1032, 852, 810 cm^{-1} ; HRMS (ESI/APCI) m/z calculated for $\text{C}_x\text{H}_x\text{N}_x\text{O}_x$ [$\text{M} + \text{H}^+$]: 214.1206, found, 214.1232.



Trifloxyenamine 385: To a flame-dried, 25 mL flask with stir bar was added eburnamonine (**91**) (258 mg, 0.877 mmol, 1.0 equiv) and THF (4.4 mL). The flask was cooled to $-78\text{ }^\circ\text{C}$ before 1M LiHMDS in THF (1.23 mL, 1.23 mmol, 1.4 equiv) was added dropwise via syringe pump over 30 minutes. The reaction mixture was then stirred at $-78\text{ }^\circ\text{C}$ for 1 hour, during which time the solution turned from light yellow to orange. HMPA (305 μL , 1.75 mmol, 2.0 equiv) was added dropwise and stirred at $-78\text{ }^\circ\text{C}$ for 10 minutes, during which time the solution turned dark brown. *N*-phenyl triflimide (438 mg, 1.23 mmol, 1.4 equiv) in THF (1.0 mL) was then added dropwise. The reaction mixture was stirred at $-78\text{ }^\circ\text{C}$ for 1.5 hours, then allowed to warm slowly to $23\text{ }^\circ\text{C}$ over 14.5 hours.

The reaction mixture was quenched with water, transferred to a separatory funnel, and extracted with diethyl ether (5X). The combined organics were washed with 10% sodium hydroxide, dried with potassium carbonate, and concentrated in vacuo. Flash column chromatography (30 \rightarrow 40 \rightarrow 50% ethyl acetate/hexanes) afforded trifloxyenamine **385** (266 mg, 71% yield) as a colorless oil, which then solidified to an amorphous white solid after letting stand in the freezer ($-20\text{ }^\circ\text{C}$) for at least 24 hours. ^1H NMR (400 MHz, CDCl_3) δ 7.66 (dt, $J = 8.3, 0.9$ Hz, 1H), 7.47 (dt, $J = 7.6, 1.0$ Hz, 1H), 7.27 – 7.22 (m, 2H), 7.18 (ddd, $J = 8.2, 7.2, 1.0$ Hz, 1H), 5.03 (s, 1H), 4.28 (s, 1H), 3.38 (dd, $J = 13.8, 5.8$ Hz, 1H), 3.27 (td, $J = 13.8, 12.6, 5.2$ Hz, 1H), 3.00 (dddd, $J = 17.2, 11.3, 6.0, 2.9$ Hz, 1H), 2.75 – 2.59 (m, 2H), 2.52 (dd, $J = 16.2, 5.1$ Hz, 1H), 2.13 – 1.97 (m, 1H), 1.76 (dq, $J = 14.8, 7.5$ Hz, 1H), 1.57 (d, $J = 13.7$ Hz, 1H), 1.46 (dt, $J = 13.5, 3.2$ Hz, 1H), 1.15 (td, $J = 13.7, 3.7$ Hz, 1H), 1.01 (t, $J = 7.5$ Hz, 3H); δ ^{13}C NMR (101 MHz, CDCl_3) δ 138.9, 133.3, 129.1, 123.5, 121.5, 120.3, 118.9, 117.1, 112.2, 110.7, 105.3, 55.2, 51.7,

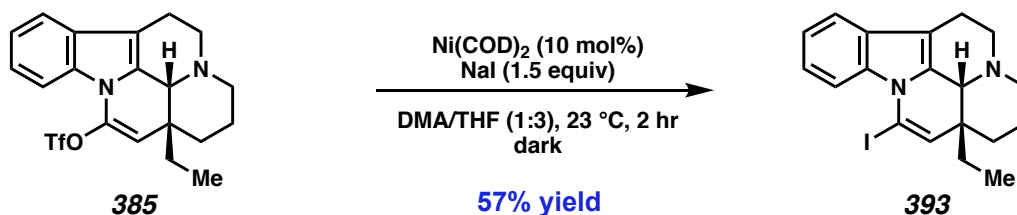
45.3, 39.6, 30.6, 27.9, 20.5, 16.3, 9.0. IR (Neat Film, NaCl); HRMS (ESI/APCI) m/z calculated for $C_xH_xN_xO_x [M + H^+]$: 427.1303, found, 427.1309; $[\alpha]_D^{22.2}$ 38.7° (*c.* 0.07, $CHCl_3$).



Alkenyl bromide 392: To an oven-dried 1-dram vial with stir bar in a nitrogen-filled glove box was added nickel (II) acetate tetrahydrate (1.2 mg, 0.0050 mmol, 0.1 equiv), zinc dust (0.6 mg, 0.01 mmol, 0.2 equiv), 1,5-cyclooctadiene (1.2 μ L, 0.01 mmol, 0.1 equiv), and lithium bromide (8.2 mg, 0.075 equiv, 1.5 mmol). DMA (0.05 mL) and THF (0.15 mL) was added and the reaction was stirred at 26 °C for 5 minutes. Trifloxyenamine **385** (22.7 mg, 0.050 mmol, 1.0 equiv) was added and the reaction was stirred in the dark for 2 hours.

The reaction was removed from the glovebox and quenched with saturated ammonium chloride. The solution was extracted with diethyl ether (3X). The combined organics were washed with brine, dried with sodium sulfate, and concentrated in vacuo. Preparative TLC (40% ethyl acetate in hexanes) afforded alkenyl bromide **385** (10.3 mg, 59% yield) as a colorless oil. 1H NMR (400 MHz, $CDCl_3$) δ 8.25 – 8.19 (m, 1H), 7.44 (dt, $J = 7.7, 1.0$ Hz, 1H), 7.23 – 7.11 (m, 2H), 5.40 (s, 1H), 4.17 (s, 1H), 3.34 (ddd, $J = 13.7, 6.1, 0.8$ Hz, 1H), 3.24 (ddd, $J = 13.7, 11.3, 5.3$ Hz, 1H), 3.00 (dddd, $J = 16.3, 11.4, 6.1, 2.8$ Hz, 1H), 2.61 (dd, $J = 8.8, 2.8$ Hz, 2H), 2.54 – 2.46 (m, 1H), 1.93 – 1.75 (m, 2H), 1.73 – 1.63 (m, 1H), 1.51 (dt, $J = 13.8, 3.3$ Hz, 1H), 1.40 (dp, $J = 13.2, 3.1$ Hz, 1H), 1.13 (td, $J = 13.7, 3.7$ Hz, 1H), 0.99 (t, $J = 7.5$ Hz, 3H); ^{13}C NMR (101 MHz, $CDCl_3$) δ 135.2, 132.8, 129.2, 122.2, 121.2, 120.8, 118.5, 113.2, 111.7, 109.1, 56.4, 51.5, 45.1, 40.7, 29.2, 27.5, 20.6, 16.4, 8.8; IR (Neat Film, NaCl) 2931, 1699, 1605, 1452, 1371, 1269, 1065, 739 cm^{-1} ;

HRMS (ESI/APCI) m/z calculated for $C_{19}H_{22}N_2Br$ $[M + H^+]$: 357.0966, found, 357.0974. $[\alpha]_D^{22.2}$ 13.0° (c 0.27, $CHCl_3$).

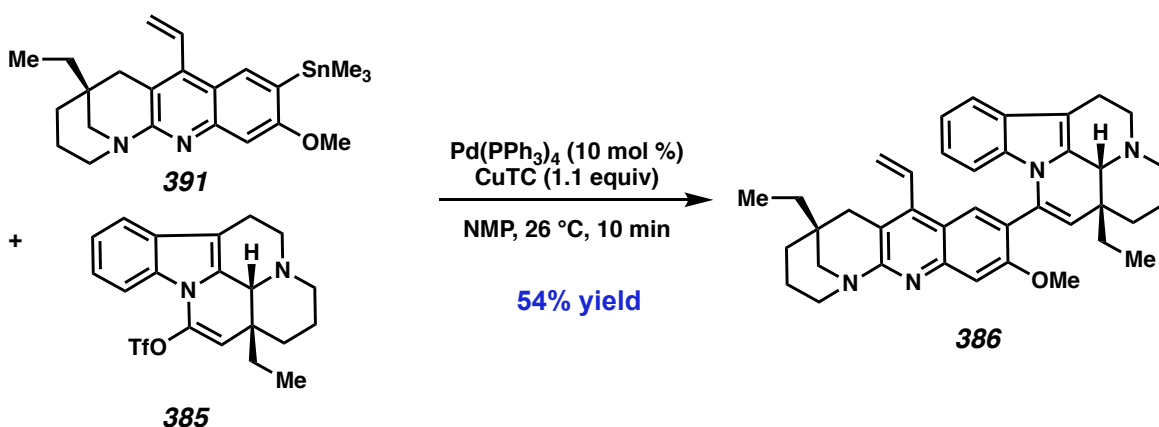


Alkenyl iodide 393: To an oven-dried 1-dram vial with stir bar in a nitrogen-filled glove box was added trifloxyenamine **385** (20.0 mg, 0.050 mmol, 1.0 equiv), *bis*(1,5-cyclooctadiene)nickel (0) (1.3 mg, 0.0050 mmol, 0.1 equiv), and a 3:1 mixture of THF/DMA (0.2 mL). Sodium iodide (10.3 mg, 0.070 equiv, 1.5 mmol) was added, the reaction was removed from the glovebox and stirred in the dark at 23°C for 2 hours.

The reaction was quenched with saturated ammonium chloride. The solution was extracted with diethyl ether (3X). The combined organics were washed with brine, dried with sodium sulfate, and concentrated in vacuo. Preparative TLC (50% ethyl acetate/ hexanes) afforded alkenyl iodide **393** (10.7 mg, 52% yield) as a colorless oil. 1H NMR (400 MHz, $CDCl_3$) δ 8.35 (d, $J = 8.4$ Hz, 1H), 7.50 – 7.39 (m, 1H), 7.20 (dtd, $J = 27.0, 7.3, 1.2$ Hz, 2H), 5.81 (s, 1H), 4.19 (s, 1H), 3.42 – 3.21 (m, 2H), 3.00 (dddd, $J = 17.3, 11.3, 6.2, 2.7$ Hz, 1H), 2.70 – 2.44 (m, 3H), 1.83 (qd, $J = 7.5, 1.6$ Hz, 2H), 1.69 (q, $J = 12.8$ Hz, 1H), 1.50 (dt, $J = 13.7, 3.2$ Hz, 1H), 1.39 (dp, $J = 13.0, 3.1$ Hz, 1H), 1.12 (td, $J = 13.7, 3.7$ Hz, 1H), 0.99 (t, $J = 7.4$ Hz, 3H).; ^{13}C NMR (101 MHz, $CDCl_3$) δ 135.9, 131.9, 129.2, 121.7, 120.8, 118.5, 112.9, 108.5, 79.3, 56.7, 51.4, 44.9, 42.1, 29.9, 28.8, 27.4, 20.5, 16.4, 8.7; IR (Neat Film, NaCl) 2930, 2860, 1589, 1451, 1364, 1271, 1171, 744 cm^{-1} ; HRMS (ESI/APCI) m/z calculated for $C_{19}H_{22}N_2I$ $[M + H^+]$: 405.0828, found, 405.0822. $[\alpha]_D^{22.2}$ -7.0° (c 0.41, $CHCl_3$).



Vinylquinoline stannane 391. To an oven-dried 1-dram vial in a nitrogen filled glove box was added vinylquinoline **318** (25.0 mg, 0.065 mmol, 1.0 equiv), *tetrakis*-(triphenylphosphine)palladium (0) (7.6 mg, 0.0065 mmol, 0.10 equiv) and toluene (0.42 mL). Hexamethylditin (20.0 μL , 0.153 mmol, 1.5 equiv) was added dropwise. The flask was sealed, removed from the glovebox, and heated to 90 $^\circ\text{C}$ for 1.5 hours. Upon completion, the reaction mixture was subjected directly to flash column chromatography (0% \rightarrow 10% \rightarrow 15% acetone/hexanes) to afford stannane **391** (21.2 mg, 70% yield) as a bright yellow oil. ^1H NMR (400 MHz, CDCl_3) δ 8.01 (s, 1H), 7.19 (s, 1H), 6.91 – 6.80 (m, 1H), 5.86 (dd, $J = 11.7, 1.9$ Hz, 1H), 5.56 (dd, $J = 18.0, 1.8$ Hz, 1H), 3.89 (s, 3H), 3.82 – 3.71 (m, 1H), 3.23 – 3.12 (m, 1H), 3.06 (dd, $J = 13.2, 2.1$ Hz, 1H), 2.98 – 2.91 (m, 1H), 2.71 (d, $J = 17.7$ Hz, 1H), 2.59 – 2.49 (m, 1H), 1.75 (dd, $J = 13.2, 3.1$ Hz, 1H), 1.59 – 1.49 (m, 1H), 1.35 (q, $J = 7.4$ Hz, 3H), 1.28 (m, 1H), 0.95 (t, $J = 7.6$ Hz, 3H), 0.30 (s, 9H). ^{13}C NMR (101 MHz, CDCl_3) δ 164.3, 161.6, 149.4, 143.3, 133.4, 132.2, 132.1, 122.6, 121.6, 119.6, 104.6, 104.5, 57.8, 55.9, 55.6, 36.9, 36.3, 35.4, 30.8, 19.6, 7.4, -8.9; IR (Neat Film, NaCl) 2918, 1596, 1555, 1455, 1404, 1364, 1210, 1051, 768; HRMS (ESI/APCI) m/z calculated for $\text{C}_{23}\text{H}_{33}\text{N}_2\text{OSn}$ [$\text{M} + \text{H}^+$]: 473.1615, found, 473.1626. $[\alpha]_{\text{D}}^{22.4}$ 115.1 $^\circ$ (c 0.23, CHCl_3).



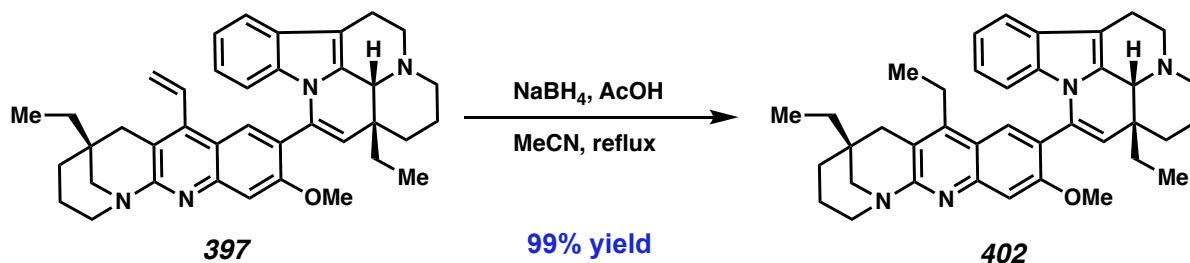
Vinyl dimer 386. To an oven-dried 1-dram vial in a nitrogen filled glove box was added triflate **385** (21.0 mg, 0.0491 mmol, 1.1 equiv), followed by a solution of stannane **391** (21.0 mg, 0.0445 mmol, 1.0 equiv) in NMP, which had been previously degassed through subjugation to five freeze-pump-thaw cycles. The solution was allowed to stir in the glovebox for five minutes. *Tetrakis*(triphenylphosphine) palladium (0) (5.2 mg, 0.0045 mmol, 0.10 equiv) and copper (I) thiophene-2-carboxylate (9.3 mg, 0.0491 mmol, 1.1 equiv) were added in single portions in quick succession. The reaction mixture was allowed to stir at glovebox temperature (26 °C) for 10 minutes, during which the solution turned from yellow to light brown.

The vial was removed from the glovebox, diluted with ethyl acetate, and quenched with saturated sodium bicarbonate. The aqueous layer was extracted with ethyl acetate (3X), before the combined organics were washed with brine (2X), dried with sodium sulfate, and concentrated in vacuo. The crude mixture was passed through a pad of silica gel (eluting with 5% methanol in dichloromethane) to remove excess NMP, and the eluent was concentrated again in vacuo. Preparative TLC (7% methanol/dichloromethane) afforded vinyl dimer **386** (14.1 mg, 54% yield, 4:1 mixture of atropisomers) as a light yellow foam.

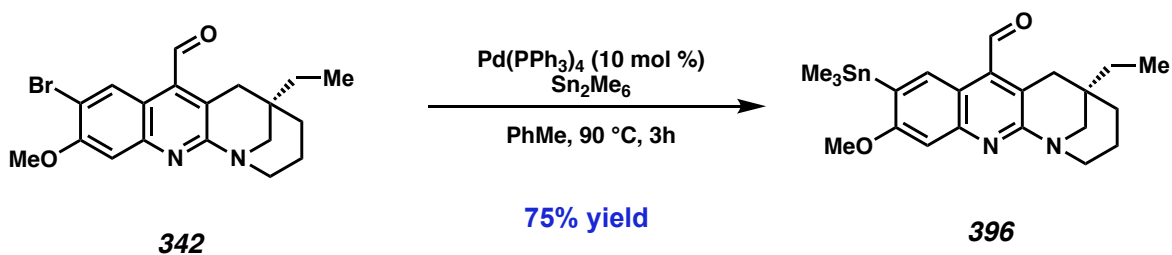
Major atropisomer: ^1H NMR (400 MHz, C_6D_6) δ 8.33 (s, 1H), 7.60 (s, 1H), 7.58 – 7.47 (m, 1H), 7.09 (ddd, $J = 7.9, 7.1, 1.0$ Hz, 1H), 6.87 (ddd, $J = 8.4, 7.1, 1.3$ Hz, 1H), 6.70 (dt, $J = 8.4, 0.9$ Hz, 1H), 6.60 – 6.49 (m, 1H), 5.46 (dd, $J = 11.7, 1.9$ Hz, 1H), 5.35 (dd, $J = 17.9, 1.9$ Hz, 1H), 5.25 (s, 1H), 4.41 (d, $J = 2.5$ Hz, 1H), 4.25 – 4.14 (m, 1H), 3.15 – 3.05 (m, 2H), 3.12 (s, 3H), 3.05 – 2.95 (m, 1H), 2.94 – 2.73 (m, 3H), 2.65 – 2.56 (m, 1H), 2.54 – 2.36 (m, 3H), 2.33 – 2.21 (m, 1H), 2.06 – 1.94 (m, 1H), 1.93 – 1.77 (m, 1H), 1.76 – 1.62 (m, 1H), 1.51 – 1.38 (m, 2H), 1.34 – 1.26 (m, 2H), 1.26 – 1.15 (m, 3H), 1.09 – 1.00 (m, 2H), 1.00 – 0.92 (m, 3H) 0.79 – 0.73 (m, 3H). ^{13}C NMR (101 MHz, C_6D_6) δ 163.1, 159.3, 150.2, 143.6, 135.6, 134.9, 132.5, 132.0, 131.5, 129.7, 126.9, 122.6, 122.5, 122.1, 120.1, 119.4, 118.6, 118.2, 111.5, 107.9, 107.5, 57.8, 57.0, 56.1, 55.4, 52.0, 45.5, 37.6, 37.6, 37.2, 36.1, 35.4, 30.7, 30.3, 28.0, 21.2, 20.0, 16.8, 9.0, 7.3.

Minor atropisomer: ^1H NMR (400 MHz, C_6D_6) δ 8.32 (s, 1H), 7.74 (s, 1H), 7.58 – 7.47 (m, 2H), 6.76 – 6.60 (m, 2H), 6.39 (dd, $J = 17.9, 11.7$ Hz, 1H), 5.30 – 5.21 (m, 2H), 5.19 (s, 1H), 4.28 (s, 1H), 4.25 – 4.14 (m, 1H), 3.36 (s, 3H), 3.15 – 3.05 (m, 2H), 3.05 – 2.95 (m, 1H), 2.94 – 2.73 (m, 3H), 2.65 – 2.56 (m, 1H), 2.54 – 2.36 (m, 3H), 2.33 – 2.21 (m, 1H), 2.06 – 1.94 (m, 1H), 1.93 – 1.77 (m, 1H), 1.76 – 1.62 (m, 1H), 1.51 – 1.38 (m, 2H), 1.34 – 1.26 (m, 2H), 1.26 – 1.15 (m, 3H), 1.09 – 1.00 (m, 2H), 1.00 – 0.92 (m, 3H) 0.73 – 0.66 (m, 3H). ^{13}C NMR (101 MHz, C_6D_6) δ 163.2, 159.2, 149.8, 143.7, 135.1, 134.5, 130.0, 129.6, 127.8, 125.6, 122.9, 121.9, 121.9, 120.6, 120.0, 119.9, 119.1, 118.8, 113.3, 112.4, 109.0, 108.1, 57.7, 56.9, 56.8, 55.5, 52.2, 45.4, 37.6, 37.1, 36.0, 35.3, 28.9, 27.6, 20.9, 20.1, 16.8, 9.1, 8.7, 7.3.

IR: 2930, 2854, 1618, 1453, 1417, 1371, 1226, 1216, 1195, 752 cm. HRMS (ESI/APCI) m/z calculated for $\text{C}_{39}\text{H}_{45}\text{N}_4\text{O}$ $[\text{M} + \text{H}^+]$: 585.3515, found, 585.3582. $[\alpha]_{\text{D}}^{22.4}$ 131.0° (c 0.45, CHCl_3).

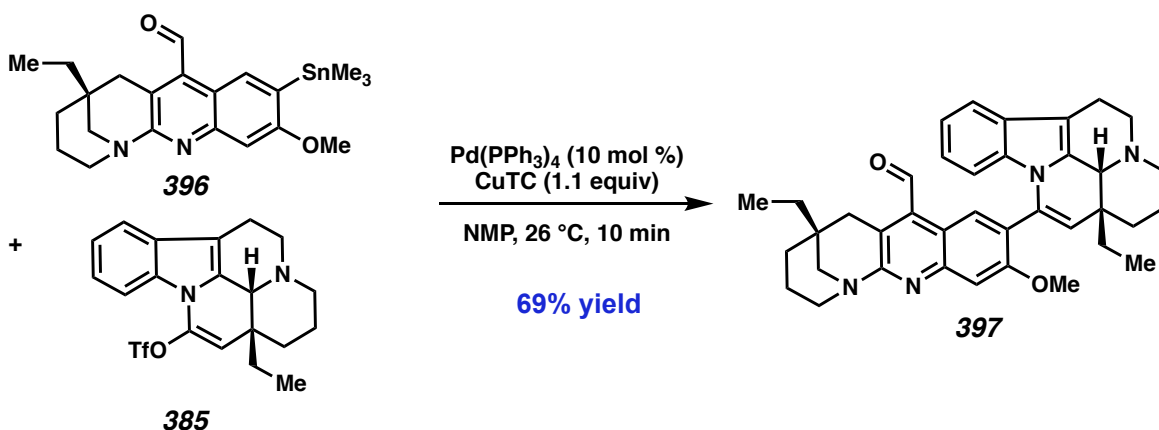


Ethylquinoline 402. To a flame-dried, one-dram vial with stir bar was charged vinyl dimer **392** (1.0 mg, 0.0017 mmol, 1.0 equiv) and methanol (0.17 mL). Sodium borohydride (6.4 mg, 0.17 mmol, 100.0 equiv) was added and the reaction was heated to 60 °C for 20 minutes. The reaction mixture was cooled to room temperature, quenched with saturated sodium bicarbonate, and extracted with ethyl acetate (3X). The combined organic extracts were dried with sodium sulfate and concentrated *in vacuo*. Preparative TLC (7% methanol/dichloromethane) afforded ethyl quinoline **402** (1.0 mg, 99% yield) as an amorphous white solid. Product characterization data was not obtained due to the Spring 2020 COVID-19 shutdown of research facilities.



Formylquinoline stannane 396. To a flame-dried 1-dram vial in a nitrogen filled glove box was added formylquinoline **342** (122.0 mg, 0.315 mmol, 1.0 equiv), *tetrakis*(triphenylphosphine) palladium (0) (37.0 mg, 0.0320 mmol, 0.10 equiv) and toluene (2.1 mL). Hexamethylditin (98.0 μL , 0.473 mmol, 1.5 equiv) was added dropwise. The vial was sealed, removed from the glovebox, and heated to 90 °C for 3 hours. Upon completion, the reaction mixture was subjected directly to flash column chromatography (0%→10%→15% acetone/hexanes) to afford formylquinoline

stannane **396** (112.1 mg, 75% yield) as a bright yellow oil. ^1H NMR (600 MHz, CDCl_3) δ 11.03 (s, 1H), 8.43 (s, 1H), 7.23 (s, 1H), 3.91 (s, 3H), 3.81 (d, $J = 13.6$ Hz, 1H), 3.25 – 3.17 (m, 2H), 3.13 (dd, $J = 13.3, 2.2$ Hz, 1H), 3.02 – 2.95 (m, 2H), 1.78 (d, $J = 13.5$ Hz, 1H), 1.64 – 1.57 (m, 1H), 1.40 (q, $J = 7.6$ Hz, 2H), 1.33 (hept, $J = 4.2$ Hz, 1H), 0.99 (t, $J = 7.6$ Hz, 3H), 0.34 (s, 9H). ^{13}C NMR (101 MHz, CDCl_3) δ 194.2, 164.5, 162.4, 150.0, 135.8, 134., 131.3, 125.9, 118.2, 104.7, 57.3, 56.2, 55.6, 36.0, 35.3, 31.1, 30.7, 19.7, 7.4, -8.8. IR (Neat Film, NaCl) 2924, 2852, 2363, 1698, 1596, 1456, 1403, 1363, 1211, 1046, 758 cm^{-1} ; HRMS (ESI/APCI) m/z calculated for $\text{C}_x\text{H}_x\text{N}_x\text{O}_x$ [$\text{M} + \text{H}^+$]: 475.1408, found, 475.1434. $[\alpha]_{\text{D}}^{22.4}$ 142.7° (c 0.09, CHCl_3).



Formyl dimer 397. To a flame-dried 10 mL round-bottom flask with stir bar in a nitrogen filled glove box was added triflate **385** (30.0 mg, 0.0698 mmol, 1.1 equiv), followed by a solution of stannane **396** (30.0 mg, 0.0634 mmol, 1.0 equiv) in NMP (1.25 mL), which had been previously degassed through subjugation to five freeze-pump-thaw cycles. The solution was allowed to stir in the glovebox for five minutes. *Tetrakis*(triphenylphosphine) palladium (0) (7.3 mg, 0.0064 mmol, 0.10 equiv) and copper (I) thiophene-2-carboxylate (13.3 mg, 0.0698 mmol, 1.1 equiv) were

added in a single portion in quick succession. The reaction mixture was allowed to stir at glovebox temperature (26 °C) for 10 minutes, during which the solution turned from yellow to light brown.

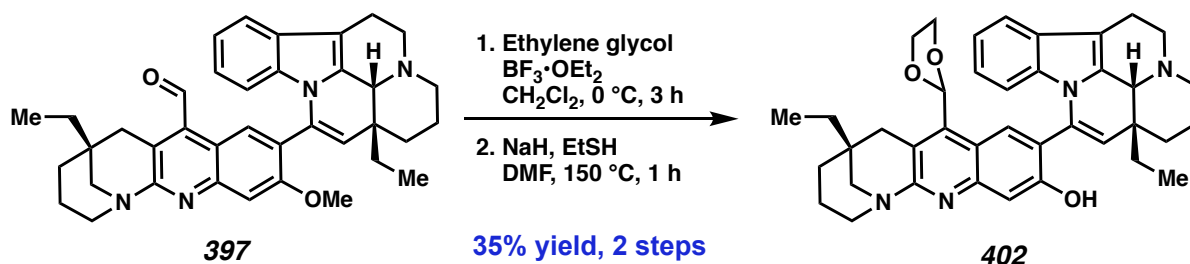
The vial was removed from the glovebox, diluted with ethyl acetate, and quenched with saturated sodium bicarbonate. The aqueous layer was extracted with ethyl acetate (3X), before the combined organics were washed with brine (2X), dried with sodium sulfate, and concentrated in vacuo. The crude mixture was passed through a pad of silica gel (eluting with 5% methanol in dichloromethane) to remove excess NMP, and the eluent was concentrated again in vacuo. Preparative TLC (7% methanol/dichloromethane) afforded formyl dimer **397** (25.5 mg, 69% yield) as a light yellow foam.

Major atropisomer: ^1H NMR (400 MHz, CDCl_3) δ 11.01 (s, 1H), 8.49 (s, 1H), 7.44 – 7.37 (m, 1H), 7.33 (s, 1H), 7.01 – 6.91 (m, 1H), 6.79 – 6.68 (m, 1H), 6.09 (dt, $J = 8.4, 0.9$ Hz, 1H), 5.14 (s, 1H), 4.41 (s, 1H), 3.94 – 3.82 (m, 1H), 3.61 (s, 3H), 3.49 – 3.34 (m, 2H), 3.32 – 3.14 (m, 3H), 3.14 – 2.94 (m, 3H), 2.90 – 2.69 (m, 2H), 2.66 – 2.53 (m, 1H), 1.95 (dp, $J = 29.2, 7.3$ Hz, 2H), 1.85 – 1.75 (m, 2H), 1.72 – 1.55 (m, 2H), 1.54 – 1.23 (m, 6H), 1.01 (q, $J = 7.6$ Hz, 6H). ^{13}C NMR (101 MHz, CDCl_3) δ 193.5, 163.5, 159.1, 149.2, 134.8, 134.3, 131.1, 130.7, 128.9, 127.5, 127.1, 126.2, 121.6, 119.6, 119.0, 118.2, 117.3, 111.8, 107.7, 107.1, 57.1, 56.7, 56.3, 56.0, 52.1, 45.4, 37.5, 35.9, 35.9, 35.2, 30.8, 30.0, 27.6, 20.8, 20.0, 16.6, 9.0, 7.4.

Minor atropisomer: ^1H NMR (400 MHz, CDCl_3) δ 10.85 (s, 1H), 8.39 (s, 1H), 7.46 (s, 1H), 7.44 – 7.37 (m, 1H), 7.01 – 6.91 (m, 1H), 6.79 – 6.68 (m, 1H), 6.21 (dt, $J = 8.4, 0.9$ Hz, 1H), 5.01 (s, 1H), 4.41 (s, 1H), 3.94 – 3.82 (m, 1H), 3.87 (s, 3H), 3.49 – 3.34 (m, 2H), 3.32 – 3.14 (m, 3H), 3.14 – 2.94 (m, 3H), 2.90 – 2.69 (m, 2H), 2.66 – 2.53 (m, 1H), 1.95 (dp, $J = 29.2, 7.3$ Hz, 1H), 1.85 – 1.75 (m, 3H), 1.72 – 1.55 (m, 2H), 1.54 – 1.23 (m, 6H), 1.01 (q, $J = 7.6$ Hz, 6H). ^{13}C NMR (101 MHz, CDCl_3) δ 193.5, 163.5, 159.1, 149.2, 134.3, 131.3, 131.1, 130.2, 128.9, 127.5, 127.1, 126.2,

121.6, 119.6, 119.0, 118.2, 117.3, 111.8, 107.7, 107.1, 57.1, 56.7, 56.3, 56.0, 52.0, 45.4, 37.5, 35.9, 35.9, 35.2, 30.8, 30.0, 27.6, 20.8, 20.0, 16.6, 9.0, 7.4.

IR: 2923, 1694, 1456, 1214, 1042, 754, 744 cm^{-1} HRMS (ESI/APCI) m/z calculated for $\text{C}_{38}\text{H}_{43}\text{N}_4\text{O}_2$ $[\text{M} + \text{H}^+]$: 587.3386, found, 587.3368. $[\text{M} + \text{H}^+]$; $[\alpha]_{\text{D}}^{22.4}$ 381.8° (c 0.32, CHCl_3).



Phenol 402: To a flame dried, 10-mL round-bottom flask with stir bar was added a solution of formyl dimer **397** (23.8 mg, 0.405 mmol, 1.0 equiv) in dichloromethane (2.7 mL). Ethylene glycol was added (50 μL , 0.41 mmol, 10.0 equiv) before the reaction was cooled to 0°C . Boron trifluoride diethyl etherate (23 μL , 0.41 mmol, 10.0 equiv) was added dropwise and the reaction was stirred for 2 hours. Additional ethylene glycol (50 μL , 0.41 mmol, 1.0 equiv) was then added and the reaction was stirred for an additional 1 hour.

After the reaction was complete, as determined by LCMS, the flask was warmed to room temperature and quenched with 1M NaOH. The solution was transferred to a separatory funnel, the organic layer was separated, and the aqueous layer was extracted with ethyl acetate (3X). The combined organic extracts were washed with brine, dried with sodium sulfate, and concentrated in vacuo. The combined organic extracts were filtered through a plug of silica gel, eluting with 10% methanol in dichloromethane. The eluent was concentrated in vacuo, transferred to a one-dram vial, dried under high vacuum for 30 minutes, and used directly in the next reaction.

The crude material was charged with a stir bar, placed under nitrogen atmosphere, and charged with a freshly prepared solution of 0.4M sodium ethanethiol in DMF (2.0 mL, 0.810 mmol, 20.0 equiv). A teflon-lined cap was quickly added, and the reaction was heated to 150 °C for 10 minutes. Upon completion of the reaction, the vial was cooled to room temperature, quenched with 1:1 30% ammonium hydroxide solution/brine, and extracted with ethyl acetate (5X). The combined organic extracts were washed with 10% lithium chloride solution, brine, and water, dried with sodium sulfate, and concentrated in vacuo. Preparative TLC (8% methanol/dichloromethane) afforded phenol **402** (9.0 mg, 36% yield) as a light, yellow oil.

Major atropisomer: ^1H NMR (400 MHz, CDCl_3) δ 8.14 (s, 1H), 7.86 (s, 1H), 7.36 – 7.30 (m, 1H), 6.87 (t, $J = 7.4$ Hz, 1H), 6.36 (s, 1H), 6.28 (t, $J = 7.8$ Hz, 1H), 5.86 (d, $J = 8.5$ Hz, 1H), 5.17 (s, 1H), 4.39 (s, 1H), 4.36 – 4.26 (m, 2H), 4.22 – 4.10 (m, 1H), 3.87 – 3.82 (m, 1H), 3.45 – 3.29 (m, 3H), 3.12 (td, $J = 13.2, 3.4$ Hz, 1H), 3.06 – 2.98 (m, 1H), 2.84 – 2.74 (m, 3H), 2.69 (d, $J = 11.2$ Hz, 2H), 2.53 (dd, $J = 37.2, 15.8$ Hz, 1H), 2.20 – 2.14 (m, 1H), 2.04 – 1.82 (m, 2H), 1.81 – 1.60 (m, 3H), 1.60 – 1.30 (m, 6 H), 1.01 (dt, $J = 11.4, 7.4$ Hz, 3H), 0.92 (dt, $J = 15.1, 7.5$ Hz, 3H). ^{13}C NMR (101 MHz, CDCl_3) δ 160.6, 155.9, 148.9, 137.2, 134.7, 134.6, 130.9, 128.5, 126.7, 126.3, 124.7, 121.6, 119.5, 118.9, 117.8, 117.6, 113.3, 111.2, 107.1, 100.7, 65.6, 65.6, 56.6, 55.8, 55.6, 51.6, 45.2, 37.3, 36.0, 35.1, 35.0, 30.5, 29.8, 27.6, 20.8, 19.5, 16.6, 8.9, 7.4.

Minor atropisomer: ^1H NMR (600 MHz, CDCl_3) δ 8.04 (s, 1H), 7.60 (s, 2H), 7.43 (d, $J = 7.8$ Hz, 1H), 7.02 (t, $J = 7.3$ Hz, 1H), 6.85 – 6.80 (m, 1H), 6.43 (d, $J = 8.4$ Hz, 1H), 6.18 (s, 1H), 4.36 – 4.26 (m, 1H), 4.22 – 4.10 (m, 3H), 3.91 (d, $J = 13.6$ Hz, 1H), 3.87 – 3.82 (m, 2H), 3.72 (td, $J = 7.7, 6.4$ Hz, 1H), 3.45 – 3.29 (m, 1H), 3.20 (td, $J = 13.0, 3.3$ Hz, 1H), 3.12 (td, $J = 13.2, 3.4$ Hz, 1H), 3.06 – 2.98 (m, 1H), 2.93 (d, $J = 17.6$ Hz, 1H), 2.84 – 2.74 (m, 3H), 2.69 (d, $J = 11.2$ Hz, 2H), 2.56 (dd, $J = 37.2, 15.8$ Hz, 1H), 2.04 – 1.82 (m, 1H), 1.81 – 1.60 (m, 3H), 1.60 – 1.30 (m,

6 H), 1.01 (dt, $J = 11.4, 7.4$ Hz, 3H), 0.92 (dt, $J = 15.1, 7.5$ Hz, 3H). ^{13}C NMR (101 MHz, CDCl_3) δ 162.3, 154.6, 148.5, 137.7, 134.3, 131.9, 131.2, 128.9, 127.0, 125.1, 122.4, 121.8, 119.9, 119.8, 118.4, 117.8, 113.5, 111.7, 108.1, 100.4, 65.4, 64.9, 56.7, 56.5, 56.0, 37.5, 35.3, 32.1, 31.9, 30.9, 29.5, 29.4, 27.6, 22.8, 20.0, 16.7, 14.3, 8.9, 7.4.

IR: 2924, 1614, 1455, 1214, 968, 757, HRMS (ESI/APCI) m/z calculated for $\text{C}_{39}\text{H}_{44}\text{N}_4\text{O}_3$ [$\text{M} + \text{H}^+$]: 617.3492, found, 617.3477. $[\alpha]_{\text{D}}^{22.4}$ 6.4° (c 0.50, CHCl_3).

0.4M Sodium Ethanethiol Stock Solution. To a flame-dried 25-mL round bottom flask with stir bar was added DMF (10 mL) and thioethanol (0.29 mL). Sodium hydride (160 mg, 60% dispersion in mineral oil) was added portionwise. The solution was then stirred for 10 minutes prior to use. Freshly prepared solutions of sodium ethanethiol tend to result in a cleaner reaction profile and shorter reaction times.

3.8.3 Computational Details

All quantum mechanical calculations were performed with ORCA version 4.2.0.¹ Geometry optimizations and frequency calculations were carried out with the Becke's three parameter B3LYP global hybrid generalized gradient approximation (hybrid-GGA) density functional paired with Becke–Johnson damped D4 dispersion corrections (henceforth referred to as D4). For optimization and frequency calculation, all atoms are described with the split valence def2-SV(P) basis set. Thermal corrections (at 298 K, 1 atm standard state) were calculated from the unscaled vibrational frequencies at this level of theory. The Quasi-RRHO method was applied to correct for the breakdown of the harmonic oscillator approximation for low frequency vibrations. All stationary points are characterized by the appropriate number of imaginary vibrational modes (zero for optimized geometries). Triple- \otimes quality single point calculations were

carried out on all stationary points with the B3LYP-D4 density functional with the def2-TZVPP basis set¹¹ on all atoms. The SMD implicit solvation model for THF was employed in these single point calculations to include effects of solvation (CDS corrections included). Gas phase single point calculations were carried out for comparison. Thermal corrections obtained at the previous level of theory are then applied to these solvated electronic energies to obtain the reported free energies (G_{298}). Henceforth this level of theory is denoted as B3LYP-D4/def2-TZVPP-SMD(THF)/B3LYP-D4/def2-SV(P).

The resolution of identity (RI) and chain-of-spheres (keyword = RIJCOSX) approximations were utilized for coulomb and exchange integrals, respectively. The fitted def2/J auxiliary basis sets was employed. The finest integration grid settings (Grid7, GridX9, NoFinalGrid) were utilized in all calculations.

3.8.4 Additional References

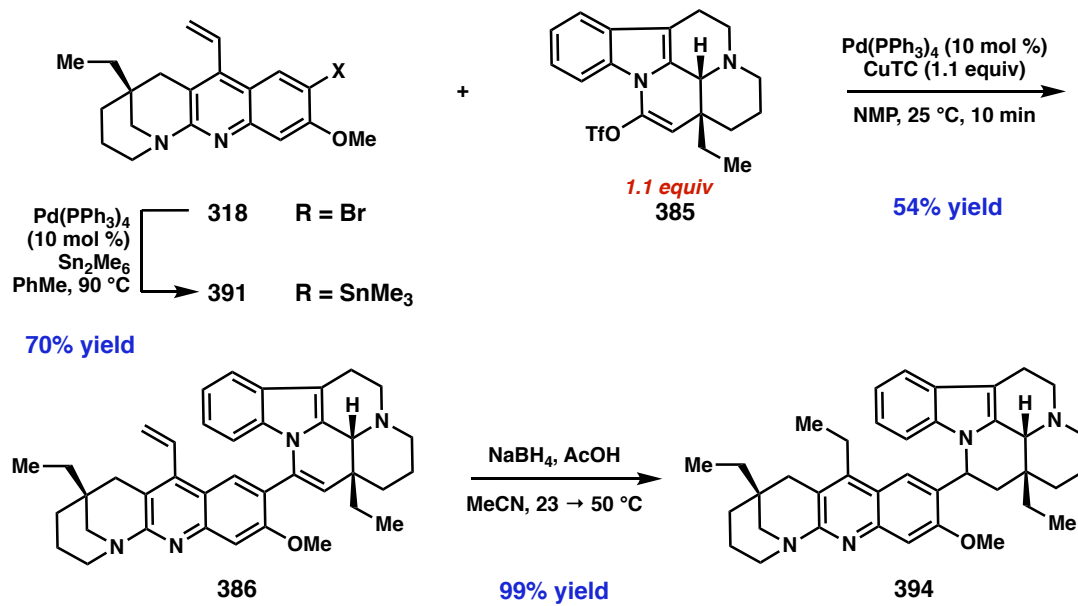
- (1) Pangborn, A. M.; Giardello, M. A.; Grubbs, R. H.; Rosen, R. K.; Timmers, F. J. *Organometallics* **1996**, *15*, 1518–1520.
- (2) Fulmer, G.R, Miller, A.J.M.; Sherden, N.H.; Gottlieb, H.E.; Nudelman, A.; Stoltz, B.M.; Bercaw, J.E.; Goldberg, K.I. *Organometallics* **2010**, *29*, 2176–2179.
- (3) Allred, G. D.; Liebeskind, L. S. *J. Am. Chem. Soc.* **1996**, *118*, 2748–2749.
- (4) Dai, J-K.; Dan, W-J.; Du, H-T.; Zhang, J-W.; Wang, J-R *Bioorg. Med. Chem. Lett.* **2016**, *26*, 580–583.

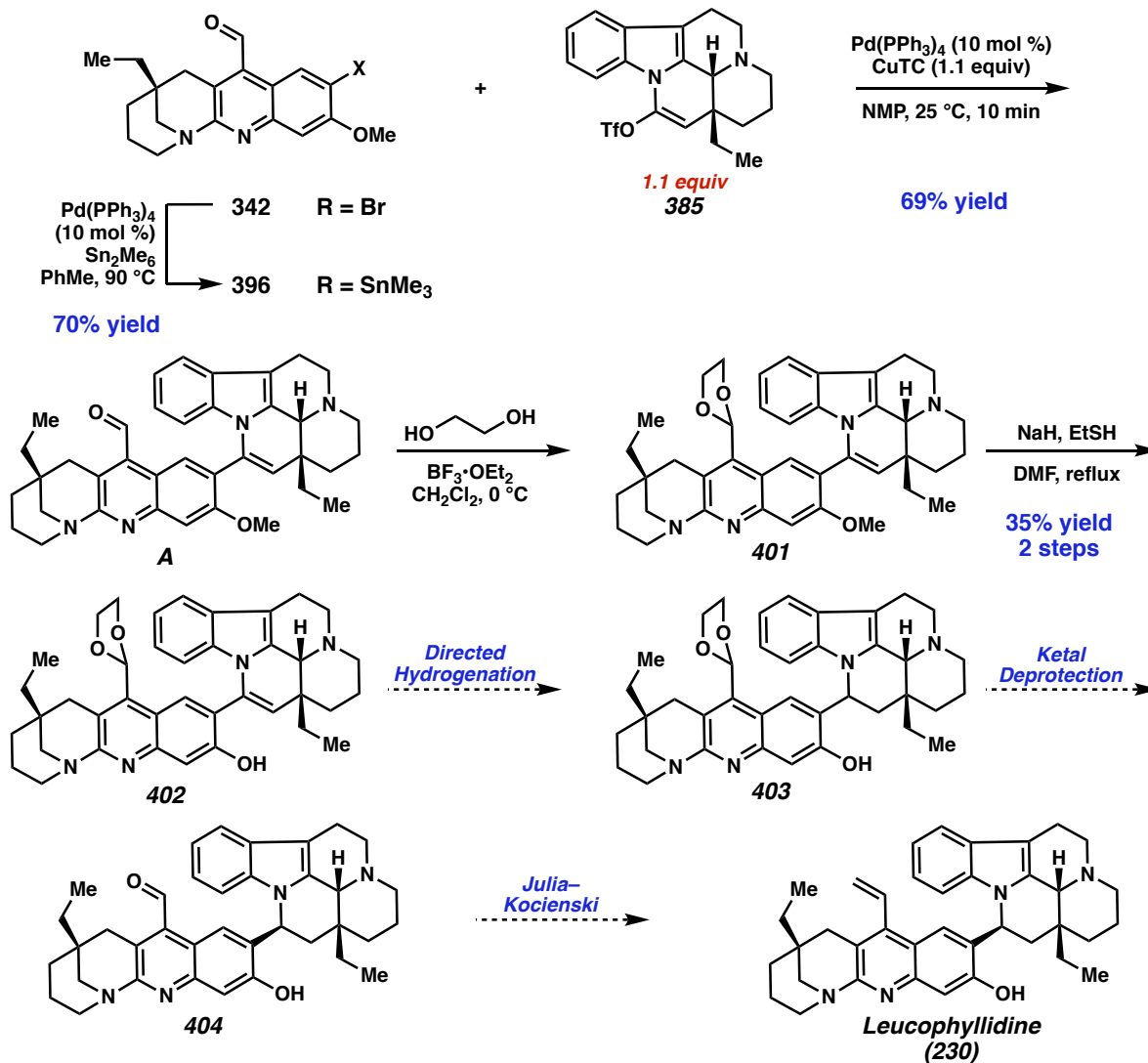
APPENDIX 3

Synthetic Summary for Chapter 3:

Progress towards a Convergent

Total Synthesis of Leucophyllidine

Scheme A3.1. Vinyl Stille coupling and undesired reduction

Scheme A3.2. Formyl Stille coupling and proposed endgame

APPENDIX 4

Spectra Relevant to Chapter 3:

Progress toward a Convergent

Total Synthesis of Leucophyllidine

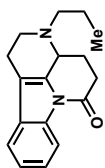
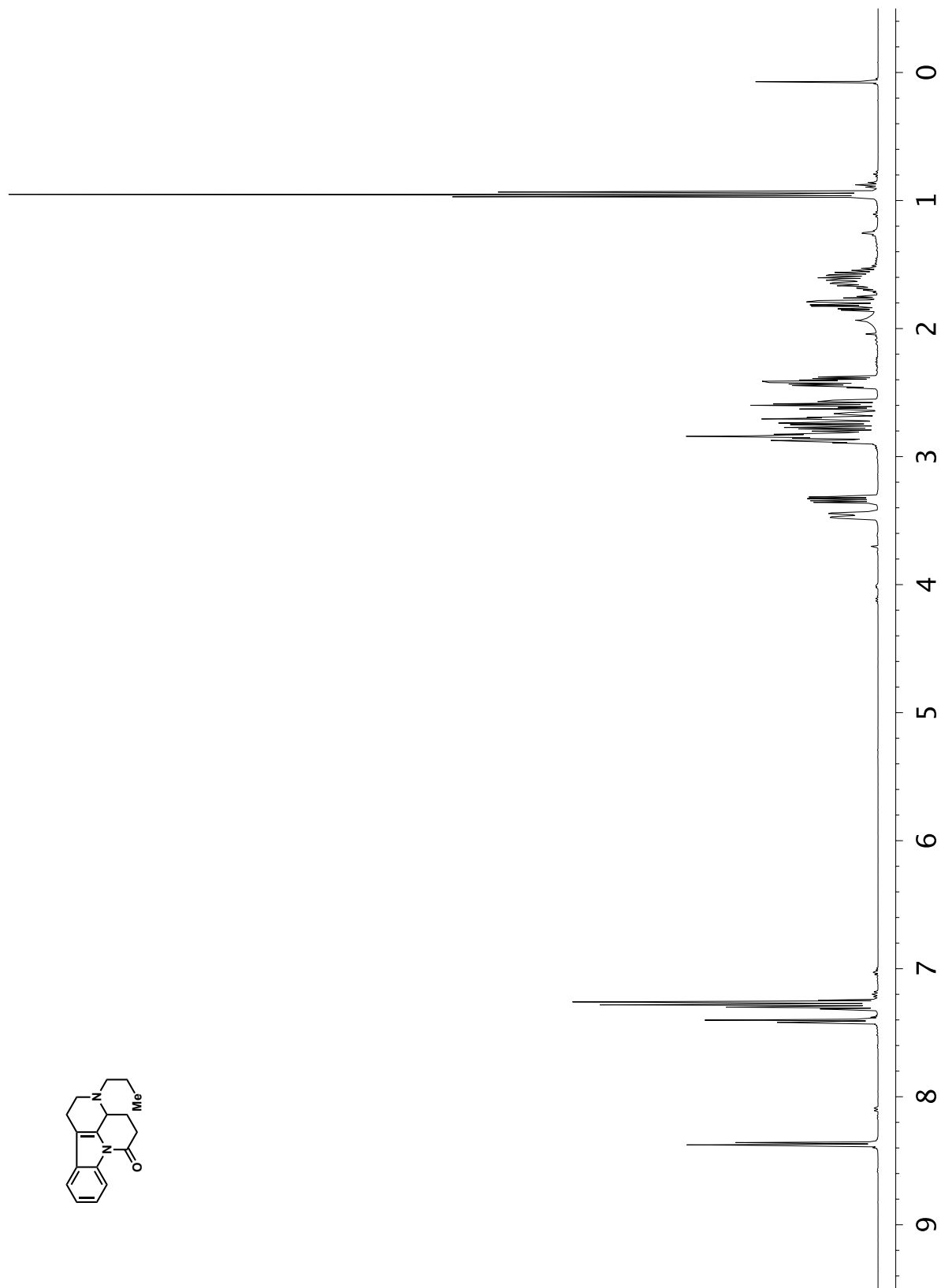


Figure A4.1 ^1H NMR (400 MHz, CDCl_3) of compound **364**.

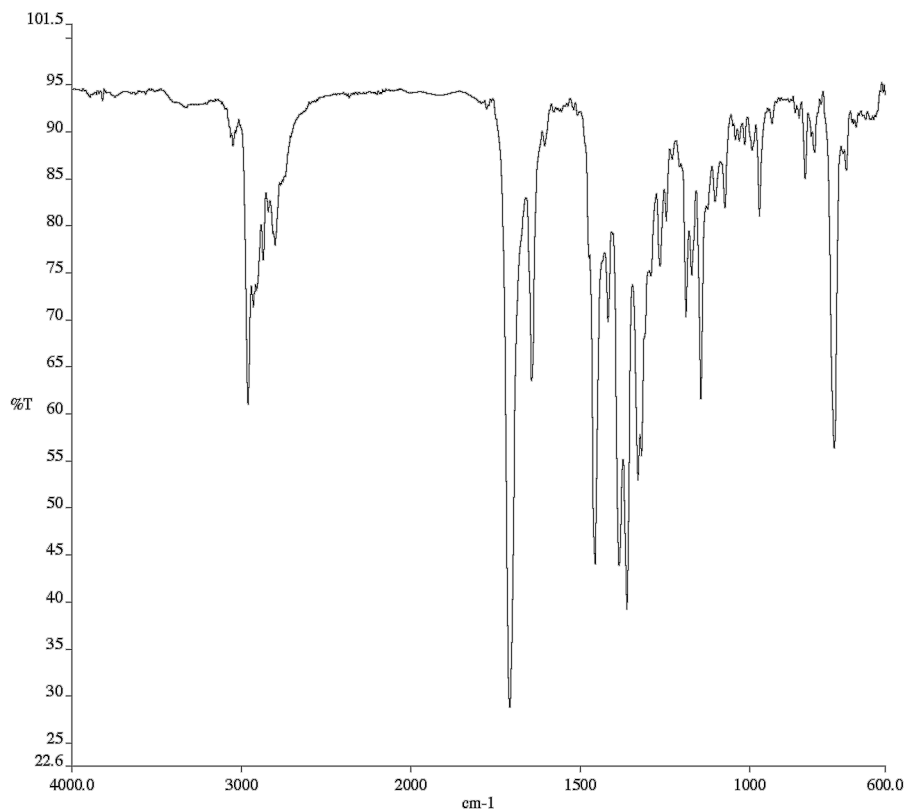


Figure A4.2. Infrared spectrum (Thin Film, NaCl) of compound **364**.

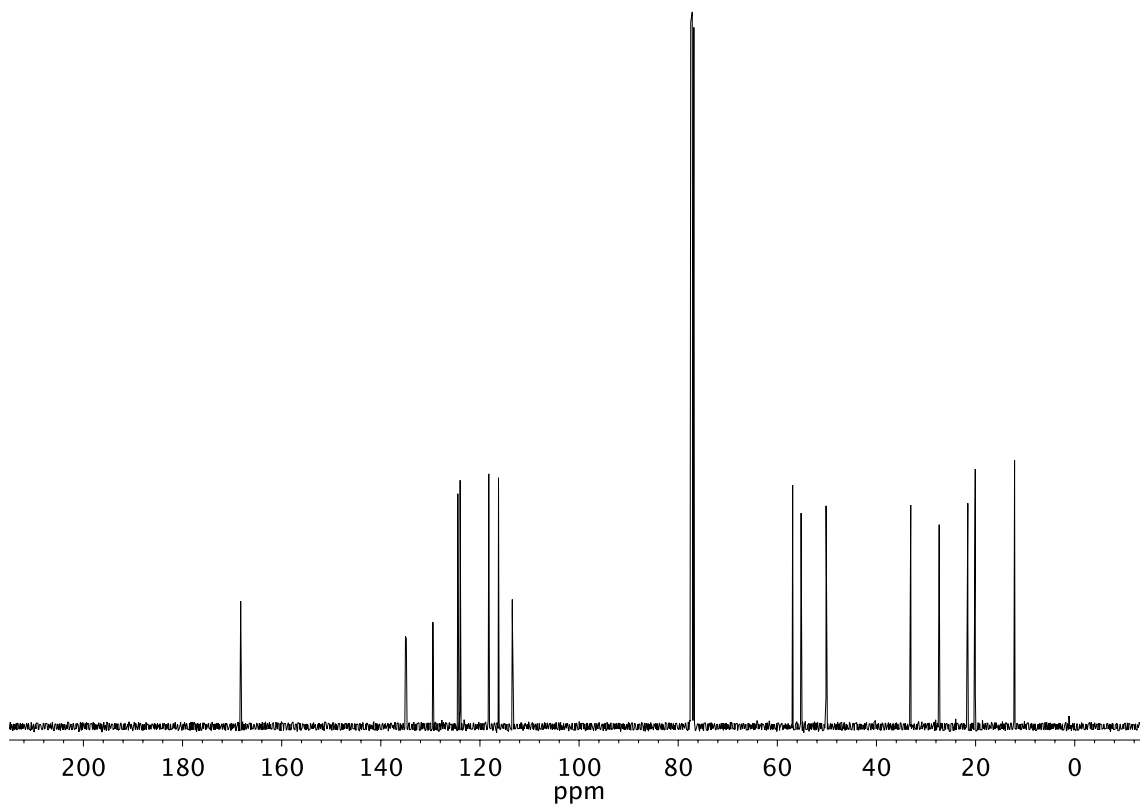


Figure A4.3. ¹³C NMR (101 MHz, CDCl₃) of compound **364**.

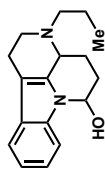
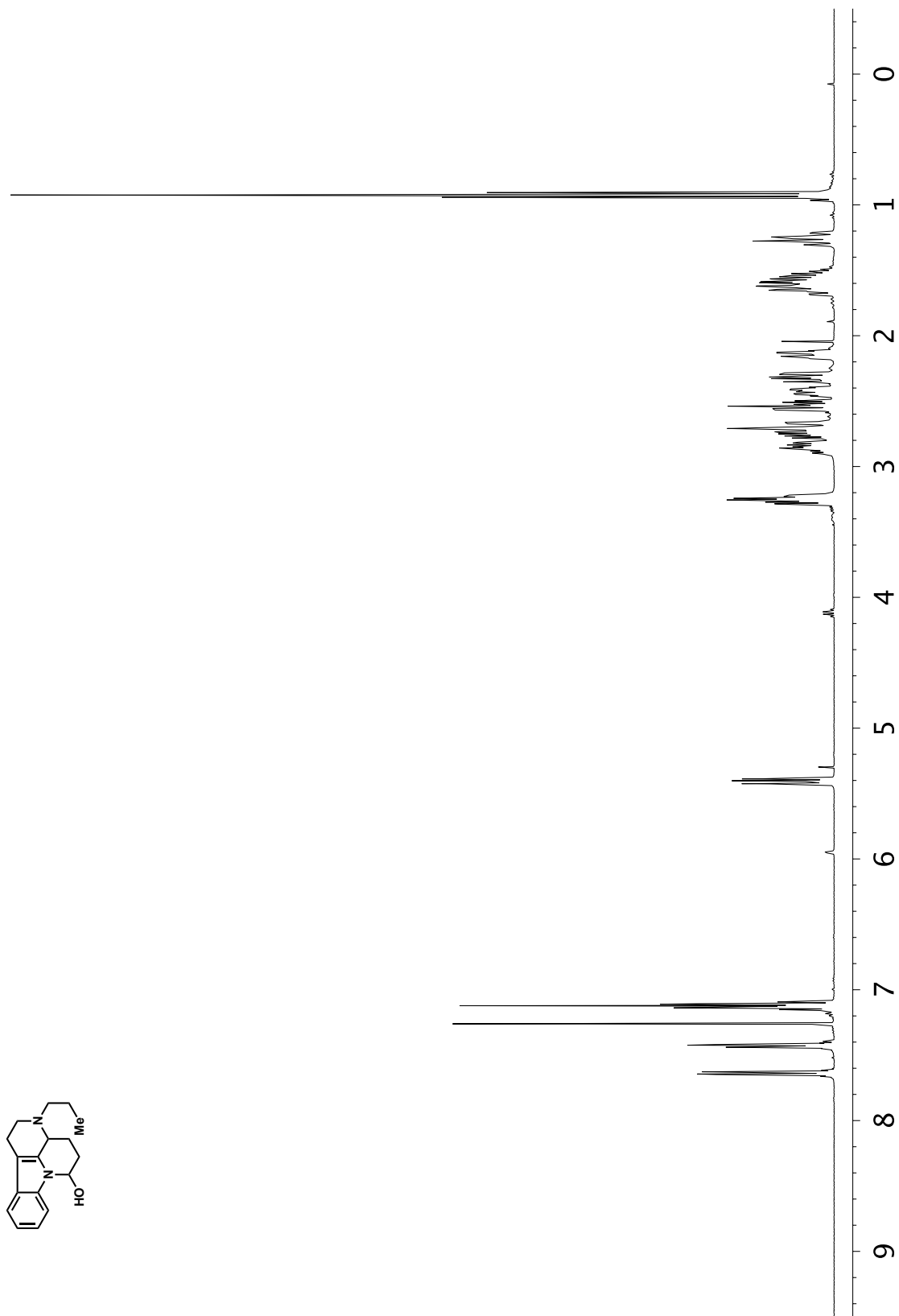


Figure A4.4. ¹H NMR (400 MHz, CDCl₃) of compound 364.

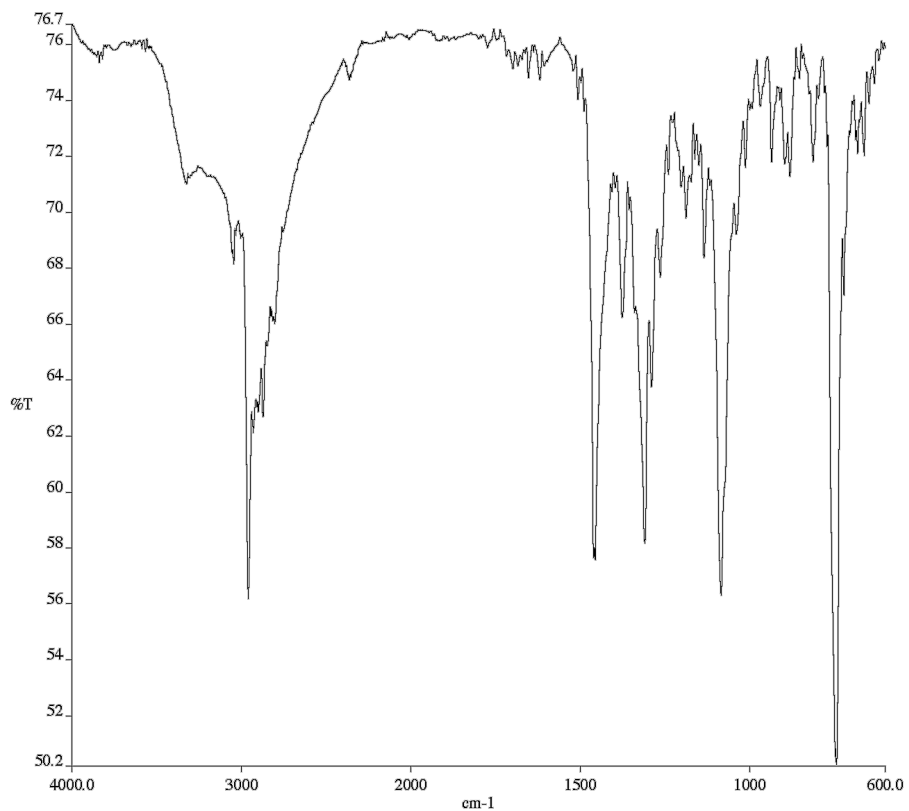


Figure A4.5. Infrared spectrum (Thin Film, NaCl) of compound **364**.

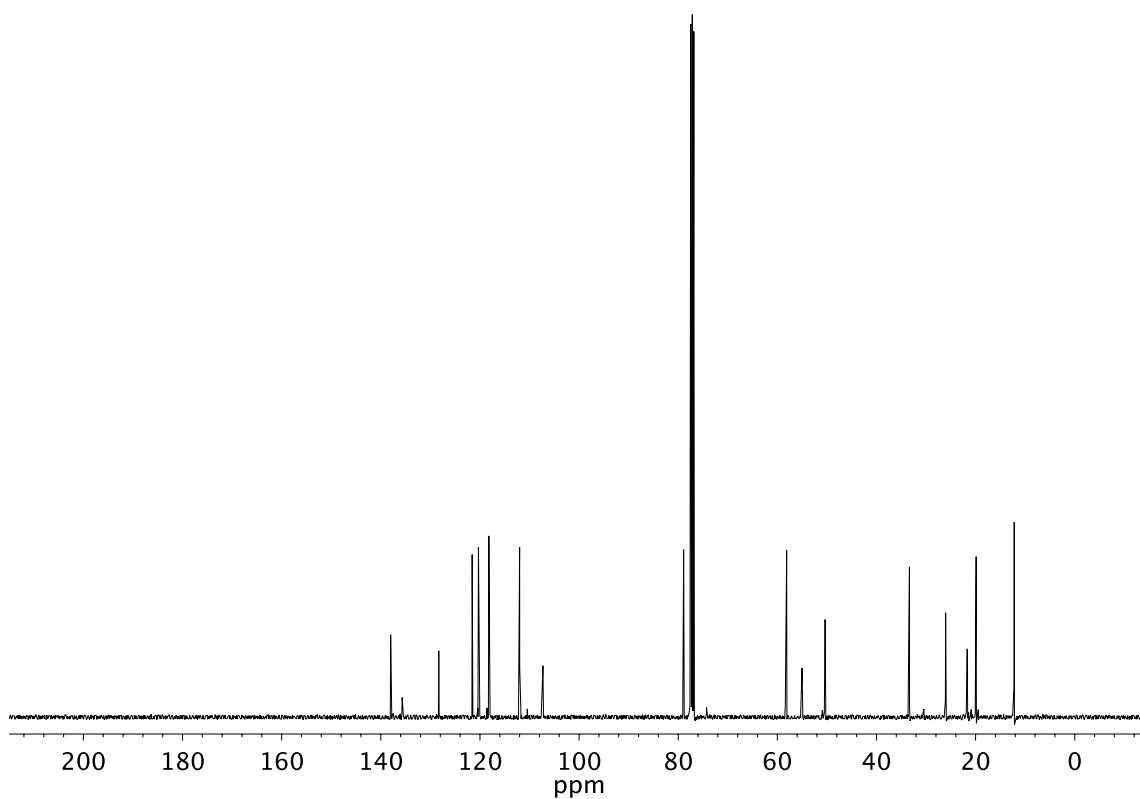


Figure A4.6. ¹³C NMR (101 MHz, CDCl₃) of compound **364**.

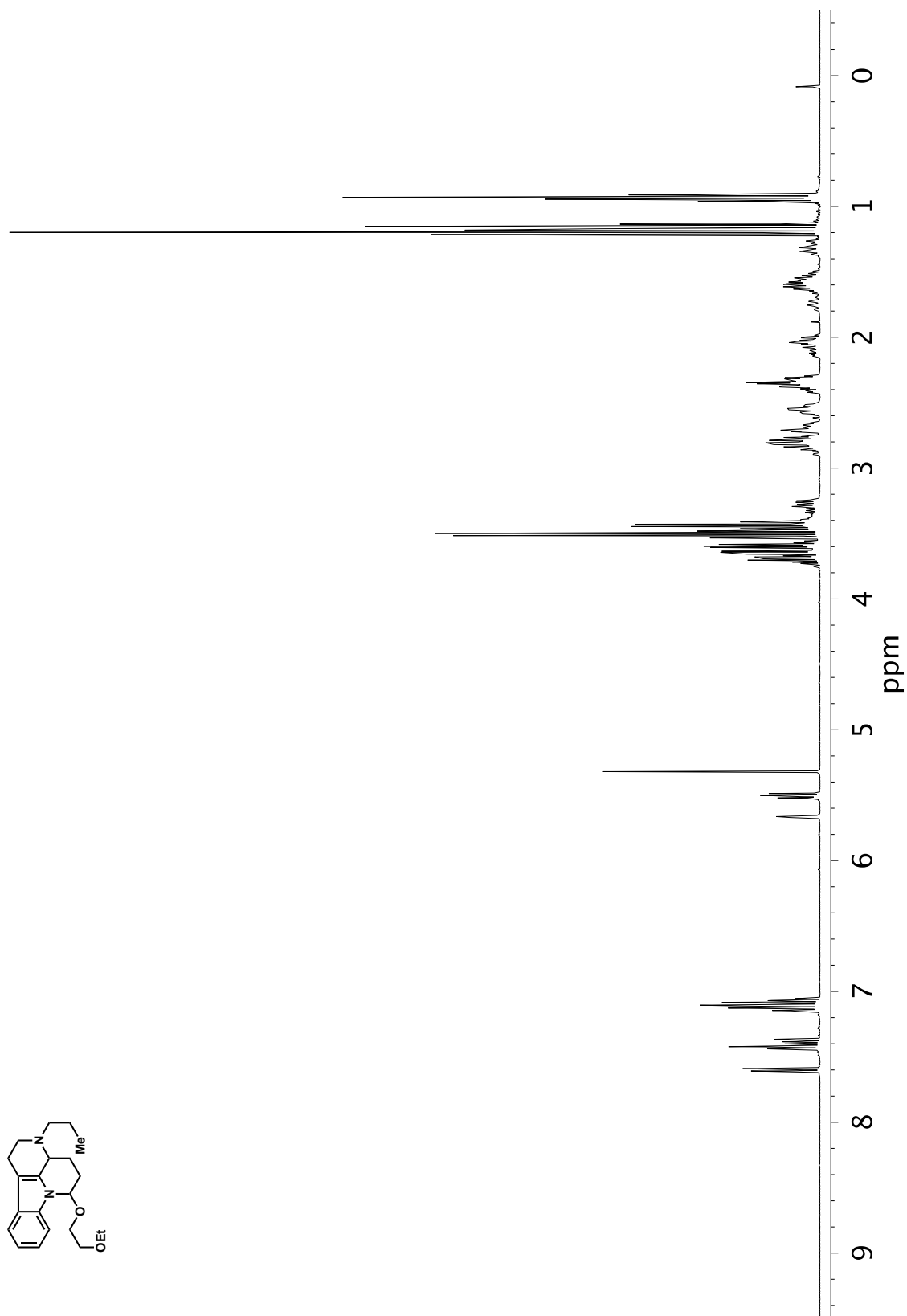


Figure A4.7. $^1\text{H NMR}$ (400 MHz, CD_2Cl_2) compound **379c**.

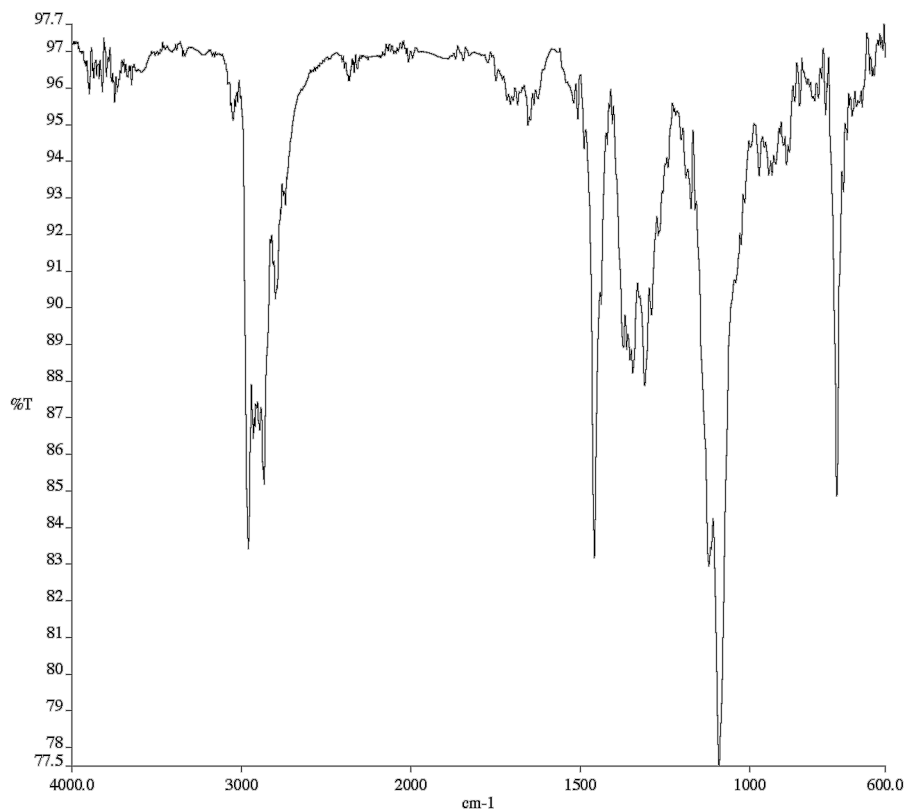


Figure A4.8. Infrared spectrum (Thin Film, NaCl) of compound **379c**.

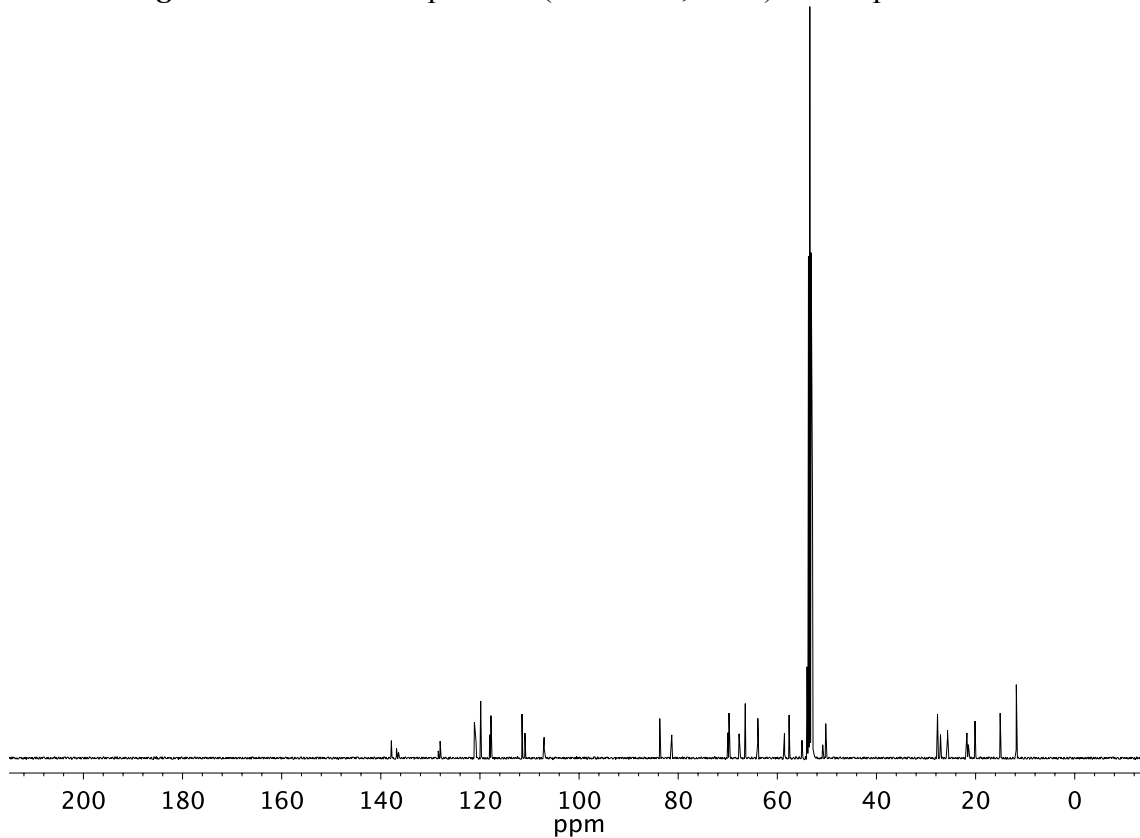


Figure A4.9. ¹³C NMR (101 MHz, CD₂Cl₂) of compound **379c**.

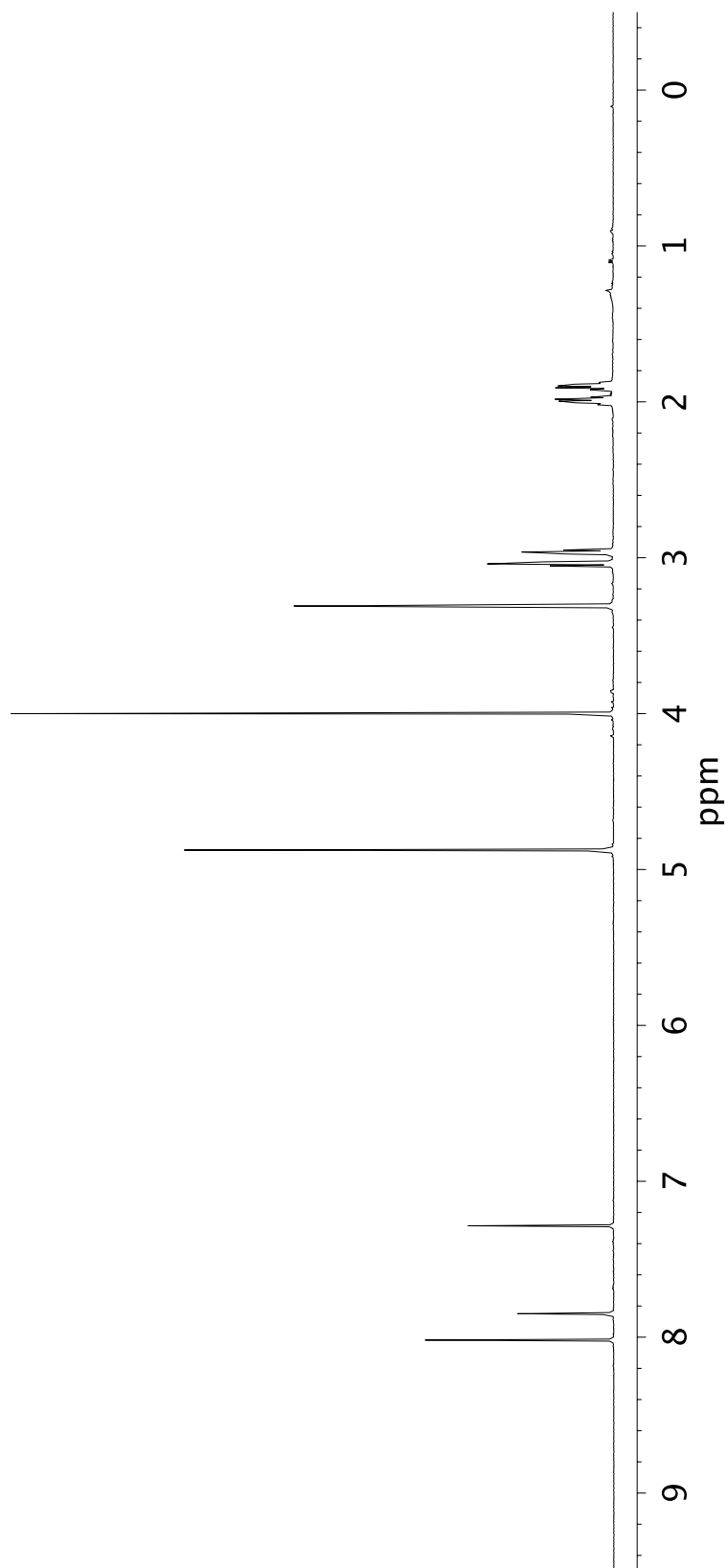
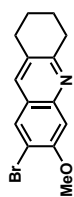


Figure A4.10. ¹H NMR (400 MHz, CDCl₃) of compound 367.

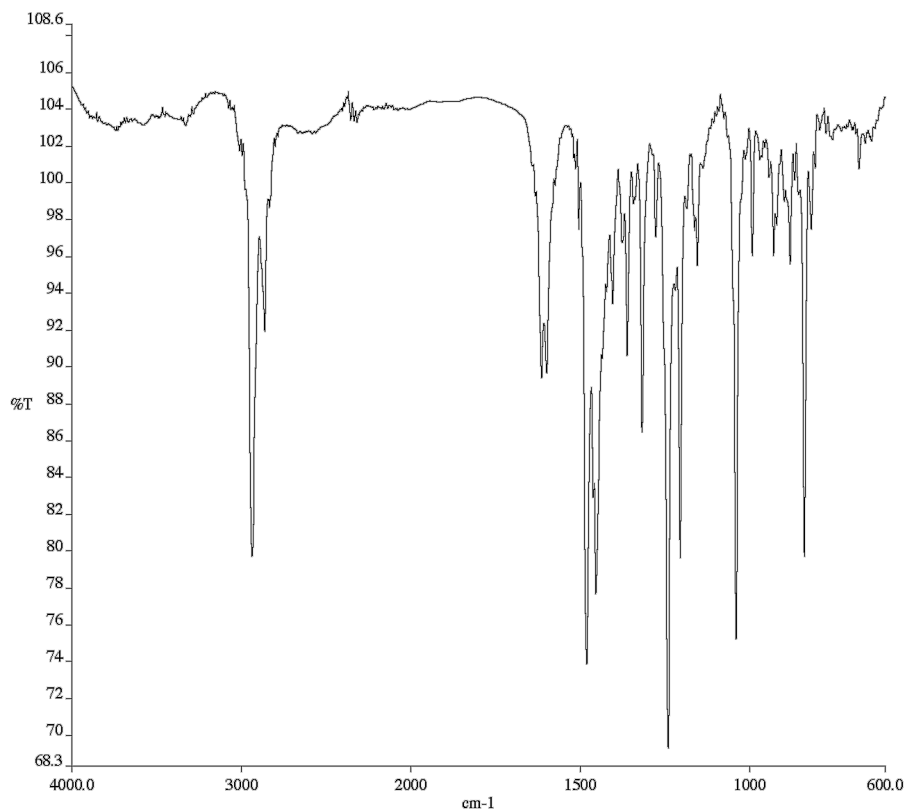


Figure A4.11. Infrared spectrum (Thin Film, NaCl) of compound **367**.

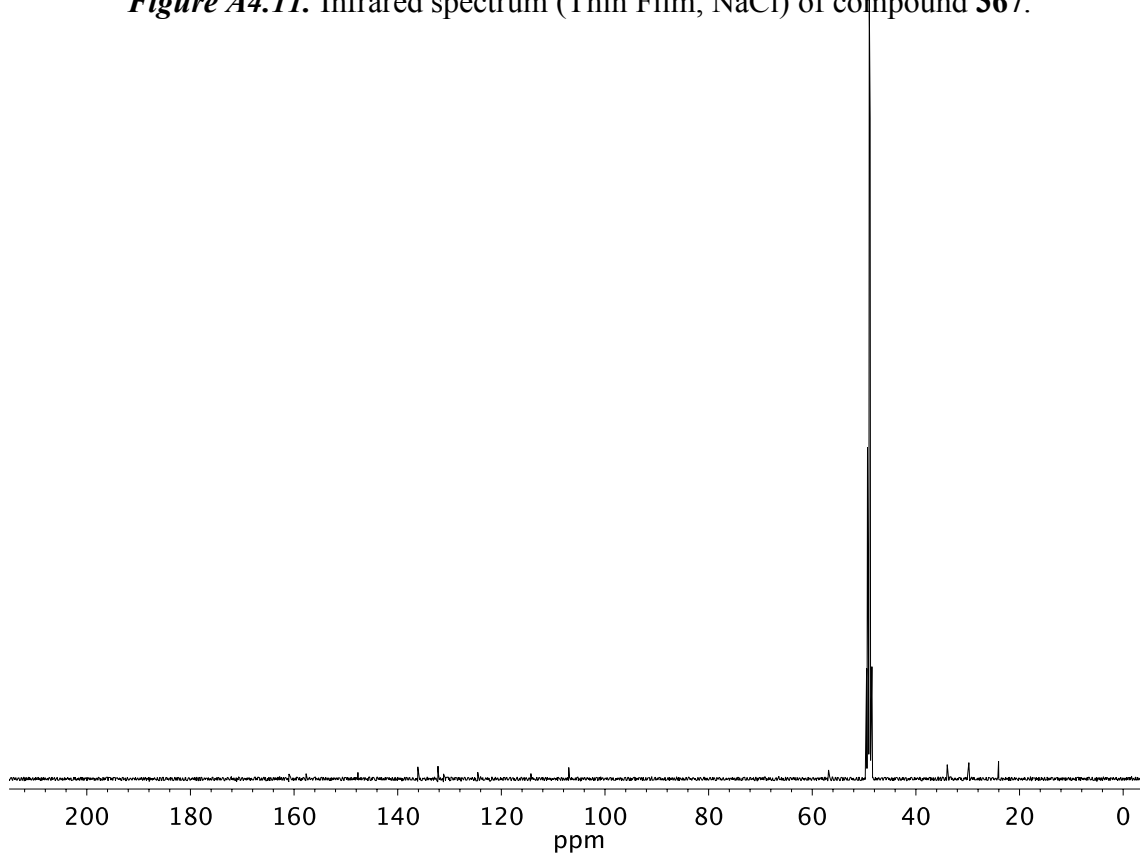


Figure A4.12. ¹³C NMR (101 MHz, CDCl₃) of compound **367**.

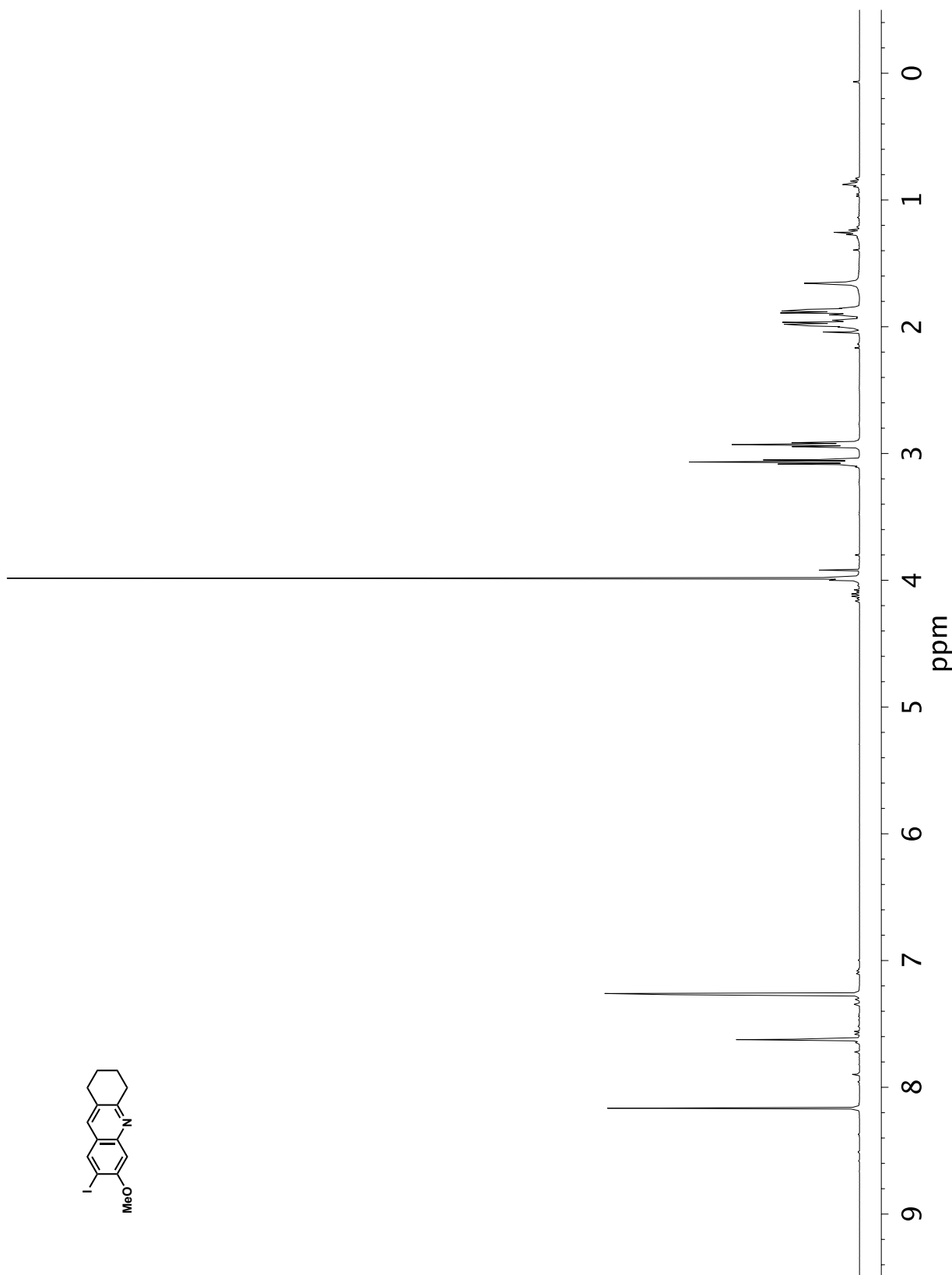


Figure A4.13. ¹H NMR (400 MHz, CDCl₃) of P compound **380**.

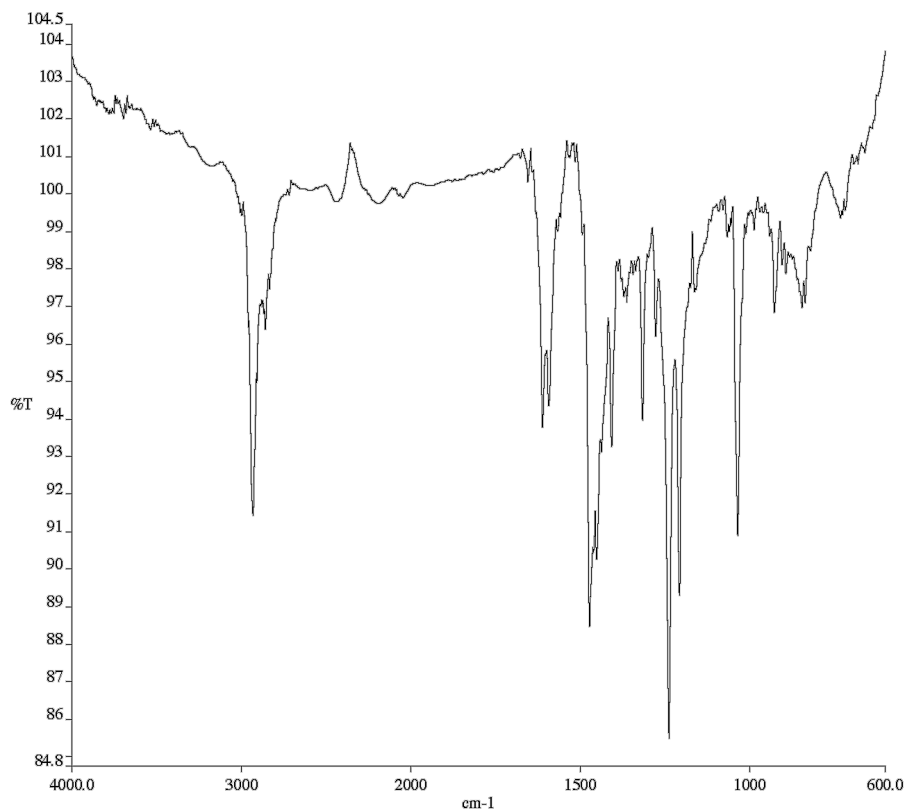


Figure A4.14. Infrared spectrum (Thin Film, NaCl) of compound **380**.

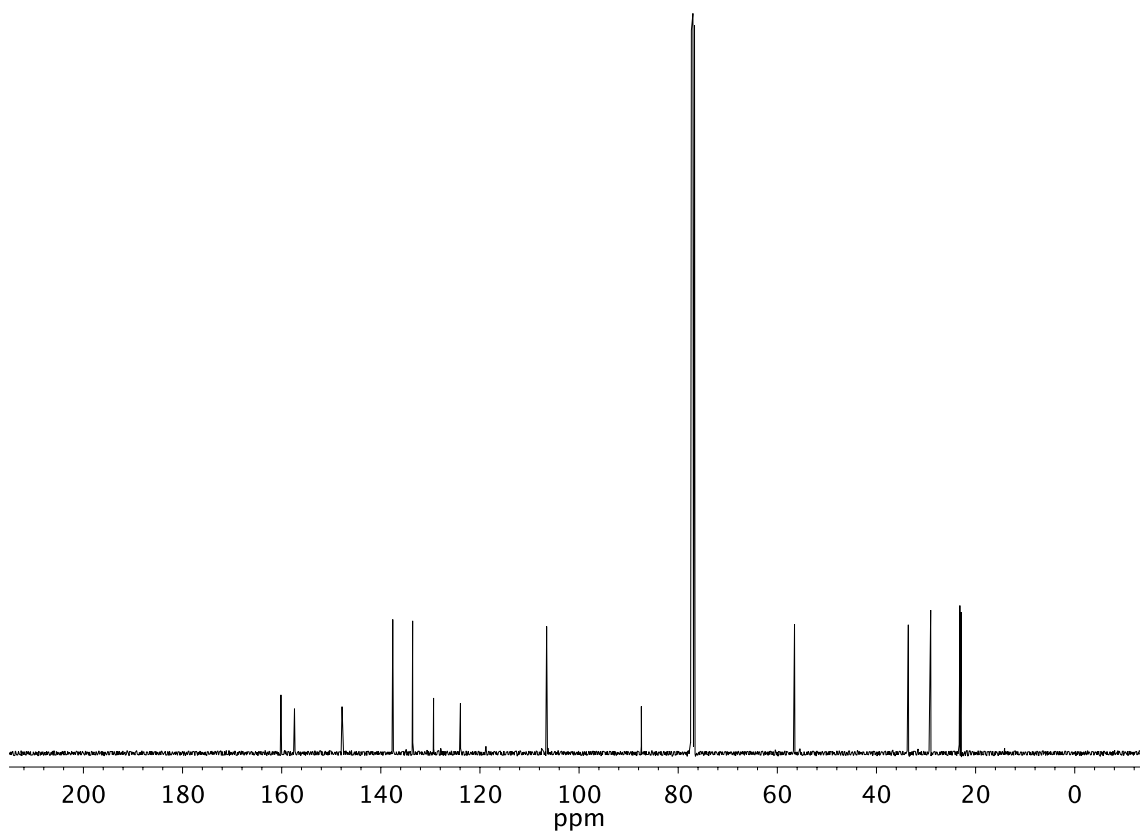


Figure A4.15. ¹³C NMR (101 MHz, CDCl₃) of compound **380**.

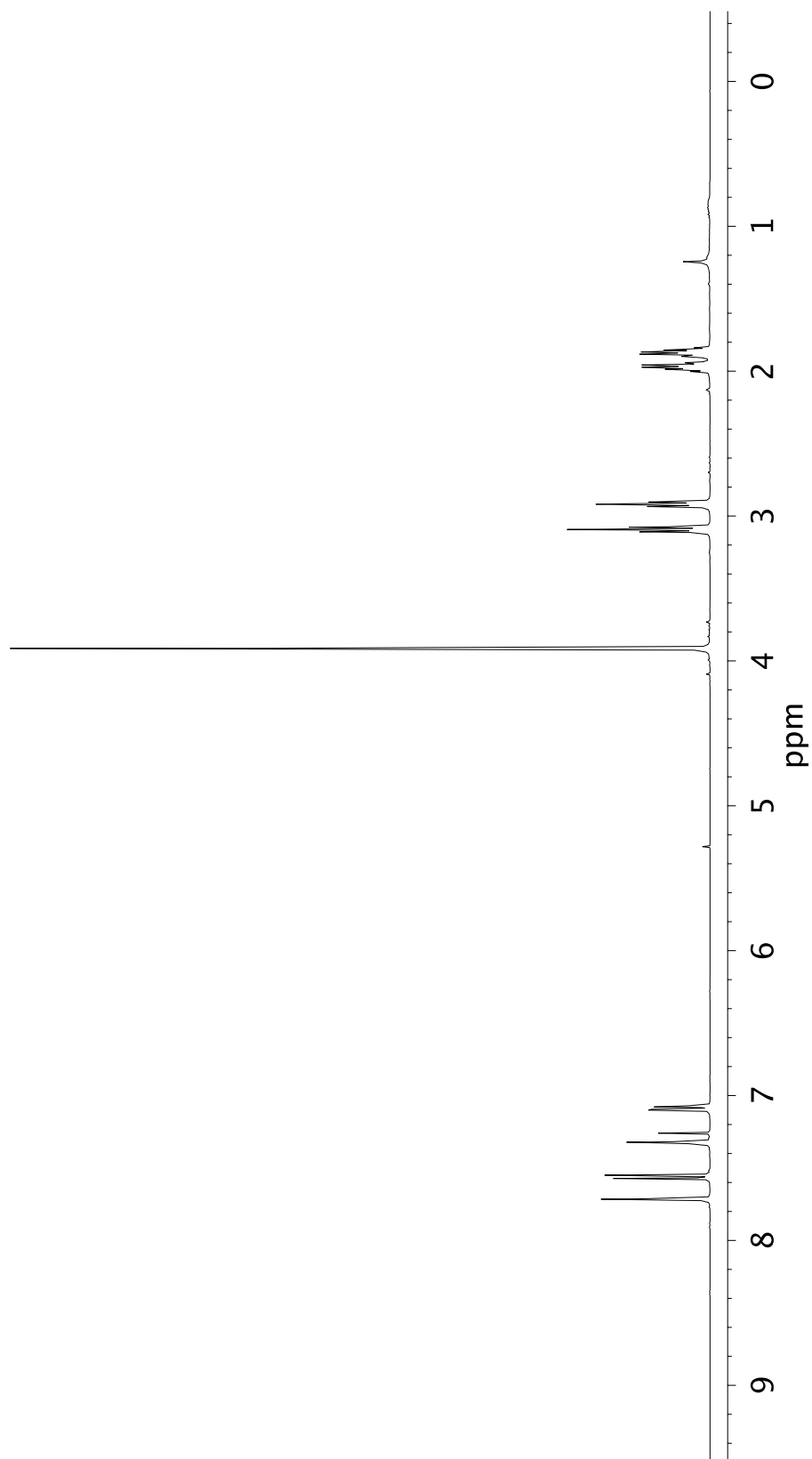
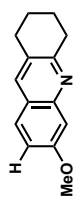


Figure A4.16. ¹H NMR (400 MHz, CDCl₃) of P compound **381**.

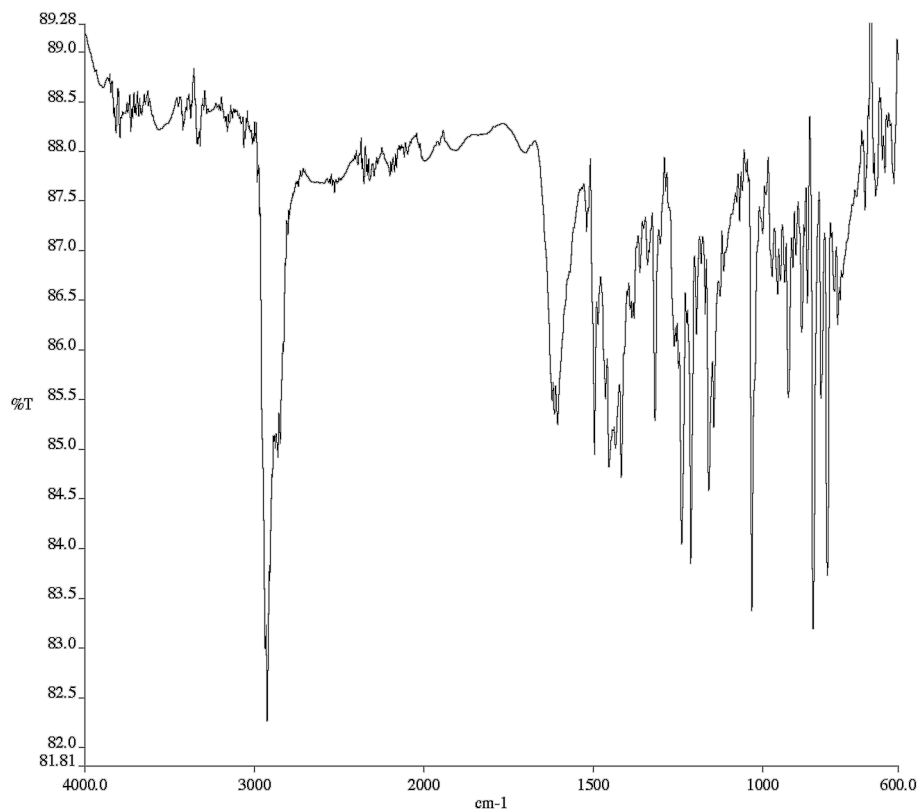


Figure A4.17. Infrared spectrum (Thin Film, NaCl) of compound **361**.

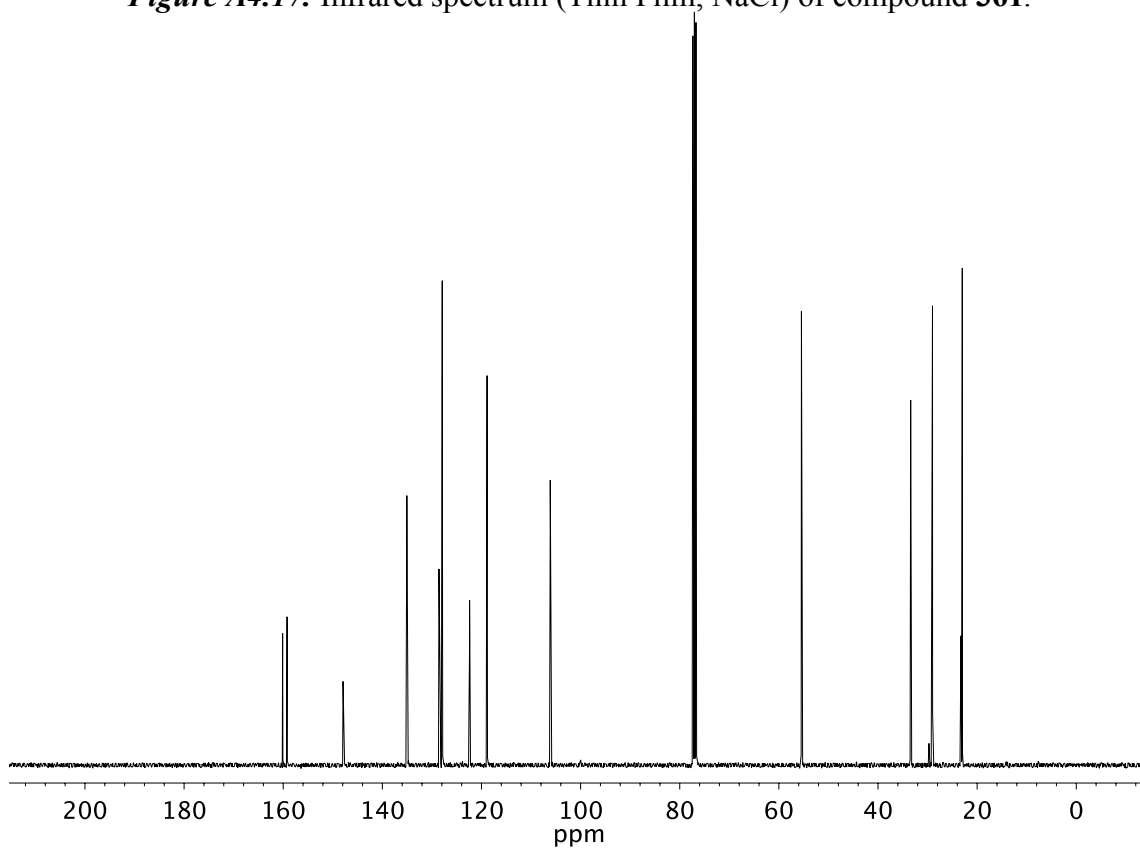
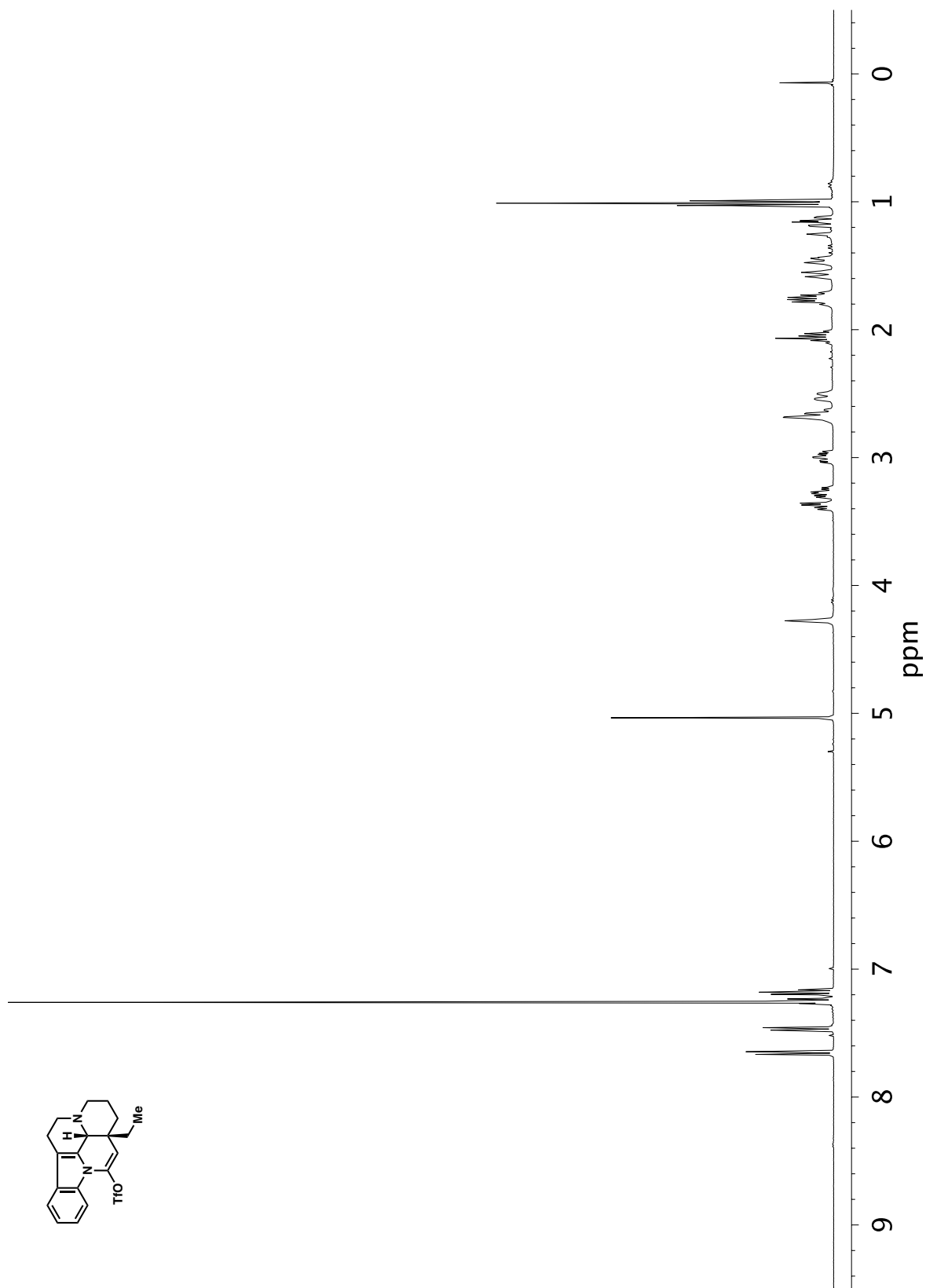


Figure A4.18. ¹³C NMR (101 MHz, CDCl₃) of compound **361**.



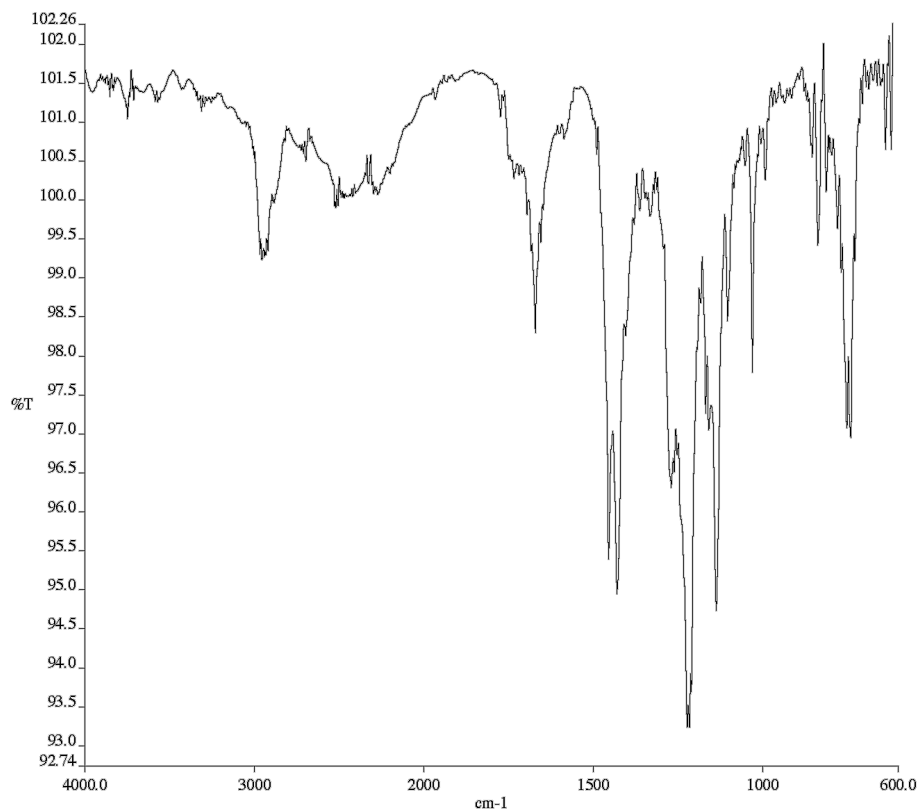


Figure A4.20. Infrared spectrum (Thin Film, NaCl) of compound **385**.

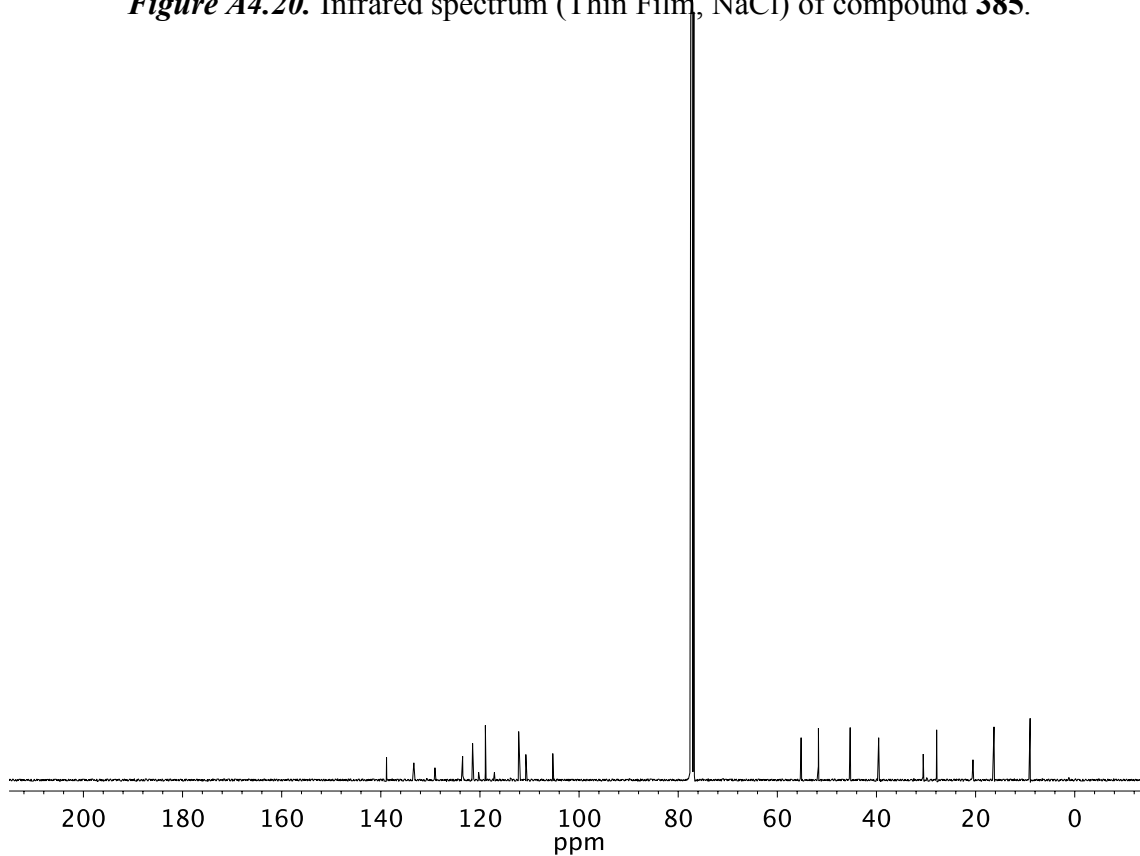


Figure A4.21. ¹³C NMR (101 MHz, CDCl₃) of compound **385**.

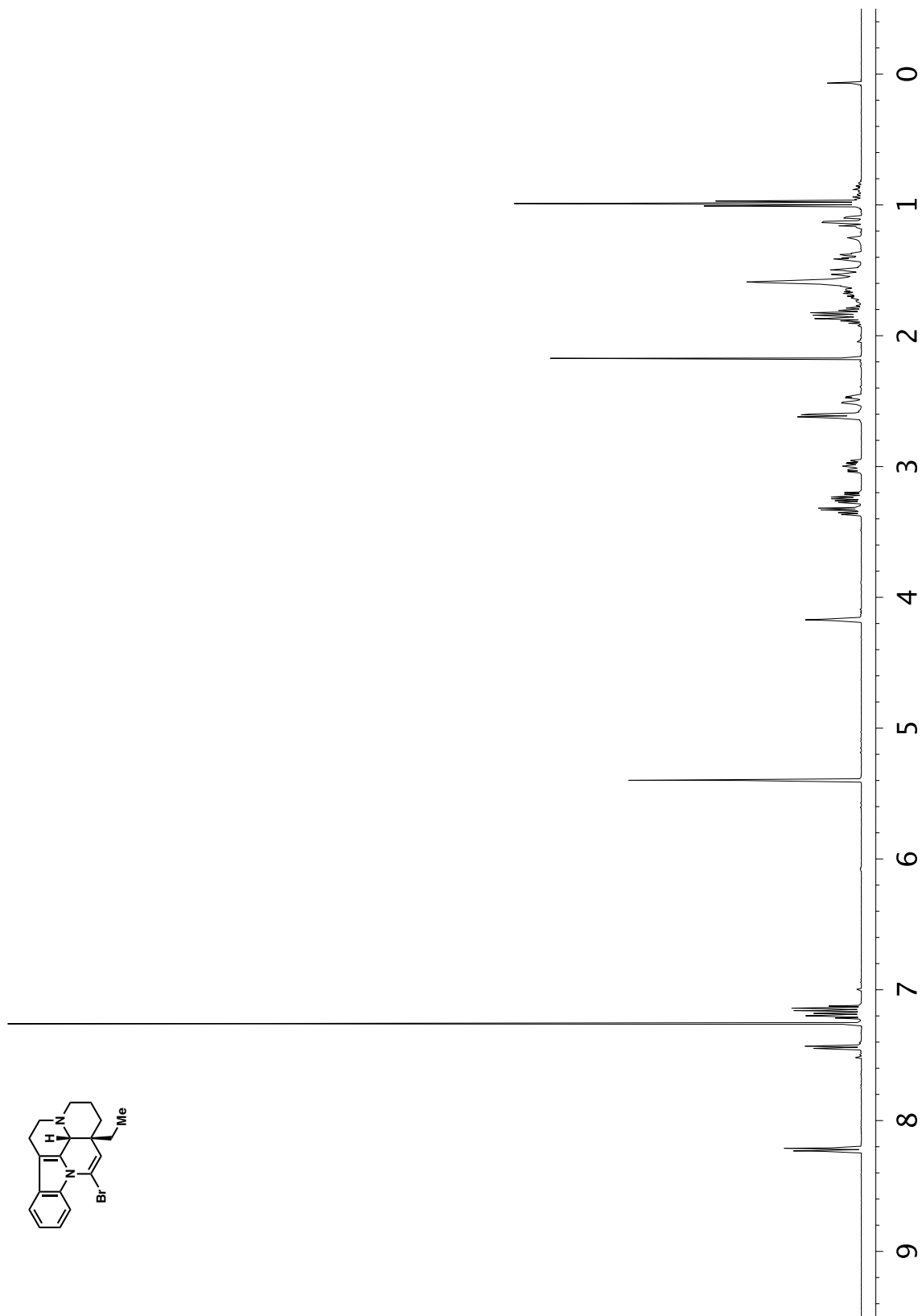


Figure A4.22 ^1H NMR (400 MHz, CDCl_3) of compound 392.

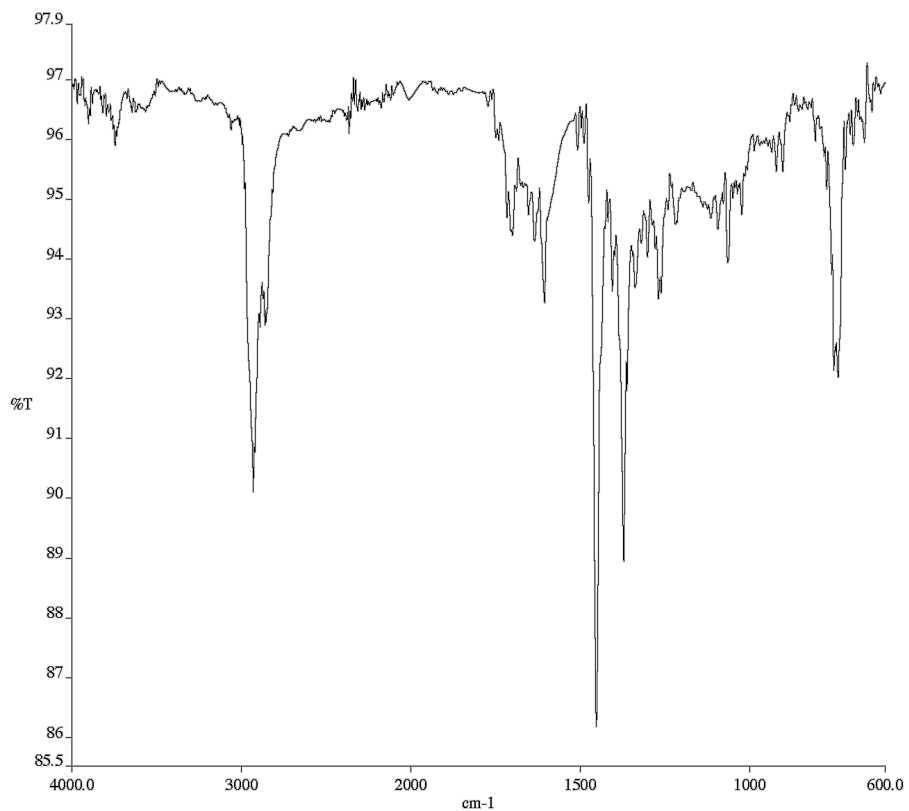


Figure A4.23 Infrared spectrum (Thin Film, NaCl) of compound **392**.

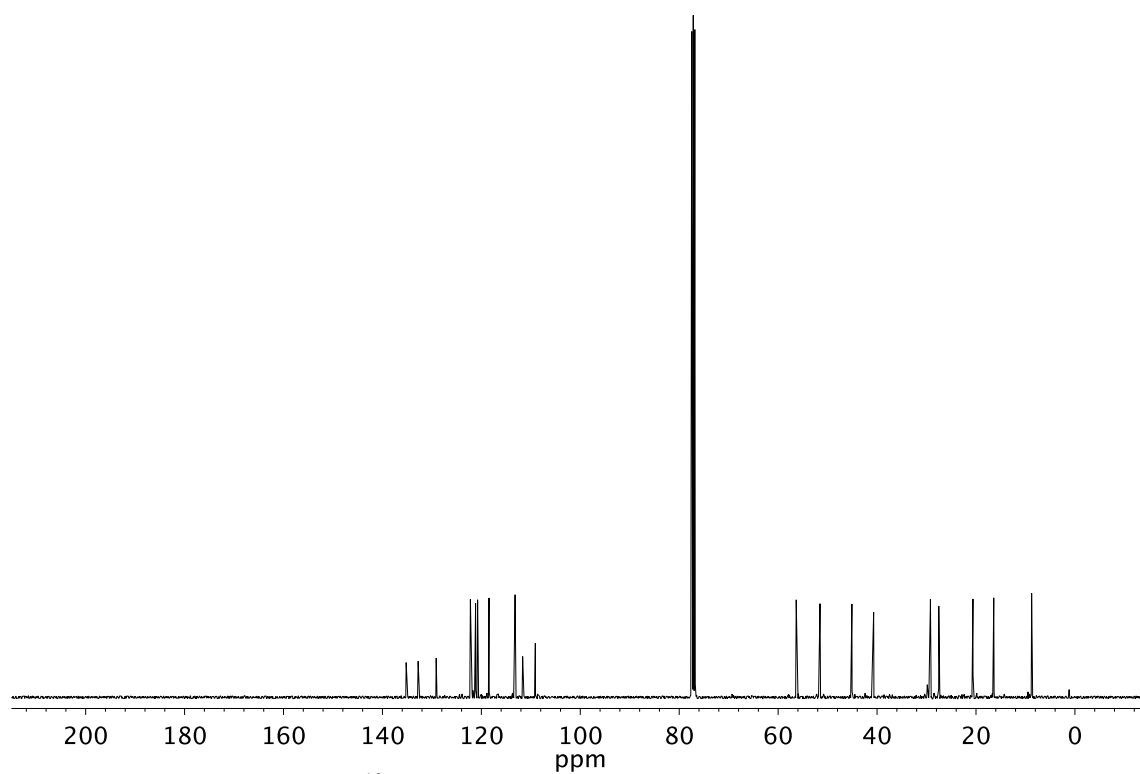


Figure A4.24 ¹³C NMR (101 MHz, CDCl₃) of compound **392**.

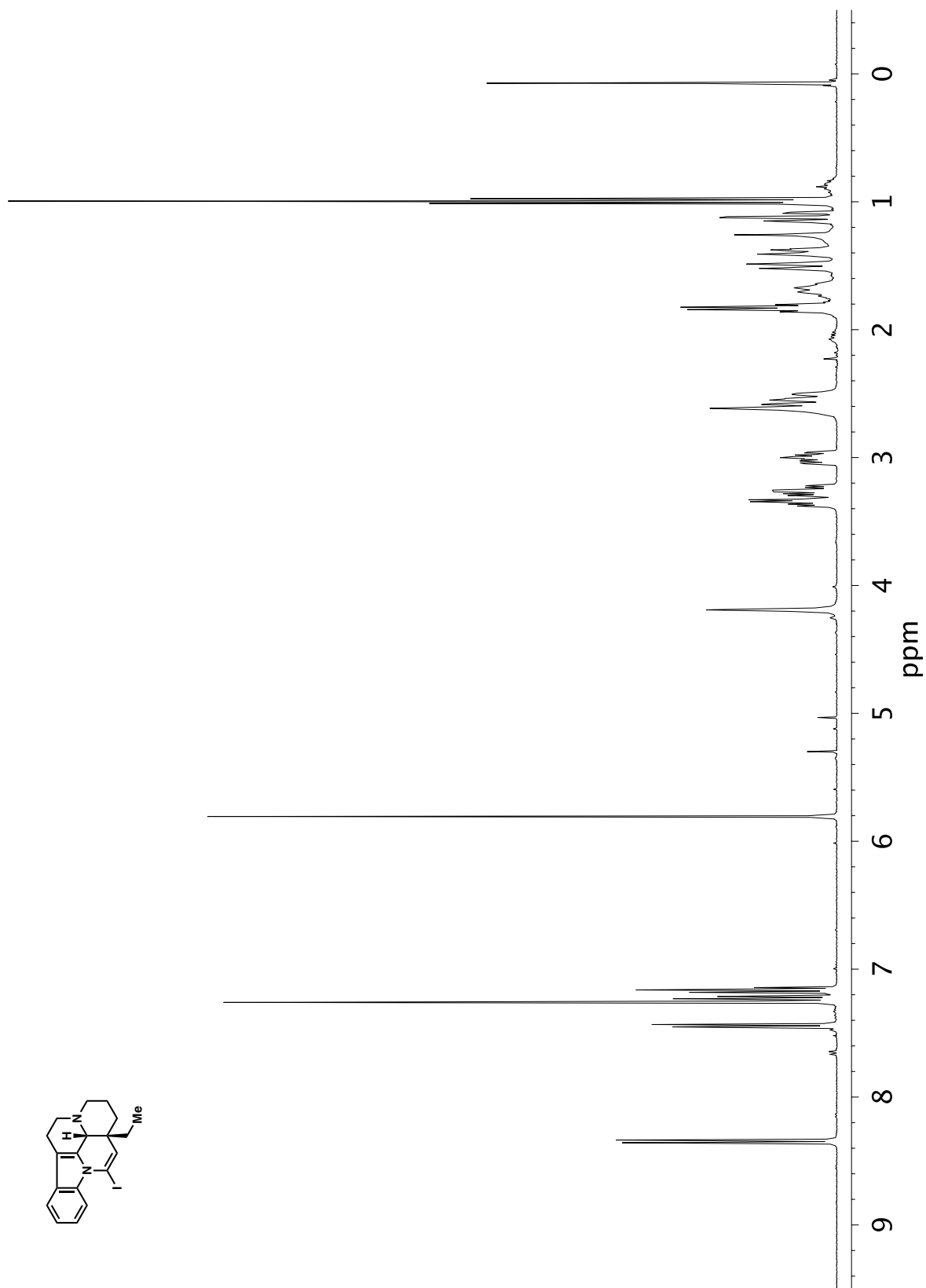


Figure A4.25 ^1H NMR (600 MHz, CD_2Cl_2) of compound **393**.

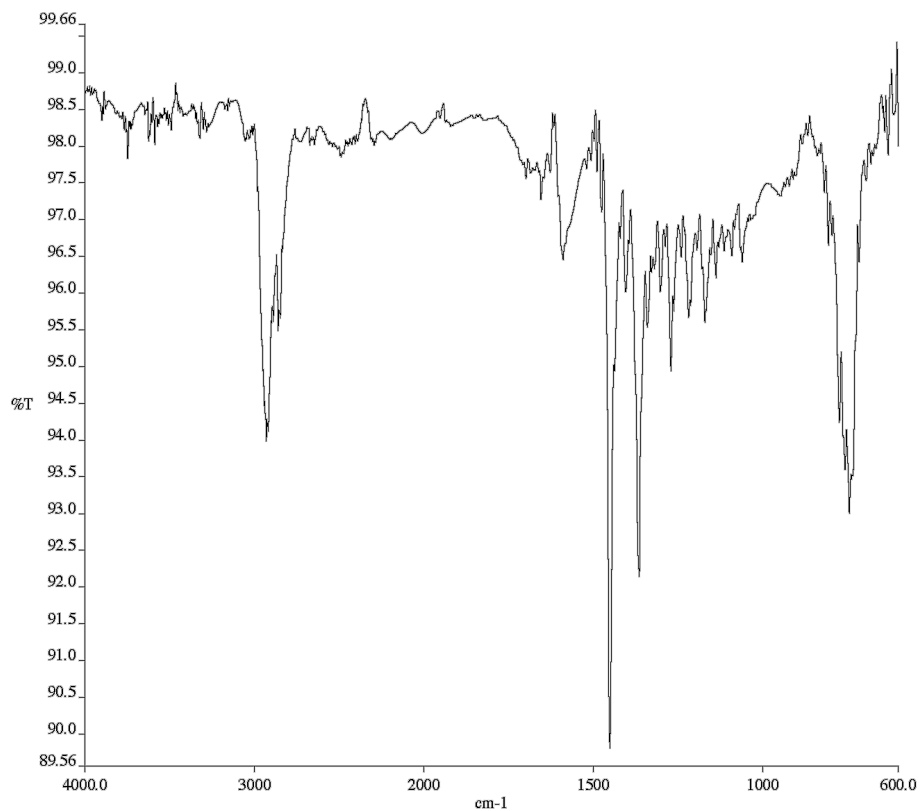


Figure A4.26 Infrared spectrum (Thin Film, NaCl) of compound **391**.

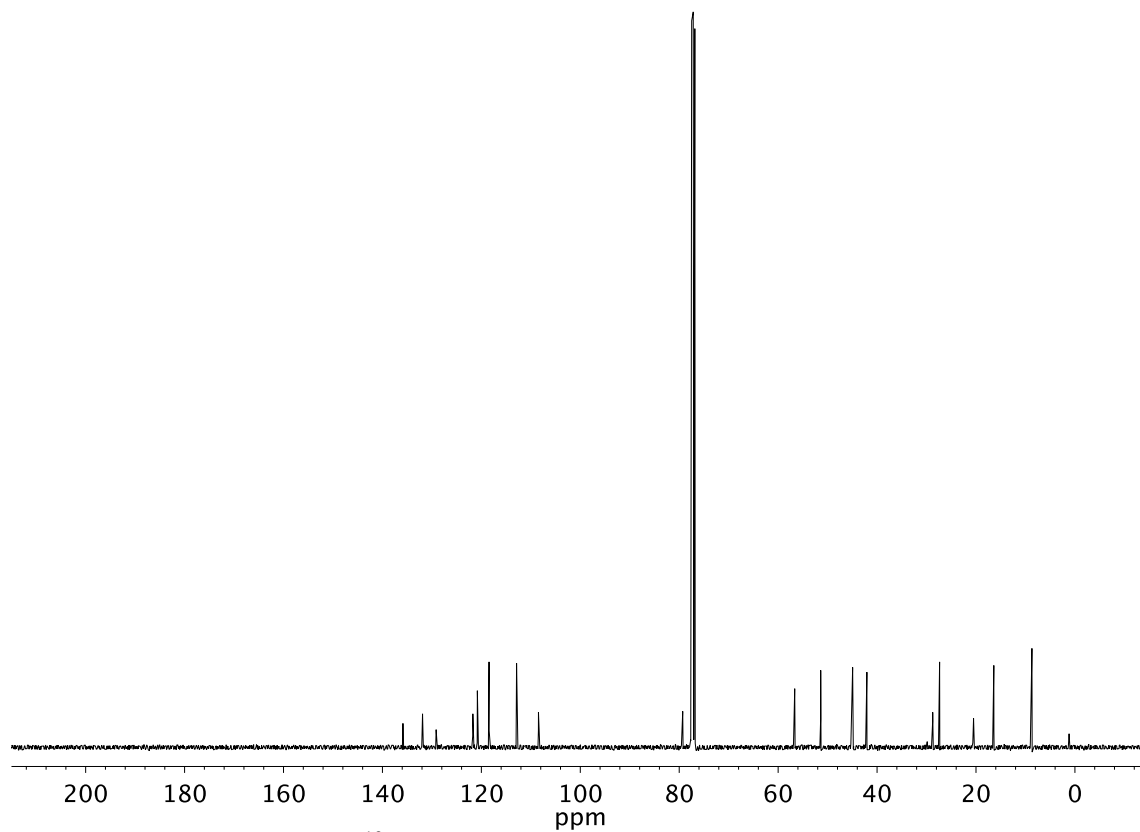


Figure A4.27 ¹³C NMR (101 MHz, CDCl₃) of compound **391**.

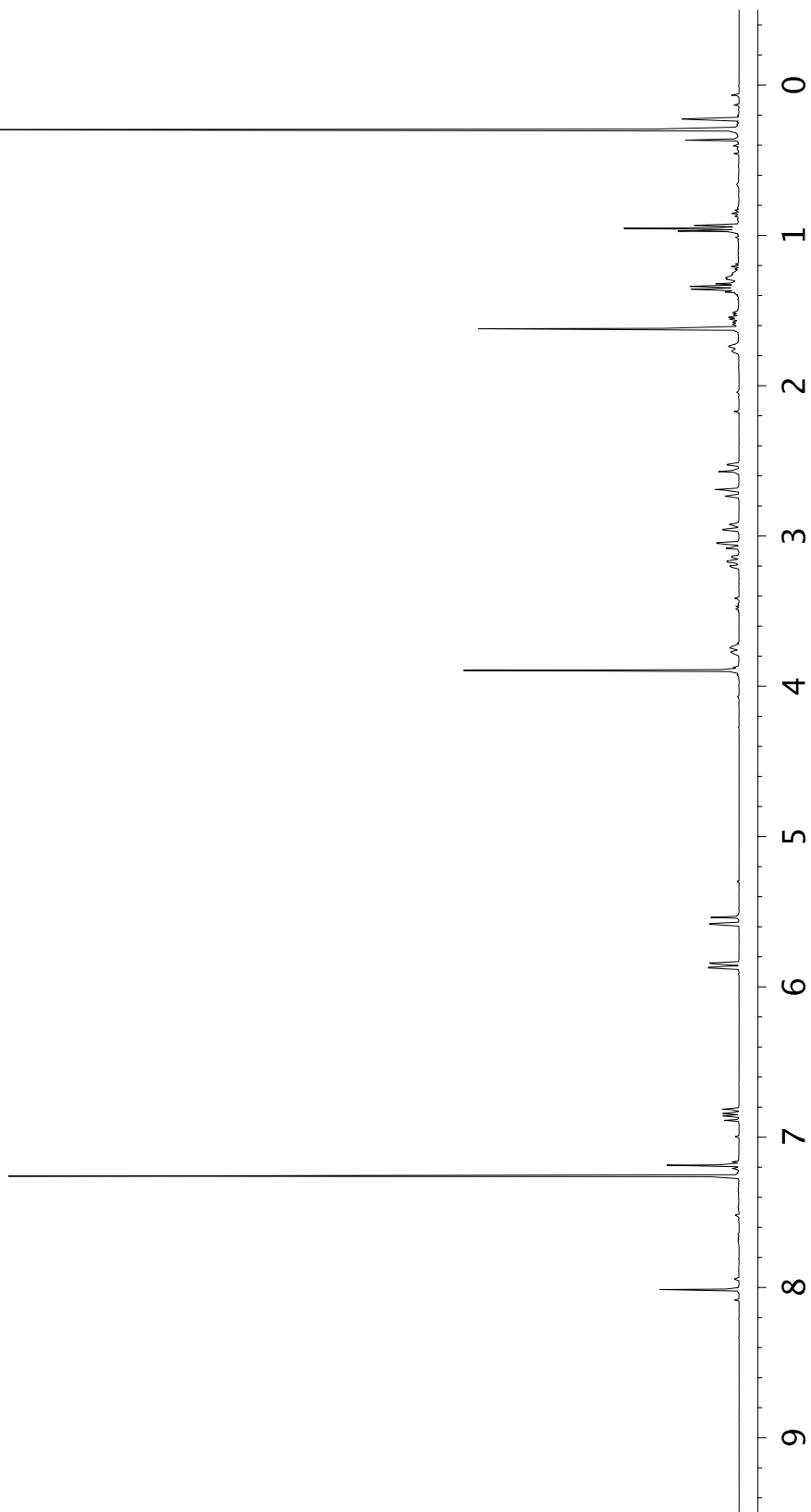
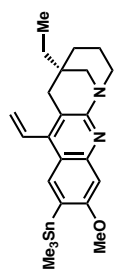


Figure A4.28 ^1H NMR (400 MHz, CDCl_3) of compound 391.

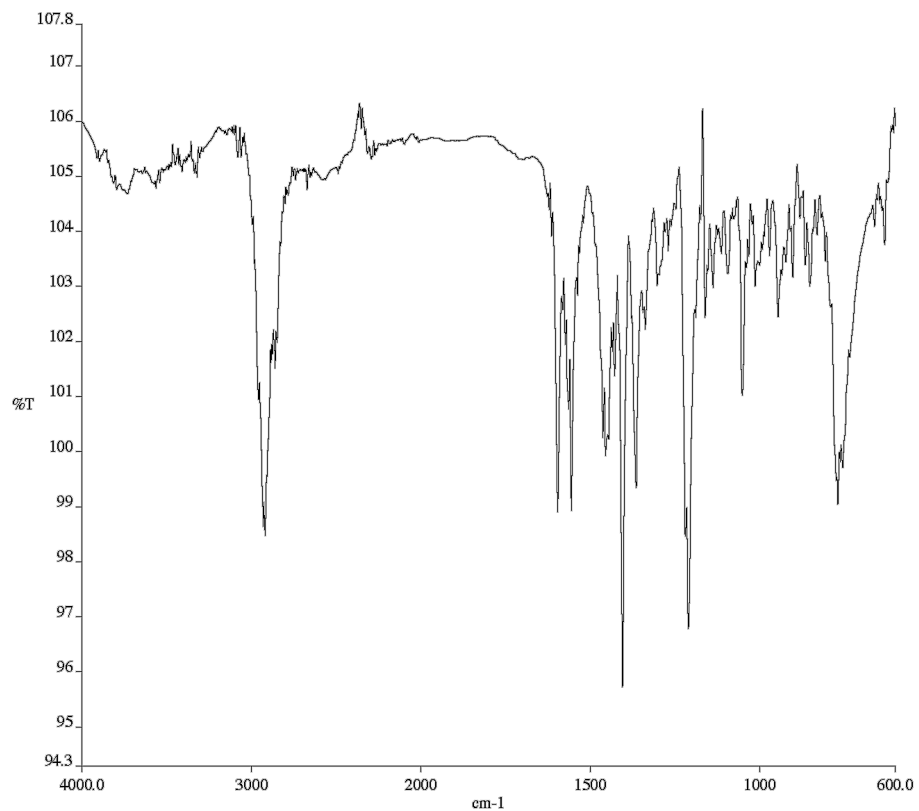


Figure A4.29 Infrared spectrum (Thin Film, NaCl) of compound **391**.

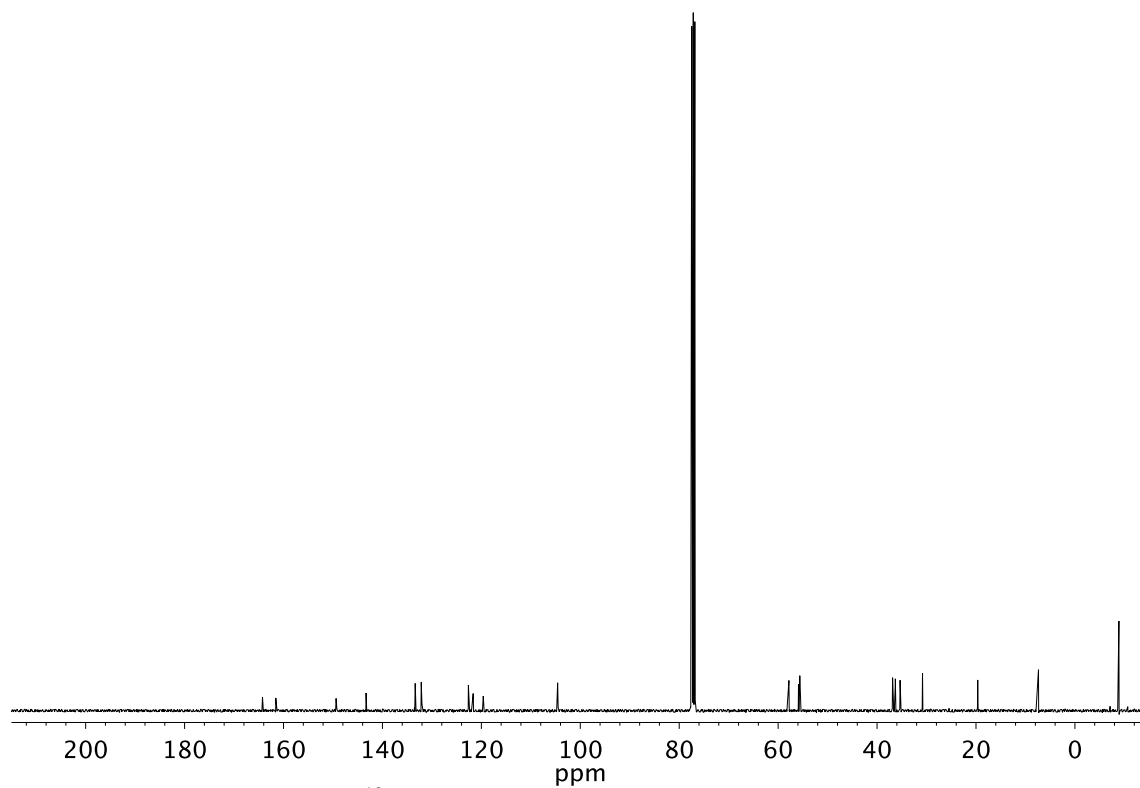


Figure A4.30 ¹³C NMR (101 MHz, CDCl₃) of compound **391**.

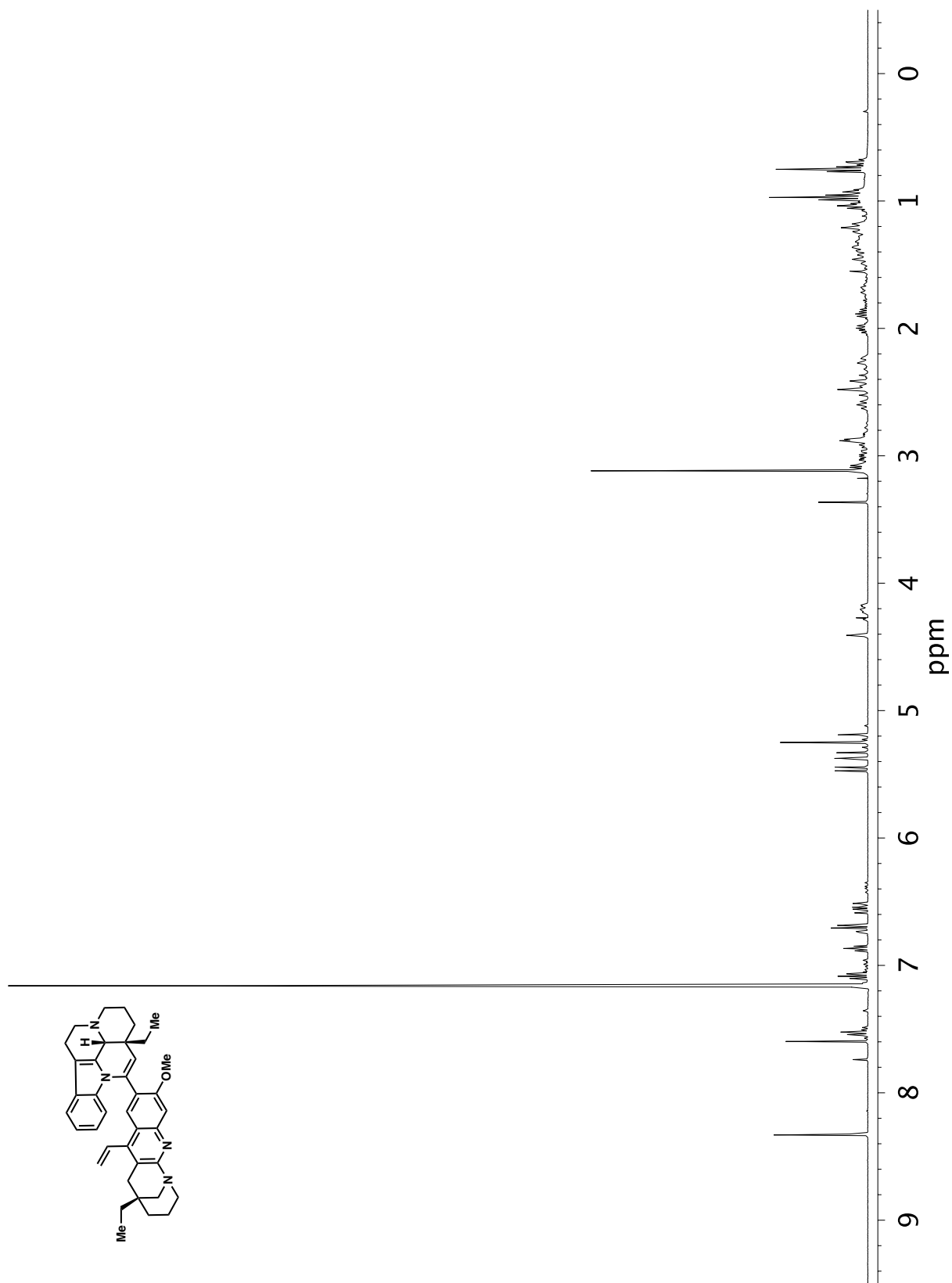


Figure A4.31 ^1H NMR (400 MHz, C_6D_6) of compound **386**.

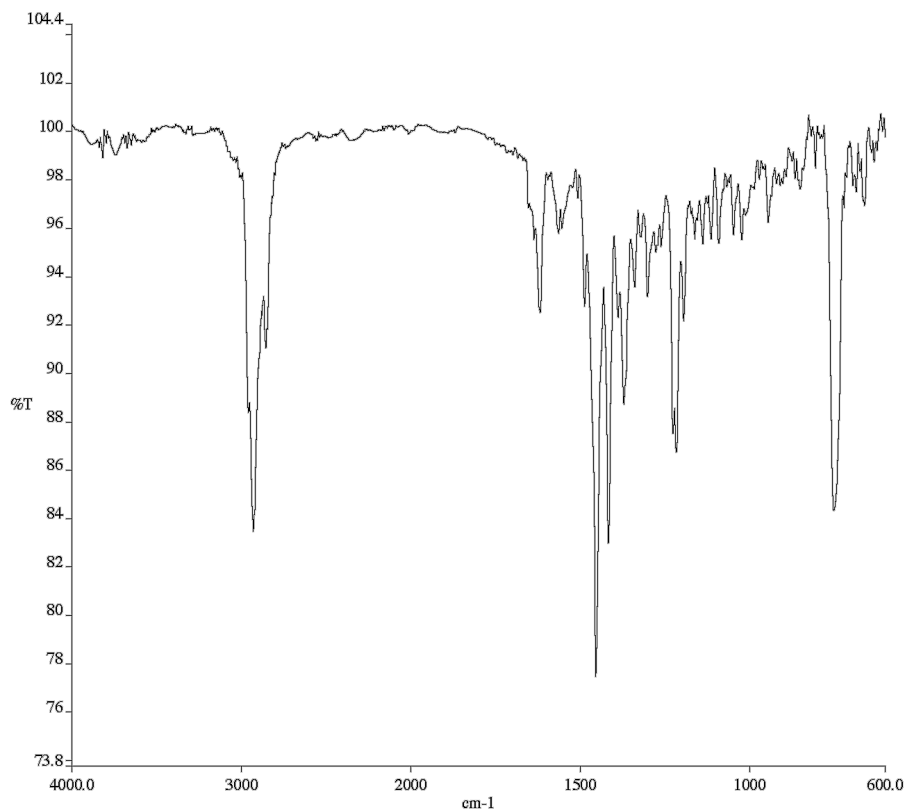


Figure A4.32 Infrared spectrum (Thin Film, NaCl) of compound **386**.

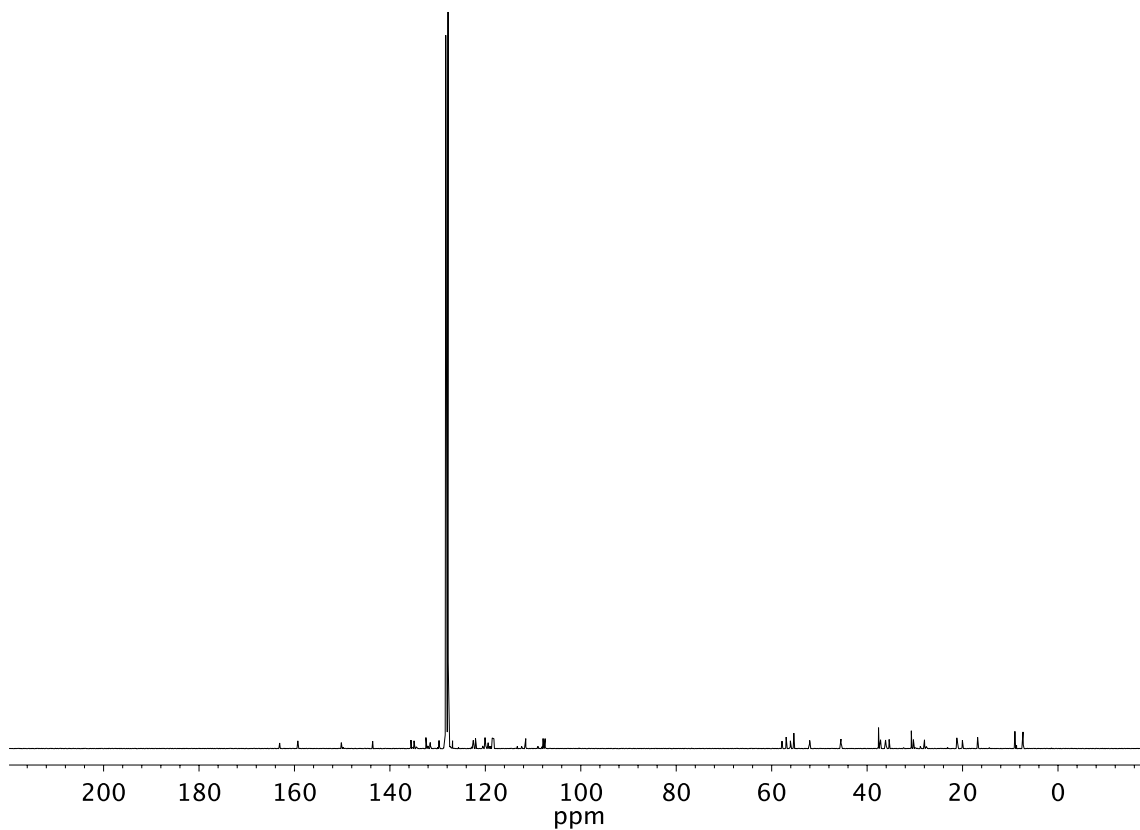


Figure A4.33 ¹³C NMR (101 MHz, C₆D₆) of compound **386**.

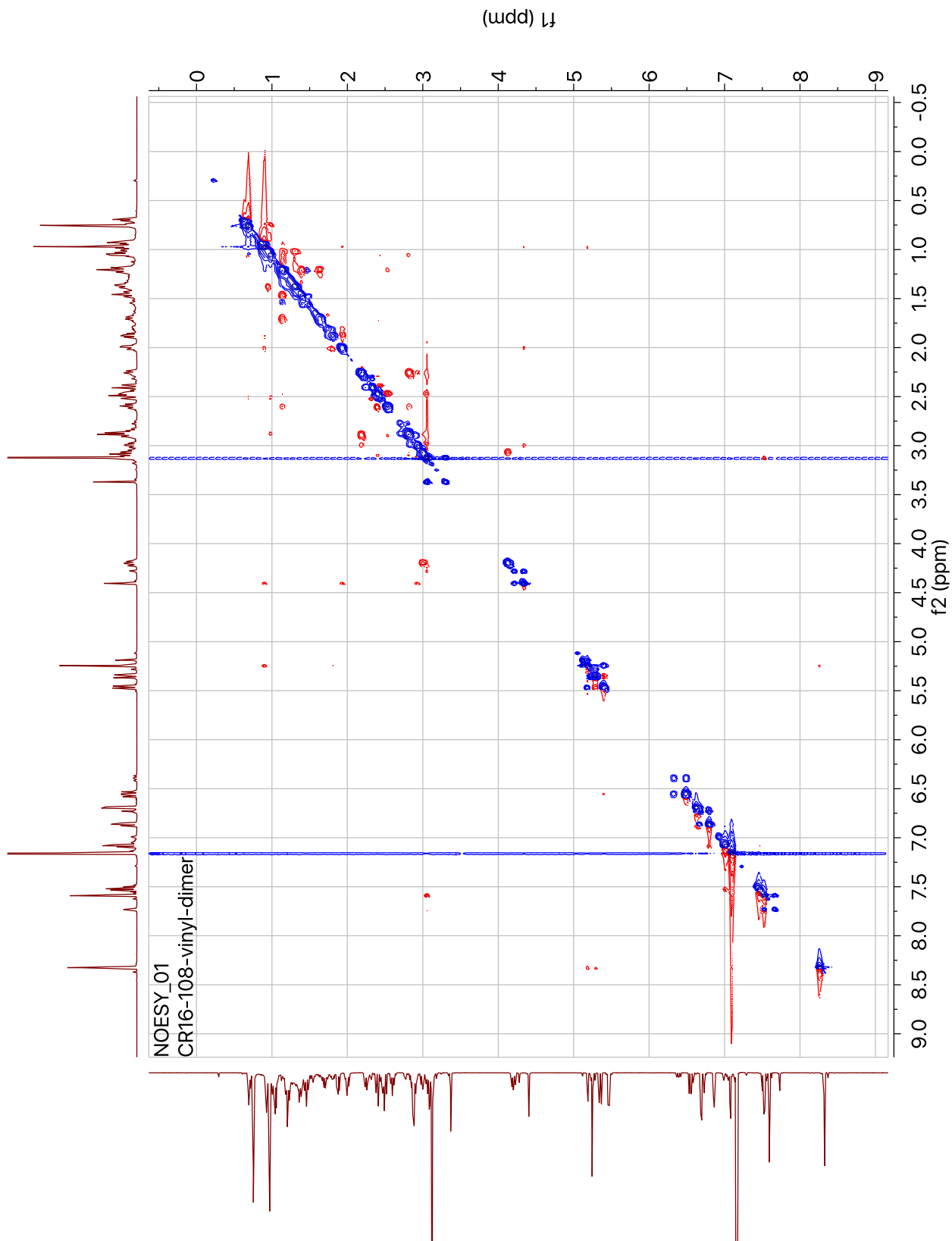


Figure A4.34 NOESY (600 MHz, C₆D₆) of compound **386**.

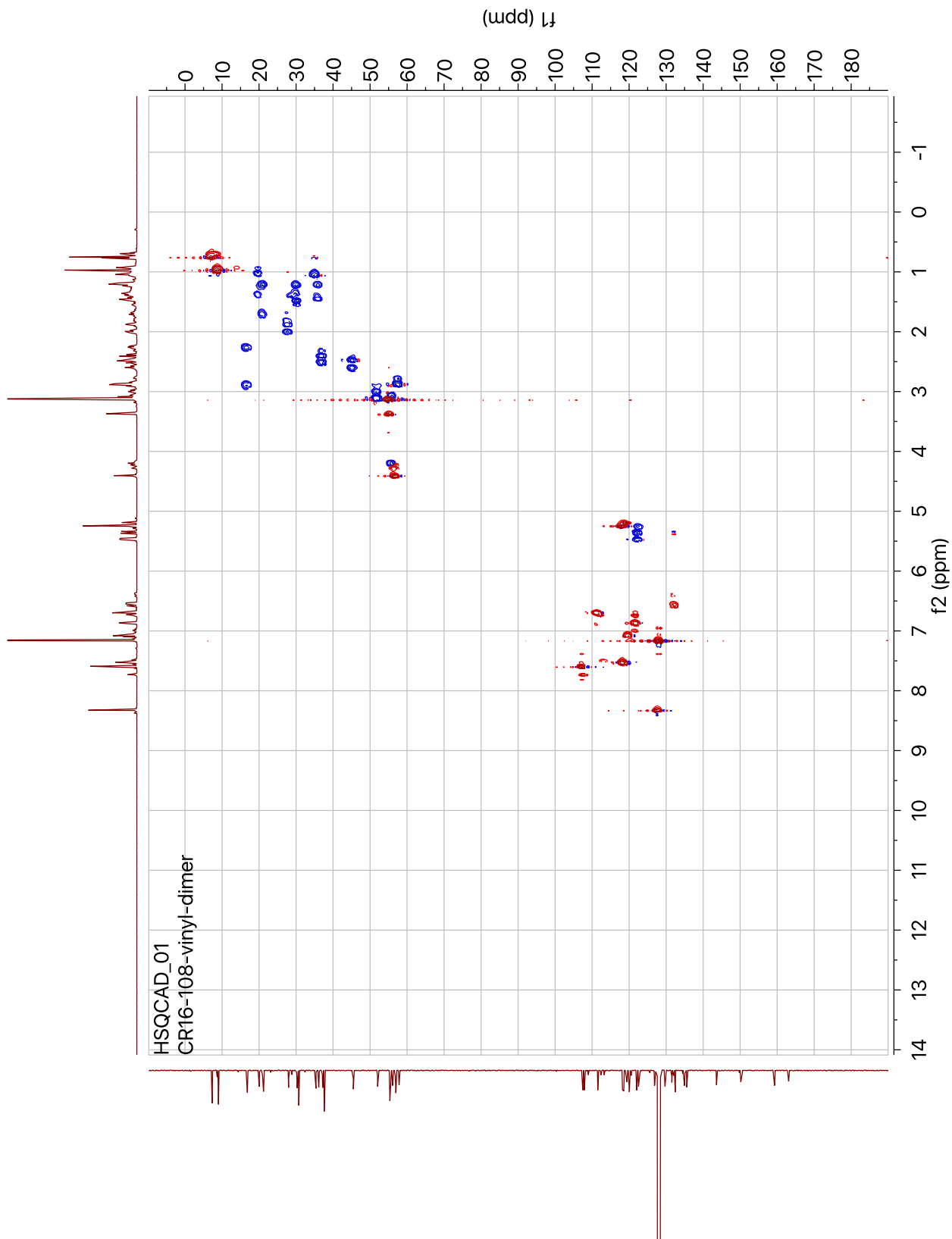


Figure A4.35 HSQC (600 MHz, C_6D_6) of compound 386.

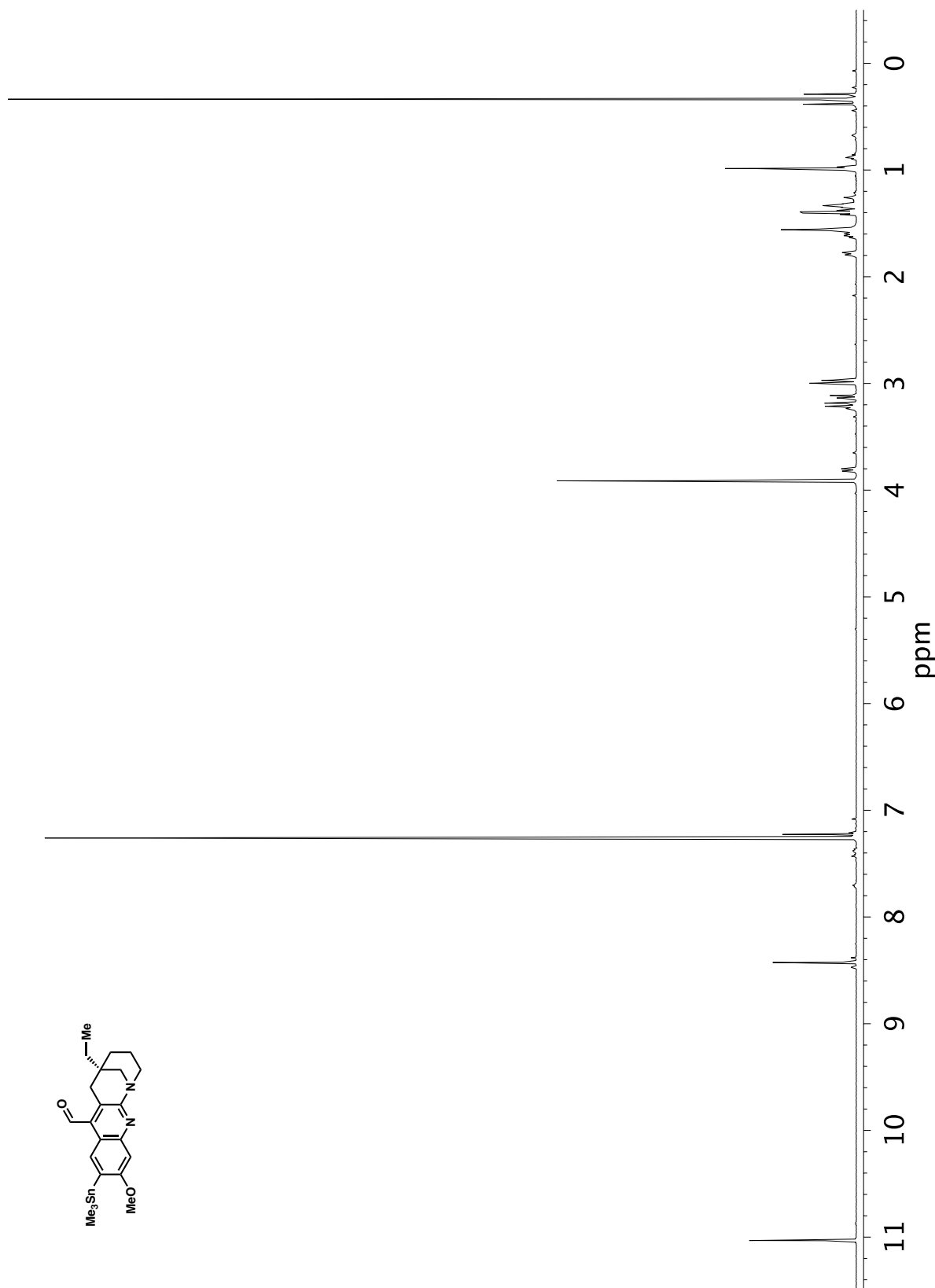


Figure A4.36 ^1H NMR (400 MHz, CDCl_3) of compound 396.

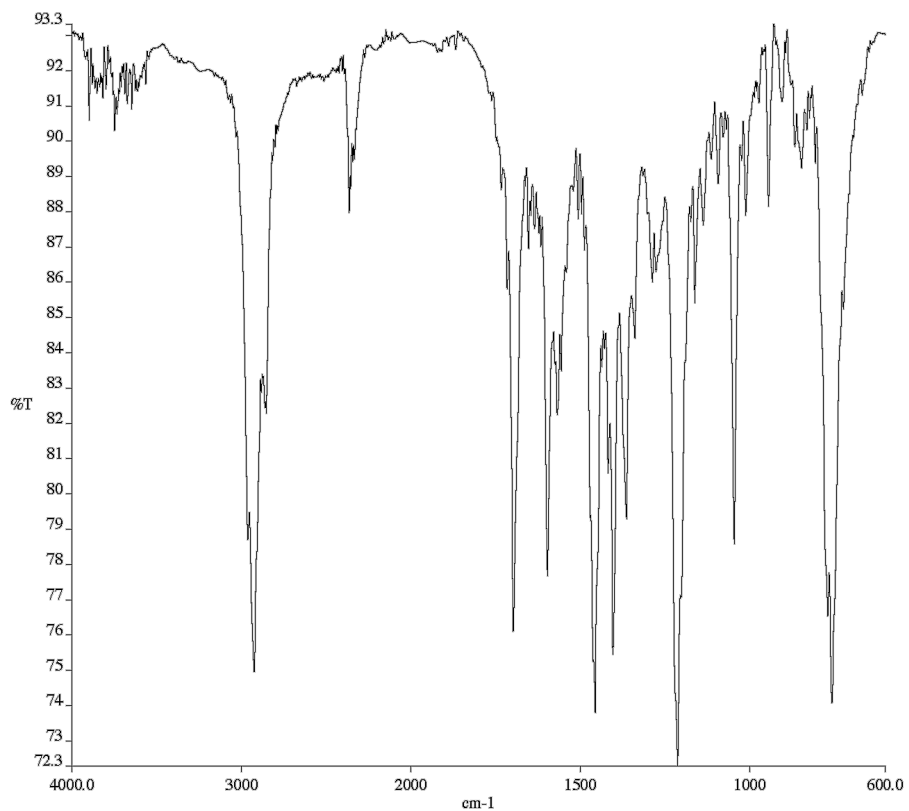


Figure A4.37 Infrared spectrum (Thin Film, NaCl) of compound **396**.

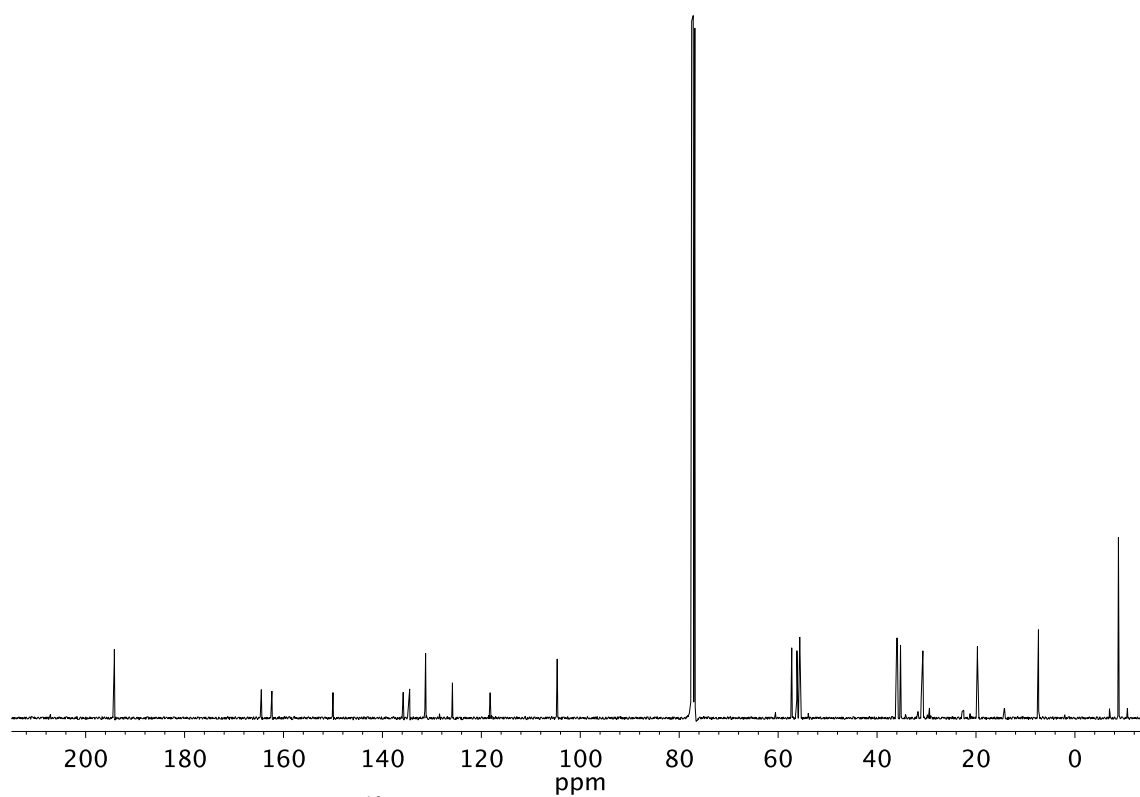


Figure A4.38 ¹³C NMR (101 MHz, CDCl₃) of compound **396**.

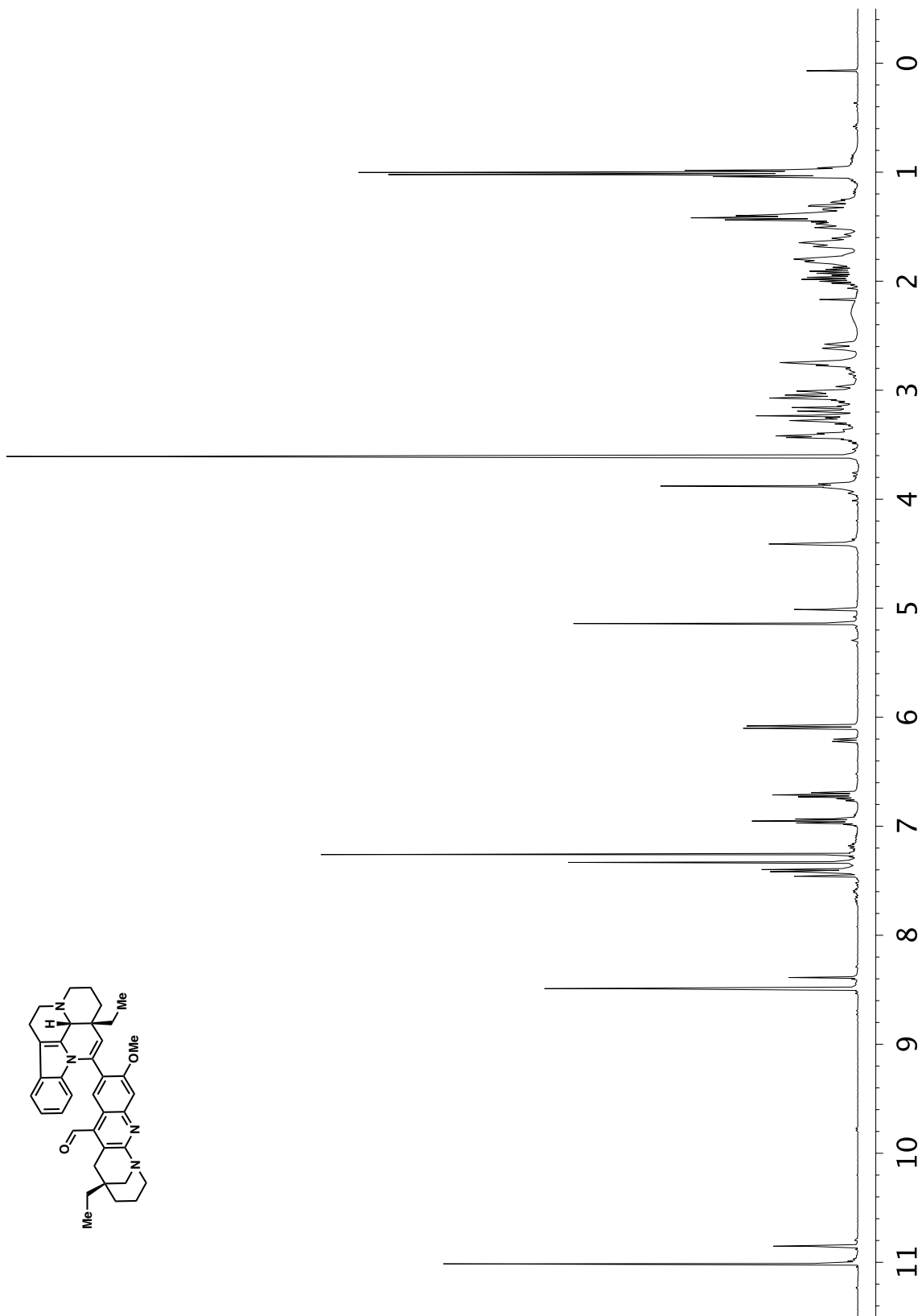


Figure A4.39 ^1H NMR (400 MHz, CDCl_3) of compound 397.

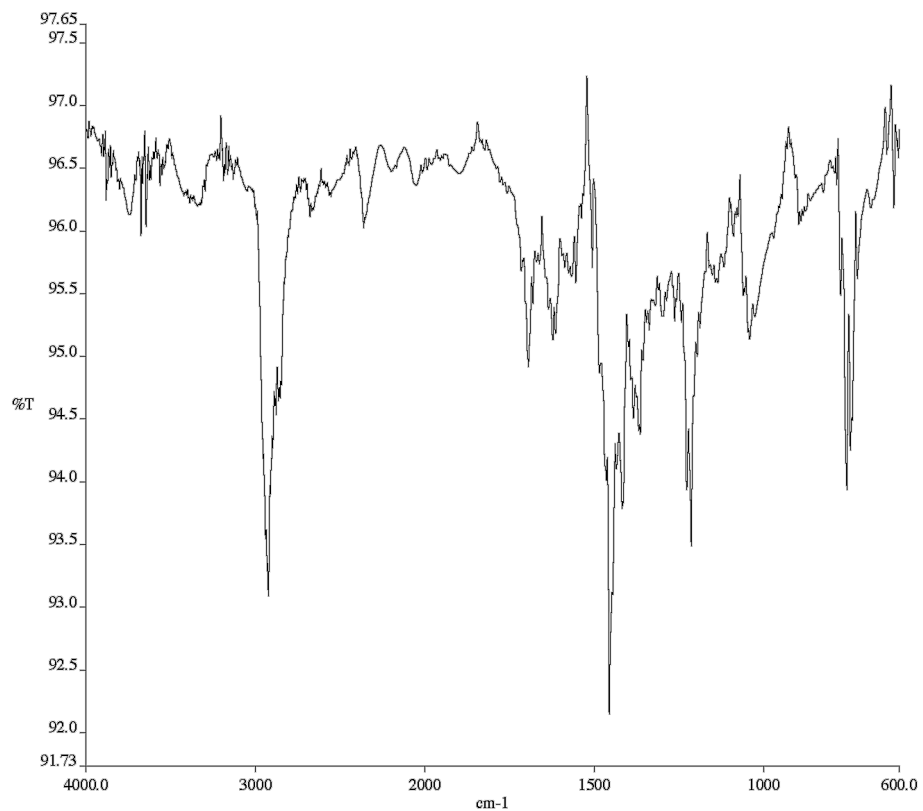


Figure A4.40 Infrared spectrum (Thin Film, NaCl) of compound **397**.

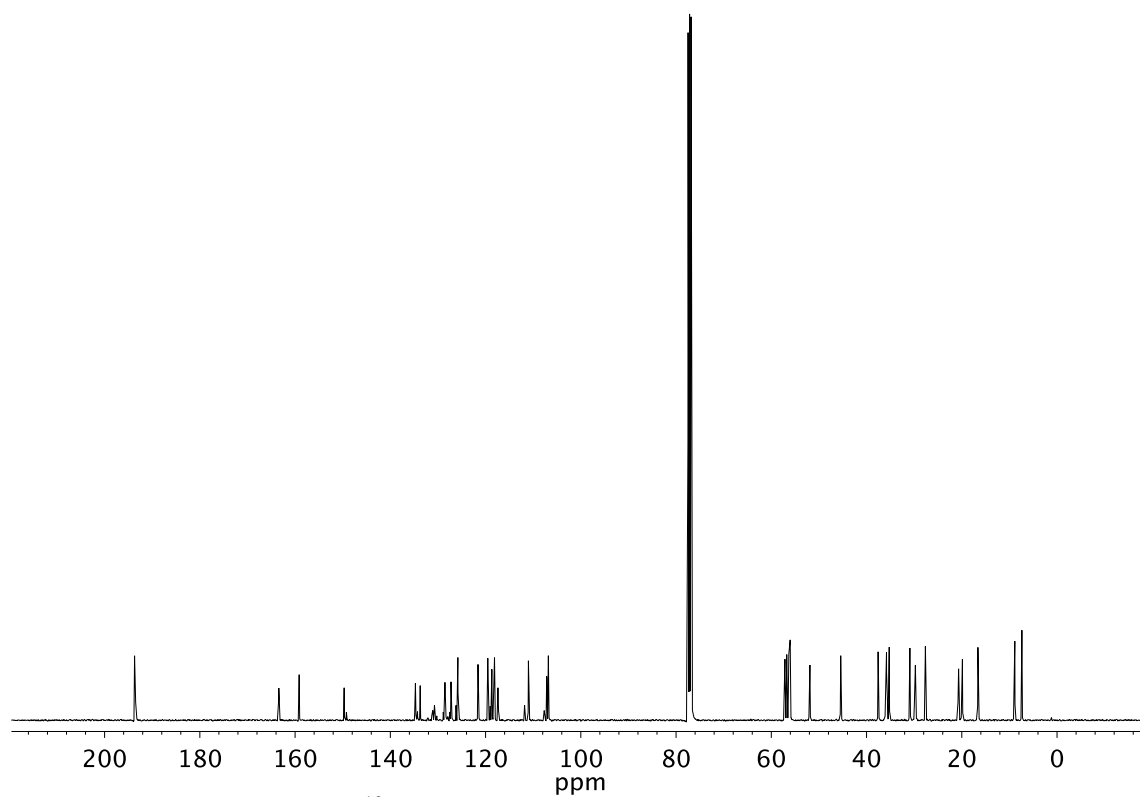
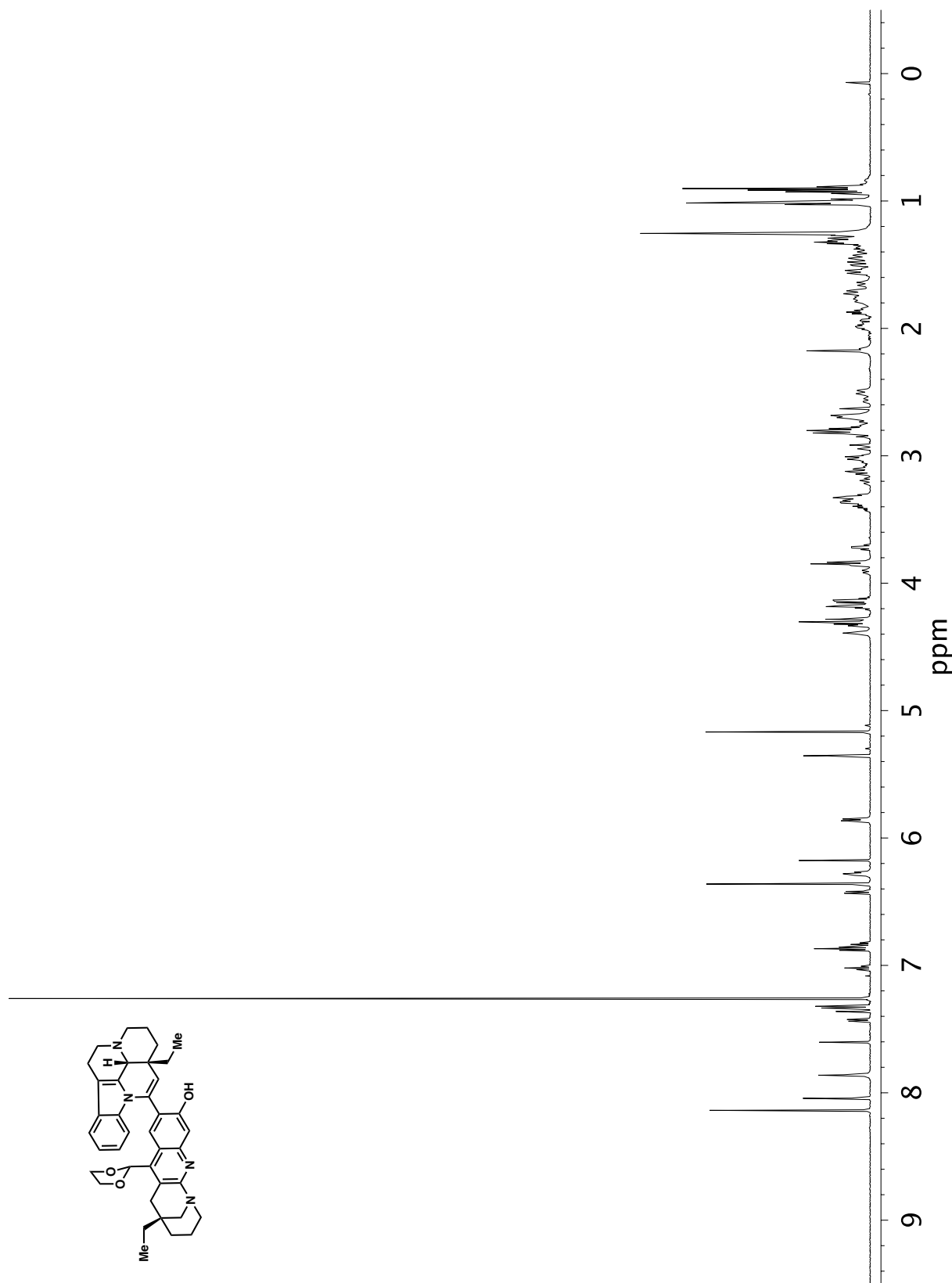


Figure A4.41 ¹³C NMR (101 MHz, CDCl₃) of compound **397**.



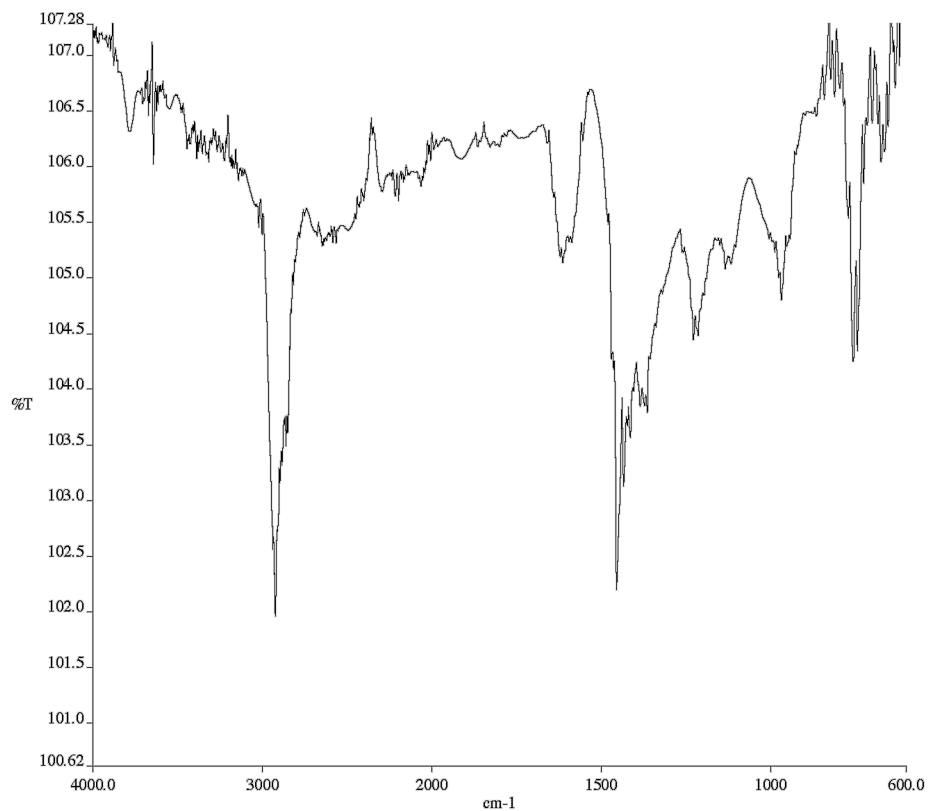


Figure A4.43 Infrared spectrum (Thin Film, NaCl) of compound **402**.

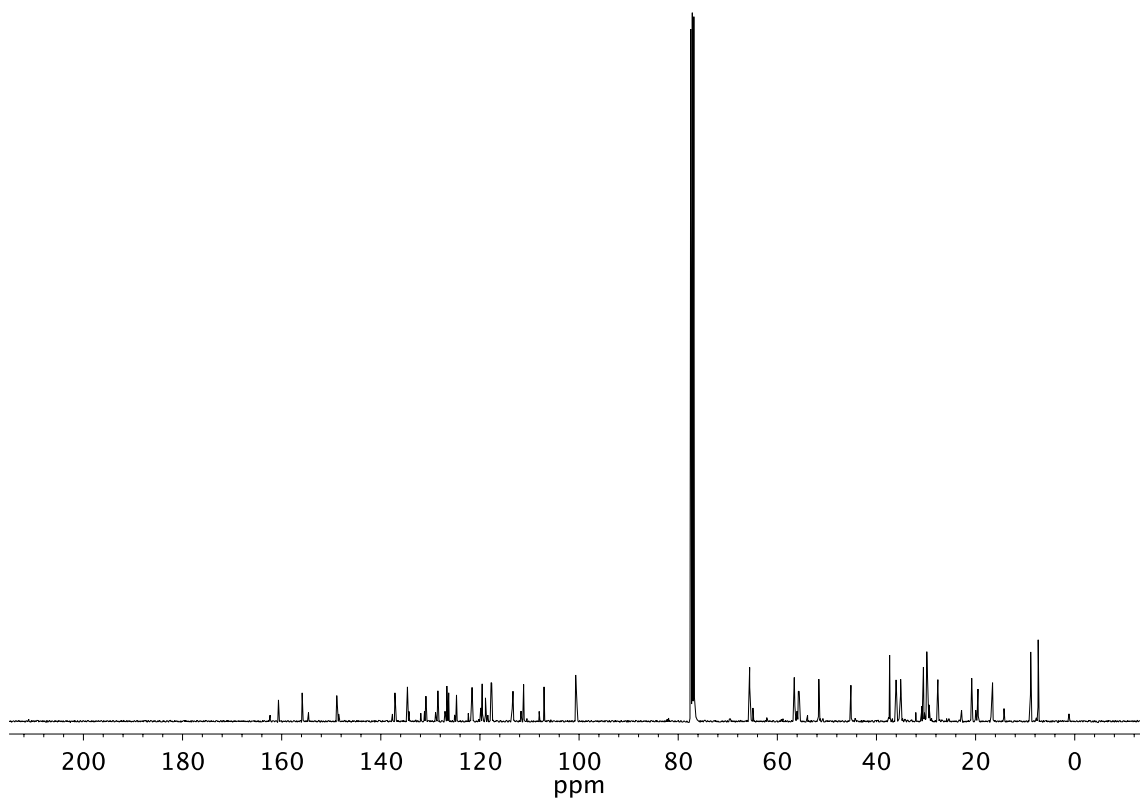


Figure A4.44 ^{13}C NMR (101 MHz, CDCl_3) of compound **403**.

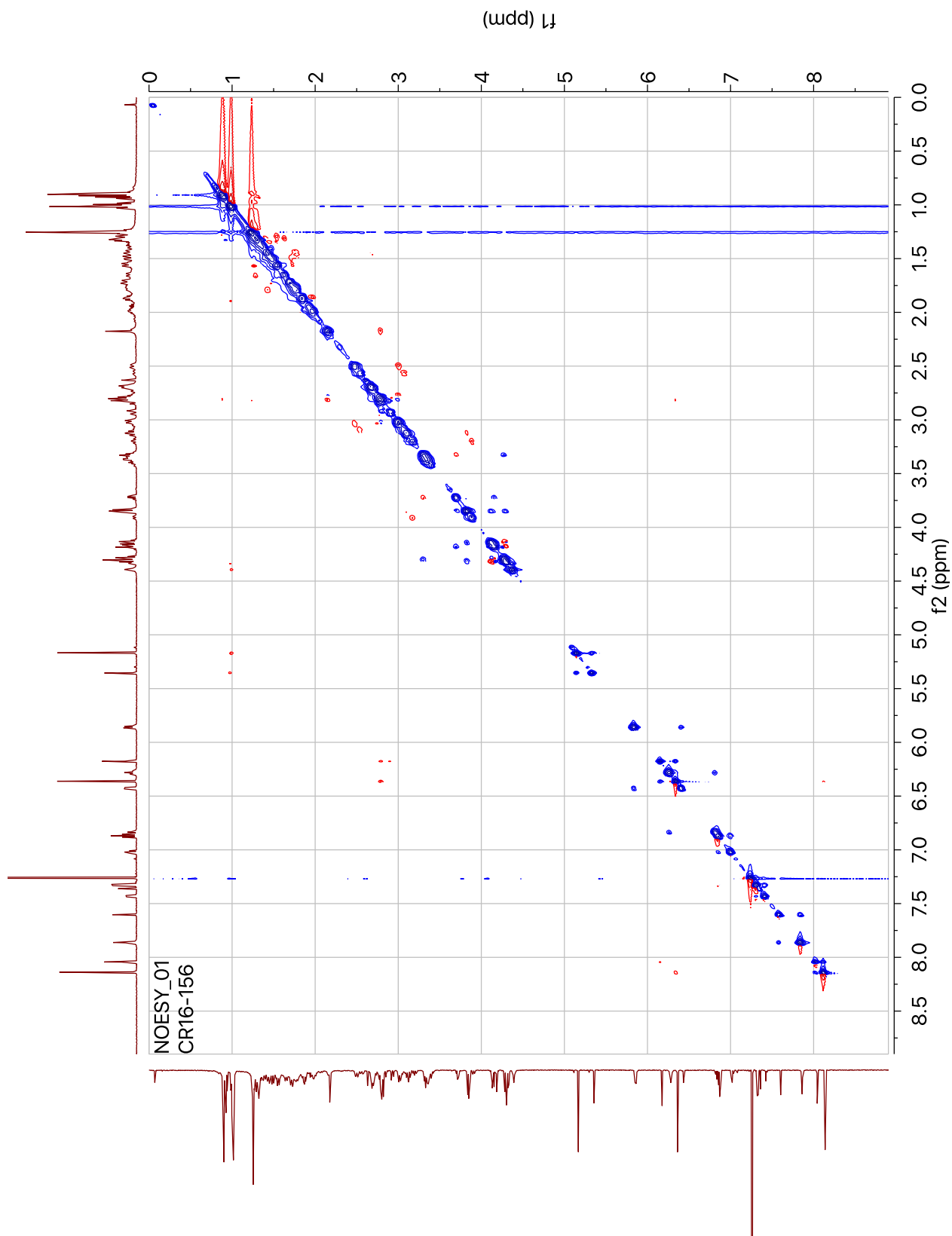


Figure A4.45 NOESY (600 MHz, CDCl_3) of compound **403**.

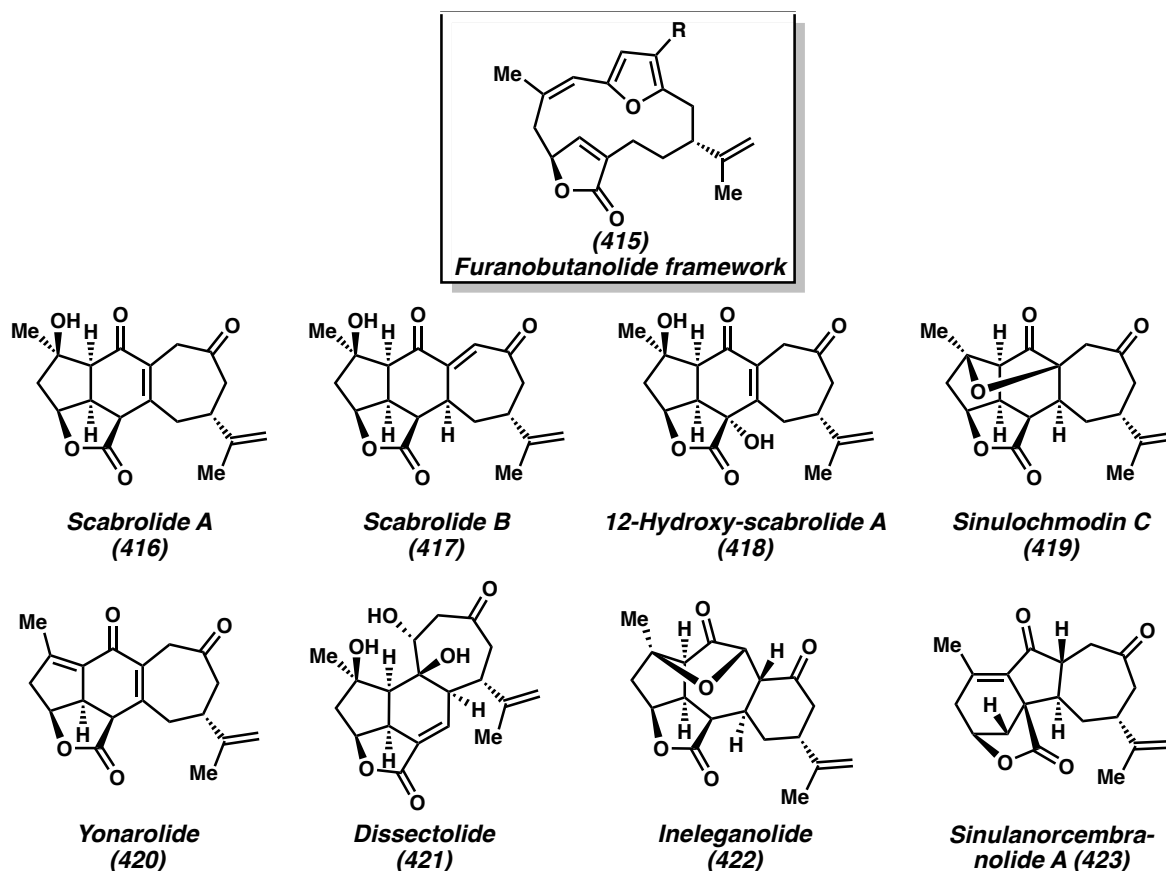
CHAPTER 4

The Total Synthesis of (-)-Scabrolide A

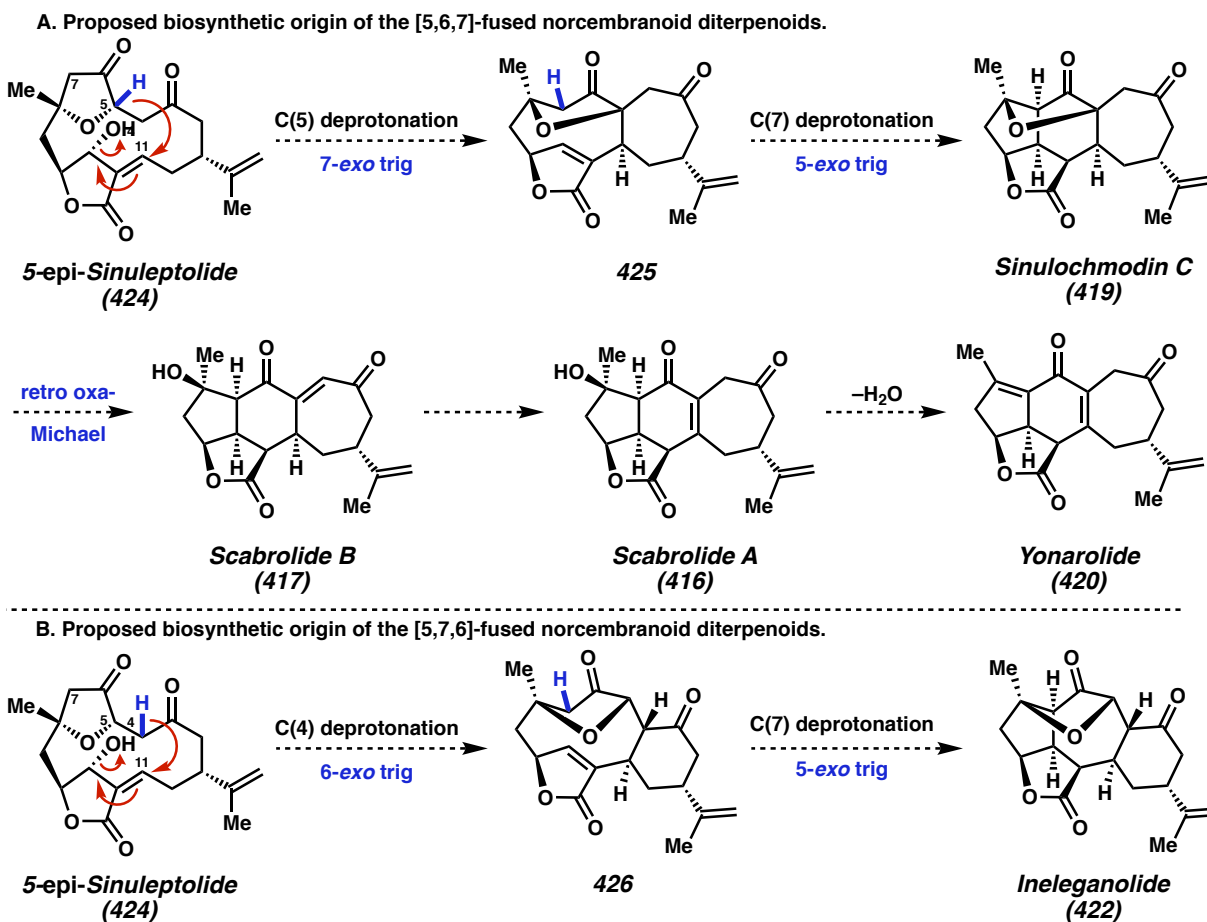
4.1 INTRODUCTION

4.1.1. Isolation, Bioactivity, and Biosynthetic Hypotheses

The soft corals of the genus *Sinularia* have attracted immense scientific interest as a fertile source of bioactive natural products. The rich chemodiversity of compounds isolated from these marine organisms has inspired a substantial body of research from natural products chemists, synthetic chemists, and biochemists alike.¹ *Sinularia*-derived secondary metabolites demonstrate an exceptional array of macrocyclic and polycyclic architectures noted for their various fused ring systems and complicated patterns of oxidation.² Biologically, these compounds display potent biological activities such as cytotoxicity, which is hypothesized to account for the low natural predation of the parent organisms.³

Figure 4.1. Furanobutenolide-derived norcembranoid diterpenoids.

The furanobutenolide-derived cembranoid and norcembranoid diterpenoids are a particular subclass which has attracted significant attention within the synthetic community. The name arises from the furanobutenolide scaffold (**415**) from which the C₂₀ cembranoid (R = Me, CHO, COOMe) and C₁₉ norcembranoid (R = H) diterpenoids arise (Figure 4.1).² This intermediate serves as a biogenic precursor for the various tricyclic norcembranoid frameworks observed in these natural products; these include the fused-[5,6,7] ring system observed in scabrolide A (**416**),⁴ scabrolide B (**417**),⁴ 12-hydroxyscabrolide A (**418**),⁵ sinulochmodin C (**419**),⁶ yonarolide (**420**),⁷ and dissectolide (**421**),⁸ the fused-[5,7,6] ring system observed in ineleganolide (**422**),⁹ the fused-[6,5,7] ring system observed in sinulanorcembranolide A (**423**),¹⁰ and several bridged variants.

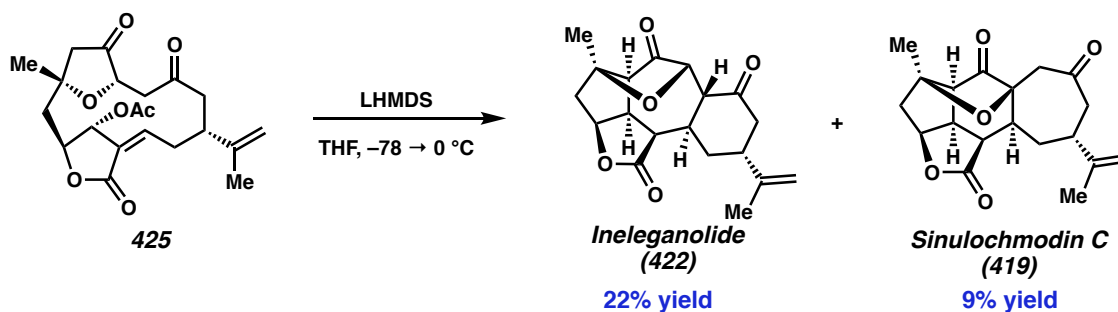
Scheme 4.1. Proposed biosynthesis of fused tricyclic norcembranoid diterpenoids.

Biosynthetically, the diverse set of ring systems are hypothesized to arise from a series of transannular Michael additions from 5-*epi*-sinuleptolide (**424**) (Scheme 4.1A). Deprotonation at C(5), for example, is believed to promote a 7-*exo*-trig cyclization with concomitant elimination of the allylic alcohol to establish butenolide **425**. Deprotonation at C(7) then initiates a 5-*exo* trig cyclization to establish the fused-[5,6,7] core of sinulochmodin C (**419**). A retro oxa-Michael addition then generates scabrolide B (**417**), which can isomerize to scabrolide A (**416**) and eliminate to yonarolide (**420**).^{1,2}

In contrast, deprotonation at C(4) of 5-*epi*-sinulariolide (**424**) and subsequent 6-*exo*-trig cyclization is believed to generate isomeric tricycle **426**, which upon C(7) deprotonation and 5-

exo-trig cyclization generates the fused-[5,7,6] core of ineleganolide (**422**) (Scheme 4.1B).^{1,2} These hypotheses are supported by research by Pattenden and coworkers,¹¹ who reported in 2011 that treatment of 5-*epi* sinulariolide with LHMDS generated a mixture of ineleganolide (**422**) and sinulochmodin C (**419**) (Scheme 4.2).

Scheme 4.2. Pattenden's semi-synthesis of ineleganolide and sinulochmodin C (2011).



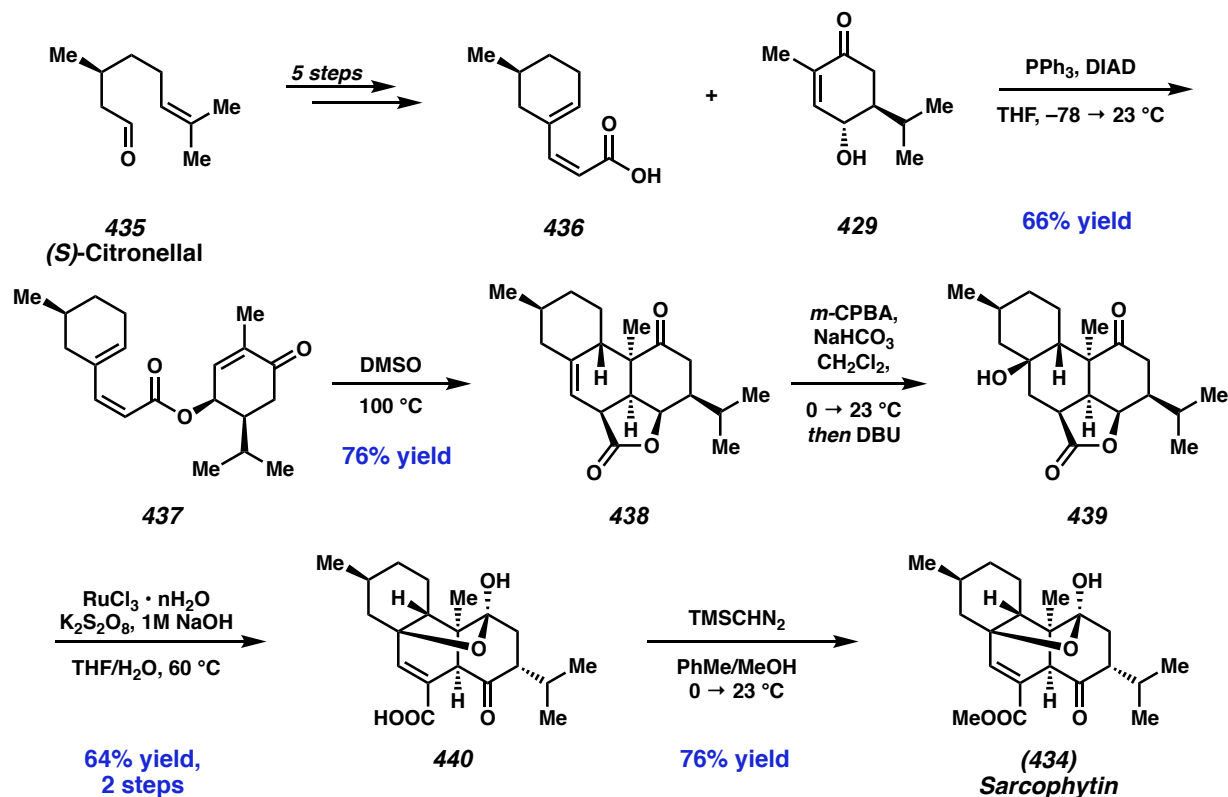
4.1.2. Previous Synthetic Efforts toward Polycyclic (Nor)cembranoid Diterpenoids

Cembranoid and norcembranoid diterpenoids have been the subject of extensive synthetic efforts over the years. However, it was not until the late 2010's that the first of these natural products succumbed to total synthesis, highlighting the difficulty accessing these targets. By examining the strategies implemented in successful synthetic efforts, we gained key insight to guide our own eventual synthetic strategy.

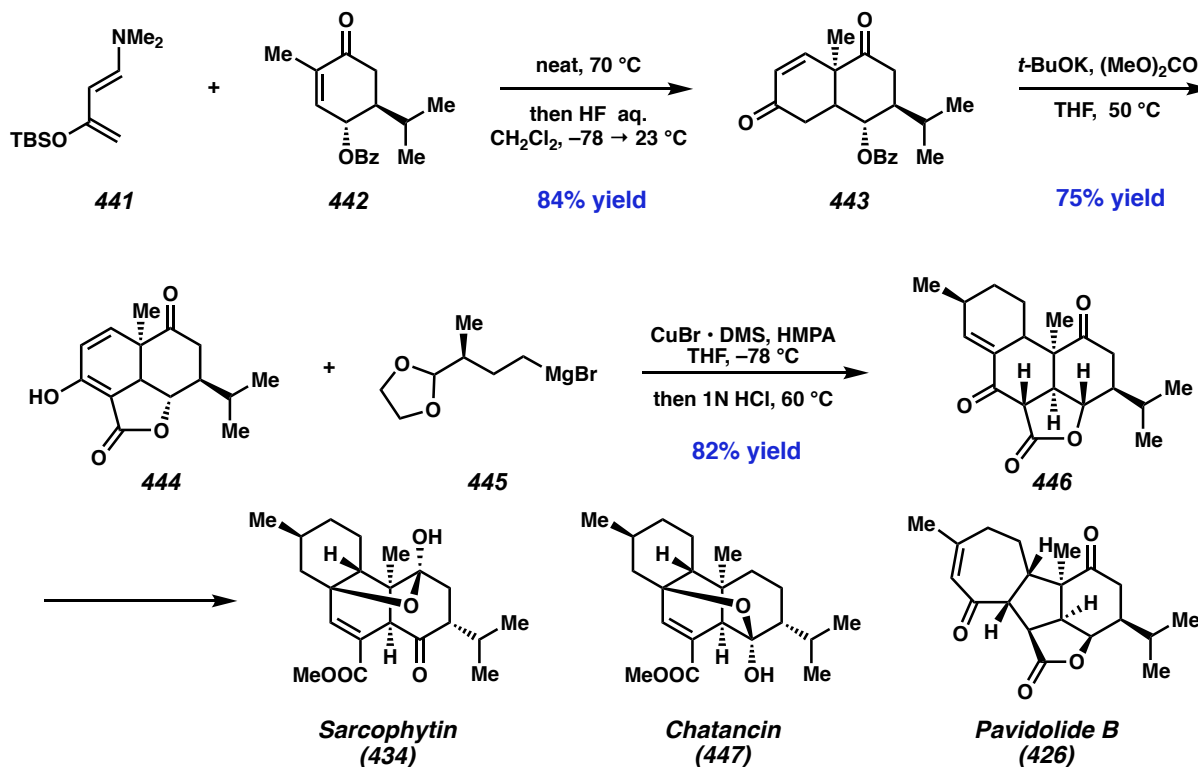
In 2017, Yang and coworkers¹² disclosed the first total synthesis of a cembranoid diterpenoid pavidolide B (**426**). (*E,E*)-2,4-hexadienal **427** is advanced in 5 steps to cyclopropane **428** via an asymmetric domino Michael addition (Scheme 4.3). This is coupled through a convergent Mitsunobu reaction with allylic alcohol **429**, available in two steps from (*R*)-carvone, to access key ester **430**. This substrate then undergoes a photoredox-catalyzed [3+2] cycloaddition to afford tricycle **431** in 50% yield as a single diastereomer before subsequent decarboxylation and

hemiaminal formation, and epimerization of the isopropyl fragment. Alkylation with TMS-diazomethane then advances this intermediate to sarcophytin (**434**).

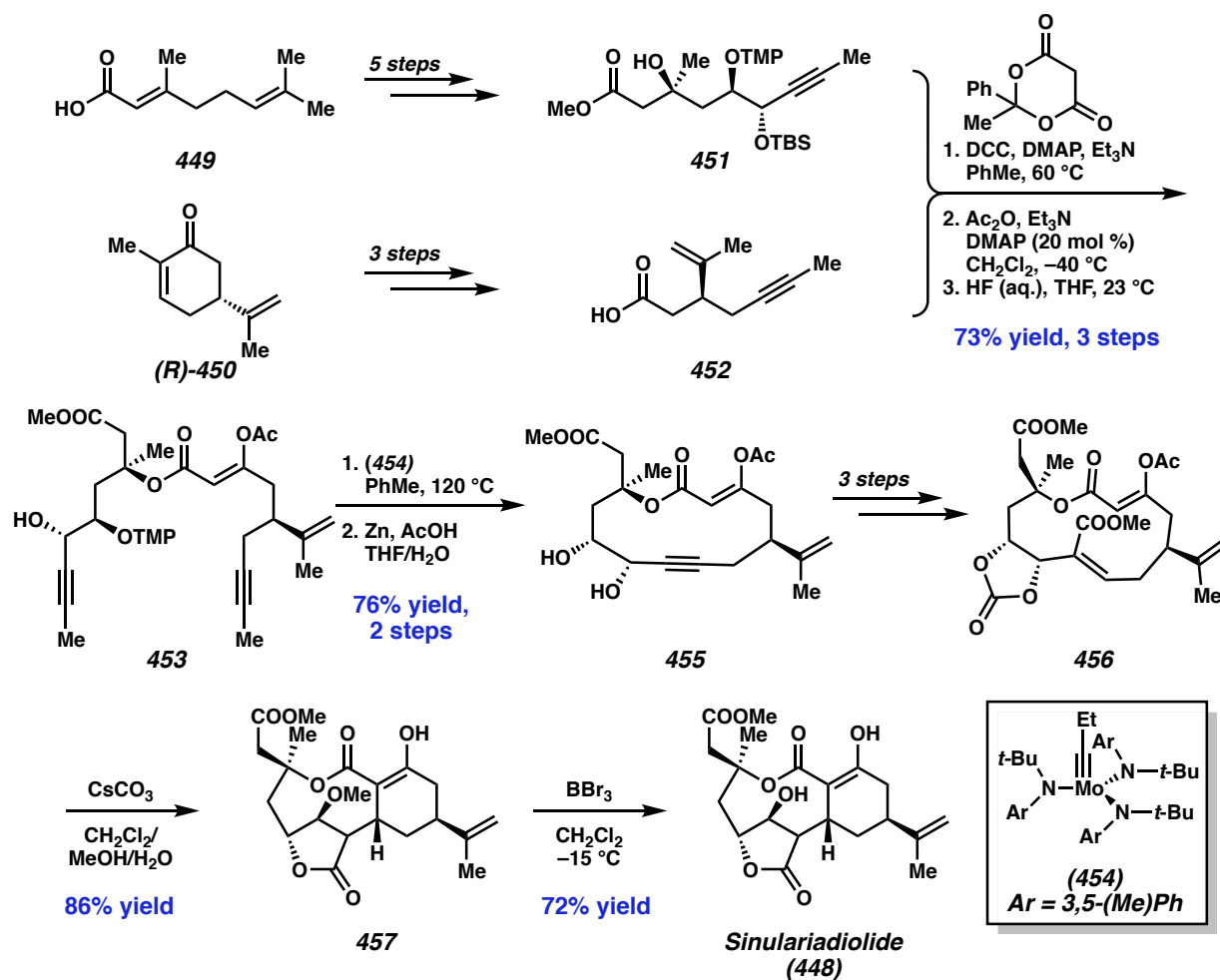
Scheme 4.4. *Carriera's asymmetric synthesis of sarcophytin (2018).*



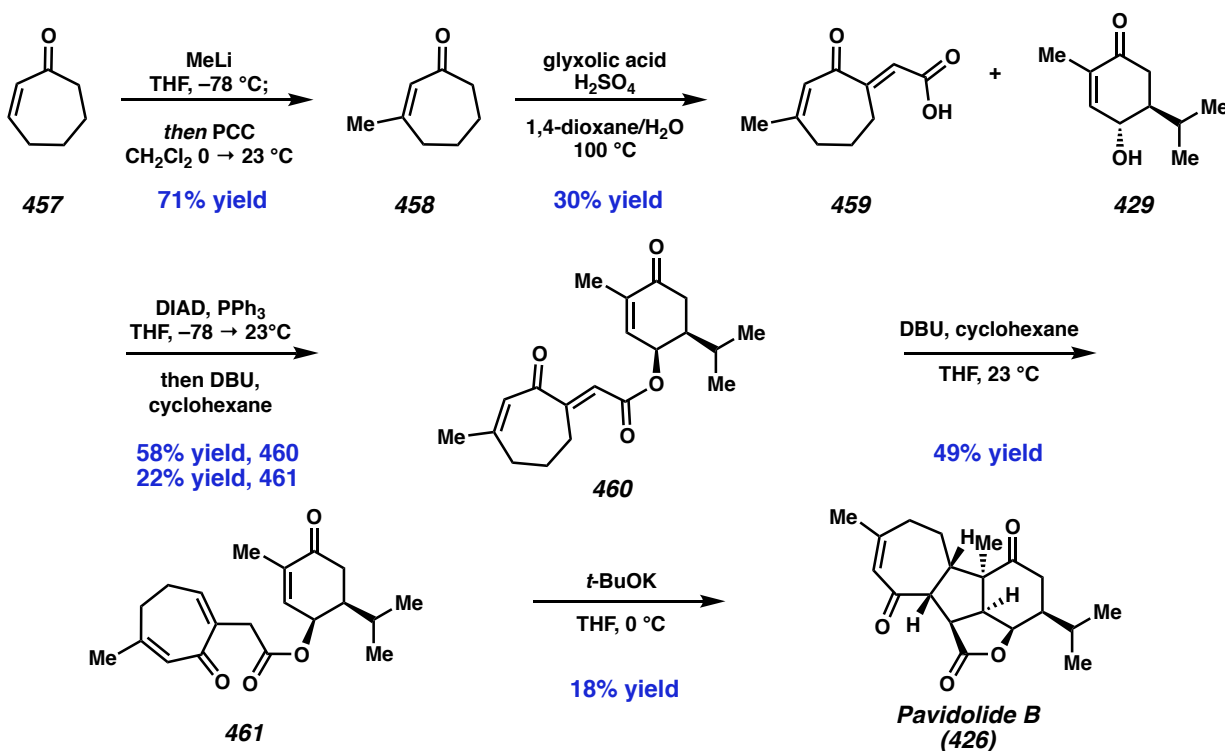
Later that year, Ding and coworkers¹⁴ disclosed a divergent route to several polycyclic cebranoids (Scheme 4.5). A formal [4+2] cycloaddition between Rawal's diene **441** and carvone-derivative **442** affords bicycle **443** in 84% yield. This is followed by a lactonization using dimethyl carbonate to afford ester **444**, which is subjected to Helquist annulation¹⁵ with Grignard **445** to afford key carbocyclic intermediate **446**. This would serve as a divergence point for the synthesis of multiple cebranoids including, sarcophytin (**434**), chatancin (**447**), and pavidolide B (**426**).

Scheme 4.5. Ding's asymmetric synthesis of several cembranoids (2018).

In 2019, the Fürstner group¹⁶ completed the first total synthesis of a polycyclic norcembranoid in the natural product sinulariadiolide (**448**). Geranic acid (**449**) is advanced to enantioenriched tertiary alcohol **451** through a five-step sequence involving an organocatalyzed asymmetric oxyamination to set the absolute stereochemistry; (*R*)-carvone (**450**) is then advanced to acid **452** over three steps through an Eschenmoser-Tanabe fragmentation strategy. A convergent esterification, followed by protecting group manipulations is advanced to diyne **453** in 73% yield over three steps before a Mo-catalyzed ring-closing alkyne metathesis with catalyst (**454**) affords macrocycle **455**. This is advanced over three steps to carbonate **456**, which is converted to tricyclic core **457** through a one-pot procedure involving five individual transformations: deacetylation, transannular Michael addition, carbonate elimination, butenolide formation, and oxa-Michael addition. Demethylation with boron tribromide then accesses sinulariadiolide (**448**).

Scheme 4.6. Fürstner's asymmetric synthesis of sinulariadiolide (2019).

Finally, Zhu and coworkers¹⁷ published a four-step synthesis of pavidolide B (**426**) in early 2020. Cycloheptenone **457** is treated first with methyllithium, followed by Dauben transposition to afford methylcycloheptenone **458** (Scheme 4.7). Aldol condensation with glycolic acid affords *trans* enoic acid **459** in 30% yield, which is coupled with hydroxycarvone **429** under Mitsunobu conditions to afford a mixture of *exo*- and *endo*- enones **460** and **461**, before the *exo*- intermediate is isomerized to the *endo*- enone with additional DBU. Finally, a base-initiated double Michael addition affords pavidolide B (**426**) directly in only four steps LLS.

Scheme 4.7. Zhu's asymmetric synthesis of pavidolide B (2020).**4.1.3. Inspiration**

By analyzing the successful synthetic efforts toward (nor)cembranoid diterpenoids, several trends have become apparent. First, given the high degree of structural analogy between natural products and commercial monoterpenes, the chiral pool provides an intuitive source of starting materials for synthetic efforts.¹⁸ Second, convergent strategies are frequently exploited to install a majority, if not all, of requisite carbons at an early stage; in most cases, an esterification is frequently used to accomplish this unification prior to intramolecular C–C bond forming steps. Finally, cycloadditions or biomimetic Michael cascades are the most frequently implemented transformations for the installation of stereocomplexity in fused systems. Therefore, the design and incorporation of unsaturation within cyclization precursors is critical for execution of the most efficient routes.

Though our strategy did not afford access to ineleganolide (**422**), the tactics developed for these late-stage manipulations remained informative and provided key insights into the reactivity of complex terpenoid scaffolds. While the cyclopropanation-Cope strategy to access a [5,7,6]-ring system would only be applicable to ineleganolide (**422**), we reasoned that a strategy to access the [5,6,7]-ring system could be applied to several natural products of varying degrees of complexity (e.g. **416** – **420**), benefiting from the expertise gained through unsuccessful pathways. To develop this strategy, we elected to target the norcembranoid diterpenoid scabrolide A (**416**).

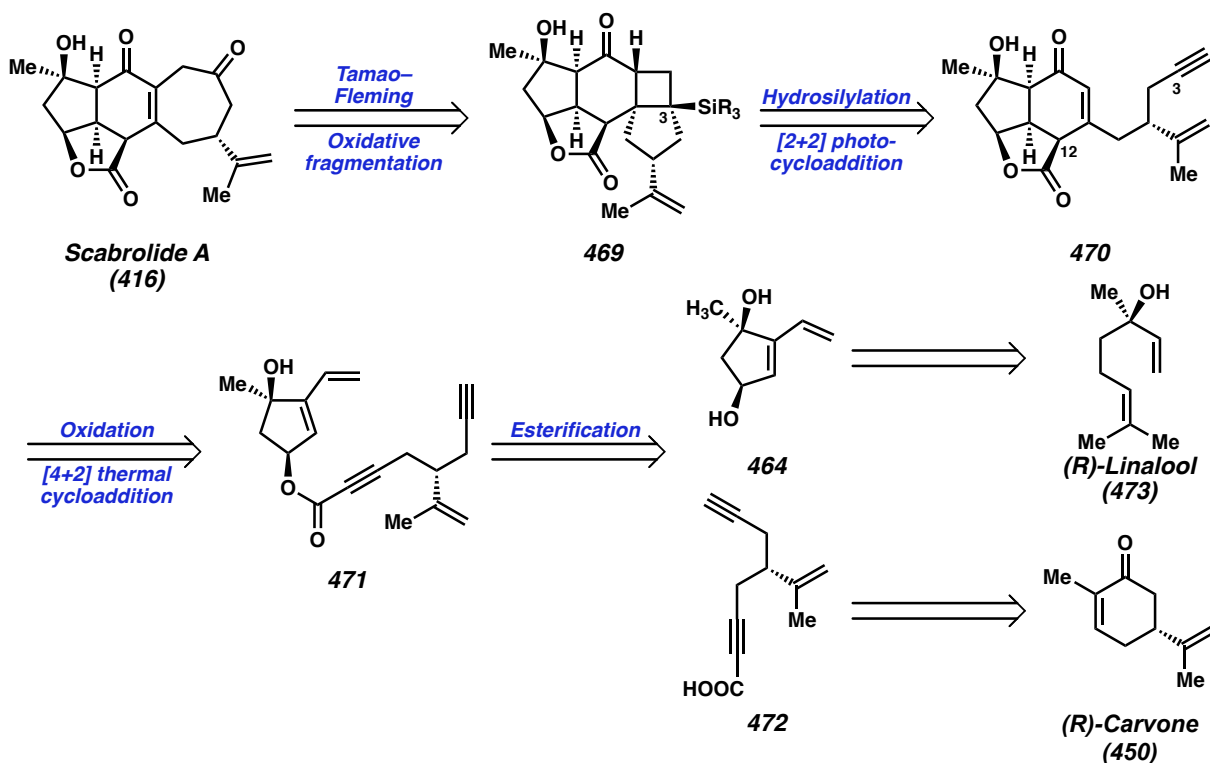
Scabrolide A (**416**) (Figure 4.1), a flagship member of the polycyclic furanobutenolide-derived natural product family, was first isolated by Sheu and coworkers from the Taiwanese soft coral *Sinularia scabra* in 2002 alongside four other novel norcembranoids (scabrolides B–D) and four known norcembranoids, including the closely related inelganolide (**422**).⁴ Since its initial isolation, **1** has been demonstrated to inhibit IL-6 and IL-12 production in vitro, suggesting its potential as an anti-inflammatory agent.⁵ Structurally, scabrolide A (**416**) is characterized by a fused [5,6,7] carbocyclic framework featuring six stereogenic centers, five of which are contiguously situated about the compact and densely functionalized western portion of the molecule. The eastern portion possesses a synthetically challenging cycloheptenone with its ketone positioned in an electronically dissonant 1,4-relationship to the central ring ketone, and a distal stereocenter in the form of an isopropenyl substituent.

4.1.4. Retrosynthetic Analysis

We envisioned that the challenging cycloheptenone moiety of scabrolide A (**416**) could arise from a Tamao-Fleming oxidation and oxidative fragmentation²⁰ of the cyclobutane moiety observed in silane **469** (Scheme 4.9); this would be generated, in turn, from a

hydrosilylation/photochemical [2+2] cycloaddition²¹ of alkyne **470**. Late-stage installation of the C(3) ketone was crucial, as a number of earlier strategies had found that the basic C(12) proton would frequently initiate an intramolecular aldol condensation.²² The central cyclohexanone would be formed through a thermal [4+2] cycloaddition and subsequent oxidative manipulations of ester **471**. Disconnection across the ester moiety provides two fragments: cyclopentadiol **464** which would serve as the diene and acyclic diyne **472** which would serve as the dienophile. These would be formed through derivatization of (-)-linalool (**473**) and (*R*)-carvone (**450**).

Scheme 4.9. Retrosynthetic analysis of scabrolide A.

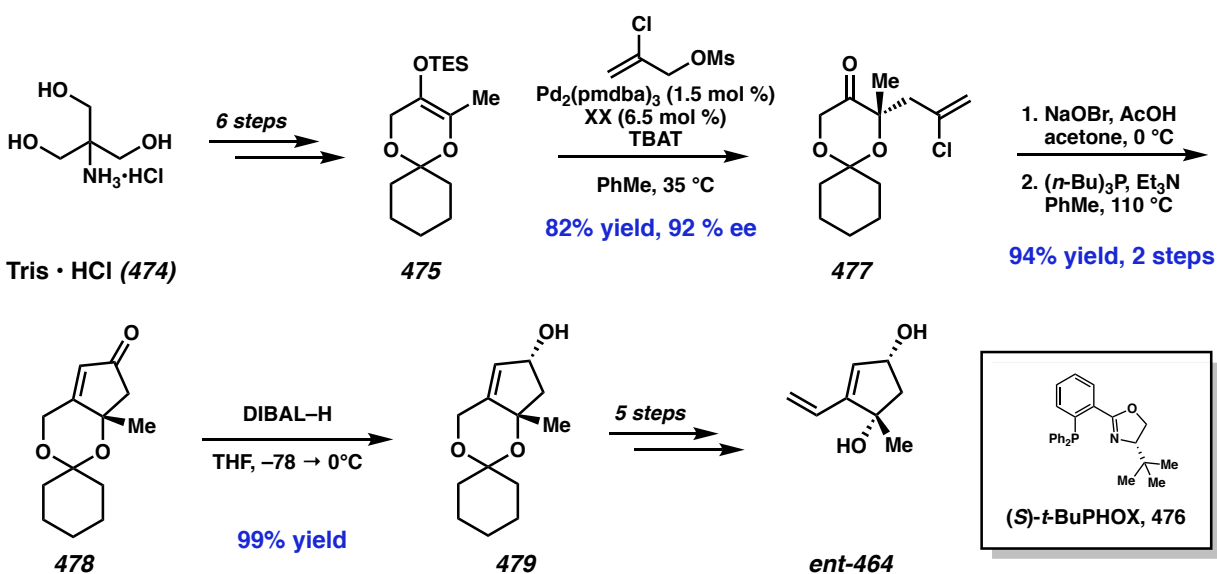


4.2 SYNTHESIS OF THE CYCLOHEXENONE CORE

4.2.1 Synthesis of the Cyclopentendiol

In 2012, our group first published a route to access cyclopentendiol **ent-464** using asymmetric catalysis.²³ Tris • HCl (**474**) is first advanced to silyl enol ether **475** over six steps (Scheme 4.10). A Pd-catalyzed allylic alkylation with 2-chloroallyl mesylate then establishes the tertiary alcohol stereogenic center of dioxolane **477** in 82% yield and 92% ee. This is then advanced through α bromination/intramolecular Wittig cyclization to cyclopenteneone **478**, before reduction with DIBAL-H forges secondary alcohol **479** as a single diastereomer. With both stereogenic centers now installed, this intermediate is advanced through five additional steps to cyclopentendiol **ent-464**.

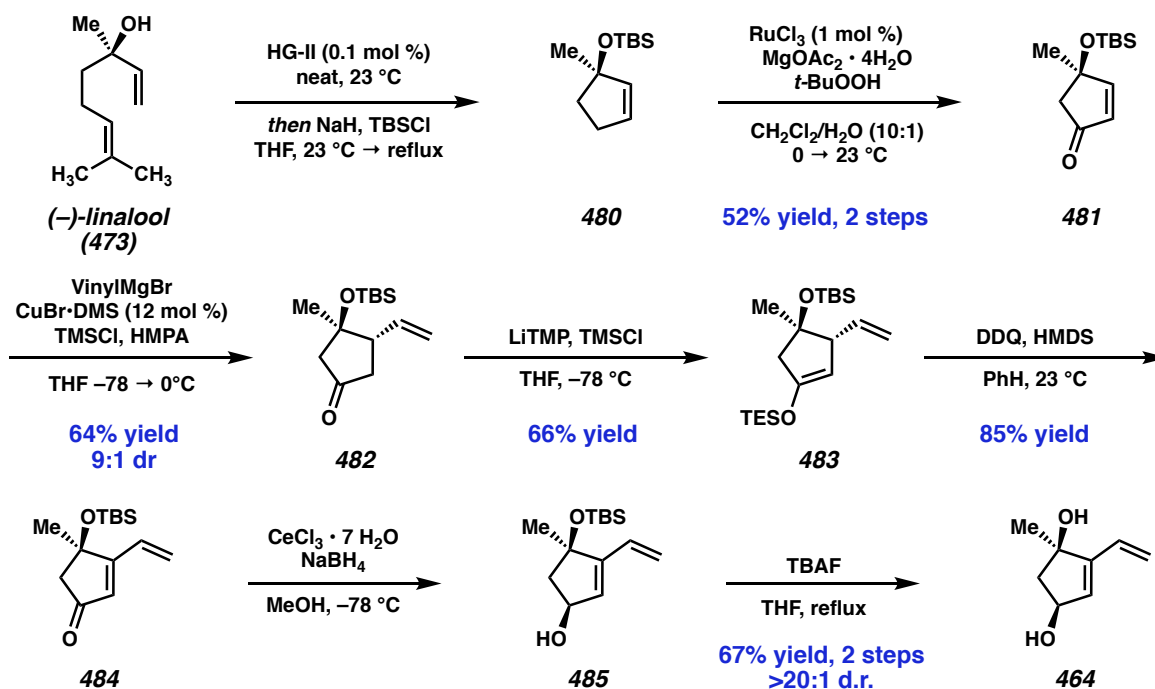
Scheme 4.10. First generation route to cyclopentendiol building block (2011).



While this approach was successfully employed to deliver the key building block on gram-scale, the route proved to be step-inefficient, as the time required to complete the sequence greatly limited material throughput. Furthermore, the established route accessed the *ent*-enantiomeric series, and to access the other enantiomer would require the synthesis of (*R*)-*t*-BuPHOX **476**

derived from a substantially more expensive D-*tert*-leucine. To circumvent these challenges, we looked to develop a revised route to our building block from chiral pool starting materials.

Scheme 4.11. Second generation synthesis of cyclopentendiol from linalool.

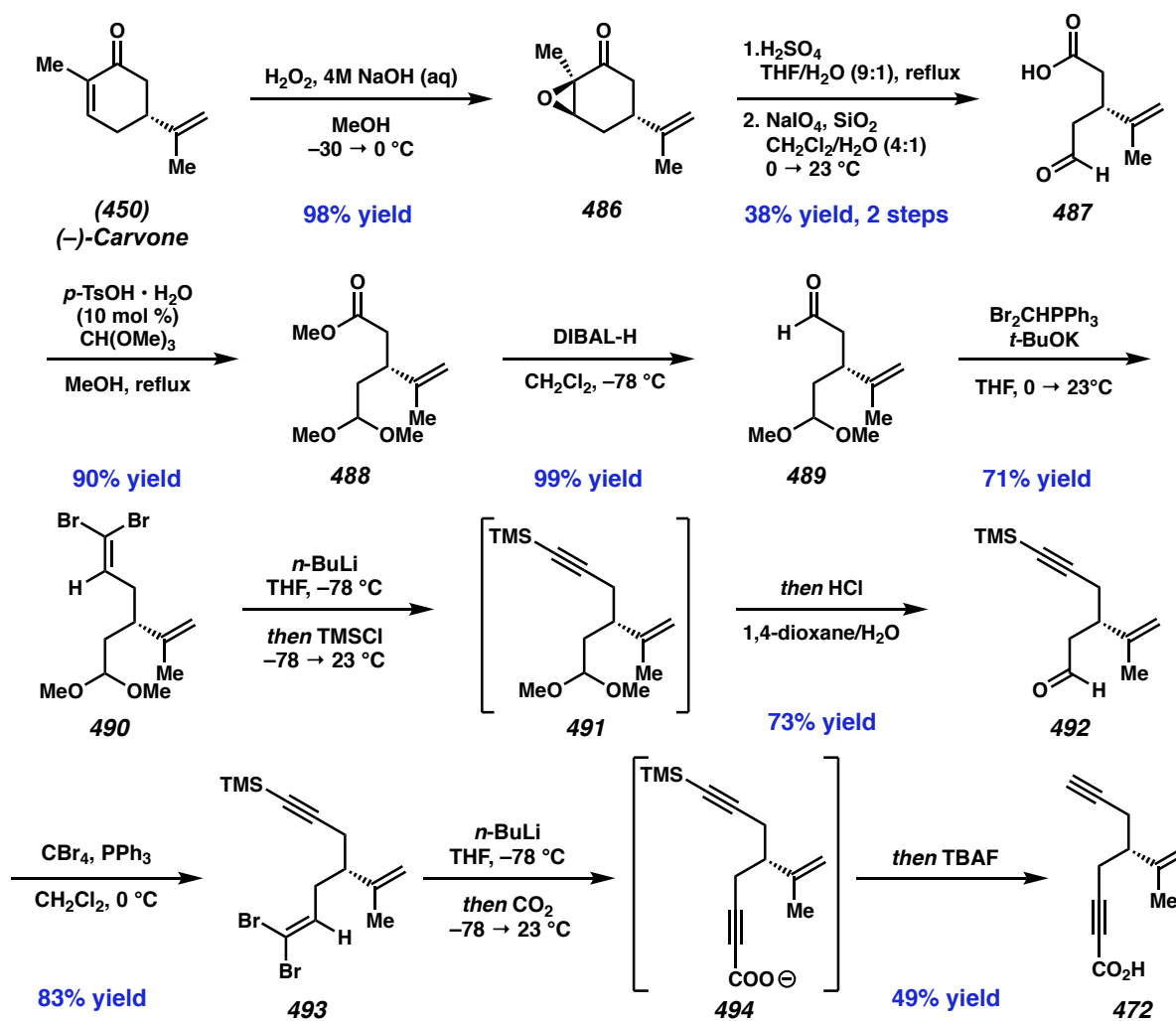


Following a procedure by Maimone and coworkers,²⁴ (-)-Linalool (**473**) is treated with Hoveyda-Grubbs II catalyst to promote a ring-closing metathesis and TBS-protected to afford cyclopentene **480** (Scheme 4.11). This intermediate is then subjected to Ru-catalyzed allylic oxidation to access key cyclopentenone **481** in 52% yield over two steps. Cu-catalyzed conjugate addition with vinyl magnesium bromide affords 1,4-addition product **482**, before transformation to the corresponding silyl enol ether **483**.²⁵ While Saegusa-Ito oxidation to dienone **484** was low yielding, we were delighted to obtain the desired product in excellent yield upon oxidation with DDQ.²⁶ Secondary alcohol **485** is forged through a diastereoselective Luche reduction before TBAF-mediated deprotection of the tertiary alcohol affords key building block **464** in seven steps

from commercial material. This sequence provides equivalent amounts of material to our previously published sequence²³ in fewer than half the number of steps.

4.2.2 Synthesis of the Acyclic Diyne

Scheme 4.12. Synthesis of acyclic diyne from carvone



Following a procedure described by Mulzer²⁷, we begin with nucleophilic epoxidation of (*R*)-carvone (450) to form epoxide 486 in 98% yield (Scheme 4.12). This is hydrolyzed using refluxing aqueous acid before oxidative cleavage affords the nearly-symmetrical acid 487.

Simultaneous Fischer esterification/acetal protection of the aldehyde affords fragment **488** which is subsequently reduced with DIBAL-H to afford differentially protected dialdehyde **489** in five steps.

Aldehyde **489** is first converted to *gem*-dibromide **490** under Wittig conditions. *n*-BuLi then promotes the Corey-Fuchs elimination, and the resultant alkynyllithium is quenched with TMSCl, generating acetylide **491**. Subsequent treatment with aqueous acid then cleaves the acetal in one-pot, affording aldehyde **492** in 73% yield. In a similar fashion, aldehyde **493** is converted to dibromide **494** before Corey-Fuchs elimination generates an alkynyllithium species that is quenched with carbon dioxide to afford carboxylate **494**. Subjugation to TBAF deprotects the acetylide in one-pot and generates diyne **472** in 49% yield.

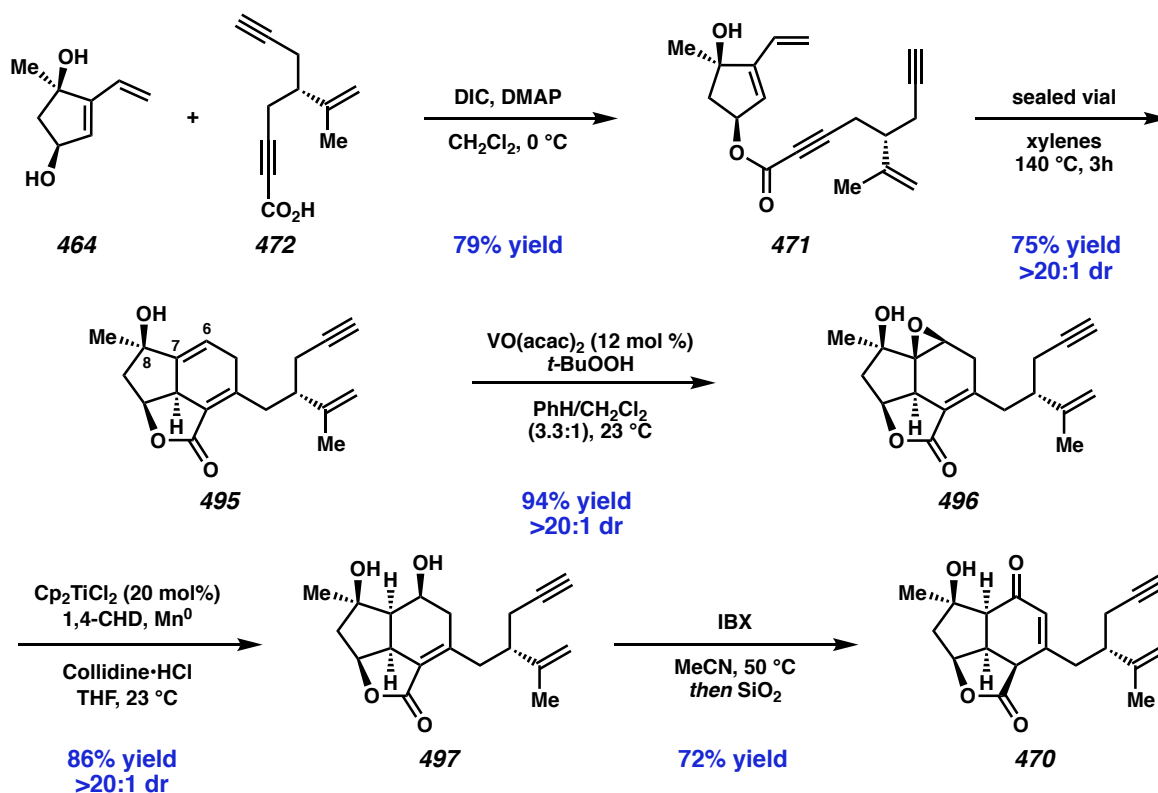
4.2.3 Convergent Esterification/Diels-Alder

With both fragments in hand, we turned our attention to the synthesis of the central six-membered ring (Scheme 4.13). Equimolar quantities of diol **464** and acid **472** could be effectively coupled under Steglich esterification conditions²⁸ generating Diels-Alder precursor **471** in 79% yield. Gratifyingly, we found that heating this intermediate for three hours in xylenes afforded cyclohexadiene **495** in 75% yield as a single diastereomer.

Following the precedent of our ineleganolide route,¹⁸ directed epoxidation with vanadium afforded selective epoxidation of the Δ -6,7 olefin in 94% yield as a single diastereomer²⁹ **496** before reductive cleavage with catalytic Ti³⁰ generated secondary alcohol **497** stereoselectively. The oxidation of secondary alcohol **497** proved to be unexpectedly challenging, with our previously optimized DMP conditions providing inconsistent and poorly scalable yields. Other mild and robust oxidations (e.g., TPAP/NMO,³¹ CuOTf/ABNO/O₂³²) failed to effect this transformation in

synthetically useful yields. After further screening, we discovered that IBX in MeCN at 50 °C was uniquely effective in providing enone **470** in good yield with olefin migration occurring spontaneously upon purification on silica gel. We attribute this challenging oxidation to two factors: 1) steric hindrance, as the alcohol is buried in the concave face of intermediate **497**, and 2) potential hydrogen bonding within the *syn*-1,3-diol, which confers further stability.

Scheme 4.13. Thermal [4+2] cycloaddition and oxidative manipulations.



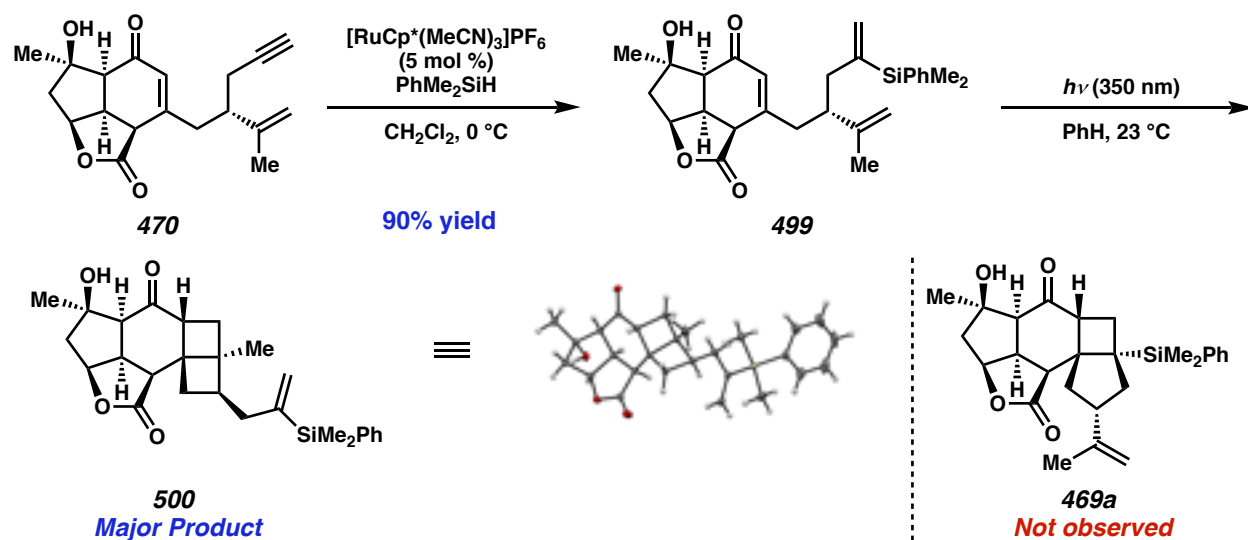
4.3 SYNTHESIS OF THE CYCLOHEPTENONE RING

4.3.1 Initial Investigations of the Photochemical [2+2] Cycloaddition

With the western hemisphere of the natural product complete, we turned our attention to the appendage of the seven-membered ring. While Trost's Ru-catalyzed hydrosilylation³³ produced vinyl silane **499** in excellent yield (Scheme 4.14), we were disappointed to see that the

subsequent photocycloaddition upon irradiation with 350 nm light primarily yielded formation of the fused [5,6,4,4] system **500**, which was confirmed through x-ray crystallography. No detectable quantity of the desired [5,6,4,5]-system **469a** was observed. While we were aware that this undesired enone-isopropenyl olefin cycloaddition could occur, we predicted that the strained nature of these products would occlude formation in significant quantity. The exclusive formation of intermediate **500** indicated that optimization to select for desired tetracycle **469a** was unlikely.

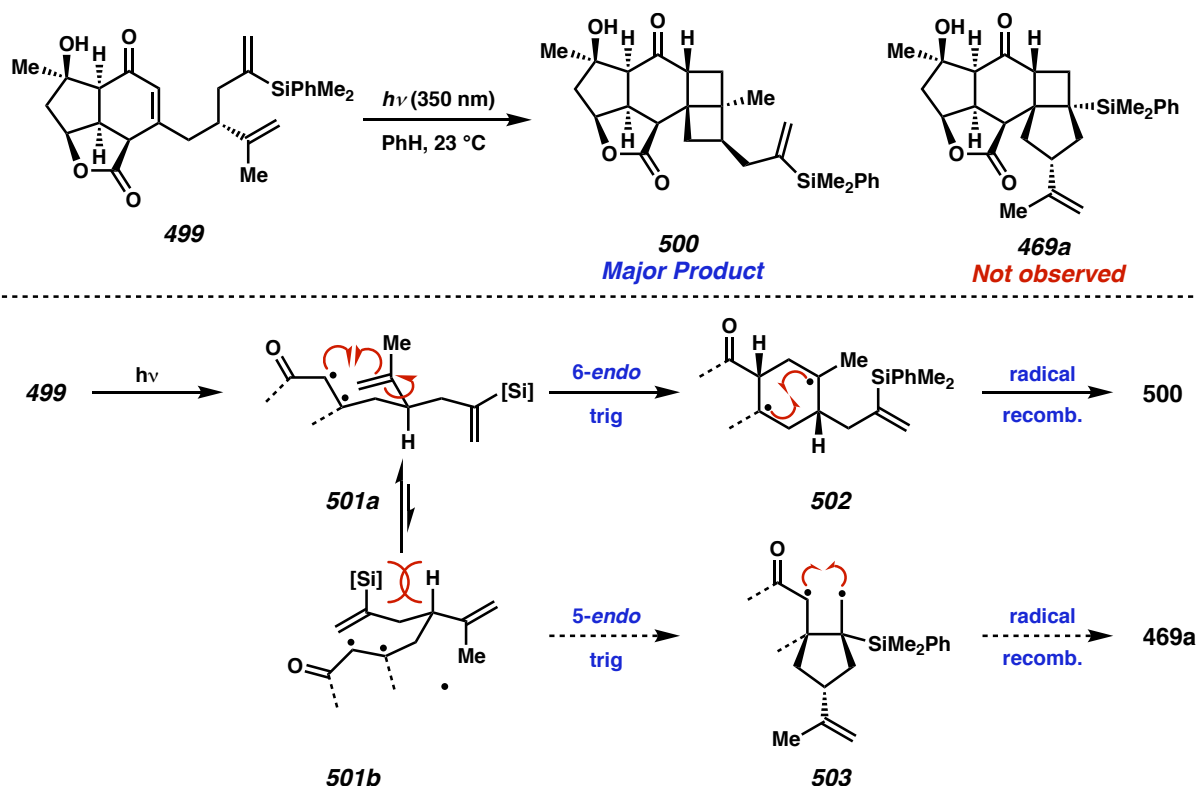
Scheme 4.14. Hydrosilylation and unexpected photocycloaddition



Mechanistically, photoexcitation of enone **499** generates a triplet-state enone, best represented as a diradical species which can exist in a variety of conformers (Scheme 4.15). Conformation **501a** would enable facile 6-*exo*-trig cyclization onto the isopropenyl fragment to generate 1,4-diradical **502** before radical recombination would then collapse to the observed [4,4]-fused ring system **500**; though enone-olefin photocycloadditions heavily favor five-membered ring formation, this reactivity has been previously observed for 1,1-disubstituted olefins.³⁴ To obtain the desired product, the diradical would likely need to adopt conformation **501b** prior to 5-*exo* trig cyclization to primary radical **503** prior to recombination; it is likely that this large

dimethylphenylsilyl substituent creates undesired steric interactions, which dissuades the adoption of this conformation.

Scheme 4.15. Mechanistic rationale for the observed photocycloaddition



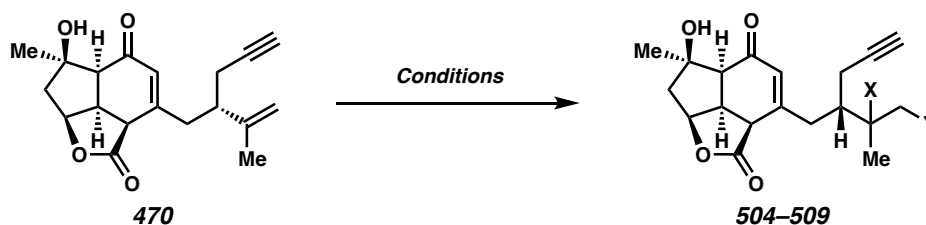
4.3.2 Development of an Olefin Protection Strategy

To avoid this competitive reactivity, we elected to modify our route slightly by functionalizing the isopropenyl fragment prior to hydrosilylation; by removing this problematic unsaturation temporarily, we could realize our key cycloaddition/fragmentation sequence before unveiling this olefin at a later stage.

We first attempted to perform a Mukaiyama hydration (Table 4.1, Entry 1), but were disappointed to observe enone reduction as the major product (*vide infra*). Hydrotrifluoroacetoxylation led to no reaction (Entry 2) while hydrochlorination with Brønsted

acid (Entry 3) or Snyder's reagent³⁵ (Entry 4) produced dehydration products. Sharpless dihydroxylation (Entry 5 and 6) led to modest diastereoselectivity, but a complex mixture of other products was also formed.

Table 4.1. Optimization of the isopropenyl protection strategy.



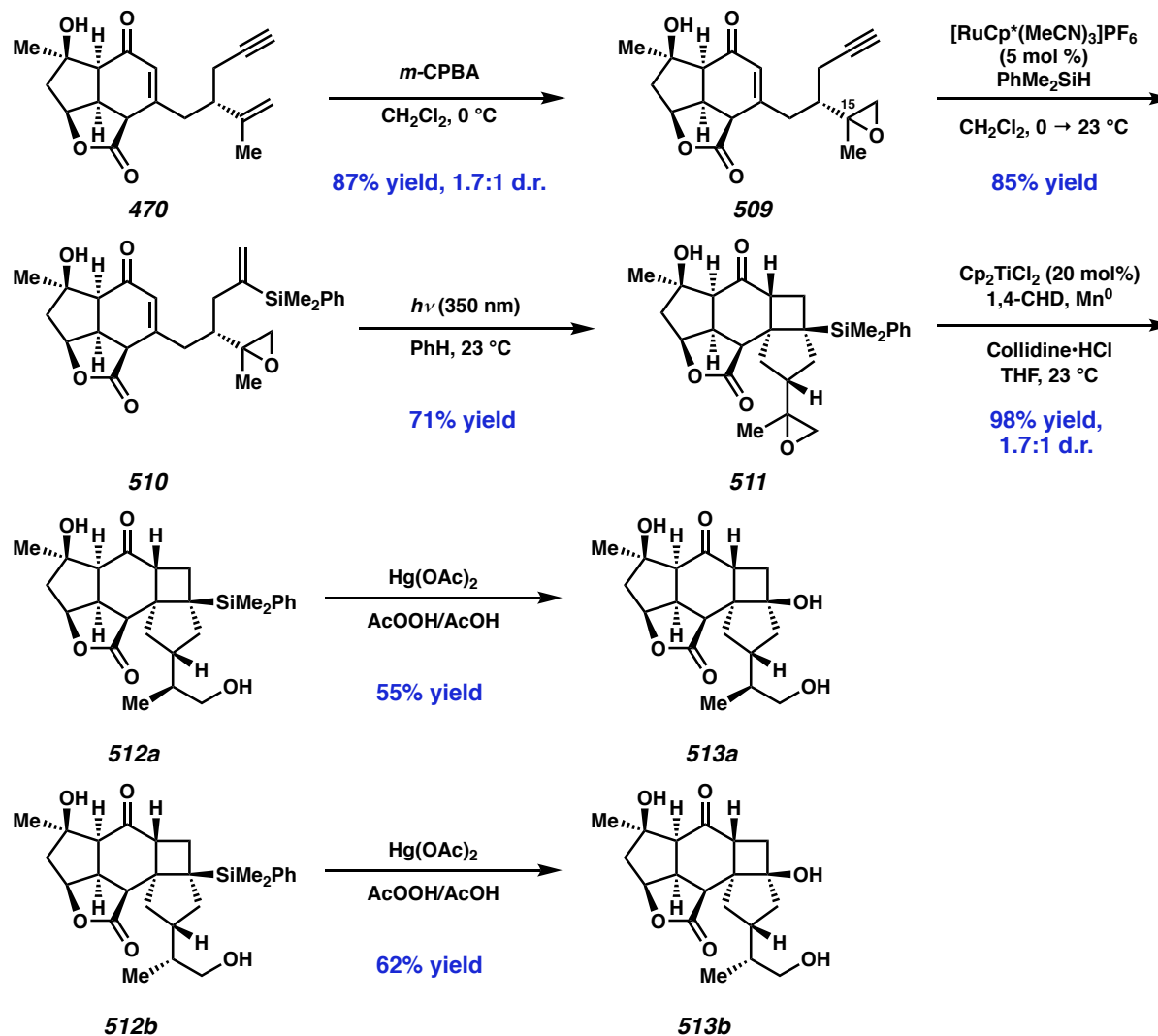
Entry	X	Y	Conditions	Result
1	OH	H	Mn(dpm) ₃ (15 mol %), PhSiH ₃ , <i>i</i> -PrOH, 23 °C	Enone reduction
2	OTFA	H	TFA (5 equiv), CH ₂ Cl ₂ , 0 → 23 °C	No reaction
3	Cl	H	AcCl, EtOH, 23 °C	Dehydration
4	Cl	H	dppe • SbCl ₅ • Cl ₂ , wet MeNO ₂ , 23 °C	Dehydration
5	OH	OH	AD-mix β, tBuOH/H ₂ O (1:1), 23 °C	18% yield, 2:1 d.r.
6	OH	OH	AD-mix α, tBuOH/H ₂ O (1:1), 23 °C	20% yield, 3:1 d.r.
7	-O-		<i>m</i> CPBA, CH ₂ Cl ₂ , 0 → 23 °C	87% yield, 1.7:1 d.r.
8	-O-		<i>m</i> CPBA, CH ₂ Cl ₂ , -10 °C	44% yield, 1.4:1 d.r.
9	-O-		Shi's Catalyst, Oxone, 1,4-dioxane/H ₂ O, 0 → 23 °C	50% yield, 1.5:1 d.r.
10	-O-		(<i>R,R</i>)-Jacobsen's Catalyst, NaOCl, 1,4-dioxane/H ₂ O, 0 → 23 °C	No reaction
11	-O-		(<i>S,S</i>)-Jacobsen's Catalyst, NaOCl, 1,4-dioxane/H ₂ O, 0 → 23 °C	No reaction

We were delighted, however, to see that epoxidation with *m*-CPBA occurred cleanly in high yield but poor d.r. (Entry 7). Performing the reaction at lower temperature lead to decreases in yield and d.r. (Entry 8). Though Shi's catalyst had been reported to promote diastereoselective epoxidation of other carvone derivatives,³⁶ we were disappointed to see no improvement with our system (Entry 9). Jacobsen epoxidations³⁷ with both enantiomers of catalyst (Entry 10 and 11) likewise produced no observable epoxidized products.

4.3.3 Synthesis of the Cyclobutanol

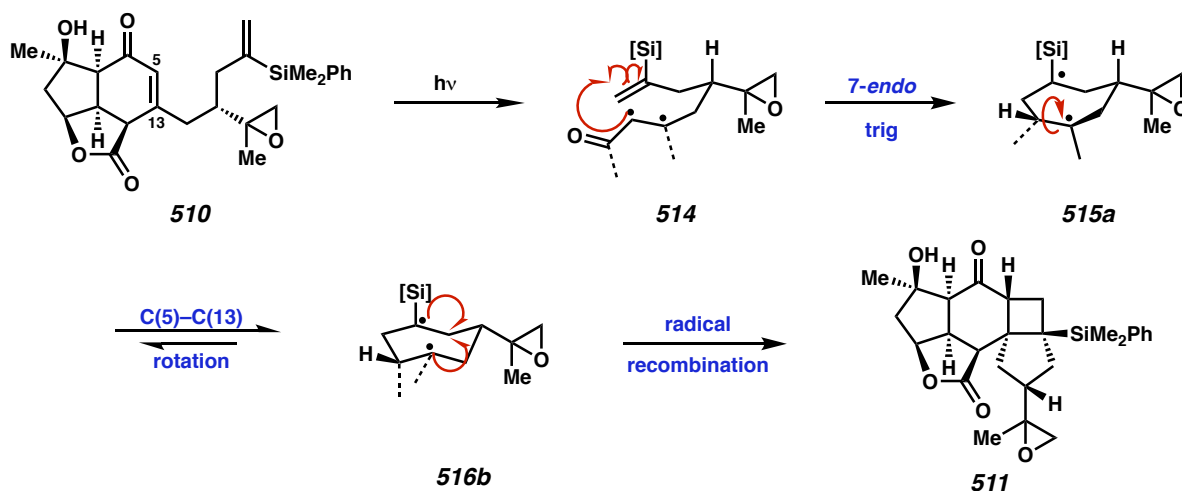
Though the diastereoselectivity of the epoxidation could not be improved, epoxide mixture **509** was carried forward through the hydrosilylation (**509** → **510**, Scheme 4.16). To our delight, the subsequent photocycloaddition occurred smoothly, accessing cyclobutane **511** as a mixture of epoxide epimers. Reductive cleavage with titanium then generates a separable mixture of primary alcohols **512a** and **512b** in 1.7:1 d.r.³⁸ Both intermediates can then be oxidized under Tamao-Fleming conditions to cyclobutanols **513a** and **513b**.

Scheme 4.16. [2+2] photocycloaddition and subsequent oxidation.



Interestingly, the crystal structures display both intermediates as *trans*-fused cyclobutanols which would not be possible under the 5-*exo* trig mechanism previously hypothesized. Mechanistically, this observation can be explained by invoking a mechanism in which an initial 7-*endo* trig between C(4) and C(5) of **514** occurs from the convex α -face of the molecule generating diradical **515a** (Scheme 4.17). This long-lived radical species does not recombine until rotation of the C(5)–C(13) bond to conformation **515b** occurs preceding recombination of the 1,4-diradical from the β -face; this prevents severe steric interactions between the bulky phenyldimethylsilyl substituent and the cyclohexanone ring generating *trans*-fused product **511**. Similar stereochemical outcomes (i.e. preferential formation of *trans*-fused adducts) have been reported in analogous systems³⁹ presumably due to the presence of substitution at the internal position of the reacting olefin.

Scheme 4.17. Mechanistic rationale for the *trans*-fused cyclobutane

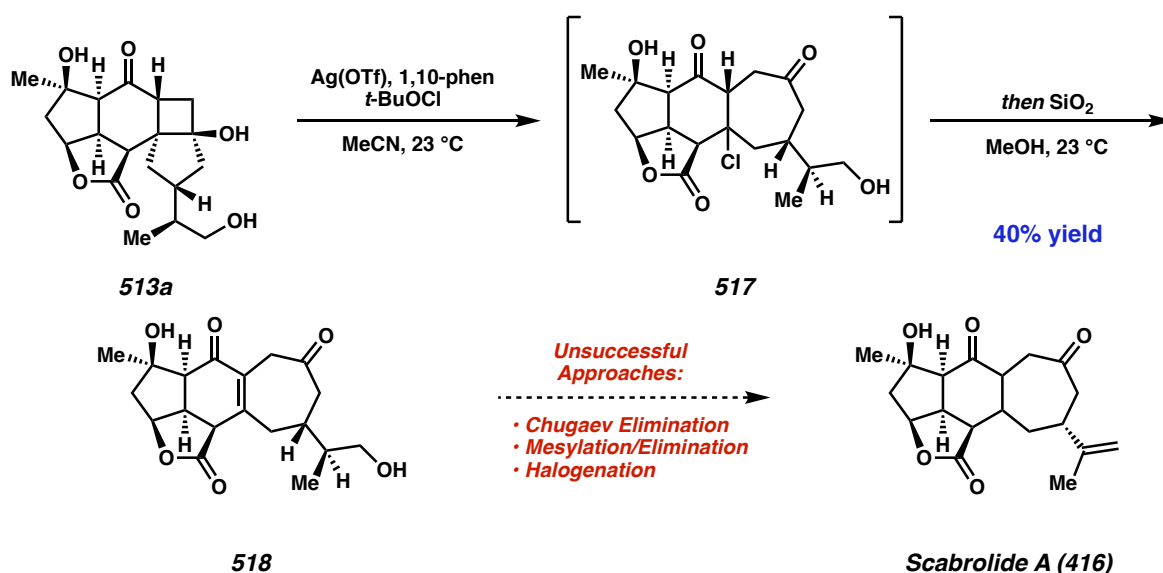


4.3.4 Oxidative Fragmentation of the Cyclobutanol

Oxidation product **513a** was subjected to an Ag-mediated fragmentation⁴⁰ generating a chlorinated intermediate that was tentatively characterized as β -chloroketone **517**. Treatment with

silica gel in methanol promoted elimination to cyclohexenone **518** (Scheme 4.18). We then investigated a number of methods to eliminate the primary alcohol including Chugaev elimination conditions, mesylation, brominations, iodination, Burgess' reagent⁴¹ and Martin's sulfurane,⁴² though all were ultimately unsuccessful. We attribute this challenging elimination to steric hindrance of the unactivated C(15) proton, which is "hexyl"-like. We therefore limited our future efforts to unimolecular eliminations.

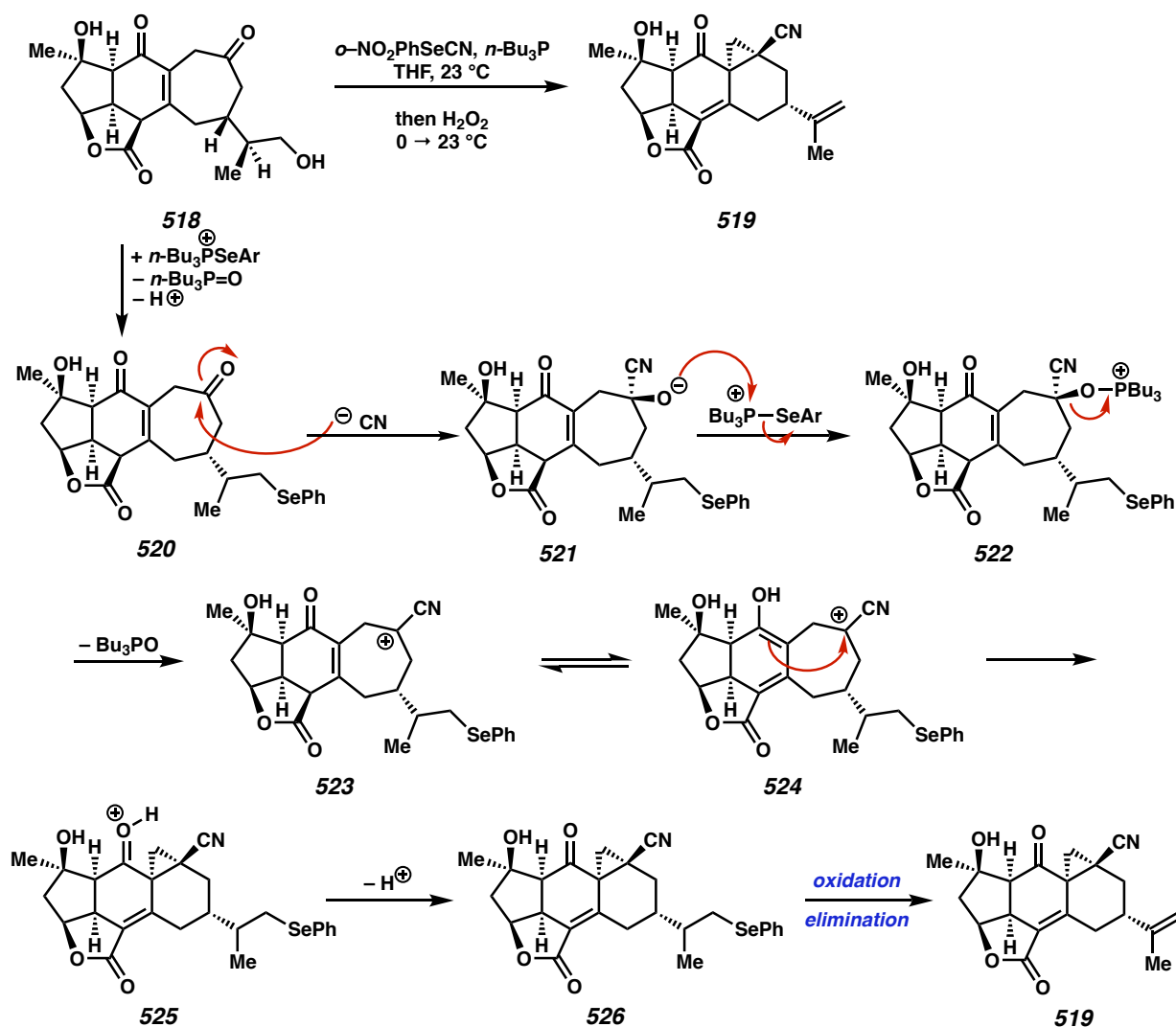
Scheme 4.18. Failed fragmentation/elimination approach.



Turning our attention to the Grieco⁴³ elimination, we were delighted to see that these conditions were highly amenable to elimination in this complex system. However, our major product was an intriguing ring-contracted cyclopropane **519** with no isolable quantity of scabrolide A (**416**) (Scheme 4.19). Mechanistically, we hypothesize that following displacement of the primary alcohol to selenide **520**, adventitious cyanide forms cyanohydrin **521** that reacts with a second equivalent of the selenophosphonium species, generating oxophosphonium **522**. This subsequently undergoes E1 elimination to the corresponding tertiary carbocation **523**. The vinylogous β -ketoester, which is in ready equilibrium with the enol species **524**, quenches the

carbocation which, upon deprotonation, generates cyclopropane **525**. Addition of peroxide then completes the oxidation/intramolecular elimination sequence of the Grieco dehydration to generate the isolated species **519**.

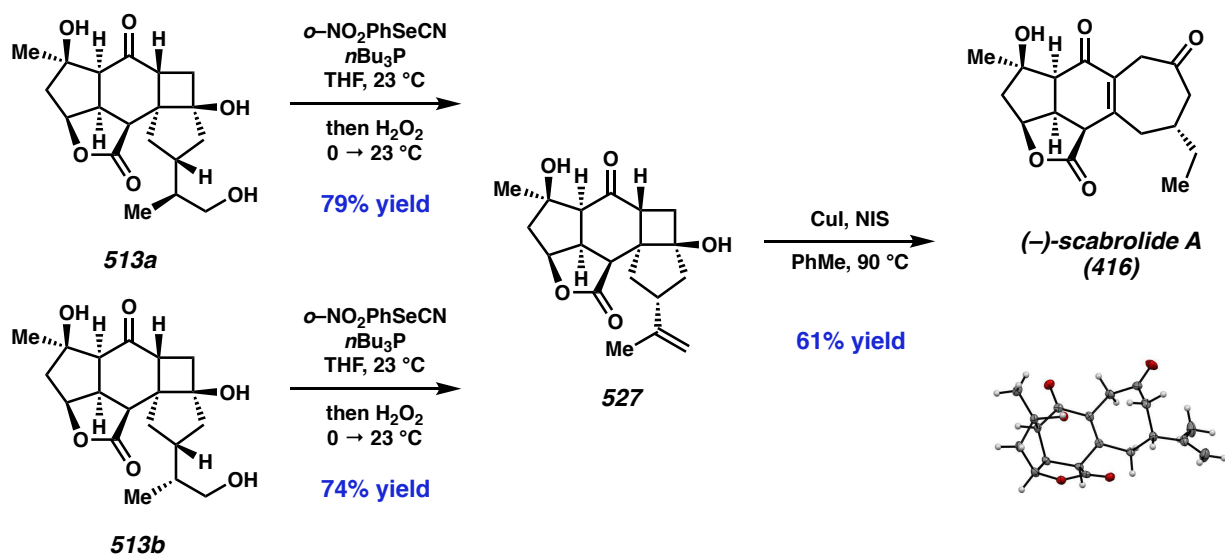
Scheme 4.19. Unexpected ring contraction and proposed mechanism.



Given the proclivity of these systems to engage in transannular reactivity, we decided to change the order of steps in order to obviate the need to perform reactions in the presence of the highly reactive cycloheptenone. Grieco elimination of both **513a** and **513b** successfully promoted elimination, converging the material to isopropenyl cyclobutanol **527** (Scheme 4.20). Though the

silver-mediated conditions created a complex mixture of products, we discovered that CuI/NIS conditions⁴⁴ successfully promoted a one-pot fragmentation/elimination to access scabrolide A (416) in a single operation.

Scheme 4.20. Completion of scabrolide A.



4.4 CONCLUDING REMARKS

In summary, we have disclosed the first total synthesis of the norcembranoid diterpenoid (-)-scabrolide A. To our knowledge, this report constitutes the first total synthesis of any member of the polycyclic C₁₉ furanobutenolide-derived norcembranoid diterpenoid family, a class of natural products that have evaded synthetic efforts for the more than two decades since their initial isolation. The route exploits the convergent esterification and subsequent intramolecular Diels–Alder cycloaddition of two enantiopure fragments to introduce each of the 19 carbon atoms of the natural product. An initially unsuccessful [2+2] cycloaddition was enabled by an unconventional olefin protection strategy, which allows for the correct regiochemical outcome of this key reaction. Finally, a late-stage oxidative cyclobutanol fragmentation was employed to furnish the

cycloheptenone ring and complete the total synthesis. Efforts are currently ongoing to extend this strategy toward the synthesis of other norecembranoid diterpenoids, and progress will be reported in due course.

4.5 REFERENCES

-
- (1) Craig II, R.A.; Stoltz, B.M. *Chem. Rev.* **2017**, *117*, 7878–7909
 - (2) Li, Y.; Pattenden, G. *Nat. Prod. Rep.* **2011**, *28*, 1269–1310. b) Li, Y.; Pattenden, G. *Nat. Prod. Rep.* **2011**, *28*, 429–440.
 - (3) a) Montaser, R.; Luesch, H.; *Future Med. Chem.* **2011**, *3*, 1473–1489. b) Berrue, F.; Kerr, R.G. *Nat. Prod. Rep.* **2009**, *26*, 681–710. c) Kamel, H.N.; Slattery, M.; *Pharm. Biol.* **2005**, *43*, 253–269.
 - (4) Sheu, J.; Ahmed, A. F.; Shiue, R.; Dai, C.; Kuo, Y.; *J. Nat. Prod.* **2002**, *65*, 1904–1908.
 - (5) Thao, N.P.; Nam, N.H. Cuong, N.X.; Quang, T.H.; Tung, P.T.; Dat, L.D.; Chae, D.; Kim, S.; Koh, Y-S.; Kiem, P.V. *Bioorg. Med. Chem. Lett.* **2013**, *23*, 228–231.
 - (6) Tseng, Y.-J.; Ahmed, A.F.; Dai, C.-F.; Chiang, M.Y.; Sheu, J.-H. *Org. Lett.* **2005**, *7*, 3813–3816.
 - (7) Iguchi, K.; Kajiyama, K.; Yamada, Y. *Tetrahedron Lett.* **1995**, *36*, 8807–8808.
 - (8) Kobayashi, M.; Rao, K.M.C.A.; Krishna, M.M.; Anjaneyulu, V.; *J. Chem. Res. (S)* **1995**, 188–189.
 - (9) Duh, C.-Y.; Wang, S.-K.; Chia, M.-C.; Chiang, M.Y. *Tetrahedron Lett.* **1999**, *40*, 6033–6035.
 - (10) Yen, W.-H.; Su, Y.-D.; Chang, Y.-C.; Chen, Y.-H.; Dai, C.-F.; Wen, Z.-H.; Su, J.-H.; Sung, P.-J. *Tetrahedron Lett.* **2013**, *54*, 2267–2270.
 - (11) Li, Y.; Pattenden, G. *Tetrahedron* **2011**, *67*, 10045–10052.
 - (12) Zhang, P-P.; Yan, Z-M.; Li, Y-H.; Gong, J-X.; Yang, Z *J. Am. Chem. Soc.* **2017**, *139*, 13989–13992.
 - (13) Nannini, L.J.; Nemat, S.J.; Carrieria, E.M. *Angew. Chem. Int. Ed.* **2018**, *57*, 823–826.

-
- (14) He, C.; Xuan, J.; Rao, P.; Xie, P.-P.; Hong, X.; Lin, X.; Ding, H. *Angew. Chem. Int. Ed.* **2018**, *58*, 5100–5014.
- (15) Marfat, A.; Helquist, P. *Tetrahedron Lett.* **1978**, *44*, 4217–4720.
- (16) Meng, Z.; Fürstner, A. *J. Am. Chem. Soc.* **2019**, *141*, 805–809.
- (17) Zhu, Y.; Romero, E.L.; Srinivas, K.; Noriega, E. *ChemRxiv.* **2020**, Preprint. DOI: 10.26434/chemrxiv.11560137.v1
- (18) Brill, Z.G.; Condakes, M.L.; Ting, C.P.; Maimone, T.J. *Chem. Rev.* **2017**, *117*, 11753–11795.
- (19) a) Craig II, R.A.; Roizen, J.L.; Smith, R.C.; Jones, A.C.; Virgil, S.C.; Stoltz, B.M. *Chem Sci.* **2017**, *8*, 507–514. b) Craig II, R.A.; Smith, R.C.; Roizen, J.L.; Jones, A.C.; Virgil, S.C.; Stoltz, B.M. *J. Org Chem.* **2018**, *83*, 3467–3485. c) Craig II, R.A.; Smith, R.C.; Roizen, J.L.; Jones, A.C.; Virgil, S.C.; Stoltz, B.M. *J. Org Chem.* **2019**, *84*, 7772–7746.
- (20) For reviews of cyclobutane fragmentation strategies in synthesis see (a) Oppolzer, W. *Acc. Chem. Res.* **1982**, *15*, 135–141. (b) Winkler, J. D.; Bowen, C. M.; Liotta, F. *Chem. Rev.* **1995**, *95*, 2003–2020.
- (21) For reviews of [2+2] photocycloadditions see: (a) Crimmins, M.T. *Chem. Rev.* **1988**, *88*, 1453–1473. (b) Sarkar, D.; Bera, N.; Ghosh, S. *Eur. J. Org. Chem.* **2020**, 1310–1326. (c) Hoffman, N. *Chem. Rev.* **2008**, *108*, 1052–1103. (d) Kärkäs M. D.; Porco, J. A., Jr.; Stephenson, C. R. J. *Chem. Rev.* **2016**, *116*, 9683–0747.
- (22) Loskot, S.A. *Ph. D. Dissertation.* California Institute of Technology **2019**.
- (23) Craig, R. A., II; Roizen, J. L.; Smith, R. C.; Jones, A. C.; Stoltz, B. M. *Org. Lett.* **2012**, *14*, 5716–5719.

-
- (24) a) Brill, Z. G.; Grover, H. K.; Maimone, T. J. *Science*, **2016**, *352*, 1078–1082. b) Thatch, D.Q.; Brill, Z.G.; Grover, H.K. Esguerra, K.V.; Thompson, J.K.; Maimone, T.J. *Angew. Chem. Int. Ed.* **2020**, *59*, 1532–1535.
- (25) Though the conjugate addition product could be directed trapped as the TES enol ether on small scale, we found that yields were significantly lower than the two step sequence when multigram quantities of starting material were utilized.
- (26) Ryu, I.; Murai, S.; Hatayama, Y.; Sonada, N. *Tetrahedron Lett.* **1978**, *37*, 3455–3458
- (27) Weinstabl, H.; Gaich, T.; Mulzer, J. *Org. Lett.* **2012**, *14*, 2834–2837.
- (28) Neises, B.; Steglich, W. *Angew. Chem. Int. Ed.* **1978**, *17*, 522–524.
- (29) Direct conversion of epoxide **496** to ketone **470** through Meinwald rearrangement was attempted but ultimately proved unsuccessful.
- (30) Gansäuer, A.; Bluhm, H.; Pierobon, M. *J. Am. Chem. Soc.* **1998**, *120*, 12849–12859.
- (31) Griffith, W. P.; Ley, S. V.; Whitcombe, G. P.; White, A. D. *J. Chem. Soc., Chem. Commun.* **1987**, *21*, 1625–1627.
- (32) Steves, J. E.; Stahl, S. S. *J. Am. Chem. Soc.* **2013**, *135*, 15742–15745.
- (33) Trost, B.M.; Ball, Z.T. *J. Am. Chem. Soc.* **2005**, *127*, 17644–17655.
- (34) (a) Srinivasan, R.; Carlough, K. H. *J. Am. Chem. Soc.* **1967**, *89*, 4932–4936. (b) Liu, R. S. H.; Hammond, G. S. *J. Am. Chem. Soc.* **1967**, *89*, 4936–4944. (c) Wolff, S.; Agosta, W. C. *J. Org. Chem.* **1981**, *46*, 4821–4825. (d) Wolff, S.; Agosta, W. C. *J. Chem. Soc., Chem. Commun.* **1981**, 118–120. (e) Wolff, S.; Agosta, W. C. *J. Am. Chem. Soc.* **1983**, *105*, 1292–1299.
- (35) Schevenels, F.T.; Shen, M.; Snyder, S.A. *J. Am. Chem. Soc.* **2017**, *139*, 6329–6337.

-
- (36) Wang, K-Y.; Liu, D-D.; Sun, T-W.; Lu, Y.; Zhang, S-L.; Li, Y-H.; Han, Y.X.; Liu, H-Y.; Peng, C.; Wang, Q-Y.; Chen, J-H.; Yang, Z. *J. Org. Chem.* **2018**, *83*, 6907–6923.
- (37) Fristrup, P.; Dideriksen, B.B.; Tanner, D.; Norrby, P-O. *J. Am. Chem. Soc.* **2005**, *127*, 13672–13679.
- (38) It is unusual for the starting material and product both have the same diastereomeric ratios, as the Ti-catalyzed epoxide opening invokes a radical intermediate, which should ablate all stereochemical information. This suggests the substrate may invoke “memory of chirality” with hydrogen radical addition occurring very quickly
- (39) For similar examples, see: (a) Corey, E. J.; Mitra, R. B.; Uda, H. *J. Am. Chem. Soc.* **1963**, *86*, 485–492. (b) Pirrung, M. C. *J. Am. Chem. Soc.* **1979**, *101*, 7130–7131. (c) Pirrung, M. C. *J. Am. Chem. Soc.* **1981**, *103*, 82–87.
- (40) Huang, F-Q.; Xie, J.; Sun, J-G.; Wang, Y-W.; Dong, X.; Qi, LW.; Zhang, B. *Org. Lett.* **2016**, *18*, 684–687.
- (41) Atkins, G.M.; Burgess, E.M. *J. Am. Chem. Soc.* **1968**, *90*, 4744 – 4745.
- (42) (a) Martin, J. C.; Arhart, R. J. *J. Am. Chem. Soc.* **1971**, *93*, 2339–2341; (b) Martin, J. C.; Arhart, R. J. *J. Am. Chem. Soc.* **1971**, *93*, 2341–2342; (c) Martin, J. C.; Arhart, R. Li, J.J. *J. Am. Chem. Soc.* **1971**, *93*, 4327–4329. (d) Martin, J. C.; Arhart, R. J.; Franz, J. A.; Perozzi, E. F.; Kaplan, L. J. *Org. Synth.* **1977**, *57*, 22–26.
- (43) Grieco, P. A.; Gilman, S.; Nishizawa, M. *J. Org. Chem.* **1976**, *41*, 1485–1486.
- (44) Takasu, K.; Nagao, S.; Ihara, M. *Tetrahedron Lett.* **2005**, *46*, 1005–1008.

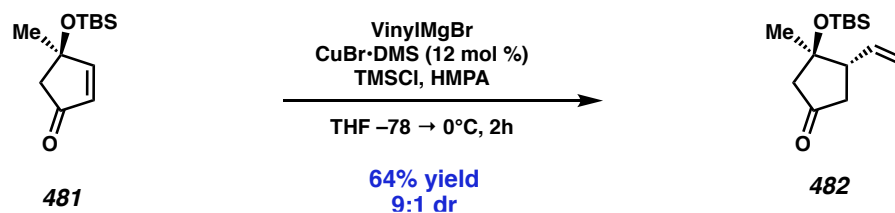
4.6 EXPERIMENTAL SECTION

4.6.1 Materials and Methods

Unless otherwise stated, reactions were performed in flame-dried glassware under a nitrogen atmosphere using dry, deoxygenated solvents. Solvents were dried by passage through an activated alumina column under argon.¹ Reaction progress was monitored by thin-layer chromatography (TLC). TLC was performed using E. Merck silica gel 60 F254 precoated glass plates (0.25 mm) and visualized by UV fluorescence quenching, *p*-anisaldehyde, or KMnO₄ staining. Silicycle SiliaFlash® P60 Academic Silica gel (particle size 40–63 μm) was used for flash chromatography. ¹H NMR spectra were recorded on Varian Inova 500 MHz and 600 MHz and Bruker 400 MHz spectrometers and are reported relative to residual CHCl₃ (δ 7.26 ppm), C₆D₆ (δ 7.16 ppm) or CD₃OD (δ 3.31 ppm). ¹³C NMR spectra were recorded on a Varian Inova 500 MHz spectrometer (125 MHz) and Bruker 400 MHz spectrometers (100 MHz) and are reported relative to CHCl₃ (δ 77.16 ppm), C₆D₆ (δ 128.06 ppm) or CD₃OD (δ 49.01 ppm). Data for ¹H NMR are reported as follows: chemical shift (δ ppm) (multiplicity, coupling constant (Hz), integration). Multiplicities are reported as follows: s = singlet, d = doublet, t = triplet, q = quartet, p = pentet, sept = septuplet, m = multiplet, br s = broad singlet, br d = broad doublet. Data for ¹³C NMR are reported in terms of chemical shifts (δ ppm). IR spectra were obtained by use of a Perkin Elmer Spectrum BXII spectrometer or Nicolet 6700 FTIR spectrometer using thin films deposited on NaCl plates and reported in frequency of absorption (cm⁻¹). Optical rotations were measured with a Jasco P-2000 polarimeter operating on the sodium D-line (589 nm), using a 100 mm path-length cell. High resolution mass spectra (HRMS) were obtained from the Caltech Mass Spectral Facility using a JEOL JMS-600H High Resolution Mass Spectrometer in fast atom bombardment (FAB+) or electron ionization (EI+) mode, or using an Agilent 6200 Series TOF with an Agilent

G1978A Multimode source in electrospray ionization (ESI+), atmospheric pressure chemical ionization (APCI+), or mixed ionization mode (MM: ESI-APCI+).

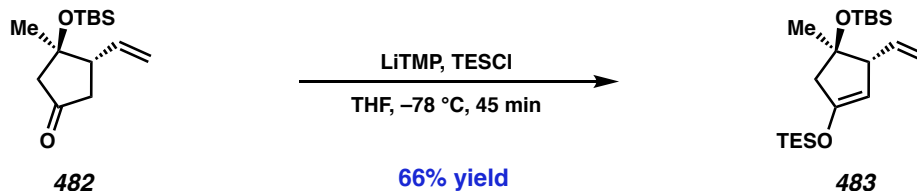
4.6.2 Experimental Procedures



Vinylcyclopentanone 482: To a flame-dried 500 mL three-necked flask is added CuBr • DMS (543 mg, 2.65 mmol, 0.12 equiv). The flask is evacuated and back-filled three times with argon, and charged with THF (110 mL). The solution is cooled to $-78\text{ }^{\circ}\text{C}$ and vinylmagnesium bromide in THF (1.0 M, 26.5 mL, 1.2 equiv) is added. The flask is equipped with an addition funnel and stirred at $-78\text{ }^{\circ}\text{C}$ for 30 minutes, during which time the solution turned from dark to red-brown. In a separate 100 mL flask, enone **481**, prepared according to the procedure of Maimone², (5.0 g, 22.1 mmol, 1.0 equiv) is dissolved in THF (22.1 mL). HMPA (10.97 mL, 66.1 mmol, 3.0 equiv) and TMSCl (6.94 mL, 55.2 mmol, 2.5 equiv) are added at room temperature, and stirred for 5 minutes. This solution is transferred to the addition funnel and slowly added to the flask over 1 hour; an internal temperature no greater than $-70\text{ }^{\circ}\text{C}$ should be maintained and the solution will turn orange to yellow to dark brown.

Upon complete addition, the reaction is stirred at $-78\text{ }^{\circ}\text{C}$ for an additional hour, then warmed to $0\text{ }^{\circ}\text{C}$. Saturated aq NH_4Cl (125 mL) is added before stirring at $0\text{ }^{\circ}\text{C}$ for 1 hour. The layers are separated and the aqueous layer is extracted with diethyl ether (3X). The combined organics are washed with brine, dried with MgSO_4 , and concentrated under reduced pressure. Flash column chromatography (10 → 20% Et_2O /Hexanes) affords the title compound (3.59 g, 64% yield, 9:1 mixture of diastereomers) as a yellow oil.

Major Diastereomer: ^1H NMR (400 MHz, CDCl_3) δ 5.81 (ddd, $J = 17.1, 10.4, 7.4$ Hz, 1H), 5.26 – 4.92 (m, 2H), 2.89 (dtd, $J = 8.1, 6.7, 1.2$ Hz, 1H), 2.64 (ddd, $J = 18.7, 8.2, 1.1$ Hz, 1H), 2.39 (d, $J = 17.8$ Hz, 1H), 2.32 (dd, $J = 17.6, 1.1$ Hz, 1H), 2.17 (dd, $J = 18.7, 6.6, 1.1$ Hz, 1H), 1.27 (s, 3H), 0.85 (s, 6H), 0.10 (d, $J = 8.0$ Hz, 6H); ^{13}C NMR (100 MHz, CDCl_3) δ 216.2, 136.9, 116.6, 79.7, 53.5, 52.8, 42.2, 25.7, 24.2, 18.0, -2.2, -2.4; IR (Neat film, NaCl) 2956, 2930, 2857, 1750, 1471, 1462, 1402, 1378, 1257, 1162, 1114, 1025, 997, 918, 836, 774, 617 cm^{-1} ; HRMS (FAB+) m/z calc'd for $\text{C}_{14}\text{H}_{27}\text{O}_2\text{Si}$ $[\text{M}+\text{H}]^+$: 255.1780, found 255.1784; $[\alpha]_{\text{D}}^{25.0} -30.0^\circ$ (c 1.0, CHCl_3).

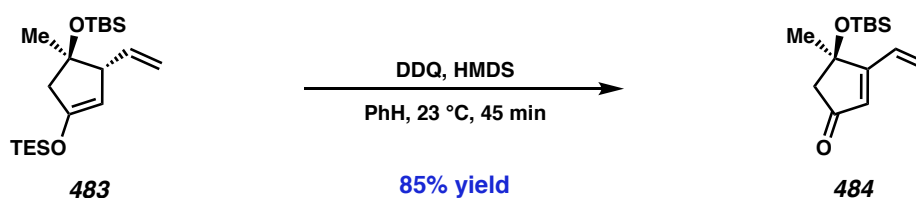


Silyl Enol Ether 483: A 500 mL round-bottom flask is soaked in a base bath overnight, then washed, flame-dried, and placed under nitrogen atmosphere. The flask is charged with 2,2,6,6-tetramethylpiperidine (4.01 mL, 23.63 mmol, 1.2 equiv) and THF (108 mL) before it is cooled to -78 °C. *n*-BuLi (9.30 mL of 2.33 M, 1.1 equiv) is added to the flask, then stirred at 0 °C for 1 hr. The flask is cooled to -78 °C and charged with TESCO (3.96 mL, 23.6 mmol, 1.2 equiv), then stirred for 5 minutes. Using a syringe pump, vinylcyclopentanone **482** (5.00 g, 19.69 mmol, 1.0 equiv) in THF (20 mL) is added dropwise over 1 hour.

Upon complete addition, the reaction is stirred until complete by TLC (15 minutes.) Triethylamine (5 mL) is added and the reaction is quenched with a saturated aqueous sodium bicarbonate solution, and gradually warmed to 23 °C. The layers are separated and the aqueous layer is extracted with hexanes (5X). The combined organics are washed with water and 0.1 M citric acid solution, dried with sodium sulfate, and concentrated under reduced pressure. Flash

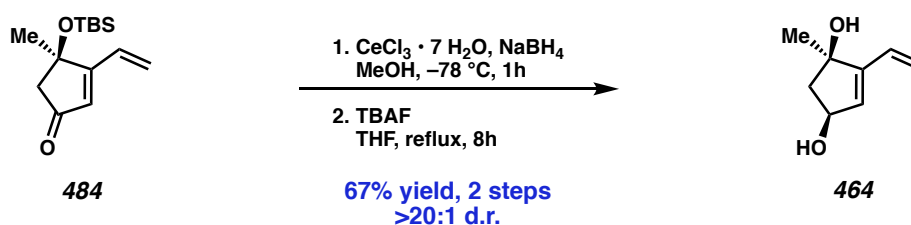
column chromatography (2.5% Et₂O/Hexanes) affords the title compound (4.78 g, 12.96 mmol, 66% yield, 9:1 mixture of diastereomers) as a colorless oil.

Major diastereomer: ¹H NMR (400 MHz, C₆D₆) δ 5.81 (ddd, *J* = 17.1, 10.1, 7.9 Hz, 1H), 5.16 (ddd, *J* = 17.1, 2.2, 1.2 Hz, 1H), 5.05 (ddd, *J* = 10.1, 2.2, 0.9 Hz, 1H), 4.66 (q, *J* = 1.8 Hz, 1H), 3.42 (ddq, *J* = 6.6, 2.3, 1.2 Hz, 1H), 2.68 (dt, *J* = 15.7, 1.6 Hz, 1H), 2.41 (dt, *J* = 15.7, 1.4 Hz, 1H), 1.27 (s, 3H), 1.04 – 0.99 (m, 18H), 0.73 – 0.61 (m, 6H), 0.15 (s, 3H), 0.14 (s, 3H); ¹³C NMR (100 MHz, C₆D₆) δ 153.9, 139.3, 115.2, 103.2, 81.9, 59.9, 50.7, 26.8, 26.3, 18.5, 7.2, 5.5, -2.0, -1.9. IR (Neat film, NaCl) 3078, 2955, 2933, 2477, 2856, 1647, 1459, 1360, 1334, 1250, 1226, 1135, 1091, 1018 1004, 918, 834, 799, 774, 746 cm⁻¹; HRMS (FAB+) *m/z* calc'd for C₂₀H₃₉O₂Si₂ [M-H]⁺: 367.2489, found 367.2489; [α]^{D25.0} -66.8° (*c* 1.0, CHCl₃).



Dienone 484: A 1 L round-bottomed flask is charged with silyl enol ether **483** (5.80 g, 15.76 mmol, 1.0 equiv) in benzene (310 mL). HMDS is added dropwise via syringe and the resulting solution is stirred for 5 minutes. DDQ (7.87 g, 34.67 mmol, 2.2 equiv) is added in a single portion, and the reaction is stirred for 45 minutes, during which time it turns from black to bright red. Celite (30 g) is added to the reaction, then concentrated and dried on high vacuum for 1 h. Flash column chromatography (1% → 10% Et₂O/Hexanes) affords the title compound as a gold oil (3.35 g, 13.27 mmol, 84% yield) along with triethylsilanol as a coeluted impurity (1.16 g as determined by ¹H NMR). A pure sample for characterization is obtained by preparative TLC (30% Et₂O/Hexane). ¹H NMR (400 MHz, CDCl₃) δ 6.56 (ddd, *J* = 17.8, 11.1, 0.8 Hz, 1H), 6.14 – 5.99 (m, 2H), 5.70

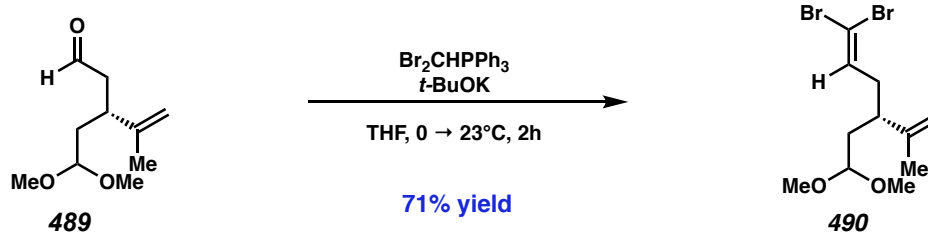
(dd, $J = 11.1, 1.5$ Hz, 1H), 2.70 (dd, $J = 17.9, 0.7$ Hz, 1H), 2.57 (d, $J = 17.8$ Hz, 1H), 1.53 (d, $J = 0.6$ Hz, 3H), 0.86 (s, 9H), 0.13 (s, 3H), 0.07 (s, 3H). ^{13}C NMR (100 MHz, CDCl_3) δ 205.0, 175.9, 129.0, 126.5, 125.5, 78.8, 53.2, 29.2, 25.8, 18.1, -2.3, -2.7; IR (Neat film, NaCl) 2955, 2930, 2857, 1709, 1603, 1473, 1361, 1336, 1253, 1232, 1206, 1159, 1074, 1004, 938, 862, 834, 776 cm^{-1} ; HRMS (FAB+) m/z calc'd for $\text{C}_{14}\text{H}_{25}\text{O}_2\text{Si}$ $[\text{M}+\text{H}]^+$: 253.1624, found 253.1622; $[\alpha]_{\text{D}}^{25.0} -92.1^\circ$ (c 0.2, CHCl_3).



Diol XX: A 500-mL round-bottom flask is charged with dienone **484** (2.69 g, 10.67 mmol, 1.0 equiv) in MeOH (110 mL) and cooled to -78°C . $\text{CeCl}_3 \cdot 7 \text{H}_2\text{O}$ (5.17 g, 13.87 mmol, 1.3 equiv) is added, and the solution is stirred for 5 minutes before NaBH_4 (534 mg, 13.87 mmol, 1.3 equiv) is added in a single portion. The reaction is stirred at -78°C for 1 hour, warmed to room temperature, and quenched with saturated, aqueous ammonium chloride. The mixture is concentrated on a rotary evaporator to remove methanol, transferred to a separatory funnel, and extracted with diethyl ether (3X). The combined organics are washed with brine, dried with MgSO_4 , and concentrated to afford an orange oil which is used directly in the next step without further purification.

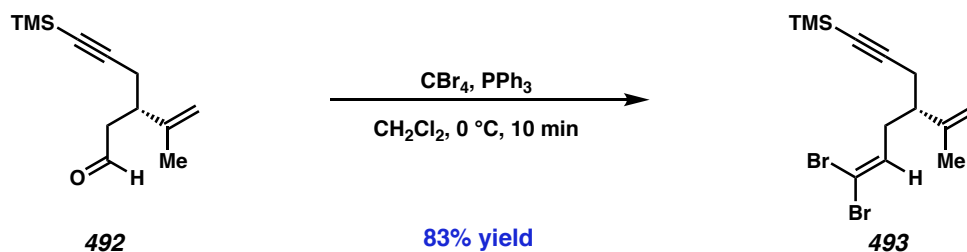
To a 500 mL flame-dried flask is added the crude reduction product in THF (150 mL). 1M TBAF in THF (15.0 mL equiv, 15.0 mmol, 1.4 equiv) is added dropwise by syringe. The flask is equipped with a reflux condenser and heated to reflux for 8 h. After completion as judged by TLC, the reaction is cooled to 23°C and quenched with brine. The mixture is extracted with ethyl acetate

(5X) before the combined organic layers are washed with brine, dried with Na_2SO_4 , and concentrated under reduced pressure onto silica gel. The mixture is purified by flash column chromatography (50 \rightarrow 75% \rightarrow 100% ethyl acetate/hexanes) to afford the title compound (1.17 g, 8.35 mmol, 78% yield over two steps) as an amorphous white solid. All spectral data for **11** was found to be in good accordance with literature values.³



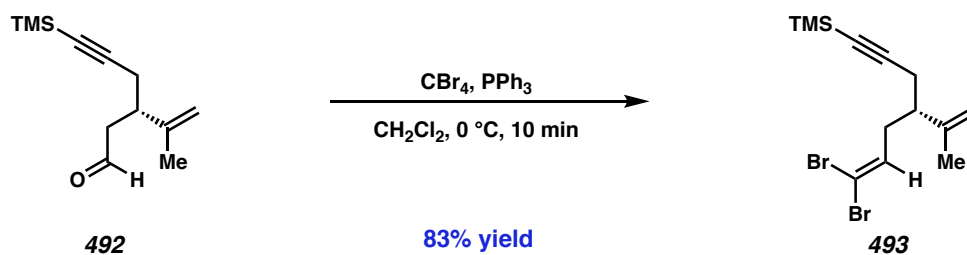
Dibromide 490: A 500 mL round-bottom flask is charged with $\text{Br}_2\text{CHPh}_3\text{Br}\cdot\text{MeCN}$ (55.6 g, 100.0 mmol, 1.4 equiv; prepared according to the method of Mulzer)⁴ and THF (238 mL, 0.3 M). The reaction mixture is cooled to 0°C and $t\text{-BuOK}$ (9.6 g, 85.7 mmol, 1.2 equiv) is added in one portion. This mixture is stirred 1.5 h at 0°C and then warmed to 23°C and stirred an additional 30 min. The mixture is cooled to 23°C and aldehyde **489** (13.3 g, 71.4 mmol, 1.0 equiv) is added dropwise via syringe. The dark suspension is stirred for 2 h at 0°C until no aldehyde is detected by TLC. The mixture is quenched with saturated, aqueous NH_4Cl and partitioned between water and Et_2O . The aqueous phase is extracted with Et_2O (3X). The organic extracts are combined, washed with brine, dried over magnesium sulfate, filtered through a sand/cotton plug and concentrated under reduced pressure. The crude residue is purified by flash chromatography (Dry load crude on Celite; 20% Et_2O /Hexanes) to afford the title compound (20.9 g, 61.1 mmol, 86% yield) as a red/orange oil: $^1\text{H NMR}$ (400 MHz, CDCl_3) 6.30 (t, $J = 7.0$ Hz, 1H), 4.83 (dt, $J = 2.9, 1.5$ Hz, 1H), 4.77 (dt, $J = 1.9, 0.8$ Hz, 1H), 4.36 – 4.28 (m, 1H), 3.32 (s, 3H), 3.30 (s, 3H), 2.43 –

2.30 (m, 1H), 2.24 – 2.07 (m, 2H), 1.72 – 1.62 (m, 5H); ^{13}C NMR (125 MHz, CDCl_3) 145.7, 137.0, 113.0, 102.9, 89.2, 53.3, 52.7, 42.0, 36.9, 35.7, 18.6; IR (Neat film, NaCl) 3073, 2948, 2829, 1645, 1440, 1377, 1191, 1127, 1060, 896, 787 cm^{-1} ; HRMS (FAB+) m/z calc'd for $\text{C}_{11}\text{H}_{17}\text{O}_2\text{Br}_2$ [$\text{M}-\text{H}$] $^+$: 340.9575, found 340.9579; $[\alpha]_{\text{D}}^{25.0} - 4.5^\circ$ (c 1.0, CHCl_3).



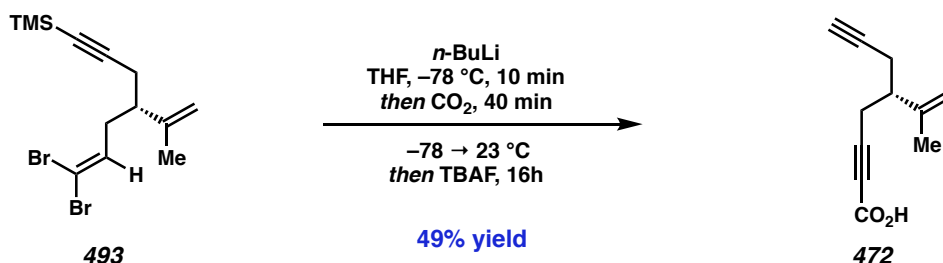
Aldehyde 492: A 500 mL round-bottom flask is charged with dibromide **490** (16.6 g, 48.5 mmol, 1.0 equiv) in THF (100 mL, 0.5 M), and cooled to -78°C . *n*-BuLi (2.3 M in hexanes; 42.2 mL, 97.1 mmol, 2.0 equiv) is added dropwise over 10 min, and the mixture is allowed to stir for 15 min at -78°C after which complete consumption of dibromide **490** is observed by TLC. TMSCl (18.5 mL, 145.5 mmol, 3.0 equiv) is added dropwise to the reaction mixture, which is then allowed to gradually warm to 23°C over 2 h. The mixture is then cooled to 0°C and water (100 mL) is added followed by 1,4-dioxane (50 mL). HCl (36% w/w, 40 mL, 10.0 equiv) is added and the reaction mixture is warmed to room temperature and allowed to stir for 16 h. NaHCO_3 (sat. aq.) is added until the pH of the solution is roughly 7. The reaction mixture is partitioned between water and Et_2O , and extracted with Et_2O (3X). The combined organic extracts are washed with brine, dried over sodium sulfate, and concentrated to afford an orange oil which is purified by flash chromatography (10% Et_2O /Hexanes). The title compound (7.37 g, 35.4 mmol, 73% yield) is isolated as a pale-yellow oil: ^1H NMR (400 MHz, CDCl_3) δ 9.70 (dd, $J = 2.4, 1.6$ Hz, 1H), 4.83 – 4.80 (m, 1H), 4.79 – 4.76 (m, 1H), 2.89 – 2.77 (m, 1H), 2.68 (ddd, $J = 16.8, 6.1, 1.7$ Hz, 1H), 2.52

(ddd, $J = 16.7, 8.4, 2.5$ Hz, 1H), 2.40 (dd, $J = 16.9, 5.8$ Hz, 1H), 2.29 (dd, $J = 17.0, 7.9$ Hz, 1H), 1.70 (dd, $J = 1.5, 0.9$ Hz, 3H), 0.11 (s, 9H); ^{13}C NMR (100 MHz, CDCl_3) 201.6, 145.4, 112.3, 104.5, 87.3, 46.3, 40.2, 24.8, 20.3, 0.1; IR (Neat film, NaCl) 3077, 2959, 2900, 2827, 2720, 1727, 1648, 1430, 1408, 1377, 1250, 1024, 1038, 896, 760, 644 cm^{-1} ; HRMS (MM: ESI-APCI+) m/z calc'd for $\text{C}_{12}\text{H}_{21}\text{OSi}$ $[\text{M}+\text{H}]^+$ 209.1356, found 209.1352.; $[\alpha]_{\text{D}}^{25.0} -13.5^\circ$ (c 1.0, CHCl_3).



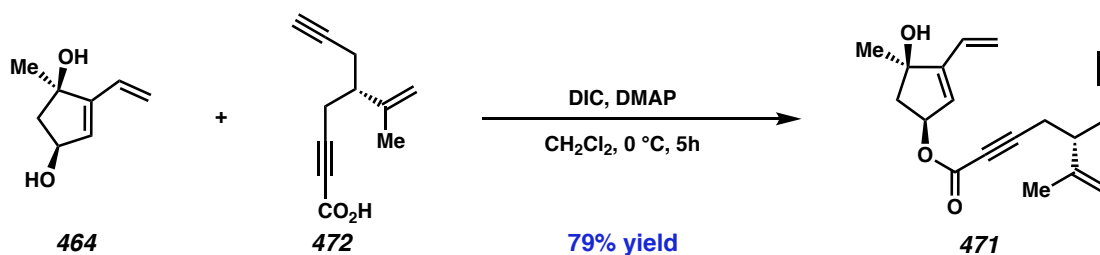
Dibromide 493: A 500 mL round-bottom flask is charged with triphenylphosphine (50.4 g, 192.0 mmol, 4.0 equiv) in CH_2Cl_2 (96 mL). The solution is cooled to 0°C , and CBr_4 (31.8 g, 96.0 mmol, 2.0 equiv) is added in one portion. The colorless solution immediately changes to yellow/orange in color. The mixture is allowed to stir for 10 min at 0°C , after which aldehyde **492** (10.0 g, 48.0 mmol, 1.0 equiv) is added via syringe. The aldehyde is consumed immediately, as judged by TLC. The reaction mixture is then quenched with water, and partitioned between water and CH_2Cl_2 . The aqueous phase is extracted with CH_2Cl_2 (3X), and the combined organic extracts are washed with brine and dried over MgSO_4 . The crude is concentrated onto SiO_2 , loaded onto a column, and purified by flash chromatography (5% Et_2O /Hexanes) to afford the title compound (14.48 g, 39.8 mmol, 83% yield) as a yellow oil: ^1H NMR (400 MHz, CDCl_3) 6.34 (t, $J = 6.9$ Hz, 1H), 4.84 (p, $J = 1.5$ Hz, 1H), 4.76 (dt, $J = 1.7, 0.8$ Hz, 1H), 2.47 – 2.16 (m, 5H), 1.69 (dd, $J = 1.5, 0.8$ Hz, 3H), 0.14 (s, 9H); ^{13}C NMR (100 MHz, CDCl_3) 145.4, 136.9, 112.7, 105.1, 89.5, 86.75, 44.9, 35.8,

24.7, 19.7, 0.3; IR (Neat film, NaCl) 2958, 2922, 2176, 1646, 1441, 1248 cm^{-1} ; HRMS (EI+) m/z calc'd for $\text{C}_{13}\text{H}_{20}\text{SiBr}_2$ [$\text{M}+\bullet$] 363.9681, found 363.9668; $[\alpha]_{\text{D}}^{25.0} +4.1^\circ$ (c 1.0, CHCl_3).



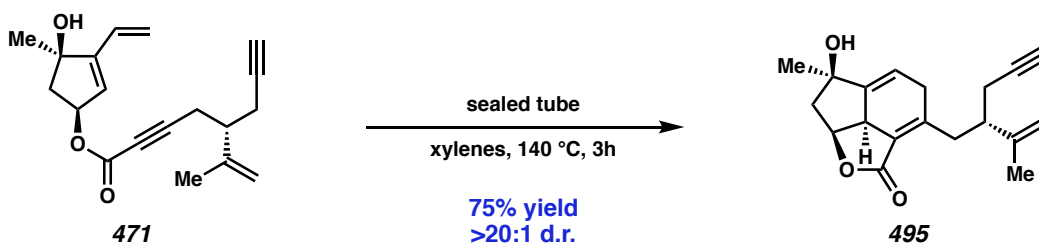
Ynoic Acid 472: A 250 mL round bottom flask was charged with dibromide **493** (9.27 g, 25.45 mmol, 1.0 equiv) in THF (52 mL). The solution was cooled to -78°C , and $n\text{-BuLi}$ (2.3 M in hexanes; 16.6 mL, 38.18 mmol, 1.5 equiv) was added dropwise. After 10 min, dibromide **493** had been completely consumed (as judged by TLC), and the reaction was then sparged with CO_2 from a balloon passing through a drying tube full of Dryrite. The solution was allowed to warm to 23°C over 30 min with continuous sparging with CO_2 . The solution was then sparged with N_2 for 10 min at 23°C , followed by the addition of TBAF (1.0 M in THF; 50.9 mL, 50.9 mmol, 2.0 equiv). The solution was allowed to stir for 16 h at 23°C after which TMS-protected substrate remained, as judged by LCMS. TBAF (25.5 mL, 25.5 mmol, 1.0 equiv) was added, and the reaction was stirred an additional 1 h at 23°C . The reaction was quenched with sat. aq. NaHCO_3 , diluted with water and EtOAc, and extracted with EtOAc (1X). The aqueous extract was then acidified with conc. HCl until a cloudy precipitate was observed. The aqueous was then extracted with EtOAc (3X). The combined organic extracts were then washed with brine and dried over MgSO_4 . Concentration under reduced pressure afforded the title compound (2.20 g, 12.5 mmol, 49% yield) as a pale orange oil which was found to be pure by NMR and used in the subsequent step without further purification: ^1H NMR (400 MHz, CDCl_3) δ 10.98 (s, 1H), 4.92 (p, $J = 1.4$ Hz, 1H), 4.84

(q, $J = 1.0$ Hz, 1H), 2.71 – 2.47 (m, 3H), 2.41 (d, $J = 2.7$ Hz, 1H), 2.40 – 2.39 (m, 1H), 2.01 (t, $J = 2.6$ Hz, 1H), 1.73 (dd, $J = 1.5, 0.8$ Hz, 3H); ^{13}C NMR (100 MHz, CDCl_3) δ 158.4, 144.1, 113.1, 90.3, 81.6, 74.1, 70.6, 43.7, 22.5, 22.4, 20.2; IR (Neat film, NaCl) 3302, 2928, 2643, 2236, 2119, 1964, 1416, 1244, 1078, 899, 775, 792, 759, 641, 648 cm^{-1} ; HRMS (MM: ESI-APCI+) m/z calc'd for $\text{C}_{11}\text{H}_{13}\text{O}_2$ $[\text{M}+\text{H}]^+$: 177.0910, found 177.0916; $[\alpha]_{\text{D}}^{25.0} -1.6^\circ$ (c 1.0, CHCl_3).

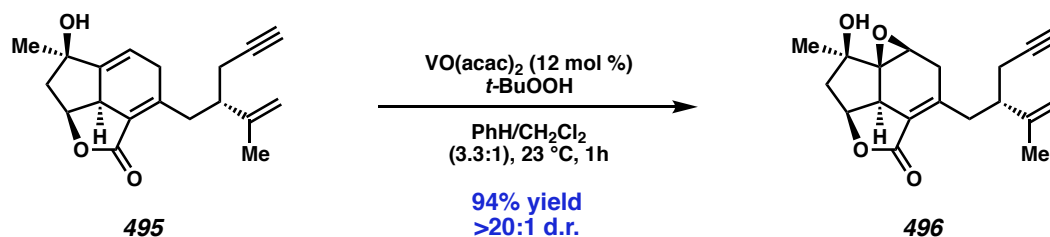


Ester XX: A 250 mL round bottom flask is charged with diol **464** (1.03 g, 7.35 mmol, 1.0 equiv), acid **472** (1.30 g, 7.35 mmol, 1.0) and DMAP (90 mg, 0.735 mmol, 0.10 equiv) in CH_2Cl_2 (74 mL). The solution is cooled to 0°C , and DIC (1.15 mL, 7.35 mmol, 1.0 equiv) is added dropwise. The reaction is stirred for 2 h while gradually warming to 23°C , and then stirred an additional 3 h at 23°C . The mixture is then partitioned between CH_2Cl_2 and H_2O , and the aqueous phase is extracted with CH_2Cl_2 (3X). The organic extracts are washed with brine, dried over Na_2SO_4 , and concentrated. The crude residue was purified by flash chromatography (0% \rightarrow 5% \rightarrow 10% \rightarrow 15% \rightarrow 20% EtOAc/Hexanes) to afford the title compound (1.74 g, 5.83 mmol, 79% yield) as a colorless oil: ^1H NMR (400 MHz, CDCl_3) δ 6.43 – 6.20 (m, 1H), 5.82 (d, $J = 2.4$ Hz, 1H), 5.78 (dd, $J = 17.8, 1.7$ Hz, 1H), 5.64 – 5.49 (m, 1H), 5.33 (dd, $J = 11.2, 1.6$ Hz, 1H), 4.92 (p, $J = 1.4$ Hz, 1H), 4.84 (dd, $J = 1.4, 0.8$ Hz, 1H), 2.77 – 2.46 (m, 4H), 2.44 – 2.39 (m, 2H), 2.05 (dd, $J = 14.7, 4.4$ Hz, 1H), 2.01 (t, $J = 2.6$ Hz, 1H), 1.74 (dd, $J = 1.5, 0.8$ Hz, 3H), 1.44 (s, 3H); ^{13}C NMR (100 MHz, CDCl_3) δ 153.5, 151.8, 144.3, 129.0, 126.1, 119.6, 113.0, 87.6, 81.7, 81.1, 77.1, 74.5,

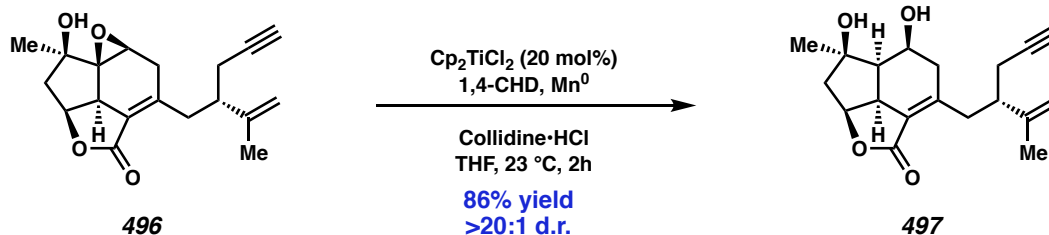
70.5, 49.0, 43.8, 26.8, 22.5, 22.4, 20.3; IR (Neat film, NaCl) 3396, 2938, 2235, 1708, 1252, 1071, 942, 752 cm^{-1} ; HRMS (MM: ESI-APCI+) m/z calc'd for $\text{C}_{19}\text{H}_{23}\text{O}_3$ $[\text{M}+\text{H}]^+$: 299.1642, found 299.1632; $[\alpha]_{\text{D}}^{25.0} -130.8^\circ$ (c 1.0, CHCl_3).



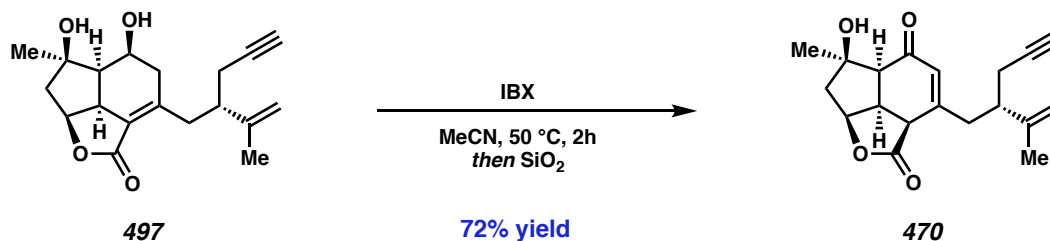
Cyclohexadiene 495: Ester **471** (804 mg, 2.69 mmol, 1.0 equiv) is dissolved in xylenes (270 mL). This solution is divided between two 500 mL Schlenk flasks. Each flask is subjected to three freeze-pump-thaw cycles, and then back-filled with nitrogen. The flasks are sealed, heated to 140 $^\circ\text{C}$, and stirred for 3 h. The flasks are then cooled to ambient temperature and the reaction mixtures are combined in a 2 L round-bottom flask. The solvent is removed under reduced pressure, and the resulting solid is purified by flash chromatography (30% \rightarrow 40% \rightarrow 50% EtOAc/Hexanes) to afford the title compound (604 mg, 2.02 mmol, 75% yield) as a flakey white solid: ^1H NMR (400 MHz, CDCl_3) δ 5.84 (ddd, $J = 6.4, 3.0, 1.9$ Hz, 1H), 4.97 (ddd, $J = 9.1, 8.0, 7.0$ Hz, 1H), 4.77 (t, $J = 1.7$ Hz, 1H), 4.69 – 4.65 (m, 1H), 3.31 (t, $J = 9.8$ Hz, 1H), 3.12 – 2.98 (m, 2H), 2.83 – 2.61 (m, 2H), 2.63 – 2.41 (m, 2H), 2.33 (d, $J = 2.6$ Hz, 1H), 2.32 (dd, $J = 2.7, 1.4$ Hz, 1H), 2.00 (t, $J = 2.6$ Hz, 1H), 1.69 (dd, $J = 1.4, 0.8$ Hz, 3H), 1.67 – 1.60 (m, 1H), 1.41 (d, $J = 1.1$ Hz, 3H); δ ^{13}C NMR (100 MHz, CDCl_3) δ 168.2, 155.9, 152.0, 146.1, 125.5, 116.5, 112.8, 82.9, 80.0, 75.3, 69.7, 49.8, 45.7, 45.7, 35.3, 26.7, 22.9, 18.8 cm^{-1} ; IR (Neat film, NaCl) 3305, 2967, 2920, 2360, 2118, 1730, 1647, 1447, 1374, 1358, 1290, 1219, 1045, 1018, 896, 632 cm^{-1} ; HRMS (MM: ESI-APCI+) m/z calc'd for $\text{C}_{19}\text{H}_{23}\text{O}_3$ $[\text{M}+\text{H}]^+$: 299.1642, found 299.1631. $[\alpha]_{\text{D}}^{25.0} -87.4^\circ$ (c 0.5, CHCl_3).



Epoxide 18: A 500 mL round-bottom flask is charged with Diels–Alder adduct **495** (1.75 g, 5.87 mmol, 1.0 equiv) in a mixture of CH_2Cl_2 (59 mL) and benzene (196 mL). $\text{VO}(\text{acac})_2$ is added (117 mg, 0.440 mmol, 0.075 equiv) in one portion, and the mixture is stirred 10 min at 23 °C until it is pale-green in color. TBHP (5.0 M in decane, 2.30 mL, 11.74 mmol, 2.0 equiv) is added dropwise via syringe, and the mixture becomes deep-red in color. The mixture is stirred at 23 °C for 1 h, at which point no starting material remained, as judged by TLC. The reaction mixture is poured directly onto a flash column and purified by flash chromatography (0% → 50% → 70% → 80% EtOAc/Hexanes) to afford the title compound (1.73 g, 5.50 mmol, 94% yield) as an amorphous white solid. ^1H NMR (400 MHz, CDCl_3) δ 4.90 – 4.77 (m, 3H), 3.78 (d, $J = 3.4$ Hz, 1H), 3.40 – 3.18 (m, 2H), 2.87 (dd, $J = 16.7, 3.4$ Hz, 1H), 2.62 – 2.43 (m, 3H), 2.41 – 2.26 (m, 3H), 2.06 – 1.95 (m, 2H), 1.74 (t, $J = 1.1$ Hz, 3H), 1.46 – 1.41 (m, 3H); ^{13}C NMR (100 MHz, CDCl_3) δ 168.9, 149.9, 146.1, 120.7, 112.5, 82.9, 76.6, 73.6, 69.8, 69.7, 51.8, 50.1, 45.7, 44.8, 36.7, 36.6, 22.7, 22.7, 19.4; IR (Neat film, NaCl) 3474, 3267, 1735, 1655, 1421, 1358, 1195, 1120, 1030, 901, 793, 674 cm^{-1} ; HRMS (MM: ESI-APCI+) m/z calc'd for $\text{C}_{19}\text{H}_{23}\text{O}_4$ $[\text{M}+\text{H}]^+$: 315.1591, found 315.1586; $[\alpha]_{\text{D}}^{25.0} -69.8^\circ$ (c 0.5, CHCl_3).

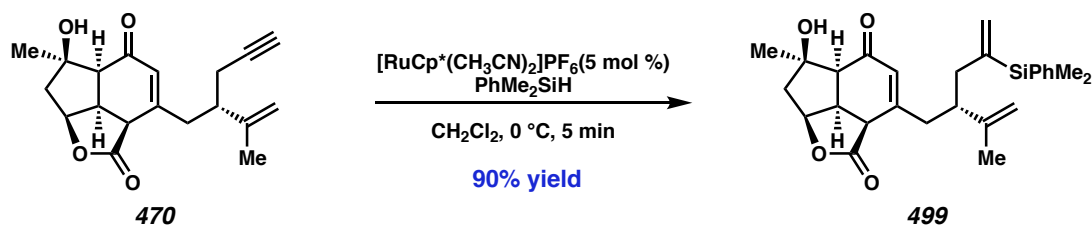


Diol 497: A 250 mL round bottom flask is charged with epoxide **496** (1.70 g, 5.41 mmol, 1.0 equiv), titanocene dichloride (269 mg, 1.08 mmol, 0.20 equiv), manganese dust (326 mg, 5.95 mmol, 1.10 equiv), and collidine·HCl (1.07 g, 6.76 mmol, 1.25 equiv) in THF (54 mL, 0.10 M). 1,4-cyclohexadiene is then added dropwise to the red suspension, which gradually changes to a blue/grey color. The suspension is stirred for 2 h at 23 °C, after which the starting material is consumed, as judged by TLC. Celite is added directly to the mixture, and the solvent is removed under reduced pressure. The resulting solid is loaded directly onto a flash column and purified by flash chromatography (40% → 50% → 60% EtOAc/Hexanes) to afford the title compound (1.47 g, 4.65 mmol, 86% yield) as an off-white solid: ^1H NMR (400 MHz, CDCl_3) 4.90 (ddd, $J = 8.1, 6.5, 3.9$ Hz, 1H), 4.83 (d, $J = 1.4$ Hz, 2H), 4.67 (td, $J = 5.4, 2.9$ Hz, 1H), 3.40 (d, $J = 6.0$ Hz, 1H), 3.37 – 3.28 (m, 1H), 3.18 (s, 1H), 3.10 (ddd, $J = 9.9, 7.9, 2.1$ Hz, 1H), 2.64 – 2.48 (m, 3H), 2.36 (dd, $J = 9.5, 7.8$ Hz, 1H), 2.32 (dd, $J = 2.7, 1.1$ Hz, 1H), 2.31 – 2.29 (m, 1H), 2.13 – 1.98 (m, 3H), 1.97 (t, $J = 2.6$ Hz, 1H), 1.80 – 1.71 (m, 3H), 1.43 (s, 3H); δ ^{13}C NMR (100 MHz, CDCl_3) δ 169.8, 151.3, 146.8, 125.2, 112.4, 83.2, 81.7, 79.4, 69.5, 68.3, 49.6, 48.4, 45.2, 44.6, 41.4, 36.8, 28.6, 22.9, 19.3; IR (Neat film, NaCl) 3296, 3076, 2116, 1738, 1731, 1668, 1424, 1375, 1360, 1306, 1223, 1198, 1105, 896 cm^{-1} ; HRMS (MM: ESI-APCI+) m/z calc'd for $\text{C}_{19}\text{H}_{25}\text{O}_4$ $[\text{M}+\text{H}]^+$: 317.1747, found 317.1761; $[\alpha]_{\text{D}}^{25.0} -11.8^\circ$ (c 0.5, CHCl_3).

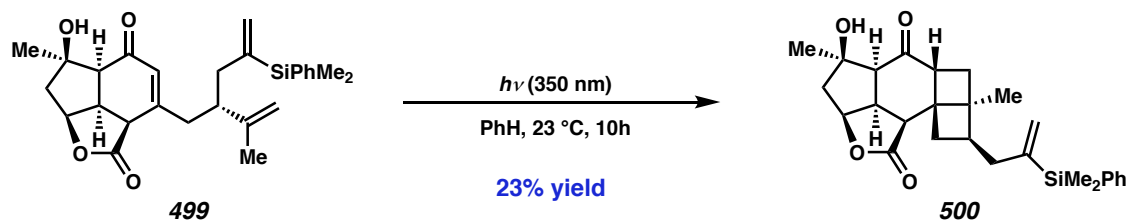


Note: The success of this procedure was found to be scale-dependent. Consequently, this reaction was run with a maximum batch size of 50 mg (**497**) per reaction flask. When run on scale, reactions were set up side-by-side, and combined for purification, as detailed below:

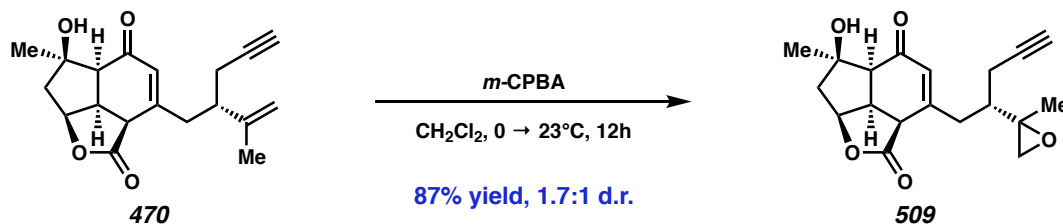
Enone 470: Diol **497** (1.0 g, 3.16 mmol, 1.0 equiv) is divided into 20 scintillation vials (not flame dried, 50 mg, 0.158 mmol per vial) each equipped with a magnetic stir bar and a septum cap. To each vial is added IBX (188 mg, 0.671 mmol, 4.25 equiv) and each vial is evacuated and back-filled with N₂. MeCN (11 mL) is added to each vial after which the vials are sealed, heated to 50 °C, and stirred for 2 h. The reactions are cooled to 23 °C, combined, and filtered over a plug of SiO₂, rinsing generously with EtOAc. The filtrate is concentrated under reduced pressure, and the residue obtained is purified by flash chromatography (30% → 40% → 50% EtOAc/Hexanes) to afford the title compound (716 mg, 2.28 mmol, 72% yield) as a white foam: ¹H NMR (400 MHz, CDCl₃) δ 6.00 (d, *J* = 1.0 Hz, 1H), 5.11 (dd, *J* = 6.7, 5.4 Hz, 1H), 4.88 – 4.81 (m, 1H), 4.78 (dt, *J* = 1.6, 0.8 Hz, 1H), 3.68 – 3.45 (m, 2H), 3.16 – 3.05 (m, 1H), 2.79 – 2.59 (m, 2H), 2.48 (d, *J* = 9.2 Hz, 1H), 2.39 – 2.28 (m, 3H), 2.03 (t, *J* = 2.6 Hz, 1H), 1.88 (dd, *J* = 15.0, 5.5 Hz, 1H), 1.71 (s, 1H), 1.67 (d, *J* = 0.7 Hz, 3H), 1.49 (s, 3H); δ ¹³C NMR (100 MHz, CDCl₃) δ 196.1, 173.6, 156.3, 145.0, 128.8, 113.6, 82.7, 82.6, 82.2, 70.5, 55.2, 47.4, 44.0, 42.1, 41.4, 38.2, 26.3, 23.9, 18.8; IR (Neat film, NaCl) 3450, 3290, 2970, 2930, 2118, 1758, 1649, 1376, 1290, 1176, 1161, 1107, 912, 735 cm⁻¹; HRMS (MM: ESI-APCI+) *m/z* calc'd for C₁₉H₂₃O₄ [M+H]⁺: 315.1591, found 315.1571; [α]_D^{25.0} -150.0° (*c* 0.5, CHCl₃).



Vinyl Silane 499: A 1-dram vial is charged with enone **470** (7.0 mg, 0.0223 mmol, 1.0 equiv) in CH_2Cl_2 (400 μL). Phenyl dimethylsilane (4 μL , 0.0267 mmol, 1.2 equiv) is added, and the mixture is cooled to 0 °C. $[\text{RuCp}^*(\text{MeCN})_3]\text{PF}_6$ (10 mg/mL stock solution 56 μL , 0.00112 mmol, 0.05 equiv) is added dropwise. Following the addition, the reaction is stirred 5 min at 0 °C, after which alkyne **470** is no longer detectable by TLC. The reaction mixture is loaded directly onto a preparatory TLC plate and purified by preparatory TLC (80% EtOAc/Hexanes) to afford the title compound (9.0 mg, 0.0200 mmol, 90% yield) as a colorless oil: ^1H NMR (400 MHz, CDCl_3) δ 7.68 – 7.46 (m, 2H), 7.39 – 7.31 (m, 3H), 5.80 (t, $J = 1.4$ Hz, 1H), 5.70 – 5.64 (m, 1H), 5.54 (d, $J = 2.8$ Hz, 1H), 5.04 (dd, $J = 7.1, 5.3$ Hz, 1H), 4.66 – 4.59 (m, 1H), 4.40 – 4.32 (m, 1H), 3.32 (td, $J = 10.6, 7.1$ Hz, 1H), 2.94 – 2.74 (m, 2H), 2.50 – 2.24 (m, 5H), 2.22 – 2.09 (m, 1H), 1.85 (dd, $J = 14.9, 5.5$ Hz, 1H), 1.52 (s, 3H), 1.47 (s, 3H), 0.41 (s, 3H), 0.39 (s, 3H); ^{13}C NMR (100 MHz, CDCl_3) δ 196.0, 173.4, 157.3, 147.7, 146.3, 138.9, 134.2, 129.0, 128.6, 128.6, 128.0, 112.7, 82.6, 82.3, 55.1, 47.3, 43.7, 42.1, 41.9, 40.5, 38.3, 26.5, 18.0, -2.7, -3.2; IR (Neat Film NaCl) 3434, 3049, 2962, 1762, 1654, 1427, 1376, 1290, 1250, 1216, 1173, 1160, 1109, 1030, 992, 933, 891, 834, 817, 776, 736, 703 cm^{-1} ; HRMS (MM: ES+) m/z calc'd for $\text{C}_{27}\text{H}_{35}\text{O}_4\text{Si}$ $[\text{M}+\text{H}]^+$: 451.2305, found 451.2314; $[\alpha]_{\text{D}}^{25.0} -106.1$ (c 0.60, CHCl_3).



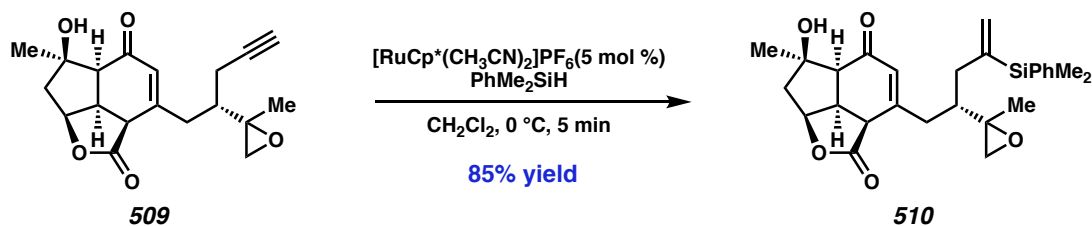
Cyclobutane XX: A 1-dram vial is charged with vinyl silane **499** (22 mg, 0.0488 mmol, 1.0 equiv) in PhH (5.0 mL). The solution is sparged with N₂ for 5 min, and placed in a photoreactor equipped with Hitachi UVA bulbs (F8T5-BLB, ~350 nm). The reaction is stirred under 350 nm irradiation for 10 h, after which no starting material remains (as judged by TLC). An ¹H NMR spectrum of the crude product shows a mixture with **21** as the major constituent. The crude white solid is purified by flash chromatography (50% EtOAc/Hexanes), followed by normal-phase (SiO₂) preparative HPLC (EtOAc/Hexanes, 7.0 mL/min, monitoring wavelength = 254 nm, isocratic–50% EtOAc/Hexanes, 10 min) then reverse-phase (C18) preparative HPLC (MeCN/H₂O, 9.0 mL/min, monitoring wavelength = 260 nm, isocratic–70% MeCN/H₂O, 10 min) to afford pure **21** (5.0 mg, 0.0111 mmol, 23 % yield). X-ray quality crystals are grown by slow cooling from *i*-PrOH: ¹H NMR (400 MHz, CDCl₃) δ 7.54 – 7.46 (m, 2H), 7.38 – 7.32 (m, 3H), 5.68 – 5.61 (m, 1H), 5.40 (d, *J* = 2.8 Hz, 1H), 4.95 (ddd, *J* = 7.0, 5.6, 1.6 Hz, 1H), 3.46 (td, *J* = 10.2, 6.7 Hz, 1H), 3.09 – 2.93 (m, 1H), 2.89 – 2.78 (m, 2H), 2.77 – 2.61 (m, 2H), 2.33 – 2.14 (m, 4H), 1.98 (dd, *J* = 14.8, 5.6 Hz, 1H), 1.94 – 1.85 (m, 1H), 1.75 (dd, *J* = 13.1, 4.3 Hz, 1H), 1.41 (s, 3H), 1.00 (s, 3H), 0.37 (s, 6H); ¹³C NMR (100 MHz, CDCl₃) δ 215.1, 175.7, 148.1, 138.2, 134.1, 129.2, 127.9, 126.9, 82.0, 81.5, 55.1, 49.2, 46.6, 46.6, 44.5, 43.5, 38.7, 38.6, 36.1, 34.1, 31.0, 27.6, 21.7, -2.8, -2.9; IR (Neat Film NaCl) 3453, 2934, 2858, 1759, 1689, 1428, 1375, 1248, 1206, 1106, 1012, 938, 858, 833, 818, 703 cm⁻¹; HRMS (MM: ES⁺) *m/z* calc'd for C₂₇H₃₅O₄Si [M+H]⁺: 451.2305, found 451.2321; [α]_D^{25.0} -113.4 ° (*c* 0.12, CHCl₃).



Epoxides 509a and 509b: A 100 mL round-bottom flask is charged with enone **470** (450 mg, 1.43 mmol, 1.0 equiv) in CH_2Cl_2 (48 mL). The solution is cooled to 0 °C, and *m*-CPBA (~70% wt/wt; 1.06 g, 4.29 mmol, 3.0 equiv) is added in one portion. The mixture is stirred while gradually warming to 23 °C over 2 h, and then stirred an additional 10 h at 23 °C, at which point **XX** has been completely consumed as judged by TLC. The reaction mixture is poured directly onto a flash column and purified by flash chromatography (50% → 60% → 70% → 80% EtOAc/Hexanes) to afford the title compounds (410 mg, 1.24 mmol, 87% yield) as a white foam. The products are isolated as a 1.7:1 mixture of diastereomers (judged by ^1H NMR). A portion of this mixture was subjected to normal phase (SiO_2) preparative HPLC (EtOAc/Hexanes, 7.0 mL/min, monitor wavelength 254 nm, 60% EtOAc/Hexanes) to obtain pure samples of the two products for the purposes of characterization:

Diastereomer 1 (minor): ^1H NMR (400 MHz, CDCl_3) δ 6.05 (d, $J = 1.4$ Hz, 1H), 5.12 (dd, $J = 6.7, 5.4$ Hz, 1H), 3.75 – 3.42 (m, 2H), 2.99 (ddt, $J = 15.6, 6.2, 1.2$ Hz, 1H), 2.76 – 2.63 (m, 2H), 2.57 (d, $J = 4.5$ Hz, 1H), 2.54 – 2.44 (m, 2H), 2.44 – 2.27 (m, 2H), 2.05 (t, $J = 2.7$ Hz, 1H), 1.99 – 1.84 (m, 2H), 1.50 (s, 3H), 1.34 (d, $J = 0.7$ Hz, 3H); ^{13}C NMR (100 MHz, CDCl_3) δ 196.0, 173.6, 156.4, 128.5, 82.9, 82.7, 81.8, 71.2, 58.6, 55.2, 54.2, 47.5, 42.6, 42.3, 42.2, 36.5, 26.4, 21.0, 18.4; IR (Neat film, NaCl) 3436, 3283, 2970, 2926, 1758, 1656, 1378, 1292, 1177, 1109, 735 cm^{-1} ; (MM: ESI-APCI+) m/z calc'd for $\text{C}_{19}\text{H}_{23}\text{O}_5$ $[\text{M}+\text{H}]^+$: 331.1545, found 331.1538; $[\alpha]_{\text{D}}^{25.0} -144.5$ (c 1.0, CHCl_3).

Diastereomer 2 (major): ^1H NMR (400 MHz, CDCl_3) δ 6.10 (t, $J = 1.6$ Hz, 1H), 5.11 (dd, $J = 7.1$, 5.4 Hz, 1H), 3.84 (dt, $J = 10.9$, 1.2 Hz, 1H), 3.76 – 3.57 (m, 1H), 3.35 – 3.16 (m, 1H), 2.70 (dd, $J = 4.6$, 0.8 Hz, 1H), 2.63 – 2.45 (m, 3H), 2.40 – 2.24 (m, 3H), 2.05 (t, $J = 2.6$ Hz, 1H), 1.95 – 1.84 (m, 2H), 1.49 (s, 3H), 1.25 (s, 3H); ^{13}C NMR (100 MHz, CDCl_3) δ 196.4, 174.1, 156.4, 129.3, 82.9, 82.9, 81.3, 71.1, 58.5, 55.5, 54.2, 47.5, 42.8, 42.8, 41.3, 38.5, 26.4, 22.5, 16.0; IR (Neat film, NaCl) 3436, 3283, 2250, 1758, 1657, 1378, 1109, 735 cm^{-1} ; HRMS (MM: ESI-APCI+) m/z calc'd for $\text{C}_{19}\text{H}_{23}\text{O}_5$ $[\text{M}+\text{H}]^+$: 331.1545, found 331.1540; $[\alpha]_D^{25.0} -83.5^\circ$ (c 1.0, CHCl_3).

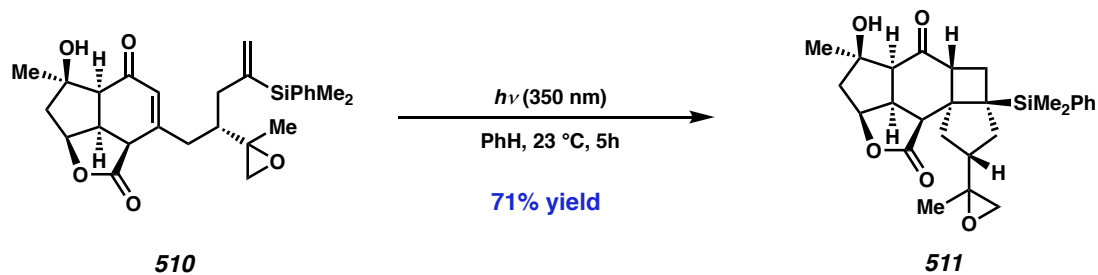


Vinyl Silanes 510a and 510b: A 250 mL round bottom flask is charged with a mixture of **509a** and **509b** (725 mg, 2.19 mmol, 1.0 equiv) in CH_2Cl_2 (22 mL). Phenyl dimethylsilane is added, and the mixture is cooled to 0 °C. $[\text{RuCp}^*(\text{MeCN})_3]\text{PF}_6$ (10 mg/mL stock solution, 5.5 mL, 0.110 mmol, 0.05 equiv) is added dropwise. Following the addition, the reaction is stirred 5 min at 0 °C, after which the starting material is no longer detectable by TLC. The reaction mixture is poured directly onto a flash column, and purified by flash chromatography (0% → 50% EtOAc/Hexanes) to afford the title compounds (870 mg, 1.86 mmol, 85% yield) as a colorless foam. The products are isolated as a 1.7:1 mixture of diastereomers (judged by ^1H NMR), which were characterized separately:

Diastereomer 1 (minor): ^1H NMR (400 MHz, CDCl_3) δ 7.54 (ddd, $J = 4.9$, 2.4, 1.7 Hz, 2H), 7.37 – 7.29 (m, 3H), 5.83 (d, $J = 1.2$ Hz, 1H), 5.71 (dd, $J = 2.3$, 1.3 Hz, 1H), 5.61 (d, $J = 2.7$ Hz, 1H), 4.99 (dd, $J = 7.0$, 5.3 Hz, 1H), 3.15 (td, $J = 10.6$, 7.0 Hz, 1H), 2.84 (ddd, $J = 14.2$, 3.3, 1.6 Hz,

1H), 2.72 (dt, $J = 13.6, 2.2$ Hz, 1H), 2.45 (d, $J = 4.7$ Hz, 1H), 2.39 (d, $J = 10.4$ Hz, 1H), 2.29 (d, $J = 15.0$ Hz, 1H), 2.20 – 1.98 (m, 5H), 1.84 (dd, $J = 15.0, 5.4$ Hz, 1H), 1.47 (s, 3H), 1.20 (s, 3H), 0.46 (s, 3H), 0.38 (s, 3H); ^{13}C NMR (100 MHz, CDCl_3) δ 195.7, 173.0, 157.2, 147.4, 139.6, 134.4, 129.2, 128.7, 128.7, 127.9, 82.7, 82.0, 58.6, 55.2, 54.9, 47.3, 42.3, 41.9, 40.4, 40.0, 36.3, 26.5, 16.6, -2.7, -3.9; IR (Neat film, NaCl) 3435, 2960, 1762, 1659, 1426, 1376, 1288, 1247, 1217, 1163, 1106, 1034, 992, 938, 838, 818, 753, 703 cm^{-1} ; HRMS (FAB+) m/z calc'd for $\text{C}_{27}\text{H}_{35}\text{O}_5\text{Si}$ $[\text{M}+\text{H}]^+$: 467.2254, found 467.2265; $[\alpha]_{\text{D}}^{25.0} -62.0^\circ$ (c 1.0, CHCl_3).

Diastereomer 2 (major): ^1H NMR (400 MHz, CDCl_3) δ 7.63 – 7.44 (m, 2H), 7.39 – 7.31 (m, 3H), 6.03 (t, $J = 1.5$ Hz, 1H), 5.73 (dt, $J = 2.4, 1.2$ Hz, 1H), 5.58 (d, $J = 2.6$ Hz, 1H), 5.07 (dd, $J = 7.1, 5.3$ Hz, 1H), 3.53 (td, $J = 10.6, 7.1$ Hz, 1H), 3.38 (dt, $J = 11.0, 1.2$ Hz, 1H), 3.23 – 3.07 (m, 1H), 2.48 (d, $J = 10.3$ Hz, 1H), 2.43 – 2.19 (m, 5H), 2.17 – 2.06 (m, 2H), 1.89 (dd, $J = 14.9, 5.5$ Hz, 1H), 1.50 (s, 3H), 1.13 (d, $J = 0.6$ Hz, 3H), 0.40 (d, $J = 0.8$ Hz, 6H); ^{13}C NMR (100 MHz, CDCl_3) δ 196.0, 173.8, 157.8, 147.0, 138.2, 134.2, 129.3, 129.3, 129.0, 128.2, 82.7, 82.5, 59.2, 55.3, 53.6, 47.5, 42.2, 42.1, 40.7, 40.2, 38.3, 26.6, 15.9, -2.8, -2.9; ; IR (Neat film, NaCl) 3439, 2924, 2854, 2282, 1758, 1656, 1428, 1373, 1291, 1266, 1248, 1214, 1164, 1108, 992, 937, 838, 821, 738 cm^{-1} ; HRMS (FAB+) m/z calc'd for $\text{C}_{27}\text{H}_{35}\text{O}_5\text{Si}$ $[\text{M}+\text{H}]^+$: 467.2254, found 467.2265; $[\alpha]_{\text{D}}^{25.0} -17.9^\circ$ (c 0.6, CHCl_3).



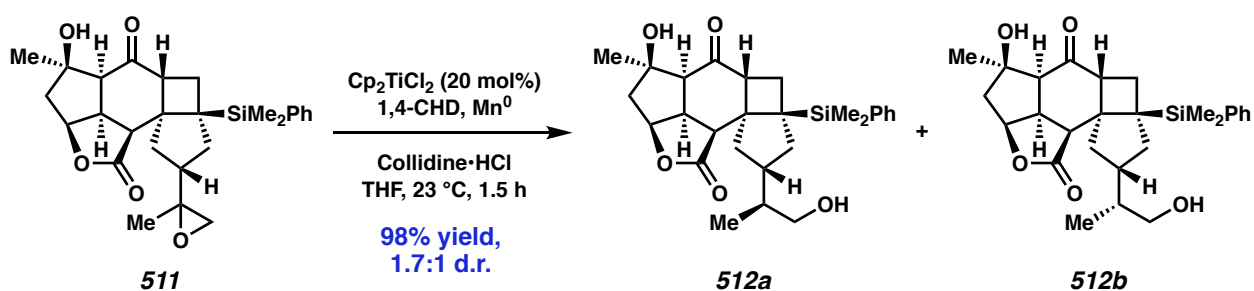
Cyclobutanes 511a and 511b: A mixture of vinyl silanes **509a** and **509b** (870 mg, 1.86 mmol, 1.0 equiv) is divided into 11 portions (79 mg each). Each portion is charged into a 40 mL scintillation vial, with PhH (34 mL). Each vial is sparged with nitrogen for 5 min, and placed in a photoreactor equipped with Hitachi UVA bulbs (F8T5-BLB, ~350 nm). The reactions are stirred under 350 nm irradiation for 5 h, after which no starting material remains (as judged by TLC). The reactions are combined in a 1 L round bottom flask, and concentrated onto Celite. The resulting solid is loaded onto a column, and purified by flash chromatography (30% → 40% → 50% → 60% → 70% → 80% EtOAc/Hexanes) to afford the title compounds (620 mg, 1.33 mmol, 71% yield) as a white solid. The products are isolated as a 1.7:1 mixture of diastereomers (judged by ^1H NMR), which were characterized separately.

*Note: The ^1H NMR spectra of these intermediates show broadened signals which were difficult to assign and integrate properly. Additionally, several signals were found to be missing from the ^{13}C NMR spectra. We attribute these observations to hindered rotation of the $-\text{Si}(\text{Me})_2\text{Ph}$ group about the highly congested cyclobutane ring. The NMR spectra are reported as observed, and the stereochemistry (and identity) of these products is assigned based upon the NMR and X-ray data obtained for **512a** and **512b**.*

Diastereomer 1 (minor): ^1H NMR (400 MHz, CDCl_3) δ 7.51 (s, 2H), 7.35 – 7.28 (m, 3H), 4.93 (s, 1H), 3.70 – 3.54 (m, 1H), 3.47 (s, 1H), 3.03 (d, $J = 9.3$ Hz, 1H), 2.70 – 2.30 (m, 4H), 1.93 (dd, J

= 15.2, 4.8 Hz, 1H), 1.68 (s, 1H), 1.45 (d, $J = 2.1$ Hz, 3H), 1.34 – 1.17 (m, 4H), 0.56 (d, $J = 18.1$ Hz, 4H); ^{13}C NMR (100 MHz, CDCl_3) δ 205.8, 134.3, 128.5, 127.6, 82.1, 81.4, 60.3, 57.6, 52.3, 50.9, 49.0, 47.7, 47.6, 40.1, 38.9, 35.0, 27.5; IR (Neat film, NaCl) 3395, 2958, 1773, 1686, 1369, 1256, 1202, 1089, 1014, 815, 776, 732 cm^{-1} ; HRMS (ES+) m/z calc'd for $\text{C}_{27}\text{H}_{35}\text{O}_5\text{Si}$ $[\text{M}+\text{H}]^+$: 467.2254, found 467.2280; $[\alpha]_{\text{D}}^{25.0} -41.1^\circ$ (c 0.19, CHCl_3).

Diastereomer 2 (major): ^1H NMR (400 MHz, CDCl_3) δ 7.59 – 7.45 (m, 2H), 7.34 – 7.28 (m, 3H), 4.92 (s, 1H), 3.60 (td, $J = 9.8, 6.2$ Hz, 1H), 3.47 (s, 1H), 3.02 (d, $J = 9.3$ Hz, 1H), 2.56 (dd, $J = 10.0, 5.3$ Hz, 3H), 2.42 – 2.31 (m, 1H), 1.94 (dd, $J = 15.1, 4.8$ Hz, 1H), 1.67 (s, 2H), 1.45 (s, 3H), 1.25 (d, $J = 1.7$ Hz, 3H), 0.53 (s, 5H); ^{13}C NMR (100 MHz, CDCl_3) δ 205.8, 134.3, 128.5, 127.7, 82.1, 81.5, 60.3, 57.1, 53.9, 50.9, 49.0, 47.7, 40.7, 38.6, 29.8, 27.5; IR (Neat film, NaCl) 3388, 2960, 2929, 1773, 1686, 1552, 1426, 1368, 1248, 1203, 1178, 1107, 1088, 817, 724, 696 cm^{-1} ; HRMS (ES+) m/z calc'd for $\text{C}_{27}\text{H}_{35}\text{O}_5\text{Si}$ $[\text{M}+\text{H}]^+$: 467.2254, found 467.1853; $[\alpha]_{\text{D}}^{25.0} -23.1^\circ$ (c 0.19, CHCl_3).



Diols 512a and 512b: A 100 mL round bottom flask is charged with a mixture of epoxides **511a** and **511b** (620 mg, 1.33 mmol, 1.0 equiv), Cp_2TiCl_2 (66 mg, 0.266 mmol, 0.20 equiv), Mn dust (80 mg, 1.46 mmol, 1.10 equiv), and collidine · HCl (262 mg, 1.66 mmol, 1.25 equiv) in THF (27 mL). To this red suspension is added 1,4-cyclohexadiene (567 μL , 599 mmol, 4.5 equiv) and the suspension gradually changes to a blue/grey color. The mixture is stirred at 23 °C for 1.5 h, after

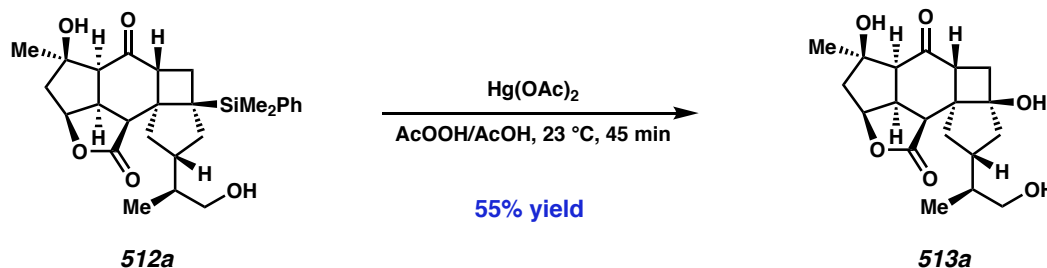
which the starting material is completely consumed, as judged by TLC. Celite is then added directly to the reaction mixture and the solvent is removed under reduced pressure. The resulting solid is loaded directly onto a flash column and purified by flash chromatography (60% → 65% → 70% → 75% → 80% → 90% → 100% EtOAc/Hexanes) to afford **XX** (385 mg, 0.781 mmol, 62% yield) and *epi-XX* (224 mg, 0.478 mmol, 36% yield) as white solids.

*Note: The ¹H NMR spectra of these intermediates show broadened signals which were difficult to assign and integrate properly. Additionally, several signals were found to be missing from the ¹³C NMR spectra. We attribute these observations to hindered rotation of the –Si(Me)₂Ph group about the highly congested cyclobutane ring. The NMR spectra are reported as observed, and the stereochemistry (and identity) of these products is assigned based upon the NMR and X-ray data obtained for **512a** and **512b**.*

512a (major): ¹H NMR (400 MHz, CD₃OD) δ 7.57 – 7.48 (m, 2H), 7.30 – 7.22 (m, 3H), 4.95 (s, 1H), 3.98 (s, 1H), 3.74 (tt, *J* = 10.1, 5.1 Hz, 1H), 3.64 (q, *J* = 10.2, 9.2 Hz, 1H), 3.52 – 3.38 (m, 1H), 3.30 – 3.15 (m, 1H), 2.76 – 1.38 (m, 11H), 1.34 (s, 3H), 1.10 – 0.83 (m, 3H), 0.52 (s, 4H); ¹³C NMR (100 MHz, CD₃OD) δ 210.1, 168.5, 151.9, 135.3, 129.2, 128.4, 108.8, 84.4, 81.6, 81.6, 67.3, 65.6, 61.9, 52.5, 45.9, 41.7, 41.5, 27.3, 15.7; IR (Neat film, NaCl) 3380, 2958, 2924, 2869, 1770, 1694, 1360, 1254, 1204, 1090, 1416, 828, 736, 730, 702 cm⁻¹; HRMS (ES+) *m/z* calc'd for C₂₇H₃₇O₅Si [M+H]⁺: 469.2410, found 469.2437; [α]_D^{25.0} –37.0 ° (*c* 0.24, CHCl₃).

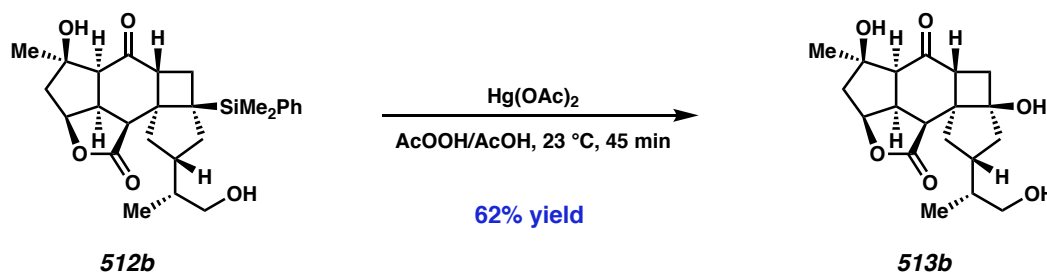
512b (major): ¹H NMR (400 MHz, CD₃OD) δ 7.58 – 7.46 (m, 2H), 7.27 (t, *J* = 3.2 Hz, 3H), 4.94 (t, *J* = 5.7 Hz, 1H), 3.81 – 3.69 (m, 1H), 3.69 – 3.58 (m, 1H), 3.48 (q, *J* = 7.1, 4.5 Hz, 1H), 3.33 (d, *J* = 13.8 Hz, 4H), 3.25 – 3.11 (m, 1H), 2.68 – 1.39 (m, 11H), 1.34 (s, 3H), 1.10 – 0.74 (m, 4H), 0.52 (d, *J* = 11.9 Hz, 5H); ¹³C NMR (100 MHz, CD₃OD) δ 210.1, 178.1, 135.3, 129.2, 128.4, 84.3,

81.6, 67.4, 61.9, 52.5, 47.8, 47.1, 47.1, 46.2, 44.1, 42.4, 41.8, 40.0, 35.9, 27.3, 15.6, -2.1, -4.9; IR (Neat film, NaCl) 3378, 2954, 2937, 2868, 2353, 1771, 1696, 1558, 1364, 1258, 1245, 1086, 827 cm^{-1} ; HRMS (ES+) m/z calc'd for $\text{C}_{27}\text{H}_{37}\text{O}_5\text{Si}$ $[\text{M}+\text{H}]^+$: 469.2410, found 469.2440; $[\alpha]_{\text{D}}^{25.0} -39.9^\circ$ (c 0.90, CHCl_3).



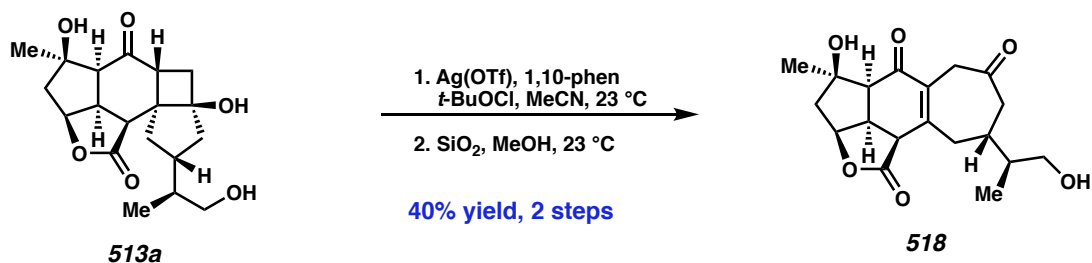
Triol 513a: A 20-mL scintillation vial is charged with **512a** (80 mg, 0.171 mmol, 1.0 equiv) and AcOOH (30% in aqueous AcOH, 3.4 mL). To this solution is added Hg(OAc)_2 (100 mg, 0.341 mmol, 2.0 equiv) in a single portion. The reaction is stirred 45 min at 23 $^\circ\text{C}$, after which no **512a** remains (as judged by LCMS). The reaction mixture is diluted with EtOAc (10 mL) and pipetted over an ice-cold mixture of sat. aq. $\text{Na}_2\text{S}_2\text{O}_3$ and sat. aq. NaHCO_3 (1:4). This aqueous solution is then extracted with EtOAc (3X), then $\text{CHCl}_3/i\text{-PrOH}$ (3:1) (2X). The organic extracts are combined and dried over Na_2SO_4 , filtered, and concentrated under reduced pressure to afford a crude solid which is purified by flash chromatography (80% \rightarrow 100% EtOAc/Hexanes) to afford the title compound (33 mg, 0.942 mmol, 55% yield) as a white solid. X-ray quality crystals were obtained by slow cooling from EtOH/ CH_2Cl_2 /Hexanes: ^1H NMR (400 MHz, CD_3OD) δ 5.16 (dd, $J = 6.2, 4.7$ Hz, 1H), 3.88 (dd, $J = 9.8, 7.7$ Hz, 1H), 3.72 (ddd, $J = 10.6, 9.3, 6.3$ Hz, 1H), 3.55 – 3.47 (m, 2H), 3.37 – 3.32 (m, 1H), 2.58 (d, $J = 10.6$ Hz, 1H), 2.35 (d, $J = 15.0$ Hz, 1H), 2.23 (dd, $J = 11.9, 9.7$ Hz, 1H), 2.19 – 1.98 (m, 3H), 1.95 (dd, $J = 15.1, 4.9$ Hz, 1H), 1.85 (ddd, $J = 12.9,$

6.1, 2.0 Hz, 1H), 1.70 (dd, $J = 13.1, 9.9$ Hz, 1H), 1.54 – 1.41 (m, 2H), 1.35 (s, 3H), 0.93 (d, $J = 6.8$ Hz, 3H); ^{13}C NMR (100 MHz, CD_3OD) δ 209.4, 181.7, 89.3, 88.2, 81.6, 67.1, 62.1, 59.0, 51.8, 51.3, 47.8, 47.3, 45.8, 41.8, 41.3, 41.2, 40.7, 27.3, 15.3; IR (Neat Film NaCl) 3308, 2936, 1694, 1371, 1217, 1184, 1120, 1016 cm^{-1} ; HRMS (MM: ESI-APCI+) m/z calc'd for $\text{C}_{19}\text{H}_{27}\text{O}_6$ $[\text{M}+\text{H}]^+$: 351.1802, found 315.1790; $[\alpha]_{\text{D}}^{25.0} -61.1^\circ$ (c 0.5, MeOH).



Triol 513b A 20-mL scintillation vial is charged with **512b** (80 mg, 0.171 mmol, 1.0 equiv) and AcOOH (30% in aqueous AcOH, 3.4 mL). To this solution is added Hg(OAc)_2 (100 mg, 0.341 mmol, 2.0 equiv) in a single portion. The reaction is stirred 45 min at 23 $^\circ\text{C}$, after which no **512b** remains (as judged by LCMS). The reaction mixture is diluted with EtOAc (10 mL) and pipetted over an ice-cold mixture of sat. aq. $\text{Na}_2\text{S}_2\text{O}_3$ and sat. aq. NaHCO_3 (1:4). This aqueous solution is then extracted with EtOAc (3X), then $\text{CHCl}_3/i\text{-PrOH}$ (3:1) (2X). The organic extracts are combined and dried over Na_2SO_4 , filtered, and concentrated under reduced pressure to afford a crude solid which is purified by flash chromatography (80% \rightarrow 100% EtOAc/Hexanes) to afford the title compound (37 mg, 0.0106 mmol, 62% yield) as a white solid. X-ray quality crystals were obtained by layer diffusion of hexanes into $\text{CH}_2\text{Cl}_2/\text{EtOH}$: ^1H NMR (400 MHz, CD_3OD) δ 5.16 (dd, $J = 6.2, 4.7$ Hz, 1H), 3.88 (dd, $J = 9.8, 7.7$ Hz, 1H), 3.79 – 3.64 (m, 1H), 3.57 – 3.45 (m, 2H), 3.40 – 3.34 (m, 1H), 2.57 (d, $J = 10.6$ Hz, 1H), 2.35 (d, $J = 15.1$ Hz, 1H), 2.28 – 2.11 (m, 2H), 2.07 (dd, $J = 11.9, 7.7$ Hz, 1H), 2.02 – 1.90 (m, 2H), 1.87 (ddd, $J = 13.0, 6.1, 2.1$ Hz, 1H), 1.68

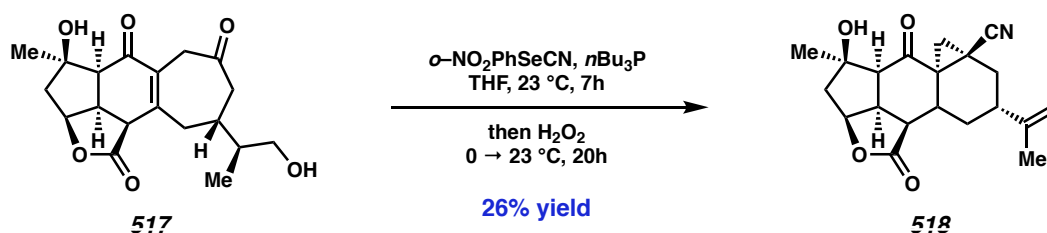
(dd, $J = 13.1, 10.2$ Hz, 1H), 1.57 – 1.43 (m, 2H), 1.35 (s, 3H), 0.94 (d, 3H); ^{13}C NMR (100 MHz, CD_3OD) δ 209.4, 181.7, 89.0, 88.2, 81.6, 66.9, 62.1, 59.3, 51.8, 51.3, 47.8, 47.3, 45.1, 41.7, 41.5, 41.4, 40.7, 27.3, 15.4; IR (Neat Film NaCl) 3464, 3292, 2953, 1720, 1693, 1372, 1190, 1104 cm^{-1} ; HRMS (MM: ESI-APCI+) m/z calc'd for $\text{C}_{19}\text{H}_{27}\text{O}_6$ $[\text{M}+\text{H}]^+$: 351.1802, found 315.1790; $[\alpha]_{\text{D}}^{25.0} -42.2^\circ$ (c 0.5, MeOH).



Diol X: To a stirred suspension of triol **513a** (21 mg, 0.0599 mmol, 1.0 equiv), AgOTf (6.0 mg, 0.0240 mmol, 0.40 equiv), and 1,10-phenanthroline (9.0 mg, 0.0479 mmol, 0.80 equiv) in acetonitrile (3.2 mL, 0.019 M) was added *t*-butyl hypochlorite (14 μL , 0.120 mmol, 2.0 equiv) at 23 °C. The suspension changed from white to red, and then to dark brown. The reaction mixture was allowed to stir at 23 °C for 12 h, after which no starting material remained (as judged by TLC and LCMS). The reaction mixture was diluted with ethyl acetate, and quenched with 5 drops of saturated aqueous sodium thiosulfate after which the dark brown color quickly dissipated. The mixture was passed directly over a short plug of silica, and the eluent was concentrated onto SiO₂ and dry loaded onto a column. The crude was purified by flash chromatography (50 – 100% ethyl acetate/hexanes) to afford an unstable intermediate (presumed to be the γ -chloroketone) which was not characterized further.

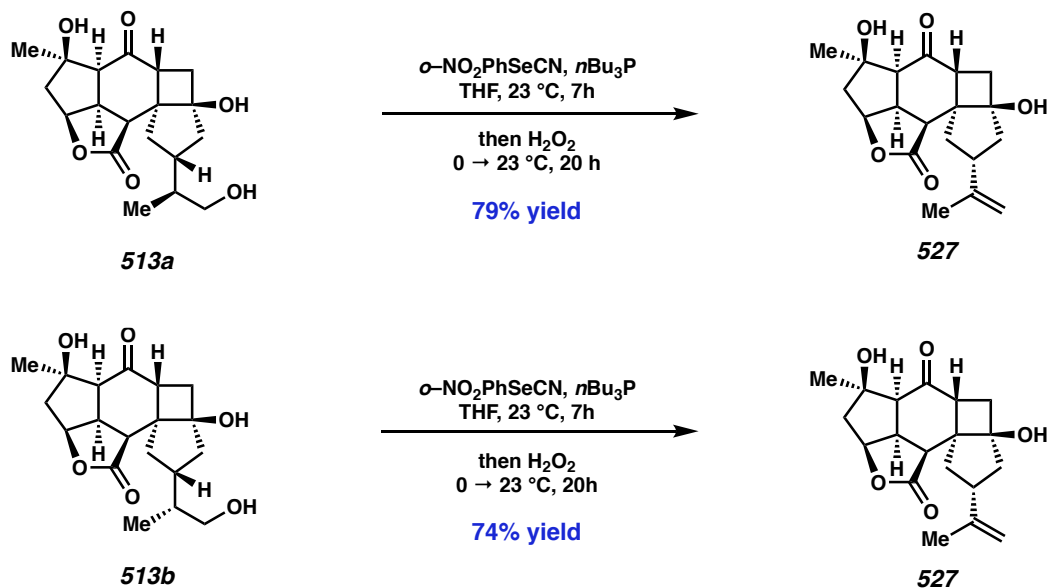
The product from the above reaction was dissolved in methanol (5 mL). TLC SiO₂ (scraped from TLC plates and crushed with a mortar and pestle) was added (c.a. 1 g). The suspension was allowed

to stir for 12 hours at 23 °C, after which the abovementioned product had been completely consumed (as judged by TLC). The methanol was removed under reduced pressure, and then resuspended in acetone (10 mL) and stirred for 1 hour. The suspension was filtered through a plug of Celite[®] and concentrated to afford diol **X** (10 mg, 40% yield) as a white solid. Product characterization data was not obtained due to the Spring 2020 COVID-19 shutdown of research facilities.



Cyclopropane 518: To a stirred solution of diol **517** (4 mg, 0.0115 mmol, 1.0 equiv) in THF (400 μL , 0.029 M) cooled to 15 °C in a nitrogen-filled glovebox was added $o\text{-NO}_2\text{PhSeCN}$ (156 mg/mL solution in THF, 25 μL , 0.0173 mmol, 1.5 equiv). To this light-brown solution was added $n\text{-Bu}_3\text{P}$ (83 mg/mL solution in THF, 42 μL , 0.0173 mmol, 1.5 equiv), at which point the solution rapidly changed to deep red in color. The reaction mixture was stirred 20 min at 15 °C and then warmed to 23 °C and stirred an additional 2 h. At this point, a small amount of starting material was detected by LCMS. An additional portion of $o\text{-NO}_2\text{PhSeCN}$ (156 mg/mL solution in THF, 8 μL , 0.00775 mmol, 0.5 equiv) was added, followed by $n\text{-Bu}_3\text{P}$ (83 mg/mL solution in THF, 14 μL , 0.00775 mmol, 0.5 equiv) at 23 °C, and the reaction was subsequently allowed to stir an additional 2 h. The reaction was removed from the glovebox and cooled to 0 °C. H_2O_2 (30%, 60 μL) was added dropwise, and the reaction was stirred 1 h at 0 °C. The mixture was allowed to warm to 23 °C, and stirred an additional 12 h. The reaction mixture was purified directly by preparative HPLC to afford

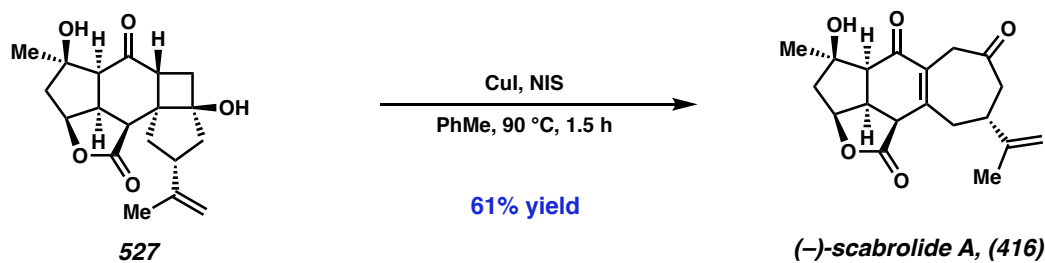
X (1 mg, 26% yield) as a white solid. Product characterization data was not obtained due to the Spring 2020 COVID-19 shutdown of research facilities.



Note: The Grieco dehydration to cyclobutanol 4a was performed using both 25 and epi-25, with both substrates providing similar yields of product. A representative procedure for this reaction is provided below:

Cyclobutanol 527: In a nitrogen filled glovebox a 1-dram vial is charged with **513a** (8.0 mg, 0.0228 mmol, 1.0 equiv) and *o*-NO₂PhSeCN (15.5 mg, 0.0685 mmol, 3.0 equiv) in THF (450 μL). To this orange solution is added *n*-Bu₃P (17 μL, 0.0685 mmol, 3.0 equiv) dropwise via syringe, at which point the reaction mixture becomes deep red/brown in color. This solution is allowed to stir in the glovebox at 23 °C for 7 h, at which point **513a** has been completely consumed, as judged by LCMS. The vial is then removed from the glovebox and cooled to 0 °C after which H₂O₂ (30% w/w, 80 μL) is cautiously added dropwise. This orange solution is then stirred while gradually warming to 23 °C over c.a. 2 h and then stirred at 23 °C an additional 18 h. The reaction is then

loaded directly onto a column and purified by flash chromatography (30% → 40% → 50% EtOAc/Hexanes) to afford the title compound (6.0 mg, 0.0181 mmol, 79% yield) as a white solid: ^1H NMR (400 MHz, CDCl_3) δ 6.08 (s, 1H), 5.14 (dd, $J = 6.1, 4.6$ Hz, 1H), 4.75 – 4.71 (m, 1H), 4.71 – 4.68 (m, 1H), 3.83 (dd, $J = 9.6, 8.0$ Hz, 1H), 3.66 – 3.56 (m, 1H), 3.36 (d, $J = 9.1$ Hz, 1H), 2.79 (ddd, $J = 15.9, 13.0, 8.0$ Hz, 1H), 2.60 (d, $J = 10.7$ Hz, 1H), 2.43 (d, $J = 15.4$ Hz, 1H), 2.34 (dd, $J = 12.1, 9.6$ Hz, 1H), 2.24 (dd, $J = 12.1, 8.0$ Hz, 1H), 2.14 (ddd, $J = 13.2, 9.8, 2.2$ Hz, 1H), 1.96 (dd, $J = 15.3, 4.8$ Hz, 1H), 1.90 – 1.78 (m, 2H), 1.74 – 1.67 (m, 5H), 1.48 (s, 3H); ^{13}C NMR (100 MHz, CDCl_3) δ 205.8, 179.2, 146.1, 109.9, 88.0, 86.0, 81.3, 60.6, 57.8, 50.3, 50.3, 47.7, 46.3, 45.3, 44.7, 40.8, 40.5, 27.6, 21.1; IR (Neat Film NaCl) 3346, 2936, 1726, 1710, 1598, 1366, 1325, 1218, 1194, 1123, 1088, 1011, 850, 822 cm^{-1} ; HRMS (MM: ESI-APCI+) m/z calc'd for $\text{C}_{19}\text{H}_{25}\text{O}_5$ $[\text{M}+\text{H}]^+$: 333.1697, found 333.1694; $[\alpha]_{\text{D}}^{25.0} -31.1^\circ$ (c 0.4, CHCl_3).



Scabrolide A (416): In a nitrogen-filled glovebox, a 1-dram vial is charged with cyclobutanol **4a** (5.0 mg, 0.0151 mmol, 1.0 equiv), CuI (22.0 mg, 0.117 mmol, 7.8 equiv) and NIS (6.7 mg, 0.0300 mmol, 2.0 equiv) in PhMe (1.5 mL). The vial is stirred at 23 °C for 5 min, and then transferred to a preheated, 90 °C aluminum block. The reaction is stirred at 90 °C for 1 h. At this point, an additional portion of NIS (3.3 mg, 0.0150 mmol, 1.0 equiv) is added, and the reaction is stirred an additional 20 min at 90 °C. The mixture is then cooled to 23 °C and filtered through a pad of Celite, washing with EtOAc. This solution is concentrated to a red film, which is directly purified by

reverse-phase (C18) preparative HPLC (MeCN/H₂O, 5.0 mL/min, monitor wavelength = 260 nm, 30% MeCN ramp to 45% MeCN over 6 min) to afford scabrolide A (3.0 mg, 0.00909 mmol, 61% yield) as a white solid. X-ray quality crystals were obtained by layer-diffusion of hexanes into a CH₂Cl₂ solution of (**416**): ¹H NMR (400 MHz, CDCl₃) δ 5.11 (dd, *J* = 7.1, 5.4 Hz, 1H), 4.87 – 4.84 (m, 1H), 4.85 – 4.82 (m, 1H), 3.70 (dd, *J* = 45.1, 17.2 Hz, 1H), 3.61 (ddd, *J* = 11.1, 10.0, 7.2 Hz, 1H), 3.51 (d, *J* = 11.3 Hz, 1H), 3.43 (dd, *J* = 17.3, 1.6 Hz, 1H), 3.18 – 3.03 (m, 1H), 2.97 – 2.80 (m, 2H), 2.68 – 2.55 (m, 2H), 2.60 (d, *J* = 10.1 Hz, 1H), 2.30 (d, *J* = 15.0 Hz, 1H), 1.93 (dd, *J* = 15.0, 5.6 Hz, 1H), 1.83 (t, *J* = 1.0 Hz, 3H), 1.50 (s, 3H); ¹³C NMR (100 MHz, CDCl₃) δ 208.2, 193.1, 173.7, 151.8, 147.2, 132.9, 111.0, 83.2, 82.3, 54.6, 47.6, 46.4, 44.8, 41.7, 41.1, 39.7, 37.3, 26.3, 21.5; IR (Neat Film NaCl) 3366, 2965, 2930, 2858, 1765, 1696, 1636, 1445, 1374, 1358, 1275, 1260, 1219, 1182, 1162, 1120, 1090, 1012, 899, 690 cm⁻¹; HRMS (MM: ESI-APCI+) *m/z* calc'd for C₁₉H₂₃O₅ [M+H]⁺: 331.1540, found 331. 1539; [α]_D^{25.0} -210.7 ° (*c* 0.39, CHCl₃).

4.6.3 Comparison of Natural and Synthetic Material

Table 4.2. Comparison of scabrolide ¹H NMR peaks to naturally-isolated material.

Synthetic scabrolide A	Isolated scabrolide A (Sheu, 2002)	Isolated scabrolide A (Liang, Guo, 2020)
400 MHz, CDCl ₃	400 MHz, CDCl ₃	400 MHz, CDCl ₃
5.11 (dd, <i>J</i> = 5.4, 7.1)	5.11 (t, <i>J</i> = 6.4)	5.11 (dd, <i>J</i> = 5.6, 7.0)
4.86 (m)	4.85 (s)	4.85 (s)
4.84 (m)	4.83 (s)	4.83 (s)
3.70 (d, <i>J</i> = 17.2)	3.70 (d, <i>J</i> = 17.2)	3.70 (d, <i>J</i> = 17.2)
3.61 (ddd, <i>J</i> = 7.2, 10.0, 11.1)	3.62 (dd, <i>J</i> = 6.4, 11.2)	3.62 (dd, <i>J</i> = 6.4, 11.2)
3.51 (d, <i>J</i> = 11.3)	3.51 (d, <i>J</i> = 11.2)	3.51 (d, <i>J</i> = 11.2)
3.43 (dd, <i>J</i> = 1.6, 17.3)	3.42 (d, <i>J</i> = 17.2)	3.42 (d, <i>J</i> = 17.2)
3.09 (m)	3.07 (q, <i>J</i> = 6.4)	3.07 (m)
2.88 (m, 2H)	2.88 (m), 2.88 (m)	2.86 (m, 2H)
2.62 (m, 2H)	2.63 (m, 2H)	2.63 (m, 2H)
2.60 (d, <i>J</i> = 10.1)	2.62 (d, <i>J</i> = 10.0)	2.62 (d, <i>J</i> = 10.0)
2.30 (d, <i>J</i> = 15.0)	2.30 (d, <i>J</i> = 15.2)	2.30 (d, <i>J</i> = 15.2)
1.93 (dd, <i>J</i> = 5.6, 15.0)	1.92 (dd, <i>J</i> = 5.6, 15.2)	1.92 (dd, <i>J</i> = 5.6, 15.2)
1.83 (s, 3h)	1.82 (s, 3H)	1.82 (s, 3H)

Table 4.3. Comparison of scabrolide ^{13}C NMR peaks to naturally-isolated material.

Synthetic scabrolide A	Isolated scabrolide A (Sheu)	Isolated Scabrolide A (Liang, Guo)
<i>100 MHz, CDCl₃</i>	<i>100 MHz, CDCl₃</i>	<i>100 MHz, CDCl₃</i>
208.2	208.3	208.2
193.1	193.1	193.2
173.7	173.7	173.7
151.8	151.7	151.8
147.2	147.1	147.3
132.9	132.7	133.0
111.0	110.8	111.0
83.2	82.9	83.1
82.3	82.2	82.3
54.6	54.5	54.6
47.6	47.4	47.6
46.4	46.3	46.5
44.8	44.6	44.8
41.7	41.6	41.7
41.1	40.9	41.1
39.7	39.5	39.7
37.3	37.2	37.4
26.3	26.1	26.3
21.5	21.3	21.5

4.6.4 Additional References

- (1) Pangborn, A. M.; Giardello, M. A.; Grubbs, R. H.; Rosen, R. K.; Timmers, F. J. *Organometallics* **1996**, *15*, 1518–1520.
- (2) Brill, Z.G.; Grover, H.K.; Maimone, T.J. *Science* **2016**, *352*, 1078–1082.
- (3) Craig, R. A., II; Roizen, J. L.; Smith, R. C.; Jones, A. C.; Stoltz, B. M. *Org. Lett.* **2012**, *14*, 5716–5719.
- (4) Weinstabl, H.; Gaich, T.; Mulzer, J. *Org. Lett.* **2012**, *14*, 2834–2837.

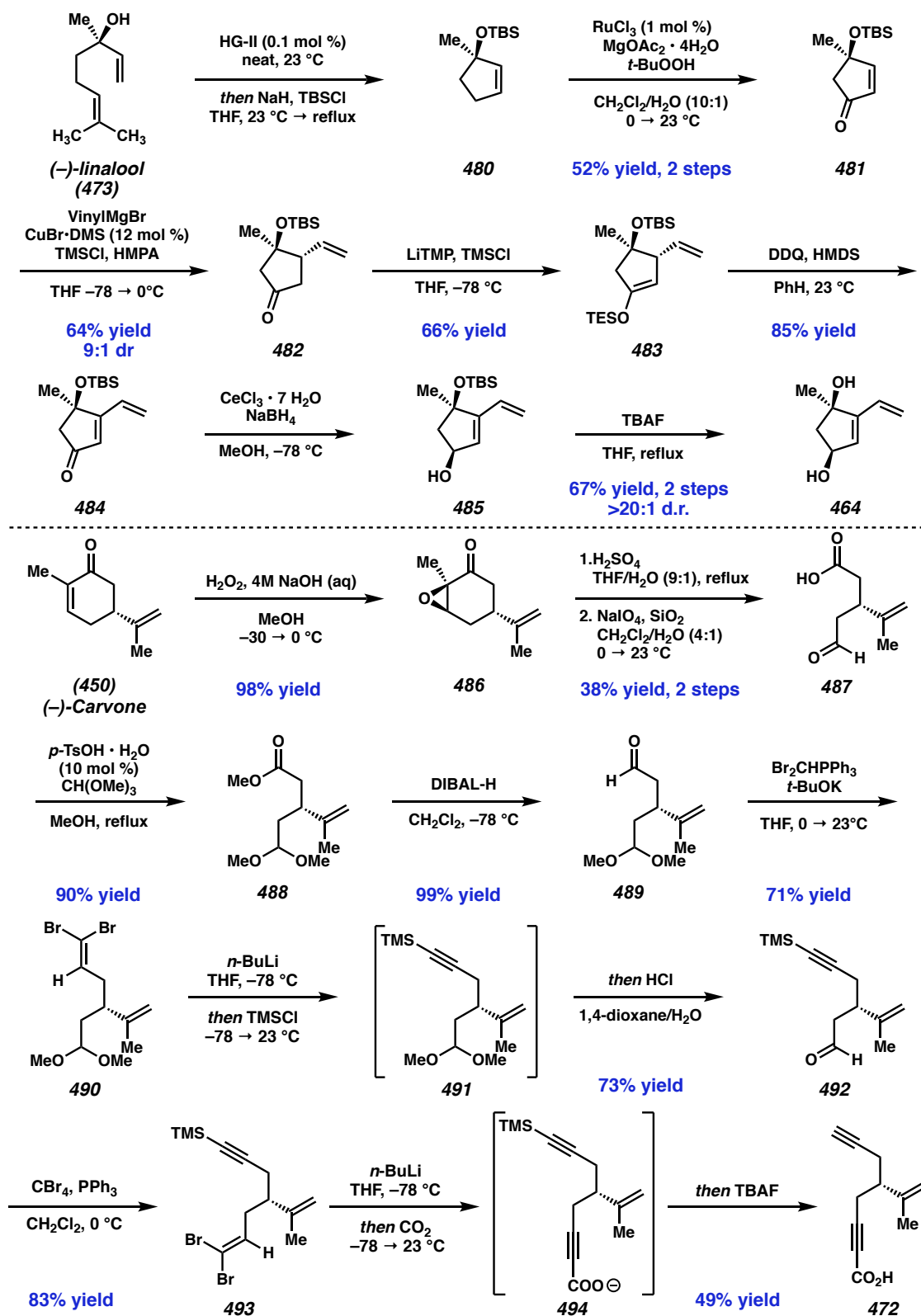
APPENDIX 7

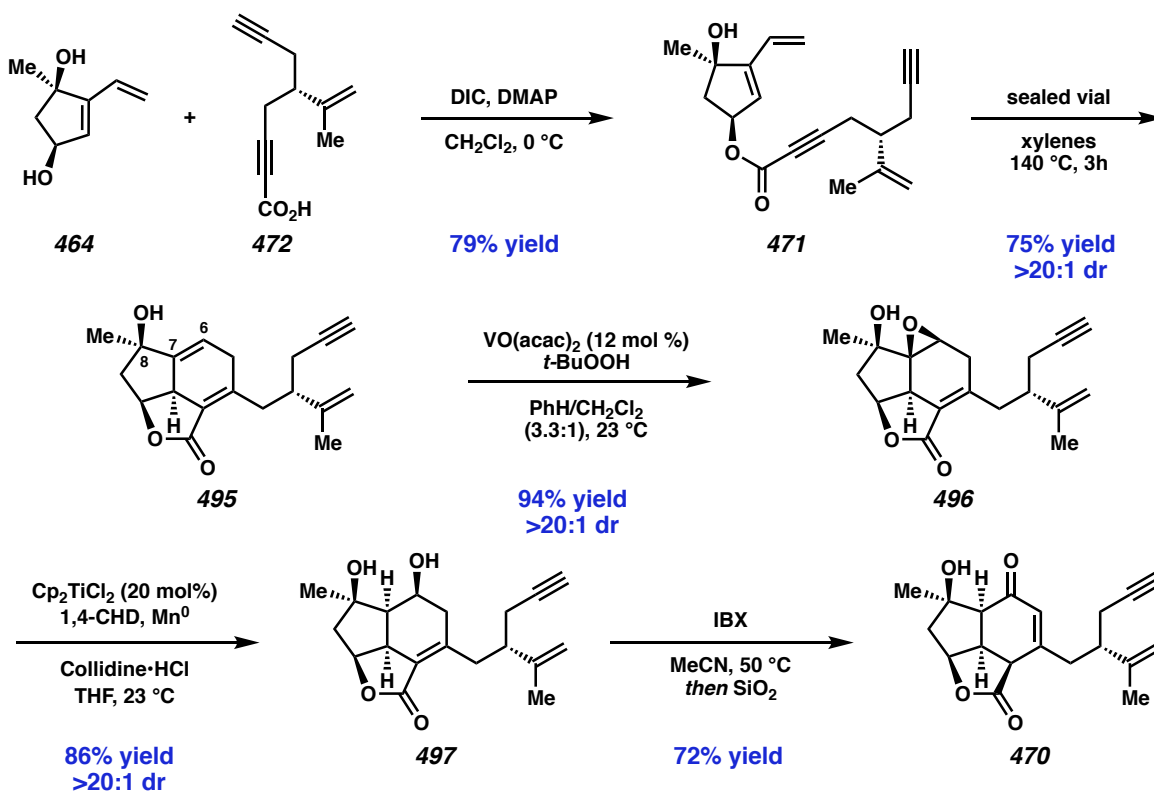
Synthetic Summary for Chapter 4:

Total Synthesis of

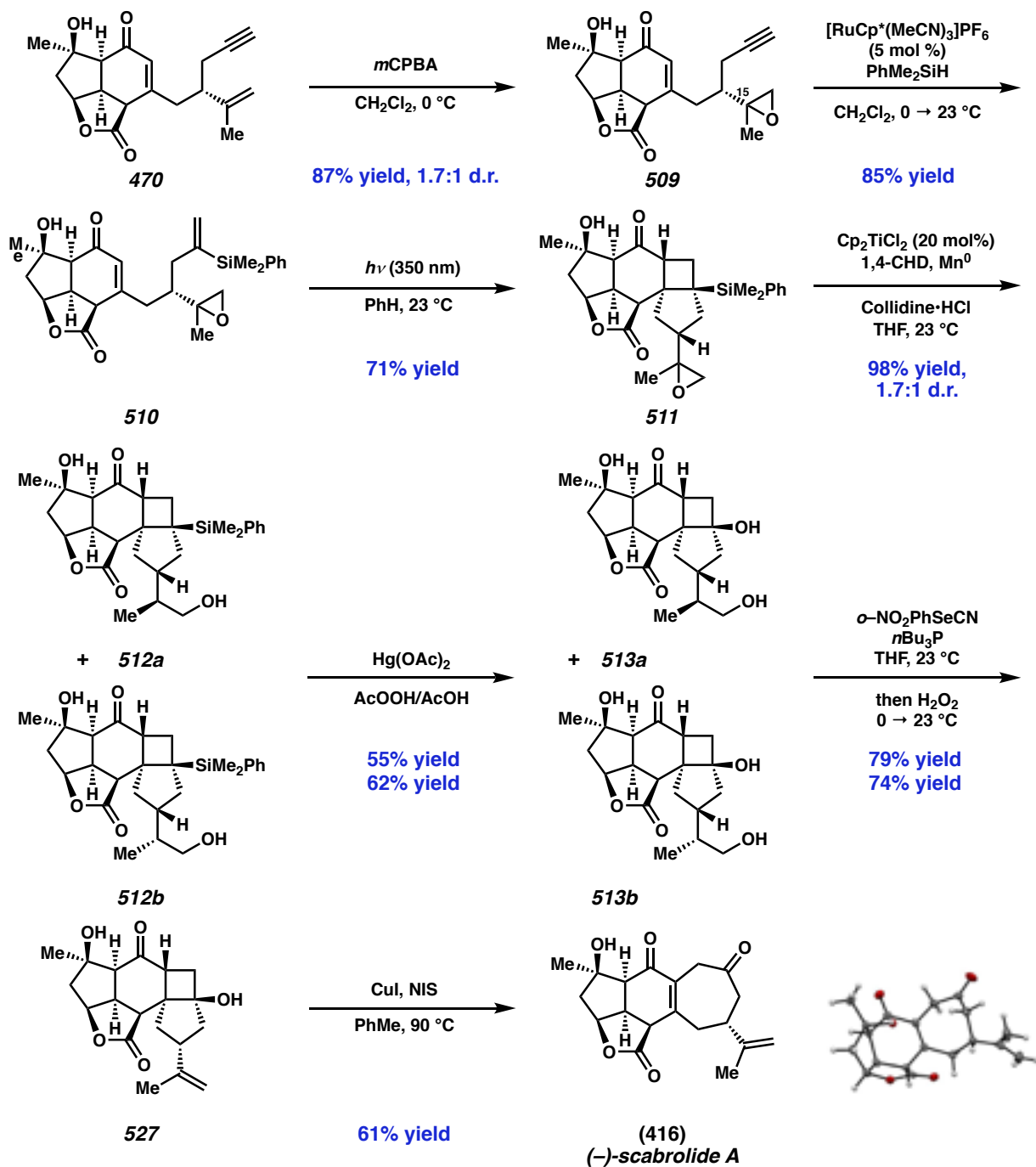
(-)-Scabrolide A

Scheme A5.1. Synthesis of esterification precursors from chiral pool starting materials.



Scheme A5.2. Synthesis of tricyclic core of (-)-scabrolide A.

Scheme A5.3. Total synthesis of (-)-scabrolide A.



APPENDIX 8

Spectra Relevant to Chapter 4:

Total Synthesis of

(-)-Scabrolide A

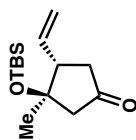
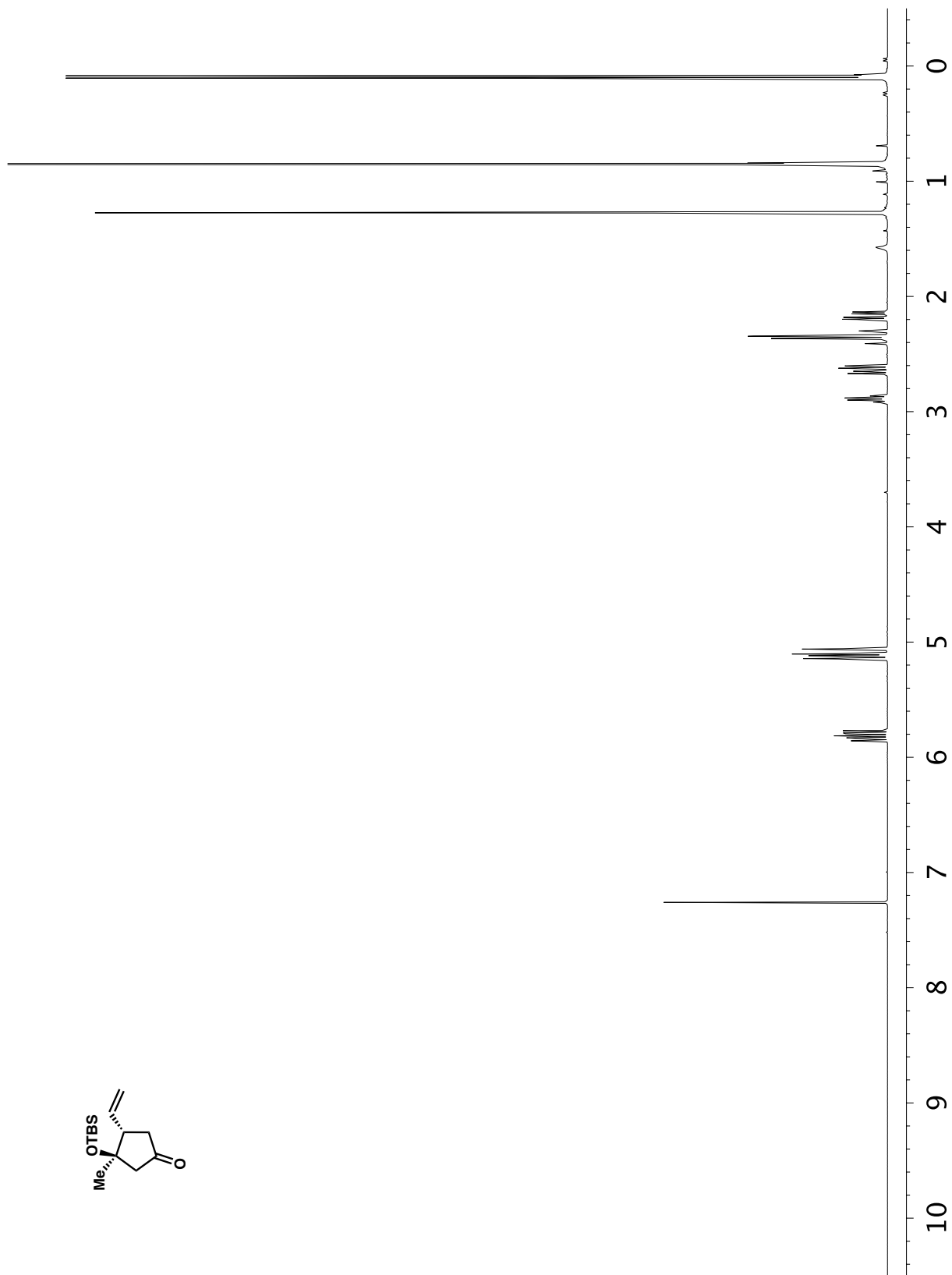


Figure A6.1 ^1H NMR (400 MHz, CDCl_3) of compound 482.

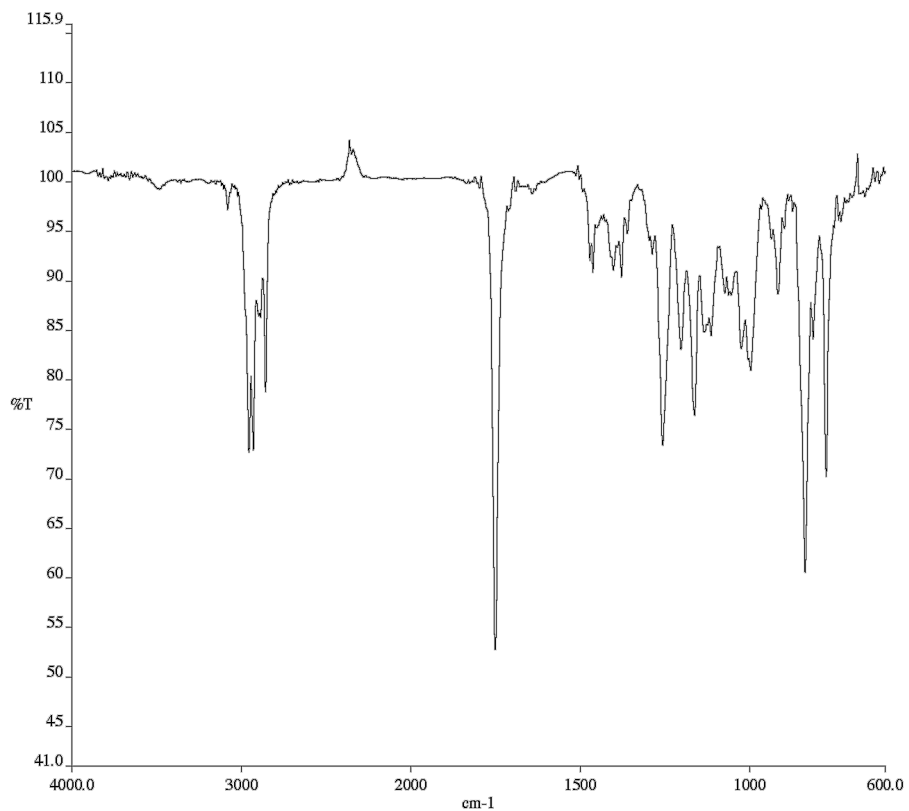


Figure A6.2 Infrared spectrum (Thin Film, NaCl) of compound **482**.

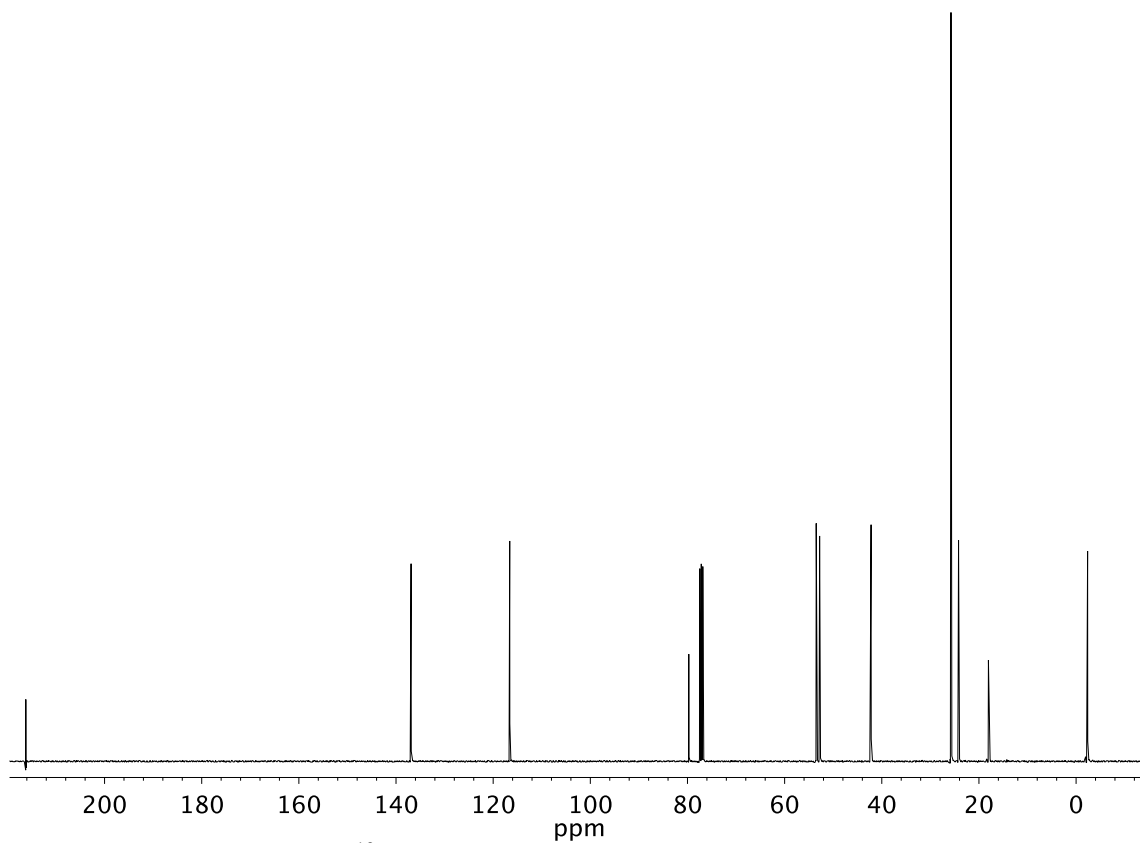


Figure A6.3 ¹³C NMR (101 MHz, CDCl₃) of compound **482**.

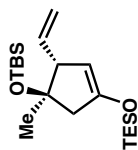
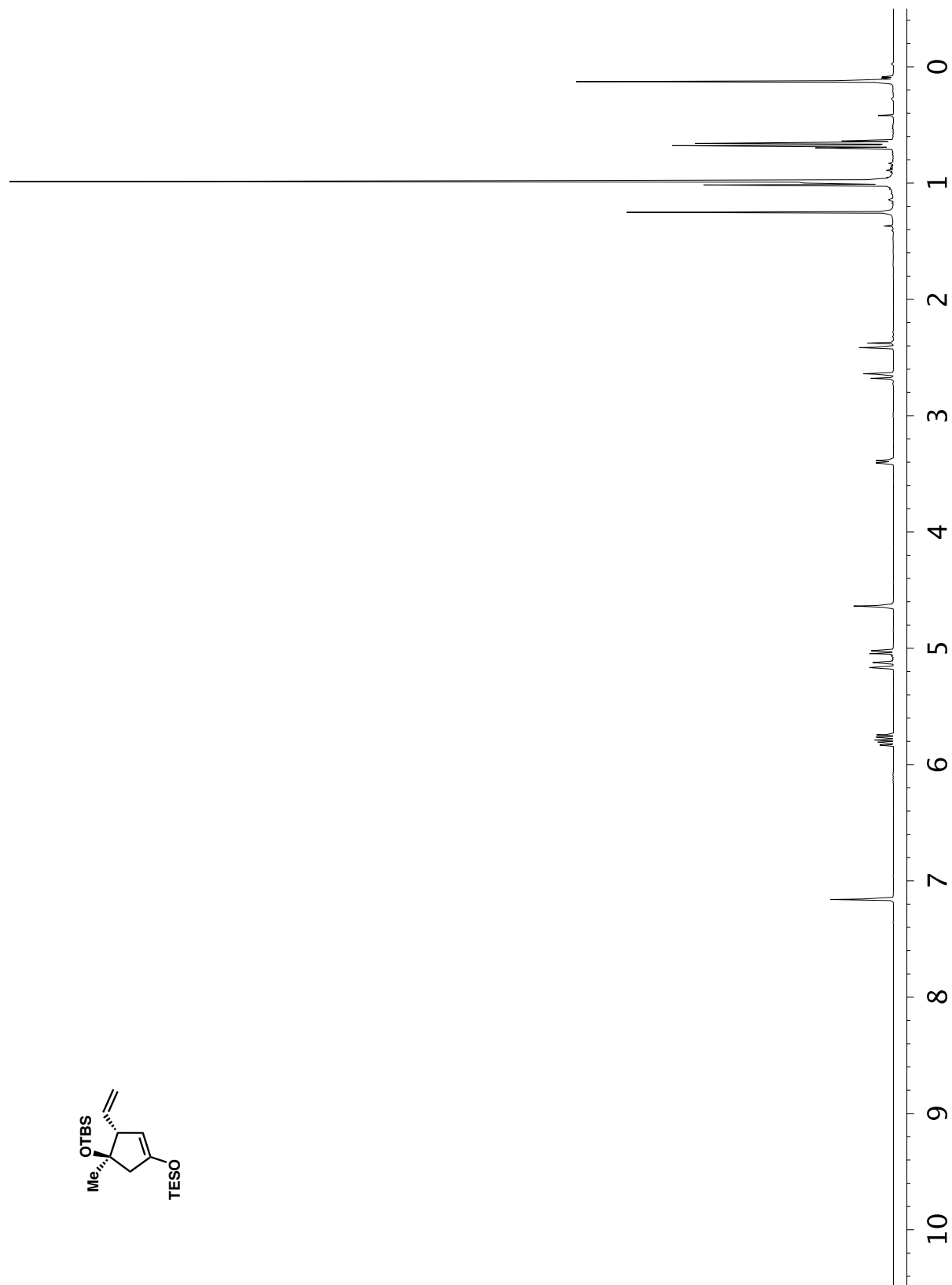


Figure A6.4 ^1H NMR (400 MHz, C_6D_6) of compound 483.

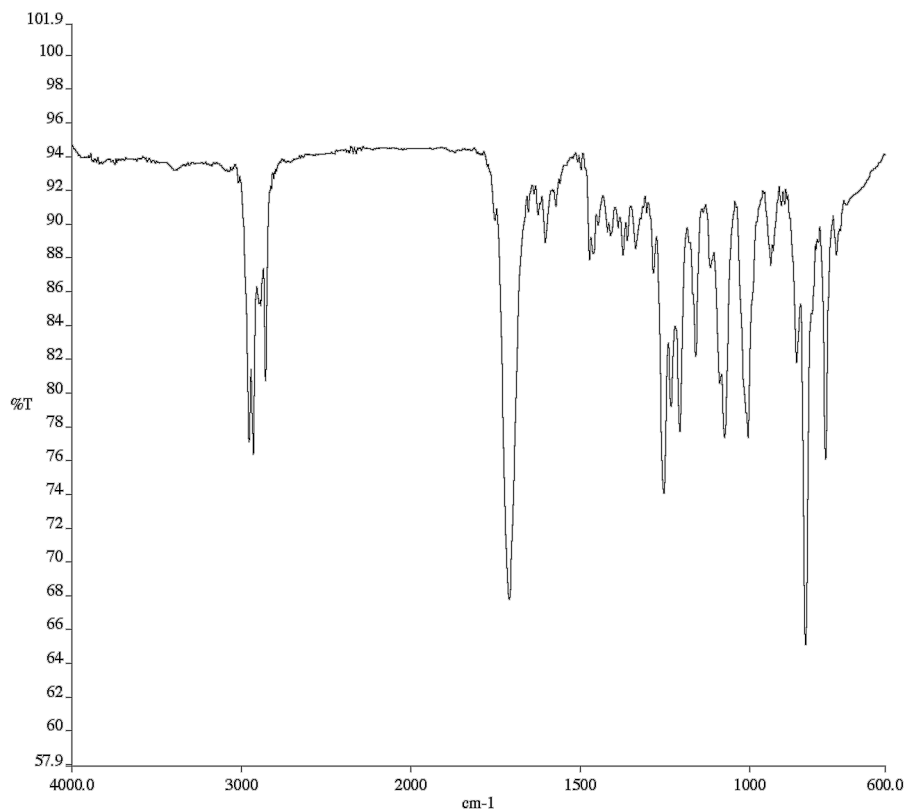


Figure A6.5 Infrared spectrum (Thin Film, NaCl) of compound **483**.

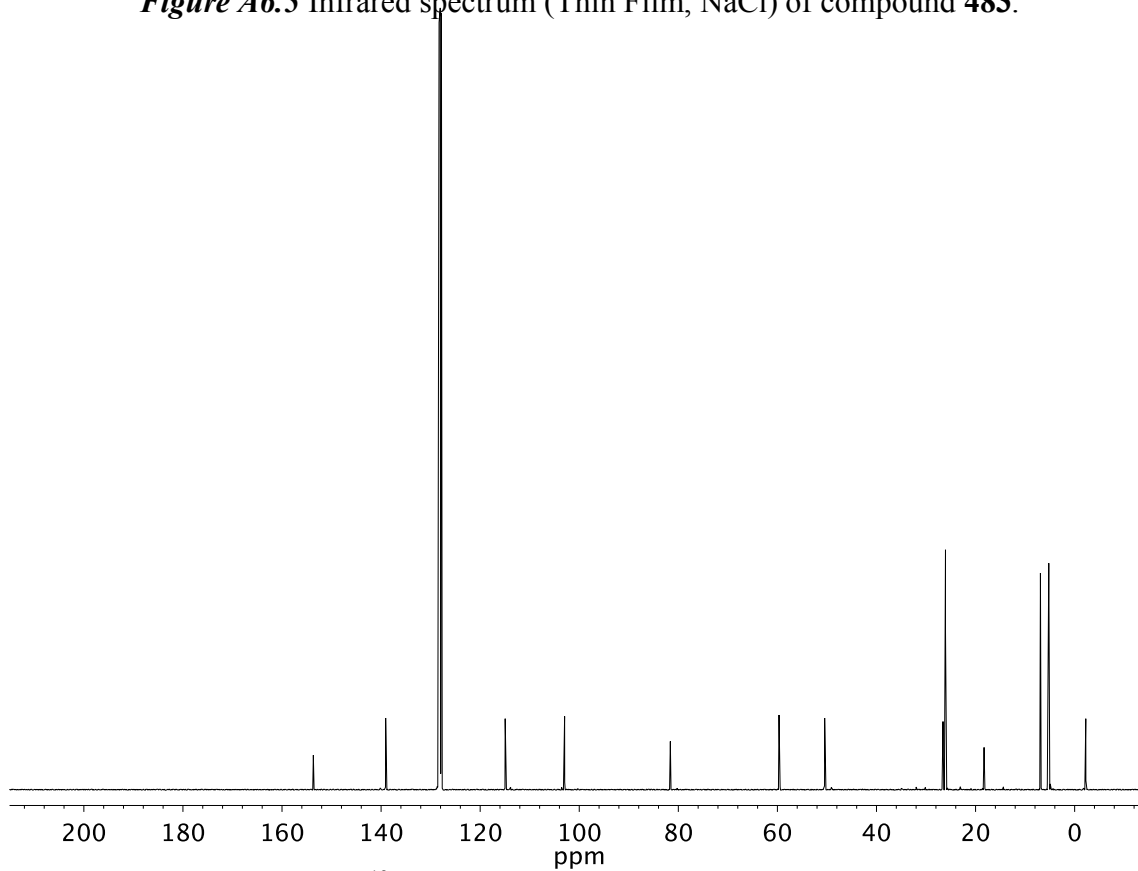


Figure A6.6 ¹³C NMR (101 MHz, C₆D₆) of compound **483**.

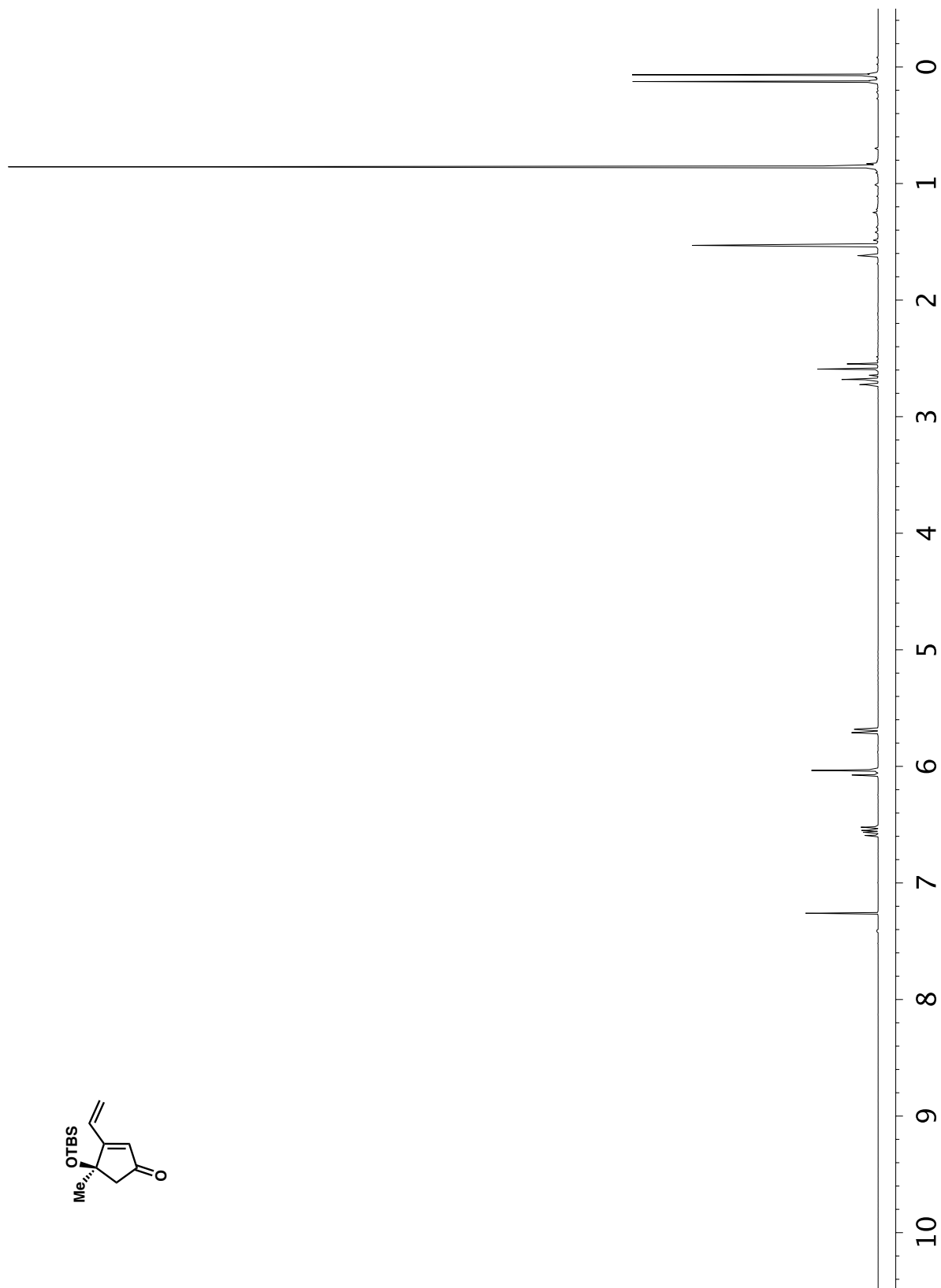


Figure A6.7 ¹H NMR (400 MHz, CDCl₃) compound 484.

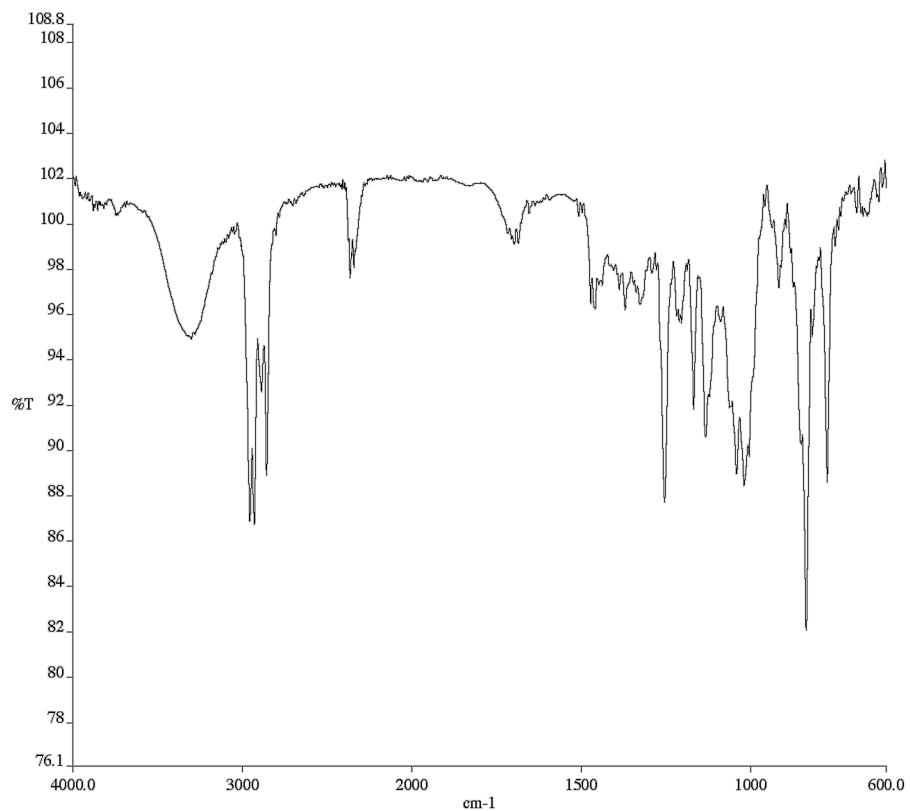


Figure A6.8 Infrared spectrum (Thin Film, NaCl) of compound **484**.

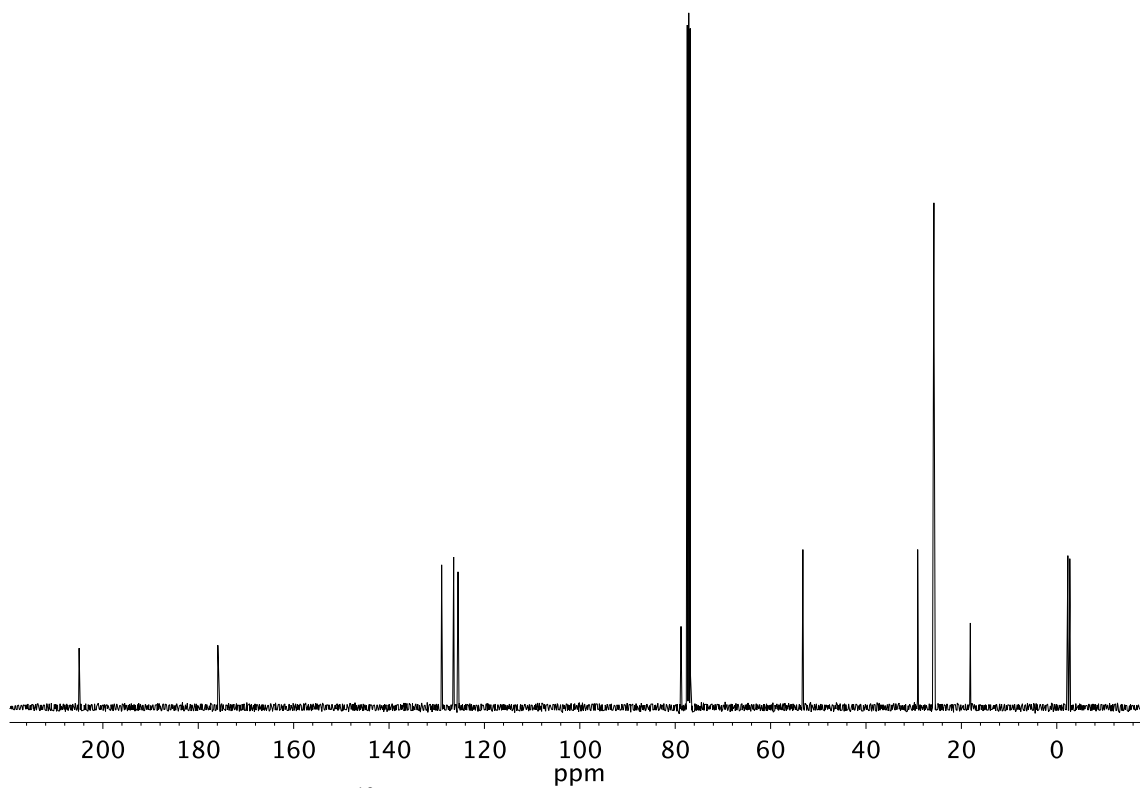


Figure A6.9 ¹³C NMR (101 MHz, CDCl₃) of compound **484**.

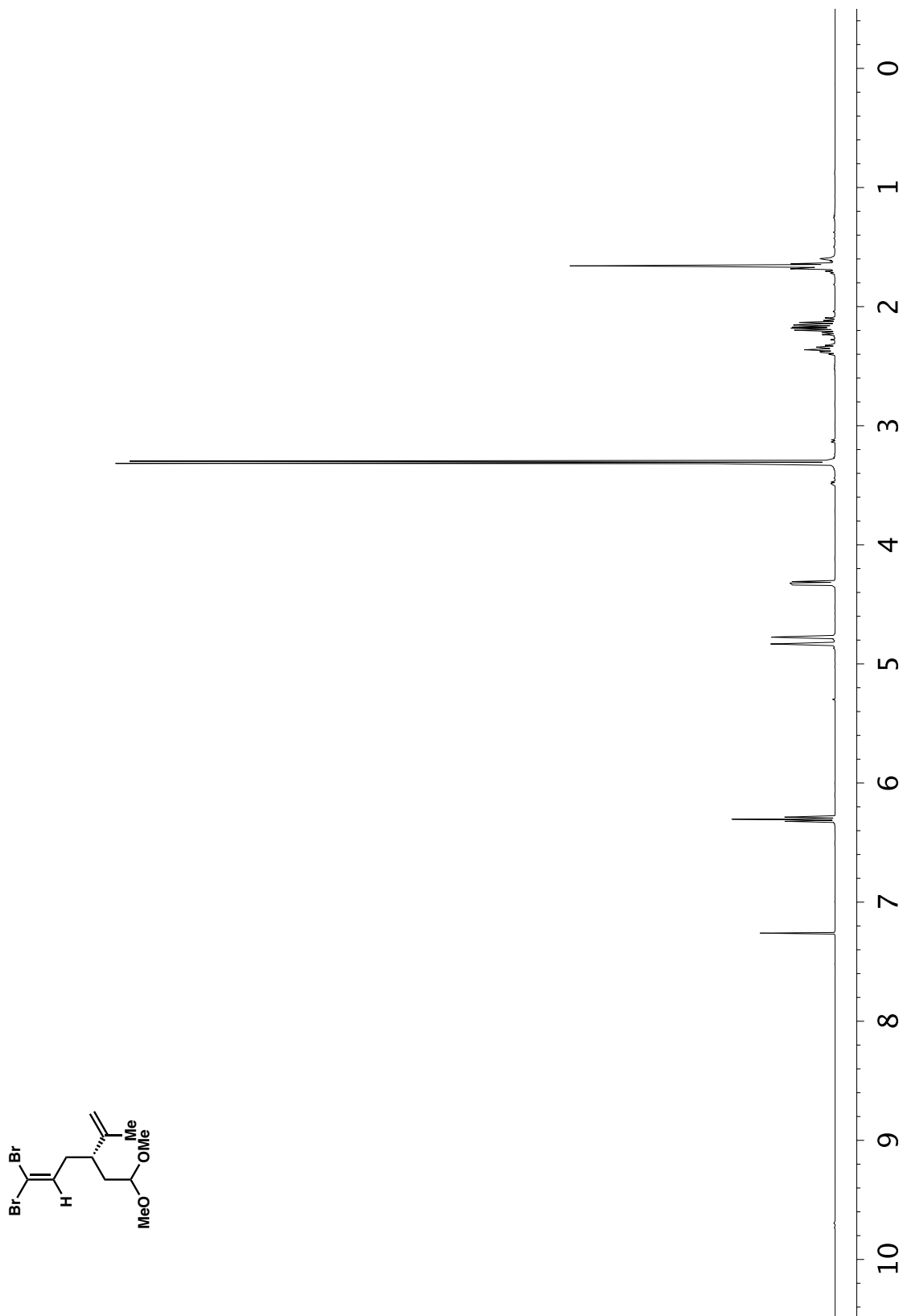


Figure A6.10 $^1\text{H NMR}$ (400 MHz, CDCl_3) of compound 490.

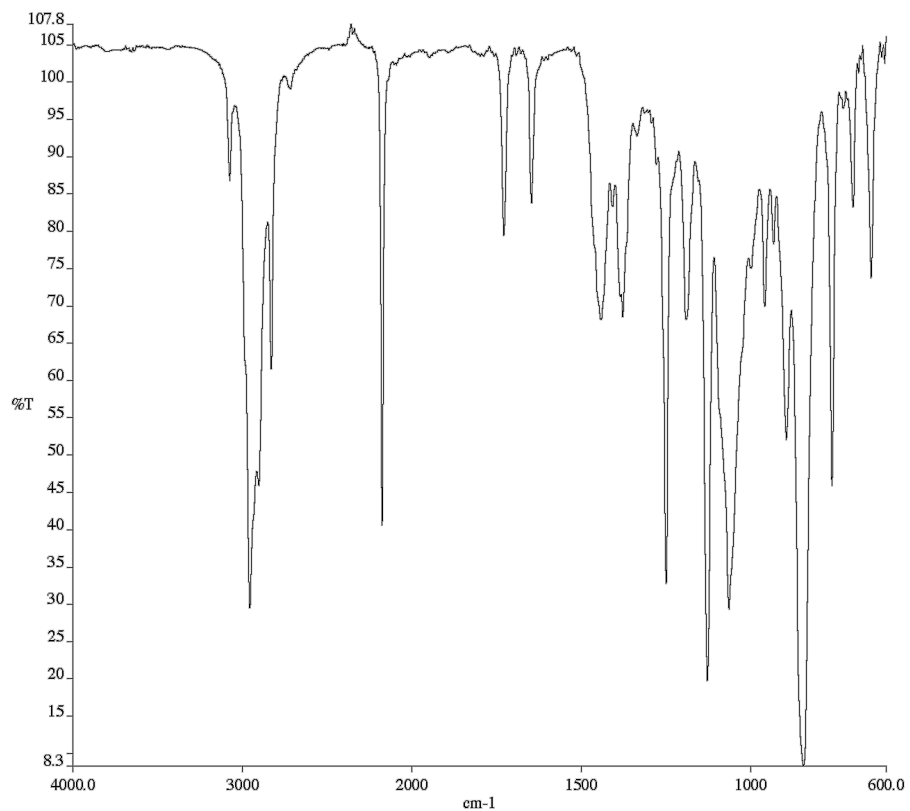


Figure A6.11 Infrared spectrum (Thin Film, NaCl) of compound **490**.

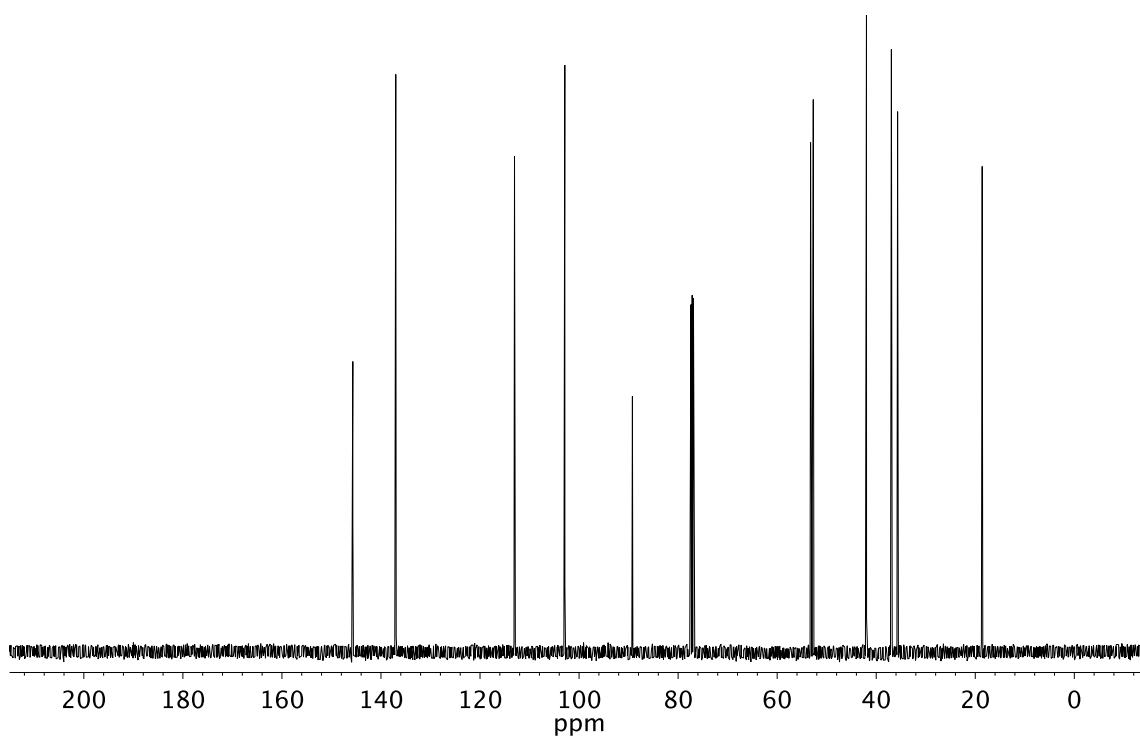


Figure A6.12 ¹³C NMR (101 MHz, CDCl₃) of compound **490**.

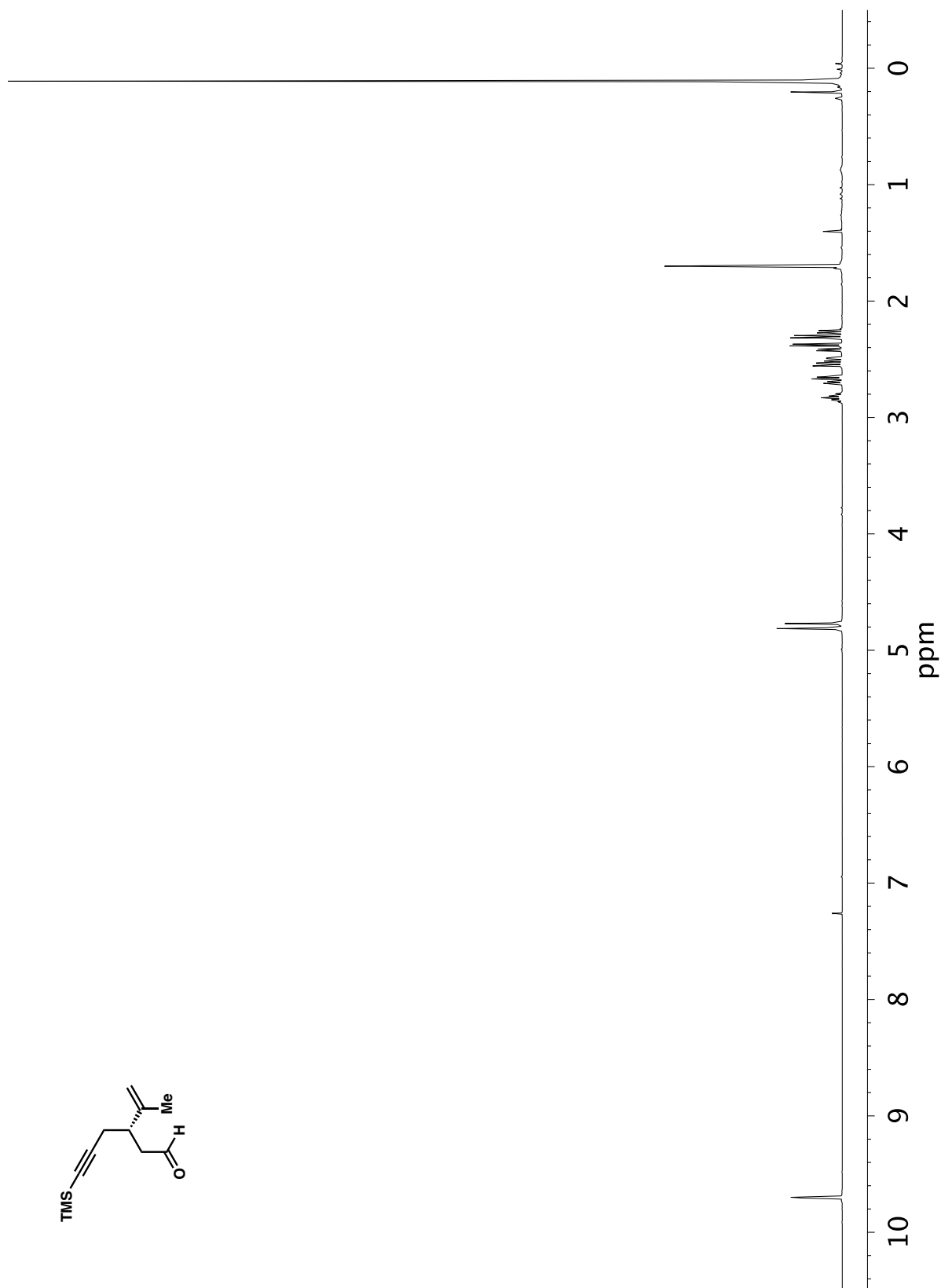


Figure A6.13 ^1H NMR (400 MHz, CDCl_3) of compound 492.

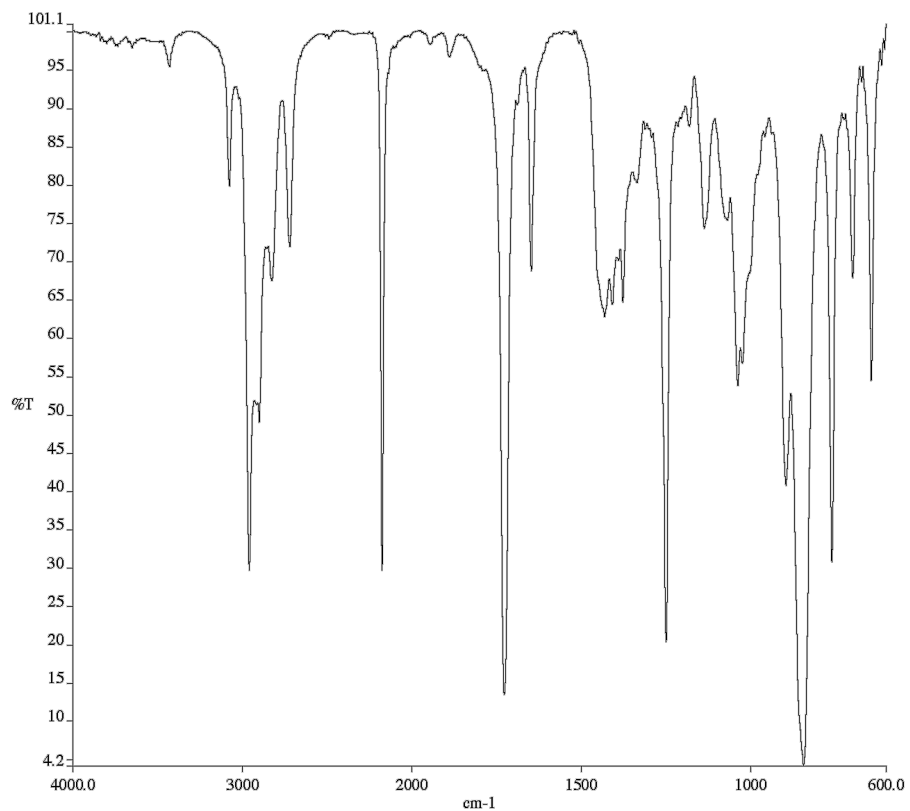


Figure A6.14 Infrared spectrum (Thin Film, NaCl) of compound **492**.

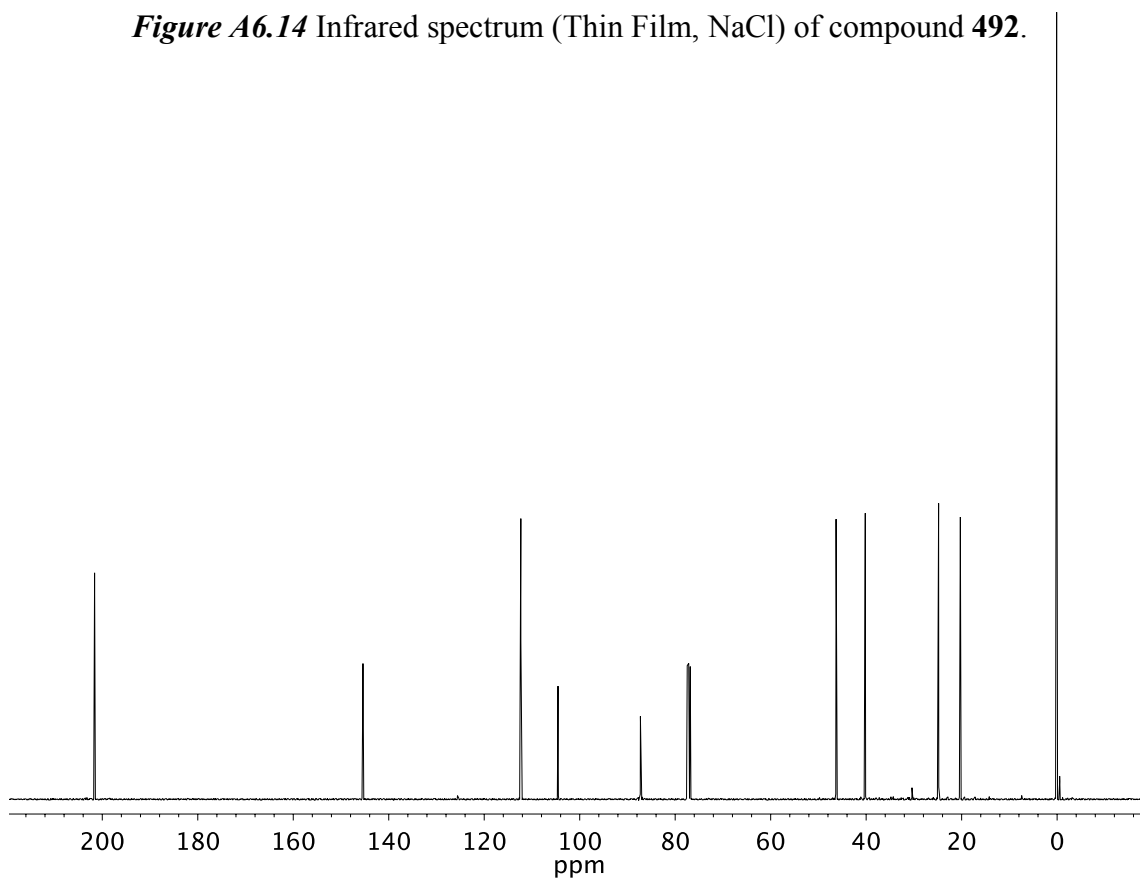


Figure A6.15 ¹³C NMR (101 MHz, CDCl₃) of compound **492**.

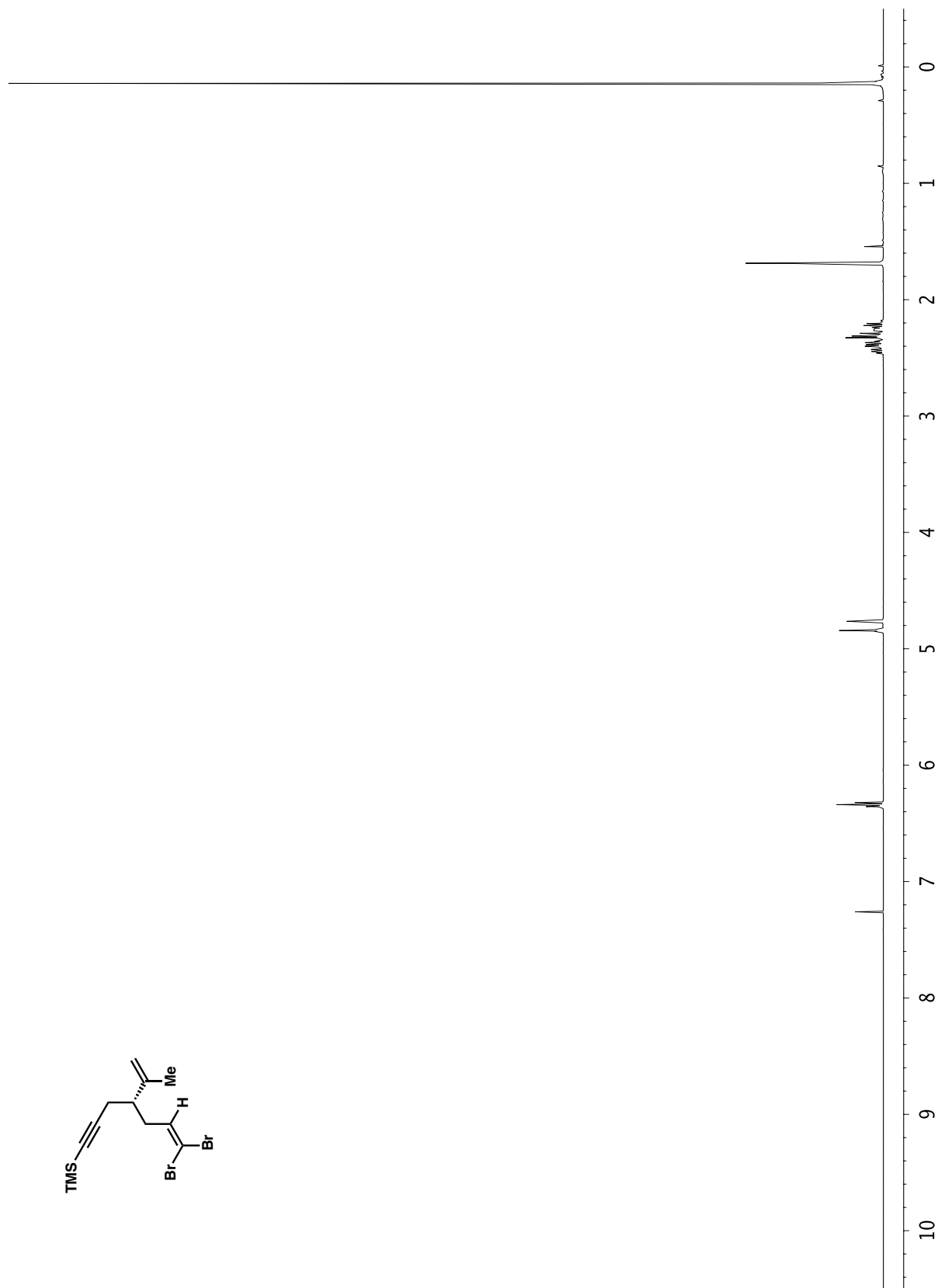


Figure A6.16 ^1H NMR (400 MHz, CDCl_3) of compound 493.

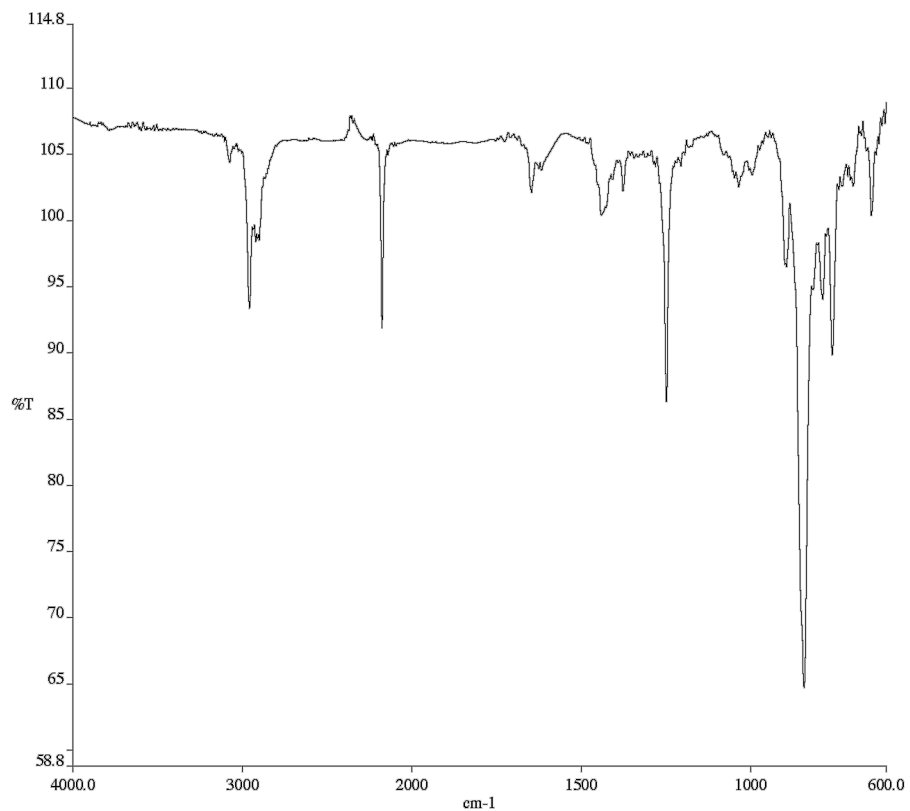


Figure A6.17 Infrared spectrum (Thin Film, NaCl) of compound **493**.

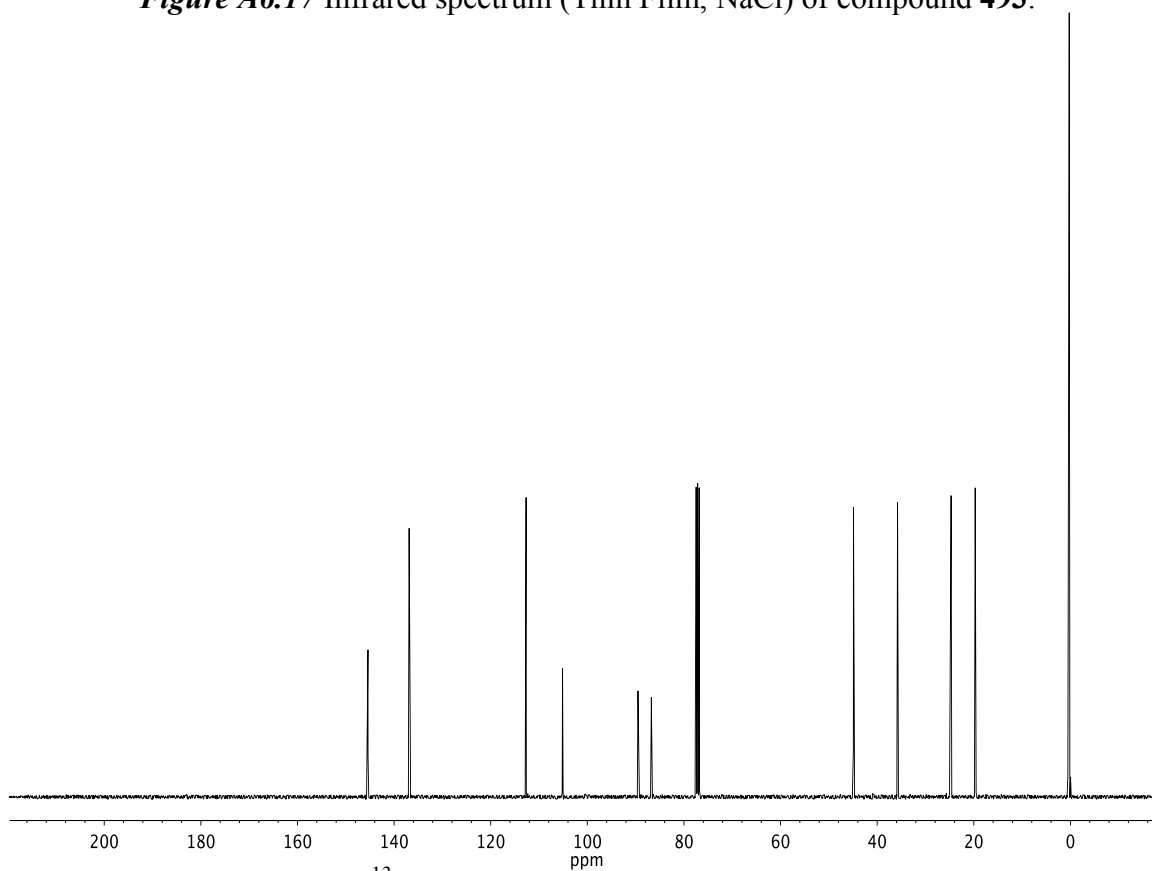


Figure A6.18 ¹³C NMR (101 MHz, CDCl₃) of compound **493**.

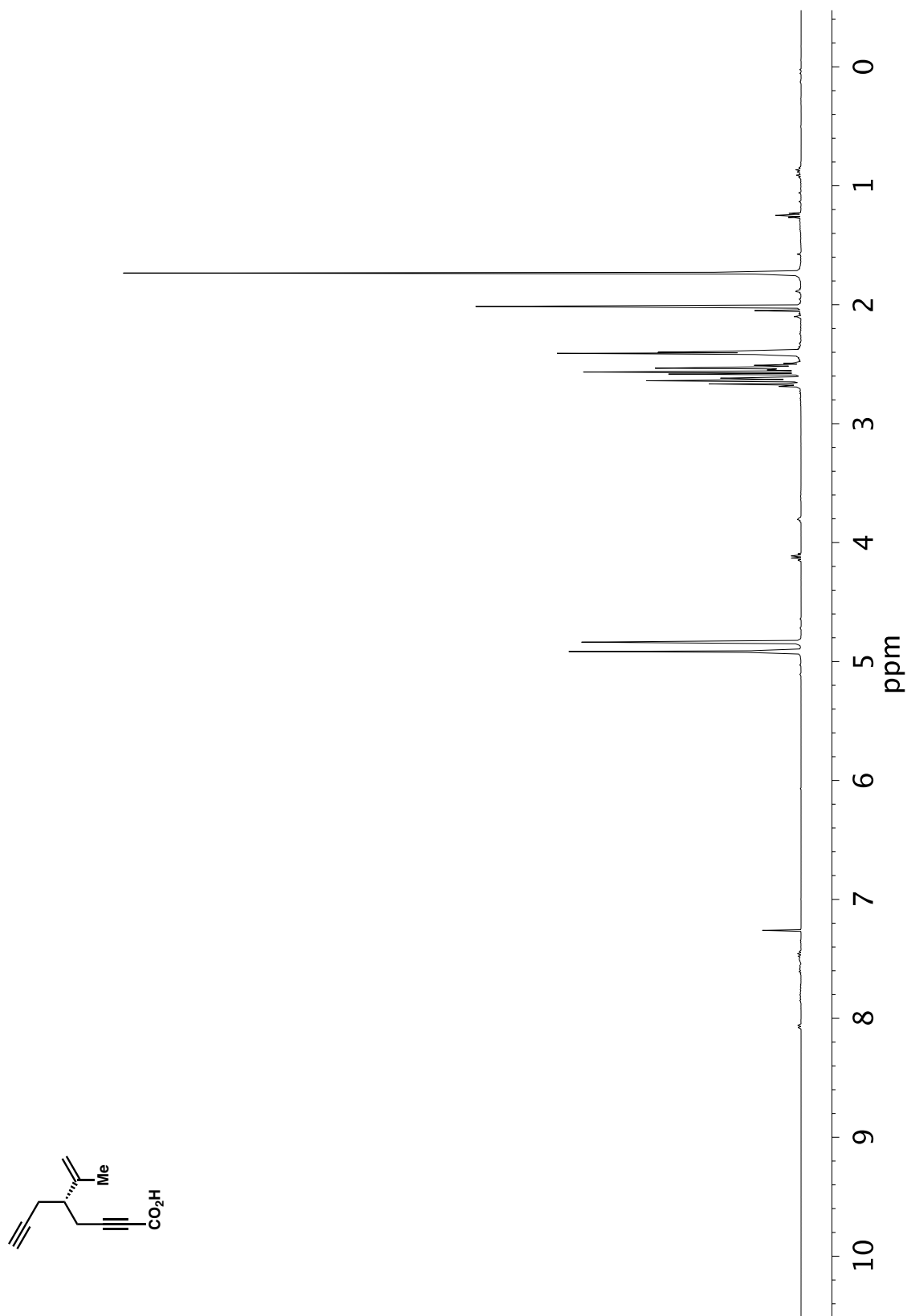


Figure A6.19 ^1H NMR (400 MHz, CDCl_3) of compound 472.

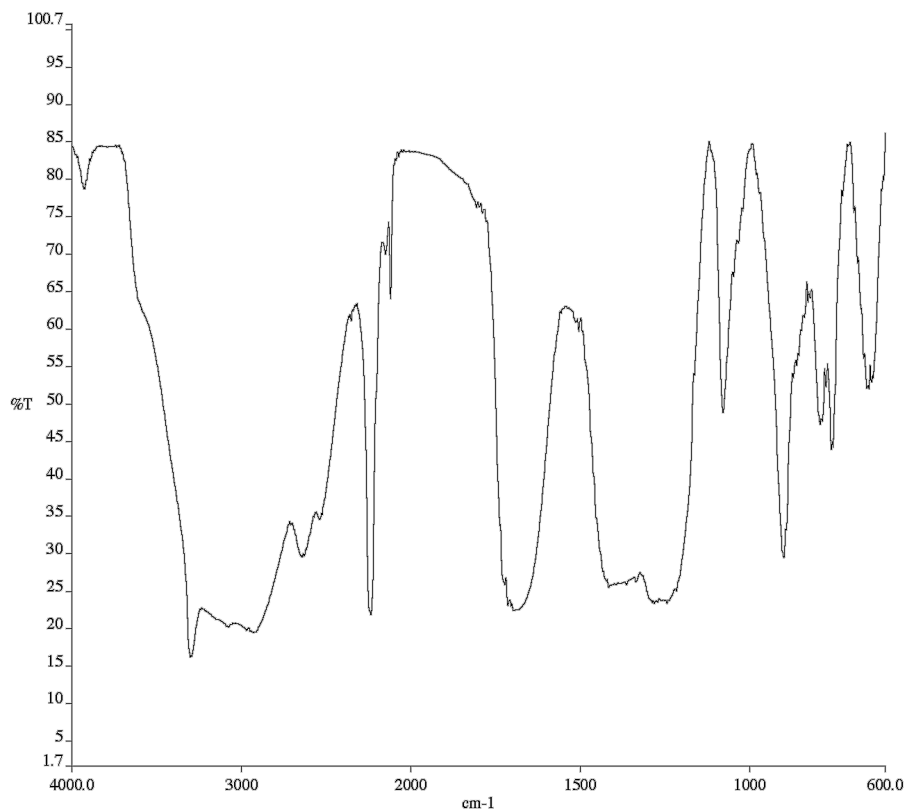


Figure A6.20 Infrared spectrum (Thin Film, NaCl) of compound **472**.

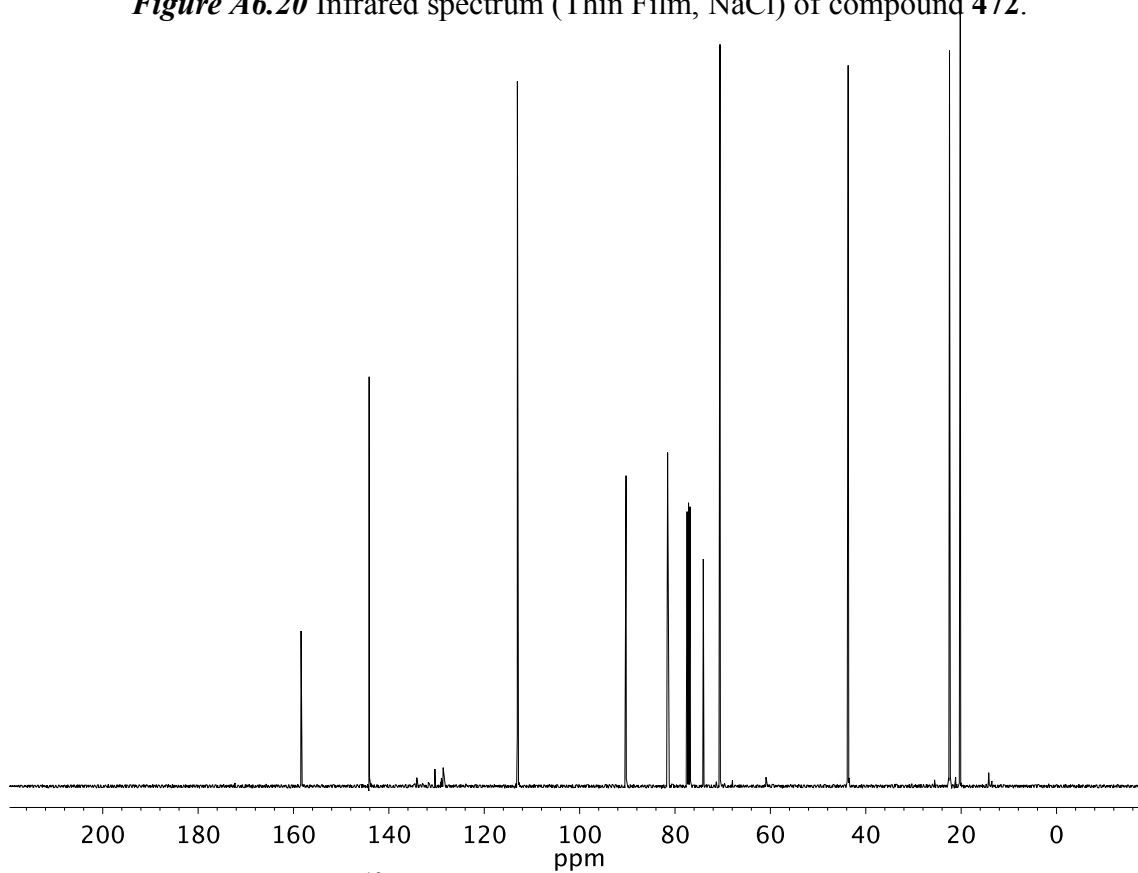


Figure A6.21 ¹³C NMR (101 MHz, CDCl₃) of compound **472**.

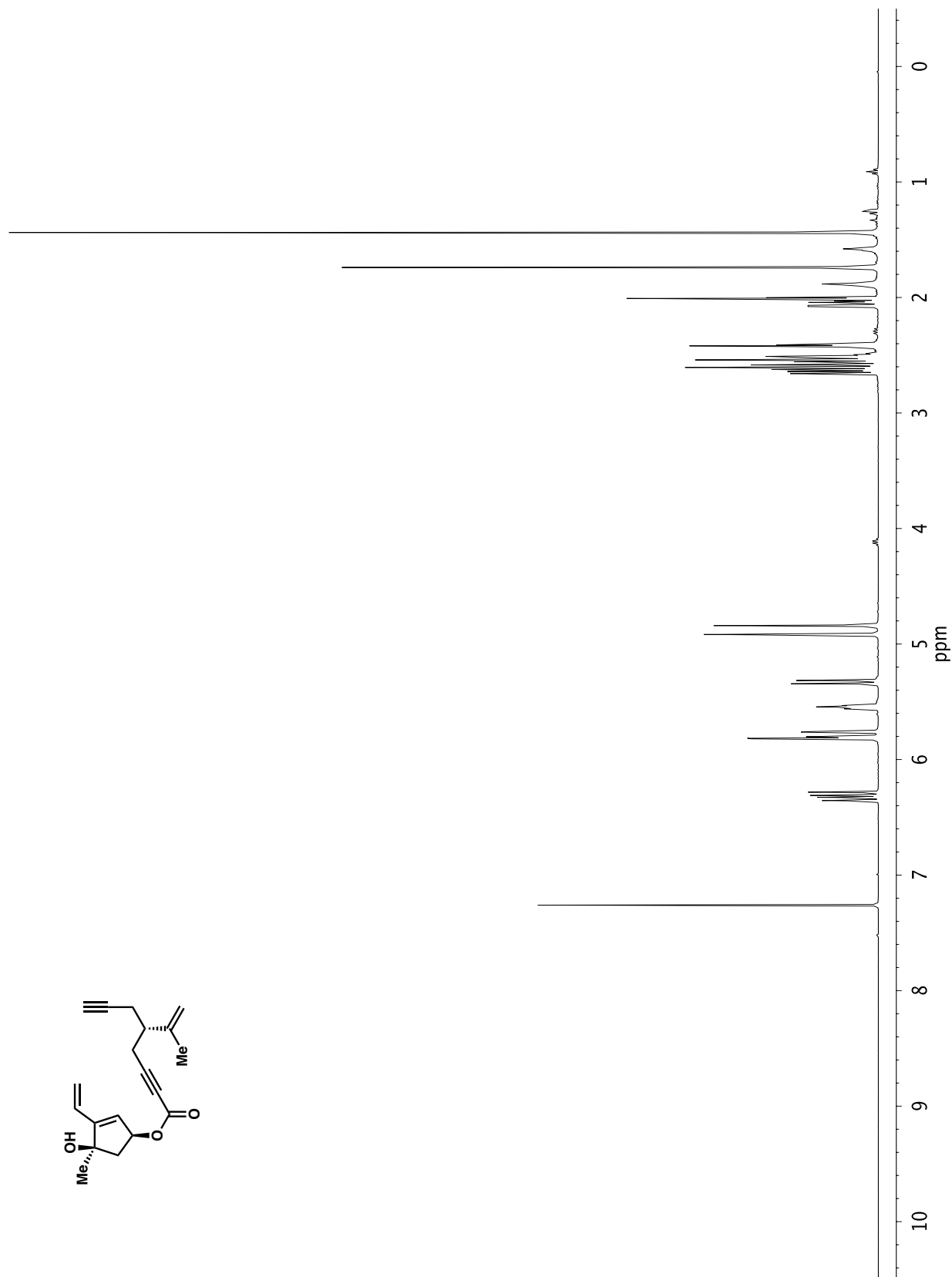


Figure A6.22 ^1H NMR (400 MHz, CDCl_3) of compound 471.

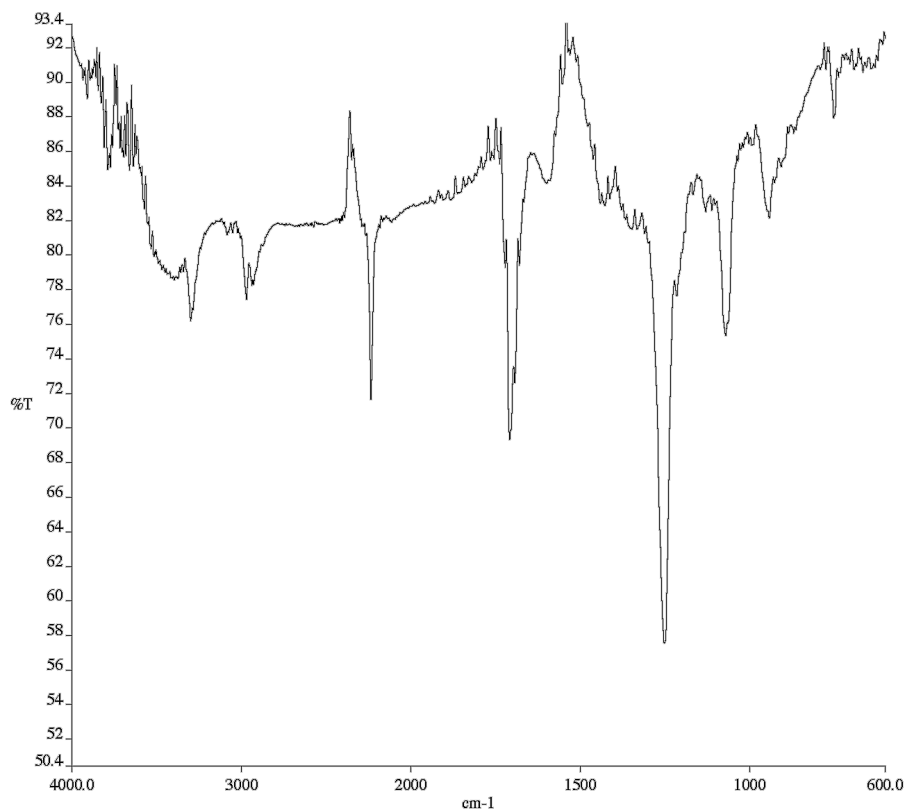


Figure A6.23 Infrared spectrum (Thin Film, NaCl) of compound **471**.

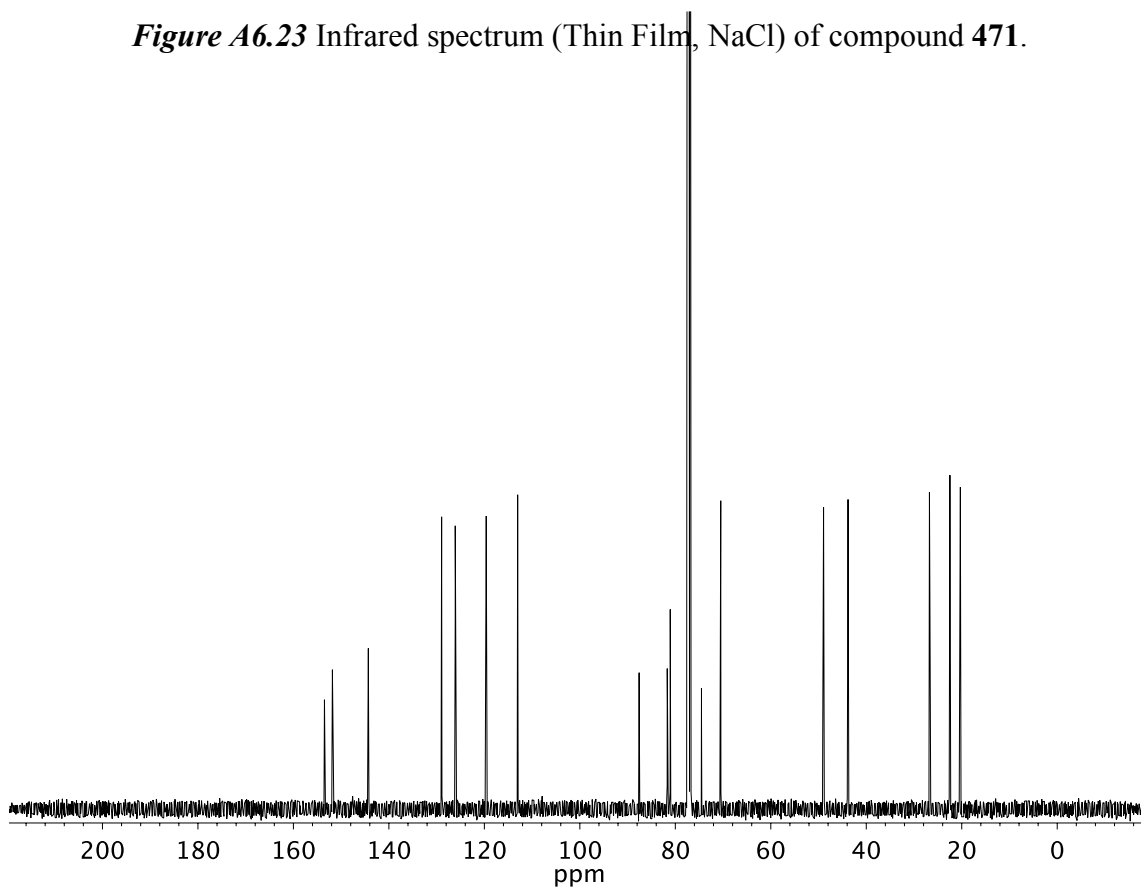


Figure A6.24 ¹³C NMR (101 MHz, CDCl₃) of compound **471**.

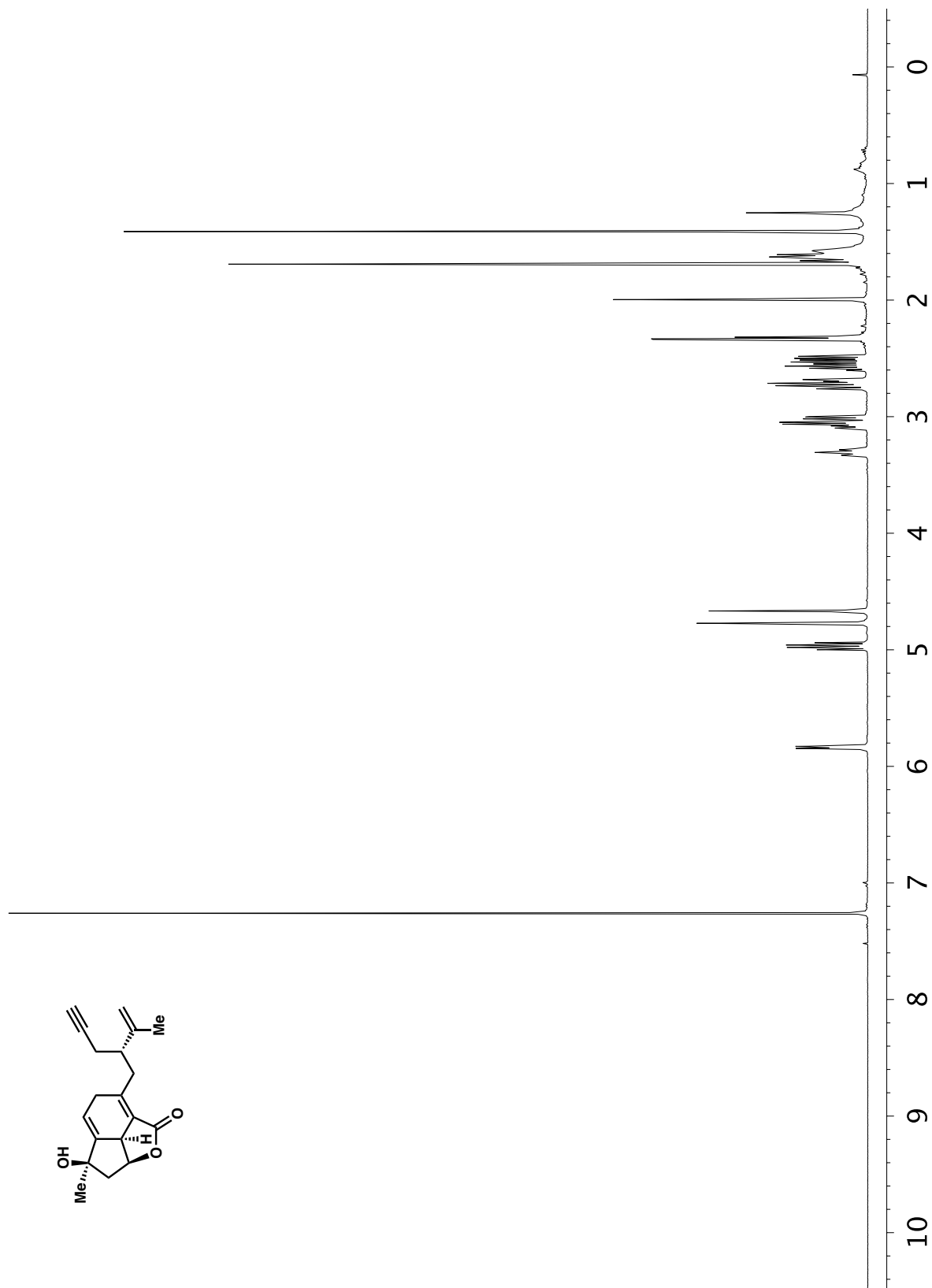


Figure A6.25 ¹H NMR (600 MHz, CD₂Cl₂) of compound 495.

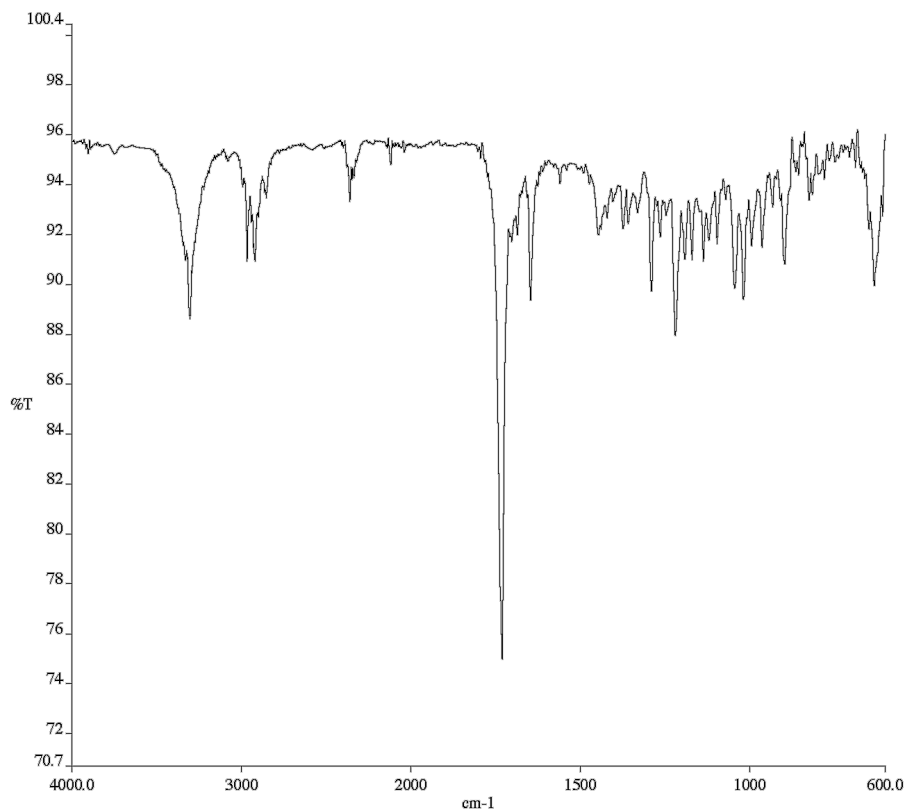


Figure A6.26 Infrared spectrum (Thin Film, NaCl) of compound **495**.

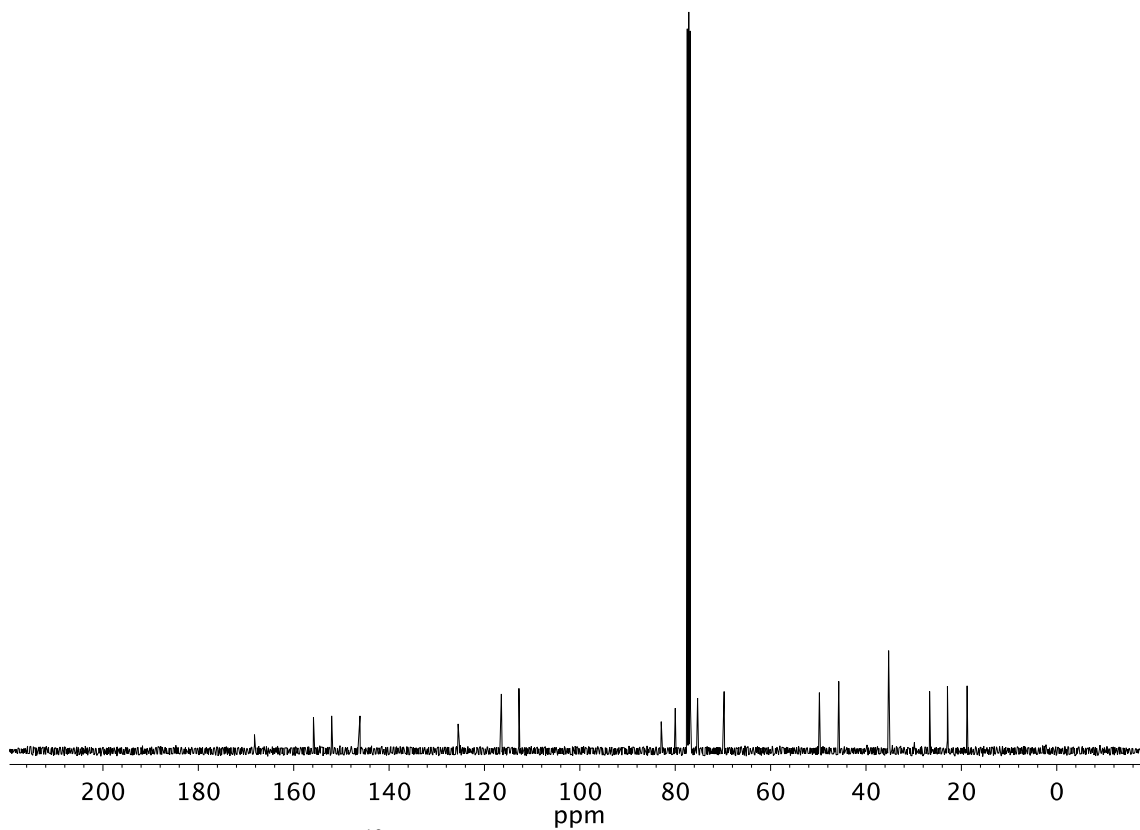


Figure A6.27 ¹³C NMR (101 MHz, CDCl₃) of compound **495**.

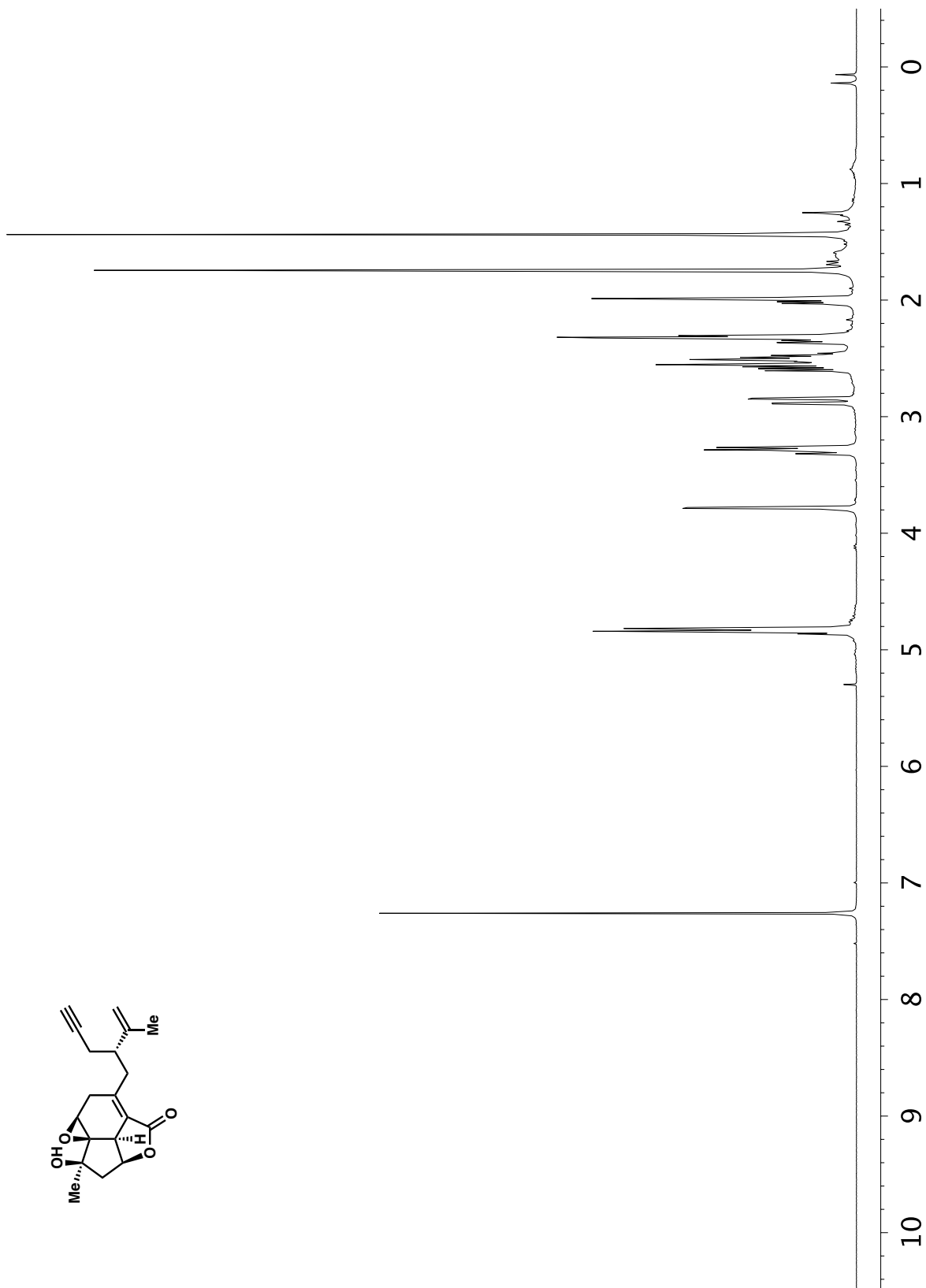


Figure A6.28 ¹H NMR (400 MHz, CDCl₃) of compound 496.

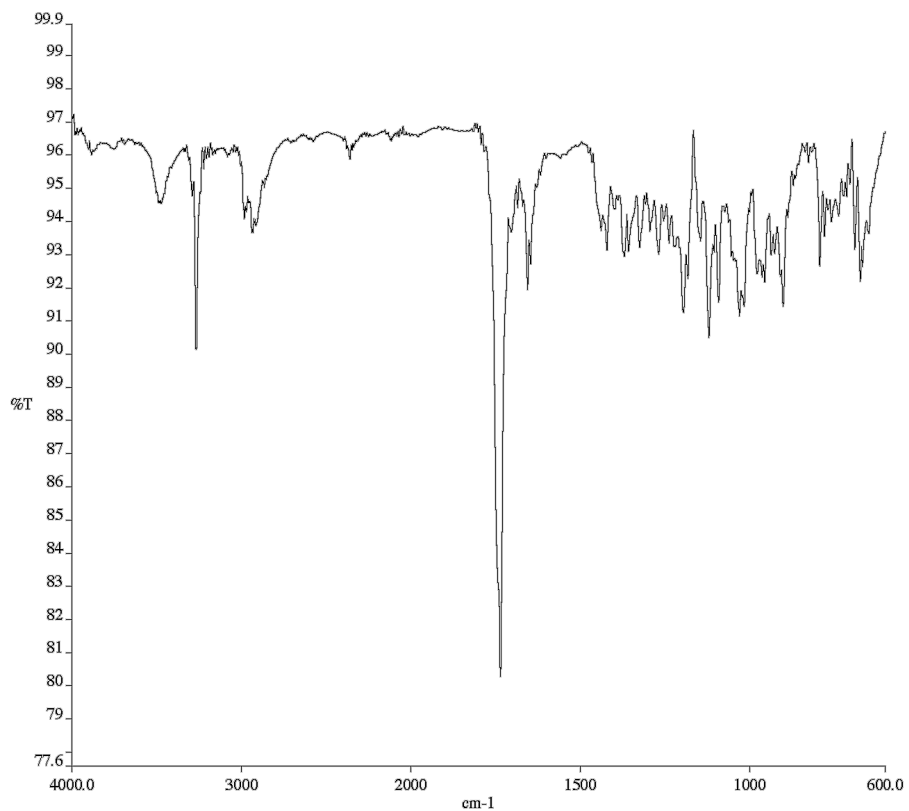


Figure A6.29 Infrared spectrum (Thin Film, NaCl) of compound **496**.

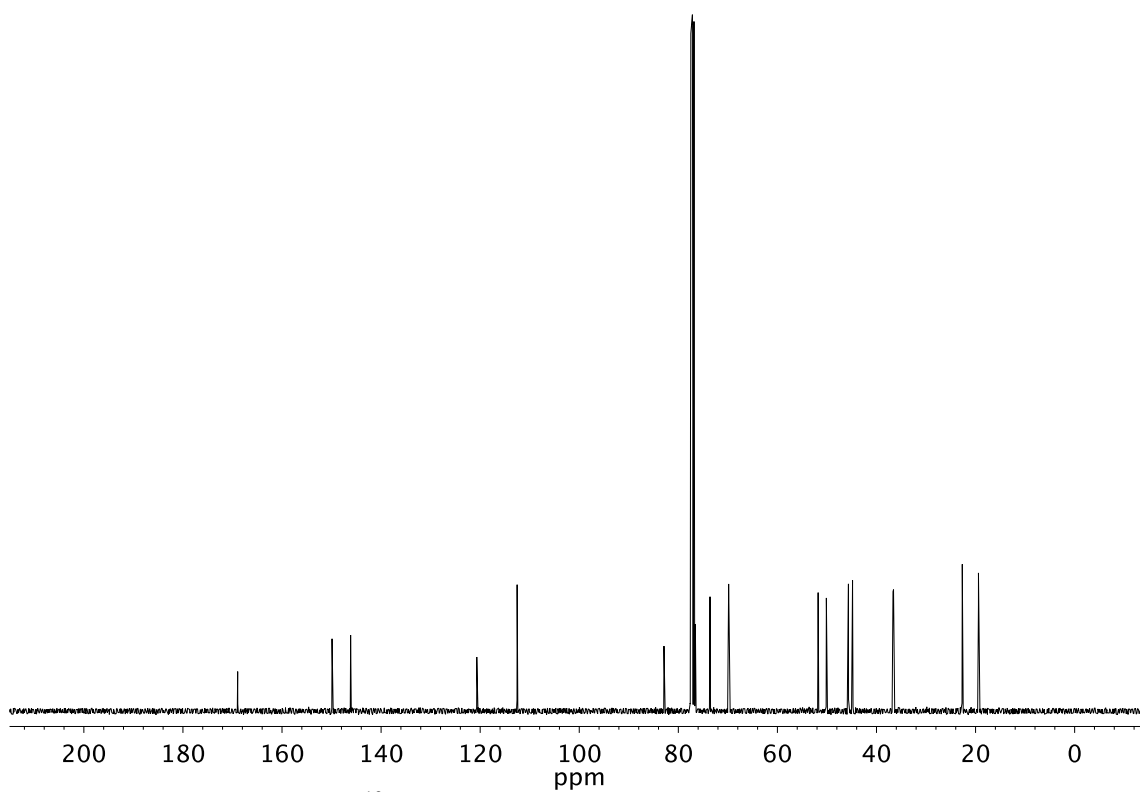


Figure A6.30 ¹³C NMR (101 MHz, CDCl₃) of compound **496**.

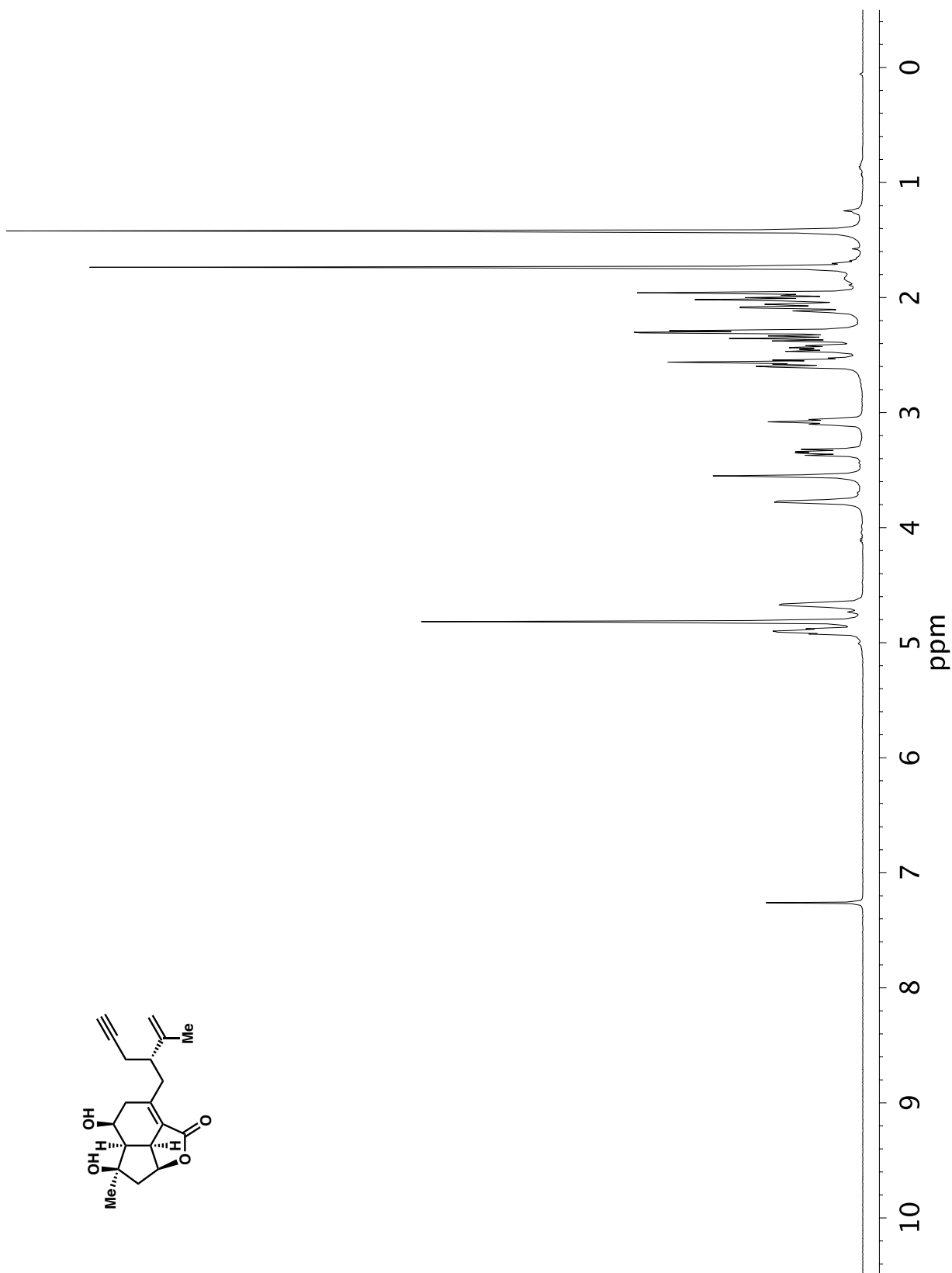


Figure A6.31 ^1H NMR (400 MHz, CDCl_3) of compound 497.

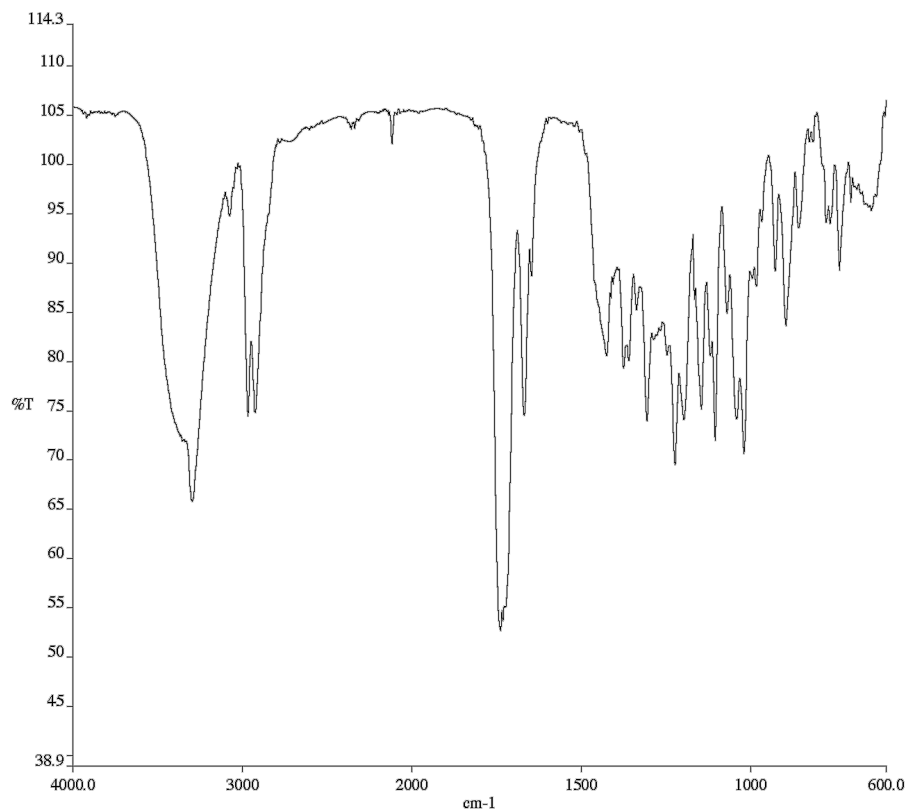


Figure A6.32 Infrared spectrum (Thin Film, NaCl) of compound **497**.

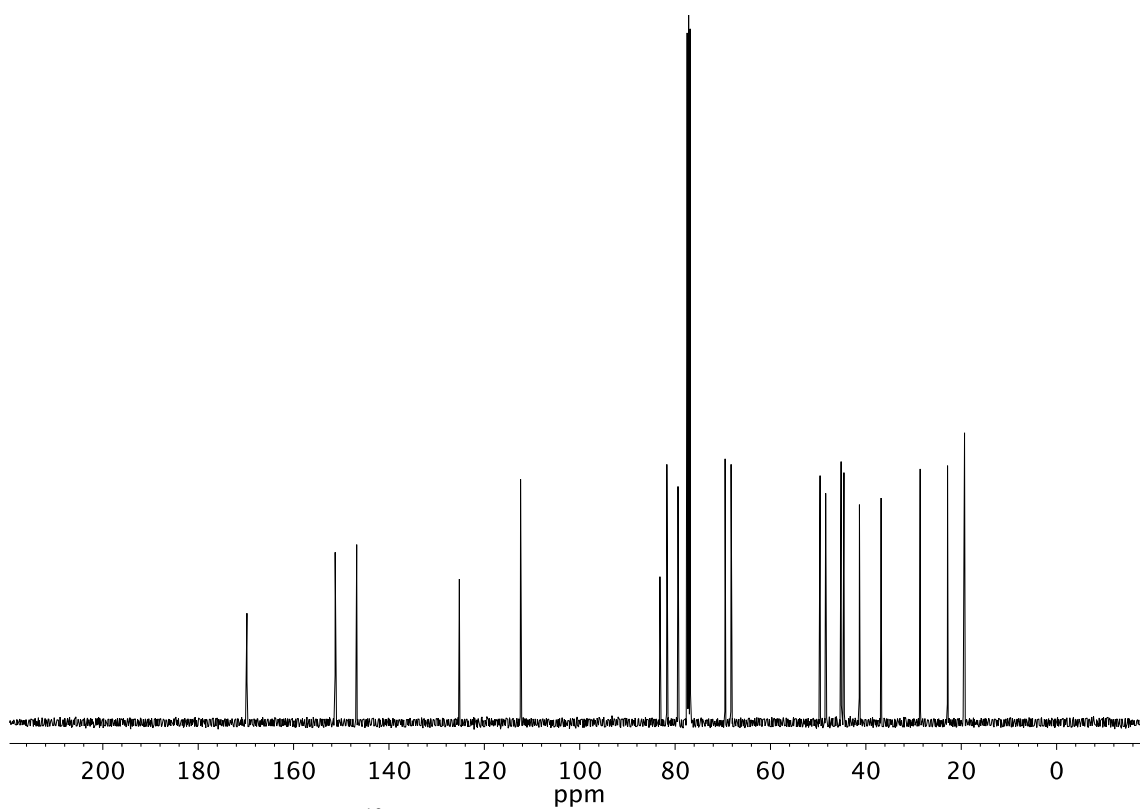


Figure A6.33 ¹³C NMR (101 MHz, CDCl₃) of compound **497**.

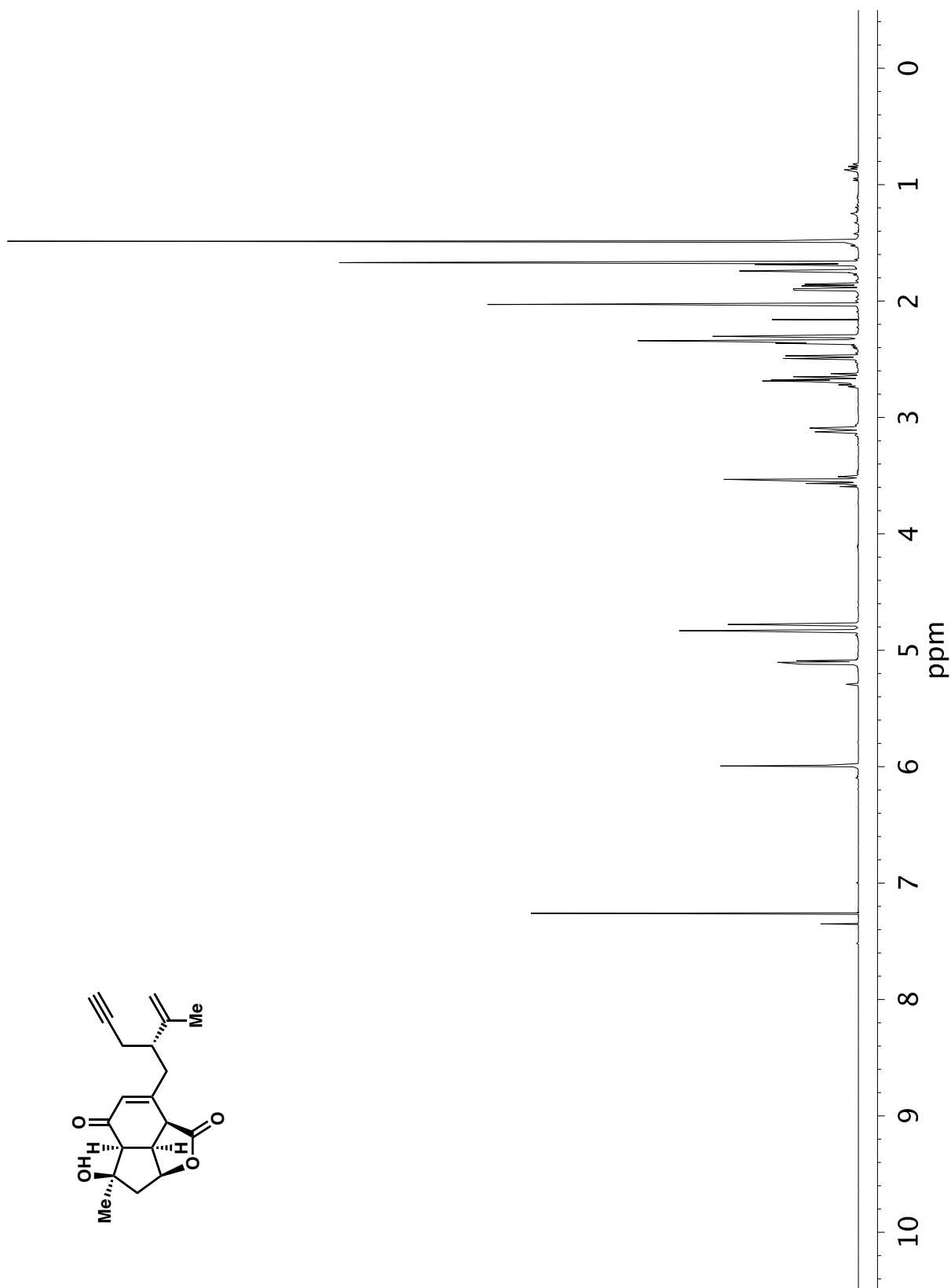


Figure A6.34 ^1H NMR (400 MHz, CDCl_3) of compound 470.

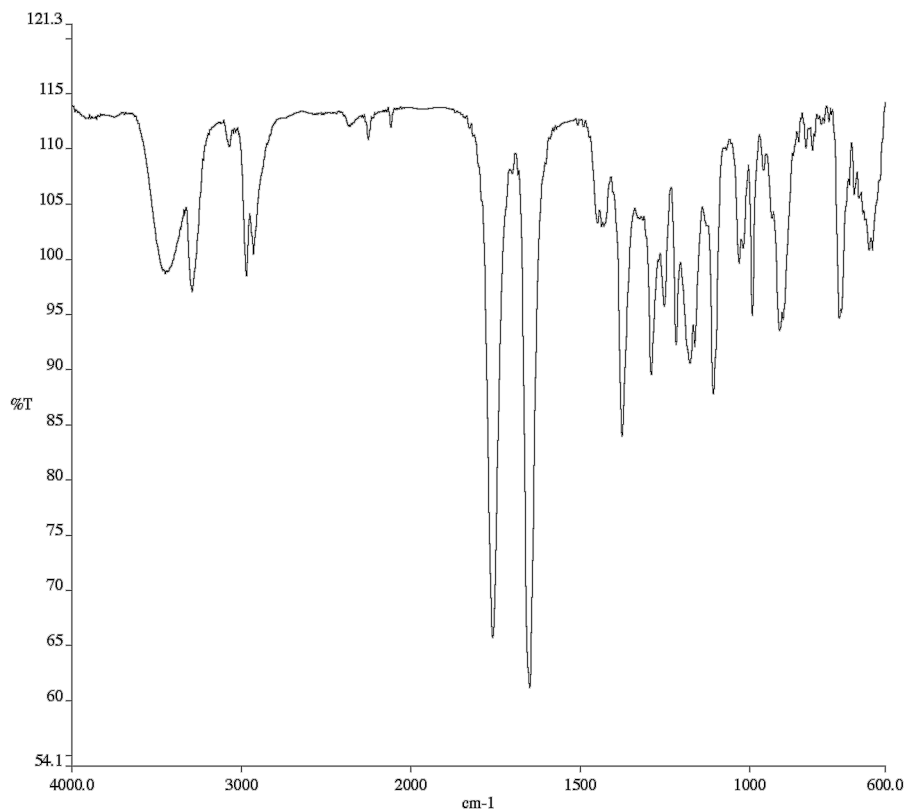


Figure A6.35 Infrared spectrum (Thin Film, NaCl) of compound **470**.

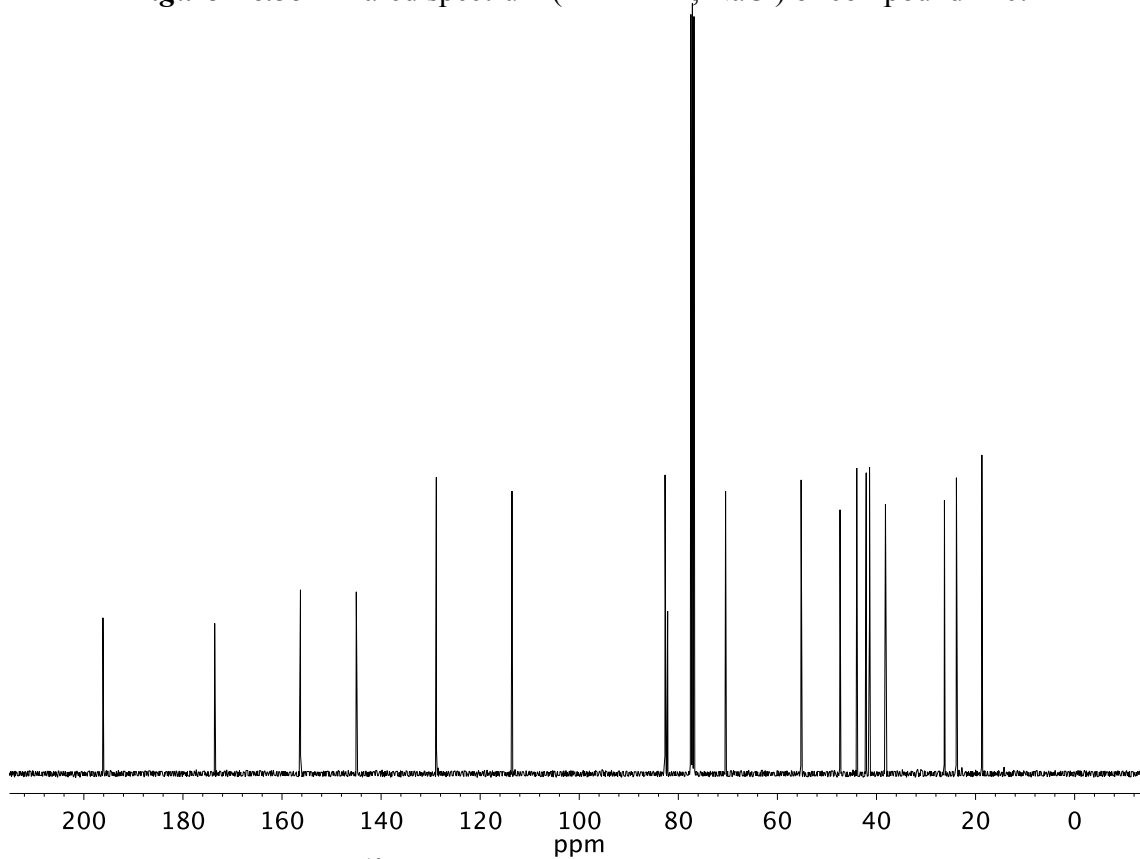


Figure A6.36 ¹³C NMR (101 MHz, CDCl₃) of compound **470**.

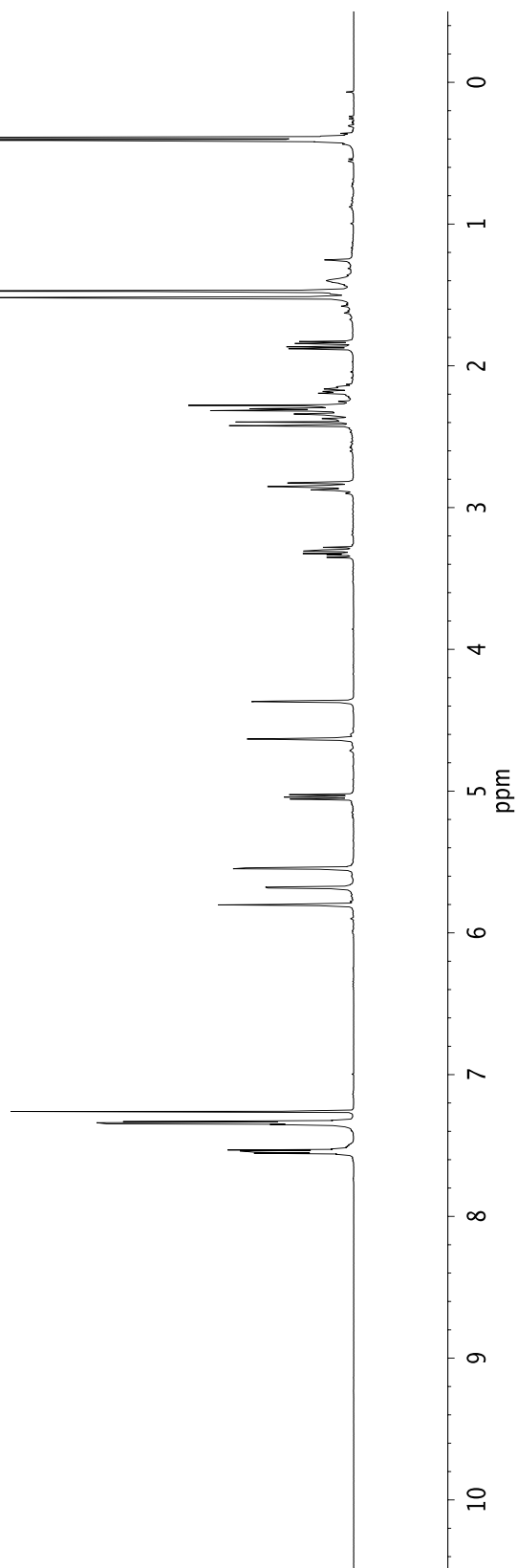
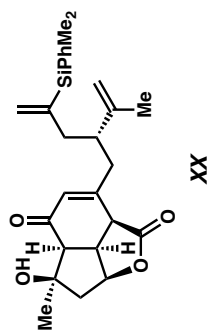


Figure A6.37 ^1H NMR (400 MHz, CDCl_3) of compound 499.

Figure A6.38 Infrared spectrum (Thin Film, NaCl) of compound **499**.

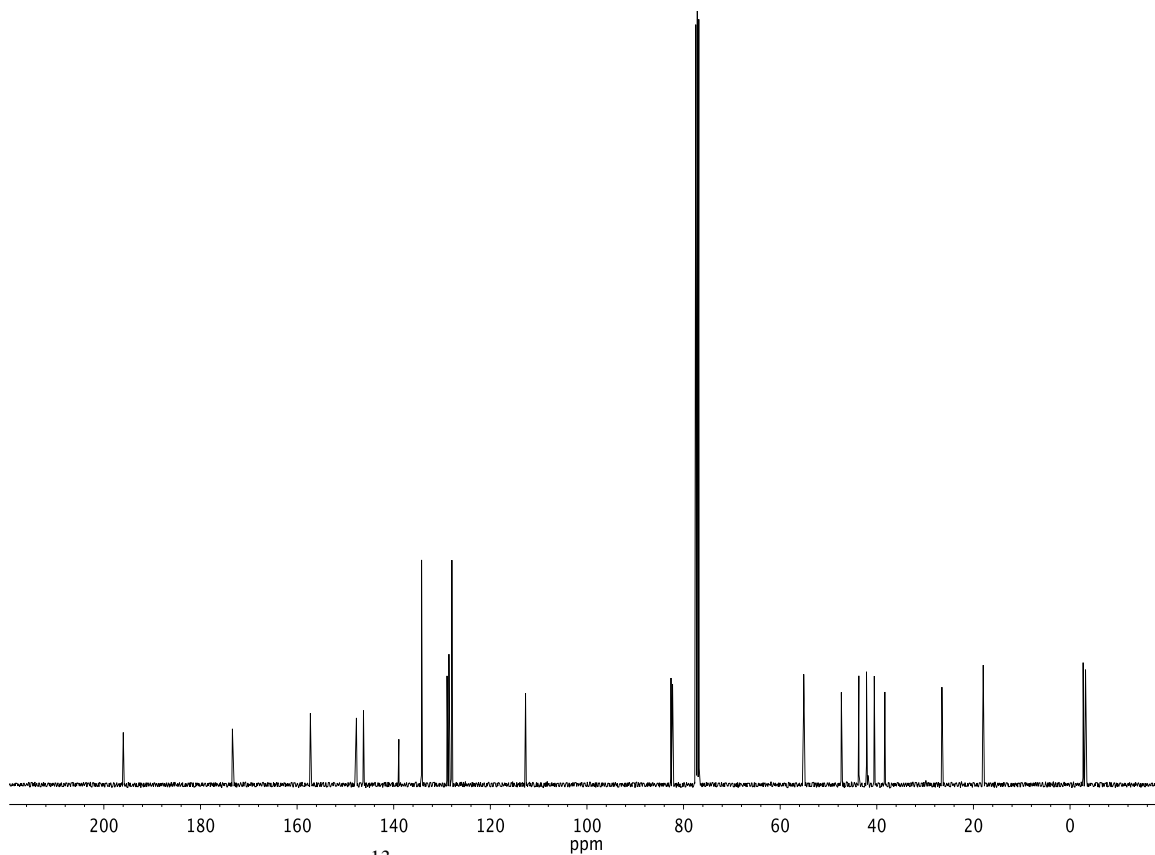


Figure A6.39 ^{13}C NMR (101 MHz, CDCl_3) of compound **499**.

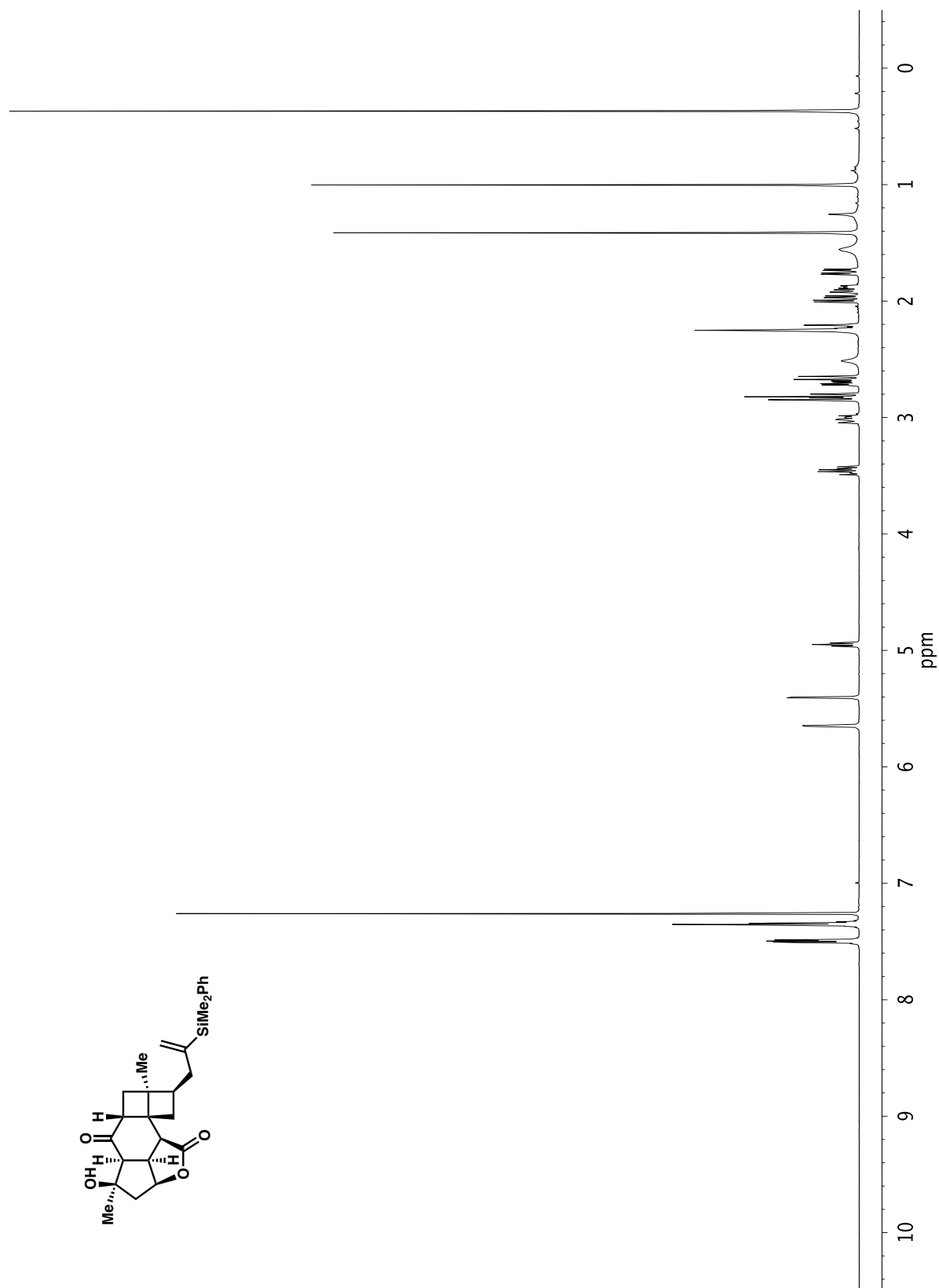


Figure A6.40 ^1H NMR (400 MHz, CDCl_3) of compound 500.

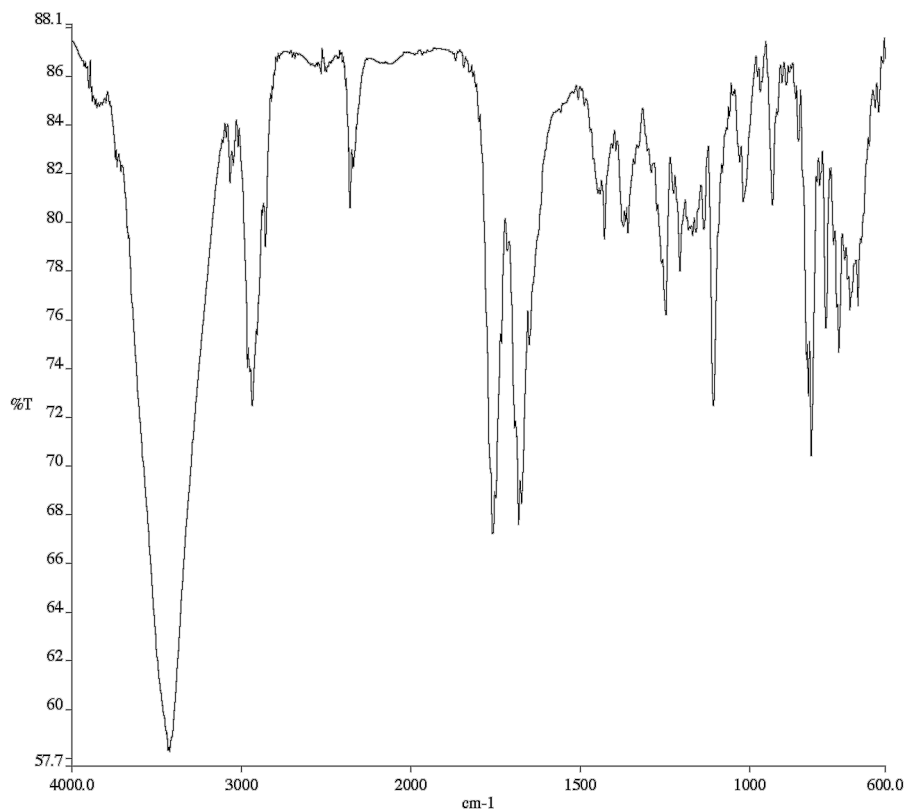


Figure A6.41 Infrared spectrum (Thin Film, NaCl) of compound **500**.

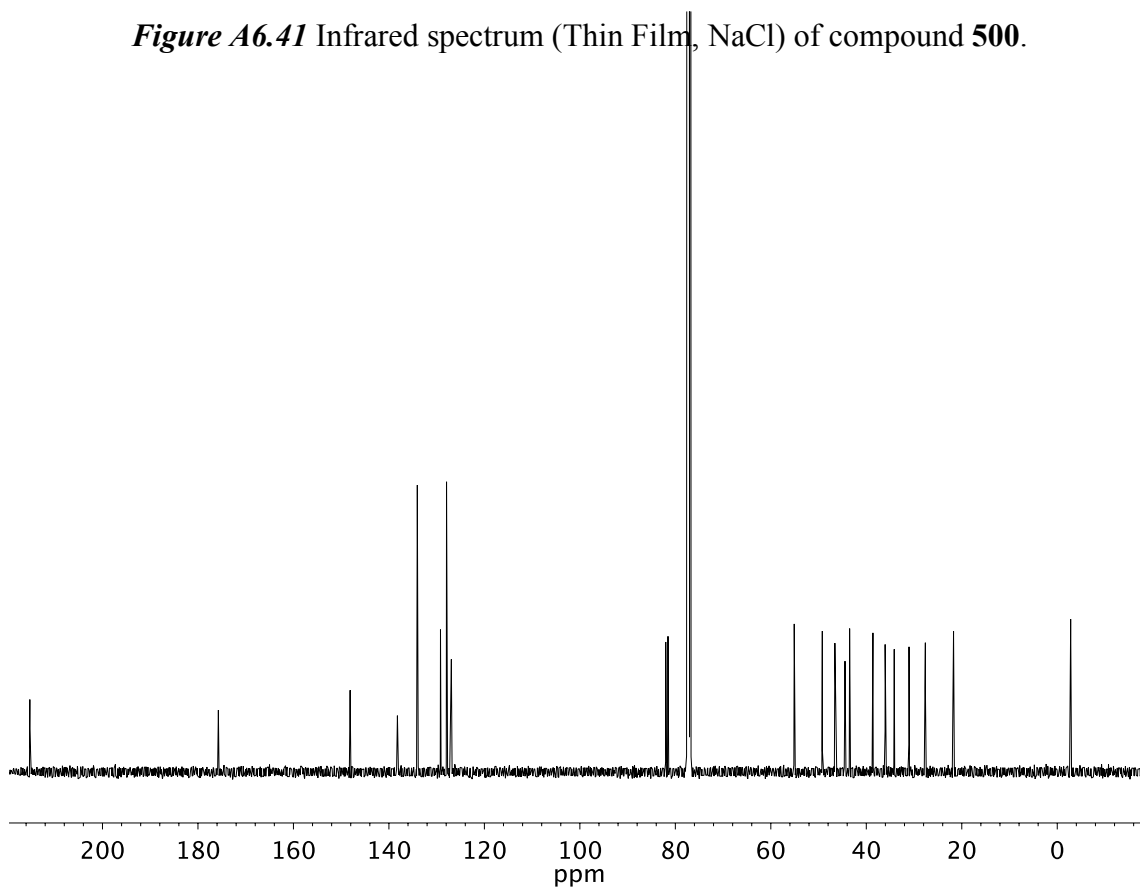


Figure A6.42 ^{13}C NMR (101 MHz, CDCl_3) of compound **500**.

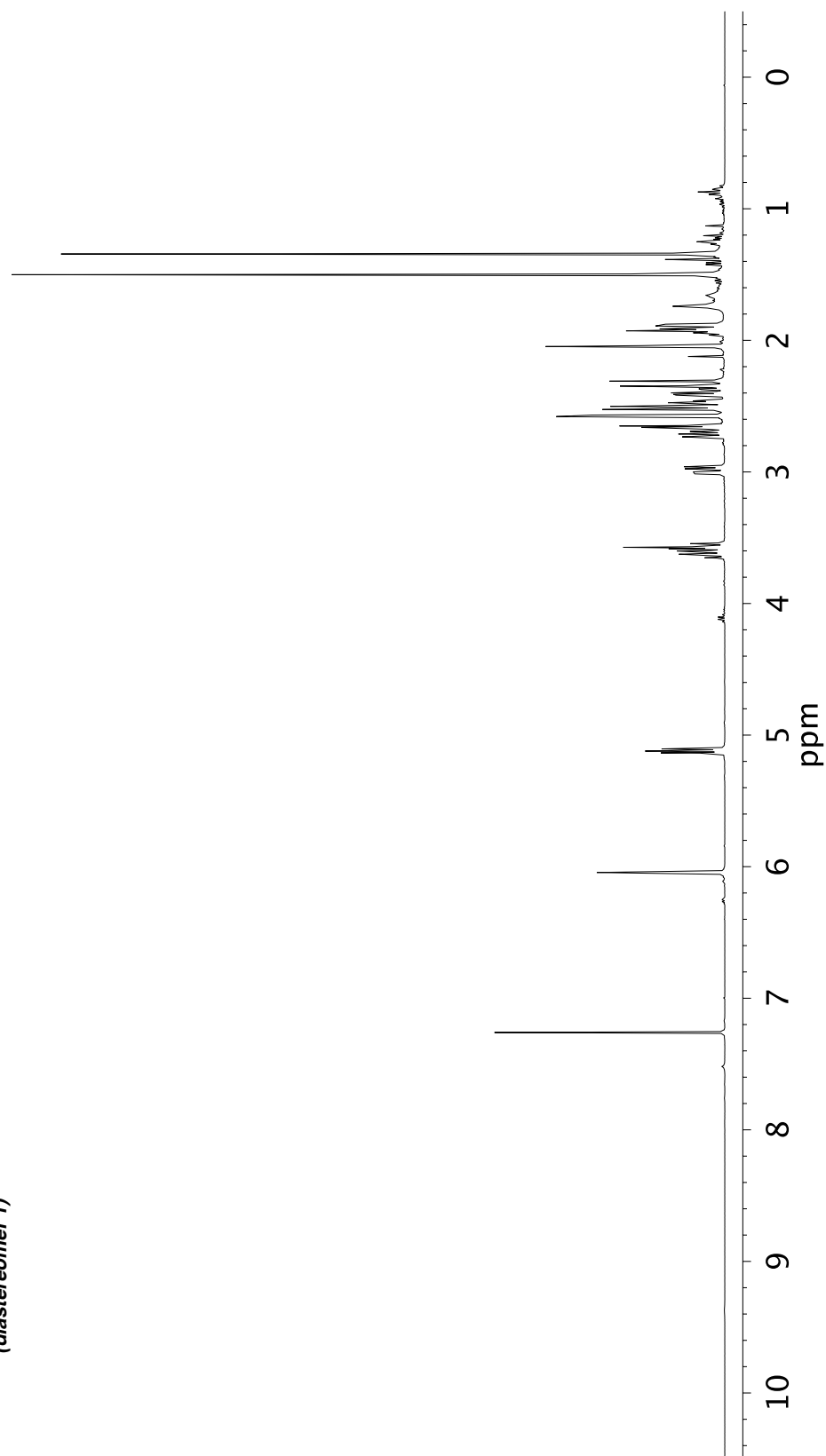
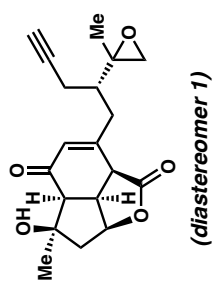


Figure A6.43 ^1H NMR (400 MHz, CDCl_3) of compound 509a.

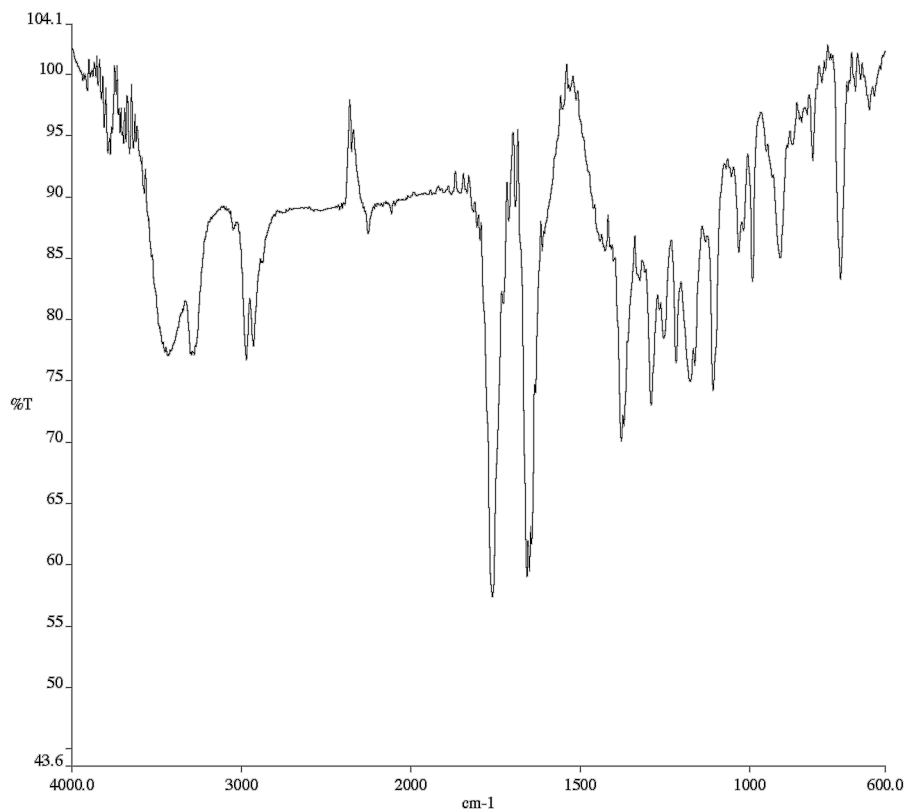


Figure A6.44 Infrared spectrum (Thin Film, NaCl) of compound **509a**.

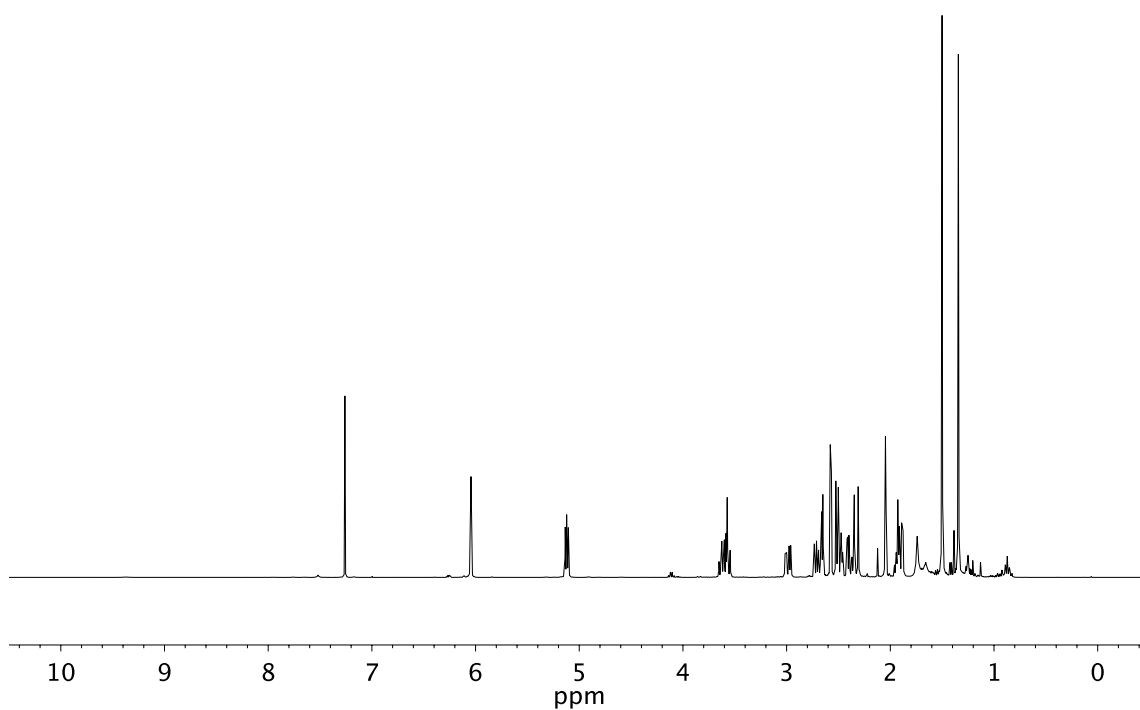


Figure A6.45 ¹³C NMR (101 MHz, CDCl₃) of compound **509a**.

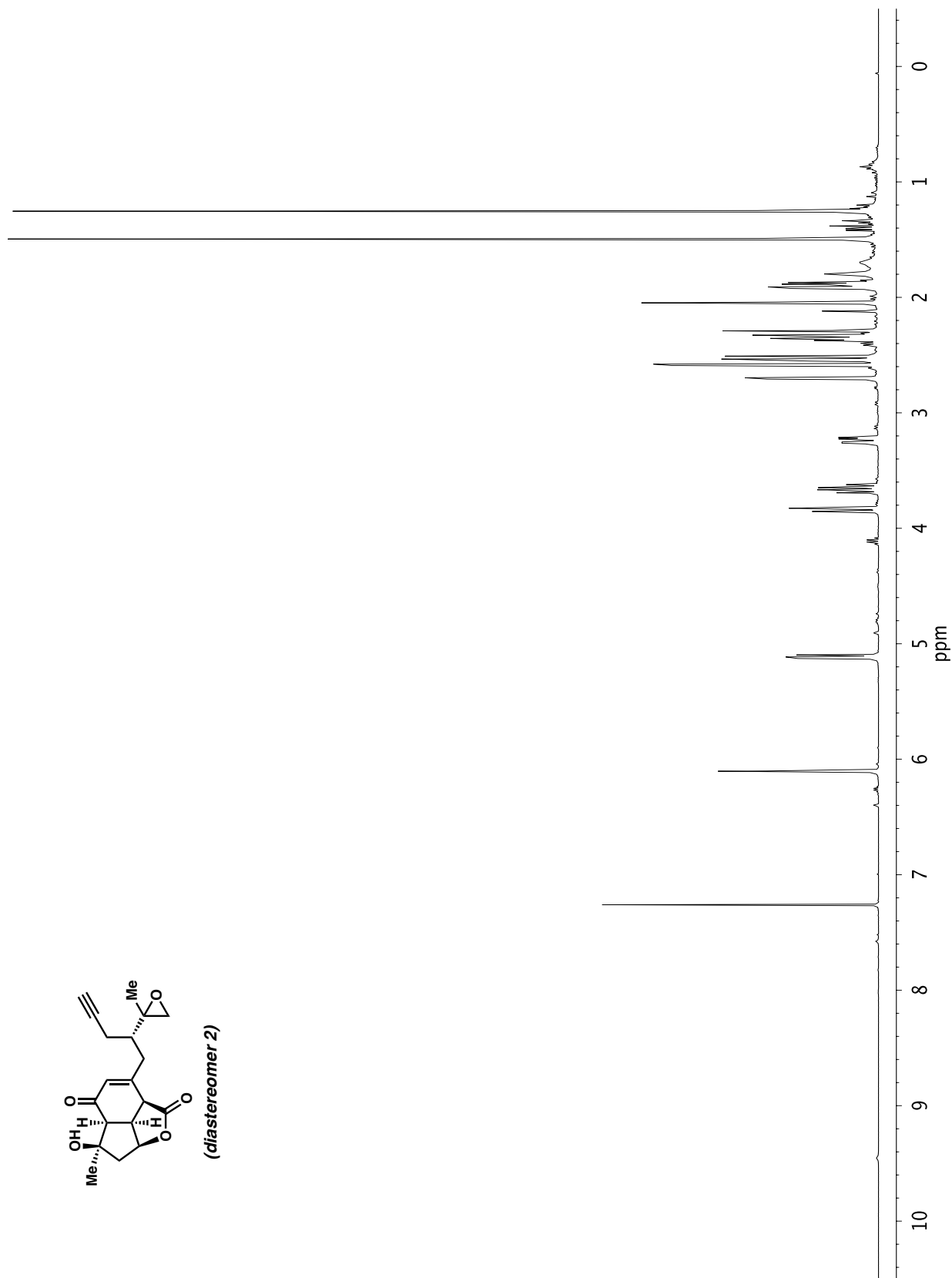


Figure A6.46 ^1H NMR (400 MHz, CDCl_3) of compound **509b**.

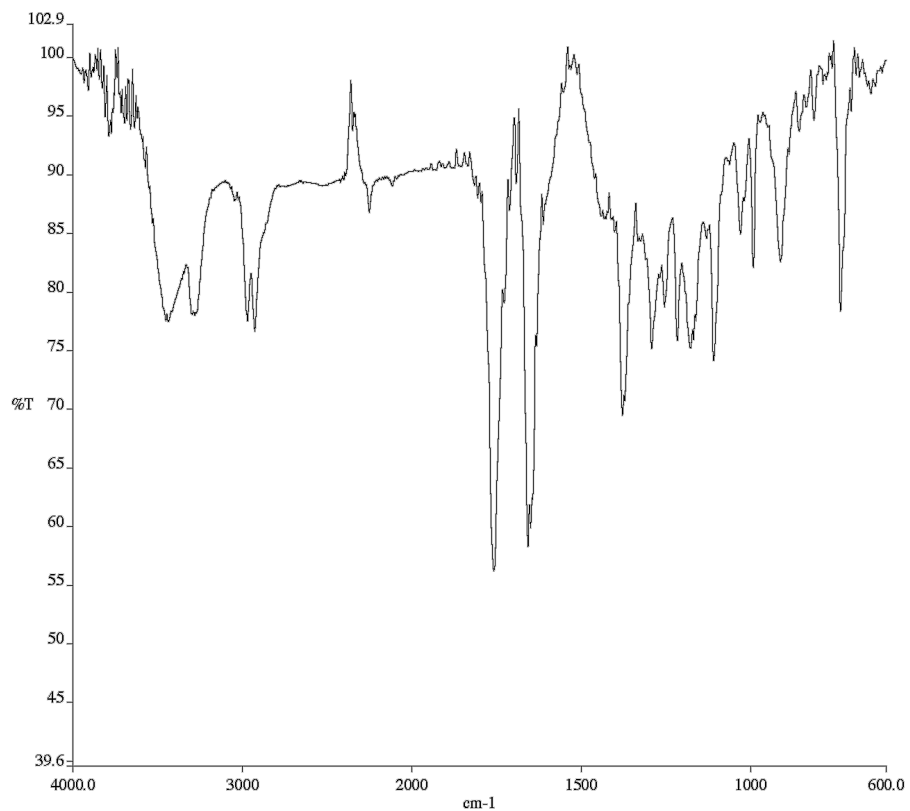


Figure A6.47 Infrared spectrum (Thin Film, NaCl) of compound **509b**.

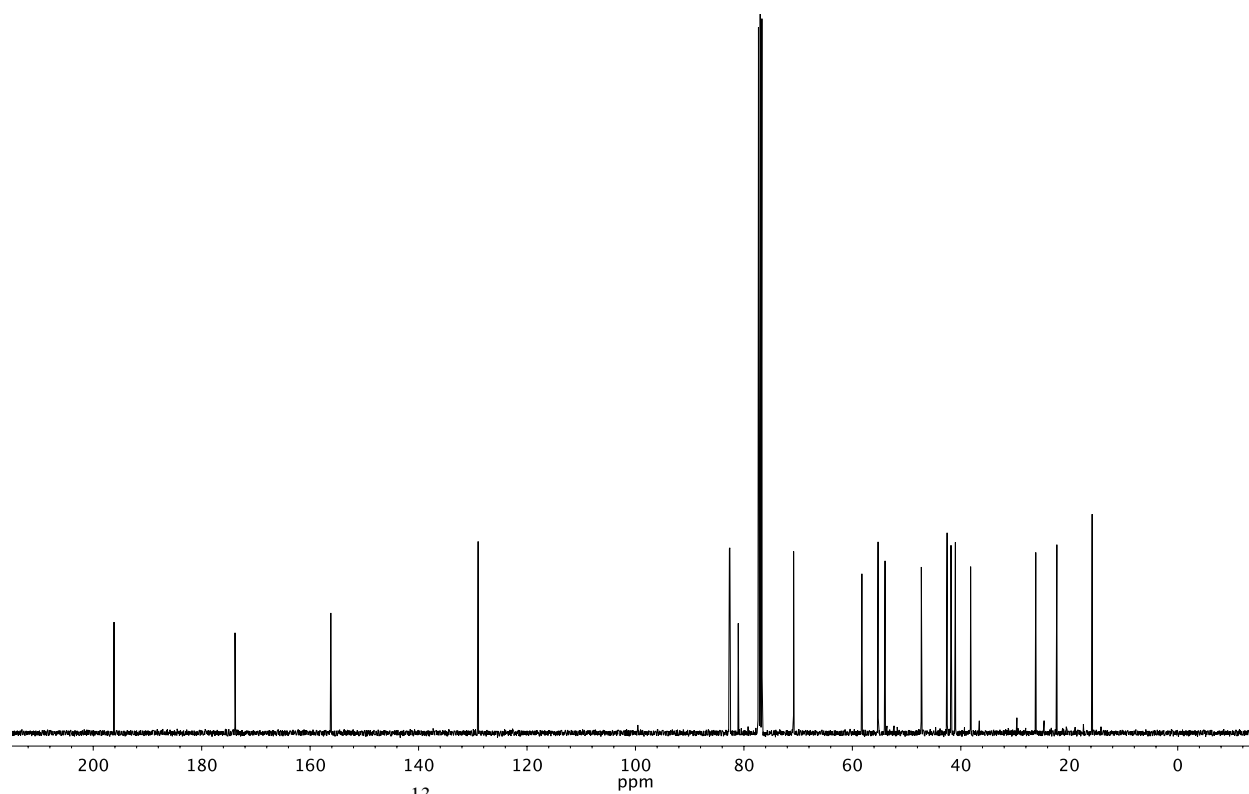


Figure A6.48 ¹³C NMR (101 MHz, CDCl₃) of compound **509b**.

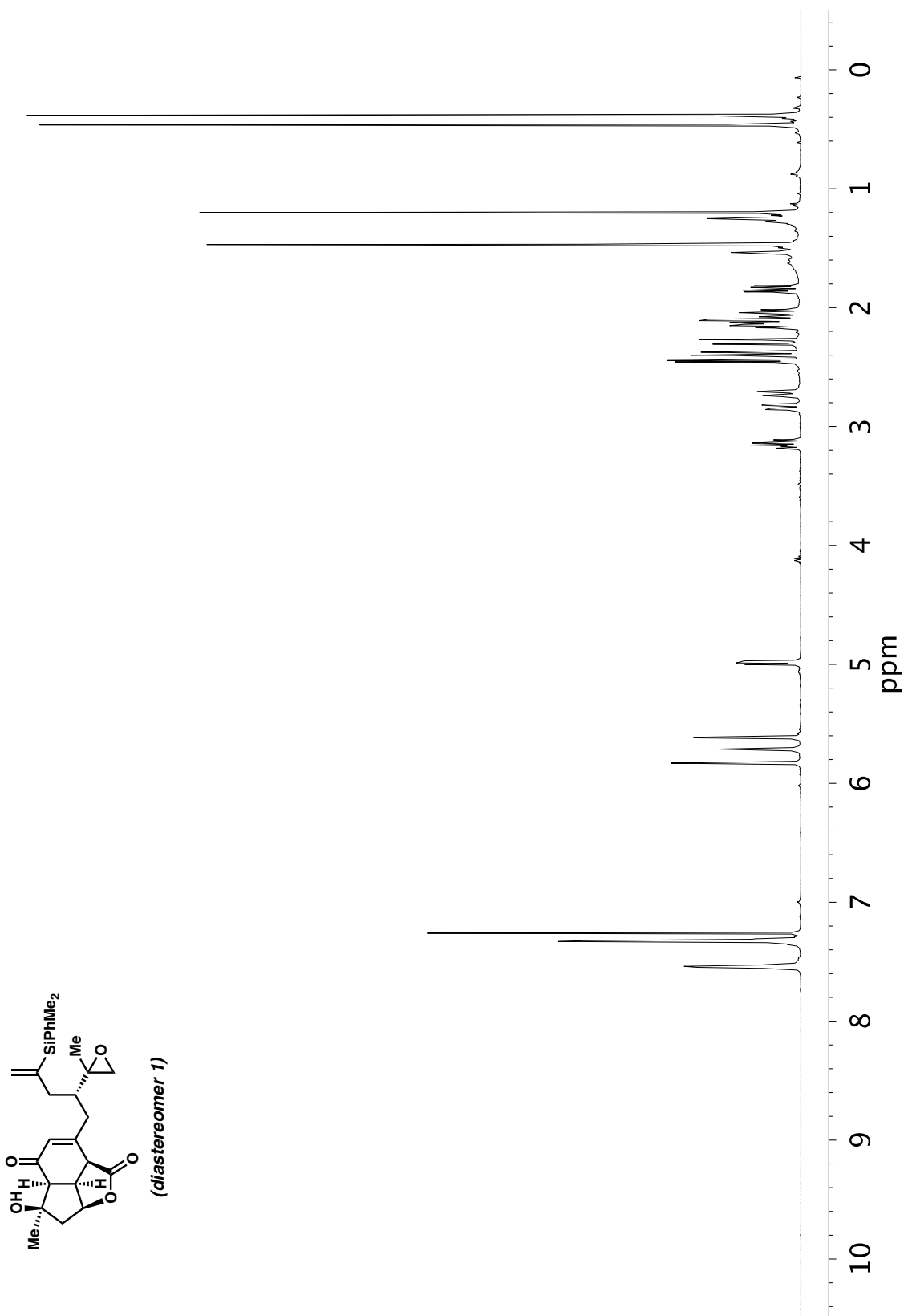


Figure A6.49 ¹H NMR (400 MHz, CDCl₃) of compound 510a.

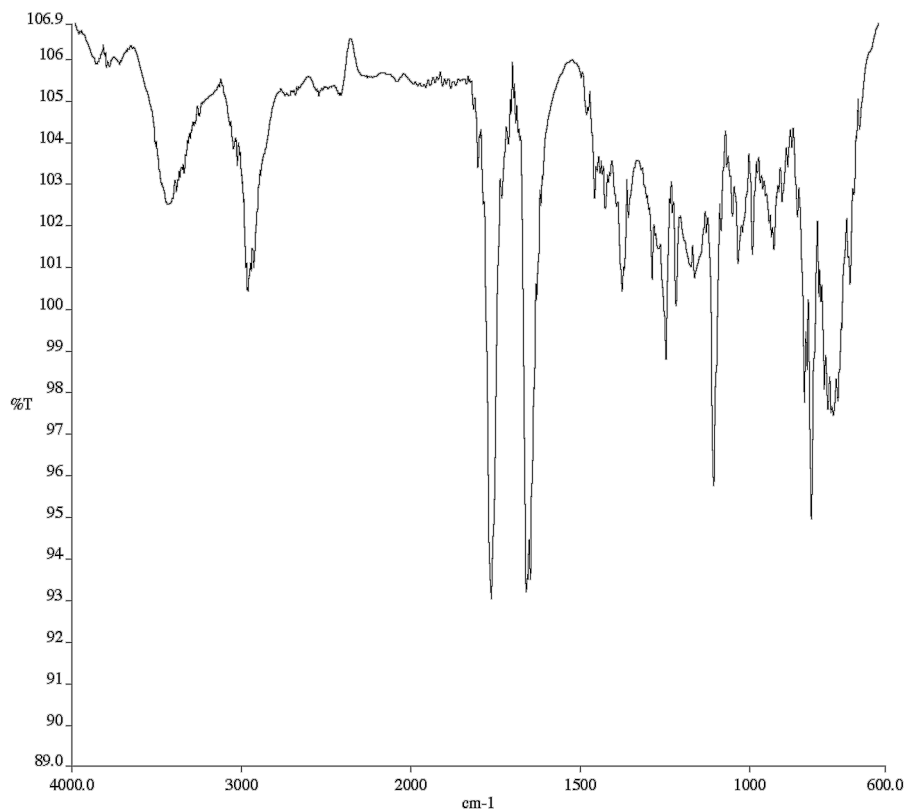


Figure A6.50 Infrared spectrum (Thin Film, NaCl) of compound **510a**.

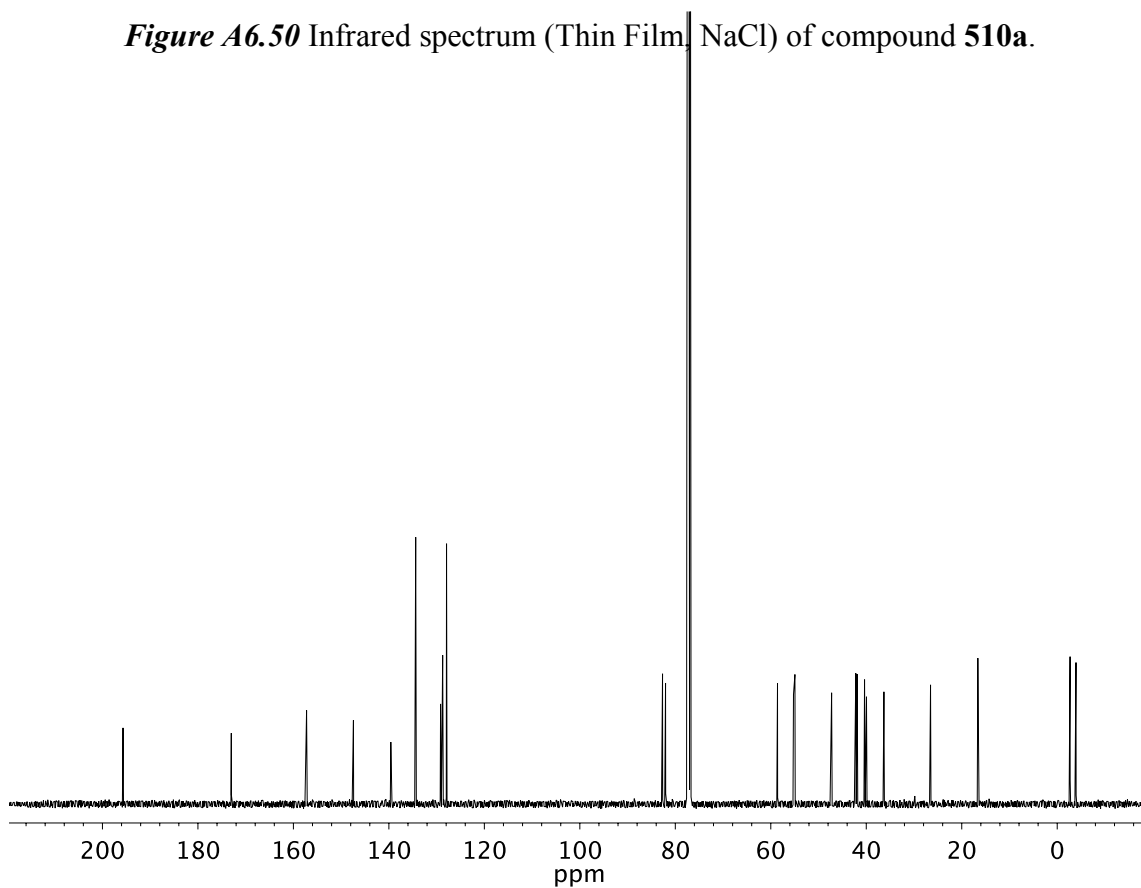


Figure A6.51 ¹³C NMR (101 MHz, CDCl₃) of compound **510a**.

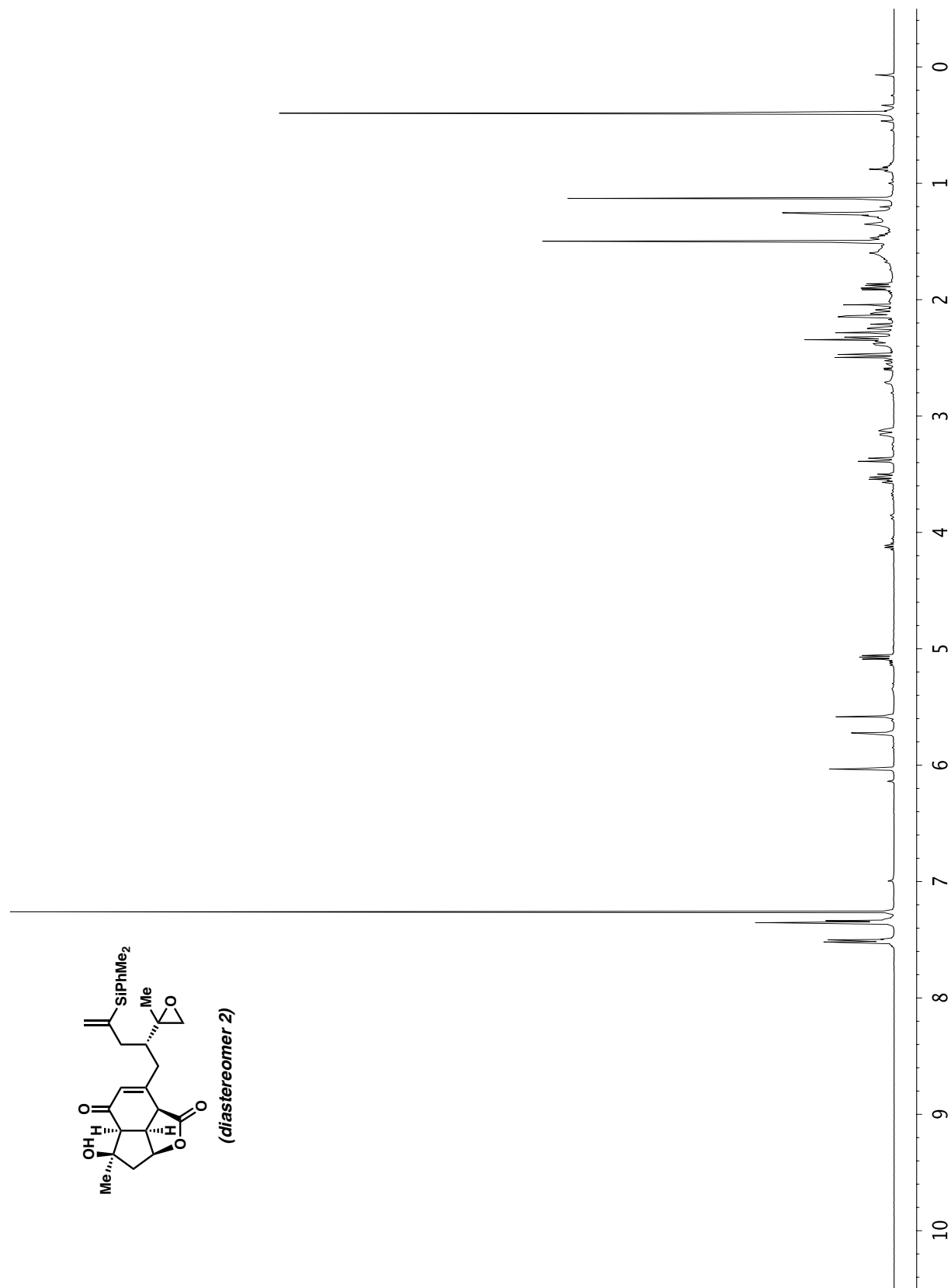


Figure A6.52 $^1\text{H NMR}$ (400 MHz, CDCl_3) of compound **510b**.

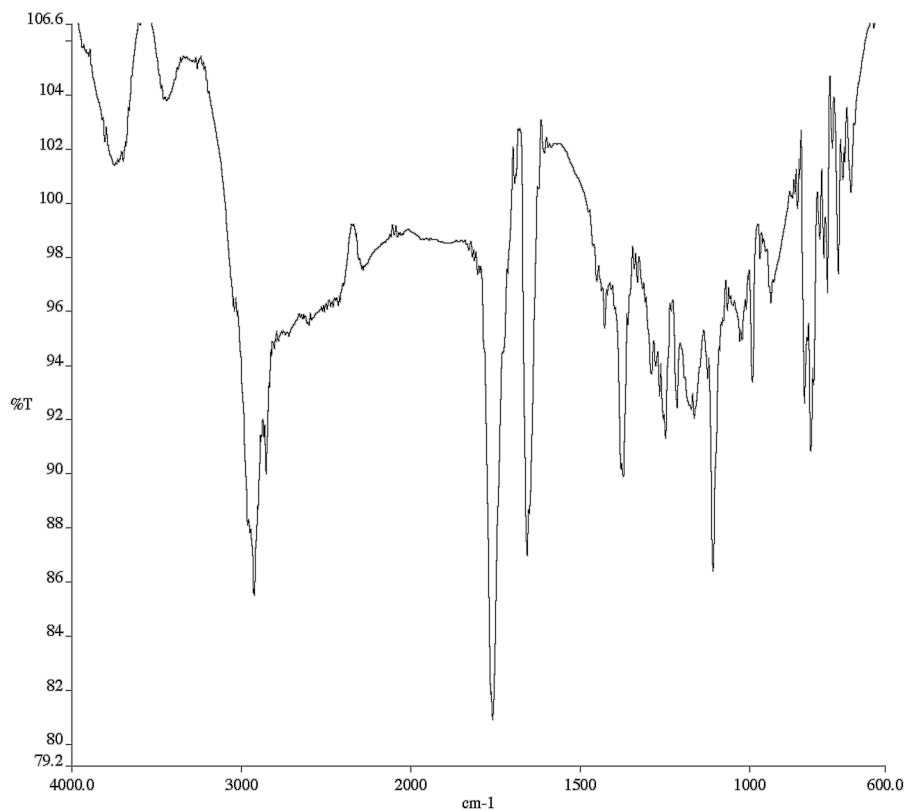


Figure A6.53 Infrared spectrum (Thin Film, NaCl) of compound **510b**.

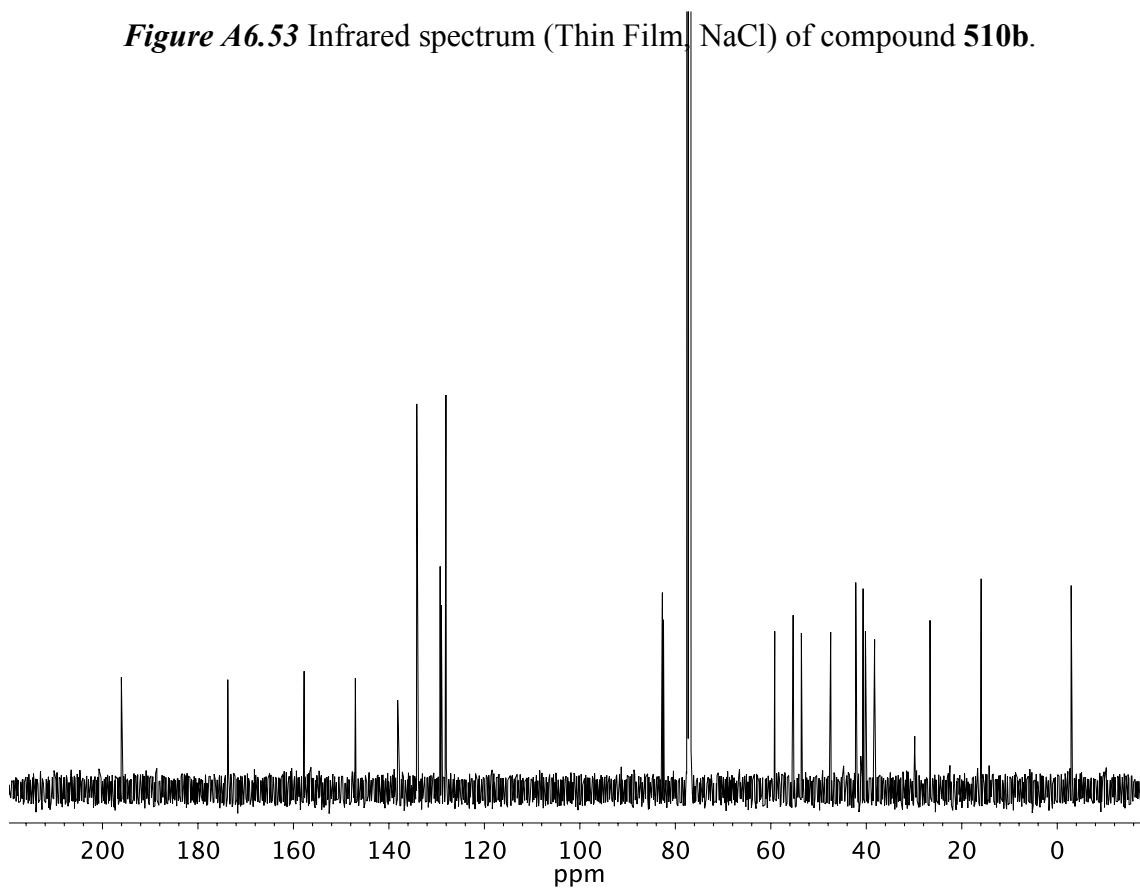


Figure A6.54 ¹³C NMR (101 MHz, CDCl₃) of compound **510b**.

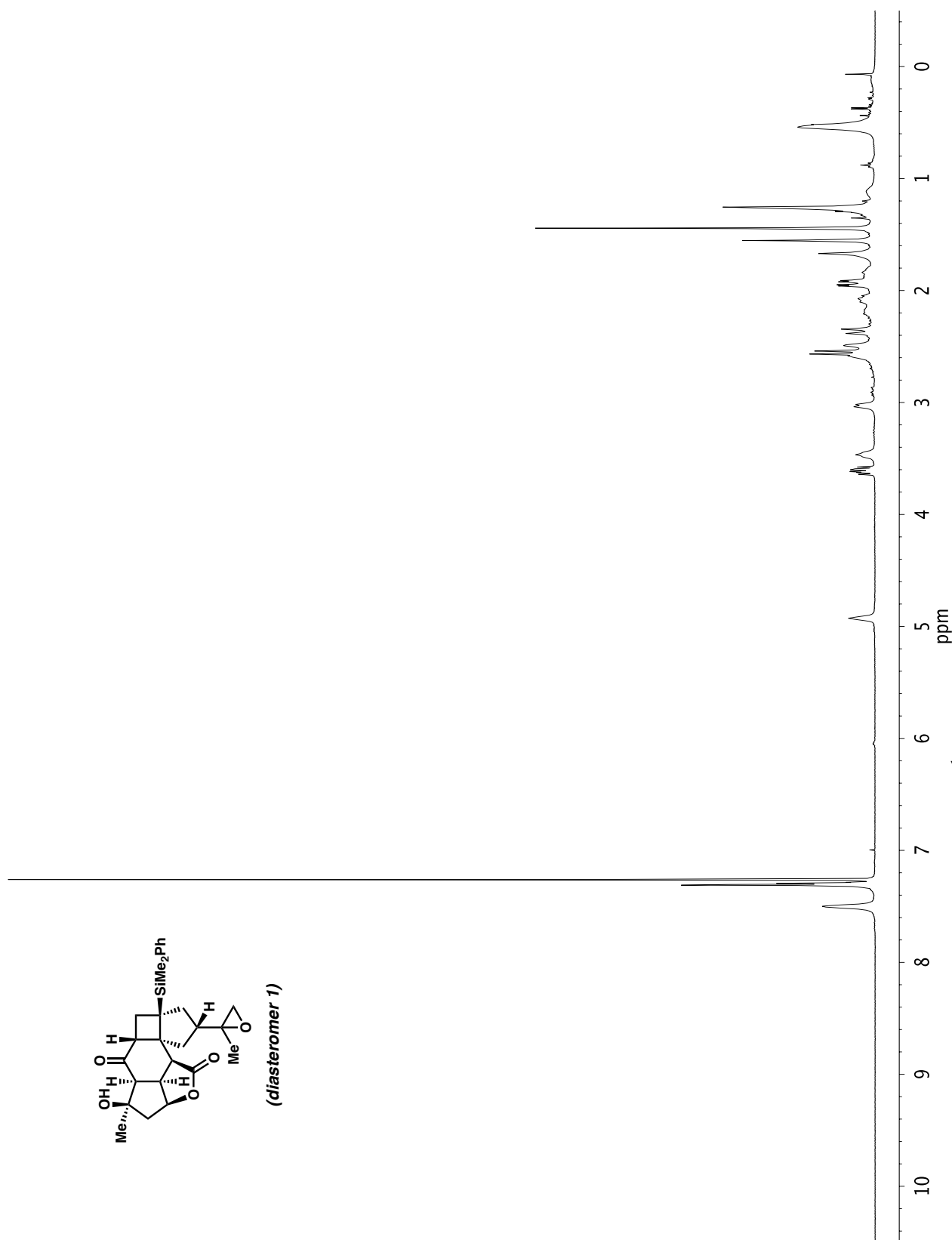


Figure A6.55 ^1H NMR (400 MHz, CDCl_3) of compound 511a.

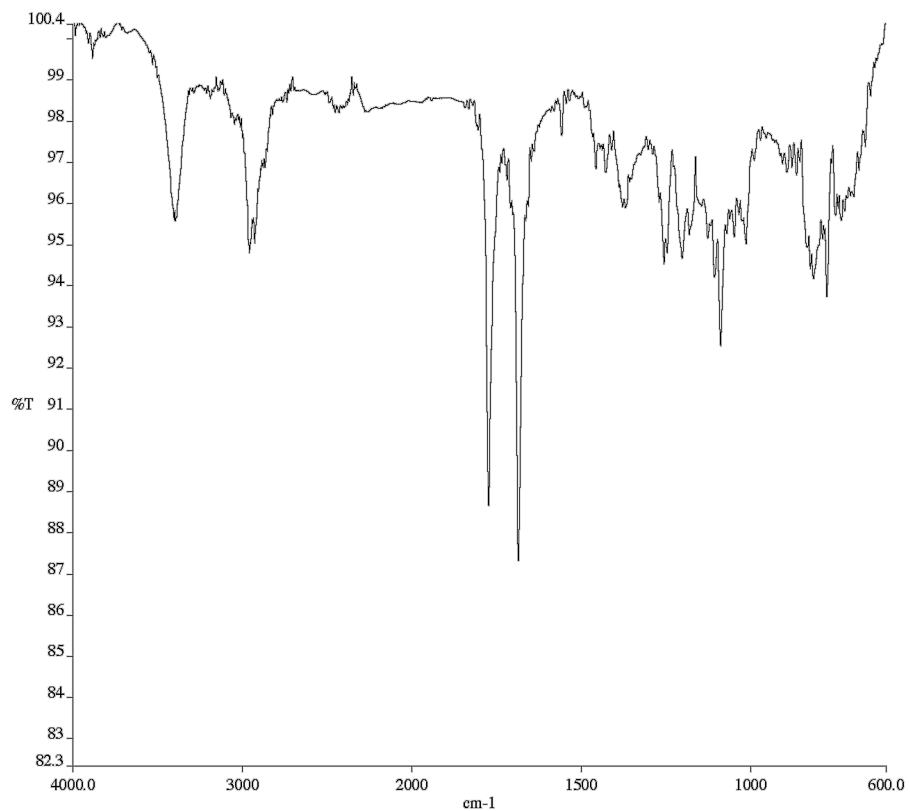


Figure A6.56 Infrared spectrum (Thin Film, NaCl) of compound **511a**.

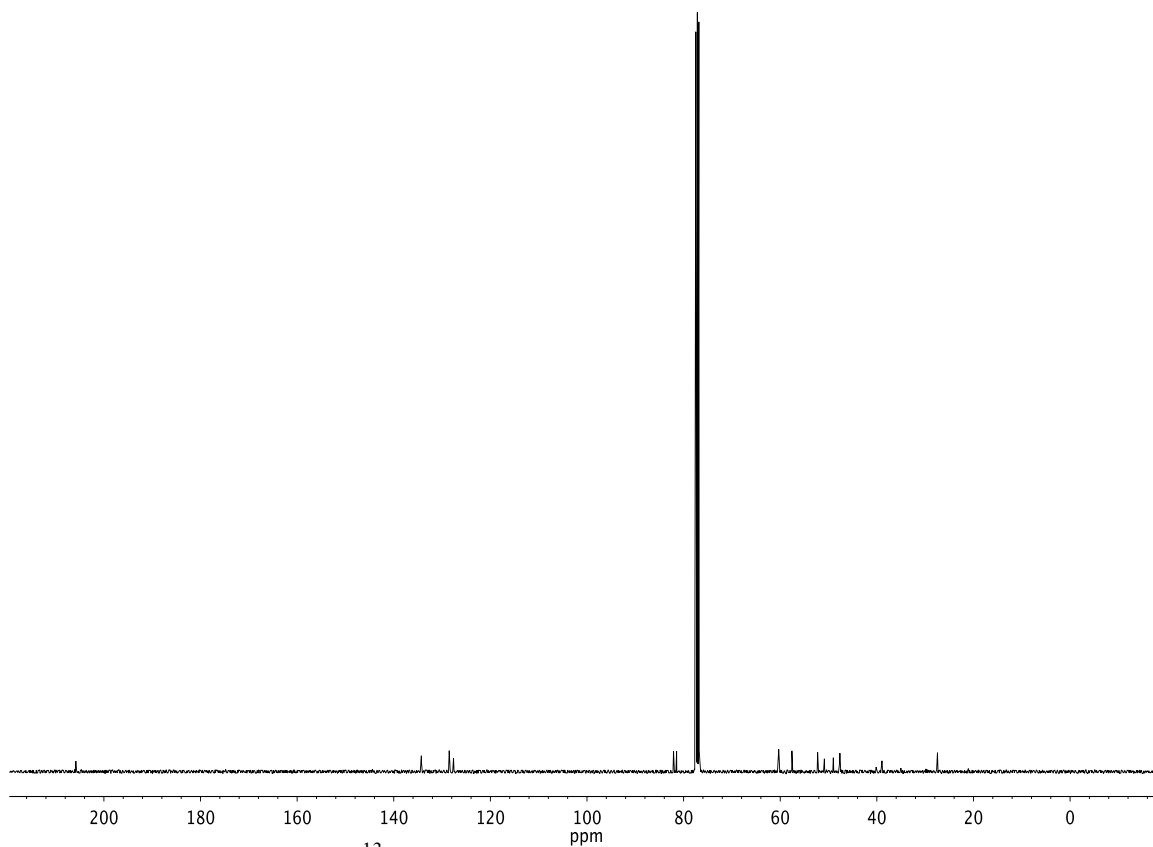


Figure A6.57 ¹³C NMR (101 MHz, CDCl₃) of compound **511a**.

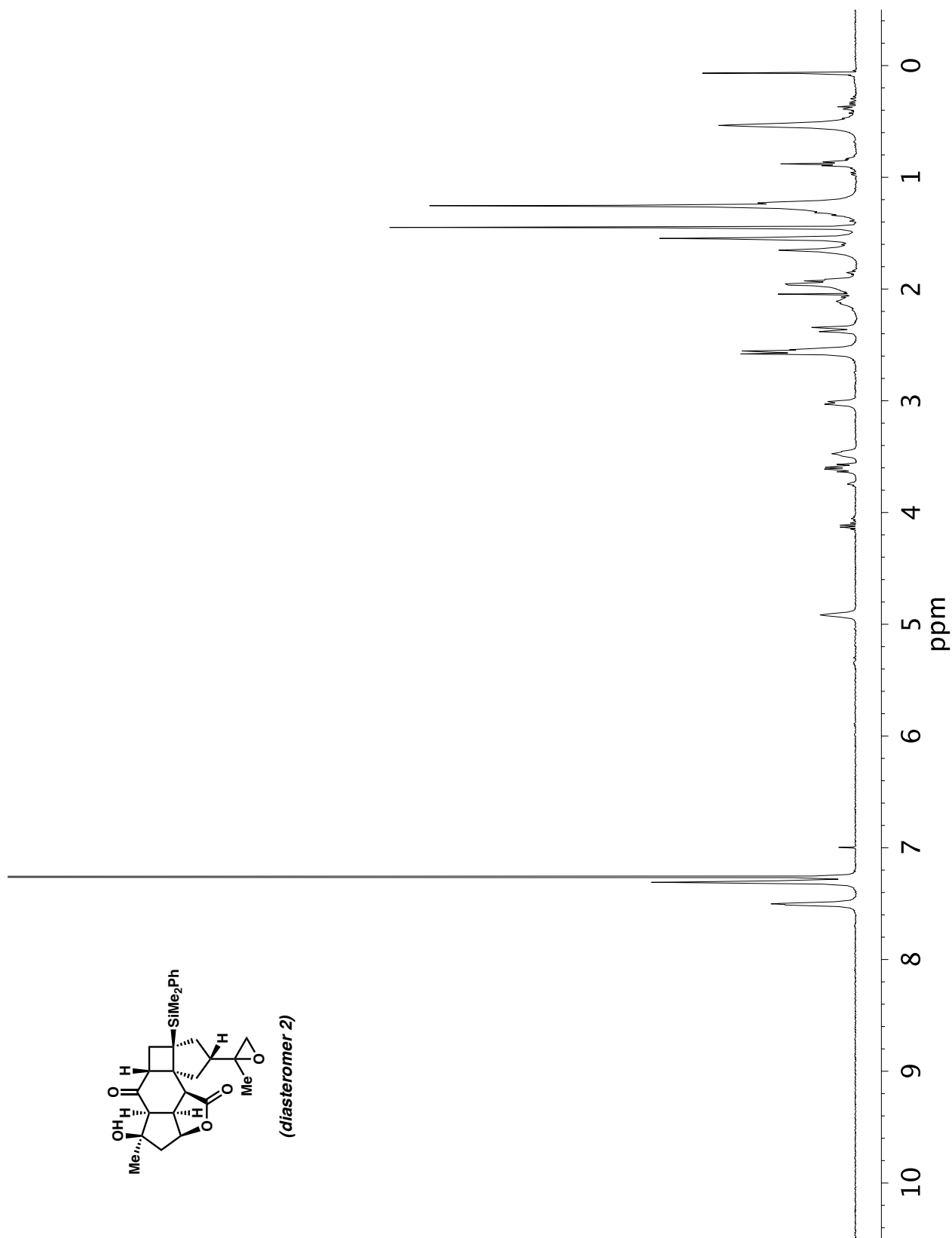


Figure A6.58 ^1H NMR (400 MHz, CDCl_3) of compound 511b.

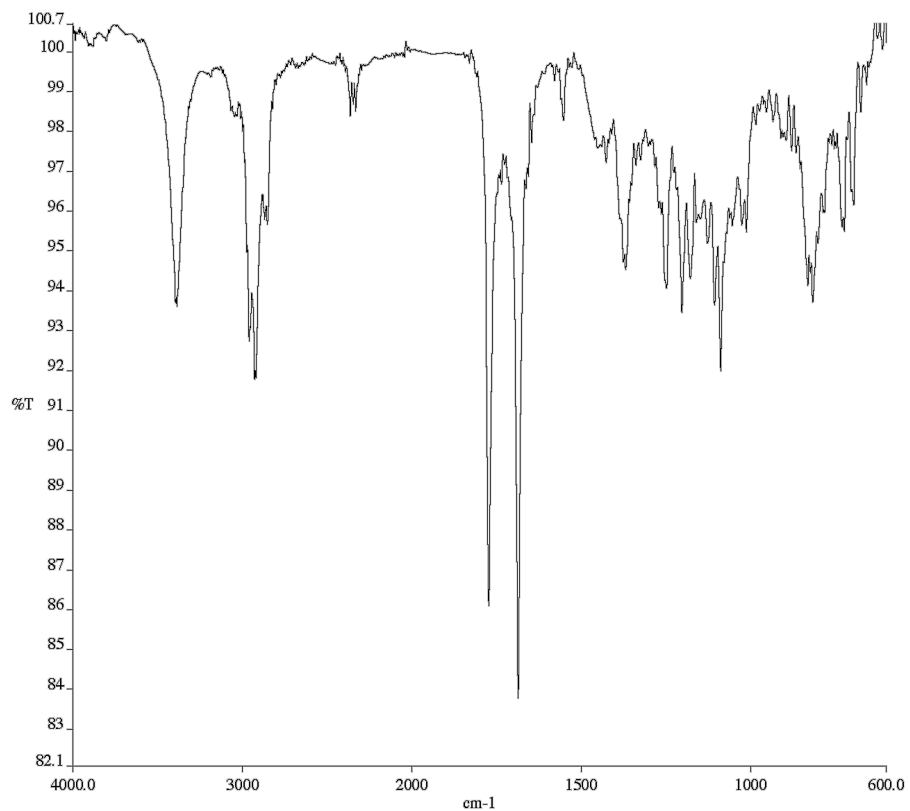


Figure A6.59 Infrared spectrum (Thin Film NaCl) of compound **511b**.

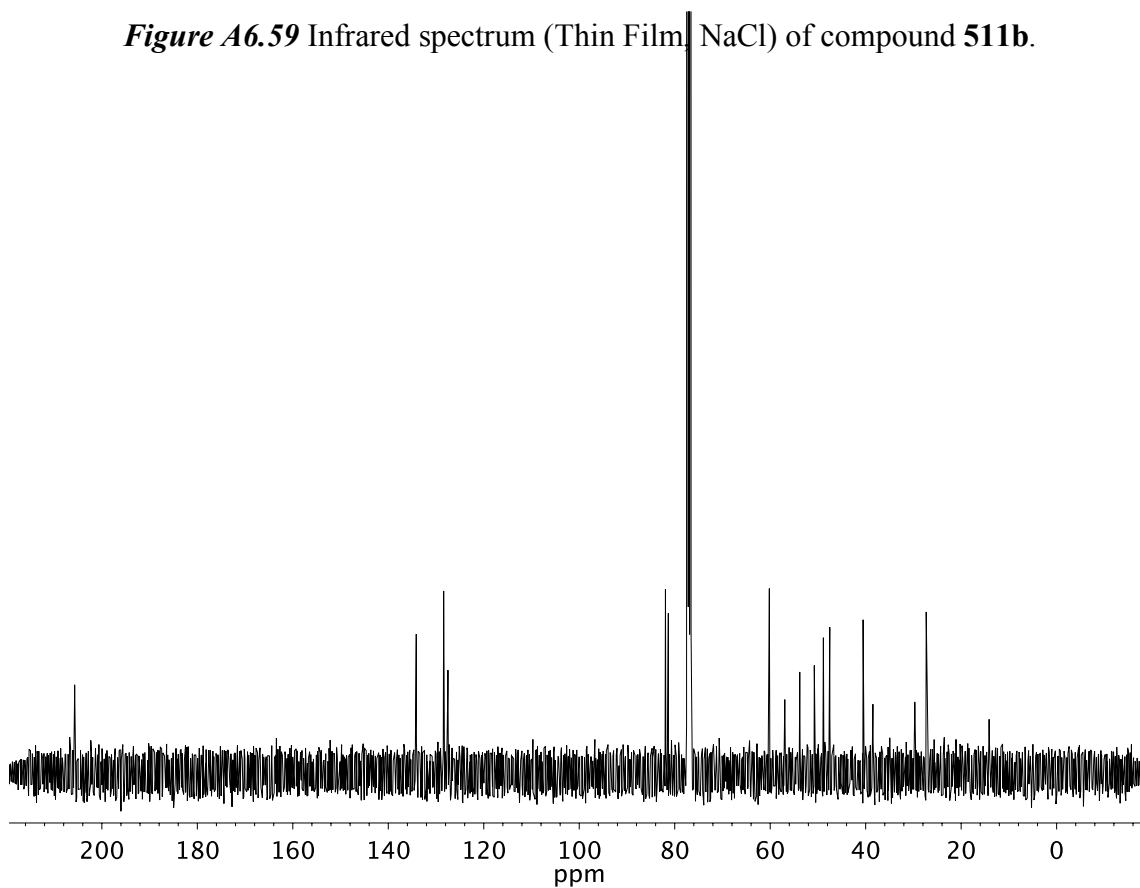


Figure A6.60 ¹³C NMR (101 MHz, CDCl₃) of compound **511b**.

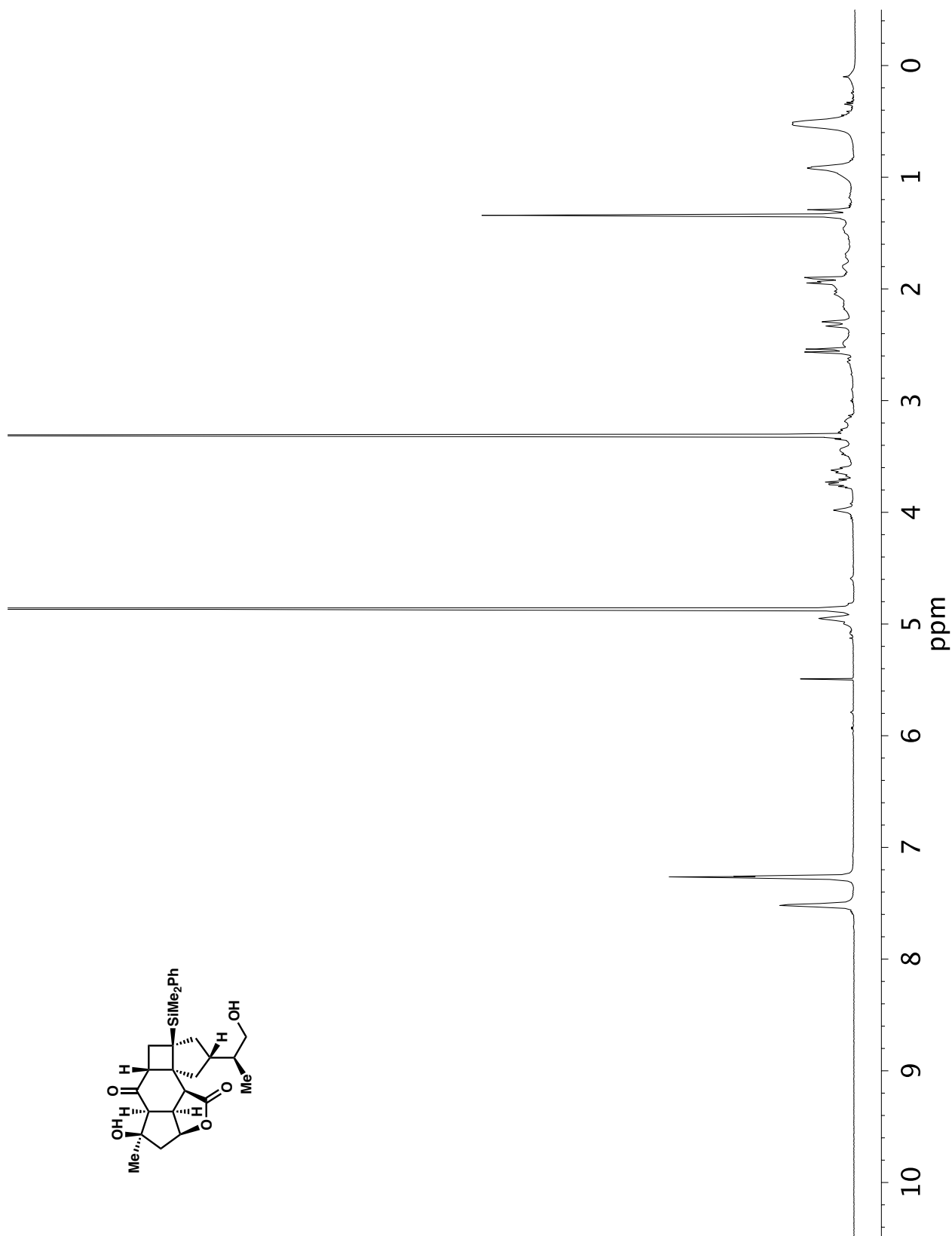


Figure A6.61 ¹H NMR (400 MHz, CDCl₃) of compound 512a.

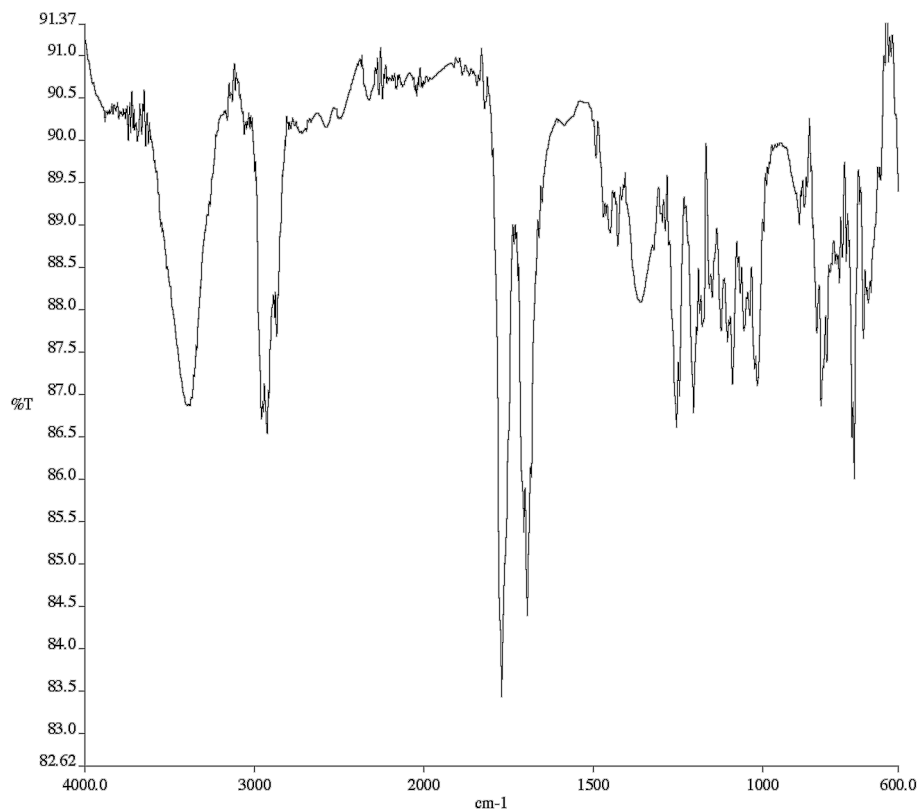


Figure A6.62 Infrared spectrum (Thin Film, NaCl) of compound **512a**.

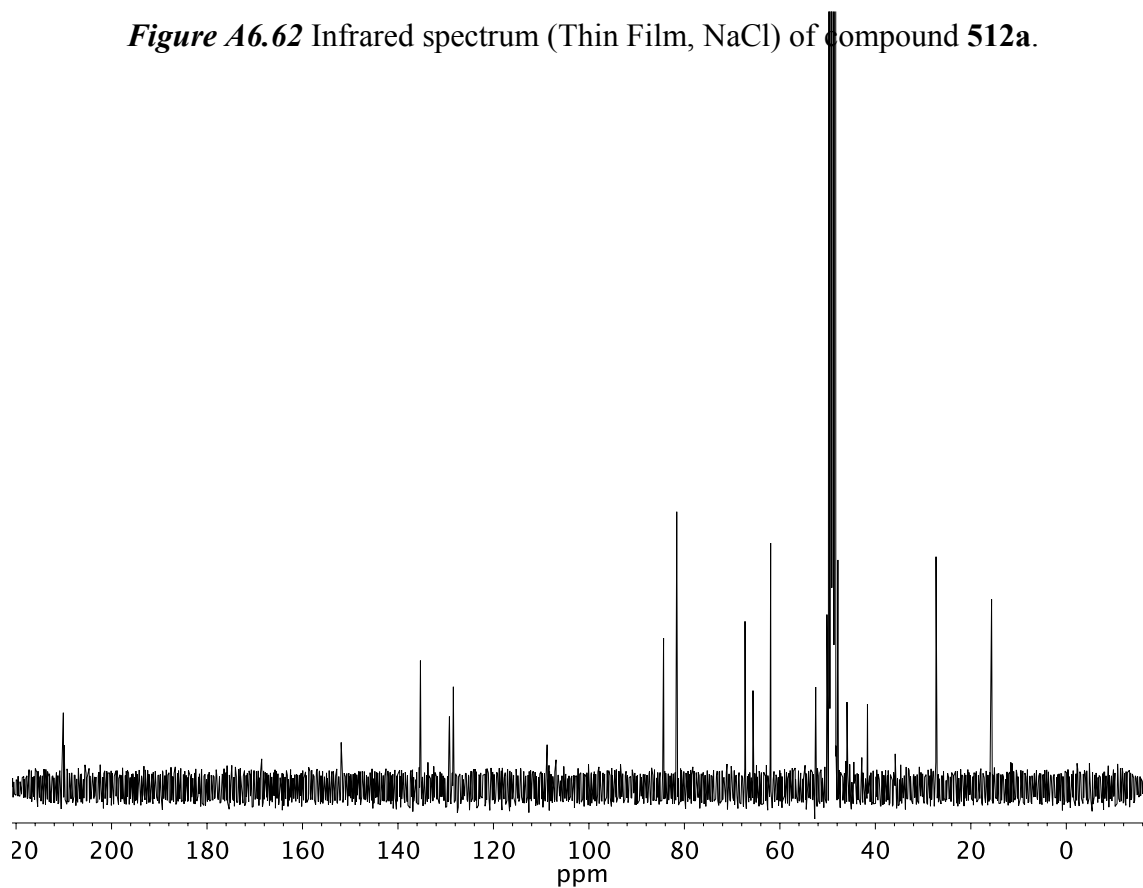


Figure A6.63 ¹³C NMR (101 MHz, CDCl₃) of compound **512a**.

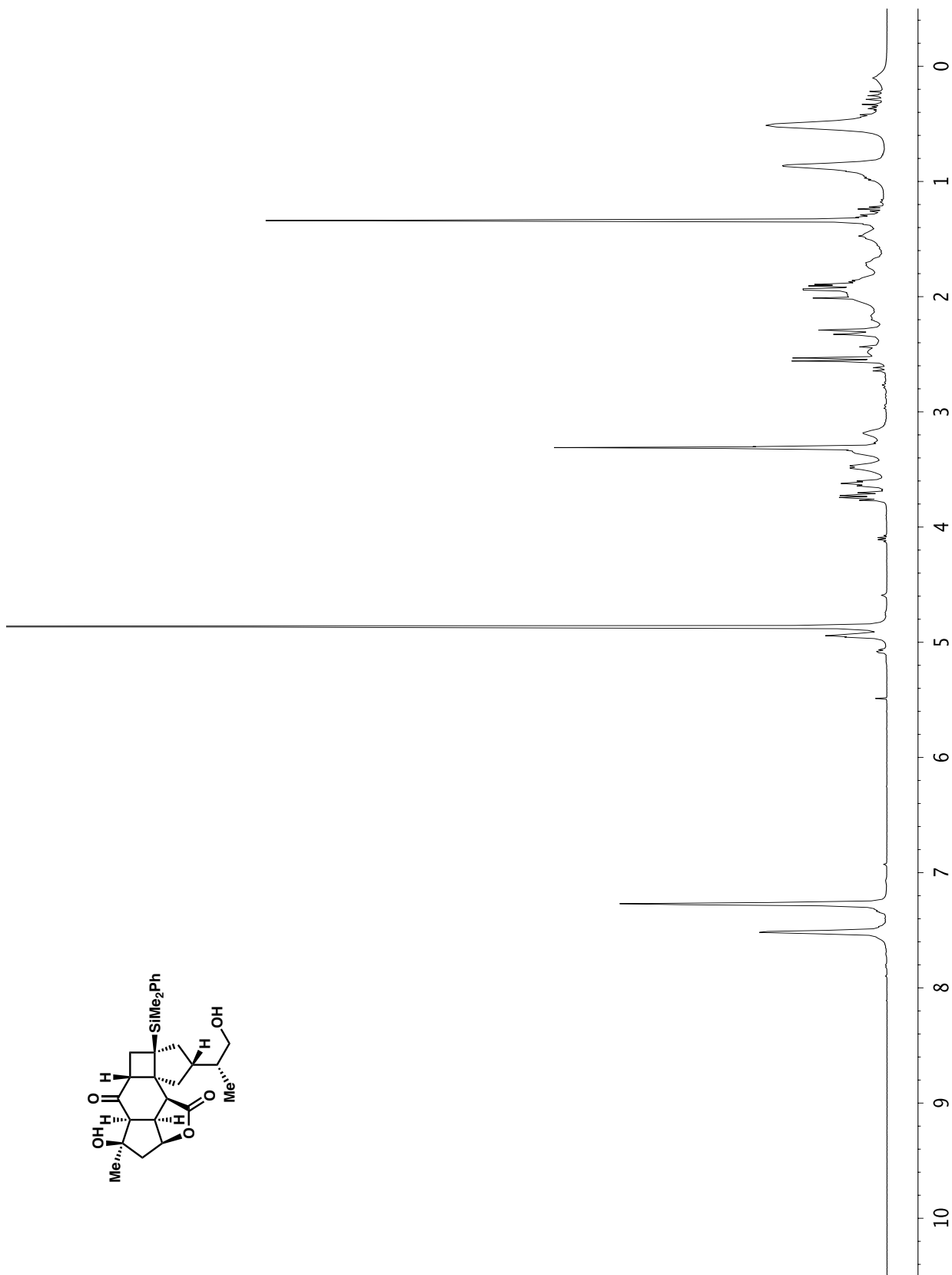


Figure A6.64 ^1H NMR (400 MHz, CD₂Cl₂) of compound **512b**.

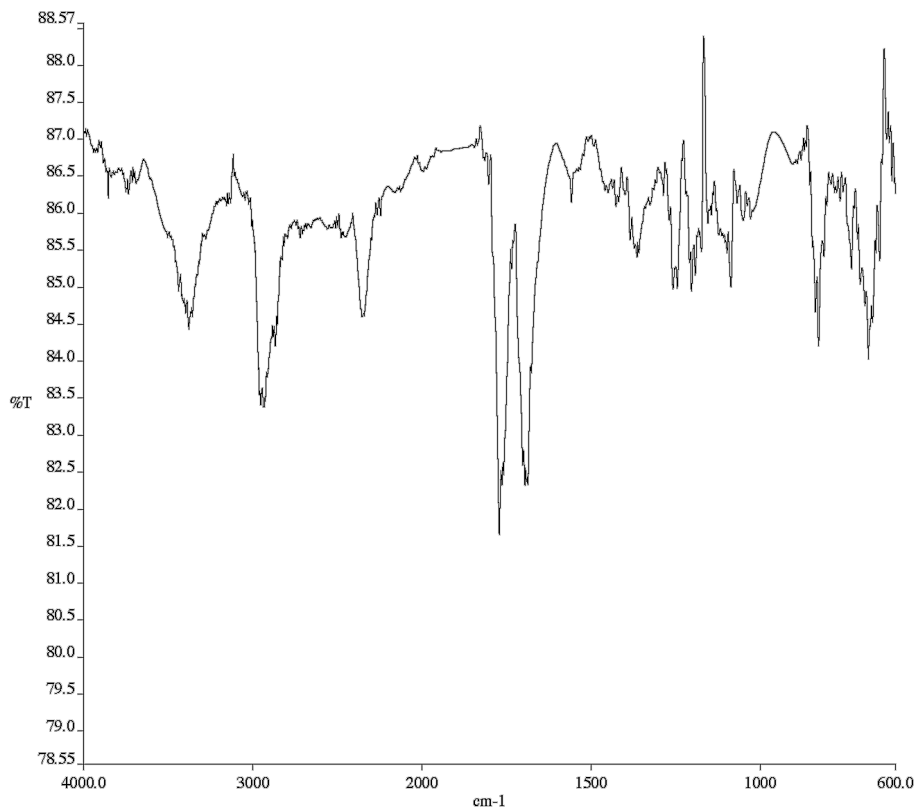


Figure A6.65 Infrared spectrum (Thin Film, NaCl) of compound **512b**.

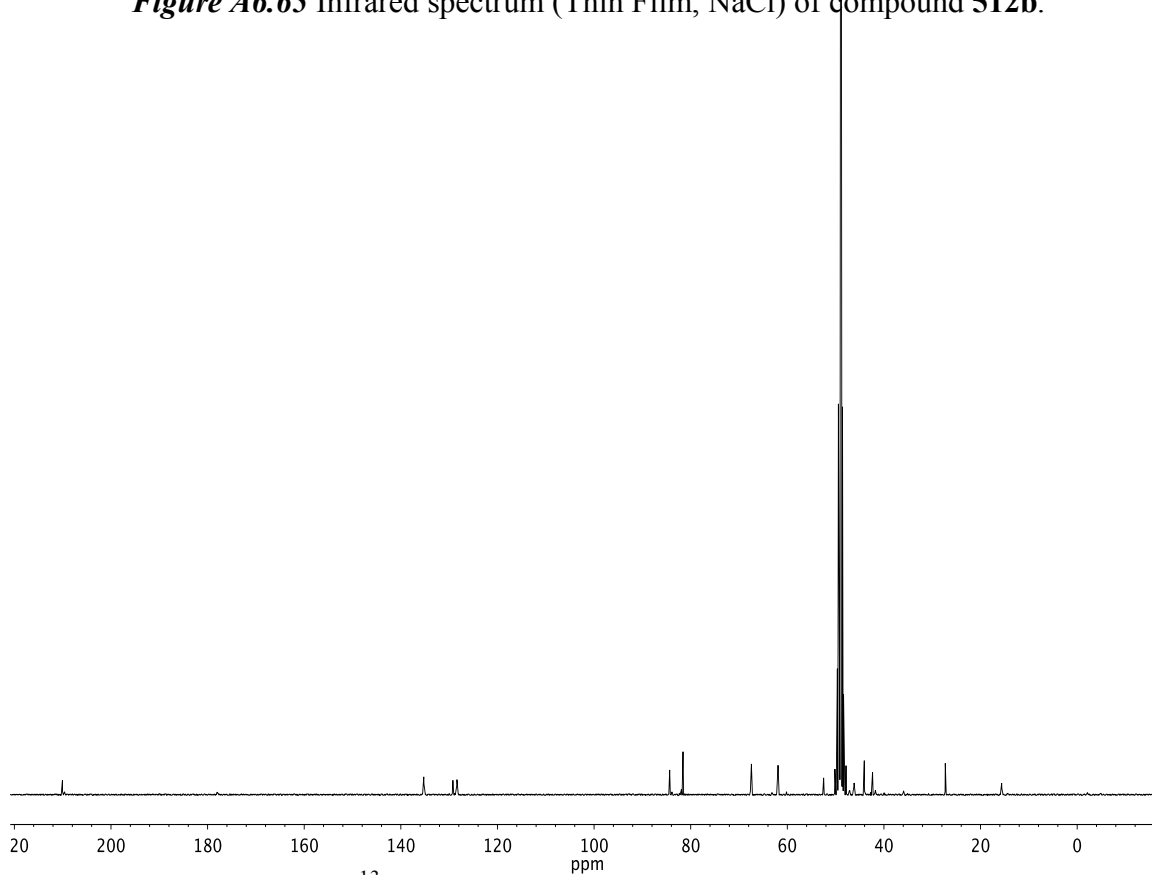


Figure A6.66 ¹³C NMR (101 MHz, CD₂Cl₂) of compound **512b**.

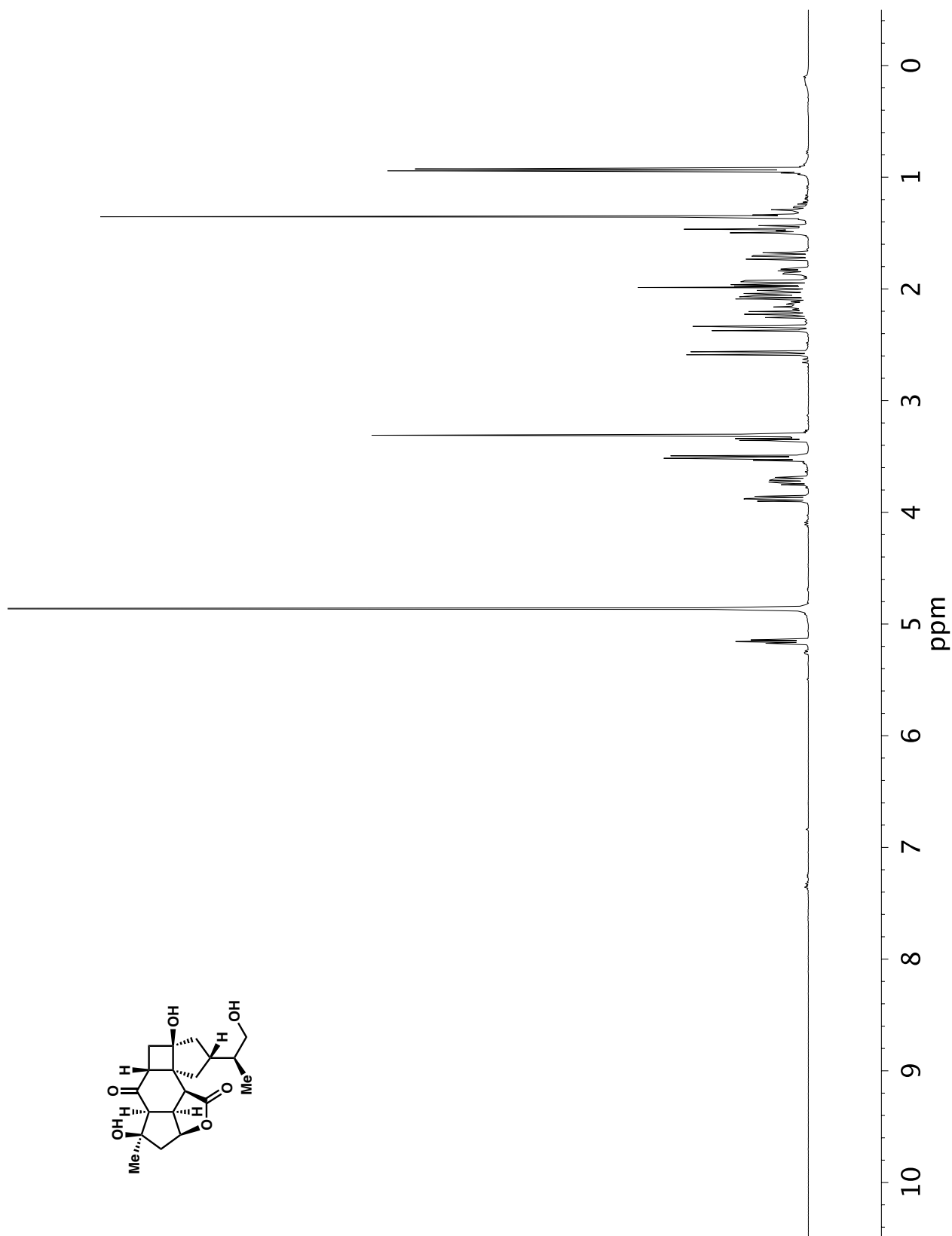


Figure A6.67 ^1H NMR (400 MHz, CDCl_3) of compound 513a.

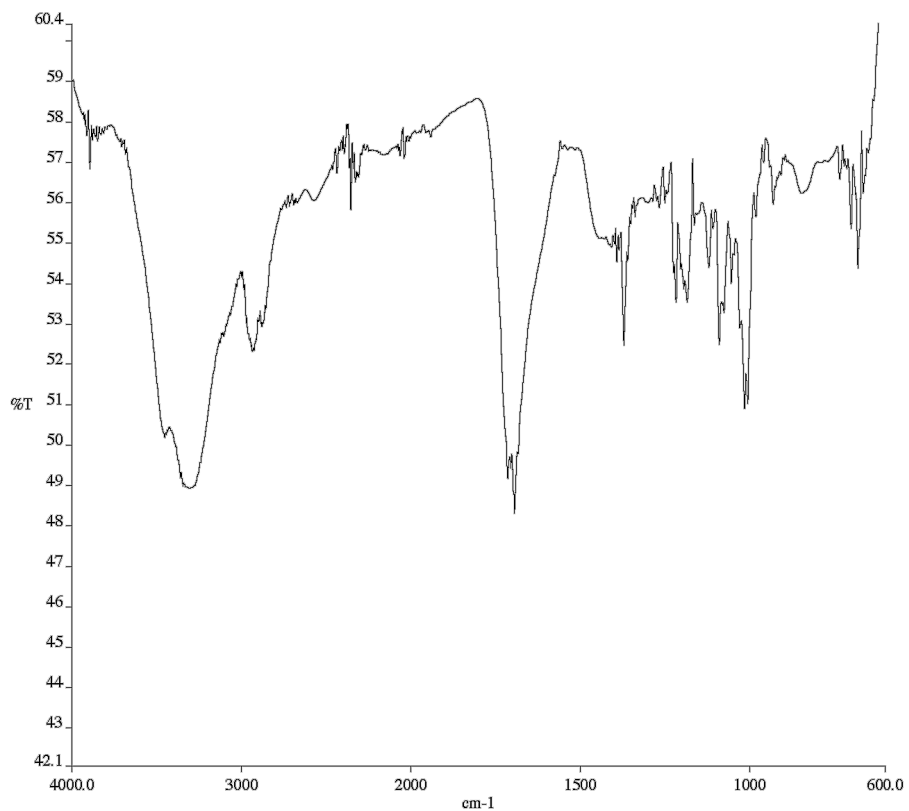


Figure A6.68 Infrared spectrum (Thin Film, NaCl) of compound **513a**.

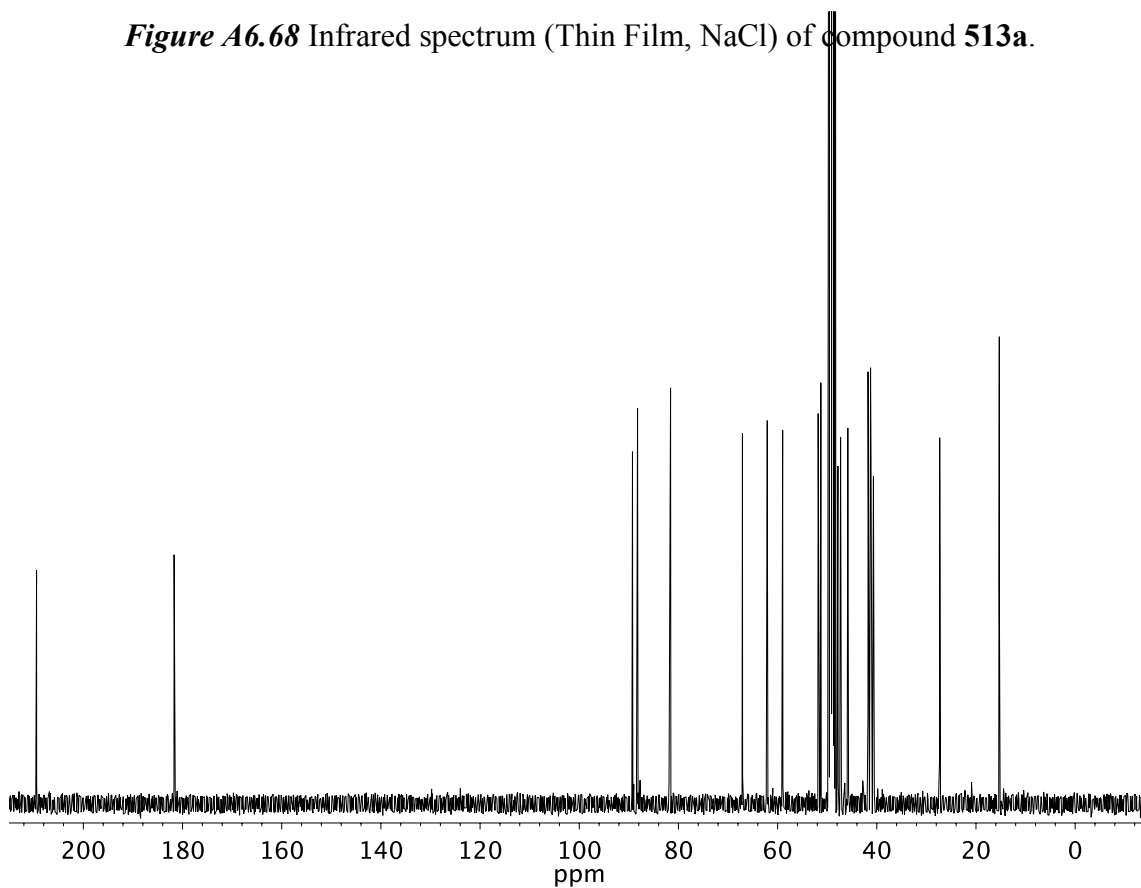


Figure A6.69 ¹³C NMR (101 MHz, CDCl₃) of compound **513a**.

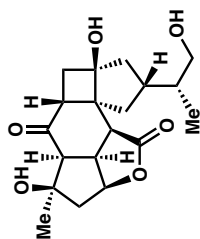
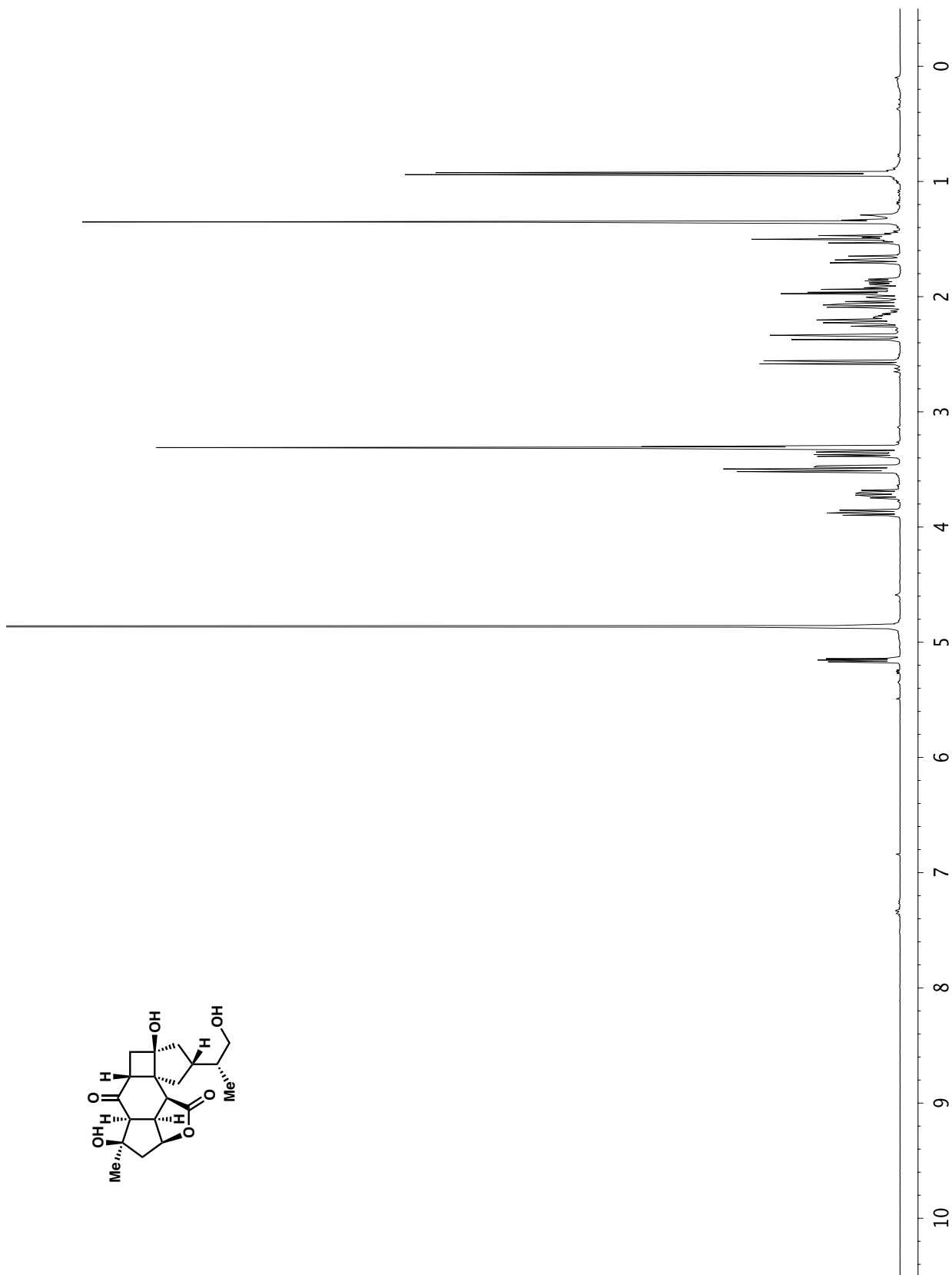


Figure A6.70 ^1H NMR (400 MHz, CDCl_3) of compound 513b.

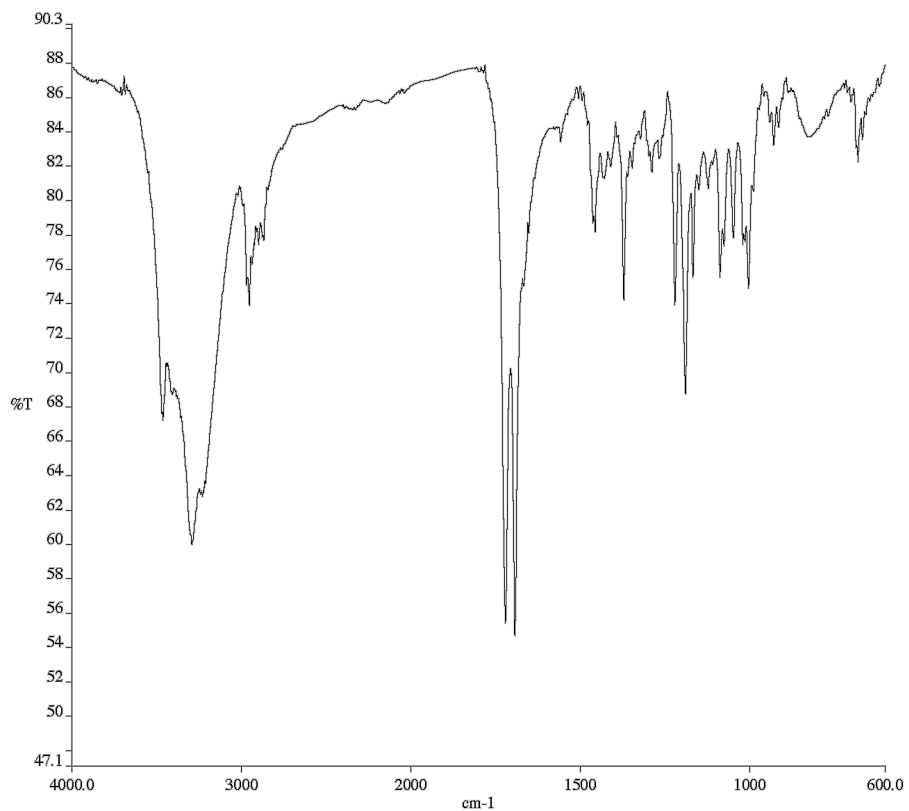


Figure A6.71 Infrared spectrum (Thin Film, NaCl) of compound **513b**.

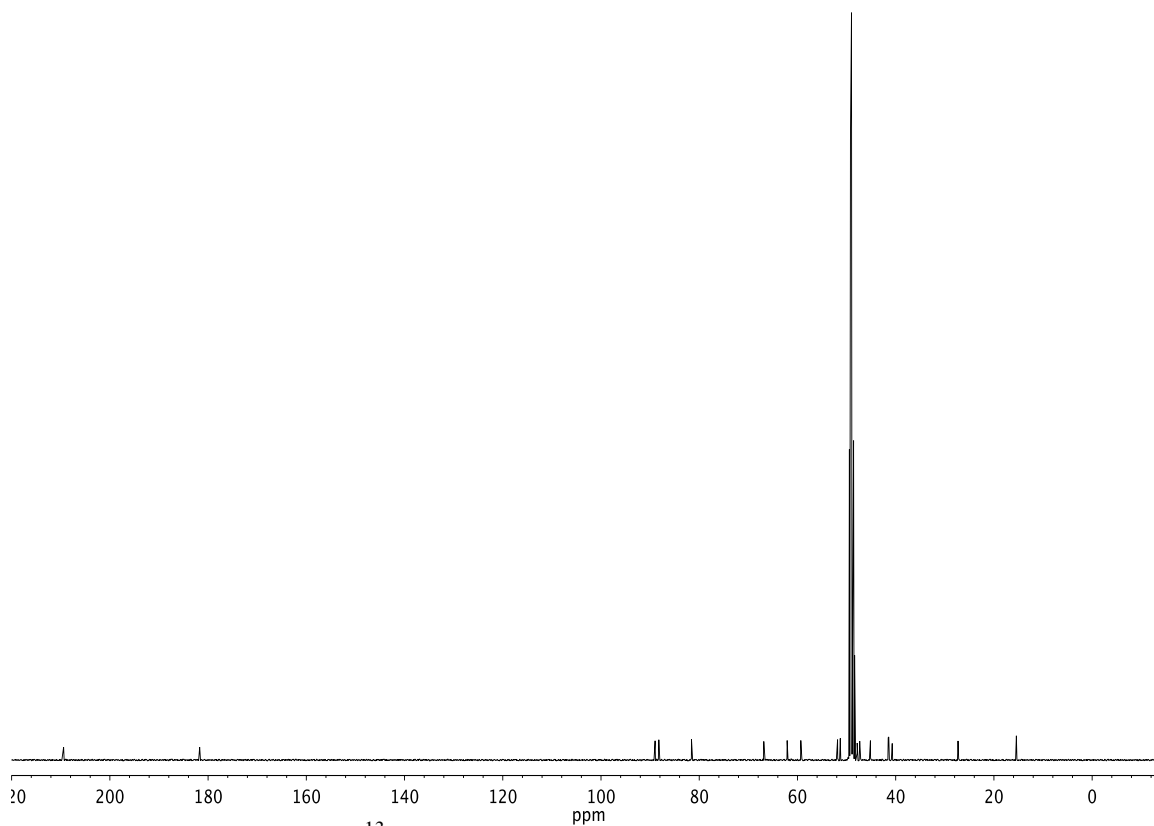
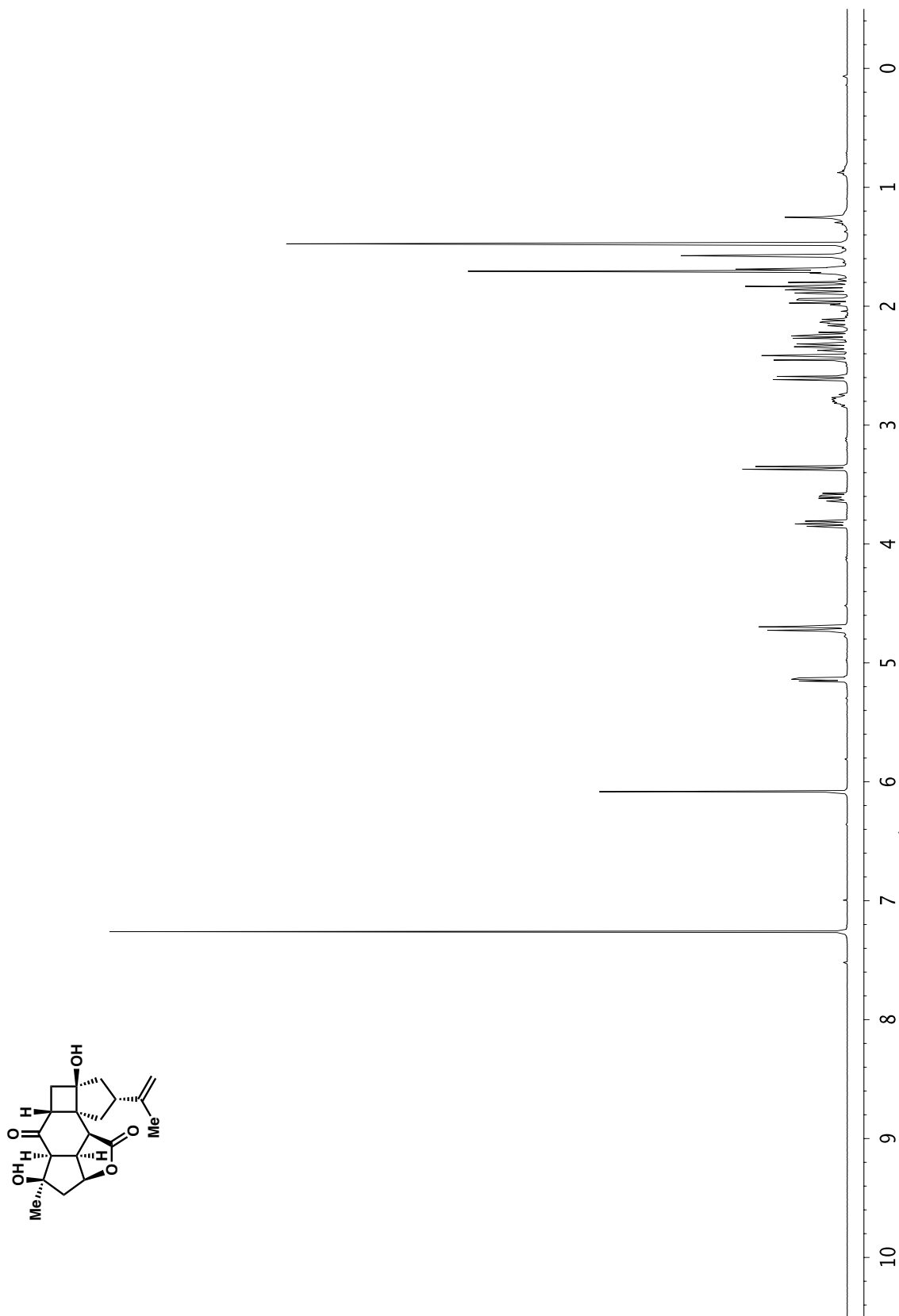


Figure A6.72 ¹³C NMR (101 MHz, CDCl₃) of compound **513b**.



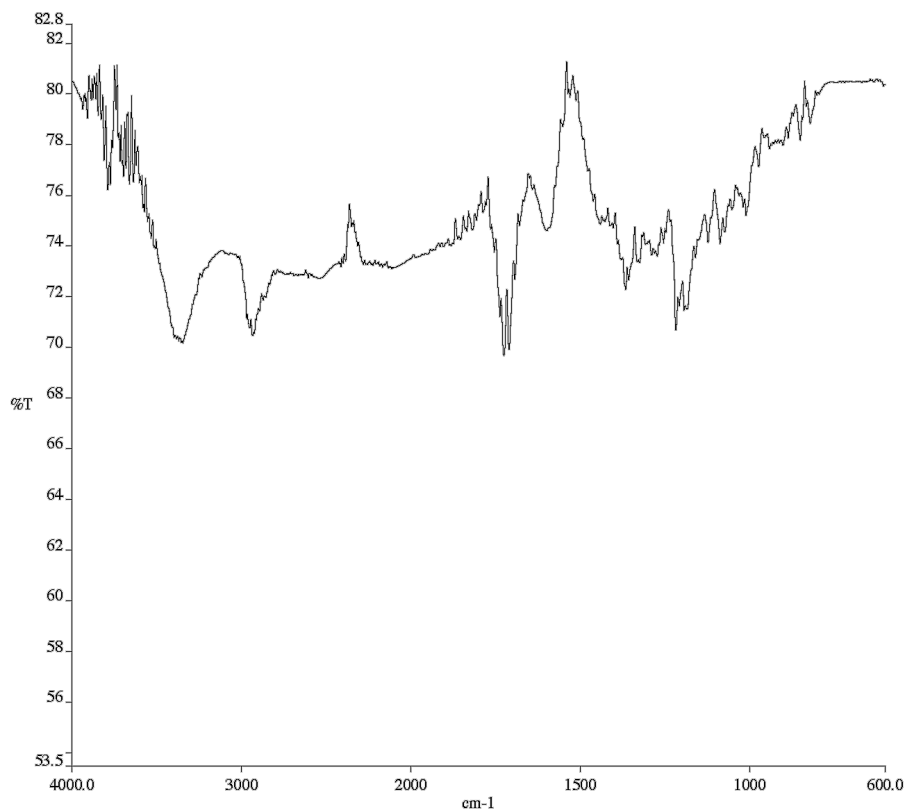


Figure A6.74 Infrared spectrum (Thin Film, NaCl) of compound **527**.

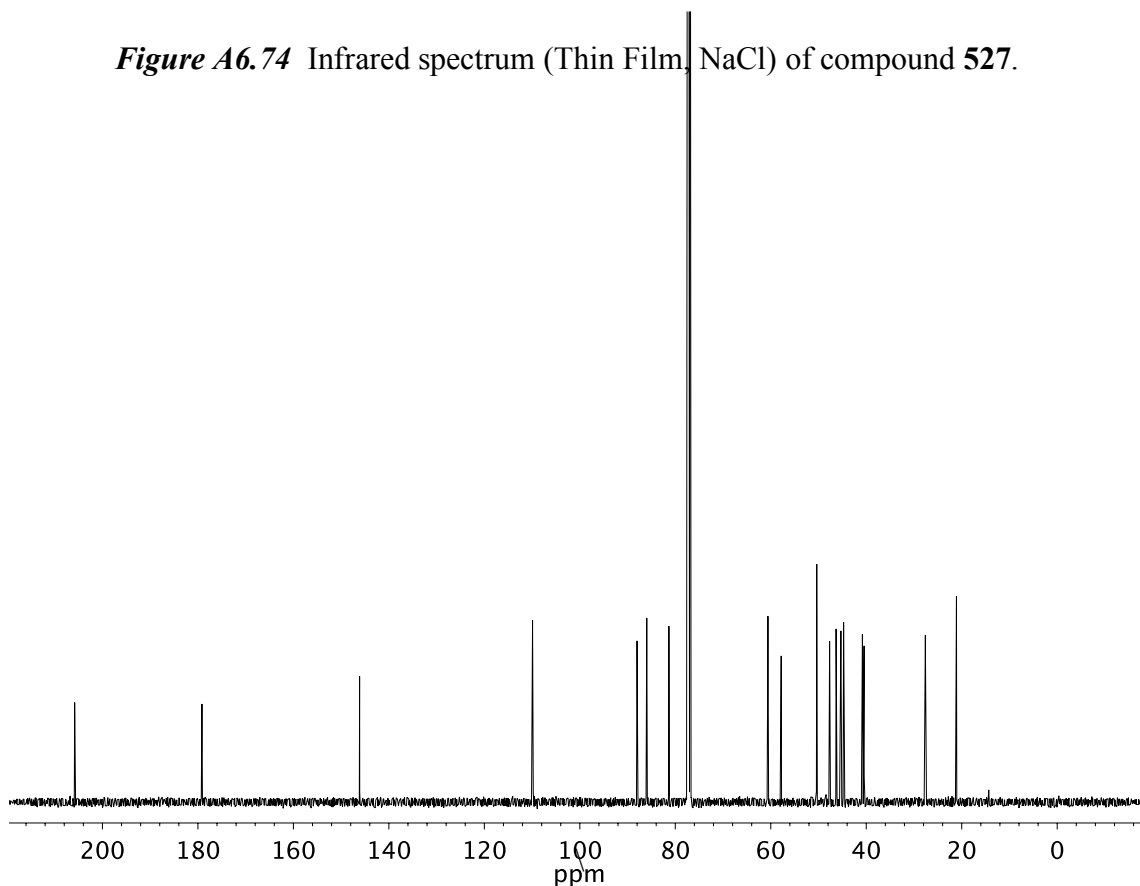


Figure A6.75 ¹³C NMR (101 MHz, CDCl₃) of compound **527**.

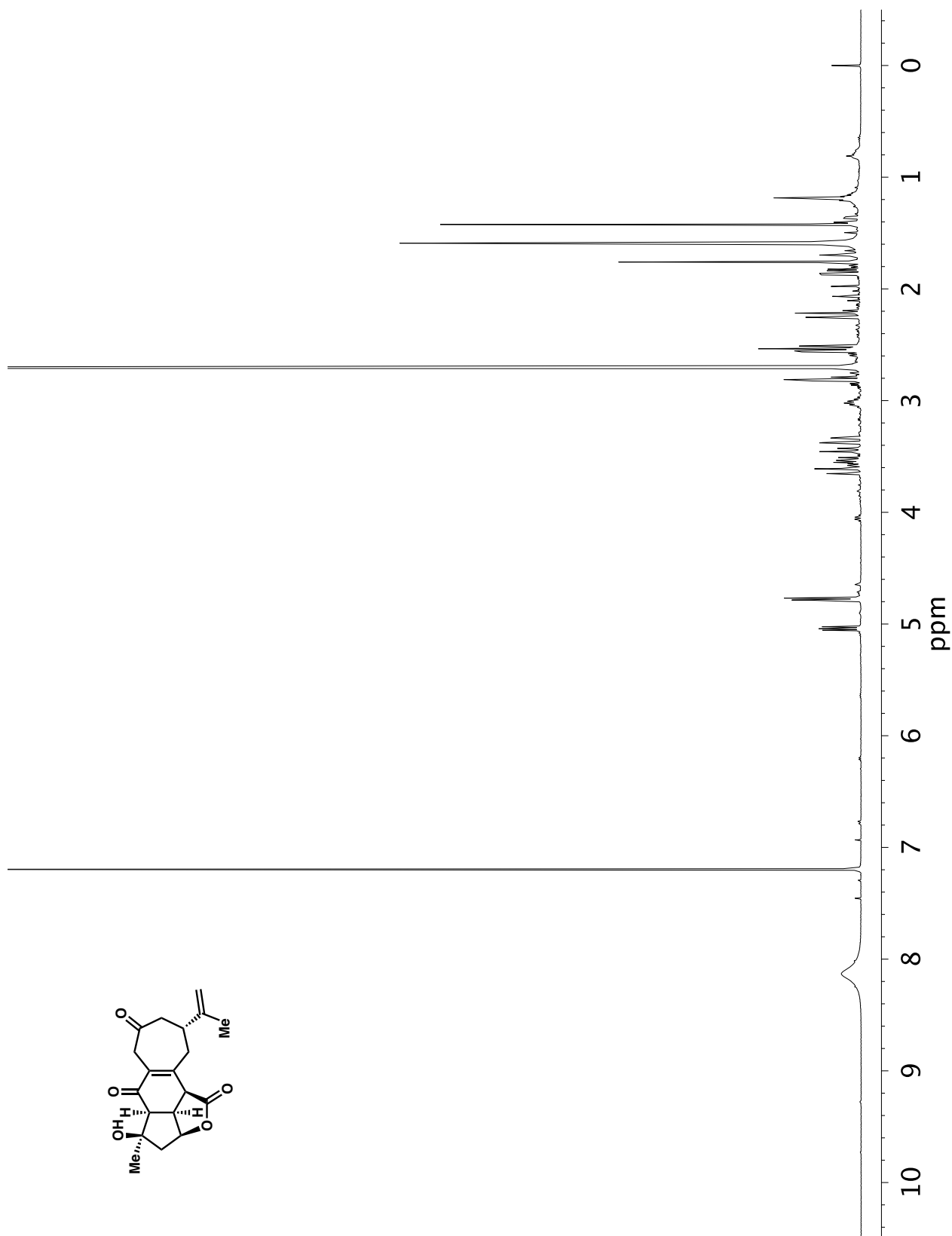


Figure A6.76 ^1H NMR (600 MHz, CDCl_3) of compound 416.

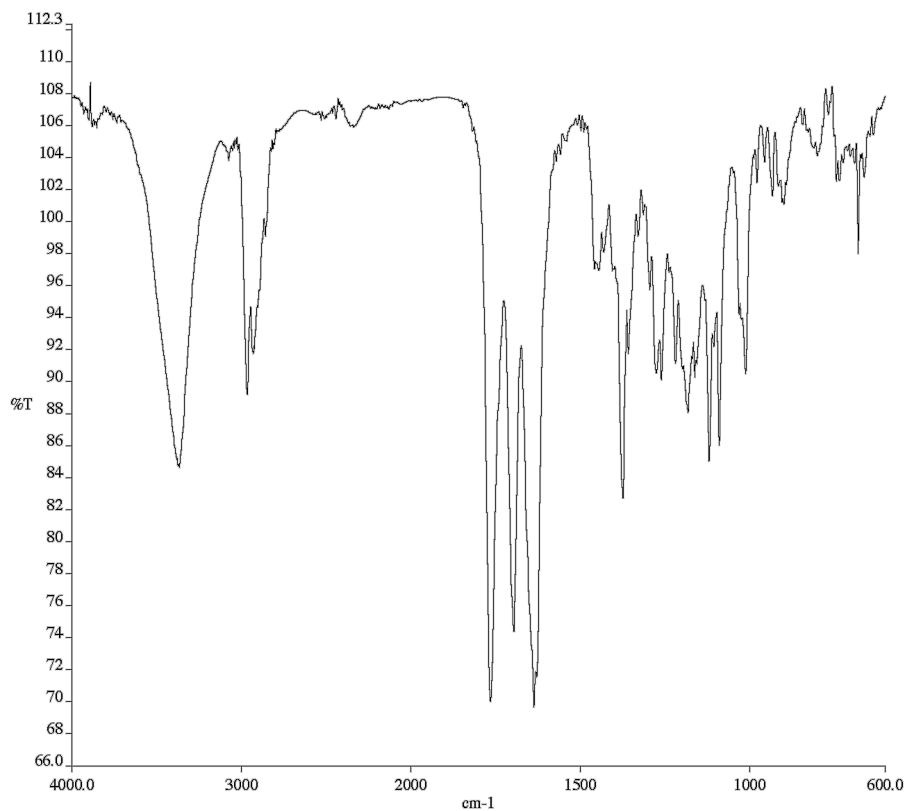


Figure A6.77 Infrared spectrum (Thin Film, NaCl) of compound **416**.

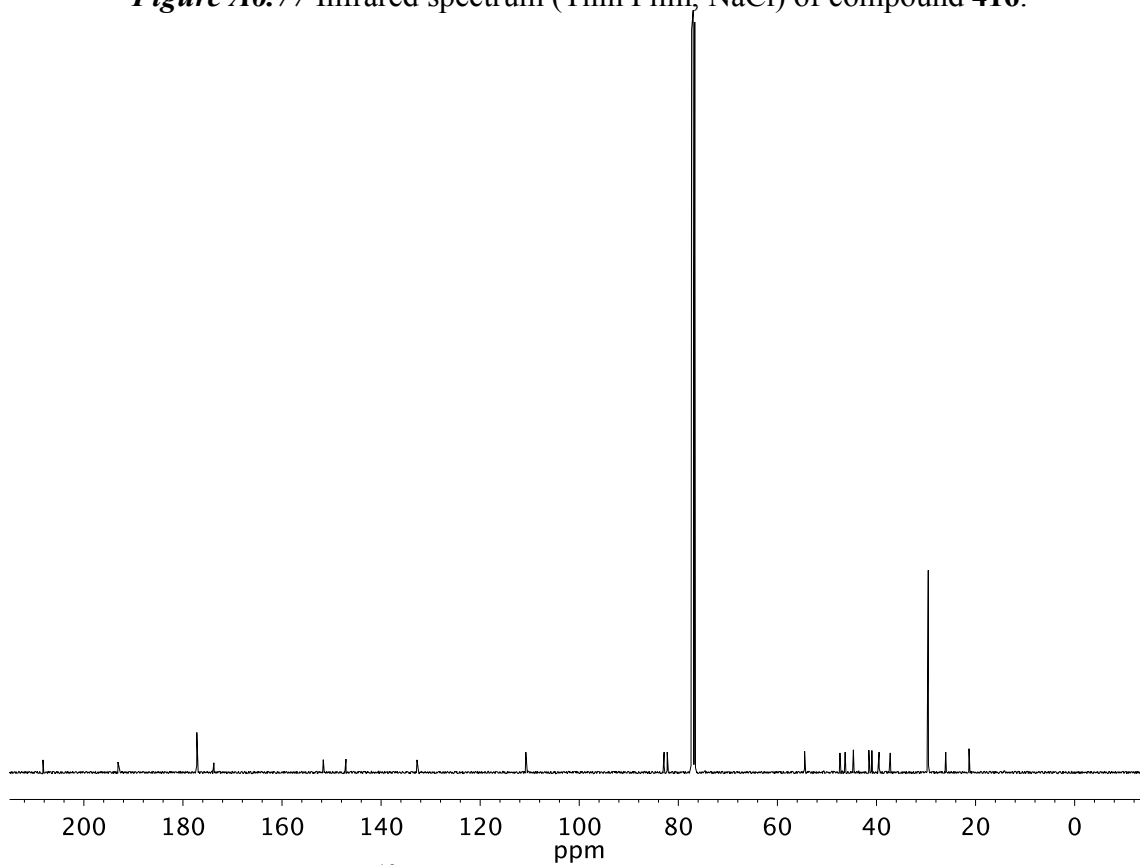


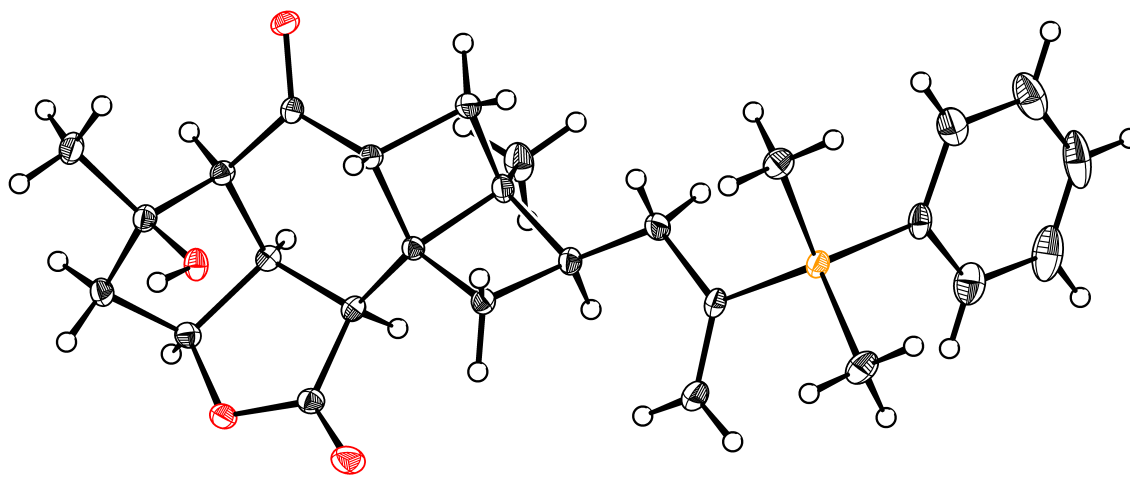
Figure A6.78 ¹³C NMR (101 MHz, CDCl₃) of compound **416**.

APPENDIX 7

X-Ray Crystallography Reports

Relevant to Chapter 4

A7.1 X-RAY CRYSTAL STRUCTURE ANALYSIS FOR DICYCLOBUTANE 500

Figure A7.1. X-Ray Coordinate of Compound **500**.**Table A7.1.** Crystal data and structure refinement for dicyclobutane **500**.

Identification code	d20010	
Empirical formula	C ₂₇ H ₃₄ O ₄ Si	
Formula weight	450.63	
Temperature	100 K	
Wavelength	0.71073 \approx	
Crystal system	Monoclinic	
Space group	P 1 21 1 (# 4)	
Unit cell dimensions	a = 6.9085(14) \approx	$\alpha = 90^\circ$
	b = 10.3765(19) \approx	$\beta = 90.920(7)^\circ$
	c = 17.058(3) \approx	$\gamma = 90^\circ$
Volume	1222.7(4) \approx^3	

Z	2
Density (calculated)	1.224 g/cm ³
Absorption coefficient	0.126 mm ⁻¹
F(000)	484
Crystal size	0.04 x 0.32 x 0.33 mm ³
Theta range for data collection	2.30 to 32.80°
Index ranges	-10 ≤ h ≤ 10, -15 ≤ k ≤ 14, -25 ≤ l ≤ 25
Reflections collected	76181
Independent reflections	8271 [R(int) = 0.0400]
Completeness to theta = 25.242°	99.9 %
Absorption correction	Semi-empirical from equivalents
Max. and min. transmission	1.0000 and 0.9658
Refinement method	Full-matrix least-squares on F ²
Data / restraints / parameters	8271 / 1 / 294
Goodness-of-fit on F ²	1.035
Final R indices [I > 2σ(I)]	R1 = 0.0401, wR2 = 0.0827
R indices (all data)	R1 = 0.0511, wR2 = 0.0865
Absolute structure parameter [Flack]	0.03(2)
Absolute structure parameter [Hooft]	0.03(2)
Extinction coefficient	n/a
Largest diff. peak and hole	0.38 and -0.28 e. ⁻³

Table A7.2. Atomic coordinates ($\times 10^5$) and equivalent isotropic displacement parameters ($\approx 2 \times 10^4$) for d20010. $U(eq)$ is defined as one third of the trace of the orthogonalized U^{ij} tensor.

	x	y	z	U(eq)
Si(1)	84284(6)	63687(4)	52641(3)	131(1)
O(1)	111852(17)	29694(12)	7683(7)	152(2)
O(2)	79881(18)	57572(12)	914(7)	147(2)
O(3)	38726(17)	51229(12)	1471(7)	144(2)
O(4)	38244(19)	62608(14)	12393(8)	225(3)
C(1)	82860(30)	50711(17)	60272(10)	171(3)
C(2)	99300(30)	44260(19)	63105(11)	232(4)
C(3)	98070(40)	34900(20)	68921(13)	321(5)
C(4)	80480(40)	31820(20)	72063(12)	351(6)
C(5)	63960(40)	38080(20)	69452(13)	352(5)
C(6)	65160(30)	47390(20)	63599(12)	262(4)
C(7)	110220(30)	66249(18)	50382(11)	186(4)
C(8)	73000(30)	78492(19)	56752(12)	216(4)
C(9)	70990(20)	58674(17)	43479(10)	146(3)
C(10)	54230(20)	64340(20)	41591(10)	198(3)
C(11)	79900(30)	48322(19)	38422(10)	187(4)
C(12)	69380(20)	45416(17)	30720(9)	143(3)
C(13)	78020(20)	35684(16)	24887(9)	141(3)
C(14)	71910(30)	21741(18)	25210(11)	229(4)
C(15)	99620(30)	38166(19)	22866(10)	171(3)
C(16)	93360(20)	44468(16)	14974(9)	125(3)
C(17)	96770(20)	35768(16)	8123(9)	112(3)
C(18)	81300(20)	34745(16)	1844(9)	119(3)
C(19)	80950(20)	46296(17)	-3905(9)	134(3)
C(20)	98020(20)	46930(20)	-9383(10)	186(3)
C(21)	61600(20)	43949(18)	-8193(10)	147(3)
C(22)	47800(20)	39861(16)	-1795(10)	131(3)
C(23)	43930(20)	53252(16)	8983(10)	136(3)
C(24)	60350(20)	33804(15)	4887(9)	115(3)
C(25)	55500(20)	41887(15)	12201(10)	116(3)

C(26)	72260(20)	44950(16)	17844(9)	109(3)
C(27)	69120(20)	55650(16)	24121(9)	129(3)

Table A7.3. Bond lengths [\approx] and angles [∞] for dicyclobutane **500**.

Si(1)-C(1)	1.8765(19)
Si(1)-C(7)	1.8576(18)
Si(1)-C(8)	1.8646(19)
Si(1)-C(9)	1.8736(17)
O(1)-C(17)	1.221(2)
O(2)-H(2)	0.8400
O(2)-C(19)	1.433(2)
O(3)-C(22)	1.451(2)
O(3)-C(23)	1.342(2)
O(4)-C(23)	1.201(2)
C(1)-C(2)	1.398(3)
C(1)-C(6)	1.399(3)
C(2)-H(2A)	0.9500
C(2)-C(3)	1.392(3)
C(3)-H(3)	0.9500
C(3)-C(4)	1.374(4)
C(4)-H(4)	0.9500
C(4)-C(5)	1.381(4)
C(5)-H(5)	0.9500
C(5)-C(6)	1.392(3)
C(6)-H(6)	0.9500
C(7)-H(7A)	0.9800
C(7)-H(7B)	0.9800
C(7)-H(7C)	0.9800
C(8)-H(8A)	0.9800
C(8)-H(8B)	0.9800
C(8)-H(8C)	0.9800
C(9)-C(10)	1.334(2)
C(9)-C(11)	1.514(2)
C(10)-H(10A)	0.9500
C(10)-H(10B)	0.9500
C(11)-H(11A)	0.9900
C(11)-H(11B)	0.9900
C(11)-C(12)	1.521(2)

C(12)-H(12)	1.0000
C(12)-C(13)	1.544(2)
C(12)-C(27)	1.547(2)
C(13)-C(14)	1.508(3)
C(13)-C(15)	1.558(2)
C(13)-C(26)	1.585(2)
C(14)-H(14A)	0.9800
C(14)-H(14B)	0.9800
C(14)-H(14C)	0.9800
C(15)-H(15A)	0.9900
C(15)-H(15B)	0.9900
C(15)-C(16)	1.552(2)
C(16)-H(16)	1.0000
C(16)-C(17)	1.498(2)
C(16)-C(26)	1.546(2)
C(17)-C(18)	1.505(2)
C(18)-H(18)	1.0000
C(18)-C(19)	1.549(2)
C(18)-C(24)	1.548(2)
C(19)-C(20)	1.518(2)
C(19)-C(21)	1.533(2)
C(20)-H(20A)	0.9800
C(20)-H(20B)	0.9800
C(20)-H(20C)	0.9800
C(21)-H(21A)	0.9900
C(21)-H(21B)	0.9900
C(21)-C(22)	1.521(2)
C(22)-H(22)	1.0000
C(22)-C(24)	1.554(2)
C(23)-C(25)	1.522(2)
C(24)-H(24)	1.0000
C(24)-C(25)	1.544(2)
C(25)-H(25)	1.0000
C(25)-C(26)	1.527(2)
C(26)-C(27)	1.560(2)
C(27)-H(27A)	0.9900

C(27)-H(27B)	0.9900
C(7)-Si(1)-C(1)	107.95(9)
C(7)-Si(1)-C(8)	111.74(9)
C(7)-Si(1)-C(9)	109.15(8)
C(8)-Si(1)-C(1)	107.66(9)
C(8)-Si(1)-C(9)	109.90(9)
C(9)-Si(1)-C(1)	110.42(8)
C(19)-O(2)-H(2)	109.5
C(23)-O(3)-C(22)	112.53(13)
C(2)-C(1)-Si(1)	122.14(14)
C(2)-C(1)-C(6)	116.87(18)
C(6)-C(1)-Si(1)	120.95(16)
C(1)-C(2)-H(2A)	119.3
C(3)-C(2)-C(1)	121.5(2)
C(3)-C(2)-H(2A)	119.3
C(2)-C(3)-H(3)	119.8
C(4)-C(3)-C(2)	120.3(2)
C(4)-C(3)-H(3)	119.8
C(3)-C(4)-H(4)	120.1
C(3)-C(4)-C(5)	119.8(2)
C(5)-C(4)-H(4)	120.1
C(4)-C(5)-H(5)	120.0
C(4)-C(5)-C(6)	120.0(2)
C(6)-C(5)-H(5)	120.0
C(1)-C(6)-H(6)	119.2
C(5)-C(6)-C(1)	121.6(2)
C(5)-C(6)-H(6)	119.2
Si(1)-C(7)-H(7A)	109.5
Si(1)-C(7)-H(7B)	109.5
Si(1)-C(7)-H(7C)	109.5
H(7A)-C(7)-H(7B)	109.5
H(7A)-C(7)-H(7C)	109.5
H(7B)-C(7)-H(7C)	109.5
Si(1)-C(8)-H(8A)	109.5
Si(1)-C(8)-H(8B)	109.5

Si(1)-C(8)-H(8C)	109.5
H(8A)-C(8)-H(8B)	109.5
H(8A)-C(8)-H(8C)	109.5
H(8B)-C(8)-H(8C)	109.5
C(10)-C(9)-Si(1)	119.42(13)
C(10)-C(9)-C(11)	122.28(16)
C(11)-C(9)-Si(1)	118.29(12)
C(9)-C(10)-H(10A)	120.0
C(9)-C(10)-H(10B)	120.0
H(10A)-C(10)-H(10B)	120.0
C(9)-C(11)-H(11A)	108.3
C(9)-C(11)-H(11B)	108.3
C(9)-C(11)-C(12)	116.09(15)
H(11A)-C(11)-H(11B)	107.4
C(12)-C(11)-H(11A)	108.3
C(12)-C(11)-H(11B)	108.3
C(11)-C(12)-H(12)	108.9
C(11)-C(12)-C(13)	120.12(14)
C(11)-C(12)-C(27)	119.48(15)
C(13)-C(12)-H(12)	108.9
C(13)-C(12)-C(27)	88.87(12)
C(27)-C(12)-H(12)	108.9
C(12)-C(13)-C(15)	114.57(14)
C(12)-C(13)-C(26)	89.81(12)
C(14)-C(13)-C(12)	119.49(14)
C(14)-C(13)-C(15)	115.87(15)
C(14)-C(13)-C(26)	122.86(15)
C(15)-C(13)-C(26)	87.81(12)
C(13)-C(14)-H(14A)	109.5
C(13)-C(14)-H(14B)	109.5
C(13)-C(14)-H(14C)	109.5
H(14A)-C(14)-H(14B)	109.5
H(14A)-C(14)-H(14C)	109.5
H(14B)-C(14)-H(14C)	109.5
C(13)-C(15)-H(15A)	113.6
C(13)-C(15)-H(15B)	113.6

H(15A)-C(15)-H(15B)	110.8
C(16)-C(15)-C(13)	90.41(12)
C(16)-C(15)-H(15A)	113.6
C(16)-C(15)-H(15B)	113.6
C(15)-C(16)-H(16)	112.6
C(17)-C(16)-C(15)	112.18(14)
C(17)-C(16)-H(16)	112.6
C(17)-C(16)-C(26)	115.32(13)
C(26)-C(16)-C(15)	89.42(12)
C(26)-C(16)-H(16)	112.6
O(1)-C(17)-C(16)	120.27(15)
O(1)-C(17)-C(18)	121.13(15)
C(16)-C(17)-C(18)	118.59(14)
C(17)-C(18)-H(18)	107.7
C(17)-C(18)-C(19)	113.56(13)
C(17)-C(18)-C(24)	115.02(13)
C(19)-C(18)-H(18)	107.7
C(24)-C(18)-H(18)	107.7
C(24)-C(18)-C(19)	104.83(13)
O(2)-C(19)-C(18)	105.62(13)
O(2)-C(19)-C(20)	111.44(14)
O(2)-C(19)-C(21)	110.55(13)
C(20)-C(19)-C(18)	114.76(14)
C(20)-C(19)-C(21)	113.17(14)
C(21)-C(19)-C(18)	100.60(13)
C(19)-C(20)-H(20A)	109.5
C(19)-C(20)-H(20B)	109.5
C(19)-C(20)-H(20C)	109.5
H(20A)-C(20)-H(20B)	109.5
H(20A)-C(20)-H(20C)	109.5
H(20B)-C(20)-H(20C)	109.5
C(19)-C(21)-H(21A)	110.8
C(19)-C(21)-H(21B)	110.8
H(21A)-C(21)-H(21B)	108.9
C(22)-C(21)-C(19)	104.71(13)
C(22)-C(21)-H(21A)	110.8

C(22)-C(21)-H(21B)	110.8
O(3)-C(22)-C(21)	109.16(14)
O(3)-C(22)-H(22)	111.3
O(3)-C(22)-C(24)	106.65(12)
C(21)-C(22)-H(22)	111.3
C(21)-C(22)-C(24)	106.87(13)
C(24)-C(22)-H(22)	111.3
O(3)-C(23)-C(25)	110.75(14)
O(4)-C(23)-O(3)	120.29(16)
O(4)-C(23)-C(25)	128.72(16)
C(18)-C(24)-C(22)	104.01(13)
C(18)-C(24)-H(24)	110.4
C(22)-C(24)-H(24)	110.4
C(25)-C(24)-C(18)	116.90(13)
C(25)-C(24)-C(22)	104.31(13)
C(25)-C(24)-H(24)	110.4
C(23)-C(25)-C(24)	104.41(13)
C(23)-C(25)-H(25)	105.9
C(23)-C(25)-C(26)	117.04(13)
C(24)-C(25)-H(25)	105.9
C(26)-C(25)-C(24)	116.77(13)
C(26)-C(25)-H(25)	105.9
C(16)-C(26)-C(13)	89.64(12)
C(16)-C(26)-C(27)	112.50(13)
C(25)-C(26)-C(13)	122.03(14)
C(25)-C(26)-C(16)	120.17(13)
C(25)-C(26)-C(27)	117.93(13)
C(27)-C(26)-C(13)	86.99(12)
C(12)-C(27)-C(26)	90.61(12)
C(12)-C(27)-H(27A)	113.5
C(12)-C(27)-H(27B)	113.5
C(26)-C(27)-H(27A)	113.5
C(26)-C(27)-H(27B)	113.5
H(27A)-C(27)-H(27B)	110.8

Symmetry transformations used to generate equivalent atoms:

Table A7.4. Anisotropic displacement parameters ($\approx 2 \times 10^4$) for dicyclobutane **500**. The anisotropic displacement factor exponent takes the form: $-2 \sum [h^2 a^* U^{11} + \dots + 2 h k a^* b^* U^{12}]$

	U ¹¹	U ²²	U ³³	U ²³	U ¹³	U ¹²
Si(1)	159(2)	129(2)	106(2)	-10(2)	21(2)	6(2)
O(1)	118(5)	178(6)	160(6)	-24(5)	17(4)	24(5)
O(2)	205(6)	121(5)	116(5)	10(4)	11(5)	-30(5)
O(3)	140(5)	149(6)	142(6)	-6(5)	-20(4)	22(4)
O(4)	247(6)	212(7)	214(6)	-56(6)	-47(5)	99(6)
C(1)	269(9)	143(8)	102(7)	-31(6)	9(6)	-29(7)
C(2)	332(10)	174(9)	190(9)	-5(7)	-24(7)	0(8)
C(3)	538(14)	193(10)	230(10)	32(8)	-100(9)	-2(9)
C(4)	682(17)	213(10)	157(9)	47(8)	-33(10)	-139(10)
C(5)	521(14)	326(12)	212(10)	7(9)	93(9)	-188(11)
C(6)	292(10)	287(11)	208(9)	1(8)	36(7)	-79(8)
C(7)	176(8)	190(9)	194(8)	0(7)	28(6)	-11(6)
C(8)	256(9)	181(9)	211(9)	-71(7)	48(7)	24(7)
C(9)	175(8)	169(8)	95(7)	-17(6)	25(6)	3(6)
C(10)	193(8)	259(9)	143(7)	-44(8)	24(6)	38(8)
C(11)	230(8)	212(9)	117(7)	-29(6)	-24(6)	88(7)
C(12)	176(7)	150(8)	103(7)	-8(6)	2(6)	21(6)
C(13)	200(8)	127(7)	94(7)	1(6)	-3(6)	25(6)
C(14)	380(11)	129(8)	177(9)	26(7)	11(8)	6(8)
C(15)	169(8)	224(9)	120(8)	-34(7)	-25(6)	64(7)
C(16)	117(7)	140(7)	117(7)	-24(6)	-9(5)	11(6)
C(17)	123(7)	106(7)	109(7)	10(6)	17(5)	-21(6)
C(18)	113(7)	126(7)	118(7)	-20(6)	0(5)	-2(6)
C(19)	133(7)	158(8)	110(7)	-11(6)	6(6)	-8(6)
C(20)	152(8)	286(9)	120(7)	-10(7)	19(6)	-22(7)
C(21)	147(7)	187(8)	108(7)	0(6)	-12(6)	-1(6)
C(22)	124(7)	138(7)	130(8)	-25(6)	-22(6)	-5(6)
C(23)	112(7)	145(8)	150(8)	2(6)	1(6)	-6(6)
C(24)	110(7)	110(7)	125(7)	-18(6)	4(6)	-24(5)
C(25)	113(7)	114(7)	121(7)	-7(6)	17(5)	-17(5)

C(26)	123(7)	104(7)	100(7)	-2(6)	-2(5)	9(6)
C(27)	162(8)	114(7)	110(7)	-23(6)	-5(6)	15(6)

Table A7.5. Hydrogen coordinates ($\times 10^4$) and isotropic displacement parameters ($\approx 2 \times 10^3$) for dicyclobutane **500**.

	x	y	z	U(eq)
H(2)	8157	6416	-185	22
H(2A)	11158	4631	6101	28
H(3)	10946	3063	7073	39
H(4)	7969	2541	7602	42
H(5)	5179	3604	7165	42
H(6)	5368	5158	6182	31
H(7A)	11550	5842	4802	28
H(7B)	11742	6823	5523	28
H(7C)	11141	7345	4670	28
H(8A)	7307	8535	5280	32
H(8B)	8038	8129	6140	32
H(8C)	5963	7662	5821	32
H(10A)	4744	6191	3693	24
H(10B)	4907	7080	4490	24
H(11A)	8064	4026	4152	22
H(11B)	9332	5093	3723	22
H(12)	5576	4284	3185	17
H(14A)	5777	2123	2544	34
H(14B)	7764	1767	2988	34
H(14C)	7635	1726	2051	34
H(15A)	10625	4419	2652	21
H(15B)	10726	3017	2223	21
H(16)	9907	5324	1425	15
H(18)	8391	2679	-127	14
H(20A)	9563	5356	-1337	28
H(20B)	9968	3855	-1194	28
H(20C)	10979	4908	-637	28
H(21A)	5698	5191	-1081	18
H(21B)	6288	3708	-1218	18
H(22)	3791	3362	-384	16

H(24)	5666	2459	570	14
H(25)	4617	3660	1526	14
H(27A)	7993	6189	2452	15
H(27B)	5656	6017	2353	15

Table A7.6. Torsion angles [$^{\circ}$] for dicyclobutane **500**.

Si(1)-C(1)-C(2)-C(3)	178.21(15)
Si(1)-C(1)-C(6)-C(5)	-177.84(16)
Si(1)-C(9)-C(11)-C(12)	-175.06(13)
O(1)-C(17)-C(18)-C(19)	-101.67(18)
O(1)-C(17)-C(18)-C(24)	137.55(16)
O(2)-C(19)-C(21)-C(22)	-69.88(17)
O(3)-C(22)-C(24)-C(18)	-116.84(13)
O(3)-C(22)-C(24)-C(25)	6.18(16)
O(3)-C(23)-C(25)-C(24)	11.88(17)
O(3)-C(23)-C(25)-C(26)	142.66(14)
O(4)-C(23)-C(25)-C(24)	-173.87(17)
O(4)-C(23)-C(25)-C(26)	-43.1(2)
C(1)-Si(1)-C(9)-C(10)	108.36(16)
C(1)-Si(1)-C(9)-C(11)	-72.16(15)
C(1)-C(2)-C(3)-C(4)	-0.3(3)
C(2)-C(1)-C(6)-C(5)	-0.1(3)
C(2)-C(3)-C(4)-C(5)	-0.2(3)
C(3)-C(4)-C(5)-C(6)	0.6(3)
C(4)-C(5)-C(6)-C(1)	-0.5(3)
C(6)-C(1)-C(2)-C(3)	0.5(3)
C(7)-Si(1)-C(1)-C(2)	-2.71(18)
C(7)-Si(1)-C(1)-C(6)	174.94(15)
C(7)-Si(1)-C(9)-C(10)	-133.12(15)
C(7)-Si(1)-C(9)-C(11)	46.36(16)
C(8)-Si(1)-C(1)-C(2)	-123.49(16)
C(8)-Si(1)-C(1)-C(6)	54.16(17)
C(8)-Si(1)-C(9)-C(10)	-10.26(18)
C(8)-Si(1)-C(9)-C(11)	169.22(14)
C(9)-Si(1)-C(1)-C(2)	116.53(15)
C(9)-Si(1)-C(1)-C(6)	-65.82(17)
C(9)-C(11)-C(12)-C(13)	175.87(15)
C(9)-C(11)-C(12)-C(27)	68.3(2)
C(10)-C(9)-C(11)-C(12)	4.4(3)
C(11)-C(12)-C(13)-C(14)	93.2(2)

C(11)-C(12)-C(13)-C(15)	-50.9(2)
C(11)-C(12)-C(13)-C(26)	-138.41(16)
C(11)-C(12)-C(27)-C(26)	139.19(15)
C(12)-C(13)-C(15)-C(16)	-101.10(15)
C(12)-C(13)-C(26)-C(16)	126.97(12)
C(12)-C(13)-C(26)-C(25)	-106.95(16)
C(12)-C(13)-C(26)-C(27)	14.41(12)
C(13)-C(12)-C(27)-C(26)	14.75(12)
C(13)-C(15)-C(16)-C(17)	-104.61(14)
C(13)-C(15)-C(16)-C(26)	12.62(13)
C(13)-C(26)-C(27)-C(12)	-14.38(12)
C(14)-C(13)-C(15)-C(16)	113.47(16)
C(14)-C(13)-C(26)-C(16)	-107.31(17)
C(14)-C(13)-C(26)-C(25)	18.8(2)
C(14)-C(13)-C(26)-C(27)	140.14(16)
C(15)-C(13)-C(26)-C(16)	12.37(12)
C(15)-C(13)-C(26)-C(25)	138.45(15)
C(15)-C(13)-C(26)-C(27)	-100.19(12)
C(15)-C(16)-C(17)-O(1)	-43.4(2)
C(15)-C(16)-C(17)-C(18)	136.71(15)
C(15)-C(16)-C(26)-C(13)	-12.41(13)
C(15)-C(16)-C(26)-C(25)	-139.99(15)
C(15)-C(16)-C(26)-C(27)	74.19(15)
C(16)-C(17)-C(18)-C(19)	78.18(18)
C(16)-C(17)-C(18)-C(24)	-42.6(2)
C(16)-C(26)-C(27)-C(12)	-102.75(14)
C(17)-C(16)-C(26)-C(13)	101.98(15)
C(17)-C(16)-C(26)-C(25)	-25.6(2)
C(17)-C(16)-C(26)-C(27)	-171.42(13)
C(17)-C(18)-C(19)-O(2)	-53.01(17)
C(17)-C(18)-C(19)-C(20)	70.15(18)
C(17)-C(18)-C(19)-C(21)	-168.04(13)
C(17)-C(18)-C(24)-C(22)	151.53(14)
C(17)-C(18)-C(24)-C(25)	37.2(2)
C(18)-C(19)-C(21)-C(22)	41.39(16)
C(18)-C(24)-C(25)-C(23)	103.80(15)

C(18)-C(24)-C(25)-C(26)	-27.1(2)
C(19)-C(18)-C(24)-C(22)	26.08(16)
C(19)-C(18)-C(24)-C(25)	-88.27(16)
C(19)-C(21)-C(22)-O(3)	88.93(15)
C(19)-C(21)-C(22)-C(24)	-26.05(17)
C(20)-C(19)-C(21)-C(22)	164.31(15)
C(21)-C(22)-C(24)-C(18)	-0.18(17)
C(21)-C(22)-C(24)-C(25)	122.84(14)
C(22)-O(3)-C(23)-O(4)	176.83(15)
C(22)-O(3)-C(23)-C(25)	-8.36(18)
C(22)-C(24)-C(25)-C(23)	-10.38(15)
C(22)-C(24)-C(25)-C(26)	-141.32(14)
C(23)-O(3)-C(22)-C(21)	-113.97(15)
C(23)-O(3)-C(22)-C(24)	1.16(17)
C(23)-C(25)-C(26)-C(13)	146.06(15)
C(23)-C(25)-C(26)-C(16)	-103.13(17)
C(23)-C(25)-C(26)-C(27)	40.9(2)
C(24)-C(18)-C(19)-O(2)	73.35(14)
C(24)-C(18)-C(19)-C(20)	-163.50(14)
C(24)-C(18)-C(19)-C(21)	-41.68(15)
C(24)-C(25)-C(26)-C(13)	-89.16(18)
C(24)-C(25)-C(26)-C(16)	21.6(2)
C(24)-C(25)-C(26)-C(27)	165.67(13)
C(25)-C(26)-C(27)-C(12)	110.60(15)
C(26)-C(13)-C(15)-C(16)	-12.32(12)
C(26)-C(16)-C(17)-O(1)	-143.85(16)
C(26)-C(16)-C(17)-C(18)	36.3(2)
C(27)-C(12)-C(13)-C(14)	-142.94(16)
C(27)-C(12)-C(13)-C(15)	72.99(15)
C(27)-C(12)-C(13)-C(26)	-14.51(12)

Symmetry transformations used to generate equivalent atoms:

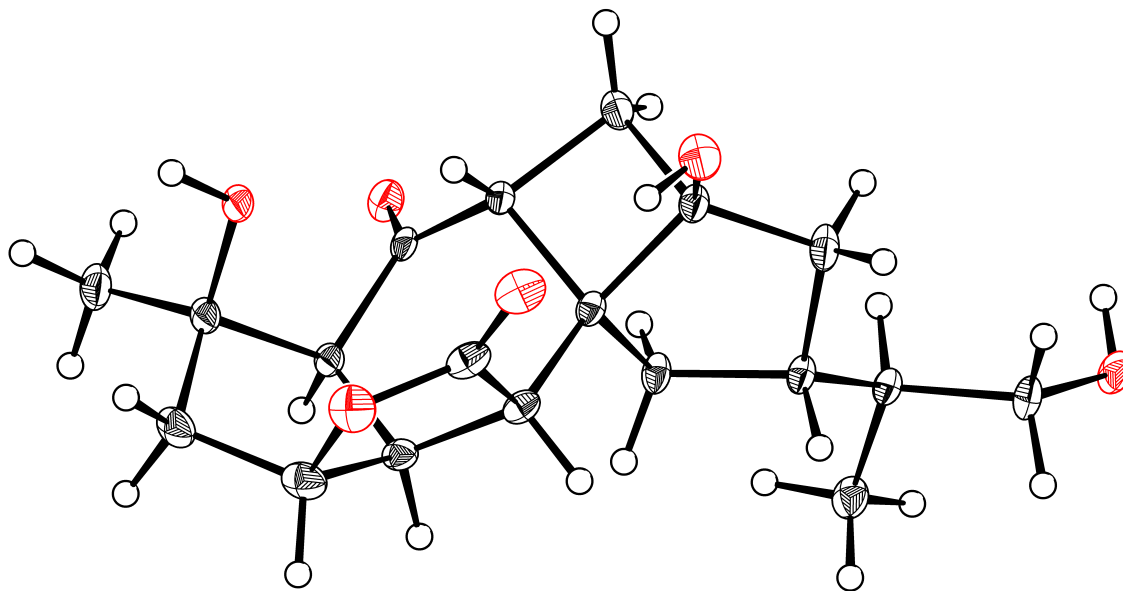
Table A7.7. Hydrogen bonds for dicyclobutane **500** [\approx and ∞].

D-H...A	d(D-H)	d(H...A)	d(D...A)	<(DHA)
O(2)-H(2)...O(1)#1	0.84	1.95	2.7880(18)	173.8

Symmetry transformations used to generate equivalent atoms:

#1 $-x+2, y+1/2, -z$

A7.3 X-RAY CRYSTAL STRUCTURE ANALYSIS FOR TRIOL 513b.

Figure A7.2. X-Ray Coordinate of Compound 513a.**Table A7.8.** Crystal data and structure refinement for triol 513a.

Identification code	d19153	
Empirical formula	C ₁₉ H ₂₆ O ₆	
Formula weight	350.40	
Temperature	100 K	
Wavelength	0.71073 Å	
Crystal system	Orthorhombic	
Space group	P2 ₁ 2 ₁ 2 ₁	
Unit cell dimensions	a = 10.221(3) Å	a = 90°
	b = 12.581(3) Å	b = 90°
	c = 13.333(4) Å	g = 90°
Volume	1714.4(8) Å ³	
Z	4	
Density (calculated)	1.358 g/cm ³	

Absorption coefficient	0.100 mm ⁻¹
F(000)	752
Crystal size	0.31 x 0.19 x 0.18 mm ³
Theta range for data collection	2.226 to 36.285°.
Index ranges	-16 ≤ h ≤ 16, -20 ≤ k ≤ 20, -22 ≤ l ≤ 22
Reflections collected	73152
Independent reflections	7997 [R(int) = 0.0477]
Completeness to theta = 25.242°	100.0 %
Absorption correction	Semi-empirical from equivalents
Max. and min. transmission	1.0000 and 0.9208
Refinement method	Full-matrix least-squares on F ²
Data / restraints / parameters	7997 / 0 / 231
Goodness-of-fit on F ²	1.069
Final R indices [I > 2σ(I)]	R1 = 0.0424, wR2 = 0.0942
R indices (all data)	R1 = 0.0592, wR2 = 0.1007
Absolute structure parameter [Flack]	0.21(16)
Absolute structure parameter [Hooft]	0.26(15)
Extinction coefficient	n/a
Largest diff. peak and hole	0.383 and -0.250 e.Å ⁻³

Table A7.9. Atomic coordinates ($\times 10^5$) and equivalent isotropic displacement parameters ($\text{\AA}^2 \times 10^4$) for triol **513a**. $U(\text{eq})$ is defined as one third of the trace of the orthogonalized U_{ij} tensor.

	x	y	z	U(eq)
O(1)	68042(10)	78131(7)	63641(8)	165(2)
O(2)	86227(11)	70321(8)	47229(8)	213(2)
O(3)	70632(11)	61684(9)	39054(7)	213(2)
O(4)	52317(11)	47286(8)	43910(8)	209(2)
O(5)	62828(10)	58461(8)	81516(7)	170(2)
O(6)	61450(11)	-568(7)	63049(8)	186(2)
C(1)	80656(12)	63996(9)	70998(9)	120(2)
C(2)	79658(13)	76259(9)	69319(10)	142(2)
C(3)	79192(15)	82417(10)	79130(11)	201(3)
C(4)	91843(14)	78776(11)	63116(11)	195(3)
C(5)	94105(14)	69305(11)	56324(11)	193(3)
C(6)	88652(12)	59459(10)	61866(9)	136(2)
C(7)	81180(12)	53340(10)	53598(9)	136(2)
C(8)	78429(13)	61948(11)	45872(10)	170(2)
C(9)	69363(12)	47732(9)	58110(9)	116(2)
C(10)	56514(13)	43122(10)	53164(10)	139(2)
C(11)	48826(13)	48194(11)	62174(10)	181(2)
C(12)	60524(12)	55734(9)	63681(9)	124(2)
C(13)	67102(12)	59314(9)	72997(9)	118(2)
C(14)	73647(13)	38142(9)	64645(9)	139(2)
C(15)	70260(13)	28115(9)	58468(9)	131(2)
C(16)	57444(15)	31051(10)	52945(11)	187(3)
C(17)	68816(13)	17984(9)	64757(9)	127(2)
C(18)	66587(14)	8454(10)	57824(10)	159(2)
C(19)	80353(15)	15980(10)	71809(10)	181(2)

Table A7.10 Bond lengths [\AA] and angles [$^\circ$] for dicyclobutane **500**

O(1)-H(1)	0.8400
O(1)-C(2)	1.4276(16)
O(2)-C(5)	1.4612(19)
O(2)-C(8)	1.3333(18)
O(3)-C(8)	1.2094(17)
O(4)-H(4)	0.8400
O(4)-C(10)	1.4075(16)
O(5)-C(13)	1.2217(15)
O(6)-H(6)	0.8400
O(6)-C(18)	1.4316(16)
C(1)-H(1A)	1.0000
C(1)-C(2)	1.5623(17)
C(1)-C(6)	1.5736(18)
C(1)-C(13)	1.5287(18)
C(2)-C(3)	1.5210(19)
C(2)-C(4)	1.528(2)
C(3)-H(3A)	0.9800
C(3)-H(3B)	0.9800
C(3)-H(3C)	0.9800
C(4)-H(4A)	0.9900
C(4)-H(4B)	0.9900
C(4)-C(5)	1.514(2)
C(5)-H(5)	1.0000
C(5)-C(6)	1.5463(18)
C(6)-H(6A)	1.0000
C(6)-C(7)	1.5464(18)
C(7)-H(7)	1.0000
C(7)-C(8)	1.5209(17)
C(7)-C(9)	1.5227(17)
C(9)-C(10)	1.5799(18)
C(9)-C(12)	1.5432(16)
C(9)-C(14)	1.5513(17)
C(10)-C(11)	1.5708(19)
C(10)-C(16)	1.5219(18)

C(11)-H(11A)	0.9900
C(11)-H(11B)	0.9900
C(11)-C(12)	1.5394(18)
C(12)-H(12)	1.0000
C(12)-C(13)	1.4825(17)
C(14)-H(14A)	0.9900
C(14)-H(14B)	0.9900
C(14)-C(15)	1.5459(17)
C(15)-H(15)	1.0000
C(15)-C(16)	1.5474(19)
C(15)-C(17)	1.5328(17)
C(16)-H(16A)	0.9900
C(16)-H(16B)	0.9900
C(17)-H(17)	1.0000
C(17)-C(18)	1.5310(17)
C(17)-C(19)	1.5290(19)
C(18)-H(18A)	0.9900
C(18)-H(18B)	0.9900
C(19)-H(19A)	0.9800
C(19)-H(19B)	0.9800
C(19)-H(19C)	0.9800
C(2)-O(1)-H(1)	109.5
C(8)-O(2)-C(5)	111.89(10)
C(10)-O(4)-H(4)	109.5
C(18)-O(6)-H(6)	109.5
C(2)-C(1)-H(1A)	107.3
C(2)-C(1)-C(6)	106.34(10)
C(6)-C(1)-H(1A)	107.3
C(13)-C(1)-H(1A)	107.3
C(13)-C(1)-C(2)	110.27(10)
C(13)-C(1)-C(6)	117.76(10)
O(1)-C(2)-C(1)	107.05(10)
O(1)-C(2)-C(3)	110.24(11)
O(1)-C(2)-C(4)	110.89(11)
C(3)-C(2)-C(1)	112.44(10)

C(3)-C(2)-C(4)	112.67(11)
C(4)-C(2)-C(1)	103.24(10)
C(2)-C(3)-H(3A)	109.5
C(2)-C(3)-H(3B)	109.5
C(2)-C(3)-H(3C)	109.5
H(3A)-C(3)-H(3B)	109.5
H(3A)-C(3)-H(3C)	109.5
H(3B)-C(3)-H(3C)	109.5
C(2)-C(4)-H(4A)	110.4
C(2)-C(4)-H(4B)	110.4
H(4A)-C(4)-H(4B)	108.6
C(5)-C(4)-C(2)	106.56(11)
C(5)-C(4)-H(4A)	110.4
C(5)-C(4)-H(4B)	110.4
O(2)-C(5)-C(4)	110.08(12)
O(2)-C(5)-H(5)	111.4
O(2)-C(5)-C(6)	105.55(11)
C(4)-C(5)-H(5)	111.4
C(4)-C(5)-C(6)	106.83(11)
C(6)-C(5)-H(5)	111.4
C(1)-C(6)-H(6A)	109.6
C(5)-C(6)-C(1)	105.44(10)
C(5)-C(6)-H(6A)	109.6
C(5)-C(6)-C(7)	103.66(10)
C(7)-C(6)-C(1)	118.41(10)
C(7)-C(6)-H(6A)	109.6
C(6)-C(7)-H(7)	109.0
C(8)-C(7)-C(6)	102.68(10)
C(8)-C(7)-H(7)	109.0
C(8)-C(7)-C(9)	116.80(11)
C(9)-C(7)-C(6)	109.92(10)
C(9)-C(7)-H(7)	109.0
O(2)-C(8)-C(7)	111.12(11)
O(3)-C(8)-O(2)	121.17(12)
O(3)-C(8)-C(7)	127.68(13)
C(7)-C(9)-C(10)	131.65(10)

C(7)-C(9)-C(12)	110.62(9)
C(7)-C(9)-C(14)	111.00(10)
C(12)-C(9)-C(10)	87.35(9)
C(12)-C(9)-C(14)	113.72(10)
C(14)-C(9)-C(10)	100.58(9)
O(4)-C(10)-C(9)	118.85(11)
O(4)-C(10)-C(11)	111.51(11)
O(4)-C(10)-C(16)	111.94(11)
C(11)-C(10)-C(9)	86.99(9)
C(16)-C(10)-C(9)	108.81(10)
C(16)-C(10)-C(11)	116.83(12)
C(10)-C(11)-H(11A)	114.0
C(10)-C(11)-H(11B)	114.0
H(11A)-C(11)-H(11B)	111.2
C(12)-C(11)-C(10)	87.80(10)
C(12)-C(11)-H(11A)	114.0
C(12)-C(11)-H(11B)	114.0
C(9)-C(12)-H(12)	108.2
C(11)-C(12)-C(9)	89.41(9)
C(11)-C(12)-H(12)	108.2
C(13)-C(12)-C(9)	109.63(10)
C(13)-C(12)-C(11)	130.45(11)
C(13)-C(12)-H(12)	108.2
O(5)-C(13)-C(1)	121.33(11)
O(5)-C(13)-C(12)	126.17(12)
C(12)-C(13)-C(1)	112.45(10)
C(9)-C(14)-H(14A)	110.6
C(9)-C(14)-H(14B)	110.6
H(14A)-C(14)-H(14B)	108.7
C(15)-C(14)-C(9)	105.80(9)
C(15)-C(14)-H(14A)	110.6
C(15)-C(14)-H(14B)	110.6
C(14)-C(15)-H(15)	108.7
C(14)-C(15)-C(16)	104.37(10)
C(16)-C(15)-H(15)	108.7
C(17)-C(15)-C(14)	114.12(10)

C(17)-C(15)-H(15)	108.7
C(17)-C(15)-C(16)	112.17(11)
C(10)-C(16)-C(15)	106.38(11)
C(10)-C(16)-H(16A)	110.5
C(10)-C(16)-H(16B)	110.5
C(15)-C(16)-H(16A)	110.5
C(15)-C(16)-H(16B)	110.5
H(16A)-C(16)-H(16B)	108.6
C(15)-C(17)-H(17)	107.5
C(18)-C(17)-C(15)	109.58(10)
C(18)-C(17)-H(17)	107.5
C(19)-C(17)-C(15)	113.53(11)
C(19)-C(17)-H(17)	107.5
C(19)-C(17)-C(18)	110.91(10)
O(6)-C(18)-C(17)	112.44(10)
O(6)-C(18)-H(18A)	109.1
O(6)-C(18)-H(18B)	109.1
C(17)-C(18)-H(18A)	109.1
C(17)-C(18)-H(18B)	109.1
H(18A)-C(18)-H(18B)	107.8
C(17)-C(19)-H(19A)	109.5
C(17)-C(19)-H(19B)	109.5
C(17)-C(19)-H(19C)	109.5
H(19A)-C(19)-H(19B)	109.5
H(19A)-C(19)-H(19C)	109.5
H(19B)-C(19)-H(19C)	109.5

Symmetry transformations used to generate equivalent atoms:

Table A7.11. Anisotropic displacement parameters ($\text{\AA}^2 \times 10^4$) for triol **513a**. The anisotropic displacement factor exponent takes the form: $-2p^2 [h^2 a^{*2} U^{11} + \dots + 2 h k a^* b^* U^{12}]$.

	U^{11}	U^{22}	U^{33}	U^{23}	U^{13}	U^{12}
O(1)	160(4)	78(3)	256(4)	18(3)	-73(4)	14(3)
O(2)	247(5)	195(5)	197(4)	86(4)	30(4)	-22(4)
O(3)	248(5)	234(5)	155(4)	65(4)	9(4)	49(4)
O(4)	240(5)	171(5)	217(5)	47(4)	-100(4)	13(4)
O(5)	207(5)	140(4)	162(4)	-7(3)	37(3)	-6(3)
O(6)	220(5)	90(4)	246(5)	18(3)	38(4)	9(3)
C(1)	129(5)	80(4)	150(5)	16(4)	-14(4)	3(4)
C(2)	145(5)	78(4)	203(5)	26(4)	-39(4)	-7(4)
C(3)	249(7)	106(5)	248(6)	-17(4)	-65(5)	-1(5)
C(4)	164(6)	138(5)	281(7)	57(5)	-14(5)	-46(4)
C(5)	148(6)	190(6)	241(6)	75(5)	30(5)	-21(5)
C(6)	119(5)	118(5)	171(5)	28(4)	6(4)	15(4)
C(7)	150(5)	119(5)	137(5)	24(4)	14(4)	37(4)
C(8)	183(6)	165(5)	161(5)	45(4)	60(4)	45(5)
C(9)	146(5)	88(4)	113(4)	2(4)	-10(4)	13(4)
C(10)	175(5)	99(5)	144(5)	-7(4)	-40(4)	12(4)
C(11)	159(5)	160(6)	224(6)	-54(5)	21(5)	-41(5)
C(12)	124(5)	96(5)	150(5)	-16(4)	10(4)	-5(4)
C(13)	138(5)	61(4)	156(5)	-1(4)	9(4)	7(4)
C(14)	199(6)	82(4)	137(5)	6(4)	-40(4)	6(4)
C(15)	180(5)	83(4)	131(5)	-6(4)	-18(4)	9(4)
C(16)	260(7)	97(5)	205(6)	-18(4)	-106(5)	11(5)
C(17)	164(5)	83(4)	135(5)	-1(4)	-2(4)	8(4)
C(18)	225(6)	89(5)	164(5)	-17(4)	14(5)	-7(4)
C(19)	215(6)	127(5)	201(6)	14(4)	-43(5)	19(5)

Table A7.12. Hydrogen coordinates ($\times 10^4$) and isotropic displacement parameters ($\text{\AA}^2 \times 10^{-3}$) for dicyclobutane **500**.

	x	y	z	U(eq)
H(1)	6684	8471	6306	25
H(4)	5784	5170	4181	31
H(6)	5423	103	6566	28
H(1A)	8603	6283	7717	14
H(3A)	7789	8999	7771	30
H(3B)	8745	8144	8275	30
H(3C)	7194	7979	8324	30
H(4A)	9046	8529	5909	23
H(4B)	9948	7989	6756	23
H(5)	10360	6843	5470	23
H(6A)	9606	5501	6439	16
H(7)	8714	4791	5058	16
H(11A)	4063	5183	6019	22
H(11B)	4732	4326	6784	22
H(12)	5924	6206	5925	15
H(14A)	8315	3845	6603	17
H(14B)	6887	3812	7111	17
H(15)	7729	2696	5337	16
H(16A)	5768	2845	4594	22
H(16B)	4982	2784	5637	22
H(17)	6081	1881	6899	15
H(18A)	6042	1052	5244	19
H(18B)	7499	647	5464	19
H(19A)	7913	917	7525	27
H(19B)	8084	2171	7677	27
H(19C)	8849	1578	6792	27

Table A7.13. Torsion angles [$^{\circ}$] for triol **513a**.

O(1)-C(2)-C(4)-C(5)	-79.58(13)
O(2)-C(5)-C(6)-C(1)	-105.80(11)
O(2)-C(5)-C(6)-C(7)	19.30(13)
O(4)-C(10)-C(11)-C(12)	-98.40(12)
O(4)-C(10)-C(16)-C(15)	137.74(11)
C(1)-C(2)-C(4)-C(5)	34.76(13)
C(1)-C(6)-C(7)-C(8)	94.36(12)
C(1)-C(6)-C(7)-C(9)	-30.62(14)
C(2)-C(1)-C(6)-C(5)	9.99(13)
C(2)-C(1)-C(6)-C(7)	-105.35(12)
C(2)-C(1)-C(13)-O(5)	-91.19(14)
C(2)-C(1)-C(13)-C(12)	91.19(12)
C(2)-C(4)-C(5)-O(2)	84.92(13)
C(2)-C(4)-C(5)-C(6)	-29.20(14)
C(3)-C(2)-C(4)-C(5)	156.31(11)
C(4)-C(5)-C(6)-C(1)	11.36(14)
C(4)-C(5)-C(6)-C(7)	136.46(11)
C(5)-O(2)-C(8)-O(3)	175.54(12)
C(5)-O(2)-C(8)-C(7)	-6.18(15)
C(5)-C(6)-C(7)-C(8)	-21.94(12)
C(5)-C(6)-C(7)-C(9)	-146.91(10)
C(6)-C(1)-C(2)-O(1)	89.94(12)
C(6)-C(1)-C(2)-C(3)	-148.85(11)
C(6)-C(1)-C(2)-C(4)	-27.15(13)
C(6)-C(1)-C(13)-O(5)	146.60(12)
C(6)-C(1)-C(13)-C(12)	-31.03(14)
C(6)-C(7)-C(8)-O(2)	18.23(13)
C(6)-C(7)-C(8)-O(3)	-163.63(13)
C(6)-C(7)-C(9)-C(10)	161.05(11)
C(6)-C(7)-C(9)-C(12)	55.47(12)
C(6)-C(7)-C(9)-C(14)	-71.76(12)
C(7)-C(9)-C(10)-O(4)	-24.01(18)
C(7)-C(9)-C(10)-C(11)	-136.98(13)

C(7)-C(9)-C(10)-C(16)	105.66(14)
C(7)-C(9)-C(12)-C(11)	155.80(10)
C(7)-C(9)-C(12)-C(13)	-70.95(12)
C(7)-C(9)-C(14)-C(15)	-106.00(11)
C(8)-O(2)-C(5)-C(4)	-123.70(12)
C(8)-O(2)-C(5)-C(6)	-8.76(15)
C(8)-C(7)-C(9)-C(10)	44.64(17)
C(8)-C(7)-C(9)-C(12)	-60.94(14)
C(8)-C(7)-C(9)-C(14)	171.83(10)
C(9)-C(7)-C(8)-O(2)	138.56(11)
C(9)-C(7)-C(8)-O(3)	-43.30(18)
C(9)-C(10)-C(11)-C(12)	21.52(9)
C(9)-C(10)-C(16)-C(15)	4.37(15)
C(9)-C(12)-C(13)-O(5)	-121.85(13)
C(9)-C(12)-C(13)-C(1)	55.64(13)
C(9)-C(14)-C(15)-C(16)	-35.43(13)
C(9)-C(14)-C(15)-C(17)	-158.22(11)
C(10)-C(9)-C(12)-C(11)	21.90(9)
C(10)-C(9)-C(12)-C(13)	155.15(10)
C(10)-C(9)-C(14)-C(15)	36.73(12)
C(10)-C(11)-C(12)-C(9)	-22.02(9)
C(10)-C(11)-C(12)-C(13)	-137.67(13)
C(11)-C(10)-C(16)-C(15)	-91.96(14)
C(11)-C(12)-C(13)-O(5)	-15.0(2)
C(11)-C(12)-C(13)-C(1)	162.49(12)
C(12)-C(9)-C(10)-O(4)	91.51(12)
C(12)-C(9)-C(10)-C(11)	-21.47(9)
C(12)-C(9)-C(10)-C(16)	-138.83(11)
C(12)-C(9)-C(14)-C(15)	128.49(11)
C(13)-C(1)-C(2)-O(1)	-38.79(13)
C(13)-C(1)-C(2)-C(3)	82.43(13)
C(13)-C(1)-C(2)-C(4)	-155.87(10)
C(13)-C(1)-C(6)-C(5)	134.19(11)
C(13)-C(1)-C(6)-C(7)	18.86(15)
C(14)-C(9)-C(10)-O(4)	-154.85(11)
C(14)-C(9)-C(10)-C(11)	92.17(10)

C(14)-C(9)-C(10)-C(16)	-25.19(13)
C(14)-C(9)-C(12)-C(11)	-78.49(12)
C(14)-C(9)-C(12)-C(13)	54.76(13)
C(14)-C(15)-C(16)-C(10)	18.65(14)
C(14)-C(15)-C(17)-C(18)	-175.42(11)
C(14)-C(15)-C(17)-C(19)	-50.80(15)
C(15)-C(17)-C(18)-O(6)	-163.03(11)
C(16)-C(10)-C(11)-C(12)	131.10(12)
C(16)-C(15)-C(17)-C(18)	66.15(14)
C(16)-C(15)-C(17)-C(19)	-169.23(11)
C(17)-C(15)-C(16)-C(10)	142.70(11)
C(19)-C(17)-C(18)-O(6)	70.85(15)

Symmetry transformations used to generate equivalent atoms:

Table A7.14. Hydrogen bonds for triol **513a**.

D-H...A	d(D-H)	d(H...A)	d(D...A)	<(DHA)
O(1)-H(1)...O(6)#1	0.84	1.93	2.7645(15)	170.3
O(4)-H(4)...O(3)	0.84	1.85	2.6841(17)	172.0
O(6)-H(6)...O(5)#2	0.84	2.01	2.8235(16)	161.6

Symmetry transformations used to generate equivalent atoms:

#1 $x, y+1, z$ #2 $-x+1, y-1/2, -z+3/2$

A7.3 X-RAY CRYSTAL STRUCTURE ANALYSIS FOR TRIOL 513b.

Figure A7.3. X-ray Crystal Structure for 513b.

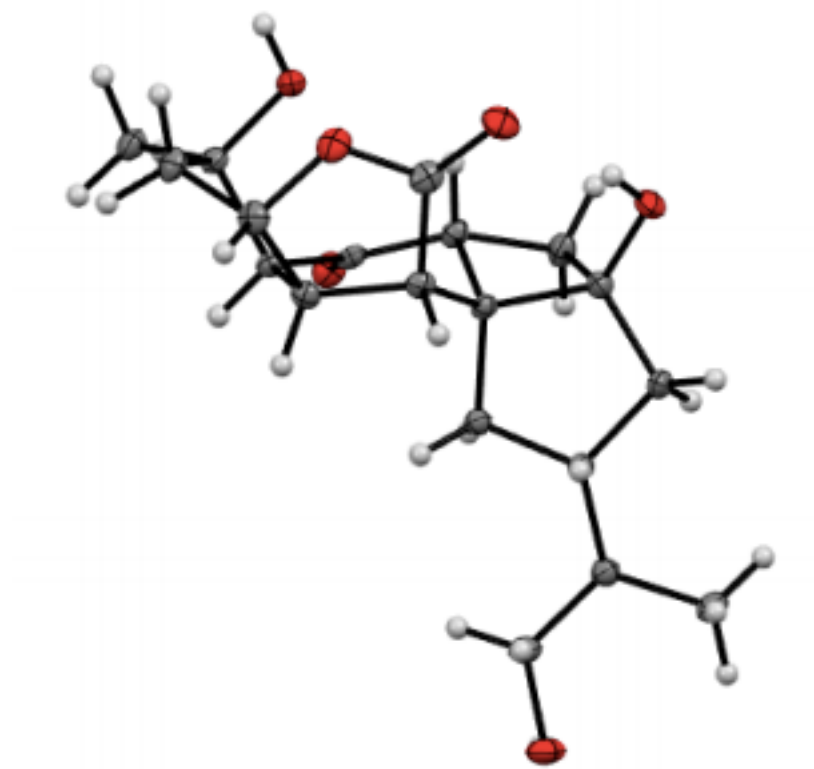


Table A7.15. X-Ray Coordinate of Compound 513b.

Identification code	V20005	
Empirical formula	C ₁₉ H ₃₂ O ₉	
Formula weight	404.44	
Temperature	100(2) K	
Wavelength	1.54178 \approx	
Crystal system	Orthorhombic	
Space group	P2 ₁ 2 ₁ 2 ₁	
Unit cell dimensions	a = 9.0245(13) \approx	$\alpha = 90^\circ$.
	b = 13.383(2) \approx	$\beta = 90^\circ$.
	c = 16.329(3) \approx	$\gamma = 90^\circ$.
Volume	1972.1(5) \approx^3	
Z	4	
Density (calculated)	1.362 Mg/m ³	
Absorption coefficient	0.906 mm ⁻¹	

F(000)	872
Crystal size	0.600 x 0.300 x 0.150 mm ³
Theta range for data collection	4.271 to 74.810°.
Index ranges	-11 ≤ h ≤ 10, -16 ≤ k ≤ 15, -19 ≤ l ≤ 20
Reflections collected	20468
Independent reflections	4017 [R(int) = 0.0461]
Completeness to theta = 67.679°	99.7 %
Absorption correction	Semi-empirical from equivalents
Max. and min. transmission	0.7538 and 0.5503
Refinement method	Full-matrix least-squares on F ²
Data / restraints / parameters	4017 / 9 / 282
Goodness-of-fit on F ²	1.087
Final R indices [I > 2σ(I)]	R1 = 0.0314, wR2 = 0.0874
R indices (all data)	R1 = 0.0315, wR2 = 0.0875
Absolute structure parameter	0.06(4)
Extinction coefficient	n/a
Largest diff. peak and hole	0.342 and -0.300 e. ⁻³

Table A7.16 Atomic coordinates ($\times 10^5$) and equivalent isotropic displacement parameters ($\approx 2 \times 10^4$) for triol **513b**. $U(\text{eq})$ is defined as one third of the trace of the orthogonalized U_{ij} tensor

	x	y	z	$U(\text{eq})$
O(1)	7488(2)	5070(1)	8786(1)	20(1)
C(1)	6251(2)	5178(1)	8340(1)	17(1)
O(2)	5331(2)	5794(1)	8528(1)	23(1)
C(2)	6244(2)	4454(1)	7623(1)	14(1)
C(3)	4778(2)	3952(1)	7419(1)	12(1)
C(4)	4938(2)	3335(1)	6621(1)	14(1)
C(5)	4168(2)	3973(1)	5960(1)	14(1)
C(6)	2780(2)	4388(1)	6396(1)	16(1)
C(16)	3800(2)	3404(1)	5169(1)	16(1)
C(17)	5215(2)	3010(1)	4767(1)	19(1)
O(3)	4944(2)	2495(1)	4010(1)	22(1)
C(18)	2929(2)	4059(2)	4575(1)	22(1)
C(7)	3164(2)	4383(1)	7305(1)	14(1)
O(4)	2807(2)	5300(1)	7691(1)	21(1)
C(8)	2599(2)	3462(1)	7821(1)	18(1)
C(9)	4188(2)	3370(1)	8165(1)	14(1)
C(10)	5111(2)	2472(1)	8330(1)	13(1)
O(5)	4650(1)	1619(1)	8426(1)	18(1)
C(11)	6770(2)	2710(1)	8379(1)	13(1)
C(12)	7370(2)	3649(1)	7898(1)	14(1)
C(13)	8371(2)	4213(1)	8507(1)	18(1)
C(14)	8646(2)	3502(2)	9217(1)	18(1)
C(15)	7232(2)	2868(1)	9288(1)	14(1)
O(6)	6066(1)	3429(1)	9662(1)	17(1)
C(19)	7469(2)	1889(1)	9746(1)	19(1)
O(1W)	4785(2)	3561(1)	2568(1)	28(1)
O(2W)	6663(2)	3854(1)	1302(1)	21(1)
O(3W)	3494(2)	756(1)	4427(1)	36(1)

Table A7.17 Bond lengths [\approx] and angles [∞] for dicyclobutane **513b**

O(1)-C(1)	1.340(2)
O(1)-C(13)	1.469(2)
C(1)-O(2)	1.210(2)
C(1)-C(2)	1.520(2)
C(2)-C(3)	1.521(2)
C(2)-C(12)	1.549(2)
C(2)-H(2)	1.0000
C(3)-C(9)	1.541(2)
C(3)-C(4)	1.549(2)
C(3)-C(7)	1.578(2)
C(4)-C(5)	1.542(2)
C(4)-H(4A)	0.9900
C(4)-H(4B)	0.9900
C(5)-C(16)	1.536(2)
C(5)-C(6)	1.544(2)
C(5)-H(5)	1.0000
C(6)-C(7)	1.525(2)
C(6)-H(6A)	0.9900
C(6)-H(6B)	0.9900
C(16)-C(18)	1.525(3)
C(16)-C(17)	1.529(3)
C(16)-H(16)	1.0000
C(17)-O(3)	1.436(2)
C(17)-H(17A)	0.9900
C(17)-H(17B)	0.9900
O(3)-H(3O)	0.80(2)
C(18)-H(18A)	0.9800
C(18)-H(18B)	0.9800
C(18)-H(18C)	0.9800
C(7)-O(4)	1.417(2)
C(7)-C(8)	1.577(2)
O(4)-H(4O)	0.82(2)
C(8)-C(9)	1.545(2)
C(8)-H(8A)	0.9900

C(8)-H(8B)	0.9900
C(9)-C(10)	1.486(2)
C(9)-H(9)	1.0000
C(10)-O(5)	1.226(2)
C(10)-C(11)	1.533(2)
C(11)-C(15)	1.557(2)
C(11)-C(12)	1.577(2)
C(11)-H(11)	1.0000
C(12)-C(13)	1.541(2)
C(12)-H(12)	1.0000
C(13)-C(14)	1.520(3)
C(13)-H(13)	1.0000
C(14)-C(15)	1.536(2)
C(14)-H(14A)	0.9900
C(14)-H(14B)	0.9900
C(15)-O(6)	1.430(2)
C(15)-C(19)	1.523(2)
O(6)-H(6O)	0.85(2)
C(19)-H(19A)	0.9800
C(19)-H(19B)	0.9800
C(19)-H(19C)	0.9800
O(1W)-H(1W1)	0.85(2)
O(1W)-H(1W2)	0.85(2)
O(2W)-H(2W1)	0.84(2)
O(2W)-H(2W2)	0.86(2)
O(3W)-H(3W1)	0.84(2)
O(3W)-H(3W2)	0.87(2)
C(1)-O(1)-C(13)	111.53(14)
O(2)-C(1)-O(1)	120.48(17)
O(2)-C(1)-C(2)	128.76(17)
O(1)-C(1)-C(2)	110.76(15)
C(1)-C(2)-C(3)	117.03(14)
C(1)-C(2)-C(12)	102.49(14)
C(3)-C(2)-C(12)	109.07(14)
C(1)-C(2)-H(2)	109.3

C(3)-C(2)-H(2)	109.3
C(12)-C(2)-H(2)	109.3
C(2)-C(3)-C(9)	110.52(13)
C(2)-C(3)-C(4)	109.79(14)
C(9)-C(3)-C(4)	115.36(14)
C(2)-C(3)-C(7)	131.85(15)
C(9)-C(3)-C(7)	87.64(13)
C(4)-C(3)-C(7)	100.48(13)
C(5)-C(4)-C(3)	104.57(13)
C(5)-C(4)-H(4A)	110.8
C(3)-C(4)-H(4A)	110.8
C(5)-C(4)-H(4B)	110.8
C(3)-C(4)-H(4B)	110.8
H(4A)-C(4)-H(4B)	108.9
C(16)-C(5)-C(4)	114.32(15)
C(16)-C(5)-C(6)	113.02(15)
C(4)-C(5)-C(6)	103.99(13)
C(16)-C(5)-H(5)	108.4
C(4)-C(5)-H(5)	108.4
C(6)-C(5)-H(5)	108.4
C(7)-C(6)-C(5)	105.26(14)
C(7)-C(6)-H(6A)	110.7
C(5)-C(6)-H(6A)	110.7
C(7)-C(6)-H(6B)	110.7
C(5)-C(6)-H(6B)	110.7
H(6A)-C(6)-H(6B)	108.8
C(18)-C(16)-C(17)	110.89(15)
C(18)-C(16)-C(5)	111.16(15)
C(17)-C(16)-C(5)	110.59(15)
C(18)-C(16)-H(16)	108.0
C(17)-C(16)-H(16)	108.0
C(5)-C(16)-H(16)	108.0
O(3)-C(17)-C(16)	113.11(16)
O(3)-C(17)-H(17A)	109.0
C(16)-C(17)-H(17A)	109.0
O(3)-C(17)-H(17B)	109.0

C(16)-C(17)-H(17B)	109.0
H(17A)-C(17)-H(17B)	107.8
C(17)-O(3)-H(3O)	104(2)
C(16)-C(18)-H(18A)	109.5
C(16)-C(18)-H(18B)	109.5
H(18A)-C(18)-H(18B)	109.5
C(16)-C(18)-H(18C)	109.5
H(18A)-C(18)-H(18C)	109.5
H(18B)-C(18)-H(18C)	109.5
O(4)-C(7)-C(6)	112.16(15)
O(4)-C(7)-C(8)	111.50(14)
C(6)-C(7)-C(8)	116.74(15)
O(4)-C(7)-C(3)	118.31(15)
C(6)-C(7)-C(3)	109.03(14)
C(8)-C(7)-C(3)	87.12(13)
C(7)-O(4)-H(4O)	112(2)
C(9)-C(8)-C(7)	87.50(13)
C(9)-C(8)-H(8A)	114.1
C(7)-C(8)-H(8A)	114.1
C(9)-C(8)-H(8B)	114.1
C(7)-C(8)-H(8B)	114.1
H(8A)-C(8)-H(8B)	111.3
C(10)-C(9)-C(3)	110.97(14)
C(10)-C(9)-C(8)	130.51(16)
C(3)-C(9)-C(8)	89.58(12)
C(10)-C(9)-H(9)	107.7
C(3)-C(9)-H(9)	107.7
C(8)-C(9)-H(9)	107.7
O(5)-C(10)-C(9)	125.92(16)
O(5)-C(10)-C(11)	121.20(16)
C(9)-C(10)-C(11)	112.88(15)
C(10)-C(11)-C(15)	109.83(13)
C(10)-C(11)-C(12)	118.35(14)
C(15)-C(11)-C(12)	105.90(13)
C(10)-C(11)-H(11)	107.4
C(15)-C(11)-H(11)	107.4

C(12)-C(11)-H(11)	107.4
C(13)-C(12)-C(2)	103.35(14)
C(13)-C(12)-C(11)	105.74(13)
C(2)-C(12)-C(11)	118.28(14)
C(13)-C(12)-H(12)	109.7
C(2)-C(12)-H(12)	109.7
C(11)-C(12)-H(12)	109.7
O(1)-C(13)-C(14)	109.94(15)
O(1)-C(13)-C(12)	105.36(14)
C(14)-C(13)-C(12)	106.27(14)
O(1)-C(13)-H(13)	111.7
C(14)-C(13)-H(13)	111.7
C(12)-C(13)-H(13)	111.7
C(13)-C(14)-C(15)	105.55(14)
C(13)-C(14)-H(14A)	110.6
C(15)-C(14)-H(14A)	110.6
C(13)-C(14)-H(14B)	110.6
C(15)-C(14)-H(14B)	110.6
H(14A)-C(14)-H(14B)	108.8
O(6)-C(15)-C(19)	110.20(15)
O(6)-C(15)-C(14)	110.70(14)
C(19)-C(15)-C(14)	113.33(14)
O(6)-C(15)-C(11)	106.36(13)
C(19)-C(15)-C(11)	112.85(15)
C(14)-C(15)-C(11)	103.01(14)
C(15)-O(6)-H(6O)	109.5(19)
C(15)-C(19)-H(19A)	109.5
C(15)-C(19)-H(19B)	109.5
H(19A)-C(19)-H(19B)	109.5
C(15)-C(19)-H(19C)	109.5
H(19A)-C(19)-H(19C)	109.5
H(19B)-C(19)-H(19C)	109.5
H(1W1)-O(1W)-H(1W2)	103(3)
H(2W1)-O(2W)-H(2W2)	105(3)
H(3W1)-O(3W)-H(3W2)	111(3)

Symmetry transformations used to generate equivalent atoms:

Table A7.18. Anisotropic displacement parameters ($\text{\AA}^2 \times 10^4$) for triol **513b**. The anisotropic displacement factor exponent takes the form: $-2 \pi^2 [h^2 a^{*2} U^{11} + 2 h k a^* b^* U^{12} + \dots]$

	U ¹¹	U ²²	U ³³	U ²³	U ¹³	U ¹²
O(1)	22(1)	15(1)	22(1)	-2(1)	-5(1)	-4(1)
C(1)	22(1)	11(1)	18(1)	2(1)	-1(1)	-5(1)
O(2)	28(1)	16(1)	25(1)	-5(1)	0(1)	1(1)
C(2)	16(1)	12(1)	13(1)	2(1)	2(1)	-1(1)
C(3)	14(1)	12(1)	10(1)	2(1)	0(1)	0(1)
C(4)	17(1)	14(1)	12(1)	0(1)	0(1)	2(1)
C(5)	18(1)	13(1)	11(1)	1(1)	-1(1)	2(1)
C(6)	19(1)	18(1)	13(1)	2(1)	-1(1)	6(1)
C(16)	18(1)	16(1)	13(1)	0(1)	-1(1)	0(1)
C(17)	23(1)	21(1)	13(1)	-3(1)	0(1)	2(1)
O(3)	34(1)	19(1)	13(1)	-3(1)	2(1)	1(1)
C(18)	28(1)	25(1)	14(1)	0(1)	-4(1)	5(1)
C(7)	15(1)	15(1)	14(1)	0(1)	1(1)	2(1)
O(4)	21(1)	22(1)	21(1)	-8(1)	-2(1)	7(1)
C(8)	14(1)	23(1)	17(1)	5(1)	0(1)	-1(1)
C(9)	14(1)	15(1)	12(1)	3(1)	-1(1)	-2(1)
C(10)	16(1)	15(1)	8(1)	1(1)	-1(1)	-2(1)
O(5)	20(1)	15(1)	20(1)	4(1)	-1(1)	-4(1)
C(11)	14(1)	14(1)	11(1)	1(1)	0(1)	-1(1)
C(12)	13(1)	15(1)	15(1)	1(1)	2(1)	-2(1)
C(13)	15(1)	18(1)	21(1)	0(1)	-1(1)	-3(1)
C(14)	14(1)	21(1)	20(1)	0(1)	-5(1)	-2(1)
C(15)	15(1)	16(1)	13(1)	-1(1)	-3(1)	0(1)
O(6)	17(1)	20(1)	13(1)	-2(1)	-1(1)	4(1)
C(19)	21(1)	19(1)	16(1)	3(1)	-4(1)	1(1)
O(1W)	25(1)	39(1)	20(1)	9(1)	5(1)	12(1)
O(2W)	22(1)	26(1)	16(1)	0(1)	-1(1)	6(1)
O(3W)	61(1)	22(1)	25(1)	0(1)	8(1)	-2(1)

Table A7.19. Hydrogen coordinates ($\times 10^4$) and isotropic displacement parameters ($\text{\AA}^2 \times 10^3$) for dicyclobutane **513b**.

	x	y	z	U(eq)
H(2)	6630	4801	7124	16
H(4A)	5995	3229	6485	17
H(4B)	4448	2676	6677	17
H(5)	4831	4546	5819	17
H(6A)	2559	5075	6207	20
H(6B)	1908	3959	6287	20
H(16)	3168	2818	5316	19
H(17A)	5892	3578	4662	22
H(17B)	5717	2549	5152	22
H(3O)	4480(30)	2009(19)	4146(18)	33
H(18A)	2013	4285	4839	33
H(18B)	2685	3673	4084	33
H(18C)	3528	4640	4422	33
H(4O)	3520(30)	5530(20)	7947(16)	31
H(8A)	1843	3633	8237	22
H(8B)	2282	2884	7485	22
H(9)	4262	3819	8653	16
H(11)	7318	2112	8171	16
H(12)	7970	3424	7418	17
H(13)	9319	4431	8245	22
H(14A)	8825	3878	9729	22
H(14B)	9516	3073	9105	22
H(6O)	6270(30)	3525(19)	10162(13)	25
H(19A)	7686	2030	10322	28
H(19B)	8302	1527	9501	28
H(19C)	6570	1480	9708	28
H(1W1)	4840(40)	3250(20)	3020(15)	42
H(1W2)	4070(30)	3960(20)	2643(19)	42
H(2W1)	6130(30)	3730(20)	1714(15)	32
H(2W2)	7530(30)	3640(20)	1429(17)	32

H(3W1)	3680(40)	690(30)	4929(15)	54
H(3W2)	3500(40)	174(19)	4180(20)	54

Table A7.20. Torsion angles [$^{\circ}$] for dicyclobutane **513b**

C(13)-O(1)-C(1)-O(2)	173.80(17)
C(13)-O(1)-C(1)-C(2)	-6.71(19)
O(2)-C(1)-C(2)-C(3)	-40.9(3)
O(1)-C(1)-C(2)-C(3)	139.63(15)
O(2)-C(1)-C(2)-C(12)	-160.19(19)
O(1)-C(1)-C(2)-C(12)	20.37(18)
C(1)-C(2)-C(3)-C(9)	-57.69(19)
C(12)-C(2)-C(3)-C(9)	57.98(18)
C(1)-C(2)-C(3)-C(4)	173.93(14)
C(12)-C(2)-C(3)-C(4)	-70.40(17)
C(1)-C(2)-C(3)-C(7)	48.3(2)
C(12)-C(2)-C(3)-C(7)	164.02(16)
C(2)-C(3)-C(4)-C(5)	-103.66(16)
C(9)-C(3)-C(4)-C(5)	130.68(15)
C(7)-C(3)-C(4)-C(5)	38.30(16)
C(3)-C(4)-C(5)-C(16)	-164.03(14)
C(3)-C(4)-C(5)-C(6)	-40.33(17)
C(16)-C(5)-C(6)-C(7)	149.27(15)
C(4)-C(5)-C(6)-C(7)	24.73(18)
C(4)-C(5)-C(16)-C(18)	175.24(16)
C(6)-C(5)-C(16)-C(18)	56.5(2)
C(4)-C(5)-C(16)-C(17)	-61.13(19)
C(6)-C(5)-C(16)-C(17)	-179.83(15)
C(18)-C(16)-C(17)-O(3)	-54.5(2)
C(5)-C(16)-C(17)-O(3)	-178.33(15)
C(5)-C(6)-C(7)-O(4)	132.31(15)
C(5)-C(6)-C(7)-C(8)	-97.27(17)
C(5)-C(6)-C(7)-C(3)	-0.71(19)
C(2)-C(3)-C(7)-O(4)	-24.0(3)
C(9)-C(3)-C(7)-O(4)	91.77(16)
C(4)-C(3)-C(7)-O(4)	-152.87(15)
C(2)-C(3)-C(7)-C(6)	105.8(2)
C(9)-C(3)-C(7)-C(6)	-138.51(15)
C(4)-C(3)-C(7)-C(6)	-23.14(17)

C(2)-C(3)-C(7)-C(8)	-136.90(18)
C(9)-C(3)-C(7)-C(8)	-21.17(12)
C(4)-C(3)-C(7)-C(8)	94.19(13)
O(4)-C(7)-C(8)-C(9)	-98.27(15)
C(6)-C(7)-C(8)-C(9)	131.00(15)
C(3)-C(7)-C(8)-C(9)	21.11(12)
C(2)-C(3)-C(9)-C(10)	-70.31(18)
C(4)-C(3)-C(9)-C(10)	54.98(19)
C(7)-C(3)-C(9)-C(10)	155.46(14)
C(2)-C(3)-C(9)-C(8)	155.83(15)
C(4)-C(3)-C(9)-C(8)	-78.88(16)
C(7)-C(3)-C(9)-C(8)	21.60(13)
C(7)-C(8)-C(9)-C(10)	-139.29(18)
C(7)-C(8)-C(9)-C(3)	-21.61(13)
C(3)-C(9)-C(10)-O(5)	-129.31(18)
C(8)-C(9)-C(10)-O(5)	-20.8(3)
C(3)-C(9)-C(10)-C(11)	51.09(19)
C(8)-C(9)-C(10)-C(11)	159.58(16)
O(5)-C(10)-C(11)-C(15)	-84.3(2)
C(9)-C(10)-C(11)-C(15)	95.36(17)
O(5)-C(10)-C(11)-C(12)	154.02(16)
C(9)-C(10)-C(11)-C(12)	-26.4(2)
C(1)-C(2)-C(12)-C(13)	-24.82(16)
C(3)-C(2)-C(12)-C(13)	-149.51(14)
C(1)-C(2)-C(12)-C(11)	91.56(17)
C(3)-C(2)-C(12)-C(11)	-33.1(2)
C(10)-C(11)-C(12)-C(13)	133.11(16)
C(15)-C(11)-C(12)-C(13)	9.42(18)
C(10)-C(11)-C(12)-C(2)	18.0(2)
C(15)-C(11)-C(12)-C(2)	-105.67(16)
C(1)-O(1)-C(13)-C(14)	-124.26(15)
C(1)-O(1)-C(13)-C(12)	-10.13(19)
C(2)-C(12)-C(13)-O(1)	21.90(17)
C(11)-C(12)-C(13)-O(1)	-103.05(15)
C(2)-C(12)-C(13)-C(14)	138.55(14)
C(11)-C(12)-C(13)-C(14)	13.60(18)

O(1)-C(13)-C(14)-C(15)	81.46(17)
C(12)-C(13)-C(14)-C(15)	-32.08(18)
C(13)-C(14)-C(15)-O(6)	-75.99(18)
C(13)-C(14)-C(15)-C(19)	159.61(15)
C(13)-C(14)-C(15)-C(11)	37.36(17)
C(10)-C(11)-C(15)-O(6)	-40.78(18)
C(12)-C(11)-C(15)-O(6)	88.10(15)
C(10)-C(11)-C(15)-C(19)	80.17(18)
C(12)-C(11)-C(15)-C(19)	-150.95(15)
C(10)-C(11)-C(15)-C(14)	-157.26(14)
C(12)-C(11)-C(15)-C(14)	-28.37(17)

Symmetry transformations used to generate equivalent atoms:

Table 21. Hydrogen bonds for V20005 [\approx and ∞].

D-H...A	d(D-H)	d(H...A)	d(D...A)	\angle (DHA)
O(3)-H(3O)...O(3W)	0.80(2)	1.95(2)	2.755(2)	175(3)
O(4)-H(4O)...O(2)	0.82(2)	1.93(2)	2.737(2)	168(3)
C(9)-H(9)...O(6)	1.00	2.37	2.976(2)	117.8
O(6)-H(6O)...O(2W)#1	0.85(2)	1.95(2)	2.790(2)	175(3)
O(1W)-H(1W1)...O(3)	0.85(2)	1.91(2)	2.758(2)	178(3)
O(1W)-H(1W2)...O(4)#2	0.85(2)	1.96(2)	2.799(2)	169(3)
O(2W)-H(2W1)...O(1W)	0.84(2)	1.86(2)	2.701(2)	173(3)
O(2W)-H(2W2)...O(5)#3	0.86(2)	1.96(2)	2.804(2)	168(3)
O(3W)-H(3W1)...O(1)#4	0.84(2)	2.49(3)	3.184(2)	141(3)
O(3W)-H(3W2)...O(2W)#5	0.87(2)	1.94(2)	2.814(2)	175(4)

Symmetry transformations used to generate equivalent atoms:

#1 $x, y, z+1$ #2 $-x+1/2, -y+1, z-1/2$ #3 $x+1/2, -y+1/2, -z+1$

#4 $-x+1, y-1/2, -z+3/2$ #5 $-x+1, y-1/2, -z+1/2$

A7.4 X-RAY CRYSTAL STRUCTURE ANALYSIS FOR SCABROLIDE A (416)

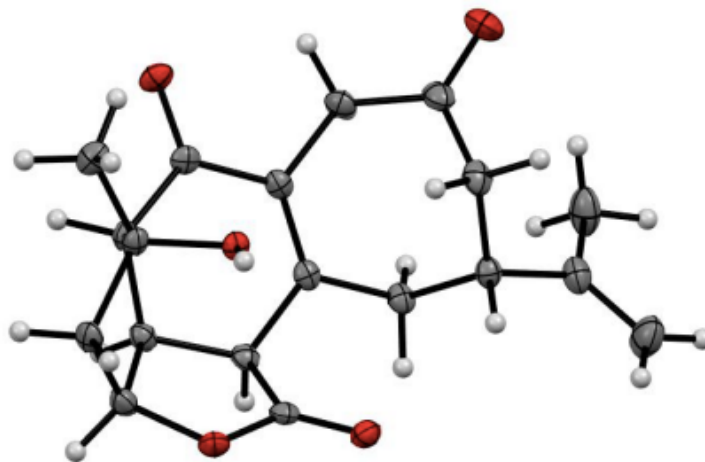


Figure A7.4. X-ray coordinate of scabrolide a (416)

Table A7.22 Crystal data and structure refinement for scabrolide A (416).

Identification code	V20018	
Empirical formula	C ₁₉ H ₂₂ O ₅	
Formula weight	330.36	
Temperature	100(2) K	
Wavelength	1.54178 \approx	
Crystal system	Orthorhombic	
Space group	P2 ₁ 2 ₁ 2 ₁	
Unit cell dimensions	a = 6.1878(4) \approx	$\alpha = 90^\circ$.
	b = 14.9676(14) \approx	$\beta = 90^\circ$.
	c = 17.511(2) \approx	$\gamma = 90^\circ$.
Volume	1621.8(3) \approx^3	
Z	4	
Density (calculated)	1.353 Mg/m ³	
Absorption coefficient	0.800 mm ⁻¹	
F(000)	704	
Crystal size	0.450 x 0.200 x 0.150 mm ³	
Theta range for data collection	3.885 to 74.514 $^\circ$.	
Index ranges	-7 \leq h \leq 7, -18 \leq k \leq 18, -20 \leq l \leq 21	
Reflections collected	14706	

Independent reflections	3306 [R(int) = 0.0575]
Completeness to theta = 67.679°	100.0 %
Absorption correction	Semi-empirical from equivalents
Max. and min. transmission	0.7538 and 0.6083
Refinement method	Full-matrix least-squares on F ²
Data / restraints / parameters	3306 / 1 / 222
Goodness-of-fit on F ²	1.048
Final R indices [I > 2σ(I)]	R1 = 0.0353, wR2 = 0.0889
R indices (all data)	R1 = 0.0369, wR2 = 0.0906
Absolute structure parameter	0.00(7)
Extinction coefficient	n/a
Largest diff. peak and hole	0.657 and -0.199 e.Å ⁻³

Table 23. Atomic coordinates ($\times 10^4$) and equivalent isotropic displacement parameters ($\times 10^3$) for V20018. $U(\text{eq})$ is defined as one third of the trace of the orthogonalized U^{ij} tensor.

	x	y	z	$U(\text{eq})$
O(1)	1620(2)	5711(1)	5387(1)	19(1)
C(1)	2687(3)	6235(1)	4894(1)	16(1)
O(2)	1762(2)	6741(1)	4470(1)	20(1)
C(2)	5129(3)	6135(1)	5002(1)	16(1)
C(3)	6351(3)	6183(1)	4262(1)	14(1)
C(4)	6411(3)	7080(1)	3873(1)	17(1)
C(5)	5192(3)	7133(1)	3101(1)	18(1)
C(16)	5851(4)	7974(2)	2674(1)	22(1)
C(17)	4347(5)	8604(2)	2509(2)	34(1)
C(18)	8117(4)	8092(2)	2448(2)	34(1)
C(6)	5415(4)	6278(2)	2609(1)	21(1)
C(7)	7669(4)	5905(1)	2542(1)	22(1)
O(3)	8577(4)	5848(1)	1932(1)	38(1)
C(8)	8816(3)	5587(2)	3257(1)	18(1)
C(9)	7470(3)	5491(1)	3974(1)	15(1)
C(10)	7522(3)	4620(1)	4364(1)	15(1)
O(4)	8720(2)	4016(1)	4141(1)	19(1)
C(11)	6084(3)	4457(1)	5040(1)	15(1)
C(12)	3939(3)	3993(1)	4811(1)	16(1)
O(5)	3102(2)	4518(1)	4189(1)	15(1)
C(19)	4176(3)	3021(1)	4572(1)	21(1)
C(13)	2585(3)	4137(1)	5535(1)	18(1)
C(14)	3075(3)	5093(1)	5780(1)	19(1)
C(15)	5399(3)	5298(1)	5486(1)	16(1)

Table 24. Bond lengths [\approx] and angles [∞] for V20018.

O(1)-C(1)	1.341(3)
O(1)-C(14)	1.462(3)
C(1)-O(2)	1.206(3)
C(1)-C(2)	1.530(3)
C(2)-C(3)	1.502(3)
C(2)-C(15)	1.522(3)
C(2)-H(2)	1.0000
C(3)-C(9)	1.345(3)
C(3)-C(4)	1.506(3)
C(4)-C(5)	1.551(3)
C(4)-H(4A)	0.9900
C(4)-H(4B)	0.9900
C(5)-C(16)	1.519(3)
C(5)-C(6)	1.549(3)
C(5)-H(5)	1.0000
C(16)-C(17)	1.356(4)
C(16)-C(18)	1.468(4)
C(17)-H(17A)	0.9500
C(17)-H(17B)	0.9500
C(18)-H(18A)	0.9800
C(18)-H(18B)	0.9800
C(18)-H(18C)	0.9800
C(6)-C(7)	1.507(3)
C(6)-H(6A)	0.9900
C(6)-H(6B)	0.9900
C(7)-O(3)	1.210(3)
C(7)-C(8)	1.515(3)
C(8)-C(9)	1.514(3)
C(8)-H(8A)	0.9900
C(8)-H(8B)	0.9900
C(9)-C(10)	1.472(3)
C(10)-O(4)	1.232(3)
C(10)-C(11)	1.501(3)
C(11)-C(15)	1.540(3)

C(11)-C(12)	1.551(3)
C(11)-H(11)	1.0000
C(12)-O(5)	1.439(2)
C(12)-C(19)	1.522(3)
C(12)-C(13)	1.535(3)
O(5)-H(5O)	0.84(2)
C(19)-H(19A)	0.9800
C(19)-H(19B)	0.9800
C(19)-H(19C)	0.9800
C(13)-C(14)	1.524(3)
C(13)-H(13A)	0.9900
C(13)-H(13B)	0.9900
C(14)-C(15)	1.558(3)
C(14)-H(14)	1.0000
C(15)-H(15)	1.0000
C(1)-O(1)-C(14)	111.70(15)
O(2)-C(1)-O(1)	122.04(19)
O(2)-C(1)-C(2)	127.36(19)
O(1)-C(1)-C(2)	110.44(17)
C(3)-C(2)-C(15)	117.69(17)
C(3)-C(2)-C(1)	112.65(16)
C(15)-C(2)-C(1)	104.94(16)
C(3)-C(2)-H(2)	107.0
C(15)-C(2)-H(2)	107.0
C(1)-C(2)-H(2)	107.0
C(9)-C(3)-C(2)	123.12(18)
C(9)-C(3)-C(4)	120.27(18)
C(2)-C(3)-C(4)	116.46(17)
C(3)-C(4)-C(5)	115.37(16)
C(3)-C(4)-H(4A)	108.4
C(5)-C(4)-H(4A)	108.4
C(3)-C(4)-H(4B)	108.4
C(5)-C(4)-H(4B)	108.4
H(4A)-C(4)-H(4B)	107.5
C(16)-C(5)-C(6)	112.80(17)

C(16)-C(5)-C(4)	109.91(17)
C(6)-C(5)-C(4)	113.52(17)
C(16)-C(5)-H(5)	106.7
C(6)-C(5)-H(5)	106.7
C(4)-C(5)-H(5)	106.7
C(17)-C(16)-C(18)	121.0(2)
C(17)-C(16)-C(5)	119.8(2)
C(18)-C(16)-C(5)	119.3(2)
C(16)-C(17)-H(17A)	120.0
C(16)-C(17)-H(17B)	120.0
H(17A)-C(17)-H(17B)	120.0
C(16)-C(18)-H(18A)	109.5
C(16)-C(18)-H(18B)	109.5
H(18A)-C(18)-H(18B)	109.5
C(16)-C(18)-H(18C)	109.5
H(18A)-C(18)-H(18C)	109.5
H(18B)-C(18)-H(18C)	109.5
C(7)-C(6)-C(5)	115.61(17)
C(7)-C(6)-H(6A)	108.4
C(5)-C(6)-H(6A)	108.4
C(7)-C(6)-H(6B)	108.4
C(5)-C(6)-H(6B)	108.4
H(6A)-C(6)-H(6B)	107.4
O(3)-C(7)-C(6)	121.7(2)
O(3)-C(7)-C(8)	119.3(2)
C(6)-C(7)-C(8)	119.01(18)
C(9)-C(8)-C(7)	117.25(18)
C(9)-C(8)-H(8A)	108.0
C(7)-C(8)-H(8A)	108.0
C(9)-C(8)-H(8B)	108.0
C(7)-C(8)-H(8B)	108.0
H(8A)-C(8)-H(8B)	107.2
C(3)-C(9)-C(10)	121.31(18)
C(3)-C(9)-C(8)	121.41(18)
C(10)-C(9)-C(8)	117.22(17)
O(4)-C(10)-C(9)	121.05(18)

O(4)-C(10)-C(11)	119.20(18)
C(9)-C(10)-C(11)	119.75(17)
C(10)-C(11)-C(15)	115.54(17)
C(10)-C(11)-C(12)	112.03(16)
C(15)-C(11)-C(12)	105.17(16)
C(10)-C(11)-H(11)	107.9
C(15)-C(11)-H(11)	107.9
C(12)-C(11)-H(11)	107.9
O(5)-C(12)-C(19)	110.42(17)
O(5)-C(12)-C(13)	110.60(16)
C(19)-C(12)-C(13)	114.45(17)
O(5)-C(12)-C(11)	105.04(15)
C(19)-C(12)-C(11)	114.65(17)
C(13)-C(12)-C(11)	100.97(16)
C(12)-O(5)-H(5O)	107(2)
C(12)-C(19)-H(19A)	109.5
C(12)-C(19)-H(19B)	109.5
H(19A)-C(19)-H(19B)	109.5
C(12)-C(19)-H(19C)	109.5
H(19A)-C(19)-H(19C)	109.5
H(19B)-C(19)-H(19C)	109.5
C(14)-C(13)-C(12)	104.79(16)
C(14)-C(13)-H(13A)	110.8
C(12)-C(13)-H(13A)	110.8
C(14)-C(13)-H(13B)	110.8
C(12)-C(13)-H(13B)	110.8
H(13A)-C(13)-H(13B)	108.9
O(1)-C(14)-C(13)	109.84(16)
O(1)-C(14)-C(15)	106.79(15)
C(13)-C(14)-C(15)	106.01(17)
O(1)-C(14)-H(14)	111.3
C(13)-C(14)-H(14)	111.3
C(15)-C(14)-H(14)	111.3
C(2)-C(15)-C(11)	114.84(16)
C(2)-C(15)-C(14)	104.14(16)
C(11)-C(15)-C(14)	105.07(16)

C(2)-C(15)-H(15) 110.8

C(11)-C(15)-H(15) 110.8

C(14)-C(15)-H(15) 110.8

Symmetry transformations used to generate equivalent atoms:

Table 25. Anisotropic displacement parameters ($\approx 2 \times 10^3$) for V20018. The anisotropic displacement factor exponent takes the form: $-2\pi^2 [h^2 a^{*2} U^{11} + \dots + 2 h k a^* b^* U^{12}]$

	U ¹¹	U ²²	U ³³	U ²³	U ¹³	U ¹²
O(1)	17(1)	21(1)	20(1)	0(1)	4(1)	5(1)
C(1)	17(1)	18(1)	14(1)	-4(1)	2(1)	1(1)
O(2)	19(1)	20(1)	21(1)	-2(1)	-1(1)	6(1)
C(2)	16(1)	18(1)	13(1)	-2(1)	-2(1)	0(1)
C(3)	11(1)	18(1)	14(1)	0(1)	-3(1)	-4(1)
C(4)	19(1)	17(1)	16(1)	0(1)	-2(1)	-3(1)
C(5)	16(1)	20(1)	17(1)	2(1)	-2(1)	-1(1)
C(16)	26(1)	23(1)	18(1)	4(1)	-3(1)	-4(1)
C(17)	34(1)	27(1)	41(1)	13(1)	4(1)	4(1)
C(18)	27(1)	38(1)	35(1)	17(1)	-1(1)	-6(1)
C(6)	24(1)	23(1)	17(1)	-1(1)	-7(1)	-3(1)
C(7)	30(1)	19(1)	17(1)	-3(1)	2(1)	0(1)
O(3)	49(1)	45(1)	20(1)	-1(1)	10(1)	14(1)
C(8)	16(1)	21(1)	19(1)	0(1)	4(1)	-1(1)
C(9)	10(1)	21(1)	14(1)	1(1)	-1(1)	-2(1)
C(10)	8(1)	19(1)	17(1)	-2(1)	-3(1)	-1(1)
O(4)	11(1)	19(1)	27(1)	0(1)	1(1)	1(1)
C(11)	12(1)	17(1)	16(1)	4(1)	-2(1)	2(1)
C(12)	11(1)	18(1)	17(1)	3(1)	0(1)	1(1)
O(5)	10(1)	18(1)	17(1)	2(1)	-1(1)	-1(1)
C(19)	15(1)	17(1)	29(1)	2(1)	0(1)	-2(1)
C(13)	14(1)	22(1)	19(1)	5(1)	3(1)	-1(1)
C(14)	17(1)	24(1)	15(1)	2(1)	3(1)	2(1)
C(15)	14(1)	21(1)	14(1)	0(1)	-1(1)	-1(1)

Table A7.26. Hydrogen coordinates ($\times 10^4$) and isotropic displacement parameters ($\text{\AA}^2 \times 10^3$) for scabrolide a (**416**)

	x	y	z	U(eq)
H(2)	5617	6652	5321	19
H(4A)	7940	7245	3785	21
H(4B)	5787	7530	4224	21
H(5)	3622	7198	3225	21
H(17A)	4754	9131	2244	41
H(17B)	2887	8518	2659	41
H(18A)	8266	8645	2153	50
H(18B)	8575	7584	2135	50
H(18C)	9025	8127	2906	50
H(6A)	4469	5811	2829	26
H(6B)	4874	6411	2089	26
H(8A)	9481	5001	3144	22
H(8B)	10006	6010	3367	22
H(11)	6869	4053	5401	18
H(5O)	1810(40)	4353(19)	4117(16)	22
H(19A)	2797	2803	4369	31
H(19B)	4593	2660	5015	31
H(19C)	5292	2972	4176	31
H(13A)	1027	4062	5425	22
H(13B)	3009	3708	5939	22
H(14)	2975	5162	6347	22
H(15)	6404	5411	5923	20

Table A7.27. Torsion angles [$^{\circ}$] for scabrolide a (**416**).

C(14)-O(1)-C(1)-O(2)	174.04(18)
C(14)-O(1)-C(1)-C(2)	-10.2(2)
O(2)-C(1)-C(2)-C(3)	-40.7(3)
O(1)-C(1)-C(2)-C(3)	143.75(16)
O(2)-C(1)-C(2)-C(15)	-169.96(19)
O(1)-C(1)-C(2)-C(15)	14.5(2)
C(15)-C(2)-C(3)-C(9)	7.3(3)
C(1)-C(2)-C(3)-C(9)	-115.0(2)
C(15)-C(2)-C(3)-C(4)	-168.25(17)
C(1)-C(2)-C(3)-C(4)	69.4(2)
C(9)-C(3)-C(4)-C(5)	71.1(3)
C(2)-C(3)-C(4)-C(5)	-113.2(2)
C(3)-C(4)-C(5)-C(16)	-165.26(18)
C(3)-C(4)-C(5)-C(6)	-37.9(3)
C(6)-C(5)-C(16)-C(17)	114.0(2)
C(4)-C(5)-C(16)-C(17)	-118.3(2)
C(6)-C(5)-C(16)-C(18)	-66.2(3)
C(4)-C(5)-C(16)-C(18)	61.6(3)
C(16)-C(5)-C(6)-C(7)	79.8(2)
C(4)-C(5)-C(6)-C(7)	-46.1(3)
C(5)-C(6)-C(7)-O(3)	-118.2(2)
C(5)-C(6)-C(7)-C(8)	62.2(3)
O(3)-C(7)-C(8)-C(9)	-167.6(2)
C(6)-C(7)-C(8)-C(9)	12.0(3)
C(2)-C(3)-C(9)-C(10)	1.6(3)
C(4)-C(3)-C(9)-C(10)	177.02(16)
C(2)-C(3)-C(9)-C(8)	-175.38(18)
C(4)-C(3)-C(9)-C(8)	0.0(3)
C(7)-C(8)-C(9)-C(3)	-57.2(3)
C(7)-C(8)-C(9)-C(10)	125.7(2)
C(3)-C(9)-C(10)-O(4)	-172.57(19)
C(8)-C(9)-C(10)-O(4)	4.6(3)
C(3)-C(9)-C(10)-C(11)	7.9(3)
C(8)-C(9)-C(10)-C(11)	-174.98(17)

O(4)-C(10)-C(11)-C(15)	155.15(18)
C(9)-C(10)-C(11)-C(15)	-25.3(2)
O(4)-C(10)-C(11)-C(12)	-84.4(2)
C(9)-C(10)-C(11)-C(12)	95.1(2)
C(10)-C(11)-C(12)-O(5)	-50.5(2)
C(15)-C(11)-C(12)-O(5)	75.75(18)
C(10)-C(11)-C(12)-C(19)	70.9(2)
C(15)-C(11)-C(12)-C(19)	-162.86(17)
C(10)-C(11)-C(12)-C(13)	-165.57(16)
C(15)-C(11)-C(12)-C(13)	-39.29(18)
O(5)-C(12)-C(13)-C(14)	-69.4(2)
C(19)-C(12)-C(13)-C(14)	165.12(17)
C(11)-C(12)-C(13)-C(14)	41.41(18)
C(1)-O(1)-C(14)-C(13)	-112.91(18)
C(1)-O(1)-C(14)-C(15)	1.6(2)
C(12)-C(13)-C(14)-O(1)	86.82(18)
C(12)-C(13)-C(14)-C(15)	-28.20(19)
C(3)-C(2)-C(15)-C(11)	-24.3(2)
C(1)-C(2)-C(15)-C(11)	101.83(19)
C(3)-C(2)-C(15)-C(14)	-138.68(17)
C(1)-C(2)-C(15)-C(14)	-12.52(19)
C(10)-C(11)-C(15)-C(2)	32.7(2)
C(12)-C(11)-C(15)-C(2)	-91.33(19)
C(10)-C(11)-C(15)-C(14)	146.55(16)
C(12)-C(11)-C(15)-C(14)	22.47(19)
O(1)-C(14)-C(15)-C(2)	7.3(2)
C(13)-C(14)-C(15)-C(2)	124.43(17)
O(1)-C(14)-C(15)-C(11)	-113.76(17)
C(13)-C(14)-C(15)-C(11)	3.33(19)

Symmetry transformations used to generate equivalent atoms:

Table A7.28. Hydrogen bonds for scabrolide a (**416**).

D-H...A	d(D-H)	d(H...A)	d(D...A)	<(DHA)
C(2)-H(2)...O(2)#1	1.00	2.53	3.461(2)	154.0
C(8)-H(8B)...O(2)#2	0.99	2.47	3.289(3)	139.6
O(5)-H(5O)...O(4)#3	0.84(2)	1.98(2)	2.815(2)	170(3)
C(19)-H(19C)...O(4)	0.98	2.64	3.270(3)	122.7
C(15)-H(15)...O(3)#4	1.00	2.58	3.123(3)	113.7

Symmetry transformations used to generate equivalent atoms:

#1 $x+1/2, -y+3/2, -z+1$ #2 $x+1, y, z$ #3 $x-1, y, z$

#4 $-x+3/2, -y+1, z+1/2$

COMPREHENSIVE BIBLIOGRAPHY

- Achenbach, H.; Schaller, E. *Chem. Ber.* **1976**, *109*, 3527–3536.
- Ahond, A.; Cavé, A.; Kan-Fan, C.; Housson, H-P.; de Rostolan, J.; Portier, P. *J. Am. Chem. Soc.* **1968**, *90*, 5622.
- Aissa C. *J. Org. Chem.* **2006**, *71*, 360–363.
- Allred, G. D.; Liebeskind, L. S. *J. Am. Chem. Soc.* **1996**, *118*, 2748–2749.
- Antitumor Bisindole Alkaloids from *Catharanthus roseus* (L.). *The Alkaloids*; Brossi, A., Suffness, M., Eds.; Academic Press Inc.: San Diego, 1990; Vol. 37, Chapters 3 and 4, pp 133-204.
- Arkin, M.R.; Wells J.A. *Nat. Rev. Drug. Discov.* **2004**, *3*, 301-317.
- Atkins, G.M.; Burgess, E.M. *J. Am. Chem. Soc.* **1968**, *90*, 4744 – 4745.
- Bartlett, M. F.; Taylor, W. I. *J. Am. Chem. Soc.* **1960**, *82*, 5941–5942.
- Bartlett, M.F.; Taylor, W.I.; Hamet, R. *C.R. Acad. Sci. Paris.* **1959**, *249*, 1259.
- Barton, J.E.D.; Harley-Mason, J.; *J. Chem. Soc. Chem. Comm.* **1965**, 298–299.
- Behenna D.C.; Liu Y.; Yurino T.; Kim J.; White D.E.; Virgil S.C.; Stoltz B.M. *Nature Chem.* **2012**, *4*, 130–133.
- Behenna, D.C.; Mohr, J.T.; Sherden, N.H.; Marinescu, S.C.; Harnet, A.M.; Tani, K.; Seto, M.; Ma, S.; Novák, Z.; Krout, M.R.; McFadden, R.M.; Roizen, J.L.; Enquist, J.A.; White, D.E.; Levine, S.R.; Petrova, K.V.; Iwashita, A.; Virgil, S.C.; Stoltz, B.M. *Chem. –Eur. J.* **2011**, *17*, 14199–14223.
- Berube, G.; *Curr. Med. Chem.* **2006**, *13*, 131–154.
- Bi, Y.; Cook, J.M. *Tetrahedron Lett.* **1993**, *34*, 4501–4504.
- Bi, Y.; Cook, J.M.; *Tetrahedron Lett.* **1994**, *35*, 3877–3878.

- Bi, Y.; Zhang, L.-H.; Hamaker, L.K.; Cook, J.M. *J. Am. Chem. Soc.* **1994**, *116*, 9027–9041.
- Bólsing, E.; Klätte, F.; Rosentreter, V.; Winterfeldt, E. *Chem. Ber.* **1979**, *112*, 1902–1912.
- Boon, B.A.; Boger, D.L. *J. Am. Chem. Soc.* **2019**, *141*, 14349–14355.
- Bornman, W.G.; Kuehne, M.E. *J. Org. Chem.* **1992**, *57*, 1752–1760.
- Bose, D.S.; Kumar, K.K.; Reddy, A.V.N. *Synth. Commun.*, **33**, 445–450.
- Brill, Z. G.; Grover, H. K.; Maimone, T. J. *Science*, **2016**, *352*, 1078–1082.
- Brill, Z.G.; Condakes, M.L.; Ting, C.P.; Maimone, T.J. *Chem. Rev.* **2017**, *117*, 11753–11795.
- Bruno, D.; Lesma, G.; Mauro, M.; Palmisano, G.; Passarella, D. *J. Org. Chem.* **1995**, *60*, 2506–2513.
- Büchi, G.; Manning, R.E.; Monti, S.A. *J. Am. Chem. Soc.* **1964**, *85*, 1893–1894.
- Büchi, G.; Manning, R.E.; Monti, S.A. *J. Am. Chem. Soc.* **1964**, *86*, 4631–4641.
- Burke, D.E.; Cook, J.M.; LeQuesne, P. *J. Am. Chem. Soc.* **1973**, *95*, 546–552.
- Burke, D.E.; Cook, J.M.; LeQuesne, P. *J. Chem. Soc. Chem. Commun.* **1972**, 697.
- Burke, D.E.; Cook, J.M.; LeQuesne, P. *J. Chem. Soc. Chem. Commun.* **1972**, 678.
- Burke, D.E.; DeMarkey, C.A.; LeQuesne, P.W.; Cook, J.M. *J. Chem. Soc. Chem. Commun.* **1972**, 1346–1347.
- Burke, M.D.; Schreiber, S.L. *Angew. Chem. Int. Ed.* **2004**, *43*, 46–58.
- Caille, S.; Crockett, R.; Ranganathan, K.; Wang, X.; Woo, J.C.S.; Walker, S.D. *J. Org. Chem.* **2011**, *76*, 5198–5206.
- Cartier, D.; Lévy, J.; LeMen, J. *Bull. Soc. Chim. Fr.* **1976**, 1961.
- Castedo, L.; Harley-Mason, J.; Leeny, T.J. *J. Chem. Soc. Chem. Comm.* **1968**, 1168.
- Chapman, L.M.; Beck, J.C.; Wu, L.; Reisman, S.E. *J. Am. Chem. Soc.* **2016**, *138*, 9803–9806.
- Chem.* **2017**, *9*, 1165–1169.

- Cleve, A.; Fritzscheimer, K.-H.; Klar, U.; Müller-Fahrnow, Neef, G.; Ottow, E.; Schwede, W. *Tetrahedron* **1996**, *52*, 1529–1542.
- Coperet C.; Adolfsson H.; Chiang J.P.; Yudin A.K.; Sharpless K.B. *Tetrahedron Lett.* **1998**, *39*, 761–764.
- Cordell, G.A.; Saxton, J.E. Bisindole Alkaloids. In *The Alkaloids: Chemistry and Physiology*; Manske, R.H.F., Rodrigo, R.G.A., Eds.; Academic Press: New York, 1981; pp 1–295.
- Corey, E. J.; Mitra, R. B.; Uda, H. *J. Am. Chem. Soc.* **1963**, *86*, 485–492. (b) Pirrung, M. C. *J. Am. Chem. Soc.* **1979**, *101*, 7130–7131. (c) Pirrung, M. C. *J. Am. Chem. Soc.* **1981**, *103*, 82–87.
- Corey, E.J.; Cheng, X-M. *The Logic of Chemical Synthesis*; John Wiley & Sons: New York, 1989; pp 1-99.
- Costerousse, G.; Buendia, J.; Toromanoff, E.; Martell, J.; *J. Bull. Soc. Chim. Fr.* **1978**, II-355.
- Cox, P.A.; Leach, A.G.; Campbell, A.D.; Lloyd-Jones, G.C. *J. Am. Chem. Soc.* **2016**, *138*, 9145–9157.
- Cox, P.A.; Reid, M.; Leach, A.G.; Campbell, A.D.; King, E.J.; Lloyd-Jones, G.C. *J. Am. Chem. Soc.* **2017**, *139*, 13156 – 13165.
- Crabtree, R.H. *Acc. Chem. Res.* *12*, 331–338.
- Crabtree, R.H.; Iridium. In *The Handbook of Homogeneous Hydrogenation*; de Vries, J.G.; Elsevier, C.J. (Eds.); Wiley-VCH: Weinheim, Germany, 2007. pp 31–43.
- Craig II, R.A.; Roizen, J.L.; Smith, R.C.; Jones, A.C.; Virgil, S.C.; Stoltz, B.M. *Chem Sci.* **2017**, *8*, 507–514.
- Craig II, R.A.; Smith, R.C.; Roizen, J.L.; Jones, A.C.; Virgil, S.C.; Stoltz, B.M. *J. Org Chem.* **2018**, *83*, 3467–3485.

- Craig II, R.A.; Smith, R.C.; Roizen, J.L.; Jones, A.C.; Virgil, S.C.; Stoltz, B.M. *J. Org Chem.* **2019**, *84*, 7772–7746.
- Craig II, R.A.; Stoltz, B.M. *Chem. Rev.* **2017**, *117*, 7878–7909
- Craig, R. A., II; Roizen, J. L.; Smith, R. C.; Jones, A. C.; Stoltz, B. M. *Org. Lett.* **2012**, *14*, 5716–5719.
- Crimmins, M.T. *Chem. Rev.* **1988**, *88*, 1453–1473
- Czibula, L.; Nemes, A.; Visky, G.; Farkas, M.; Szombathelyi, Z.; Kárpáti, E.; Sohár, P.; Kessel, M. Kreidl, J. *Liebigs Annalen der Chemie* **1993**, *3*, 221–230.
- D.C.; *Phytother. Res.* **1992**, *6*, 121.
- Dai, J-K.; Dan, W-J.; Du, H-T.; Zhang, J-W.; Wang, J-R. *Bioorg. Med. Chem. Lett.* **2016**, *26*, 580–583.
- Deguchi, J.; Shoji, T.; Nugroho, A.; Hirasawa, Y.; Hosoya, T. Shirota, O.; Awang, K.; Hadi, A.H.A.; Morita, H. *J. Nat. Prod.* **2010**, *73*, 1727–1729.
- Duh, C.-Y.; Wang, S.-K.; Chia, M.-C.; Chiang, M.Y. *Tetrahedron Lett.* **1999**, *40*, 6033–6035.
- Duncton, M.A.J. *Med. Chem.. Commun.* **2011**, *2*, 1135–1161.
- Edwankar, C.R.; Edwankar, R.V.; Namjoshi, O.A.; Rallapalli, S.K.; Yang, J.; Cook, J.M. *Curr. Opin. Drug. Discov. Devel.* **2009**, *12*, 752-771.
- Edwankar, C.R.; Edwankar, R.V.; Rallapali, S.; Cook, J.M. *Nat. Prod. Commun.* **2008**, *3*, 1837-1870.
- Enders, D.; Shilvock, J.P. *Chem. Soc. Rev.* **2000**, *29*, 359–373.
- Esmond, R.W.; LeQuesne, P.W. *J. Am. Chem. Soc.* **1980**, *102*, 7116–7117.
- Farina, V.; Krishnan, B. *J. Am. Chem. Soc.* **1991**, *113*, 9585-9595. b) Farina, V.; Krishnan, B.; Marshall, D.R.; Roth, G.P. *J. Org. Chem.* **1993**, *58*, 5434-5444.

- Feng, X-Z.; Liu, G.; Kan, C.; Portier, P.; Kan, S-W. *J. Nat. Prod.* **1989**, *52*, 928–933.
- Ferrali, A.; Guarna, A.; Lo Galbo, F.; Occhiato, E.G. *Tetrahedron Lett.* **2004**, 5271–5274.
- Fier, P.S.; Hartwig, J.F. *Science* **2013**, *342*, 956–960. (b) Fier, P.S.; Hartwig, J.F. *J. Am. Chem. Soc.* **2014**, *136*, 10139–10147.
- Fillon, H.; Gosmini, C.; Périchon, J. *J. Am. Chem. Soc.* **2003**, *125*, 3867–3870.
- Fristrup, P.; Dideriksen, B.B.; Tanner, D.; Norrby, P-O. *J. Am. Chem. Soc.* **2005**, *127*, 13672–13679.
- Fukuyama, T.; Chen, X.; Peng, G. *J. Am. Chem. Soc.* **1994**, 3127–3128.
- Fulton T.J.; Chen A.Y.; Stoltz B.M. *ChemRxiv. Preprint. DOI: 10.26434/chemrxiv.11900331.v1*.
- Gan, C-Y.; Robinson, W.T.; Etoh, T.; Hayashi, M.; Komiyama, K.; Kam, T-S. *Org. Lett.* **2009**, *11*, 3962 – 3965.
- Gannick, R.L.; LeQuesne, P.W. *J. Am. Chem. Soc.* **1978**, *100*, 4213–4219.
- Gansäuer, A.; Bluhm, H.; Pierobon, M. *J. Am. Chem. Soc.* **1998**, *120*, 12849–12859.
- Ghosh, A. K.; Kawahama, R. *J. Org. Chem.* **2000**, *65*, 5433–5435.
- Gmeiner, P.; Feldman, P. L.; Chu-Moyer, M. Y.; Rapoport, H. *J. Org. Chem.* **1990**, *55*, 3068–3074.
- Gotoh, H.; Sears, J.E.; Eschenboser, A.; Boger, D.L. *J. Am. Chem. Soc.* **2012**, *134*, 13240-13243.
- Grieco, P. A.; Gilman, S.; Nishizawa, M. *J. Org. Chem.* **1976**, *41*, 1485–1486.
- Griffith, W. P.; Ley, S. V.; Whitcombe, G. P.; White, A. D. *J. Chem. Soc., Chem. Commun.* **1987**, *21*, 1625–1627.
- Hakam, K.; Thielmann, M.; Thielmann, T.; Winterfeldt, E. *Tetrahedron* **1987**, *43*, 2035–2044.
- Han-ya, Y.; Tokuyama, H.; Fukuyama, T. *Angew. Chem. Int. Ed.* **2011**, *50*, 4884–4887.
- Hassan, H.; Mohammed, S.; Robert, F.; Landais, Y. *Org. Lett.* **2015**, *17*, 4518–4521.

He, C.; Xuan, J.; Rao, P.; Xie, P.-P.; Hong, X.; Lin, X.; Ding, H. *Angew. Chem. Int. Ed.* **2018**, *58*, 5100–5014.

He, F.; Bo, Y.; Atlom, J.D.; Corey, E.J. *J. Am. Chem. Soc.* **1999**, *121*, 6771–6772.

Hermann, J. L.; Cregge, R. J.; Richman, J. E.; Kieczkowski, G. R.; Normandin, S. N.; Quesada, M. L.; Semmelhack, C. L.; Poss, A. J.; Schlessinger, R. H. *J. Am. Chem. Soc.* **1979**, *101*, 1540–1544.

Heath-Brown, B.; Philpott, P. *J. Chem. Soc.* **1965** 7185–7193.

Hesse, M.; Bodmer, F.; Gemenden, C.; Joshi, B.; Taylor, W.; Schmid, H. *Helv. Chim. Acta* **1966**, *49*, 1173–1182.

Hesse, M.; Dimeric Alkaloids (Bis-alkaloids). In *Alkaloids: Nature's Curse or Blessing?*; Wiley-VCH/Weinheim: New York, 2002; pp 91-114.

Hirasawa, Y.; Arai, H.; Rahman, A.; Kusumawati, I.; Zaini, N.C.; Shirota, O.; Morita, H.

Hoffman, N. *Chem. Rev.* **2008**, *108*, 1052–1103.

Hofstra, J.L.; Poremba, K.E.; Shomozono, A.M.; Reisman, S.E. *Angew. Chem. Int. Ed.* **2019**, *58*, 14901–14905.

Huang, F-Q.; Xie, J.; Sun, J-G.; Wang, Y-W.; Dong, X.; Qi, L.W.; Zhang, B. *Org. Lett.* **2016**, *18*, 684–687.

Huff C.A.; Cohen R.D.; Dykstra K.D.; Steckfuss E.; DiRocco D.A.; Krska S.W.; *J. Org. Chem.* **2016**, *81*, 6980 – 6987.

Iguchi, K.; Kajiyama, K.; Yamada, Y. *Tetrahedron Lett.* **1995**, *36*, 8807–8808.

Ihara, M.; Takahashi, M.; Taniguchi, N.; Yasui, K.; Niitsuma, H.; Fukumoto, K. *J. Chem. Soc., Perkin Trans. 1*, **1991**, 525–535.

Irie, K.; Ban, Y. *Heterocycles* **1981**, *15*, 201–206.

- Irie, K.; Okita, M.; Wakamatsu, T.; Ban, Y. *Nouv. J. Chem.* **1980**, *4*, 275.
- Ishikawa, H.; Colby, D.A.; Boger, D.L. *J. Am. Chem. Soc.* **2008**, *130*, 420–421. b)
- Ishikawa, H.; Colby, D.A.; Seto, S.; Va, P.; Tam, A.; Kakei, H.; Rayl, T.J.; Hwang, I.; Boger, D.L. *J. Am. Chem. Soc.* **2009**, *131*, 4904–4916.
- Ishikawa, H.; Elliot, G.I.; Velcicky, J.; Choi, Y.; Boger, D.L. *J. Am. Chem. Soc.* **2006**, *128*, 10596–10612.
- Ishiyama, T.; Murata, M.; Miyaura, N. *J. Org. Chem.* **1995**, *60*, 7508–7510.
- Iwabuchi, Y.; Hayashi, M.; Satoh, A.; Shibuya, M.; Ogasawara, K. *Heterocycles* **2009**, *77*, 855–863.
- Iwasaki, K.; Wan, K.K.; Oppedisano, A.; Crossley, S.W.M.; Shenvi, R.A. *J. Am. Chem. Soc.* **2014**, *136*, 1300–1303.
- Jamison, C.R.; Badillo, J.J.; Lipshultz, J.M.; Comito, R.J.; Macmillan, D.W.C. *Nature*
- Jones, S.B.; Simmons, B.; Mastracchio, A.; MacMillan, D.W.C. *Nature* **2011**, *475*, 183–188.
- Kalaus, G.; Malkieh, N.; Katona, I.; Kajtar-Peredy, M.; Koritsanszky, T.; Kalman, A.; Szabo, L.; Szantay, C. *J. Org. Chem.* **1985**, *50*, 3760–3767.
- Kam, T-S.; Choo, Y-M. Bisindole Alkaloids. In *The Alkaloids: Chemistry and Biology*; Cordell, G.A. Ed.; Elsevier/Academic Press: New York, 2006; pp 181–387.
- Kärkäs M. D.; Porco, J. A., Jr.; Stephenson, C. R. *J. Chem. Rev.* **2016**, *116*, 9683–0747.
- Katiritzky, A.R.; Khan, G.R.; Schwarz, O.A. *Tetrahedron Lett.* **1984**, *25*, 1223–1226.
- Kazmierski, I.; Gosmini, C.; Paris, J-M.; Périchon, J. *Tetrahedron Lett.* **2003**, *44*, 6417–6420.
- Keawpradub, N.; Houghton, P.J.; Eno-Amuoquaye, E.; Burke, P.J. *Planta. Med.* **1997**, *63*, 97–101.
- Keawpradub, N.; Kirby, G.C.; Steele, J.C.P.; Houghton, P.J.; *Planta. Med.* **1999**, *65*, 690–694.

- Kim, A.N.; Ngamnithiporn, A.; Welin, E.R.; Daiger, M.T.; Grünanger, C.U.; Bartberger, M.D.; Virgil, S.C.; Stoltz, B.M. *ACS Catal.* **2020**, *10*, 3241–3248.
- Kim, K.E.; Li, J.; Stoltz, B.M.; Grubbs R.H.; *J. Am. Chem. Soc.* **2016**, *138*, 13179 – 13182.
- Kingston, G.I.; Gerhart, B.B.; Ionescu, F. *Tetrahedron Lett.* **1976**, *17*, 649–652.
- Kitajima, M.; Takayama, H. Monoterpenoid Bisindole Alkaloids. In *The Alkaloids: Chemistry and Biology*; Knölker, H-J. Ed.; Elsevier/Academic Press: Cambridge, MA, 2016; pp 259–310.
- Knox, J.R.; Slobbe, J. *Aust. J. Chem.* **1975**, *28*, 1813–1823.
- Kobayashi, M.; Rao, K.M.C.A.; Krishna, M.M.; Anjaneyulu, V.; *J. Chem. Res. (S)* **1995**, 188–189.
- Kobayashi, S.; Ueda, T.; Fukuyama, T. *Synlett* **2000**, 883–886.
- Kolmar, S.S.; Mayer, J.M. *J. Am. Chem Soc.* **2017**, *129*, 10687–10692.
- Korch, K. M., Loskot, S. A. and Stoltz, B. M. (2017). Asymmetric Synthesis of Quaternary Stereocenters via Metal Enolates. In *PATAI'S Chemistry of Functional Groups*, Z. Rappoport (Ed.). doi:10.1002/9780470682531.pat0858.
- Kuboyama, T.; Yokoshima, S.; Tokuyama, H.; Fukuyama, T. *J. Am. Chem. Soc.* **2004**, *101*, 11966–11970.
- Kuehne, M.E.; Giacobbe, T.J. *J. Org. Chem.* **1968**, *33*, 3359–3369.
- Kuehne, M.E.; Matson, P.A.; Bornmann, W.G. *J. Org. Chem.* **1991**, *56*, 513–528.
- Kutney, J.P.; Beck, J.; Bylsma, F.; Cretney, W.J. *J. Am. Chem. Soc.* **1968**, *90*, 4504–4505
- Kutney, J.P.; Beck, J.F.; Nelson, V.R.; Sood, R.S. *J. Am. Chem. Soc.* **1971**, *92*, 255–257.
- Kutney, J.P.; Choi, L.S.L.; Nakao, J.; Tsukamoto, H.; McHugh, M.; Boulet, C.A. *Heterocycles* **1988**, *27*, 1845–1853.

- Kutney, J.P.; Hibino, T.; Jahngen, E.; Okutani, T.; Ratcliffe, A.H.; Treasurywala, A.M.; Wunderly, S. *Helv. Chim. Acta.* **1976**, *59*, 2858–2882.
- Kutney, J.P.; Ratcliffe, A.H.; Treasurywala, A.M.; Wunderly, S. *Heterocycles* **1975**, *3*, 639–639.
- Lachkkr, D.; Denizot, N.; Bernadat, G.; Ahamada, K.; Beniddir, M.A.; Dumontet, V.; Gallard, J-F.; Guillot, R.; Leblanc, K.; N'ngang, E.O.; Turpin, V.; Kouklovsky, C.; Poupon, E.; Evanno, L. Vincent, G. *Nature Chem.* **2017**, *9*, 793–798.
- Lancefield, C.S.; Zhou, L.; Lébl, T.; Slawin, A.M.Z.; Westwood, N.J. *Org. Lett.* **2012**, *14*, 6166–6169.
- Langlois, N. Guéritte, F.; Langlois, Y.; Potier, P. *J. Am. Chem. Soc.* **1976**, *98*, 7017–7024.
- Lavaud, C.; Massiot, G.; Vercauteren, J; Le Men-Olivier, L. *Phytochemistry*, **1982**, *21*, 445–446.
- Le Gall, E.; Haurena, C.; Sengmany, S.; Martens, T.; Troupel, M. *J. Org. Chem.* **2009**, *20*, 7970–7973.
- Le Gall, E.; Troupel, M.; Nédélec, J-Y. *Tetrahedron* **2006**, *62*, 9953–9965.
- Leggans, E.K.; Barker, T.J.; Duncan, K.K.; Boger, D.L. *Org. Lett.* **2012**, *14*, 1428–1431.
- Léonard, N.G.; Chirik, P.J. *ACS Catal.* **2018**, *8*, 342–348.
- Lett.* **2007**, *9*, 4737–4740.
- Li, H.; Chen, Q.; Lu, Z.; Li, A. *J. Am. Chem. Soc.* **2016**, *138*, 15555–15558. b) Furstner, A.; Funel, J-A.; Tremblay, M.; Bouchez, L.C.; Nevado, C.; Waser, M.; Ackerstaff, J.; Stimson, C.C. *Chem Comm.* **2008**, 2873 – 2875.
- Li, L. Chen, Z.; Zhang, X.; Jia, Y. *Chem. Rev.* **2018**, *118*, 3752-3832
- Li, Y.; Pattenden, G. *Nat. Prod. Rep.* **2011**, *28*, 1269–1310. b) Li, Y.; Pattenden, G. *Nat Prod Rep.* **2011**, *28*, 429–440.
- Li, Y.; Pattenden, G. *Tetrahedron* **2011**, *67*, 10045–10052.

- Liao, X.; Zhou, H.; Wearing, X.Z.; Ma, J.; Cook, J.M. *Org Lett.* **2005**, *7*, 3501–3504.
- Liao, X.; Zhou, H.; Yu, J.; Cook, J.M. *J. Org. Chem.* **2006**, *71*, 8884–8890.
- Lindovska, P.; Movassaghi, M. *J. Am. Chem. Soc.* **2017**, *139*, 17590–17596.
- Littke, A.F.; Fu, G.C. *Angew. Chem. Int. Ed.* **1999**, *38*, 2411–2413.
- Liu, R. S. H.; Hammond, G. S. *J. Am. Chem. Soc.* **1967**, *89*, 4936–4944.
- Liu, X. *Ph.D. Thesis, The University of Wisconsin-Wilwaukee*, **2002**.
- Liu, X.; Deschamp, J.R.; Cook, J.M. *Org. Lett.* **2002**, *4*, 3339–3342.
- Liu, X.; Wang, T.; Xu, Q.; Ma, C.; Cook, J.M. *Tetrahedron Lett.* **2000**, *41*, 6299–6303.
- Liu, X.; Zhang, C.; Lio, X. Cook, J.M. *Tetrahedron Lett.* **2002**, *43*, 7373–7377.
- Liu, Y.; Han, S-J.; Liu, W-B.; Stoltz, B.M. *Acc. Chem. Res.* **2015**, *48*, 740–751.
- Lo, J.C.; Yabe, Y.; Baran, P.S. *J. Am. Chem. Soc.* **2014**, *136*, 1304–1307.
- Londregan A.T.; Jennings S.; Wei L. *Org. Lett.* **2011**, *13*, 1840–1843
- Loskot, S.A. *Ph. D. Dissertation*. California Institute of Technology **2019**.
- Lounasmaa, M.; Berner, M.; Brunner, M.; Soumalainen, H.; Tolvanen, A. *Tetrahedron* **1998**, *54*, 10205–10216.
- Lounasmaa, M.; Karvinen, E. *Heterocycles* **1992**, *34*, 1773–1782.
- Lounasmaa, M.; Nemes, A.; *Tetrahedron* **1982**, *38*, 223–243.
- Lounasmaa, M.; Tolvanen, A. In *The Alkaloids*; Cordell, G. A., Ed.; Academic Press: New York, **1992**; Vol. 42, p 1.
- Lowry, M. S.; Goldsmith, J. I.; Slinker, J. D.; Rohl, R.; Pascal, R. A.; Malliaras, G. G.; Bernhard, S. *Chem. Mater.* **2005**, *17*, 5712–5719. (b) Prier, C.K.; Rankic, D.A.; MacMillan, D.W.C. *Chem. Rev.* **2015**, *113*, 5322–5363.
- Ma, X.; Herzon, S.B. *Chem. Sci.* **2015**, *6*, 6250–6255.

- Magnus, P.; Brown, P.; *J. Chem. Soc. Chem. Comm.* **1985**, 184–186.
- Magnus, P.; Gallagher, T.; Brown, P.; Huffman, J.C. *J. Am. Chem. Soc.* **1984**, *106*, 2105–2114.
- Magnus, P.; Mendoza, J.S.; Stamford, A.; Ladlow, M.; Willis, P. *J. Am. Chem. Soc.* **1992**, *114*, 10232–10245.
- Magnus, P.; Pappalardo, P.; Southwell, I. *Tetrahedron* **1986**, *42*, 3215–3222.
- Mangenev, P.; Andriamialisoa, R.Z.; Langlois, N.; Langlois, Y. *J. Am. Chem. Soc.* **1979**, *101*, 2243–2245.
- Marco-Contelles, J.; Perez-Mayoral, E.; Samadi, A.; do Carmo Carrieras, M.; Soriano, E. *Chem. Rev.* **2009**, *109*, 2652–2671.
- Marfat, A.; Helquist, P. *Tetrahedron Lett.* **1978**, *44*, 4217–4720.
- Martin, J. C.; Arhart, R. J. *J. Am. Chem. Soc.* **1971**, *93*, 2339–2341
- Martin, J. C.; Arhart, R. J. *J. Am. Chem. Soc.* **1971**, *93*, 2341–2342
- Martin, J. C.; Arhart, R. J.; Franz, J. A.; Perozzi, E. F.; Kaplan, L. J. *Org. Synth.* **1977**, *57*, 22–26.
- Martin, J. C.; Arhart, R. Li, J.J. *J. Am. Chem. Soc.* **1971**, *93*, 4327–4329.
- Marziale, A.N.; Duquette, D.C.; Craig II, R.A.; Kim, K.E.; Liniger, M.; Numajira Y.; Stoltz, B.M. *Adv. Synth Catal.* **2015**, *357*, 2238 – 2245.
- McDougal, N.T.; Streuff, J.; Mukherjee, H.; Virgil, S.C.; Stoltz, B.M. *Tetrahedron Lett.* **2010**, *51*, 5550–5554.
- Medley, J.W; Movassaghi, M. *Angew. Chem. Int. Ed.* **2012**, *51*, 4572–4576.
- Mejia-Oneto, J.M.; Padwa, A.; *Org. Lett.* **2006**, *8*, 3275–3278.
- Meng, Z.; Fürstner, A. *J. Am. Chem. Soc.* **2019**, *141*, 805–809.
- Meyers, A. I.; Romine, J.; Robichaud, A. J. *Heterocycles* **1990**, *30*, 339–340.

- Miyazaki, T.; Yokoshima, S.; Simizu, S.; Osada, H.; Tokuyama, H.; Fukuyama, T. *Org. Montaser, R.; Luesch, H.; Future Med. Chem.* **2011**, *3*, 1473–1489. b) Berrue, F.; Kerr, R.G. *Nat. Prod. Rep.* **2009**, *26*, 681–710. c) Kamel, H.N.; Slattery, M.; *Pharm. Biol.* **2005**, *43*, 253–269.
- Morales, S.; Guijarro, F.G.; Garcia Ruano, J.L.; Cid, M.B. *J. Am. Chem. Soc* **2014**, *136*, 1082–1089.
- Morelli X.; Hupp T. *EMBO Rep.* **2012**, *13*, 877-879.
- Naaz, H.; Singh, S.; Pandey, V.P.; Singh, P.; Swivedi, U.N. *Indian Journal of Biochemistry & Biophysics* **2013**, *50*, 120–125.
- Naber, J.R.; Buchwald, S.L. *Adv. Synth. Catal.* **2008**, *350*, 957–961.
- Nannini, L.J.; Nemat, S.J.; Carrieria, E.M. *Angew. Chem. Int. Ed.* **2018**, *57*, 823–826.
- Neises, B.; Steglich, W. *Angew. Chem. Int. Ed.* **1978**, *17*, 522–524.
- Nicolaou, K.C.; Bulger, P.G.; Sarlah, D. *Angew. Chem. Int. Ed.* **2005**, *44*, 4442–4489.
- Nicolaou, K.C.; Chen, J.S. Haplophytine. In *Classics in total synthesis III: further targets, strategies, methods*; Wiley-VCH: Weinheim, Germany, 2011; pp. 689–718.
- Nicolaou, K.C.; Dalby, S.M.; Li, S.; Suzuki, T.; Chen, D.Y.K. *Angew. Chem. Int. Ed.* **2009**, *48*, 7616–7620.
- Nicolaou, K.C.; Dalby, S.M.; Majumder, U. *J. Am. Chem. Soc.* **2008**, *130*, 14942-14943.
- Nicolaou, K.C.; Snyder, S.A. Vinblastine. In *Classics in total synthesis II: more targets, strategies, methods*; Wiley-VCH: Weinheim, Germany, 2003; pp 505–532.
- Noble, R. L. *Lloydia* **1964**, *27*, 280.
- Noble, R. L.; Beer, C. T.; Cutts, J. H. *Ann. N.Y. Acad. Sci.* **1958**, *76*, 882.
- Node, M.; Nagasawa, H.; Fuji, K. *J. Am. Chem. Soc.* **1987**, *109*, 7901–7903.

- Node, M.; Nagasawa, H.; Fuji, K. *J. Org. Chem.* **1990**, *55*, 517–521.
- Numajiri Y. Pritchett B.P.; Chiyoda K.; Stoltz B.M. *J. Am. Chem. Soc.* **2015**, *137*, 1040–1043.
- O'Connor, S.E.; Maresh, J.J. *Nat. Prod. Rep.* **2006**, *23*, 532–547.
- Occhiato, E.G.; Trabocchi, A.; Guarna, A. *J. Org. Chem.* **2001**, *66*, 2459–2465.
- Ono, I.; Hata, N. *Bull. Chem. Soc. Jpn.* **1987**, *60*, 2891–2897.
- Oppolzer, W. *Acc. Chem. Res.* **1982**, *15*, 135–141.
- Palani, V.; Hugelshofer, C.L.; Sarpong, R. *J. Am. Chem. Soc.* **2019**, *141*, 14421–14432.
- Pandey, G.; Mishra, A.; Khamrai, J. *Org. Lett.* **2017**, *19*, 3267 – 3270.
- Potier, P.; Langlois, N.; Langlois, Y.; Guéritte, F. *J. Chem. Soc. Chem. Comm.* **1975**, 670–671.
- Prasad, K. R.; Nidhiry, J. E. *Synlett* **2012**, *23*, 1477–1480.
- Pritchett B.P.; Donckele E.J.; Stoltz B.M. *Angew. Chem. Int. Ed.* **2017**, *56*, 12624–12627.
- Pritchett B.P.; Kikuchi J.; Numajiri Y.; Stoltz B.M. *Angew Chem. Int. Ed* **2016**, *56*, 13529–13532.
- Rahman, M.T.; Tiruveedhula, V.V.N.P.B.; Cook, J.M. *Molecules* **2016**, *21* 1525–1564.
- Raie, I.D.; Rosenberger, M.; Snabo, A.G.; Willis, C.R.; Yates, P.; Zacharias, D.E.; Jeffrey, G.A.; Douglas, B.; Kirkpatrick, J.L.; Weisbach, J.A.
- Raucher, S.; Bray, B.L. *J. Org. Chem.* **1985**, *50*, 3236–3237.
- Raucher, S.; Bray, B.L.; Lawrence, R.F. *J. Am. Chem. Soc.* **1987**, *109*, 442–446.
- Renner, U.; Fritz, H. *Tetrahedron Lett.* **1964**, *6*, 283–287.
- Rieke, R.D.; Uhm, S.J.; Hudnall, P.M. *J. Chem. Soc. Chem. Comm.* **1973**, 269–270.
- Rogers, E.E.; Snyder, H.R.; Fischer, R.F.; *J. Am. Chem. Soc.* **1952**, *74*, 1987–1989.
- Ryu, I.; Murai, S.; Hatayama, Y.; Sonada, N. *Tetrahedron Lett.* **1978**, *37*, 3455–3458
- Sarkar, D.; Bera, N.; Ghosh, S. *Eur. J. Org. Chem.* **2020**, 1310–1326.

- Sasaki, Y.; Kato, D.; Boger, D.L. *J. Am. Chem. Soc.* **2010**, *132*, 13533–13544.
- Satoh, H.; Ojima, K.; Ueda, H.; Tokuyama, H. *Angew. Chem. Int. Ed.* **2016**, *55*, 15157–15161.
- Satoh, H.; Ueda, H.; Tokuyama, H. *Tetrahedron* **2013**, *69*, 89–95.
- Sawada, S., Okajima, S., Aiyama, R. Nokata, K., Furuta, T., Yokokura, T., Sugino, E., Yamaguchi, K., Miyasaka, T. *Chem. Pharm. Bull.* **1991**, *39*, 1446–1454.
- Schevenels, F.T.; Shen, M.; Snyder, S.A. *J. Am. Chem. Soc.* **2017**, *139*, 6329–6337.
- Schley, N.D.; Fu, G.C. *J. Am. Chem. Soc.* **2014**, *136*, 16588–16593.
- Schmidt, M.A.; Movassaghi, M. *Synlett.* **2008**, *3*, 313–324.
- Schultz, A. G.; Pettus, L. *J. Org. Chem.* **1997**, *62*, 6855–6861.
- Scott, D.E.; Bayly, A.R.; Abell, C.; Skidmore, J. *Nat. Rev. Drug. Discov.* **2016**, *15*, 533-550.
- Sears, J.E.; Boger, D.L. *Acc. Chem. Res.* **2015**, *48*, 653–662 and references therein.
- Shenvi, R.A.; Guerrero, C.A.; Shi, J.; Li, C-C.; Baran, P.S. *J. Am. Chem. Soc.* **2008**, *130*, 7241–7243.
- Sheu, J.; Ahmed, A. F.; Shiue, R.; Dai, C.; Kuo, Y.; *J. Nat. Prod.* **2002**, *65*, 1904–1908.
- Shono, T.; Matsumura, H.; Ogaki, M.; Onomura, O. *Chem. Lett.* **1987**, *16*, 1447–1450.
- Snyder, H.R.; Fischer, R.F.; Walker, J.F.; Els, H.E.; Nussberger, G.A. *J. Am. Chem. Soc.* **1954**, *76*, 2819–2825.
- Srinivasan, R.; Carlough, K. H. *J. Am. Chem. Soc.* **1967**, *89*, 4932–4936.
- Steven, A.; Overman, L.E. *Angew. Chem. Int. Ed.* **2007**, *46*, 5488–5508.
- Steves, J. E.; Stahl, S. S. *J. Am. Chem. Soc.* **2013**, *135*, 15742–15745.
- Sumi, S.; Matsumoto, K.; tokuyama, H.; Fukuyama, T. *Tetrahedron* **2003**, *59*, 8571–8587.
- Sumi, S.; Matusomoto, K.; Tokuyama, h.; Fukuyama, T. *Org. Let.* **2003**, *5*, 1891–1893.
- Suzuki, H.; Kondo, A.; Ogawa, T. *Chem Lett.* **1985**, *14*, 411–412.)

- Svoboda, G. H.; Nuess, N.; Gorman, M. *J. Am. Pharm. Assoc. Sci. Ed.* **1959**, *48*, 659.
- Synder, H.R.; Strohmayer, H.F.; Mooney, R.A. *J. Am. Chem. Soc.* **1958**, *80*, 3708–3710.
- Szabo, L.; Kalas, G.; Szantay C. *Archiv der Pharmazie*, **1983**, *316*, 629–638.
- Tadross, P.A.; Stoltz, B.M. *Chem. Rev.* **2012**, *112*, 3550–3577.
- Takano, S.; Hatakeyama, S.; Ogasawara, K. *Heterocycles* **1977**, *6*, 1311–1317.
- Takano, S.; Yonaga, M.; Morimoto, M.; Ogasawara, K. *J. Chem. Soc., Perkin Trans. I*, **1985**, 305–309.
- Takasu, K.; Nagao, S.; Ihara, M. *Tetrahedron Lett.* **2005**, *46*, 1005–1008.
Tetrahedron **2013**, *69*, 10869–10875.
- Thao, N.P.; Nam, N.H. Cuong, N.X.; Quang, T.H.; Tung, P.T.; Dat, L.D.; Chae, D.; Kim, S.; Koh, Y-S.; Kiem, P.V. *Bioorg. Med. Chem. Lett.* **2013**, *23*, 228–231.
- Thatch, D.Q.; Brill, Z.G.; Grover, H.K. Esguerra, K.V.; Thompson, J.K.; Maimone, T.J. *Angew. Chem. Int. Ed.* **2020**, *59*, 1532–1535.
- Tokuyama, H.; Yokoshima, S.; Yamashita, T.; Fukuyama, T.; *tetrahedron Lett.* **1998**, *39*, 3189–3192.
- Tran, Y.S.; Kwon, O. *Org. Lett.* **2005**, *7*, 4289–4291.
- Trost, B.M.; Bai, Y.; Bai, W-J.; Schultz, J.E. *J. Am. Chem. Soc.* **2019**, *141*, 4811–4814.
- Trost, B.M.; Ball, Z.T. *J. Am. Chem. Soc.* **2005**, *127*, 17644–17655.
- Tseng, Y.-J.; Ahmed, A.F.; Dai, C.-F.; Chiang, M.Y.; Sheu, J.-H. *Org. Lett.* **2005**, *7*, 3813–3816.
- Ueda, *Chem. Pharm. Bull.* **2020**, *68*, 117–128.
- Ueda, H.; Satoh, H.; Matsumoto, K.; Sugimoto, K.; Fukuyama, T.; Tokuyama, H. *Angew Chem. Int. Ed.* **2009**, *48*, 7600–7603.

- Uematsu, N.; Fujii, A.; Hashiguchi, H.; Ikariya, T.; Noyori, R. *J. Am. Chem. Soc.* **1996**, *118*, 4916–4917.
- Vander Mierde, H.; Van Der Poort, P.; Verpoort, F. *Tetrahedron Lett.* **2009**, *50*, 201–203.
- Varseev, G.N.; Maier, M.E. *Org. Lett.* **2005**, *7*, 3881–3885.
- Voloshchuk, T.; Farina, N.S.; Wauchope, O.R.; Kiprowska, M.; Haberfield, P.; Greer, A. *J. Nat. Prod.* **2004**, *67*, 1141–1146.
- Wang, K-Y.; Liu, D-D.; Sun, T-W.; Lu, Y.; Zhang, S-L.; Li, Y-H.; Han, Y.X.; Liu, H-Y.; Peng, C.; Wang, Q-Y.; Chen, J-H.; Yang, Z. *J. Org. Chem.* **2018**, *83*, 6907–6923.
- Wang, X.; Guram, A.; Caille, S.; Hu, J.; Preston, J.P.; Ronk, M.; Walker, S. *Org. Lett.* **2011**, *13*, 1881–1883.
- Wang, Z.; Ai, F.; Wang, Z.; Zhao, W.; Zhu, G.; Lin, Z.; Sun, J. *J. Am. Chem. Soc.* **2015**, *137*, 383–389.
- Wasserman, H. H.; Kuo, G.-H. *Tetrahedron Lett.* **1989**, *30*, 873–876.
- Wee, A. G. H.; Yu, Q. *J. Org. Chem.* **2001**, *66*, 8935–8943.
- Wee, A. G. H.; Yu, Q. *Tetrahedron Lett.* **2000**, *41*, 587–590.
- Weinstabl, H.; Gaich, T.; Mulzer, J. *Org. Lett.* **2012**, *14*, 2834–2837.
- Wenkert, E.; Hudlicky, T. *J. Org. Chem.* **1988**, *53*, 1953–1957.
- Wenkert, E.; Wickberg, B. *J. Am. Chem. Soc.* **1965**, *87*, 1580–1589.
- Wickens, Z.K.; Morandi, B.; Grubbs, R.H. *Angew. Chem. Int. Ed.* **2013**, *52*, 11257–11260.
- Wickens, Z.K.; Skakuj, K.; Morandi, B.; Grubbs, R.H. *J. Am. Chem. Soc.* **2014**, *136*, 890–893.
- Winkler, J. D.; Bowen, C. M.; Liotta, F. *Chem. Rev.* **1995**, *95*, 2003–2020.
- Wolff, S.; Agosta, W. C. *J. Chem. Soc., Chem. Commun.* **1981**, 118–120.
- Wolff, S.; Agosta, W. C. *J. Org. Chem.* **1981**, *46*, 4821–4825.

- Wolff, S.; Agosta, W. C. *J. Am. Chem. Soc.* **1983**, *105*, 1292–1299.
- Woodward, R.B.; Wendler, N.L.; Brutschy, F.J. *J. Am. Chem. Soc.* **1945**, *67*, 1425–1429.
- Wright, C.W.; Allen, D.; Cai, Y.; Philipson, J.D.; Said, I.M.; Kirby, G.C.; Warhurst,
- Wu, P.; Givskov, M.; Nielsen, T.E. *Chem. Rev.* **2019**, *119*, 11245–11290.
- Wüstenberg, B.; Pfaltz, A. *Adv. Synth. Cat.* **2008**, *350*, 174–178.
- Xan, H; Stoltz, B.M.; Corey E.J.; *J. Am. Chem. Soc.* **1999**, *121*, 7600 – 7605.
- Xia, S.; Yang, B.; Li, G.; Zhu, X.; Wang, A.; Zhu. *J. Polym. Chem.* **2011**, *2*, 2356–2359.
- Xu, Z.; Wang, Q.; Zhu, J. *Chem. Soc. Rev.* **2018**, *47*, 7882–7898.
- Yang, C.C.; Chang, H.T.; Fang, J.M. *J. Org. Chem.* **1993**, *58*, 3100–3105.
- Yates, P.; MacLachlan, F.N.; Rai, I.D.; Rosenberger, M.; Szabo, A.G.; Willis, C.R.; Cava, M.P.; Behforouz, M.; Lakshmikantham, M.V.; Zeiger, W. *J. Am. Chem. Soc.* **1973**, *95*, 7842–7850.
- Yen, W.-H.; Su, Y.-D.; Chang, Y.-C.; Chen, Y.-H.; Dai, C.-F.; Wen, Z.-H.; Su, J.-H.; Sung, P.-J. *Tetrahedron Lett.* **2013**, *54*, 2267–2270.
- Yokoshima, S.; Ueda, T.; Kobayashi, S.; Sato, A.; Kuboyama, T.; Tokuyama, H.; Fukuyama, T. *J. Am. Chem. Soc.* **2002**, *124*, 2137–2139.
- Yu, J.; Wearing, X.Z.; Cook, J.M. *J. Org. Chem.* **2005**, *70*, 3963–3979.
- Zhang, L.-H.; Cook, J. *Heterocycles* **1988**, *27*, 2795–2802.
- Zhang, P-P.; Yan, Z-M.; Li, Y-H.; Gong, J-X.; Yang, Z *J. Am. Chem. Soc.* **2017**, *139*, 13989–13992.
- Zhao, S.; Lio, X.; Wang, T.; Flippen-Anderson, J.; Cook, J.M. *J. Org. Chem.* **2003**, *68*, 6279–6295.

Zhu, Y.; Romero, E.L.; Srinivas, K.; Noriega, E. *ChemRxiv*. **2020**, Preprint. DOI:

10.26434/chemrxiv.11560137.v1

ABOUT THE AUTHOR

Christopher Elias Reimann was born in New York City on May 11, 1993 but raised in the great state of New Jersey. He is the oldest son of Robert and Susan Reimann and the older brother of twins, Cole and Gabrielle; due to a common misconception, Chris stresses he himself *does not have a twin sibling*, but rather, he has *siblings who are twins*.

Chris's love of science from an early age influenced his decision to attend Biotechnology High School, a district academy for students specializing in biomedical sciences. He then went on to attend the University of Southern California (USC), where his love of organic chemistry was cultivated by two experiences: performing undergraduate research in the lab of Professor Nicos Petasis, studying the synthesis of pro-resolving lipid mediators, and teaching recitations for the sophomore Organic Chemistry class as a Supplemental Instruction leader during his final two years. According to university records, he graduated *magna cum laude* with a B.S. in Biochemistry and a minor in Neuroscience in 2015; however, Chris maintains this was all a front to allow him to pursue his true passion, marching band, where he played trumpet and served as Drum Major¹.

Chris decided to stay in Southern California, much to the chagrin of his mother, and he began his graduate studies at the California Institute of Technology (Caltech) researching natural product synthesis in the lab of Professor Brian Stoltz. Outside of lab, Chris enjoys drinking good bourbon, decent wine, and crappy beer. His favorite hobbies include exploring LA with friends, getting his hopes up about Trojan football, playing guitar, and—as of this past spring when he couldn't be in lab—cooking.

Following graduation, he will return to the East Coast and begin work as a Senior Scientist in Early Oncology Development at AstraZeneca in Waltham, MA.

¹ Everyone thinks he was the mascot; he swears it's different.